BONE MARROW ADIPOSE TISSUE: FORMATION, FUNCTION, AND IMPACT ON HEALTH AND DISEASE

EDITED BY: William P. Cawthorn and Erica L. Scheller

PUBLISHED IN: Frontiers in Endocrinology

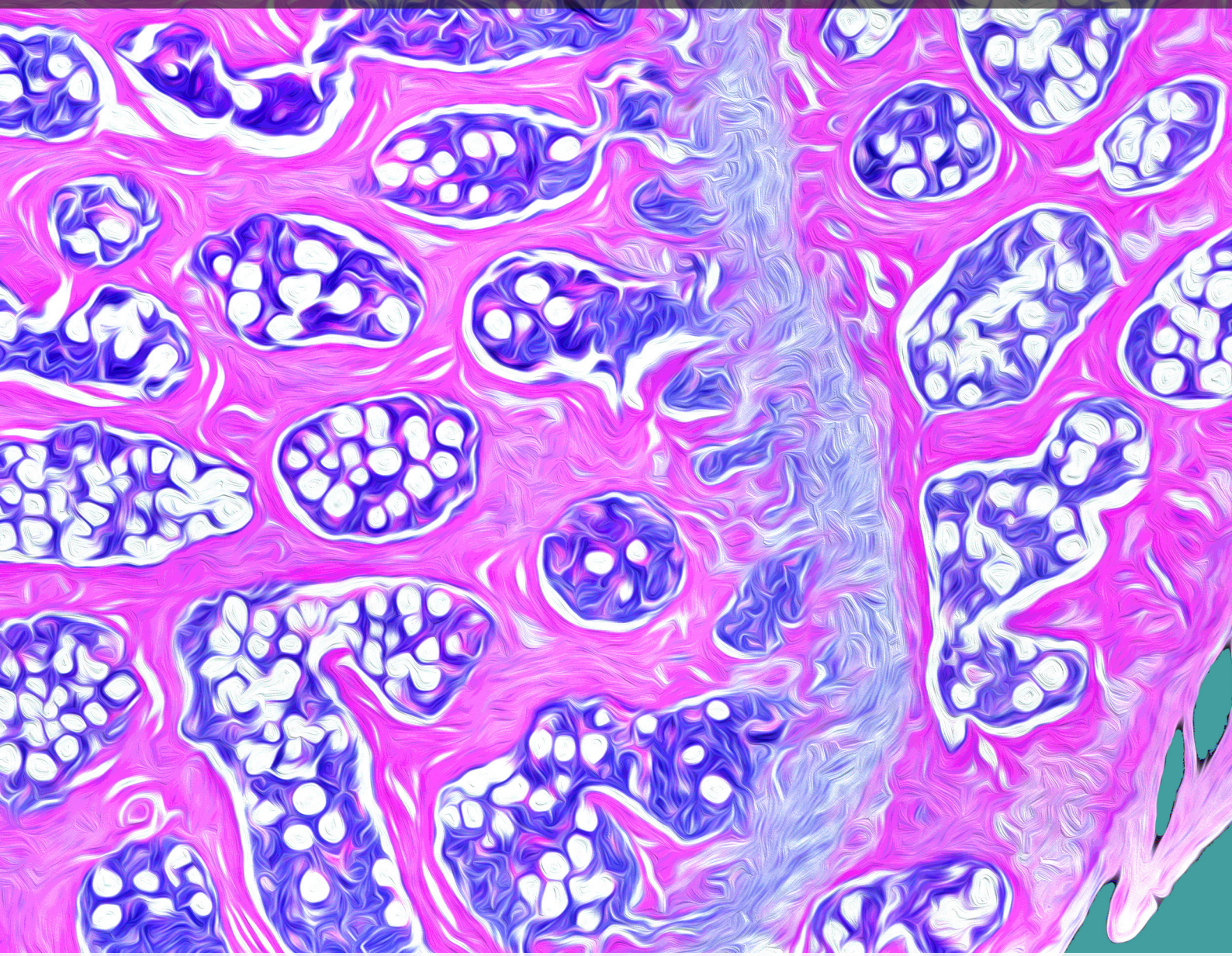

frontiers Research Topics

frontiers

ISSN 1664-8714
ISBN 978-2-88945-245-3
DOI 10.3389/978-2-88945-245-3

About Frontiers

Frontiers is more than just an open-access publisher of scholarly articles: it is a pioneering approach to the world of academia, radically improving the way scholarly research is managed. The grand vision of Frontiers is a world where all people have an equal opportunity to seek, share and generate knowledge. Frontiers provides immediate and permanent online open access to all its publications, but this alone is not enough to realize our grand goals.

Frontiers Journal Series

The Frontiers Journal Series is a multi-tier and interdisciplinary set of open-access, online journals, promising a paradigm shift from the current review, selection and dissemination processes in academic publishing. All Frontiers journals are driven by researchers for researchers; therefore, they constitute a service to the scholarly community. At the same time, the Frontiers Journal Series operates on a revolutionary invention, the tiered publishing system, initially addressing specific communities of scholars, and gradually climbing up to broader public understanding, thus serving the interests of the lay society, too.

Dedication to quality

Each Frontiers article is a landmark of the highest quality, thanks to genuinely collaborative interactions between authors and review editors, who include some of the world's best academicians. Research must be certified by peers before entering a stream of knowledge that may eventually reach the public - and shape society; therefore, Frontiers only applies the most rigorous and unbiased reviews.
Frontiers revolutionizes research publishing by freely delivering the most outstanding research, evaluated with no bias from both the academic and social point of view.
By applying the most advanced information technologies, Frontiers is catapulting scholarly publishing into a new generation.

What are Frontiers Research Topics?

Frontiers Research Topics are very popular trademarks of the Frontiers Journals Series: they are collections of at least ten articles, all centered on a particular subject. With their unique mix of varied contributions from Original Research to Review Articles, Frontiers Research Topics unify the most influential researchers, the latest key findings and historical advances in a hot research area! Find out more on how to host your own Frontiers Research Topic or contribute to one as an author by contacting the Frontiers Editorial Office: **researchtopics@frontiersin.org**

BONE MARROW ADIPOSE TISSUE: FORMATION, FUNCTION, AND IMPACT ON HEALTH AND DISEASE

Topic Editors:
William P. Cawthorn, University of Edinburgh, Edinburgh, United Kingdom
Erica L. Scheller, Washington University, United States

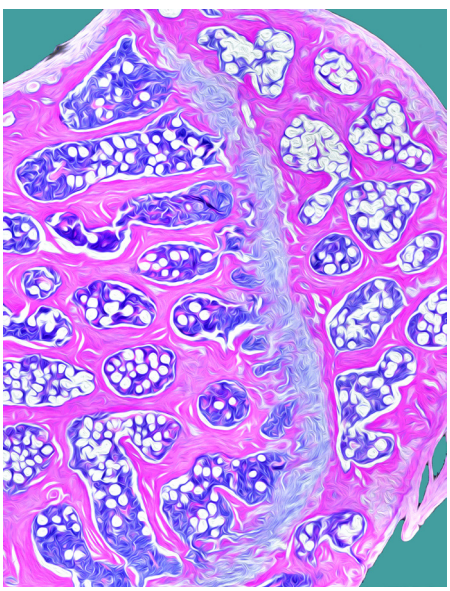

Micrograph of a rat femoral head (male FBN rat, 30-months old). The section was stained with haematoxylin and eosin. The image was then stylised in Adobe Photoshop by processing through the 'Oil Paint' Filter, followed by HDR Toning. Adipocytes (white circles) are clustered within pockets of bone marrow (purple), sorrounded by trabecular bone (pink). Tissue sectioning and staining was done by Dr. Karla Suchacki and Mr. Alexandre Lafond (University of Edinburgh), with image processing done by Dr. William Cawthorn.

Adipocytes are a major component of the bone marrow, accounting for up to 70% of total bone marrow volume in healthy humans. Indeed, this bone marrow adipose tissue (often referred to as 'MAT' or 'BMAT') accounts for at least 5% of total adipose tissue mass in lean, healthy humans, suggesting a role in normal physiology and development. Bone marrow adiposity further increases with ageing and in diverse clinical conditions, including major public health challenges such as osteoporosis. Yet despite this abundance and compelling clinical potential, bone marrow adipocytes have received surprisingly little attention from the biomedical research community.

Thankfully, this is now beginning to change. Research over the past decade has begun to increase our knowledge of BMAT, including the conditions associated with altered bone marrow adiposity and the potential physiological and pathological functions of bone marrow adipocytes. The articles within this e-Book highlight many of these recent developments, underscoring our increasing knowledge of BMAT formation and function; showcasing emerging techniques for basic and clinical BMAT analysis; and highlighting key questions and future directions for this burgeoning and increasingly diverse field.

The editors would like to express their thanks to the authors for contributing the articles within this e-Book; to the senior editors at Frontiers in Endocrinology for their guidance; and to the staff at Frontiers for their helpful input throughout.

Citation: Cawthorn, W. P., Scheller, E. L., eds. (2017). Bone Marrow Adipose Tissue: Formation, Function, and Impact on Health and Disease. Lausanne: Frontiers Media. doi: 10.3389/978-2-88945-245-3

Table of Contents

06 ***Editorial: Bone Marrow Adipose Tissue: Formation, Function, and Impact on Health and Disease***

William P. Cawthorn and Erica L. Scheller

Chapter 1 – Key Aspects of BMAT Biology in Health and Disease

09 ***Bone Marrow Adipose Tissue: To Be or Not To Be a Typical Adipose Tissue?***

Pierre Hardouin, Tareck Rharass and Stéphanie Lucas

20 ***Qualitative Aspects of Bone Marrow Adiposity in Osteoporosis***

Ana María Pino, Melissa Miranda, Carolina Figueroa, Juan Pablo Rodríguez and Clifford J. Rosen

26 ***MR-Based Assessment of Bone Marrow Fat in Osteoporosis, Diabetes, and Obesity***

Christian Cordes, Thomas Baum, Michael Dieckmeyer, Stefan Ruschke, Maximilian N. Diefenbach, Hans Hauner, Jan S. Kirschke and Dimitrios C. Karampinos

Chapter 2 – BMAT Origins and Development

33 ***The Bone Marrow-Derived Stromal Cells: Commitment and Regulation of Adipogenesis***

Michaela Tencerova and Moustapha Kassem

45 ***Fatty Infiltration of Skeletal Muscle: Mechanisms and Comparisons with Bone Marrow Adiposity***

Mark W. Hamrick, Meghan E. McGee-Lawrence and Danielle M. Frechette

52 ***Vanadate Impedes Adipogenesis in Mesenchymal Stem Cells Derived from Different Depots within Bone***

Frans Alexander Jacobs, Hanél Sadie-Van Gijsen, Mari van de Vyver and William Frank Ferris

Chapter 3 – Metabolic and Endocrine Aspects of BMAT

64 ***Changes in Skeletal Integrity and Marrow Adiposity during High-Fat Diet and after Weight Loss***

Erica L. Scheller, Basma Khoury, Kayla L. Moller, Natalie K. Y. Wee, Shaima Khandaker, Kenneth M. Kozloff, Simin H. Abrishami, Brian F. Zamarron and Kanakadurga Singer

77 ***Hypothalamic Leptin Gene Therapy Reduces Bone Marrow Adiposity in ob/ob Mice Fed Regular and High-Fat Diets***

Laurence B. Lindenmaier, Kenneth A. Philbrick, Adam J. Branscum, Satya P. Kalra, Russell T. Turner and Urszula T. Iwaniec

86 ***Marrow Adipose Tissue Expansion Coincides with Insulin Resistance in MAGP1-Deficient Mice***

Tezin A. Walji, Sarah E. Turecamo, Alejandro Coca Sanchez, Bryan A. Anthony, Grazia Abou-Ezzi, Erica L. Scheller, Daniel C. Link, Robert P. Mecham and Clarissa S. Craft

95 ***Exercise Regulation of Marrow Adipose Tissue***

Gabriel M. Pagnotti and Maya Styner

105 ***Increased Bone Marrow Adiposity in a Context of Energy Deficit: The Tip of the Iceberg?***

Olfa Ghali, Nathalie Al Rassy, Pierre Hardouin and Christophe Chauveau

112 ***Increased Circulating Adiponectin in Response to Thiazolidinediones: Investigating the Role of Bone Marrow Adipose Tissue***

Richard J. Sulston, Brian S. Learman, Bofeng Zhang, Erica L. Scheller, Sebastian D. Parlee, Becky R. Simon, Hiroyuki Mori, Adam J. Bree, Robert J. Wallace, Venkatesh Krishnan, Ormond A. MacDougald and William P. Cawthorn

Chapter 4 – BMAT and Cancer

129 ***Bone Marrow Adipose Tissue: A New Player in Cancer Metastasis to Bone***

Emma V. Morris and Claire M. Edwards

136 ***Signaling Interplay between Bone Marrow Adipose Tissue and Multiple Myeloma Cells***

Carolyne Falank, Heather Fairfield and Michaela R. Reagan

151 ***New 3D-Culture Approaches to Study Interactions of Bone Marrow Adipocytes with Metastatic Prostate Cancer Cells***

Mackenzie Katheryn Herroon, Jonathan Driscoll Diedrich and Izabela Podgorski

frontiers in Endocrinology

EDITORIAL
published: 29 May 2017
doi: 10.3389/fendo.2017.00112

Editorial: Bone Marrow Adipose Tissue: Formation, Function, and Impact on Health and Disease

William P. Cawthorn[1] and Erica L. Scheller[2]*

[1] University/British Heart Foundation Centre for Cardiovascular Science, The Queen's Medical Research Institute, University of Edinburgh, Edinburgh, United Kingdom, [2] Division of Bone and Mineral Diseases, Department of Medicine, Washington University, Saint Louis, MO, United States

Keywords: bone marrow adipocytes, bone marrow adipose tissue, bone remodeling, osteoporosis, bone marrow stromal cell, endocrinology and metabolism, bone metastases, multiple myeloma

The Editorial on the Research Topic

Bone Marrow Adipose Tissue: Formation, Function, and Impact on Health and Disease

Enthusiasm surrounding bone marrow (BM) adiposity has accelerated in recent years, motivated by numerous factors: adipocytes are abundant within the BM, BM adiposity increases in diverse pathophysiological states, and BM adipocytes can exert diverse effects both within and beyond the skeleton. This diversity has attracted a broad cross-section of scientists to the field and we are delighted to showcase their work in this special edition of *Frontiers in Endocrinology*.

WHAT'S IN A NAME?

Bone marrow adipocytes (BMAs) are large, roughly spherical cells containing a unilocular lipid droplet. They have gone by many names. Early work aptly recognized that BM has different colors, red or yellow, depending on its location—thus the terms *red marrow* and *yellow marrow* came into use (1). Red marrow consists of blood-forming cells with scattered adipocytes, whereas yellow marrow is filled almost entirely with adipocytes. It was not until 1950s–1960s that BM adipocytes became recognized as a fat depot with the potential for adipose tissue-like characteristics (2, 3). This caused the term *yellow marrow* to be replaced by "*marrow fat*" or "*fatty marrow*". Even today, radiological studies still refer to the "bone marrow fat fraction" (BMFF) as a measure of marrow lipid content (Cordes et al.); however, as marrow adipocytes gain more recognition as a distinct, functional cell type, such designations are expanding beyond references to simple lipid. Herein, several options and abbreviations are introduced, including "BMAs" (Hardouin et al.; Ghali et al.,), "marrow adipose tissue" (MAT) (Scheller et al.; Walji et al.; Pino et al.; Sulston et al.), "bone marrow adipose tissue" (BMAT) (Hardouin et al.), and the "constitutive" and "regulated" subtypes of these (i.e., cMAT/rMAT or cBMA/rBMA). Clearly, reaching a consensus on this nomenclature will be important in providing a consistent framework on which this burgeoning field can progress. Based on the publications to date and the overlap of the acronym "MAT" with "muscle adipose tissue", we propose adopting "BMAT" to refer to the tissue and "BMA" to refer to the adipocytes therein.

ORIGINS AND EXPANSION OF BMAT

Bone marrow adipose tissue develops postnatally and accounts for 50–70% of BM volume in healthy adult humans; hence, BMAT development is a normal physiological process. BMAT further accumulates with aging and in diverse clinical conditions, suggesting pathological implications of aberrant

OPEN ACCESS

Edited and Reviewed by:
Jonathan H. Tobias, University of Bristol, United Kingdom

****Correspondence:***
William P. Cawthorn
w.cawthorn@ed.ac.uk

Specialty section:
This article was submitted to Bone Research, a section of the journal Frontiers in Endocrinology

Received: *02 May 2017*
Accepted: *09 May 2017*
Published: *29 May 2017*

Citation:
Cawthorn WP and Scheller EL (2017) Editorial: Bone Marrow Adipose Tissue: Formation, Function, and Impact on Health and Disease. Front. Endocrinol. 8:112. doi: 10.3389/fendo.2017.00112

BMAT formation and function. In their comprehensive review, Hardouin et al. further discuss these issues, which underscore the need to better understand BMAT in physiology and disease. Several other articles herein provide additional focus on BMAT developmental origins and the mechanisms underlying BMAT expansion. Tencerova and Kassem review the differentiation of BMAs from BM stromal cells (BMSCs), discussing lineage tracing studies that are identifying BMSCs committed to the adipogenic lineage; signaling pathways that regulate this commitment; and the heterogeneity of committed BMSC subpopulations. The latter is underscored by Jacobs et al., whose study reveals site-specific differences in BMSC adipogenic potential, while Lindenmaier et al. provide further evidence for the important role of leptin in regulating adipogenic and osteogenic differentiation of BMSCs. Elsewhere, Hamrick et al. discuss BMAT expansion by raising a compelling question: are there common mechanisms underlying adipocyte accumulation in muscle and bone? This unique perspective highlights the many conditions with similar effects on BMAT expansion and intramuscular adipocyte accumulation, and how these common mechanisms might be targeted for therapeutic benefit.

Several other papers in this Research Topic address BMAT expansion in adverse metabolic states. As reviewed by Ghali et al., increased BMAT during caloric restriction is now well established, although the causes and consequences of this remain incompletely understood. At the other end of the metabolic spectrum, studies by Scheller et al. and by Lindenmaier et al. provide additional evidence that, in mice, BMAT accumulates during obesity, and further reveal that this is prevented by leptin treatment or weight loss. This is reminiscent of exercise's ability to prevent BMAT expansion during obesity or other conditions, as discussed by Pagnotti and Styner. Finally, Walji et al. reveal that, in *Mfap2*$^{-/-}$ mice, BMAT expansion coincides with the development of insulin resistance, but not of obesity or hyperglycemia.

Despite such progress, more research is needed to identify committed BMA progenitor(s) in humans and to clarify the mechanisms underlying gain or loss of BMAT in normal development and disease.

BMAT—GOOD, BAD, OR SOMEWHERE IN BETWEEN?

These questions regarding BMAT formation are related to a broader question: what is the function of BMAT? Given that it is a feature of normal anatomy and development, it would be surprising if BMAT did not fulfill at least some physiological functions. Yet, it also seems likely that, in adverse contexts, BMAT can contribute to disease pathogenesis. Notably, increased BMAT often coincides with decreased bone mass, suggesting that bone formation and marrow adiposity are linked. One possibility, touted throughout this Research Topic, is that a common BM progenitor undergoes adipogenesis at the expense of osteogenesis (Hardouin et al.; Pino et al.; Tencerova and Kassem; Jacobs et al.; Pagnotti and Styner). However, other contributors show that alterations in BMAT quantity do not always coincide with opposite changes in bone mass, whether in response to obesity (Scheller et al.), insulin resistance (Walji et al.), leptin treatment (Lindenmaier et al.), or caloric restriction/anorexia (Ghali et al.). Another possibility is that BMAs secrete factors to directly regulate bone remodeling, even without gross changes in BMAT quantity. Other potential secretory functions of BMAT are further explored by Sulston et al., who investigate BMAT as a source of the hormone adiponectin. Such endocrine properties might allow BMAT to act outside the skeleton, exerting systemic effects on metabolism and beyond.

A final concept gaining increasing attention is that BMAs modulate tumor growth and metastasis. Morris and Edwards provide a comprehensive review, while Falank et al. offer an in-depth focus on the interplay between BMAT and multiple myeloma cells. Complementing these articles, Herroon et al. describe novel methods for studying interactions between BMAs and prostate metastases. Together, these articles emphasize that some BMA-derived factors can stimulate tumor progression, while other secretory products can exert inhibitory effects. Targeting these mechanisms may thereby represent a novel therapeutic avenue in the battle against myeloid cancers and metastatic bone disease.

TECHNOLOGICAL ADVANCEMENTS

Recent advances in quantitative imaging of BMAs have accelerated our understanding of this relatively inaccessible fat depot in both rodents and humans. In the article by Hardouin et al., the evolution of these techniques is described in detail, including magnetic resonance imaging, proton magnetic resonance spectroscopy, and high-resolution computed tomography. In humans, synthesis, adaptation, and modification of existing techniques have allowed researchers to non-invasively monitor BMAT development and expansion in parallel with changes to the healthy and diseased skeleton (reviewed in Cordes et al.). In rodents, imaging of skeletal BMAT with osmium tetroxide and computed tomography has emerged as the current gold standard, facilitating both volumetric quantification of BMAT and spatial analysis of BMAT patterning within bone. Longitudinal application of these techniques in rodents is leveraged in this edition to demonstrate that bone loss precedes BMAT expansion in two models of obesity and diabetes (Scheller et al.; Walji et al.), leading to the conclusion that, in this context, accumulation of BMAT may be more closely linked to peripheral adipose tissue dysfunction than bone turnover.

Unlike widespread advances in imaging, techniques for robust molecular analysis and genetic manipulation of BMAs are still lacking. However, the work by Herroon et al., presented in this edition, provides a glimpse of the future possibilities. The authors detail two novel *in vitro* approaches to study the interactions of primary BM-derived adipocytes and tumor cells in a three-dimensional coculture. Given the challenges inherent in studying BMAs within their native skeletal microenvironment, *ex vivo* and *in vitro* systems that recapitulate key aspects of BMAT biology will be crucial to elucidation of BMA function.

QUALITY VS QUANTITY

Emerging evidence supports the concept that not all BMAs are created equal and that they have the potential for maladaptation

with age and disease. Indeed, it may not be the total amount of BMAT, but rather its context-specific phenotype that dictates the relationships between BMAT, bone and whole-body metabolism. In this edition, our authors highlight the ability of BMAT to undergo pathological change in diseases such as osteoporosis (Ghali et al.). Morris and Edwards also discuss the relevance of this concept for tumor metastasis, which may explain context-specific tumor-promoting and tumor-suppressive effects of BMAT. A key aspect of this phenotypic switch or maladaptation appears to be shifts in the lipid composition of BMAs (discussed in Pino et al.). While the source of these differences remains unknown, current hypotheses suggest consideration of site-specific progenitor populations (Jacobs et al.) and microenvironmental programming of both developing and mature BMAs. Future work will undoubtedly be needed to explore the differences in BMAT between skeletal sites and to determine its implications for bone loss and metabolic health.

PROSPECTUS

This edition provides a comprehensive overview of the state of the field of BM adiposity, details novel hypotheses, and provides opportunities for development and growth. Based on the work presented, it is clear that future studies are warranted to define the biological functions of BM adipocytes—having implications for bone turnover, hematopoiesis, systemic metabolic homeostasis, tumor metastasis, energy storage, and beyond.

AUTHOR CONTRIBUTIONS

WC and ES jointly wrote this editorial. ES initially wrote the section entitled "What's in a Name?", with WC then contributing further edits. WC then focused on the sections entitled "Origins and Expansion of BMAT" and "BMAT—Good, Bad, or Somewhere in between?", while ES focused on "Technological Advancements", "Quality vs Quantity," and the "Prospectus".

ACKNOWLEDGMENTS

WC and ES are grateful to all of the authors for their contributions to this Research Topic.

FUNDING

WC is supported by a Career Development Award (MR/M021394/1) from the Medical Research Council (UK) and by a Chancellor's Fellowship from the University of Edinburgh. ES is supported by grant R00-DE024178 from the National Institutes of Health.

REFERENCES

1. Piney A. The anatomy of the bone marrow. *Br Med J* (1922) 2:792–5.
2. Scheller EL, Rosen CJ. What's the matter with MAT? Marrow adipose tissue, metabolism, and skeletal health. *Ann N Y Acad Sci* (2014) 1311:14–30. doi:10.1111/nyas.12327
3. Zakaria E, Shafrir E. Yellow bone marrow as adipose tissue. *Proc Soc Exp Biol Med* (1967) 124(4):1265–8. doi:10.3181/00379727-124-31983

Conflict of Interest Statement: The authors declare that the research was conducted in the absence of any commercial or financial relationships that could be construed as a potential conflict of interest.

frontiers in Endocrinology

REVIEW
published: 30 June 2016
doi: 10.3389/fendo.2016.00085

Bone Marrow Adipose Tissue: To Be or Not To Be a Typical Adipose Tissue?

*Pierre Hardouin, Tareck Rharass and Stéphanie Lucas**

Laboratory of Pathophysiology of Inflammatory Bone Diseases PMOI, University of Littoral-Opale Coast ULCO, Boulogne sur Mer, France

Bone marrow adipose tissue (BMAT) emerges as a distinct fat depot whose importance has been proved in the bone–fat interaction. Indeed, it is well recognized that adipokines and free fatty acids released by adipocytes can directly or indirectly interfere with cells of bone remodeling or hematopoiesis. In pathological states, such as osteoporosis, each of adipose tissues – subcutaneous white adipose tissue (WAT), visceral WAT, brown adipose tissue (BAT), and BMAT – is differently associated with bone mineral density (BMD) variations. However, compared with the other fat depots, BMAT displays striking features that makes it a substantial actor in bone alterations. BMAT quantity is well associated with BMD loss in aging, menopause, and other metabolic conditions, such as anorexia nervosa. Consequently, BMAT is sensed as a relevant marker of a compromised bone integrity. However, analyses of BMAT development in metabolic diseases (obesity and diabetes) are scarce and should be, thus, more systematically addressed to better apprehend the bone modifications in that pathophysiological contexts. Moreover, bone marrow (BM) adipogenesis occurs throughout the whole life at different rates. Following an ordered spatiotemporal expansion, BMAT has turned to be a heterogeneous fat depot whose adipocytes diverge in their phenotype and their response to stimuli according to their location in bone and BM. *In vitro*, *in vivo*, and clinical studies point to a detrimental role of BM adipocytes (BMAs) throughout the release of paracrine factors that modulate osteoblast and/or osteoclast formation and function. However, the anatomical dissemination and the difficulties to access BMAs still hamper our understanding of the relative contribution of BMAT secretions compared with those of peripheral adipose tissues. A further characterization of the phenotype and the functional regulation of BMAs are ever more required. Based on currently available data and comparison with other fat tissues, this review addresses the originality of the BMAT with regard to its development, anatomy, metabolic properties, and response to physiological cues.

Keywords: fat–bone association, marrow fat, adipokine, bone marrow adiposity, skeletal adipocyte, osteoporosis, bone fragility

OPEN ACCESS

Edited by:
William Peter Cawthorn, University of Edinburgh, UK

Reviewed by:
Eleni Douni, Agricultural University of Athens, Greece
Ann Schwartz, University of California San Francisco, USA

****Correspondence:***
Stéphanie Lucas
stephanie.lucas@univ-littoral.fr

Specialty section:
This article was submitted to Bone Research, a section of the journal Frontiers in Endocrinology

Received: *03 May 2016*
Accepted: *21 June 2016*
Published: *30 June 2016*

Citation:
Hardouin P, Rharass T and Lucas S (2016) Bone Marrow Adipose Tissue: To Be or Not To Be a Typical Adipose Tissue? Front. Endocrinol. 7:85. doi: 10.3389/fendo.2016.00085

Besides being the main energy storage sites, adipose tissues have revealed through these last decades their diversity regarding their cellular composition, anatomical location, and pathophysiological properties. Indeed, adipocytes are typically classified into three categories: white, brown, and beige types (1). White adipocytes store excessive energy supply in a unilocular triglyceride droplet to release fatty acids in periods of energy depletion. White adipocytes also exert an endocrine function

through the secretions of various adipokines that mainly regulate metabolism and inflammation (2). Conversely, brown adipocytes are multilocular, rich in mitochondria, and dissipate the energy into heat through the uncoupling protein-1 (UCP-1). Their high glucose uptake and oxidative capacities make them key players in the energy balance. At last, beige (also called "brite") adipocytes are brown-like adipocytes with UCP-1 expression that arise within white fat depots in response to cold or catecholaminergic stimulation (3).

Most adipose tissues in adult humans consist of white adipose tissue (WAT) that encompasses major subcutaneous depots (85% of total adipose tissue) in the lower or abdominal body parts and visceral fat depots (~10%) with omental, mesenteric, or retroperitoneal distributions. According to that anatomical location and the pathophysiological contexts, WATs exhibit differences in their development pattern, lipogenic and lipolytic activities, "browning" ability, or endocrine functions. This is best exemplified by the development of visceral adipose tissue that is considered as a strong predictive factor for the emergence of obesity co-morbidities, notably through the secretion of pro-inflammatory cytokines and an enhanced lipolysis (4). Brown adipose tissue (BAT) exhibits a more diffuse distribution with discrete small depots. Owing to the recent reassessement of BAT in adults, stimulating BAT and beige adipocyte recruitment have become promising strategies for the management of metabolic diseases (3, 5).

In addition to WAT and BAT, bone marrow adipose tissue (BMAT) emerges as a "new" fat depot that could represent up to 5% of total fat mass in adults. The presence of BMAT – also referred to as "yellow" bone marrow (BM) – was of a long-standing knowledge but has been surprisingly disregarded for many decades. Meanwhile, bone has been revealed as a target and a regulator of energy metabolism: the two main adipokines, adiponectin and leptin, modulate bone mass through indirect and direct mechanisms (6, 7) and undercarboxylated osteocalcin, the bone-derived hormone, positively impacts on whole-body glucose metabolism (8, 9). Moreover, numerous clinical studies indicate strong relationships between BMAT amount and bone loss emphasizing its potential pathophysiological role in osteoporosis. Other lines of evidence support the involvement of BMAT in hematopoiesis regulation (10) and in the pathophysiology of myeloma (11) and bone metastases (12). Such bone–fat connections have contributed to renew interest in BMAT. Yet, the anatomical dissemination of BM fat and the difficulties to study adipocytes inside bones have considerably hampered our understanding of BM adipocyte (BMA) function and its relative contribution to pathophysiological processes compared with extramedullary fat depots. In this review, we aim at highlighting the current knowledge of BMAT development and phenotype to pinpoint its original features as an adipose tissue.

BMAT DEVELOPMENT IS BOTH PHYSIOLOGICAL AND PATHOLOGICAL

Exploration of BMAT Development

The first descriptions of "hematopoietic red BM" replacement by the "fat yellow BM" were brought by histomorphometric studies of iliac crest biopsies in humans (13, 14) or other bone sites in animals. BMAT quantification has been, thus, performed using specific but static parameters (adipocyte number and diameter, percent of adipocyte volume per tissue volume), which precludes a reliable and dynamic assessment of adipocyte evolution according to the pathophysiological conditions. Magnetic resonance imaging (MRI) has been being of considerable interest to map non-invasively the distribution of hematopoietic BM and fatty BM in clinical studies (15). Moreover, proton magnetic resonance spectroscopy (1H MRS) allows the relative assessment of the saturated and unsaturated fatty acid composition of the fat fraction to monitor the lipid content changes. Combined with bone mineral density (BMD) and bone structure measurement by dual energy X-ray absorptiometry (DEXA) and high-resolution peripheral quantitative computed tomography, respectively, MR techniques have been being instrumental to follow BMAT development and to evaluate relationship between bone quantity and BMAT amount in diverse cohorts. Finally, using the lipid affinity of the opaque agent osmium tetroxide, a three-dimensional quantification of BMAT (whole amount, individual volume, spatial distribution) can be achieved by micro- or nanocomputerized tomography (μCT, nanoCT) in animal decalcified bones (16).

Physiological BM Cellular Conversion to BMAT

Bone marrow adiposity development has been shown to be age, bone site, and gender dependent. At birth, bone cavities mainly contain active hematopoietic red marrow. BMAT accretion then occurs in an orderly and centripetal way: the process begins in the terminal phalanges around birth, continues in the appendicular skeleton (from the diaphysis to the distal and proximal extremities of the long bones) and finally arises in the axial skeleton (15, 17, 18). By the age of 25 years, BMAT is considered to occupy 50 (17) to 70% (16) of the BM volume, while hematopoietic BM is mainly restricted to the axial skeleton, ribs, sternum, and proximal metaphyses of humerus and femur. Afterward, the BM conversion into BMAT slowly progresses throughout the adulthood. Interestingly, women exhibit less BMAT amount compared with age-matched men (19, 20) prior the menopause age, while the following period is associated with a sharp increase of BM adiposity (21).

The development pattern in rodents is considered to be similar though it is far to be as well characterized as in humans. Histological studies of femur or tibia show the presence of BMA at adult age (22, 23), which further increases with aging (24, 25). Of note, the percentage of BM adiposity (or BMA density) appears low in rodents when compared with humans and varies according to the mouse strain. Moreover the presence of different BMA subsets could be suspected from early (26) to more recent studies (27, 28). However, it is with the new introduction of osmium tetroxide staining combined with μCT visualization that analysis of BMAT development has led to the first characterization of two BMA subpopulations in rodents (29). Scheller and collaborators propose to distinguish constitutive BMA (cBMA) – which arise first and early in life

in distal tibia and caudal vertebrae to constitute a rather dense fat depot – from regulated BMA (rBMA) whose formation is late, increases with age, and occurs in a more scattered way in the proximal tibia, distal femur, and lumbar vertebrae (29). Importantly, this distinction based on a spatiotemporal distribution also corresponds to a different metabolic pattern and to different bone remodeling regions (see "Specific properties of BMA versus other adipocytes"). How such classification can be extrapolated to humans is still difficult although one can suggest that cBMA reside in the feet and hands, whereas the rBMA develops in the proximal femur and lumbar vertebrae (16, 29).

BMAT Development Differs from that of Extramedullary Adipose Tissues

Formed during gestation, BAT quantity and activity are maximal at birth to provide an efficient thermogenesis during the first weeks. Beyond puberty that is characterized by an important BAT activity, cold-activated BAT incidence remains high in young adults but rapidly declines by the age of 30 to almost disappear in the elderly (30). BAT function and WAT browning also decrease with age in rodents (31) as shown in **Table 1**. Thus, the development pattern of BMAT differs from the recruitment of thermogenic adipose tissues during the lifespan and other physiological conditions [exercice, cold exposure (3, 5)], supporting that BMAT development responds to different cues.

TABLE 1 | Comparison of the main characteristics of brown adipose tissue (BAT), white adipose tissues (WAT), and bone marrow adipose tissue (BMAT) in rodents.

	BAT	WAT	BMAT
Main locations	Interscapular (32)	Subcutaneous (inguinal) and visceral (perigonadal > mesenteric > retro-peritoneal) (32)	Constitutive BMA (cBMA): distal tibia and caudal vertebrae Regulated BMA (rBMA): proximal tibia and long bones, lumbar vertebrae (29)
Mean adipocyte diameter	–	For rat[a] ~56 μm for inguinal ~74 μm for perigonadal	For rat[a] ~40 μm for caudal cBMA ~33 μm for tibia rBMA
Amount variation during			
Aging	↗ with "whitening" ↘ activity (33)	Subcutaneous ↗ Visceral ↗ (33)	↗ (mainly rBMA) (25, 29)
Calorie restriction (30%)	→ (34, 35)	Subcutaneous ↘ Visceral ↘ (34, 35) or unchanged (22, 35)	↗ (mainly rBMA) (22, 34, 35)
Cold exposure	→ ↗ activity (36, 37)	Subcutaneous ↘ with beiging ↗ (36, 37)	rBMA ↘ cBMA → (29)
High-fat diet-induced obesity	↗ with "whitening" ↘ activity (38)	Subcutaneous ↗ Visceral ↗ (39, 40)	↗ (reported for rBMA in long bones) (39–41)
Ovariectomy	→ ↘ activity (42)	Subcutaneous ↗ Visceral ↗ (42)	↗ (reported for rBMA in long bones) (27)

[a]*Values from Sprague Dawley female rats aged between 19 and 24 weeks (29, 43).*
↗ refers to "increased," ↘ refers to "decreased," → refers to "unchanged." "Whitening" refers to BAT with a changed morphology as occurrence of unilocular adipocytes with increased triglyceride storage. "Beiging" refers to WAT with a changed morphology as the occurrence of multilocular adipocytes with UCP-1 expression.

Early WAT formation is achieved through two early periods of intense precursor proliferation with adipocyte differentiation and lipogenesis in the meanwhile. By the end of adolescence, an adipocyte number set point specific to each individual is considered to be reached and to remain constant throughout life (44), with a rather low adipocyte renewal rate estimated at 8% per year (45). Indeed, the tremendous expandability of WAT primarily relies on adipocyte hypertrophy (cell size increase). Hyperplasia (cell number increase) occurs secondly when adipocyte storage capacity is exceeded and preferentially in subcutaneous AT. WAT growth is, thus, observed throughout the adult lifespan with a maximal mass achieved at middle–early old age. In advanced old age, white fat depots are redistributed with a subcutaneous fat loss in favor of visceral fat accumulation and ectopic fat deposition in other tissues (46). BMAT development with its long-lasting hyperplasia and concomitant hypertrophy (14) throughout life exhibits some striking differences compared with WAT. Moreover, BMAT amount is generally not correlated to usual anthropometric parameters of adiposity, such as waist-to-hip ratio, amount of visceral or subcutaneous fat, or even body mass index (47–49). Altogether, BMAT formation also appears independently regulated from extramedullary WAT both in humans and rodents (**Table 1**).

Adipose Tissues and Relationship with Skeletal Fragility: The Importance of BMAT Development

Beyond being a simple witness of age, diffuse or local BMAT accumulation has been described in several types of osteoporosis notably that associated with aging, menopause, anorexia nervosa, or glucocorticoid treatment. In humans, BMAT amount is even found inversely correlated with bone quantity in aged (47, 50), post-menopausal (51), and anorexia nervosa (52) subjects at various bone sites. Enhanced BMAT formation is also depicted in animal models of aging (53), ovariectomy (27), calorie restriction (22), or following glucocorticoid administration (54). Bone loss results from an altered bone remodeling with either decreased number and/or mineralizing function of osteoblasts as in senile osteoporosis, or with increased bone resorption by osteoclasts that overwhelms bone formation as in post-menopausal osteoporosis (55). BMAT is suspected to contribute to this unbalanced bone remodeling through the adipogenesis process *per se* or its paracrine activity (see Section "BM Adipogenesis" and "Specific Properties of BMA"). However, it has to be emphasized that blocking BMAT formation failed to generate any bone modification in some mouse models (56, 57).

The impact of other adipose tissues on bone has of course been the subject of intensive clinical research that led to a complex picture. Whereas inconsistent results are drawn with subcutaneous adipose tissue measurements, visceral adipose

tissue level, when directly quantitated, is often found negatively associated with BMD and bone quality (58). Indeed, excess visceral fat as in obesity is paralleled by an altered adipokine secretion with increased pro-inflammatory cytokines that have been suggested to interfere with bone remodeling (59). A positive association between BAT volume and BMD has been reported in a few studies in humans (60–62). Yet the prevalence and activity of BAT in humans remain difficult to measure. The beneficial impact of active BAT on bone has also been reported in mouse models (63, 64) and could rely on direct [derived-BAT adipokines (64)] or indirect mechanisms (61, 63). Moreover, bone fragility is a comorbidity of several metabolic diseases and BMAT evolution is obviously of interest in that context.

BMAT Development in Metabolic Diseases

Regarding with type 1 diabetes, genetically or streptozotocin-induced insulin deficiency results in increased BMAT in the long bones of mice (65). However, preventing BMAT formation does not impact on the bone loss (66) inherent to these models and the disease. Moreover, as reported in one study, BMAT content measured at different bone sites was unchanged in diabetic patients compared with control subjects (67). Thus, the involvement of BMAT in type 1 diabetes remains unclear and deserves further explorations.

The skeletal health in obesity has been a controversial subject (68, 69). However, most clinical and epidemiologic studies have reported an alteration of bone quality in obesity leading to an increased fracture incidence at specific bone sites (59, 70–72). Even though visceral adipose tissue quantity can be negatively associated with bone microarchitecture and strength (73), BMAT content has been poorly examined in obesity. So far, only one clinical study performed in obese premenopausal women has reported a positive correlation between visceral adiposity and vertebral BMAT (74). The Ob/Ob mouse model with extreme obesity due to spontaneous leptin disruption shows increased BM adipogenesis in the long bones (75). Nevertheless, this model remains complex to analyze because of the pleiotropic effects of leptin on bone and metabolism. The BMA amount in the long bones also increases in models of high-fat diet-induced obesity (39, 41, 76) (**Table 1**). However, divergent results make it difficult to conclude about the bone phenotype in these models and no associations have been drawn between metabolic parameters and the BMAT rise yet. Of note, animal age and diet duration appear to influence BMAT increment (41, 76), so that older mice would develop more quickly and at a higher level BMA.

Type 2 diabetic patients exhibit an increased fracture risk that is predominantly linked to a compromised bone quality (77, 78). In post-menopausal women, BMAT content in vertebrae is found unchanged by the diabetic state (79, 80), even though it is higher in patients who experienced prolonged hyperglycemia reflected by a HbA1c level above 7% (79).

Weight loss is well known to trigger bone loss, as exemplified in anorexia nervosa but also in bariatric surgery in obesity care (59). In anorexia nervosa (52), BMAT unexpectedly develops while subcutaneous and essentially visceral adipose tissues are extremely depleted. Bariatric surgery (81) or a 4-week-calorie restriction (82) in obese women leads to a marked or a more modest reduction of extramedullary fat depots, respectively. Yet, these decreases are not accompanied by significant changes in BMAT volume. These later studies rely on a limited number of subjects but suggest that the initial metabolic status [diabetes (81) or abdominal adipose tissue distribution (82)] can impact on the BMAT amount changes.

In summary, compared with other fat depots, BMAT could, thus, be considered as a strong and reliable indicator of bone integrity that could open new clinical perspectives in the management of osteoporosis (83). Its measurement rather easily performed using MRI should be more systematically analyzed particularly in metabolic diseases considering that most available data have been generated in animal models. In response to metabolic variations, BMAT development differs from other fat depots in both humans and rodents. Yet, it remains conceivable that BMAT expansion may not be completely independent from the WAT distribution. In this connection, BMAT accretion could be triggered when WAT redistribution occurs as in aging. However, the paradoxical situation of anorexia nervosa supports that BMAT formation is dissociated from that of other fat tissues. A mechanistic pathway shared by all physiopathological conditions to explain BMAT development is, thus, still missing.

BM Adipogenesis

Bone marrow adipogenesis of resident mesenchymal stem cell (MSC) is classically controlled through a transcriptional cascade involving the key transcriptional factors PPARγ and c/EBPα. Within the BM, MSCs reside in the perivascular compartment, at the endosteal surface, and in the marrow space. As in other tissues, BM MSCs represent a heterogeneous cell population with regard to their cell surface marker expression and differentiation potential toward the osteoblast, adipocyte, or chondrocyte lineages (84, 85). It has to be emphasized that a great diversity of adipocyte precursors (distinct MSC populations, pericyte progenitors) for WAT and BAT has been revealed and debated this last decade (3, 44, 86). Interestingly, whereas most adipocytes also develop from adipose tissue-resident progenitors, engrafted BM-derived cells have been shown to generate new adipocytes within WAT in both humans (87) and rodents (88), which argues for another interaction between BM and WAT.

Importantly, adipogenesis is well considered as a competitive process for osteoblastogenesis within the BM. Haplo-insufficiency or overexpression of PPARγ in BM progenitor cells results in increased osteoblastogenesis or adipogenesis, respectively (89). Both *in vitro* and *in vivo* studies have shown that various conditions – such as elevated glucocorticoid levels, estrogen withdrawal, oxidative stress, and immobilization – that promote adipogenesis limit osteoblastogenesis. Conversely, pro-osteogenic factors [growth hormone, insulin-like growth factor 1 (IGF1), Wnt proteins, estrogens, mechanic inputs] decrease adipogenesis (85, 89, 90). Thus, the BM MSC shift toward either lineage results from a complex interplay of systemic and local mediators.

However, the classical view of an unbalanced adipogenesis at the expense of osteoblastogenesis is challenged by other findings.

The coexistence within the mouse BM of independent precursor cells committed to each lineage has been shown (91). Both adipocytes and osteoblasts can fully develop from mouse BM MSC in a co-differentiation medium without any alteration of either lineage (92). As described in Section "Physiological BM Cellular Conversion to BMAT," a part of BMAT development occurs when the bone mass peak is achieved at human puberty and cBMA fully arise without bone loss in rodents. Bone mass can evolve independently of BM adipogenesis in some models (56, 57) or mouse strain (e.g., the C3H/HeJ strain) (93).

In this context, BMAT development cannot represent the only detrimental mechanism. BMA phenotype – which underlies its function – should be considered as a pivotal aspect in bone alterations as emphasized below.

SPECIFIC PROPERTIES OF BMA VERSUS OTHER ADIPOCYTES

Basic Anatomy of the "BMAT"

Compared with subcutaneous or visceral fat lobules composed of ~80% well-packed adipocytes, BMAs arise loosely connected and scattered among hematopoietic cells. In that respect, such adipocyte distribution may not be referred to as a true "adipose tissue". Whereas cBMA constitute a rather dense adipocyte area, rBMA are primarily located at the trabecular site where bone remodeling is active, which suggests their involvement in this process. The sympathetic cue is crucial in bone homeostasis (94) but the nerve distribution toward BMAs has not been depicted yet. Compared with hematopoietic areas, BMA-enriched regions are considered to be less vascularized with a lower perfusion as observed in the hip of normal-aged subjects (95). Moreover, vascularization could differ between cBMA and rBMA areas with, surprisingly, a higher capillary density in the cBMA regions in mouse (96).

Bone marrow adipocytes appear filled by a large unilocular lipid vacuole, a typical morphology of white adipocytes. Human BMA diameter can vary from 40 to 65 μm according to the fat infiltration (14), the cellular composition of BM (97), or the analyzed age (14, 98). BMAs are, thus, smaller than subcutaneous and visceral adipocytes in both humans and rodents, with cBMA larger than rBMA (**Table 1**).

A White or Brown/Beige Phenotype?

Determining the white or brown/brite phenotype of BMA is crucial with regard to a better understanding of their regulation and function. The development factors (**Table 1**) and the unilocular morphology of BMAs are more reminiscent of a white adipocyte. However, the preferential distribution of BM adiposity in the appendicular skeleton following a temperature gradient led some authors to propose a thermogenic role for the adipocytes (99, 100). Several gene markers specific for the "brown/beige" lineage were found expressed in the whole tibia BM in young mice. Based on the expression of both white and brown markers upon rosiglitazone treatment, although UCP-1 expression was barely detected, the authors proposed that BMAT has the two phenotypes (101). A high glucose uptake detected within the BM of cold-exposed patients combined with the immuno-detection of UCP-1 protein in the BMA of very young mice convincingly support the potential presence of functional brown/beige BMA in vertebrae (102). However, these results are contradicted by other studies. Several genes of the fatty acid oxidation pathway were found more weakly expressed in isolated BMA from long bones in comparison with isolated visceral adipocytes in mouse (23). Similarly, human BMA isolated from the iliac crest had lower mRNA levels of typical markers of the brown phenotype compared with subcutaneous adipocytes (103). Importantly, a long-term cold exposure of mice led to a marked decline of BMA density in tibiae but a concomitant browning of other WAT depots (29). Altogether, one may suggest that the BMA phenotype varies according to their localization: BMAs that arise in the long bones most likely belong to the white lineage, whereas some BMAs in the vertebrae can exhibit brown-like features. The presence of such thermogenic adipocytes could explain the disappearance of the "yellow BM" in the caudal vertebrae during a temperature rise (104). Indeed, hematopoiesis remains quite efficient in the vertebra BM and brown adipocytes have been proposed to support myelopoiesis through the secretion of some specific adipokines (102).

Most studies characterizing BMA have been performed from long bones or iliac crest samples and have raised some puzzling specificities regarding their paracrine/endocrine and metabolic properties.

Secretory Profile of BMA

The two main adipokines adiponectin and leptin are detected in isolated mature BMA, could locally promote osteoblastogenesis, and impact on osteoclastogenesis or hematopoiesis (89). However, their mRNA expression levels were found markedly low compared with extramedullary adipocytes in adult healthy donors (103) and normal-aged mice (23).This finding may relate to a lower state of differentiation of BMA as proposed in aging mice (23). Yet BMAT explants from rabbit (distal tibia) or human patients (tibia) were shown to secrete more adiponectin than other WAT depots. Moreover, through the characterization of a mouse model of defective BM adipogenesis, BMAT was revealed as a significant source of serum adiponectin during caloric restriction (34). Even though this contribution to the calorie restriction-induced adiponectinemia rise was not confirmed in rabbits (35), this study underlies a true endocrine status of BMA which can modulate metabolism at the systemic level.

Given the importance of inflammatory factors in the bone loss of post-menopause or aging, the cytokine production by BMA has begun to be assessed. A first antibody-based array study indicates that the cytokine content of BMA diverges from that of subcutaneous adipocytes with a more pro-adipogenic and pro-apoptotic profile in aging mice (105). In another independent transcriptomic study in mice, BMAs were reported to express inflammatory genes, such as TNFα and IL6, at higher levels than visceral adipocytes (23). Surprisingly, in both studies, their expression levels were downregulated during aging, suggesting

that this pro-inflammatory profile of BMA is rather early and transient. Of note, another transcriptional analysis failed to detect any further upregulation of these genes in the BMA from normal-aged mice fed with a high-fat diet (24). Interestingly, primary human femoral BMAs express the pro-osteoclastogenic factor RANKL and mediate through a direct cell contact the differentiation of osteoclast precursors (106, 107). RANKL expression was also shown to be associated with BMA differentiation and with Pref1-expressing preadipocytes in the BM of aging mice (108).

Several *in vitro* studies using notably co-culture models (109, 110) of BM MSC-derived adipocytes and osteoblasts strongly support a deleterious paracrine role of BMA. BM MSC-derived adipocytes have also been reported to secrete factors that alter osteoblastogenesis and favor adipogenesis, such as Wnt signaling inhibitors (111) and chemerin (112) (**Figure 1**).

Metabolic Profile of BMA

Adipocytes synthesize and hydrolyze triglycerides in response to insulin and catecholamines, the respective prototypical lipogenic and lipolytic factors. Functional assays to establish the relative capacity of BMA for lipogenesis and lipolysis compared with other fat depots remain scarce due to technical difficulties. Only one early study in rabbits has reported that isolated femoral adipocytes incorporate palmitate into triglycerides at level equivalent to perirenal adipocytes (113). Catecholamine-induced lipolysis appeared lower in femur compared with omental adipose tissue in dogs (114). More indirectly, but in line with their small size, mouse BMAs were shown to express weaker expression of key genes involved in lipogenesis and lipolysis compared with visceral adipocytes (23). Moreover, the metabolic activity of BMA has been indirectly assessed by the adipocyte size and density determination and seems to vary according to their bone localization and the different subtypes in rodents. Indeed, only BMA in the lumbar spine were affected by a chronic administration of a β3-adrenergic agonist (27). In the tibia, cBMA were reported resistant to a long-term cold-induced catecholamine challenge compared with the regulated subpopulation (29). Whether these observations result from the development timing of each BMA subset, a different innervation/vascularization of the BM regions or intrinsic divergences among BMA subtypes has to be further explored. Nevertheless, the relative amount of BMAT compared with other adipose tissues supports that the metabolic influence of BMA is locally confined.

Importantly, the fatty acid composition of BMA is emerging as a key signature of their phenotype. Compared with subcutaneous adipose tissue, lipid extracts of human BM (mainly from proximal tibia or femur) display a higher proportion of saturated fatty acids and a lower amount of monounsaturated ones (115). Based on 1H MRS exploration, the unsaturation index of the

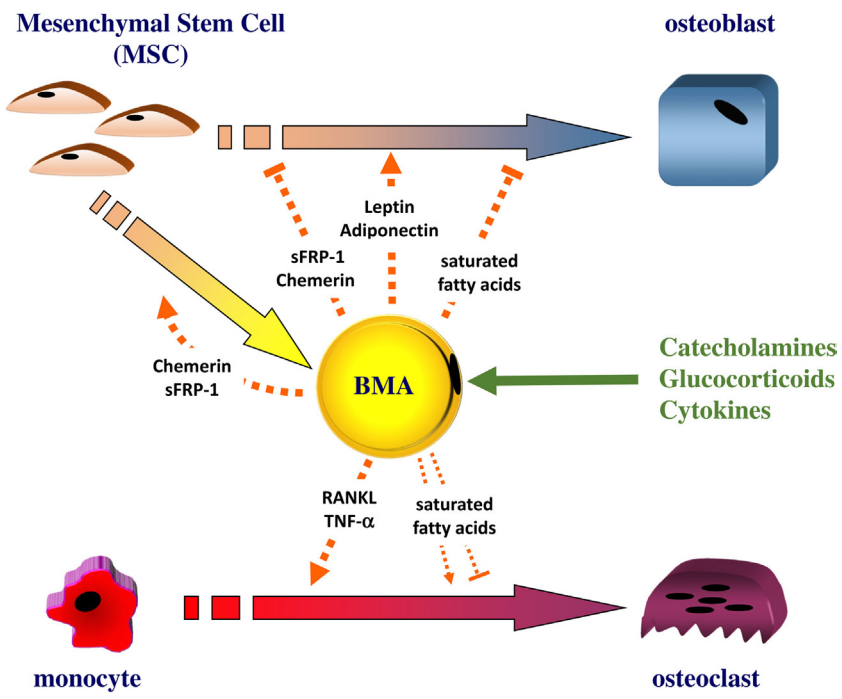

FIGURE 1 | The bone marrow adipocyte as an active cell in bone remodeling. The bone marrow adipocyte (BMA) can secrete leptin and adiponectin, which directly stimulate the proliferation and the differentiation of mesenchymal stem cell (MSC) into osteoblast. Other factors, such as the Wnt signaling inhibitor sFRP1 or chemerin, can be released by the BMA: these factors were shown to promote adipogenesis while negatively regulating osteoblastogenesis. As a source of RANKL and TNF-α, the BMA can also support osteoclastogenesis. The BMA appears enriched in saturated fatty acids that can trigger the dysfunction and apoptosis of osteoblasts. Saturated fatty acids could impact on osteoclast differentiation and survival but results are conflicting. The BMA could release these different factors in response to catecholamines, glucocorticoids, and cytokines.

vertebral fat fraction is decreased compared with controls and inversely associated with bone loss (51) or fragility fractures (80) in post-menopausal women. Moreover, in healthy adult women, a gradual increase of the unsaturation index is observed from the proximal femur to the most distal part of the tibia, suggesting a differential fatty acid distribution in the BMA subpopulations. Accordingly, this was further examined in several bone sites in rats to reveal a higher unsaturation index in cBMA compared with regulated ones (29). These studies strongly support that BMA associated with bone alterations preferentially store saturated fatty acids. This has a strong pathophysiological relevance since *in vitro* chronic exposure of osteoblasts to saturated fatty acids triggers their dysfunction and apoptosis (116–118). Results are conflicting for the resorbing cells since saturated fatty acids were reported either to reduce osteoclastogenesis (119) or to exert beneficial effects on mature osteoclasts by preventing their apoptosis (120). Though the amount of fatty acids released by BMA appears rather low *in vitro* (121), BMA could contribute to bone alterations through a detrimental fatty acid-mediated process referred as lipotoxicity. Moreover, a specific lipid pattern of BMA may be considered as a discriminative trait, which is rather puzzling considering that dietary fat intake usually impacts on the fatty acid composition of bone (122), adipose tissues, and blood (123). The variation in the BMA fatty acid content could reflect an adaptation to systemic metabolic alterations (79, 80) and/or an intrinsic characteristic through the expression of desaturases (29).

Regulation of BMA Function

Directly assessing the factors regulating the BMA function as done through *ex vivo* experiments with other fat depots is hampered by the dissemination and the scarcity of BMAT in animal models. Alternatively, indirect measurements of BMA activity through the size and density determination have often been performed using long-term experimentations (27, 29, 40). However, in such studies (27, 40), experiments are often carried out while BM adipogenesis is also initiated, which may interfere with the interpretation of the mature BMA response. One may propose to perform tests when BM adiposity (and mostly rBMA) is fully developed: indeed, a few interventional studies have already uncovered for example a sensitivity to estradiol for BMAT in post-menopausal women (124, 125) or to growth hormone for tibial rBMA in dwarf rats (126). Moreover, using radiolabeled glucose or fatty acid analogs with Positron Emission Tomography imaging could be helpful to decipher the metabolic function and regulation of BMA during acute challenges. So far, information regarding the regulation of BMA function mainly comes from *in vitro* studies (**Figure 1**).

As mentioned before, like for other WAT, catecholamines or agonists of the β-adrenergic receptors stimulate fatty acid release from BMA both *in vitro* (121, 127, 128) and *in vivo* (114). Surprisingly, insulin addition does not seem necessary for human BM MSC adipogenesis and subsequent lipogenesis *in vitro* (109, 127, 129). However, insulin acutely stimulates glucose uptake (130) and modifies the adipokine pattern (127, 131) *in vitro* and in organotypic cultures supporting that BMAs are sensitive to insulin.

Dexamethasone triggers lipolysis (118) and stimulates the secretion of leptin from human BM MSC-derived adipocytes (118) or human primary cultivated BMAs (131) like reported for extramedullary white adipocytes. Regarding to adiponectin secretion, discrepancies are obtained according to the studied model (118, 131). Dexamethasone also stimulates the expression of RANKL in human primary BMAs (106).

Similarly to white adipocytes, cytokines – including notably TNFα – alter leptin secretion in two cultured models (131, 132), supporting that BMAs are also sensitive to a pro-inflammatory environment.

CONCLUSION

Bone marrow adipose tissue is metabolically distinct from other fat depots as indicated by several evidence related to its development and properties. Numerous data from clinical studies, *in vivo*, and vitro models point to an involvement of BMAT in bone remodeling resulting in bone alterations. Besides the participation of the adipogenesis process, BMAs are active cells whose phenotype is strikingly heterogeneous according to the bone site or BM area. Compared with cBMA, rBMA appear highly responsive to diverse stimuli. The first characterizations of BMA as well as their sensitivity to catecholamines and glucocorticoids support that BMA behaves more as a white-like adipocyte whose fatty acid or adipokine release could impact on BM cells (**Figure 1**). Moreover, its phenotype could also evolve when bone remodeling is altered. Owing to its specific microenvironment, it is expected that osteoblasts, osteoclasts, hematopoietic, and other bone cells reciprocally regulate BMA function. In that respect, a description of BMAT vascularization, innervation, and interaction with BM cells is needed to better comprehend its regulation. Moreover, the relative contribution of BMAT secretions compared with those of extramedullary adipose tissues remains poorly examined, which emphasizes the necessity to deepen the characterization of BMA. So far considering the different physiopathological situations of BMAT development together has not led to a shared hypothesis defining the role of BMA. This actually suggests that, as a true responsive cell, BMA function and regulation could vary according to the pathophysiological context and should be analyzed accordingly.

AUTHOR CONTRIBUTIONS

SL drafted the review. TR and SL made the figure. PH, TR, and SL contributed to the design of the review, critically revised it, approved the final version to be published, and agreed to be accountable for all aspects of the work.

ACKNOWLEDGMENT

Writing of this review was enabled by ULCO University.

FUNDING

The study was supported by ULCO University and The French Society of Rhumatology (SFR).

REFERENCES

1. Rosen ED, Spiegelman BM. What we talk about when we talk about fat. *Cell* (2014) 156:20–44. doi:10.1016/j.cell.2013.12.012
2. Fasshauer M, Blüher M. Adipokines in health and disease. *Trends Pharmacol Sci* (2015) 36:461–70. doi:10.1016/j.tips.2015.04.014
3. Peirce V, Carobbio S, Vidal-Puig A. The different shades of fat. *Nature* (2014) 510:76–83. doi:10.1038/nature13477
4. White UA, Tchoukalova YD. Sex dimorphism and depot differences in adipose tissue function. *Biochim Biophys Acta* (2014) 1842:377–92. doi:10.1016/j.bbadis.2013.05.006
5. Peng X-R, Gennemark P, O'Mahony G, Bartesaghi S. Unlock the thermogenic potential of adipose tissue: pharmacological modulation and implications for treatment of diabetes and obesity. *Front Endocrinol* (2015) 6:174. doi:10.3389/fendo.2015.00174
6. Kawai M, de Paula FJA, Rosen CJ. New insights into osteoporosis: the bone-fat connection. *J Intern Med* (2012) 272:317–29. doi:10.1111/j.1365-2796.2012.02564.x
7. Naot D, Cornish J. Cytokines and hormones that contribute to the positive association between fat and bone. *Front Endocrinol* (2014) 5:70. doi:10.3389/fendo.2014.00070
8. Karsenty G, Ferron M. The contribution of bone to whole-organism physiology. *Nature* (2012) 481:314–20. doi:10.1038/nature10763
9. Wei J, Karsenty G. An overview of the metabolic functions of osteocalcin. *Rev Endocr Metab Disord* (2015) 16:93–8. doi:10.1007/s11154-014-9307-7
10. Bianco P, Robey PG. Skeletal stem cells. *Development* (2015) 142:1023–7. doi:10.1242/dev.102210
11. Reagan MR, Liaw L, Rosen CJ, Ghobrial IM. Dynamic interplay between bone and multiple myeloma: emerging roles of the osteoblast. *Bone* (2015) 75:161–9. doi:10.1016/j.bone.2015.02.021
12. Hardaway AL, Herroon MK, Rajagurubandara E, Podgorski I. Bone marrow fat: linking adipocyte-induced inflammation with skeletal metastases. *Cancer Metastasis Rev* (2014) 33:527–43. doi:10.1007/s10555-013-9484-y
13. Meunier P, Aaron J, Edouard C, Vignon G. Osteoporosis and the replacement of cell populations of the marrow by adipose tissue. A quantitative study of 84 iliac bone biopsies. *Clin Orthop* (1971) 80:147–54. doi:10.1097/00003086-197110000-00021
14. Rozman C, Feliu E, Berga L, Reverter JC, Climent C, Ferrán MJ. Age-related variations of fat tissue fraction in normal human bone marrow depend both on size and number of adipocytes: a stereological study. *Exp Hematol* (1989) 17:34–7.
15. Hwang S, Panicek DM. Magnetic resonance imaging of bone marrow in oncology, part 1. *Skeletal Radiol* (2007) 36:913–20. doi:10.1007/s00256-007-0309-3
16. Scheller EL, Troiano N, Vanhoutan JN, Bouxsein MA, Fretz JA, Xi Y, et al. Use of osmium tetroxide staining with microcomputerized tomography to visualize and quantify bone marrow adipose tissue in vivo. *Methods Enzymol* (2014) 537:123–39. doi:10.1016/B978-0-12-411619-1.00007-0
17. Blebea JS, Houseni M, Torigian DA, Fan C, Mavi A, Zhuge Y, et al. Structural and functional imaging of normal bone marrow and evaluation of its age-related changes. *Semin Nucl Med* (2007) 37:185–94. doi:10.1053/j.semnuclmed.2007.01.002
18. Scheller EL, Rosen CJ. What's the matter with MAT? Marrow adipose tissue, metabolism, and skeletal health: marrow adipose tissue and skeletal health. *Ann N Y Acad Sci* (2014) 1311:14–30. doi:10.1111/nyas.12327
19. Kugel H, Jung C, Schulte O, Heindel W. Age- and sex-specific differences in the 1H-spectrum of vertebral bone marrow. *J Magn Reson Imaging* (2001) 13:263–8. doi:10.1002/1522-2586(200102)13:2<263::AID-JMRI1038>3.3.CO;2-D
20. Pansini V, Monnet A, Salleron J, Hardouin P, Cortet B, Cotten A. 3 Tesla (1) H MR spectroscopy of hip bone marrow in a healthy population, assessment of normal fat content values and influence of age and sex. *J Magn Reson Imaging* (2014) 39:369–76. doi:10.1002/jmri.24176
21. Griffith JF, Yeung DKW, Ma HT, Leung JCS, Kwok TCY, Leung PC. Bone marrow fat content in the elderly: a reversal of sex difference seen in younger subjects. *J Magn Reson Imaging* (2012) 36:225–30. doi:10.1002/jmri.23619
22. Devlin MJ, Cloutier AM, Thomas NA, Panus DA, Lotinun S, Pinz I, et al. Caloric restriction leads to high marrow adiposity and low bone mass in growing mice. *J Bone Miner Res* (2010) 25:2078–88. doi:10.1002/jbmr.82
23. Liu L-F, Shen W-J, Ueno M, Patel S, Kraemer FB. Characterization of age-related gene expression profiling in bone marrow and epididymal adipocytes. *BMC Genomics* (2011) 12:212. doi:10.1186/1471-2164-12-212
24. Liu L-F, Shen W-J, Ueno M, Patel S, Azhar S, Kraemer FB. Age-related modulation of the effects of obesity on gene expression profiles of mouse bone marrow and epididymal adipocytes. *PLoS One* (2013) 8:e72367. doi:10.1371/journal.pone.0072367
25. Lazarenko OP, Rzonca SO, Hogue WR, Swain FL, Suva LJ, Lecka-Czernik B. Rosiglitazone induces decreases in bone mass and strength that are reminiscent of aged bone. *Endocrinology* (2007) 148:2669–80. doi:10.1210/en.2006-1587
26. Tavassoli M, Crosby WH. Bone marrow histogenesis: a comparison of fatty and red marrow. *Science* (1970) 169:291–3. doi:10.1126/science.169.3942.291
27. Kurabayashi T, Tomita M, Matsushita H, Honda A, Takakuwa K, Tanaka K. Effects of a beta 3 adrenergic receptor agonist on bone and bone marrow adipocytes in the tibia and lumbar spine of the ovariectomized rat. *Calcif Tissue Int* (2001) 68:248–54. doi:10.1007/s002230001203
28. Devlin M, Vliet MV, Motyl K, Karim L, Brooks D, Louis L, et al. Early onset type 2 diabetes impairs skeletal acquisition in the male TALLYHO/JngJ mouse. *Endocrinology* (2014) 155:3806–16. doi:10.1210/en.2014-1041
29. Scheller EL, Doucette CR, Learman BS, Cawthorn WP, Khandaker S, Schell B, et al. Region-specific variation in the properties of skeletal adipocytes reveals regulated and constitutive marrow adipose tissues. *Nat Commun* (2015) 6:7808. doi:10.1038/ncomms8808
30. Rogers NH. Brown adipose tissue during puberty and with aging. *Ann Med* (2015) 47:142–9. doi:10.3109/07853890.2014.914807
31. Graja A, Schulz TJ. Mechanisms of aging-related impairment of brown adipocyte development and function. *Gerontology* (2015) 61:211–7. doi:10.1159/000366557
32. Waldén TB, Hansen IR, Timmons JA, Cannon B, Nedergaard J. Recruited vs. nonrecruited molecular signatures of brown, "brite," and white adipose tissues. *Am J Physiol Endocrinol Metab* (2012) 302:E19–31. doi:10.1152/ajpendo.00249.2011
33. Sellayah D, Sikder D. Orexin restores aging-related brown adipose tissue dysfunction in male mice. *Endocrinology* (2014) 155:485–501. doi:10.1210/en.2013-1629
34. Cawthorn WP, Scheller EL, Learman BS, Parlee SD, Simon BR, Mori H, et al. Bone marrow adipose tissue is an endocrine organ that contributes to increased circulating adiponectin during caloric restriction. *Cell Metab* (2014) 20:368–75. doi:10.1016/j.cmet.2014.06.003
35. Cawthorn WP, Scheller EL, Parlee SD, Pham HA, Learman BS, Redshaw CMH, et al. Expansion of bone marrow adipose tissue during caloric restriction is associated with increased circulating glucocorticoids and not with hypoleptinemia. *Endocrinology* (2016) 157:508–21. doi:10.1210/en.2015-1477
36. Lim S, Honek J, Xue Y, Seki T, Cao Z, Andersson P, et al. Cold-induced activation of brown adipose tissue and adipose angiogenesis in mice. *Nat Protoc* (2012) 7:606–15. doi:10.1038/nprot.2012.013
37. Hao Q, Yadav R, Basse AL, Petersen S, Sonne SB, Rasmussen S, et al. Transcriptome profiling of brown adipose tissue during cold exposure reveals extensive regulation of glucose metabolism. *Am J Physiol Endocrinol Metab* (2015) 308:E380–92. doi:10.1152/ajpendo.00277.2014
38. Shimizu I, Aprahamian T, Kikuchi R, Shimizu A, Papanicolaou KN, MacLauchlan S, et al. Vascular rarefaction mediates whitening of brown fat in obesity. *J Clin Invest* (2014) 124:2099–112. doi:10.1172/JCI71643
39. Halade GV, Rahman MM, Williams PJ, Fernandes G. High fat diet-induced animal model of age-associated obesity and osteoporosis. *J Nutr Biochem* (2010) 21:1162–9. doi:10.1016/j.jnutbio.2009.10.002
40. Styner M, Thompson WR, Galior K, Uzer G, Wu X, Kadari S, et al. Bone marrow fat accumulation accelerated by high fat diet is suppressed by exercise. *Bone* (2014) 64C:39–46. doi:10.1016/j.bone.2014.03.044
41. Shu L, Beier E, Sheu T, Zhang H, Zuscik MJ, Puzas EJ, et al. High-fat diet causes bone loss in young mice by promoting osteoclastogenesis through alteration of the bone marrow environment. *Calcif Tissue Int* (2015) 96(4):313–23. doi:10.1007/s00223-015-9954-z
42. Nadal-Casellas A, Proenza AM, Lladó I, Gianotti M. Effects of ovariectomy and 17-β estradiol replacement on rat brown adipose tissue mitochondrial function. *Steroids* (2011) 76:1051–6. doi:10.1016/j.steroids.2011.04.009

43. de Heredia FP, Larque E, Portillo MDP, Canteras M, Zamora S, Garaulet M. Age-related changes in fatty acids from different adipose depots in rat and their association with adiposity and insulin. *Nutrition* (2008) 24:1013–22. doi:10.1016/j.nut.2008.03.022
44. Berry R, Jeffery E, Rodeheffer MS. Weighing in on adipocyte precursors. *Cell Metab* (2014) 19:8–20. doi:10.1016/j.cmet.2013.10.003
45. Spalding KL, Arner E, Westermark PO, Bernard S, Buchholz BA, Bergmann O, et al. Dynamics of fat cell turnover in humans. *Nature* (2008) 453:783–7. doi:10.1038/nature06902
46. Cartwright MJ, Tchkonia T, Kirkland JL. Aging in adipocytes: potential impact of inherent, depot-specific mechanisms. *Exp Gerontol* (2007) 42:463–71. doi:10.1016/j.exger.2007.03.003
47. Justesen J, Stenderup K, Ebbesen EN, Mosekilde L, Steiniche T, Kassem M. Adipocyte tissue volume in bone marrow is increased with aging and in patients with osteoporosis. *Biogerontology* (2001) 2:165–71. doi:10.1023/A:1011513223894
48. Shen W, Chen J, Punyanitya M, Shapses S, Heshka S, Heymsfield SB. MRI-measured bone marrow adipose tissue is inversely related to DXA-measured bone mineral in Caucasian women. *Osteoporos Int* (2007) 18:641–7. doi:10.1007/s00198-006-0285-9
49. Di Iorgi N, Rosol M, Mittelman SD, Gilsanz V. Reciprocal relation between marrow adiposity and the amount of bone in the axial and appendicular skeleton of young adults. *J Clin Endocrinol Metab* (2008) 93:2281–6. doi:10.1210/jc.2007-2691
50. Griffith JF, Yeung DKW, Antonio GE, Lee FKH, Hong AWL, Wong SYS, et al. Vertebral bone mineral density, marrow perfusion, and fat content in healthy men and men with osteoporosis: dynamic contrast-enhanced MR imaging and MR spectroscopy. *Radiology* (2005) 236:945–51. doi:10.1148/radiol.2363041425
51. Yeung DKW, Griffith JF, Antonio GE, Lee FKH, Woo J, Leung PC. Osteoporosis is associated with increased marrow fat content and decreased marrow fat unsaturation: a proton MR spectroscopy study. *J Magn Reson Imaging* (2005) 22:279–85. doi:10.1002/jmri.20367
52. Bredella MA, Fazeli PK, Miller KK, Misra M, Torriani M, Thomas BJ, et al. Increased bone marrow fat in anorexia nervosa. *J Clin Endocrinol Metab* (2009) 94:2129–36. doi:10.1210/jc.2008-2532
53. Kajkenova O, Lecka-Czernik B, Gubrij I, Hauser SP, Takahashi K, Parfitt AM, et al. Increased adipogenesis and myelopoiesis in the bone marrow of SAMP6, a murine model of defective osteoblastogenesis and low turnover osteopenia. *J Bone Miner Res* (1997) 12:1772–9. doi:10.1359/jbmr.1997.12.11.1772
54. Li G-W, Xu Z, Chen Q-W, Chang S-X, Tian Y-N, Fan J-Z. The temporal characterization of marrow lipids and adipocytes in a rabbit model of glucocorticoid-induced osteoporosis. *Skeletal Radiol* (2013) 42:1235–44. doi:10.1007/s00256-013-1659-7
55. Marie PJ, Kassem M. Extrinsic mechanisms involved in age-related defective bone formation. *J Clin Endocrinol Metab* (2011) 96:600–9. doi:10.1210/jc.2010-2113
56. Justesen J, Mosekilde L, Holmes M, Stenderup K, Gasser J, Mullins JJ, et al. Mice deficient in 11beta-hydroxysteroid dehydrogenase type 1 lack bone marrow adipocytes, but maintain normal bone formation. *Endocrinology* (2004) 145:1916–25. doi:10.1210/en.2003-1427
57. Iwaniec UT, Turner RT. Failure to generate bone marrow adipocytes does not protect mice from ovariectomy-induced osteopenia. *Bone* (2013) 53:145–53. doi:10.1016/j.bone.2012.11.034
58. Sheu Y, Cauley JA. The role of bone marrow and visceral fat on bone metabolism. *Curr Osteoporos Rep* (2011) 9:67–75. doi:10.1007/s11914-011-0051-6
59. Shapses SA, Sukumar D. Bone metabolism in obesity and weight loss. *Annu Rev Nutr* (2012) 32:287–309. doi:10.1146/annurev.nutr.012809.104655
60. Bredella MA, Fazeli PK, Freedman LM, Calder G, Lee H, Rosen CJ, et al. Young women with cold-activated brown adipose tissue have higher bone mineral density and lower pref-1 than women without brown adipose tissue: a study in women with anorexia nervosa, women recovered from anorexia nervosa, and normal-weight women. *J Clin Endocrinol Metab* (2012) 97:E584–90. doi:10.1210/jc.2011-2246
61. Ponrartana S, Aggabao PC, Hu HH, Aldrovandi GM, Wren TAL, Gilsanz V. Brown adipose tissue and its relationship to bone structure in pediatric patients. *J Clin Endocrinol Metab* (2012) 97:2693–8. doi:10.1210/jc.2012-1589
62. Lee P, Brychta RJ, Collins MT, Linderman J, Smith S, Herscovitch P, et al. Cold-activated brown adipose tissue is an independent predictor of higher bone mineral density in women. *Osteoporos Int* (2013) 24:1513–8. doi:10.1007/s00198-012-2110-y
63. Motyl KJ, Bishop KA, DeMambro VE, Bornstein SA, Le P, Kawai M, et al. Altered thermogenesis and impaired bone remodeling in misty mice. *J Bone Miner Res* (2013) 28:1885–97. doi:10.1002/jbmr.1943
64. Rahman S, Lu Y, Czernik PJ, Rosen CJ, Enerback S, Lecka-Czernik B. Inducible brown adipose tissue, or beige fat, is anabolic for the skeleton. *Endocrinology* (2013) 154:2687–701. doi:10.1210/en.2012-2162
65. Botolin S, McCabe LR. Bone loss and increased bone adiposity in spontaneous and pharmacologically induced diabetic mice. *Endocrinology* (2007) 148:198–205. doi:10.1210/en.2006-1006
66. Botolin S, McCabe LR. Inhibition of PPARγ prevents type I diabetic bone marrow adiposity but not bone loss. *J Cell Physiol* (2006) 209:967–76. doi:10.1002/jcp.20804
67. Slade JM, Coe LM, Meyer RA, McCabe LR. Human bone marrow adiposity is linked with serum lipid levels not T1-diabetes. *J Diabetes Complications* (2012) 26:1–9. doi:10.1016/j.jdiacomp.2011.11.001
68. Reid IR. Fat and bone. *Arch Biochem Biophys* (2010) 503:20–7. doi:10.1016/j.abb.2010.06.027
69. Johansson H, Kanis JA, Odén A, McCloskey E, Chapurlat RD, Christiansen C, et al. A meta-analysis of the association of fracture risk and body mass index in women. *J Bone Miner Res* (2014) 29:223–33. doi:10.1002/jbmr.2017
70. Compston JE, Watts NB, Chapurlat R, Cooper C, Boonen S, Greenspan S, et al. Obesity is not protective against fracture in postmenopausal women: GLOW. *Am J Med* (2011) 124:1043–50. doi:10.1016/j.amjmed.2011.06.013
71. Prieto-Alhambra D, Premaor MO, Fina Avilés F, Hermosilla E, Martinez-Laguna D, Carbonell-Abella C, et al. The association between fracture and obesity is site-dependent: a population-based study in postmenopausal women. *J Bone Miner Res* (2012) 27:294–300. doi:10.1002/jbmr.1466
72. Premaor MO, Compston JE, Fina Avilés F, Pagès-Castellà A, Nogués X, Díez-Pérez A, et al. The association between fracture site and obesity in men: a population-based cohort study. *J Bone Miner Res* (2013) 28:1771–7. doi:10.1002/jbmr.1878
73. Bredella MA, Lin E, Gerweck AV, Landa MG, Thomas BJ, Torriani M, et al. Determinants of bone microarchitecture and mechanical properties in obese men. *J Clin Endocrinol Metab* (2012) 97:4115–22. doi:10.1210/jc.2012-2246
74. Bredella MA, Torriani M, Ghomi RH, Thomas BJ, Brick DJ, Gerweck AV, et al. Vertebral bone marrow fat is positively associated with visceral fat and inversely associated with IGF-1 in obese women. *Obesity (Silver Spring)* (2011) 19:49–53. doi:10.1038/oby.2010.106
75. Hamrick MW, Pennington C, Newton D, Xie D, Isales C. Leptin deficiency produces contrasting phenotypes in bones of the limb and spine. *Bone* (2004) 34:376–83. doi:10.1016/j.bone.2003.11.020
76. Doucette CR, Horowitz MC, Berry R, MacDougald OA, Anunciado-Koza R, Koza RA, et al. High fat diet increases bone marrow adipose tissue (MAT) but does not alter trabecular or cortical bone mass in C57BL/6J mice. *J Cell Physiol* (2015) 230:2032–7. doi:10.1002/jcp.24954
77. Dede AD, Tournis S, Dontas I, Trovas G. Type 2 diabetes mellitus and fracture risk. *Metabolism* (2014) 63:1480–90. doi:10.1016/j.metabol.2014.09.002
78. Saito M, Marumo K. Bone quality in diabetes. *Front Endocrinol* (2013) 4:72. doi:10.3389/fendo.2013.00072
79. Baum T, Yap SP, Karampinos DC, Nardo L, Kuo D, Burghardt AJ, et al. Does vertebral bone marrow fat content correlate with abdominal adipose tissue, lumbar spine bone mineral density, and blood biomarkers in women with type 2 diabetes mellitus? *J Magn Reson Imaging* (2012) 35:117–24. doi:10.1002/jmri.22757
80. Patsch JM, Li X, Baum T, Yap SP, Karampinos DC, Schwartz AV, et al. Bone marrow fat composition as a novel imaging biomarker in postmenopausal women with prevalent fragility fractures. *J Bone Miner Res* (2013) 28:1721–8. doi:10.1002/jbmr.1950
81. Schafer AL, Li X, Schwartz AV, Tufts LS, Wheeler AL, Grunfeld C, et al. Changes in vertebral bone marrow fat and bone mass after gastric bypass surgery: a pilot study. *Bone* (2015) 74:140–5. doi:10.1016/j.bone.2015.01.010
82. Cordes C, Dieckmeyer M, Ott B, Shen J, Ruschke S, Settles M, et al. MR-detected changes in liver fat, abdominal fat, and vertebral bone marrow

fat after a four-week calorie restriction in obese women. *J Magn Reson Imaging* (2015) 42:1272–80. doi:10.1002/jmri.24908
83. Paccou J, Hardouin P, Cotten A, Penel G, Cortet B. The role of bone marrow fat in skeletal health: usefulness and perspectives for clinicians. *J Clin Endocrinol Metab* (2015) 100:3613–21. doi:10.1210/jc.2015-2338
84. Sivasubramaniyan K, Lehnen D, Ghazanfari R, Sobiesiak M, Harichandan A, Mortha E, et al. Phenotypic and functional heterogeneity of human bone marrow- and amnion-derived MSC subsets. *Ann N Y Acad Sci* (2012) 1266:94–106. doi:10.1111/j.1749-6632.2012.06551.x
85. Abdallah BM, Kassem M. New factors controlling the balance between osteoblastogenesis and adipogenesis. *Bone* (2012) 50:540–5. doi:10.1016/j.bone.2011.06.030
86. Ma X, Lee P, Chisholm DJ, James DE. Control of adipocyte differentiation in different fat depots; implications for pathophysiology or therapy. *Front Endocrinol* (2015) 6:1. doi:10.3389/fendo.2015.00001
87. Rydén M, Uzunel M, Hård JL, Borgström E, Mold JE, Arner E, et al. Transplanted bone marrow-derived cells contribute to human adipogenesis. *Cell Metab* (2015) 22:408–17. doi:10.1016/j.cmet.2015.06.011
88. Crossno JT, Majka SM, Grazia T, Gill RG, Klemm DJ. Rosiglitazone promotes development of a novel adipocyte population from bone marrow-derived circulating progenitor cells. *J Clin Invest* (2006) 116:3220–8. doi:10.1172/JCI28510
89. Sadie-Van Gijsen H, Crowther NJ, Hough FS, Ferris WF. The interrelationship between bone and fat: from cellular see-saw to endocrine reciprocity. *Cell Mol Life Sci* (2013) 70:2331–49. doi:10.1007/s00018-012-1211-2
90. Nuttall ME, Shah F, Singh V, Thomas-Porch C, Frazier T, Gimble JM. Adipocytes and the regulation of bone remodeling: a balancing act. *Calcif Tissue Int* (2014) 94:78–87. doi:10.1007/s00223-013-9807-6
91. Post S, Abdallah BM, Bentzon JF, Kassem M. Demonstration of the presence of independent pre-osteoblastic and pre-adipocytic cell populations in bone marrow-derived mesenchymal stem cells. *Bone* (2008) 43:32–9. doi:10.1016/j.bone.2008.03.011
92. Ghali O, Broux O, Falgayrac G, Haren N, van Leeuwen JPTM, Penel G, et al. Dexamethasone in osteogenic medium strongly induces adipocyte differentiation of mouse bone marrow stromal cells and increases osteoblast differentiation. *BMC Cell Biol* (2015) 16:9. doi:10.1186/s12860-015-0056-6
93. Fazeli PK, Horowitz MC, MacDougald OA, Scheller EL, Rodeheffer MS, Rosen CJ, et al. Marrow fat and bone – new perspectives. *J Clin Endocrinol Metab* (2013) 98:935–45. doi:10.1210/jc.2012-3634
94. Karsenty G, Oury F. The central regulation of bone mass, the first link between bone remodeling and energy metabolism. *J Clin Endocrinol Metab* (2010) 95:4795–801. doi:10.1210/jc.2010-1030
95. Budzik J-F, Lefebvre G, Forzy G, El Rafei M, Chechin D, Cotten A. Study of proximal femoral bone perfusion with 3D T1 dynamic contrast-enhanced MRI: a feasibility study. *Eur Radiol* (2014) 24:3217–23. doi:10.1007/s00330-014-3340-5
96. Roche B, David V, Vanden-Bossche A, Peyrin F, Malaval L, Vico L, et al. Structure and quantification of microvascularisation within mouse long bones: what and how should we measure? *Bone* (2012) 50:390–9. doi:10.1016/j.bone.2011.09.051
97. Abella E, Feliu E, Granada I, Millá F, Oriol A, Ribera JM, et al. Bone marrow changes in anorexia nervosa are correlated with the amount of weight loss and not with other clinical findings. *Am J Clin Pathol* (2002) 118:582–8. doi:10.1309/2Y7X-YDXK-006B-XLT2
98. Allen JE, Henshaw DL, Keitch PA, Fews AP, Eatough JP. Fat cells in red bone marrow of human rib: their size and spatial distribution with respect to the radon-derived dose to the haemopoietic tissue. *Int J Radiat Biol* (1995) 68:669–78. doi:10.1080/09553009514551681
99. Gimble JM, Nuttall ME. Bone and fat: old questions, new insights. *Endocrine* (2004) 23:183–8. doi:10.1385/ENDO:23:2-3:183
100. Lecka-Czernik B. Marrow fat metabolism is linked to the systemic energy metabolism. *Bone* (2012) 50:534–9. doi:10.1016/j.bone.2011.06.032
101. Krings A, Rahman S, Huang S, Lu Y, Czernik PJ, Lecka-Czernik B. Bone marrow fat has brown adipose tissue characteristics, which are attenuated with aging and diabetes. *Bone* (2012) 50:546–52. doi:10.1016/j.bone.2011.06.016
102. Nishio M, Yoneshiro T, Nakahara M, Suzuki S, Saeki K, Hasegawa M, et al. Production of functional classical brown adipocytes from human pluripotent stem cells using specific hemopoietin cocktail without gene transfer. *Cell Metab* (2012) 16:394–406. doi:10.1016/j.cmet.2012.08.001
103. Poloni A, Maurizi G, Serrani F, Mancini S, Zingaretti MC, Frontini A, et al. Molecular and functional characterization of human bone marrow adipocytes. *Exp Hematol* (2013) 41:558–66.e2. doi:10.1016/j.exphem.2013.02.005
104. Huggins C, Blocksom BH. Changes in outlying bone marrow accompanying a local increase of temperature within physiological limits. *J Exp Med* (1936) 64:253–74. doi:10.1084/jem.64.2.253
105. Gasparrini M, Rivas D, Elbaz A, Duque G. Differential expression of cytokines in subcutaneous and marrow fat of aging C57BL/6J mice. *Exp Gerontol* (2009) 44:613–8. doi:10.1016/j.exger.2009.05.009
106. Goto H, Osaki M, Fukushima T, Sakamoto K, Hozumi A, Baba H, et al. Human bone marrow adipocytes support dexamethasone-induced osteoclast differentiation and function through RANKL expression. *Biomed Res* (2011) 32:37–44. doi:10.2220/biomedres.32.37
107. Goto H, Hozumi A, Osaki M, Fukushima T, Sakamoto K, Yonekura A, et al. Primary human bone marrow adipocytes support TNF-α-induced osteoclast differentiation and function through RANKL expression. *Cytokine* (2011) 56:662–8. doi:10.1016/j.cyto.2011.09.005
108. Takeshita S, Fumoto T, Naoe Y, Ikeda K. Age-related marrow adipogenesis is linked to increased expression of RANKL. *J Biol Chem* (2014) 289:16699–710. doi:10.1074/jbc.M114.547919
109. Clabaut A, Delplace S, Chauveau C, Hardouin P, Broux O. Human osteoblasts derived from mesenchymal stem cells express adipogenic markers upon coculture with bone marrow adipocytes. *Differentiation* (2010) 80:40–5. doi:10.1016/j.diff.2010.04.004
110. Zhang H, Lu W, Zhao Y, Rong P, Cao R, Gu W, et al. Adipocytes derived from human bone marrow mesenchymal stem cells exert inhibitory effects on osteoblastogenesis. *Curr Mol Med* (2011) 11:489–502. doi:10.2174/156652411796268704
111. Taipaleenmäki H, Abdallah BM, AlDahmash A, Säämänen A-M, Kassem M. Wnt signalling mediates the cross-talk between bone marrow derived pre-adipocytic and pre-osteoblastic cell populations. *Exp Cell Res* (2011) 317:745–56. doi:10.1016/j.yexcr.2010.12.015
112. Muruganandan S, Roman AA, Sinal CJ. Role of chemerin/CMKLR1 signaling in adipogenesis and osteoblastogenesis of bone marrow stem cells. *J Bone Miner Res* (2010) 25:222–34. doi:10.1359/jbmr.091106
113. Trubowitz S, Bathija A. Cell size and plamitate-1-14c turnover of rabbit marrow fat. *Blood* (1977) 49:599–605.
114. Tran MA, Dang TL, Berlan M. Effects of catecholamines on free fatty acid release from bone marrow adipose tissue. *J Lipid Res* (1981) 22:1271–6.
115. Griffith JF, Yeung DKW, Ahuja AT, Choy CWY, Mei WY, Lam SSL, et al. A study of bone marrow and subcutaneous fatty acid composition in subjects of varying bone mineral density. *Bone* (2009) 44:1092–6. doi:10.1016/j.bone.2009.02.022
116. Elbaz A, Wu X, Rivas D, Gimble JM, Duque G. Inhibition of fatty acid biosynthesis prevents adipocyte lipotoxicity on human osteoblasts in vitro. *J Cell Mol Med* (2010) 14:982–91. doi:10.1111/j.1582-4934.2009.00751.x
117. Gunaratnam K, Vidal C, Gimble JM, Duque G. Mechanisms of palmitate-induced lipotoxicity in human osteoblasts. *Endocrinology* (2014) 155:108–16. doi:10.1210/en.2013-1712
118. Wang D, Haile A, Jones LC. Dexamethasone-induced lipolysis increases the adverse effect of adipocytes on osteoblasts using cells derived from human mesenchymal stem cells. *Bone* (2013) 53:520–30. doi:10.1016/j.bone.2013.01.009
119. Cornish J, MacGibbon A, Lin J-M, Watson M, Callon KE, Tong PC, et al. Modulation of osteoclastogenesis by fatty acids. *Endocrinology* (2008) 149:5688–95. doi:10.1210/en.2008-0111
120. Oh S-R, Sul O-J, Kim Y-Y, Kim H-J, Yu R, Suh J-H, et al. Saturated fatty acids enhance osteoclast survival. *J Lipid Res* (2010) 51:892–9. doi:10.1194/jlr.M800626
121. Lucas S, Clabaut A, Ghali O, Haren N, Hardouin P, Broux O. Implication of fatty acids in the inhibitory effect of human adipocytes on osteoblastic differentiation. *Bone* (2013) 55:429–30. doi:10.1016/j.bone.2013.04.010
122. During A, Penel G, Hardouin P. Understanding the local actions of lipids in bone physiology. *Prog Lipid Res* (2015) 59:126–46. doi:10.1016/j.plipres.2015.06.002
123. Hodson L, Skeaff CM, Fielding BA. Fatty acid composition of adipose tissue and blood in humans and its use as a biomarker of dietary intake. *Prog Lipid Res* (2008) 47:348–80. doi:10.1016/j.plipres.2008.03.003

124. Syed FA, Oursler MJ, Hefferan TE, Peterson JM, Riggs BL, Khosla S. Effects of estrogen therapy on bone marrow adipocytes in postmenopausal osteoporotic women. *Osteoporos Int* (2008) 19:1323–30. doi:10.1007/s00198-008-0574-6
125. Limonard EJ, Veldhuis-Vlug AG, van Dussen L, Runge JH, Tanck MW, Endert E, et al. Short-term effect of estrogen on human bone marrow fat. *J Bone Miner Res* (2015) 30:2058–66. doi:10.1002/jbmr.2557
126. Gevers EF, Loveridge N, Robinson ICAF. Bone marrow adipocytes: a neglected target tissue for growth hormone. *Endocrinology* (2002) 143:4065–73. doi:10.1210/en.2002-220428
127. Laharrague P, Larrouy D, Fontanilles AM, Truel N, Campfield A, Tenenbaum R, et al. High expression of leptin by human bone marrow adipocytes in primary culture. *FASEB J* (1998) 12:747–52.
128. Dicker A, Le Blanc K, Aström G, van Harmelen V, Götherström C, Blomqvist L, et al. Functional studies of mesenchymal stem cells derived from adult human adipose tissue. *Exp Cell Res* (2005) 308:283–90. doi:10.1016/j.yexcr.2005.04.029
129. Zhao X-Y, Chen X-Y, Zhang Z-J, Kang Y, Liao W-M, Yu W-H, et al. Expression patterns of transcription factor PPARγ and C/EBP family members during in vitro adipogenesis of human bone marrow mesenchymal stem cells. *Cell Biol Int* (2015) 39:457–65. doi:10.1002/cbin.10415
130. Franchini M, Monnais E, Seboek D, Radimerski T, Zini E, Kaufmann K, et al. Insulin resistance and increased lipolysis in bone marrow derived adipocytes stimulated with agonists of toll-like receptors. *Horm Metab Res* (2010) 42:703–9. doi:10.1055/s-0030-1261872
131. Uchihashi K, Aoki S, Shigematsu M, Kamochi N, Sonoda E, Soejima H, et al. Organotypic culture of human bone marrow adipose tissue. *Pathol Int* (2010) 60:259–67. doi:10.1111/j.1440-1827.2010.02511.x
132. Laharrague P, Truel N, Fontanilles AM, Corberand JX, Pénicaud L, Casteilla L. Regulation by cytokines of leptin expression in human bone marrow adipocytes. *Horm Metab Res* (2000) 32:381–5. doi:10.1055/s-2007-978658

Conflict of Interest Statement: The authors declare that the research was conducted in the absence of any commercial or financial relationships that could be construed as a potential conflict of interest.

frontiers in Endocrinology

HYPOTHESIS AND THEORY
published: 25 October 2016
doi: 10.3389/fendo.2016.00139

Qualitative Aspects of Bone Marrow Adiposity in Osteoporosis

*Ana María Pino[1], Melissa Miranda[1], Carolina Figueroa[2], Juan Pablo Rodríguez[1] and Clifford J. Rosen[2]**

[1] Laboratory of Cell Biology, INTA, University of Chile, Santiago, Chile, [2] Maine Medical Center, Portland, ME, USA

The function of marrow adipocytes and their origin has not been defined although considerable research has centered on their presence in certain conditions, such as osteoporosis. Less work has focused on the qualitative aspects of marrow fat. Bone marrow serum is composed of multiple nutrients that almost certainly relate to functional aspects of the niche. Previous studies using non-invasive techniques have shown that osteoporotic individuals have more marrow fat and that the ratio of saturated: unsaturated fatty acid is high. We recently reported that bone marrow sera from osteoporotic patients with fracture showed a switch toward decreased content of total saturated versus unsaturated fatty acids, compared to patients without fracture highlighting a dynamic relationship between the composition of fatty acids in the bone microenvironment and the metabolic requirements of cells. The relative distribution of fatty acids differed considerably from that in the serum providing further evidence that energy utilization is high and that marrow adipocytes may contribute to this pool. Whether these lipids can affect osteoblast function in a positive or negative manner is still not certain but will require further investigation.

Keywords: lipids, fatty acids, unsaturated, bone marrow cells, bone marrow examination, adipocytes

OPEN ACCESS

Edited by:
Xinhua Qu,
Shanghai Ninth People's Hospital, China

Reviewed by:
Jan Tuckermann,
University of Ulm, Germany
Jawed Akhtar Siddiqui,
University of Nebraska Medical Center, USA

****Correspondence:***
Clifford J. Rosen
cjrofen@gmail.com

Specialty section:
This article was submitted to Bone Research, a section of the journal Frontiers in Endocrinology

Received: *04 August 2016*
Accepted: *10 October 2016*
Published: *25 October 2016*

Citation:
Pino AM, Miranda M, Figueroa C, Rodríguez JP and Rosen CJ (2016) Qualitative Aspects of Bone Marrow Adiposity in Osteoporosis. Front. Endocrinol. 7:139. doi: 10.3389/fendo.2016.00139

THE BONE MARROW MICROENVIROMENT

In adults, the rigid bone structure of the cortex encloses a dynamic and flexible cell organization sustaining continuous bone and bone marrow stroma remodeling, as well as blood formation. These processes rest on preserving specific adult stem cells (SCs) that are characterized by their capacity for self-renewal and multilineage differentiation. These unique properties of SCs are not only cell-autonomous *in vivo*, but also controlled by their surrounding microenvironment, which is currently called the SC niche. The original Schofield's proposition for hematopoietic stem cells (HSCs) in the bone marrow emphasized the input from other marrow cells types to maintain SCs behavior and prevent maturation (1). Such cell- depending interactions provide a specialized microenvironment ("niche") that allows cell lodging while maintaining self-renewal of SCs; loss of such an association would lead to cell differentiation. At present, the niche concept has been assumed to explain the behavior of SCs in several tissue types while evolving to take account of specific cell types, anatomical sites, soluble molecules, signaling cascades and gradients, as well as physical factors, such as weight bearing, shear stress, oxygen tension, and temperature (2–5). Among the most studied somatic SCs in mammals are the HSC and mesenchymal stromal/stem cells (MSCs) that integrate a unique niche in the bone marrow made of heterotypic SC pairs (6). Therefore, the bone marrow niche concept comprises a complex microenvironment, providing spatial and temporal coordinated signals to support SC function; balanced inputs from the niche can sustain homeostatic SC self-renewal and differentiation, but under pathological conditions they could constrain SCs functioning.

MESENCHYMAL STEM CELLS OR MARROW STROMAL CELLS

In the bone marrow, MSCs mainly localize lining blood vessels, in particular on the sinusoids, the characteristic vessels of bone marrow microcirculation (7, 8), often in close association with HSCs (6, 9, 10). Then, the sinusoidal wall brings together both HSCs and MSCs, framing and sustaining a mutual niche (6, 11). Such perivascular localization has also been demonstrated for MSCs in several tissues through the body, which support the proposition that MSCs are fundamental to the healing of many tissues. MSCs in the bone marrow are ontogenically distinct populations taking over various biological functions, such as niches for HSCs (6, 12, 13), progenitor cells for bone formation during bone remodeling or repair (14), for cartilage and adipocyte formation, and vascular support (15–17).

Ex vivo, hMSCs are relatively easy to obtain from a small bone marrow aspirate and they can simply be isolated from other marrow nucleated cells by their adherence to plastic dishes. Subsequently, these cells can be expanded under *in vitro* conditions in which they display varying proliferation and differentiation potential; however, as cells are expanded consecutively under standard conditions, they lose some of these capacities. Clonal analysis demonstrated that MSCs obtained from the bone marrow are a heterogeneous mixture of cells that differ in their stage of lineage commitment and extent of differentiation (18–21). Therefore, MSCs populations in the bone marrow or those that are isolated and maintained in culture are not homogeneous, but rather assemble progenitor cells with diverse biological properties, such that not all MSCs are alike.

In theory, the lineage fate of MSCs appears to be determined during cell "commitment," at very early stages of cell differentiation. During this almost unknown period, both intrinsic (genetic) and environmental (local and/or systemic) conditions interplay to outline the cell's fate toward one of the possible lineages. Factors, such as age (22), culture condition (23), microenvironment (24), mechanical strain (25), and some pathologies (26, 27), appear to affect the intrinsic activity of MSCs.

Multilineage differentiation capacity has been related to wide range gene expression at intermediary levels, which along cell commitment and differentiation shifts to a selective mode of restricted genes expressed at high level (21, 28–30). Several fundamental signaling pathways participate in regulating the lineage commitment of MSCs, including transforming growth factor-beta (TGFβ)/bone morphogenic protein (BMP) signaling, wingless type MMTV integration site (Wnt) signaling, Hedgehogs (Hh), Notch, and fibroblast growth factors (FGFs) (31, 32).

RELATIONSHIP BETWEEN THE OSTEO/ ADIPOGENIC PROCESSES THE OBESITY THEORY OF OSTEOPOROSIS

The formation, maintenance, and repair of bone tissue depend on fine-tuned interlinks in the activities of cells derived from the two SC types housed in the bone marrow interstice, above described. HSCs along the myeloid differentiation lineage generate osteoclasts (33), whereas osteoblasts derive from MSCs, which are also progenitor cells for adipocytes (34). Bone diseases, such as osteopetrosis, osteopenia, and osteoporosis, show imbalance between bone formation and resorption (33).

Since MSCs can generate several cell types, the control of lineage commitment of MSCs appears critical. Alteration in such control has been observed in some bone diseases resulting in abnormal bone remodeling, which show divergent commitment of MSCs to adipocytes and osteoblasts. For instance, increased marrow fat content has been demonstrated in osteoporosis patients, the most common bone remodeling disorder (35, 36). Also, this alteration of the osteo/adipogenic processes is observed in other bone loss conditions, such as aging, immobilization, microgravity, ovariectomy, diabetes, and glucocorticoid or thiazolidinedione treatments, highlighting the harmful consequence of marrow adipogenesis in osteogenic disorders (37–39).

Osteoblasts and adipocytes originate from a common precursor, MSCs; preserving bone tissue requires adequate osteoblastic differentiation while minimizing adipogenesis. Commitment and differentiation of MSCs into a specific phenotype *in vivo* is postulated to be controlled by hormonal and local factors (paracrine/autocrine) regulating the expression and/or activity of master differentiation genes (32, 40). Research on MSCs differentiation *in vitro* showed that activation of PPARγ2 and C/EBPs match to the master transcription factors for adipogenic differentiation (41–43), while Runx2 and osterix are required for osteogenic differentiation (44). PPARγ2 positively regulates adipocyte differentiation while acting as a dominant negative regulator of osteogenic differentiation (45, 46). By contrast, an increase in bone mass density was observed in PPARγ2-deficient mice model (47). On the other hand, Runx2 expression by MSCs inhibits their differentiation into adipocytes, as shown by experiments in Runx2/calvarial cells, which spontaneously differentiate into adipocytes (48). However, due to the heterogeneity of the earliest MSC, cell expression of only adipogenic or osteogenic markers is unlikely. Indeed, osterix positive marrow adipocytes have been shown in lineage tracing studies, and marrow adipocytes can be traced to peroxiredoxin 1 (Rosen, personal communication). Moreover, some Runx2-positive cells isolated in high marrow adiposity states also have large lipid droplets and express perilipin (49).

Thus, in most cases, there is a reciprocal relationship in the regulation of these differentiation processes whose alteration would facilitate adipose accretion in the bone marrow, at the expense of osteoblast formation, decreasing bone mass (50–52). Such altered conditions would prevail in the bone marrow of osteoporotic patients and other bone loss conditions, disrupting the activities of MSCs and their microenvironment (37, 40, 50). This proposition has been termed the obesity theory of osteoporosis.

According to this proposition, observations in iliac crest biopsies from elderly women show considerable accumulation of adipocytes; i.e., 70–80% of the total marrow volume in osteoporotic patients, compared to that of healthy elderly women. More recently, observations done by magnetic resonance imaging (MRI) allowed similar conclusion in patients with low bone density (53–55). However, the origin of marrow adipocytes and their true nature has been more difficult to discern.

HUMAN BONE MARROW FAT

In newborn mammals, there is scarce marrow fat; however, adipocyte number increases with age such that in humans older than 30 years, most of the femoral cavity is occupied by adipose tissue (56). The function of human marrow fat was largely overlooked; at first, it was considered "filler" for the void left by trabecular bone during aging or after radiation treatments. Early observations from the 1970s highlighted the different characteristics between adipocytes within the red and yellow marrow, suggesting that marrow adipocytes may have a region-specific lipid composition (57, 58). In humans, adipocytes accumulate within the yellow marrow at or slightly before birth, regardless of prematurity, and accelerate between 4 and 8 weeks of age (59, 60). Early adipose tissue is established in distal skeletal regions, including the hands, feet, and distal tibia. This is often called constitutive marrow fat. After attaining some bulk, distal marrow adipose tissue histologically resembles peripheral white adipose tissue, and is relatively devoid of active hematopoiesis. During adulthood, marrow fat accretion continues in areas of red, hematopoietic marrow (61), which show histologically single adipocytes interspersed with sites of active hematopoiesis. These regions appear to be spatially distinct in rats and mice; but in human, both types of adipose tissue may allocate in the same skeletal region (62).

In a recent study in mice, Scheller et al. (62) related region-specific fat differences in development to functional differences, such as regulation, adipocyte size, lipid composition, gene expression, and genetic determinants of marrow adipocytes, proposing that distal fat areas embody constitutive marrow adipose tissue (cMAT), while proximal adipose tissue contains regulated marrow adipose tissue (rMAT). Although cMAT showed histologic similarities with white extra-medullar adipose tissue (WAT), the lipid composition, cold regulation, and gene expression of WAT is more related to that of rMAT, concluding that lipid metabolism in WAT and rMAT adipocytes may be similar. Of note, cMAT showed increased unsaturation index compared to both, rMAT and WAT. Scheller's study and those of others highlight that not all marrow adipocytes are equivalent, sustaining connotation for the marrow niche and its relationship to skeletal and whole-body metabolism.

Bone marrow fat has a role in systemic and local energy metabolism (63–66). When dysfunctional, it may disrupt the complex relationships in the bone marrow microenvironment, constraining functioning of both HSCs and MSCs, and thereby affecting their progeny (67, 68).

Bone marrow adipocytes have endocrine, autocrine, and paracrine effects; the activity of these cells on neighboring marrow result from the production of adipokines, steroids, cytokines, and free fatty acids (51, 64, 69–71), which could sustain or suppress the hematopoietic and osteogenic processes (10, 50, 51, 63, 64, 72).

The modification of bone marrow adipose tissue, either in size or function, may have similar consequences to that of extra medullary fat, which by unbalanced production of signaling products underlay in several human diseases, including obesity, lipodystrophy, atherogenesis, diabetes, and inflammation.

MARROW FAT COMPOSITION AND OSTEOPOROSIS

Current information on bone marrow fat points to diverse adipocytes that have development-dependent skeletal distribution, showing distinct properties, such as lipid composition, gene expression, and probably subjected to different peripheral and local regulation. Underlying the relationship between such bone marrow fat and bone function is a balance in the number and quality of adipose cells; hence, the interest in characterizing bone marrow fat and searching for the quality of human marrow fat, for instance, in a bone remodeling disorder like osteoporosis.

Skeletal and marrow cells utilize fatty acids as substrates for their energy needs (73), although the contribution of marrow adipocytes to such requirements is most unknown; as it is the role of fatty acids stored in the marrow adipocytes in bone remodeling and hematopoiesis. Moreover, the lipid composition in the interstitial compartment surrounding bone marrow cells, its physiological significance, its variation under a bone stress situation, or its relationship with systemic lipids are undefined.

Studies on the composition of bone marrow fat suggested that it could have clinical relevance, in addition to marrow fat size and volume. Such conclusion is derived from *in situ* non-invasive MRI-based analysis of bone marrow, in patients with chronic diseases, such as osteoporosis (54), type 2 diabetes mellitus (74), or diabetic and non-diabetic women with prevalent fragility fractures (75). These studies demonstrated significantly lower unsaturation of bone marrow lipids in patients than corresponding controls. Moreover, Patsch and colleagues showed that low unsaturation and high saturation levels of lipids was accentuated in diabetic patients with prevalent fractures (75).

Physiological levels of molecules in the human bone marrow milieu are practically unknown; measurement has been particularly difficult not only because of tissue seclusion, but because of the complicated anatomy and blood perfusion of bone requiring invasive bone marrow sampling. Thus, knowledge on the availability to bone marrow cells of metabolites or regulatory compounds is scarce, limited to some pathologic condition or estimated from measurements in plasma (69, 76–78). A soluble fraction, named "bone marrow serum (BMS)," obtained after spinning human bone marrow aspirates allows measurement of physiologically significant concentrations in the bone cell microenvironment, which are dissimilar from circulating plasma or whole blood (70, 79, 80).

In such fraction, we tested the hypothesis that BMS reflects the uniqueness of the marrow compartment in respect to the sequestration and utilization of fatty acids, by studying the composition of total soluble fatty acids in BMS and plasma samples from control and osteoporotic women with and without hip fracture (81). Results revealed a specific pattern of fatty acid composition in the bone marrow milieu that was characterized by higher saturated and decreased unsaturated fatty acids, compared to that of the circulation. The proportion of fatty acids in the BMS varied in the range of lipids in plasma, but its relative levels of unsaturated and saturated fatty acids compares well to those observed in the human marrow fat tissue (62, 75, 82), implying a distinct lipid content in BMS that replicates relevant fatty acids derived from

the activity of adipocytes and other marrow cells, rather than those provided by blood plasma. The lipid content in BMS of all women studied suggests an active exchange of lipids between marrow cells; thus, the surplus of saturated fatty acids in BMS could result from palmitic and stearic acids supplied mainly by adipocytes, while marrow cells apparently preserve their pool of unsaturated fatty acids, except for oleic acid that is higher in BMS than in plasma (81).

By contrast, when the content of fatty acids in BMS and blood plasma was evaluated according to women's bone mass density, no consistent differences in fatty acid composition were apparent in BMS, nor in plasma, which is analogous to former observations on the composition of bone fat tissue (53, 54, 74). Notwithstanding, there was a trend toward higher saturation and lower unsaturation in BMS fatty acids as compared to plasma. The analysis of the relative proportion of individual fatty acids suggests an active distribution of unsaturated fatty acids.

The former conclusion is supported by further analysis of data on the composition of fatty acids in both BMS and plasma in the osteoporosis group, in relation to the presence or not of a hip fracture (**Figure 1**). A switch toward decreased content of total saturated versus unsaturated fatty acids was observed in BMS of women with fractures, emphasizing a dynamic relationship between the composition of fatty acid in the bone microenvironment and the metabolic requirements of cells. In women with fractures, stearic acid content significantly decreased concomitant with increased oleic acid content, implying a substrate to product relationship to fulfill specific requirements for unsaturated fatty acids. Moreover, increased activity of cyclooxygenase (COX), COX-2 could be proposed from the total removal of polyunsaturated eicosatrienoic and arachidonic fatty acids (81).

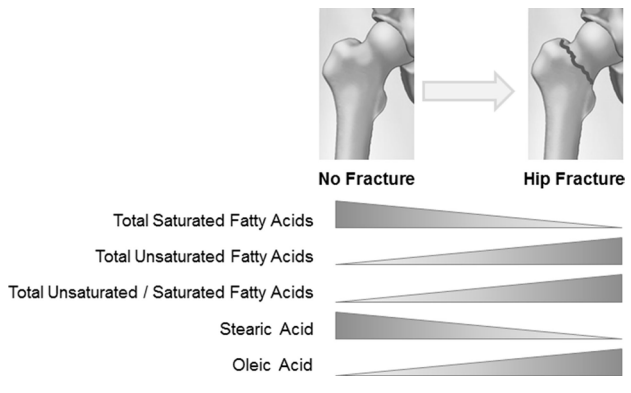

FIGURE 1 | Relationship between hip fracture and fatty acid composition in the bone marrow serum of osteoporotic women.

It is difficult to define the origin (adipocyte or other marrow cell production) and type of lipids that change the fatty acid content of the BMS fraction after fracture, in part because the measurement was limited to the total fatty acid pool in the soluble fraction of the bone marrow. After a hip fracture bone cell metabolism may change in order to provide extra energy for damage repair by osteoblasts, or to suppress excessive inflammation. Interestingly, the lipid fraction in BMS of fractured women appears adjust to such conditions, thus diminished level of saturated fatty acid could result from increased supply of energetic substrate to marrow cells (bone, fat, and hematopoietic), while an increased exchange of oleic and polyunsaturated fatty acids could be related to their regulatory functions.

In conclusion, in this report, we summarize evidence on the role that adipocytes may play in the bone marrow in health and disease. Bone marrow adipose tissue appears as distinct from other extra marrow fat tissues, heterogeneous in its development, and allocated in subpopulations that seem to have different physiological properties. The regulation of the number and quality adipocytes is a necessity to preserve a functional bone marrow microenvironment to sustain SCs. In a bone disease like osteoporosis, there is increased differentiation of the precursor MSCs toward adipocytes, altering the local marrow microenvironment but leading to bone loss. In addition to fat mass, the quality of lipids could also participate in disrupting local regulation; hence, the interest in knowing the fatty acid composition of marrow adipose tissue. The measurement of the fat composition in BMS portrays a dynamic exchange of fatty acids in this fraction implying the connotation of locally produced lipids. The fatty acid composition in the BMS is enriched in saturated fatty acids and decreased in unsaturated fatty acids, as compared to blood plasma. Therefore, it is clear that qualitative aspects of marrow adiposity provide significant insights into the metabolism of the bone marrow niche, and may offer clues as to the pathophysiology of bone diseases, such as osteoporosis.

ETHICS STATEMENT

This study was approved by the INTA, University of Chile IRB.

AUTHOR CONTRIBUTIONS

JR did the research and helped prepare the manuscript. AP did the background work. CF also performed some of the experiments.

FUNDING

This work was supported by a grant from the Fondo Nacional de Ciencia y Tecnología (FONDECYT·#1160214) and NIDDK R24 092759.

REFERENCES

1. Schofield R. The relationship between the spleen colony-forming cell and the haemopoietic stem cell. *Blood Cells* (1978) 4:7–25.
2. Eliasson P, Rehn M, Hammar P, Larsson P, Sirenko O, Flippin LA, et al. Hypoxia mediates low cell-cycle activity and increases the proportion of longterm-reconstituting hematopoietic stem cells during in vitro culture. *Exp Hematol* (2010) 38:301–10. doi:10.1016/j.exphem.2010.01.005
3. Kulkeaw K, Ishitani T, Kanemaru T, Fucharoen S, Sugiyama D. Cold exposure down-regulates zebrafish hematopoiesis. *Biochem Biophys Res Commun* (2010) 394:859–64. doi:10.1016/j.bbrc.2010.01.047
4. Adamo L, Naveiras O, Wenzel PL, McKinney-Freeman S, Mack PJ, Gracia-Sancho J, et al. Biomechanical forces promote embryonic haematopoiesis. *Nature* (2009) 459:1131–5. doi:10.1038/nature08073
5. Guzmán A, García C, Marín AP, Tortajada A, Ruiz MT, Fernández de Henestrosa AR, et al. Formation of micronucleated erythrocytes in mouse

bone-marrow under conditions of hypothermia is not associated with stimulation of erythropoiesis. *Mutat Res* (2008) 656:8–13. doi:10.1016/j.mrgentox.2008.06.016
6. Méndez-Ferrer S, Michurina TV, Ferraro F, Mazloom AR, Macarthur BD, Lira SA, et al. Mesenchymal and haematopoietic stem cells form a unique bone marrow niche. *Nature* (2010) 466:829–34. doi:10.1038/nature09262
7. Kiel MJ, Yilmaz OH, Iwashita T, Yilmaz OH, Terhorst C, Morrison SJ. SLAM family receptors distinguish hematopoietic stem and progenitor cells and reveal endothelial niches for stem cells. *Cell* (2005) 121:1109–21. doi:10.1016/j.cell.2005.05.026
8. Kiel MJ, Morrison SJ. Maintaining hematopoietic stem cells in the vascular niche. *Immunity* (2006) 25:862–4. doi:10.1016/j.immuni.2006.11.005
9. Sacchetti B, Funari A, Michienzi S, Di Cesare S, Piersanti S, Saggio I, et al. Self-renewing osteoprogenitors in bone marrow sinusoids can organize a hematopoietic microenvironment. *Cell* (2007) 131:324–36. doi:10.1016/j.cell.2007.08.025
10. Omatsu Y, Sugiyama T, Kohara H, Kondoh G, Fujii N, Kohno K, et al. The essential functions of adipo-osteogenic progenitors as the hematopoietic stem and progenitor cell niche. *Immunity* (2010) 33:387–99. doi:10.1016/j.immuni.2010.08.017
11. Bianco P. Minireview: the stem cell next door: skeletal and hematopoietic stem cell "niches" in bone. *Endocrinology* (2011) 152:2957–62. doi:10.1210/en.2011-0217
12. Isern J, García-García A, Martín AM, Arranz L, Martín-Pérez D, Torroja C, et al. The neural crest is a source of mesenchymal stem cells with specialized hematopoietic stem cell niche function formation. *Elife* (2014) 2014(3):e03696. doi:10.7554/eLife.03696
13. Ehninger A, Trumpp A. The bone marrow stem cell niche grows up: mesenchymal stem cells and macrophages move in. *J Exp Med* (2011) 208(3):421–8. doi:10.1084/jem.20110132
14. Blair HC, Zaidi M, Schlesinger PH. Mechanisms balancing skeletal matrix synthesis and degradation. *Biochem J* (2002) 364:329–41. doi:10.1042/bj20020165
15. Pittenger MF, Mackay AM, Beck SC, Jaiswal RK, Douglas R, Mosca JD, et al. Multilineage potential of adult human mesenchymal stem cells. *Science* (1999) 284:143–7. doi:10.1126/science.284.5411.143
16. Hegner B, Weber M, Dragun D, Schulze-Lohoff E. Differential regulation of smooth muscle markers in human bone marrow-derived mesenchymal stem cells. *J Hypertens* (2005) 23:1191–202. doi:10.1097/01.hjh.0000170382.31085.5d
17. Tao H, Han Z, Han Z-C, Li Z. Proangiogenic features of mesenchymal stem cells and their therapeutic applications. *Stem Cells Int* (2016) 2016:1314709. doi:10.1155/2016/1314709
18. Muraglia A, Cancedda R, Quarto R. Clonal mesenchymal progenitors from human bone marrow differentiate in vitro according to a hierarchical model. *J Cell Sci* (2000) 113:1161–6.
19. Kuznetsov SA, Krebsbach PH, Satomura K, Kerr J, Riminucci M, Benayahu D, et al. Single-colony derived strains of human marrow stromal fibroblasts form bone after transplantation in vivo. *J Bone Miner Res* (1997) 12:1335–47. doi:10.1359/jbmr.1997.12.9.1335
20. Digirolamo CM, Stokes D, Colter D, Phinney DG, Class R, Prockop DJ. Propagation and senescence of human marrow stromal cells in culture: a simple colony-forming assay identifies samples with the greatest potential to propagate and differentiate. *Br J Haematol* (1999) 107:275–81. doi:10.1046/j.1365-2141.1999.01715.x
21. Baksh D, Song L, Tuan RS. Adult mesenchymal stem cells: characterization, differentiation, and application in cell and gene therapy. *J Cell Mol Med* (2004) 8:301–16. doi:10.1111/j.1582-4934.2004.tb00320.x
22. Zhou S, Greenberger JS, Epperly MW, Goff JP, Adler C, Leboff MS, et al. Age-related intrinsic changes in human bone marrow-derived mesenchymal stem cells and their differentiation to osteoblasts. *Aging Cell* (2008) 7:335–43. doi:10.1111/j.1474-9726.2008.00377.x
23. Kultere B, Friedl G, Jandrositz A, Sánchez-Cabo F, Prokesch A, Paar C, et al. Gene expression profiling of human mesenchymal stem cells derived from bone marrow during expansion and osteoblast diff erentiation. *BMC Genomics* (2007) 8:70. doi:10.1186/1471-2164-8-70
24. Kuhn NZ, Tuan RS. Regulation of stemness and stem cell niche of mesenchymal stem cells: implications in tumorigenesis and metastasis. *J Cell Physiol* (2010) 222:268–77. doi:10.1002/jcp.21940
25. McBride SH, Falls T, Knothe Tate ML. Modulation of stem cell shape and fate B: mechanical modulation of cell shape and gene expression. *Tissue Eng Part A* (2008) 14:1573–80. doi:10.1089/ten.tea.2008.0113
26. Seebach C, Henrich D, Tewksbury R, Wilhelm K, Marzi I. Number and proliferative capacity of human mesenchymal stem cells are modulated positively in multiple trauma patients and negatively in atrophic nonunions. *Calcif Tissue Int* (2007) 80:294–300. doi:10.1007/s00223-007-9020-6
27. Hofer EL, Labovsky V, La Russa V, Vallone VF, Honegger AE, Belloc CG, et al. Mesenchymal stromal cells, colony-forming unit fibroblasts, from bone marrow of untreated advanced breast and lung cancer patients suppress fi broblast colony formation from healthy marrow. *Stem Cells Dev* (2010) 19:359–70. doi:10.1089/scd.2008.0375
28. Song L, Webb NE, Song Y, Tuan RS. Identification and functional analysis of candidate genes regulating mesenchymal stem cell self-renewal and multipotency. *Stem Cells* (2006) 24:1707–18. doi:10.1634/stemcells.2005-0604
29. Zipori D. The stem state: Plasticity is essential, whereas self-renewal and hierarchy are optional. *Stem Cells* (2005) 23:719–26. doi:10.1634/stemcells.2005-0030
30. Zipori D. The stem state: mesenchymal plasticity as a paradigm. *Curr Stem Cell Res Ther* (2006) 1:95–102. doi:10.2174/157488806775269133
31. Chen Q, Shou P, Zheng C, Jiang M, Cao G, Yang Q, et al. Fate decision of mesenchymal stem cells: adipocytes or osteoblasts? *Cell Death Differ* (2016) 23(7):1128–39. doi:10.1038/cdd.2015.168
32. Muruganandan S, Roman AA, Sinal CJ. Adipocyte differentiation of bone marrow-derived mesenchymal stem cells: cross talk with the osteoblastogenic program. *Cell Mol Life Sci* (2009) 66:236–53. doi:10.1007/s00018-008-8429-z
33. Teitelbaum SL. Bone resorption by osteoclasts. *Science* (2000) 289:1504–8. doi:10.1126/science.289.5484.1504
34. Caplan AI. Mesenchymal stem-cells. *J Orthop Res* (1991) 9:641–50. doi:10.1002/jor.1100090504
35. Meunier P, Aaron J, Edouard C, Vignon G. Osteoporosis and replacement of cell populations of marrow by adipose tissue – a quantitative study of 84 iliac bone biopsies. *Clin Orthop Relat Res* (1971) 80:147–54. doi:10.1097/00003086-197110000-00021
36. Justesen J, Stenderup K, Ebbesen EN, Mosekilde L, Steiniche T, Kassem M. Adipocyte tissue volume in bone marrow is increased with aging and in patients with osteoporosis. *Biogerontology* (2001) 2:165–71. doi:10.1023/A:1011513223894
37. Moerman EJ, Teng K, Lipschitz DA, Lecka-Czernik B. Aging activates adipogenic and suppresses osteogenic programs in mesenchymal marrow stroma/stem cells: the role of PPARg 2 transcription factor and TGF-β/BMP signaling pathways. *Aging Cell* (2004) 3:379–89. doi:10.1111/j.1474-9728.2004.00127.x
38. Zayzafon M, Gathings WE, McDonald JM. Modeled microgravity inhibit osteogenic differentiation of human mesenchymal stem cells and increases adipogenesis. *Endocrinology* (2004) 145:2421–32. doi:10.1210/en.2003-1156
39. Forsen L, Meyer HE, Midthjell K, Edna TH. Diabetes mellitus and the incidence of hip fracture: results from the Nord-Trondelag Health Survey. *Diabetologia* (1999) 42:920–5. doi:10.1007/s001250051248
40. Nuttall M, Gimble JM. Controlling the balance between osteoblastogenesis and adipogenesis and the consequent therapeutic implications. *Curr Opin Pharmacol* (2004) 4:290–4. doi:10.1016/j.coph.2004.03.002
41. Lefterova MI, Zhang Y, Steger DJ, Schupp M, Schug J, Cristancho A, et al. PPARgamma and C/EBP factors orchestrate adipocyte biology via adjacent binding on a genome-wide scale. *Genes Dev* (2008) 22:2941–52. doi:10.1101/gad.1709008
42. Cao Z, Umek RM, McKnight SL. Regulated expression of three C/EBP isoforms during adipose conversion of 3T3-L1 cells. *Genes Dev* (1991) 5:1538–52. doi:10.1101/gad.5.9.1538
43. Kim J, Ko J. A novel PPARgamma2 modulator sLZIP controls the balance between adipogenesis and osteogenesis during mesenchymal stem cell differentiation. *Cell Death Differ* (2014) 21:1642–55. doi:10.1038/cdd.2014.80
44. Komori T. Regulation of osteoblast differentiation by transcription factors. *J Cell Biochem* (2006) 99:1233–9. doi:10.1002/jcb.20958
45. Lecka-Czernik B, GubriJ I, Moerman EA, Kajkenova O, Lipschitz DA, Manolagas SC, et al. Inhibition of Osf2/Cbaf1 expression and terminal osteoblast differentiation by PPAR-gamma2. *J Cell Biochem* (1999) 74:357–71. doi:10.1002/(SICI)1097-4644(19990901)74:3<357::AID-JCB5>3.0.CO;2-7
46. Jeon MJ, Kim JA, Kwon SH, Kim SW, Park KS, Park SW, et al. Activation of peroxisome proliferator-activated receptor-γ inhibits the Runx2-mediated

transcription of osteocalcin in osteoblasts. *J Biol Chem* (2003) 278:23270–7. doi:10.1074/jbc.M211610200
47. Cock TA, Back J, Elefteriou F, Karsenty G, Kastner P, Chans S, et al. Enhanced bone formation in lipodystrophic PPARγ*hyp/hyp* mice relocates haematopoiesis to the spleen. *EMBO Rep* (2004) 5:1007–12. doi:10.1038/sj.embor.7400254
48. Kobayashi H, Gao Y, Ueta C, Yamaguchi A, Komori T. Multiline-age diff erentiation of Cbfa1-defi cient calvarial cells in vitro. *Biochem Biophys Res Commun* (2000) 273:630–6. doi:10.1006/bbrc.2000.2981
49. McGee-Lawrence ME, Carpio LR, Schulze RJ, Pierce JL, McNiven MA, Farr JN, et al. Hdac3 deficiency increases marrow adiposity and induces lipid storage and glucocorticoid metabolism in osteochondroprogenitor cells. *J Bone Miner Res* (2016) 31(1):116–28. doi:10.1002/jbmr.2602
50. Rosen CJ, Bouxsein ML. Mechanisms of disease: is osteoporosis the obesity of bone? *Nat Clin Pract Rheumatol* (2006) 2:35–43. doi:10.1038/ncprheum0070
51. Rosen CJ, Ackert-Bicknell C, Rodriguez JP, Pino AM. Marrow fat and the bone microenvironment: developmental, functional and pathological implications. *Crit Rev Eukaryot Gene Expr* (2009) 19:109–24. doi:10.1615/CritRevEukarGeneExpr.v19.i2.20
52. Rodríguez JP, Astudillo P, Rios S, Pino AM. Involvement of adipogenic potential of human bone marrow mesenchymal stem cells (MSCs) in osteoporosis. *Curr Stem Cell Res Ther* (2008) 3:208–18. doi:10.2174/157488808785740325
53. Griffith JF, Yeung DKW, Ahuja AT, Choy CWY, Mei WY, Lam SSL, et al. A study of bone marrow and subcutaneous fatty acid composition in subjects of varying bone mineral density. *Bone* (2009) 44:1092–6. doi:10.1016/j.bone.2009.02.022
54. Yeung DK, Griffith JF, Antonio GE, Lee FK, Woo J, Leung PC. Osteoporosis is associated with increased marrow fat content and decreased marrow fat unsaturation: a proton MR spectroscopy study. *J Magn Reson Imaging* (2005) 22(2):279–85. doi:10.1002/jmri.20367
55. Blake GM, Griffith JF, Yeung DK, Leung PC, Fogelman I. Effect of increasing vertebral marrow fat content on BMD measurement, T-Score status and fracture risk prediction by DXA. *Bone* (2009) 44:495–501. doi:10.1016/j.bone.2008.11.003
56. Moore SG, Dawson KL. Red and yellow marrow in the femur: age related changes in appearance at MR imaging. *Radiology* (1990) 175(1):219–23. doi:10.1148/radiology.175.1.2315484
57. Tavassoli M. Ultrastructural development of bone marrow adipose cell. *Acta Anat* (1976) 94:65–77. doi:10.1159/000144545
58. Tavassoli M. Marrow adipose cells. Histochemical identification of labile and stable components. *Arch Pathol Lab Med* (1976) 100:16–8.
59. Scheller EL, Rosen CJ. What's the matter with MAT? Marrow adipose tissue, metabolism, and skeletal health. *Ann N Y Acad Sci* (2014) 1311:14–30. doi:10.1111/nyas.12327
60. Emery JL, Follett GF. Regression of bone-marrow haemopoiesis from the terminal digits in the foetus and infant. *Br J Haematol* (1964) 10:485–9. doi:10.1111/j.1365-2141.1964.tb00725.x
61. Kricun ME. Red-yellow marrow conversion: its effect on the location of some solitary bone lesions. *Skeletal Radiol* (1985) 14:10–9. doi:10.1007/BF00361188
62. Scheller EL, Doucette CR, Learman BS, Cawthorn WP, Khandaker S, Schell B, et al. Region-specific variation in the properties of skeletal adipocytes reveals regulated and constitutive marrow adipose tissues. *Nat Commun* (2015) 6:7808. doi:10.1038/ncomms8808
63. Krings A, Rahman S, Huang S, Lu Y, Czernik PJ, Lecka-Czernik B. Bone marrow fat has brown adipose tissue characteristics, which are attenuated with aging and diabetes. *Bone* (2011) 50(2):546–52. doi:10.1016/j.bone.2011.06.016
64. Lecka-Czernik B. Marrow fat metabolism is linked to the systemic energy metabolism. *Bone* (2012) 50(2):534–9. doi:10.1016/j.bone.2011.06.032
65. Wren TA, Chung SA, Dorey FJ, Bluml S, Adams GB, Gilsanz V. Bone marrow fat is inversely related to cortical bone in young and old subjects. *J Clin Endocrinol Metab* (2011) 96(3):782–6. doi:10.1210/jc.2010-1922
66. Di Iorgi N, Mo AO, Grimm K, Wren TA, Dorey F, Gilsanz V. Bone acquisition in healthy young females is reciprocally related to marrow adiposity. *J Clin Endocrinol Metab* (2010) 95(6):2977–82. doi:10.1210/jc.2009-2336
67. Naveiras O, Nardi V, Wenzel PL, Hauschka PV, Fahey F, Daley GQ. Bone-marrow adipocytes as negative regulators of the haematopoietic microenvironment. *Nature* (2009) 460:259–63. doi:10.1038/nature08099
68. Clabaut A, Delplace S, Chauveau C, Hardouin P, Broux O. Human osteoblasts derived from mesenchymal stem cells express adipogenic markers upon coculture with bone marrow adipocytes. *Differentiation* (2010) 80:40–5.
69. Lee WY, Kang MI, Oh ES, Oh KW, Han JH, Cha BY, et al. The role of cytokines in the changes in bone turnover following bone marrow transplantation. *Osteoporos Int* (2002) 13:62–8. doi:10.1007/s198-002-8339-5
70. Pino AM, Ríos S, Astudillo P, Fernández M, Figueroa P, Seitz G, et al. Concentration of adipogenic and pro inflammatory cytokines in the bone marrow supernatant fluid of osteoporotic women. *J Bone Min Res* (2010) 25:492–8. doi:10.1359/jbmr.090802
71. Ahima RS, Flier JS. Adipose tissue as an endocrine organ. *Trends Endocrinol Metab* (2000) 11(8):327–32. doi:10.1016/S1043-2760(00)00301-5
72. Kawai M, de Paula FJ, Rosen CJ. New insights into osteoporosis: the bone-fat connection. *J Intern Med* (2012) 272(4):317–29. doi:10.1111/j.1365-2796.2012.02564.x
73. Niemeier A, Niedzielska D, Secer R, Schilling A, Merkel M, Enrich C, et al. Uptake of postprandial lipoproteins into bone in vivo: impact on osteoblast function. *Bone* (2008) 43(2):230–7. doi:10.1016/j.bone.2008.03.022
74. Baum T, Yap SP, Karampinos DC, Nardo L, Kuo D, Burghardt AJ, et al. Does vertebral bone marrow fat content correlate with abdominal adipose tissue, lumbar spine bone mineral density, and blood biomarkers in women with type 2 diabetes mellitus? *J Magn Reson Imaging* (2012) 35(1):117–24. doi:10.1002/jmri.22757
75. Patsch JM, Li X, Baum T, Yap SP, Karampinos DC, Schwartz AV, et al. Bone marrow fat composition as a novel imaging biomarker in postmenopausal women with prevalent fragility fractures. *J Bone Min Res* (2013) 28(8):1721–8. doi:10.1002/jbmr.1950
76. Wiig H, Berggreen E, Borge BA, Iversen PO. Demonstration of altered signaling responses in bone marrow extracellular fluid during increased hematopoiesis in rats using a centrifugation method. *Am J Physiol Heart Circ Physiol* (2004) 286:H2028–34. doi:10.1152/ajpheart.00934.2003
77. Iversen PO, Wiig H. Tumor necrosis factor A and adiponectin in bone marrow interstitial fluid from patients with acute myeloid leukemia inhibit normal hematopoiesis. *Clin Cancer Res* (2005) 11:6793–9. doi:10.1158/1078-0432.CCR-05-1033
78. Khosla S, Peterson JM, Egan K, Jones JD, Riggs BL. Circulating cytokine levels in osteoporotic and normal women. *J Clin Endocrinol Metab* (1994) 79:707–11. doi:10.1210/jcem.79.3.8077350
79. Xian L, Wu X, Pang L, Lou M, Rosen CJ, Qiu T, et al. Matrix IGF-1 maintains bone mass by activation of mTOR in mesenchymal stem cells. *Nat Med* (2012) 18(7):1095–101. doi:10.1038/nm.2793
80. Li X, Shet K, Rodriguez JP, Pino AM, Kurhanewicz J, Schwartz A, et al. Unsaturation level decreased in bone marrow lipids of postmenopausal women with low bone density using high resolution HRMAS NMR. *Presented at: 34th Annual Conference of American Society of Bone Mineral Research (ASBMR); Oct 9–12*. Minneapolis, MN, USA (2012).
81. Miranda M, Pino AM, Fuenzalida K, Rosen CJ, Seitz G, Rodríguez JP. Characterization of fatty acid composition in bone marrow fluid from postmenopausal women: modification after hip fracture. *J Cell Biochem* (2016) 117(10):2370–6. doi:10.1002/jcb.25534
82. Yeung DKW, Lamb SL, Griffith JF, Chanc ABW, Chend Z, Tsang PH, et al. Analysis of bone marrow fatty acid composition using high-resolution proton NMR spectroscopy. *Chem Phys Lipids* (2008) 151:103–9. doi:10.1016/j.chemphyslip.2007.10.006

Conflict of Interest Statement: The authors declare that the research was conducted in the absence of any commercial or financial relationships that could be construed as a potential conflict of interest.

frontiers in Endocrinology

MINI REVIEW
published: 27 June 2016
doi: 10.3389/fendo.2016.00074

MR-Based Assessment of Bone Marrow Fat in Osteoporosis, Diabetes, and Obesity

Christian Cordes[1], Thomas Baum[1], Michael Dieckmeyer[1], Stefan Ruschke[1], Maximilian N. Diefenbach[1], Hans Hauner[2], Jan S. Kirschke[3] and Dimitrios C. Karampinos[1]*

[1] Department of Diagnostic and Interventional Radiology, Klinikum rechts der Isar, Technische Universität München, Munich, Germany, [2] Else Kröner Fresenius Center for Nutritional Medicine, Klinikum rechts der Isar, Technische Universität München, Munich, Germany, [3] Section of Diagnostic and Interventional Neuroradiology, Klinikum rechts der Isar, Technische Universität München, Munich, Germany

Bone consists of the mineralized component (i.e., cortex and trabeculae) and the non-mineralized component (i.e., bone marrow). Most of the routine clinical bone imaging uses X-ray-based techniques and focuses on the mineralized component. However, bone marrow adiposity has been also shown to have a strong linkage with bone health. Specifically, multiple previous studies have demonstrated a negative association between bone marrow fat fraction (BMFF) and bone mineral density. Magnetic resonance imaging (MRI) and magnetic resonance spectroscopy (MRS) are ideal imaging techniques for non-invasively investigating the properties of bone marrow fat. In the present work, we first review the most important MRI and MRS methods for assessing properties of bone marrow fat, including methodologies for measuring BMFF and bone marrow fatty acid composition parameters. Previous MRI and MRS studies measuring BMFF and fat unsaturation in the context of osteoporosis are then reviewed. Finally, previous studies investigating the relationship between bone marrow fat, other fat depots, and bone health in patients with obesity and type 2 diabetes are presented. In summary, MRI and MRS are powerful non-invasive techniques for measuring properties of bone marrow fat in osteoporosis, obesity, and type 2 diabetes and can assist in future studies investigating the pathophysiology of bone changes in the above clinical scenarios.

Keywords: bone marrow, magnetic resonance imaging, magnetic resonance spectroscopy, osteoporosis, diabetes, obesity

OPEN ACCESS

Edited by:
William Peter Cawthorn, University of Edinburgh, UK

Reviewed by:
Graham J. Galloway, Translational Research Institute, Australia
Miriam A. Bredella, Massachusetts General Hospital, USA

****Correspondence:***
Christian Cordes
c.cordes@tum.de

Specialty section:
This article was submitted to Bone Research, a section of the journal Frontiers in Endocrinology

Received: *19 April 2016*
Accepted: *14 June 2016*
Published: *27 June 2016*

Citation:
Cordes C, Baum T, Dieckmeyer M, Ruschke S, Diefenbach MN, Hauner H, Kirschke JS and Karampinos DC (2016) MR-Based Assessment of Bone Marrow Fat in Osteoporosis, Diabetes, and Obesity. Front. Endocrinol. 7:74. doi: 10.3389/fendo.2016.00074

INTRODUCTION

Bone consists of the mineralized (i.e., cortex and trabeculae) and the non-mineralized component (i.e., bone marrow). The interaction of the mineralized and non-mineralized components plays an important role in bone loss pathophysiology. Quantitative measurements of the mineralized component have been traditionally performed by using dual-energy-X-ray-absorptiometry (DXA) or quantitative computed tomography (QCT) assessing bone mineral density (BMD) (1). BMD is used in clinical routine to determine osteoporosis-associated fracture risk. Osteoporosis is defined as a skeletal disorder characterized by compromised bone strength predisposing an individual to an increased risk for fractures (2). It is classified as a public health problem, since osteoporosis-related fractures are associated with a reduction in quality of life and an increased

morbidity and mortality (3, 4). However, BMD accounts for only 60–70% of the variation in bone strength (5) and the BMD values of subjects with and without osteoporotic fracture overlap (6). Measurements of trabecular bone microstructure, based on high-resolution imaging techniques, in addition to BMD have shown to improve the prediction of the variation in bone strength (7–9).

Despite the focus on the mineralized bone component for osteoporosis diagnostics, recent studies have highlighted the potential role of the non-mineralized bone component in bone health (10–14). Bone marrow fills the cavities of trabecular bone and it primarily consists of adipocytes (yellow marrow regions) or adipocytes and hematopoietic red blood cells (red marrow regions). It is well known that osteoporosis is associated with an increased bone marrow fat mass due to a shift of differentiation of mesenchymal stem cells to adipocytes rather than to osteoblasts (11, 13, 15). Multiple studies have shown that higher bone marrow fat fraction (BMFF) values are associated with lower BMD values (12, 14, 16–26).

Bone marrow fat has a distinctly different function compared to other white and brown adipose tissue depots or ectopic fat depots in the human body (27) and might play a role in the pathophysiology of metabolic disorders. Metabolic diseases, including obesity and diabetes, are known to have a complex and still poorly understood relationship to bone health. There seems to be a higher fracture-related morbidity in obese than in non-obese women (28), and more fractures in diabetic than in healthy subjects (29–32). In addition, there is a growing interest to study the relationship between bone marrow fat mass and fat in other depots regarding obesity and type 2 diabetes mellitus (T2DM).

In this context, imaging biomarkers are emerging to non-invasively study the properties of the non-mineralized component of bone (33). Dual-energy CT (DECT) allows to simultaneously determine bone marrow fat and BMD (34). In contrast to DECT, magnetic resonance (MR) allows the quantitative assessment of bone marrow without radiation exposure. MR enables reliable measurements of bone marrow water-fat and fatty acid composition with different methods including magnetic resonance imaging (MRI) and magnetic resonance spectroscopy (MRS) (35, 36).

The purpose of the present work is to review the currently available literature on MR-based assessment of bone marrow fat in the context of osteoporosis, T2DM, and obesity.

MR-BASED ASSESSMENT OF BONE MARROW FAT

Literature Research

Electronic searches in PubMed (http://www.ncbi.nlm.nih.gov/pubmed) were performed up to March 2015 to identify relevant studies for this review. No starting date was entered for the electronic search to obtain the entire literature available in PubMed. Search terms used included "Bone Marrow," "Bone Marrow Fat," "Bone Marrow Adipose Tissue," "Magnetic Resonance Imaging," "Magnetic Resonance Spectroscopy," "Osteoporosis," "Obesity," and "Diabetes." The search was restricted to studies in humans. The reference lists of relevant articles were also screened.

MR Methods

T1-weighted imaging (T1WI), MRS, and chemical shift encoding-based water–fat imaging have been previously used to assess BMFF.

T1-Weighted Imaging

T1-weighted imaging is not technically demanding and has been mostly applied on the pelvis, hip, and spine. A recent study has even introduced a score analog to the DEXA *t*-score based on the mean signal-to-noise ratio of the L1–L4 vertebral bodies in T1WI (37). Measurements of bone marrow fat volume have been also proposed by applying thresholds on T1WI to extract bone marrow fat voxels (25). The applied threshold was usually set at the same gray-scale level as subcutaneous adipose tissue. The intra- and interobserver reproducibility for the assessment of bone marrow fat volume in T1WI images expressed as coefficient of variation (CV) amounted 0.9% (intraobserver) and 2.2% (interobserver) (for the post-processing) (38). The main error source for the calculation of bone marrow fat volume based on T1WI results from partial volume effects and threshold selection, especially in regions with red marrow.

Magnetic Resonance Spectroscopy

Proton-MRS (1H-MRS) is considered as the MR gold standard for bone marrow fat quantification (**Figure 1**). Point-resolved spectroscopy (PRESS) and stimulated echo acquisition mode (STEAM) single-voxel 1H-MRS sequences have been most commonly used for the characterization of the fat spectrum in the bone marrow at the pelvis, spine, and hip. Based on MR spectra, fat fraction and fatty acid composition parameters can be determined (36). The average CV of vertebral BMFF was reported to be 1.7% (on the same day with repositioning). Griffith et al. recruited 36 subjects who underwent MRS in the femoral neck and head, as well as in the subtrochanteric region of the femoral shaft to measure bone marrow fat content (39). They found the best reproducibility (between two measurements within 1 week) in the femoral head (interclass correlation 0.85), followed by the femoral shaft (interclass correlation 0.83), and the femoral neck (interclass correlation 0.78). Another recent study that examined reproducibility of 1H-MRS vertebral BMFF found a CV of 9.9% (SD 0.08) for a 6-week reproducibility and a CV of 12.3% (SD 0.10) for a 6-month reproducibility (40).

However, most of the above studies did not account for the difference in T2 relaxation times between the water- and fat components and measured a signal-weighted fat fraction at a single echo time (TE), dependent on the employed TE value and field strength. A multi-TE MRS measurement combined with T2 estimation routines instead removes the confounding effects of water–fat T2 differences and results in the proton density fat fraction (PDFF), which is independent of the employed experimental settings (41).

In addition, bone marrow spectra are characterized by strongly overlapping water and fat peaks due to susceptibility effects from the trabecular bone (41, 42): water and olefinic fat peaks overlap significantly, especially in the spine. The *a priori* knowledge of the chemical structure of triglycerides can be employed to improve the robustness of water peak extraction

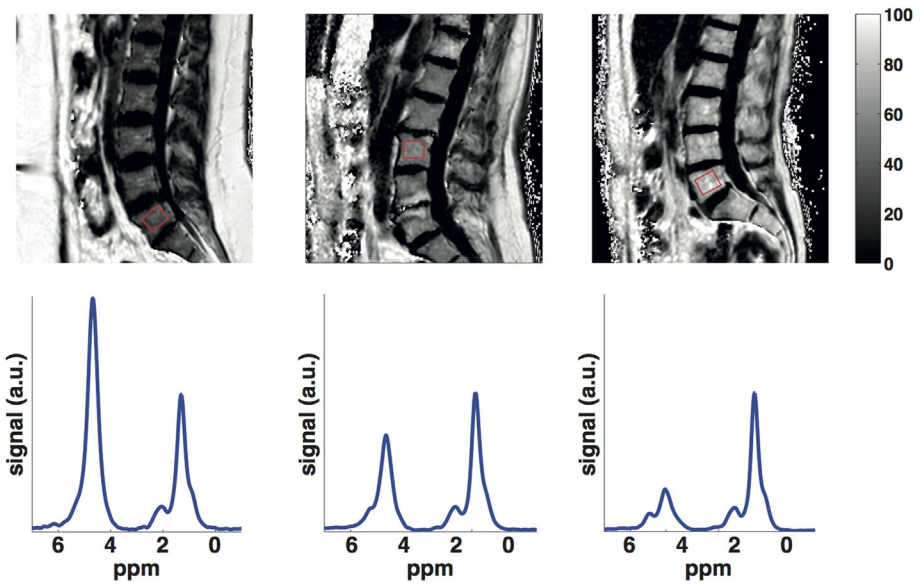

FIGURE 1 | Lumbar vertebral bone marrow PDFF maps (first row) and single-voxel MR spectra (second row) in a young subject (25 years), an old subject (60 years) with normal BMD (spine t-score = 3.7) and an old subject (60 years) with osteoporosis (spine *t*-score = −3). Bone marrow PDFF increases with age and lower BMD: the young subject had a PDFF on the L5 vertebral body (red box) equal to 32.4%, the old subject with normal BMD had a PDFF on the L3 vertebral body (red box) equal to 48.9% and the old subject with osteoporosis had a PDFF on the L5 vertebral body (red box) equal to 67.5%.

by constraining the area of the olefinic fat peak to the main fat peaks (41–43). However, the quantification of fat unsaturation relies on the extraction of the olefinic fat peak on an individual spectrum basis and remains a major technical challenge in the presence of a strong water peak (i.e., in the spine). Previous studies measuring vertebral bone marrow fat unsaturation based on short-TE spectra have reported moderate reproducibility values (same day, with repositioning) (36). Increasing the TE (44) or adding diffusion-weighting (45, 46) have been recently proposed to reduce the water peak height and more robustly extract the olefinic peak in vertebral bone marrow spectra.

Water–Fat Imaging

In contrast to single-voxel MRS, chemical shift encoding-based water–fat imaging allows the spatially resolved assessment of the BMFF (**Figure 1**). High-resolution BMFF mapping is highly advantageous due to the heterogeneous distribution of bone marrow in most regions (e.g., proximal femur, spine). However, several confounding factors have to be considered when measuring bone marrow PDFF by using water–fat imaging, including the presence of multiple peaks in the fat spectrum (47, 48), T1-bias (49, 50) and T2*-decay effects (47, 51). The presence of trabecular bone most importantly shortens the T2* of water and fat components, inducing a rapid decay of the measured gradient echo signal with echo time (42, 52). After correcting for T2* decay effects, a good agreement was reported *in vivo* between MRS-based and imaging-based PDFF in both the proximal femur (42) and spine (52).

An *ex vivo* study was performed in trabecular bone specimens filled with water–fat emulsions of different fat fractions, showing an excellent agreement between imaging-based PDFF and the known PDFF of the emulsions (53). To validate the results of bone marrow water–fat imaging with a non-MRI reference, Arentsen et al. (54) and MacEwan et al. (55) performed studies comparing water–fat imaging with histological examinations. Water–fat imaging in both studies resulted in vertebral BMFF and water fraction values, which showed good correlation ($r = 0.76$–0.77) with the histological results.

As water–fat imaging methodologies become more broadly available, studies have been recently performed to evaluate the significance of a spatially resolved fat fraction map (56–60). In a recent study, Baum et al. investigated whole body spine water–fat imaging on 28 healthy subjects (56). They found an increased BMFF from the cervical to the lumbar level. Absolute precision error amounted to 1.7% on the average.

Despite a considerable amount of literature using MR methods to assess bone marrow properties in the pelvis and the long bones, vertebral bone marrow remains the region most extensively investigated in bone marrow studies of aging, osteoporosis, diabetes, and obesity (**Table 1**).

Bone Marrow Fat in Aging

The BMFF is well known to increase with age (**Figure 1**). The exact age dependence has been shown to differ between male and female subjects (61–63). A recent study has also emphasized the importance of T2-correction when using MRS to investigate the age dependence of BMFF (41). However, less is known about the age dependence of bone marrow fat unsaturation. Huovinen et al. recently investigated bone marrow fat unsaturation in young adults (15–27 years) (64). Thirty-five young adults from 27 to 35 years were included in their study, and they showed an increase of bone marrow fat unsaturation with age. The results

TABLE 1 | Summary of MR-based studies investigating vertebral bone marrow fat properties in osteoporosis, diabetes, and obesity.

Study	Subjects	MR technique and bone marrow fat parameters	Main results for bone marrow fat
Osteoporosis			
Yeung et al. (26)	53 women	MRS for fat fraction and unsaturation	Higher fat fraction and lower fat unsaturation in osteoporotic than osteopenic and normal subjects
Griffith et al. (19)	90 men	MRS for fat fraction	Higher fat fraction in osteoporotic than osteopenic and normal subjects
Griffith et al. (20)	103 women	MRS for fat fraction	Higher fat fraction in osteoporotic than osteopenic and normal subjects
Patsch et al. (66)	69 women	MRS for fat fraction and unsaturation	Fat unsaturation negatively associated with prevalence of fragility fractures
Kühn et al. (57)	51 subjects	Water-fat imaging for PDFF	Higher PDFF in osteoporotic than normal subjects
Karampinos et al. (21)	10 specimens	MRS for fat fraction (*ex vivo*)	Fat fraction negatively associated with failure load
Diabetes and obesity			
Bredella et al. (70)	47 women	MRS for fat fraction	Fat fraction positively associated with visceral fat volume
Baum et al. (16)	26 women	MRS for fat fraction and unsaturation	Fat unsaturation lower in diabetics compared to non-diabetics
Bredella et al. (67)	35 men	MRS for fat fraction	Fat fraction negatively associated with bone strength parameters
Bredella et al. (68)	106 women	MRS for fat fraction	Fat fraction positively associated with intra-hepatic and intramyocellar lipids
Bredella et al. (69)	79 women	MRS for fat fraction	Fat fraction increased after growth hormone therapy
Cordes at al. (72)	20 women	MRS for fat fraction	Fat fraction unchanged after a 4-week calorie restriction in obesity, but fat fraction changes associated with subcutaneous fat volume before intervention
Schafer et al. (22)	11 women	MRS for fat fraction	Fat fraction decreased only in diabetics after a gastric bypass surgery

suggest an association of bone marrow fat unsaturation with age in early adulthood and may represent the normal maturation of bone marrow.

Bone Marrow Fat in Osteoporosis

Bone Marrow Fat Fraction

The MR-based vertebral bone marrow fat parameter studied most frequently in the context of osteoporosis is the fat fraction. Representative data from the authors own work, using a methodology similar to Baum et al. (65) and highlighting the effect of age and osteoporosis on bone-marrow fat fraction, are shown in **Figure 1**.

Most previous studies evaluating the relationship between BMD and BMFF have been based on single-voxel MRS. Griffith et al. performed a study in 103 female subjects to investigate the association between bone marrow fat and osteoporosis *in vivo* (20). They acquired DXA to stratify the group into healthy ($n = 18$), osteopenic ($n = 30$), and osteoporotic subjects ($n = 55$). MRS was performed at L3. The vertebral marrow fat fraction was significantly increased in osteoporotic subjects (67.8 ± 8.5%) compared with healthy subjects (59.2 ± 10.0%). Similar results were found in men. In another study, 90 men (42 subjects with normal BMD, 23 osteopenic, and 17 osteoporotic subjects) were recruited and obtained a measurement of the bone marrow fat content in L3 using MRS (19). The vertebral marrow fat fraction was significantly increased in subjects with osteoporosis (58.2 ± 7.8%) and osteopenia (55.7 ± 10.2%) compared to subjects with normal BMD (50.5 ± 8.7%).

Karampinos et al. recently examined ten vertebrae from human cadavers using MRS to assess BMFF, multi-detector computed tomography (MDCT) to determine BMD and trabecular bone microstructure parameters, and biomechanical testing to assess vertebral bone strength (21). They reported significant correlations between the MRS-based fat fraction and MDCT-based parameters (up to $r = -0.72$), and MRS-based fat fraction and vertebral failure load ($r = -0.77$). Thus, this study demonstrated that bone marrow fat volume is negatively associated with both bone microstructure and bone strength. However, further studies with larger number of specimens are needed in order to investigate whether the BMFF has an effect on bone strength after correcting for the contribution of BMD.

Kühn et al. performed one of the first bone marrow high-resolution fat fraction mapping studies in patients with osteoporosis. Their study included 51 patients who underwent DXA as well as water-fat imaging of the lumbar spine (57). According to the DXA results, the participants were divided into three subgroups: 92 healthy, 47 osteopenic, and 34 osteoporotic. The obtained PDFF was greater in osteoporotic than healthy vertebrae (62.4 ± 11.0% versus 56.3 ± 14.8%). Thus, water–fat imaging could be an alternative to the most commonly used MRS to assess bone marrow fat in the context of osteoporosis.

Bone Marrow Fat Unsaturation

The second MR-based bone marrow fat parameter, which has been linked to bone matrix loss, is bone marrow fat unsaturation. Yeung et al. analyzed bone marrow fat composition in the context of osteoporosis (26). They included 53 women over 60 years of age and 12 young controls in their study. The subjects underwent DXA and MRS of the lumbar spine. Interestingly, the fat unsaturation level was significantly decreased in osteoporotic (0.091 ± 0.013) and osteopenic (0.097 ± 0.014) subjects compared to healthy subjects (0.114 ± 0.016) and young controls (0.127 ± 0.031). Patsch et al. investigated the vertebral bone marrow fat composition in diabetic and non-diabetic postmenopausal women with and without fragility fractures (66). In consistency with Yeung et al., the prevalence of fragility fractures

was associated with −1.7% lower unsaturation levels and +2.9% higher saturation levels.

Bone Marrow Fat in T2DM

Baum et al. performed a study on 26 subjects, including 13 non-diabetic and 13 treated diabetic women (16). The subjects underwent blood parameter analysis including plasma glucose and HbA1c. Images from mid T12 to mid L4 were acquired using MDCT to obtain SAT (subcutaneous adipose tissue), VAT (visceral adipose tissue), and TAT (total adipose tissue). MRS was obtained at L1, L2, and L3 to assess BMFF and unsaturation. The mean vertebral BMFF was similar in the diabetic women and the healthy controls (69.3 ± 7.5% versus 67.5 ± 6.1%; $P > 0.05$). However, the mean unsaturation level was significantly lower in the diabetic group (6.7 ± 1.0% versus 7.9 ± 1.6%; $P < 0.05$). Adjusted SAT and TAT correlated significantly with mean vertebral bone marrow fat content in the whole study population ($r = 0.538$ and $r = 0.466$; $P < 0.05$). Interestingly, significant correlations of mean vertebral bone marrow fat content with adjusted VAT and HbA1c were observed only in the diabetic group ($r = 0.642$ and $r = 0.825$; $P < 0.05$).

Similar results to the study by Baum et al. (16) were reported by Patsch et al. (66): diabetes was associated with a −1.3% lower unsaturation and +3.3% higher saturation levels. Diabetics with fractures showed the lowest marrow unsaturation and highest saturation. Therefore, the authors suggested that vertebral bone marrow fat unsaturation beyond fat fraction might have a potential for assessing the BMD-independent fracture risk.

Bone Marrow Fat in Obesity

Bone marrow fat fraction has been shown to be a negative predictor of bone microarchitecture and mechanical properties in obese men (67). BMFF has been also shown to be positively associated with ectopic and serum lipid levels in obese men and women (68) and to increase after a 6-month growth hormone administration in obese women (69).

To get further insight into the relationship between bone marrow fat and obesity, Bredella et al. performed a study in 47 pre-menopausal women (70). The authors measured IGF-1 and growth hormone blood levels, and performed MRS at L4 and MDCT scans at the level of L4 for VAT determination. The vertebral BMFF was positively associated with VAT and inversely associated with IGF-1. The authors concluded that visceral fat might have detrimental effects on bone health, which may be mediated in part by IGF-1 as an important regulator of the fat and bone lineage. Wongdee et al. concluded in a recent review that obesity and insulin resistance because of hyperglycemia in T2DM may induce osteoblast and osteoclast dysfunction with a resulting lower bone turnover (71). However, the underlying cellular and molecular mechanisms of insulin resistance in osteoblasts, osteoclasts, and osteocytes remain unknown and require further investigation.

Cordes et al. examined a group of twenty obese women who underwent a 4 week calorie restriction of 800 kcal/day (72). They performed MRS of the bone marrow and liver. Furthermore, they determined blood fat values and acquired two-point Dixon images of the abdomen to measure SAT and VAT. Despite a significant reduction of the body mass index (BMI), SAT, VAT, triglycerides, and LDL (low density lipoproteins)-cholesterol, they observed no significant reduction of the vertebral BMFF. However, absolute BMFF changes were positively associated with SAT volume ($r = 0.489$) and negatively associated with non-adipose tissue volume ($r = -0.493$) before dietary intervention (67).

Schafer et al. examined the changes of the BMFF and bone mass after gastric bypass surgery (22). They included eleven women (six diabetic, five non-diabetic) who underwent bariatric surgery (Roux-y-gastric-bypass) and underwent L3/L4 MRS, anthropometric measurements, whole body fat, and BMD measurements. VAT was determined on a single slice at the level of L4 using MDCT. In consistency with previous studies, they reported a positive correlation between age and bone marrow fat content. Interestingly, mean bone marrow fat decreased (−7.5%, $p = 0.05$) in the diabetic subjects, while the non-diabetic women showed only a small change (+0.9%, $p = 0.84$). Despite the small sample size, this study highlighted that bone marrow fat behaves differently compared to other fat depots in patients without diabetes after gastric bypass surgery.

CONCLUSION AND PERSPECTIVES

In summary, MR-based assessment of bone marrow fat provides interesting insights into the pathophysiology of osteoporosis, T2DM, and obesity as well as the association of bone and metabolic disturbances. Currently available MR methods including MRS and water–fat imaging enable the non-invasive extraction of the BMFF and unsaturation. Very little is known about the underlying mechanisms. Furthermore, new research questions are evolving on the role of bone marrow adipocytes in bone remodeling, hematopoietic stem cell differentiation, and whole body homeostasis (73, 74), on novel non-invasive MR biomarkers specific to the distribution, composition, microstructure, and function of bone marrow adipocytes requiring further investigations.

AUTHOR CONTRIBUTIONS

Collection of literature: CC, TB, and DK. Development of technical parts: MD, SR, MND, and DK. Development of clinical parts: CC, TB, HH, JK, and DK. Manuscript preparation/revision: CC, TB, MD, SR, MND, HH, JK, and DK.

FUNDING

This work has received funding from Philips Healthcare (to DK), the European Research Council (ERC) under the European Union's Horizon 2020 research and innovation programme [grant agreement No 677661, ProFatMRI (to DK)] and the Deutsche Forschungsgemeinschaft [DFG BA 4085/2-1 (to JK) and BA 4906/1-1 (to TB)]. This work was supported by the German Research Foundation (DFG) and the Technical University of Munich (TUM) in the framework of the Open Access Publishing Program.

REFERENCES

1. Kanis JA. Assessment of fracture risk and its application to screening for postmenopausal osteoporosis: synopsis of a WHO report. *Osteoporos Int* (1994) 4:368–81. doi:10.1007/BF01622200
2. NIH Consensus. Development panel on osteoporosis prevention, diagnosis, and therapy, March 7-29 2000: highlights of the conference. *South Med J* (2001) 94(6):569–73. doi:10.1097/00007611-200106000-00005
3. Barcenilla-Wong AL, Chen JS, Cross MJ, March LM. The impact of fracture incidence on health related quality of life among community-based postmenopausal women. *J Osteoporos* (2015) 2015:717914. doi:10.1155/2015/717914
4. Bleibler F, Rapp K, Jaensch A, Becker C, König H-H. Expected lifetime numbers and costs of fractures in postmenopausal women with and without osteoporosis in Germany: a discrete event simulation model. *BMC Health Serv Res* (2014) 14:284. doi:10.1186/1472-6963-14-284
5. Ammann P, Rizzoli R. Bone strength and its determinants. *Osteoporos Int* (2003) 14(Suppl 3):S13–8. doi:10.1007/s00198-002-1345-4
6. Schuit S, van der Klift M, Weel AE, de Laet CE, Burger H, Seeman E, et al. Fracture incidence and association with bone mineral density in elderly men and women: the Rotterdam study. *Bone* (2004) 34:195–202. doi:10.1016/j.bone.2003.10.001
7. Baum T, Karampinos DC, Liebl H, Rummeny EJ, Waldt S, Bauer JS. High-resolution bone imaging for osteoporosis diagnostics and therapy monitoring using clinical MDCT and MRI. *Curr Med Chem* (2013) 20(38):4844–52. doi:10.2174/09298673113206660279
8. Krug R, Burghardt AJ, Majumdar S, Link TM. High-resolution imaging techniques for the assessment of osteoporosis. *Radiol Clin North Am* (2010) 48(3):601–21. doi:10.1016/j.rcl.2010.02.015
9. Wehrli FW, Song HK, Saha PK, Wright AC. Quantitative MRI for the assessment of bone structure and function. *NMR Biomed* (2006) 19(7):731–64. doi:10.1002/nbm.1066
10. Devlin MJ, Rosen CJ. The bone-fat interface: basic and clinical implications of marrow adiposity. *Lancet Diabetes Endocrinol* (2015) 3(2):141–7. doi:10.1016/S2213-8587(14)70007-5
11. Fazeli PK, Horowitz MC, MacDougald OA, Scheller EL, Rodeheffer MS, Rosen CJ, et al. Marrow fat and bone – new perspectives. *J Clin Endocrinol Metab* (2013) 98(3):935–45. doi:10.1210/jc.2012-3634
12. Paccou J, Hardouin P, Cotten A, Penel G, Cortet B. The role of bone marrow fat in skeletal health: usefulness and perspectives for clinicians. *J Clin Endocrinol Metab* (2015) 100(10):3613–21. doi:10.1210/jc.2015-2338
13. Rosen CR, Bouxsein ML. Mechanisms of disease: is osteoporosis the obesity of bone? *Nature* (2006) 2:35–43. doi:10.1038/ncprheum0070
14. Schwartz AV. Marrow fat and bone: review of clinical findings. *Front Endocrinol* (2015) 6:40. doi:10.3389/fendo.2015.00040
15. Zhao LJ, Jiang H, Papasian CJ, Maulik D, Drees B, Hamilton J, et al. Correlation of obesity and osteoporosis: effect of fat mass on the determination of osteoporosis. *J Bone Miner Res* (2008) 23(1):17–29. doi:10.1359/jbmr.070813
16. Baum T, Yap SP, Karampinos DC, Nardo L, Kuo D, Burghardt AJ, et al. Does vertebral bone marrow fat content correlate with abdominal adipose tissue, lumbar spine bone mineral density, and blood biomarkers in women with type 2 diabetes mellitus? *J Magn Reson Imaging* (2012) 35(1):117–24. doi:10.1002/jmri.22757
17. Cohen A, Shen W, Dempster DW, Zhou H, Recker RR, Lappe JM, et al. Marrow adiposity assessed on transiliac crest biopsy samples correlates with noninvasive measurement of marrow adiposity by proton magnetic resonance spectroscopy (1H-MRS) at the spine but not the femur. *Osteoporos Int* (2015) 26(10):2471–8. doi:10.1007/s00198-015-3161-7
18. Di Iorgi N, Rosol M, Mittelman SD, Gilsanz V. Reciprocal relation between marrow adiposity and the amount of bone in the axial and appendicular skeleton of young adults. *J Clin Endocrinol Metab* (2008) 93(6):2281–6. doi:10.1210/jc.2007-2691
19. Griffith JF, Yeung DK, Antonio GE, Lee FK, Hong AW, Wong SY, et al. Vertebral bone mineral density, marrow perfusion, and fat content in healthy men and men with osteoporosis: dynamic contrast-enhanced MR imaging and MR spectroscopy. *Radiology* (2005) 236(3):945–51. doi:10.1148/radiol.2363041425
20. Griffith JF, Yeung DK, Antonio GE, Wong SY, Kwok TC, Woo J, et al. Vertebral marrow fat content and diffusion and perfusion indexes in women with varying bone density: MR evaluation. *Radiology* (2006) 241(3):831–8. doi:10.1148/radiol.2413051858
21. Karampinos DC, Ruschke S, Gordijenko O, Grande Garcia E, Kooijman H, Burgkart R, et al. Association of MRS-based vertebral bone marrow fat fraction with bone strength in a human in vitro model. *J Osteoporos* (2015) 2015:152349. doi:10.1155/2015/152349
22. Schafer AL, Li X, Schwartz AV, Tufts LS, Wheeler AL, Grunfeld C, et al. Changes in vertebral bone marrow fat and bone mass after gastric bypass surgery: a pilot study. *Bone* (2015) 74:140–5. doi:10.1016/j.bone.2015.01.010
23. Schellinger D, Lin CS, Lim J, Hatipoglu HG, Pezzullo JC, Singer AJ. Bone marrow fat and bone mineral density on proton MR spectroscopy and dual-energy X-ray absorptiometry: their ratio as a new indicator of bone weakening. *AJR Am J Roentgenol* (2004) 183(6):1761–5. doi:10.2214/ajr.183.6.01831761
24. Schwartz AV, Sigurdsson S, Hue TF, Lang TF, Harris TB, Rosen CJ, et al. Vertebral bone marrow fat associated with lower trabecular BMD and prevalent vertebral fracture in older adults. *J Clin Endocrinol Metab* (2013) 98(6):2294–300. doi:10.1210/jc.2012-3949
25. Shen W, Scherzer R, Gantz M, Chen J, Punyanitya M, Lewis CE, et al. Relationship between MRI-measured bone marrow adipose tissue and hip and spine bone mineral density in African-American and Caucasian participants: the CARDIA study. *J Clin Endocrinol Metab* (2012) 97(4):1337–46. doi:10.1210/jc.2011-2605
26. Yeung DK, Griffith JF, Antonio GE, Lee FK, Woo J, Leung PC. Osteoporosis is associated with increased marrow fat content and decreased marrow fat unsaturation: a proton MR spectroscopy study. *J Magn Reson Imaging* (2005) 22(2):279–85. doi:10.1002/jmri.20367
27. Scheller EL, Rosen CJ. What's the matter with MAT? Marrow adipose tissue, metabolism, and skeletal health. *Ann N Y Acad Sci* (2014) 1311:14–30. doi:10.1111/nyas.12327
28. Compston JE, Flahive J, Hooven FH, Anderson FA Jr, Adachi JD, Boonen S, et al. Obesity, health-care utilization, and health-related quality of life after fracture in postmenopausal women: global longitudinal study of osteoporosis in women (GLOW). *Calcif Tissue Int* (2014) 94(2):223–31. doi:10.1007/s00223-013-9801-z
29. Melton LJ III, Leibson CL, Achenbach SJ, Therneau TM, Khosla S. Fracture risk in type 2 diabetes: update of a population-based study. *J Bone Miner Res* (2008) 23(8):1334–42. doi:10.1359/jbmr.080323
30. Napoli N, Strotmeyer ES, Ensrud KE, Sellmeyer DE, Bauer DC, Hoffman AR, et al. Fracture risk in diabetic elderly men: the MrOS study. *Diabetologia* (2014) 57(10):2057–65. doi:10.1007/s00125-014-3289-6
31. Schwartz AV, Sellmeyer DE, Ensrud KE, Cauley JA, Tabor HK, Schreiner PJ. Older women with diabetes have an increased risk of fracture: a prospective study. *J Clin Endocrinol Metab* (2001) 86(1):32–8. doi:10.1210/jcem.86.1.7139
32. Vestergaard P, Rejnmark L, Mosekilde L. Relative fracture risk in patients with diabetes mellitus, and the impact of insulin and oral antidiabetic medication on relative fracture risk. *Diabetologia* (2005) 48(7):1292–9. doi:10.1007/s00125-005-1786-3
33. Duque G. Bone and fat connection in aging bone. *Curr Opin Rheumatol* (2008) 20(4):429–34. doi:10.1097/BOR.0b013e3283025e9c
34. Bredella MA, Daley SM, Kalra MK, Brown JK, Miller KK, Torriani M. Marrow adipose tissue quantification of the lumbar spine by using dual-energy ct and single-voxel (1)H MR spectroscopy: a feasibility study. *Radiology* (2015) 277(1):230–5. doi:10.1148/radiol.2015142876
35. Hu HH, Kan HE. Quantitative proton MR techniques for measuring fat. *NMR Biomed* (2013) 26(12):1609–29. doi:10.1002/nbm.3025
36. Li X, Kuo D, Schafer AL, Porzig A, Link TM, Black D, et al. Quantification of vertebral bone marrow fat content using 3 tesla MR spectroscopy: reproducibility, vertebral variation, and applications in osteoporosis. *J Magn Reson Imaging* (2011) 33(4):974–9. doi:10.1002/jmri.22489
37. Bandirali M, Di Leo G, Papini GD, Messina C, Sconfienza LM, Ulivieri FM, et al. A new diagnostic score to detect osteoporosis in patients undergoing lumbar spine MRI. *Eur Radiol* (2015) 25(10):2951–9. doi:10.1007/s00330-015-3699-y
38. Shen W, Gong X, Weiss J, Jin Y. Comparison among T1-weighted magnetic resonance imaging, modified dixon method, and magnetic resonance spectroscopy in measuring bone marrow fat. *J Obes* (2013) 2013:298675. doi:10.1155/2013/298675
39. Griffith JF, Yeung DK, Chow SK, Leung JC, Leung PC. Reproducibility of MR perfusion and (1)H spectroscopy of bone marrow. *J Magn Reson Imaging* (2009) 29(6):1438–42. doi:10.1002/jmri.21765

40. Singhal V, Miller KK, Torriani M, Bredella MA. Short- and long-term reproducibility of marrow adipose tissue quantification by 1H-MR spectroscopy. *Skeletal Radiol* (2016) 45(2):221–5. doi:10.1007/s00256-015-2292-4
41. Dieckmeyer M, Ruschke S, Cordes C, Yap SP, Kooijman H, Hauner H, et al. The need for T(2) correction on MRS-based vertebral bone marrow fat quantification: implications for bone marrow fat fraction age dependence. *NMR Biomed* (2015) 28(4):432–9. doi:10.1002/nbm.3267
42. Karampinos DC, Melkus G, Baum T, Bauer JS, Rummeny EJ, Krug R. Bone marrow fat quantification in the presence of trabecular bone: initial comparison between water-fat imaging and single-voxel MRS. *Magn Reson Med* (2014) 71(3):1158–65. doi:10.1002/mrm.24775
43. Hamilton G, Yokoo T, Bydder M, Cruite I, Schroeder ME, Sirlin CB, et al. In vivo characterization of the liver fat (1)H MR spectrum. *NMR Biomed* (2011) 24(7):784–90. doi:10.1002/nbm.1622
44. Bingolbali A, Fallone BG, Yahya A. Comparison of optimized long echo time STEAM and PRESS proton MR spectroscopy of lipid olefinic protons at 3 tesla. *J Magn Reson Imaging* (2015) 41(2):481–6. doi:10.1002/jmri.24532
45. Ruschke S, Kienberger H, Baum T, Kooijman H, Settles M, Haase A, et al. Diffusion-weighted stimulated echo acquisition mode (DW-STEAM) MR spectroscopy to measure fat unsaturation in regions with low proton-density fat fraction. *Magn Reson Med* (2016) 75(1):32–41. doi:10.1002/mrm.25578
46. Ruschke S, Dieckmeyer M, Kooijman H, Haase A, Rummeny EJ, Bauer JS, et al., editors. Separating water and olefinic fat peaks using diffusion-weighted MRS and diffusion constraint fitting to measure vertebral bone marrow fat unsaturation. *Proc ISMRM* (Toronto) (2015). 618 p.
47. Bydder M, Yokoo T, Hamilton G, Middleton MS, Chavez AD, Schwimmer JB, et al. Relaxation effects in the quantification of fat using gradient echo imaging. *Magn Reson Imaging* (2008) 26(3):347–59. doi:10.1016/j.mri.2007.08.012
48. Yu H, Shimakawa A, McKenzie CA, Brodsky E, Brittain JH, Reeder SB. Multiecho water-fat separation and simultaneous R_2* estimation with multifrequency fat spectrum modeling. *Magn Reson Med* (2008) 60(5):1122–34. doi:10.1002/mrm.21737
49. Karampinos DC, Yu H, Shimakawa A, Link TM, Majumdar S. T1-corrected fat quantification using chemical shift-based water/fat separation: application to skeletal muscle. *Magn Reson Med* (2011) 66:1312–26. doi:10.1002/mrm.22925
50. Liu CY, McKenzie CA, Yu H, Brittain JH, Reeder SB. Fat quantification with IDEAL gradient echo imaging: correction of bias from T_1 and noise. *Magn Reson Med* (2007) 58(2):354–64. doi:10.1002/mrm.21301
51. Yu H, McKenzie CA, Shimakawa A, Vu AT, Brau AC, Beatty PJ, et al. Multiecho reconstruction for simultaneous water-fat decomposition and T_2* estimation. *J Magn Reson Imaging* (2007) 26(4):1153–61. doi:10.1002/jmri.21090
52. Karampinos DC, Ruschke S, Dieckmeyer M, Eggers H, Kooijman H, Rummeny EJ, et al. Modeling of T2* decay in vertebral bone marrow fat quantification. *NMR Biomed* (2015) 28(11):1535–42. doi:10.1002/nbm.3420
53. Gee CS, Nguyen JT, Marquez CJ, Heunis J, Lai A, Wyatt C, et al. Validation of bone marrow fat quantification in the presence of trabecular bone using MRI. *J Magn Reson Imaging* (2015) 42(2):539–44. doi:10.1002/jmri.24795
54. Arentsen L, Yagi M, Takahashi Y, Bolan PJ, White M, Yee D, et al. Validation of marrow fat assessment using noninvasive imaging with histologic examination of human bone samples. *Bone* (2015) 72:118–22. doi:10.1016/j.bone.2014.11.002
55. MacEwan IJ, Glembotski NE, D'Lima D, Bae W, Masuda K, Rashidi HH, et al. Proton density water fraction as a biomarker of bone marrow cellularity: validation in ex vivo spine specimens. *Magn Reson Imaging* (2014) 32(9):1097–101. doi:10.1016/j.mri.2014.03.005
56. Baum T, Yap SP, Dieckmeyer M, Ruschke S, Eggers H, Kooijman H, et al. Assessment of whole spine vertebral bone marrow fat using chemical shift-encoding based water-fat MRI. *J Magn Reson Imaging* (2015) 42(4):1018–23. doi:10.1002/jmri.24854
57. Kuhn JP, Hernando D, Meffert PJ, Reeder S, Hosten N, Laqua R, et al. Proton-density fat fraction and simultaneous R2* estimation as an MRI tool for assessment of osteoporosis. *Eur Radiol* (2013) 23(12):3432–9. doi:10.1007/s00330-013-2950-7
58. Li GW, Xu Z, Chen QW, Tian YN, Wang XY, Zhou L, et al. Quantitative evaluation of vertebral marrow adipose tissue in postmenopausal female using MRI chemical shift-based water-fat separation. *Clin Radiol* (2014) 69(3):254–62. doi:10.1016/j.crad.2013.10.005
59. Martin J, Nicholson G, Cowin G, Ilente C, Wong W, Kennedy D. Rapid determination of vertebral fat fraction over a large range of vertebral bodies. *J Med Imaging Radiat Oncol* (2014) 58(2):155–63. doi:10.1111/1754-9485.12143
60. Ojanen X, Borra RJ, Havu M, Cheng SM, Parkkola R, Nuutila P, et al. Comparison of vertebral bone marrow fat assessed by 1H MRS and inphase and out-of-phase MRI among family members. *Osteoporos Int* (2014) 25(2):653–62. doi:10.1007/s00198-013-2472-9
61. Griffith JF, Yeung DK, Ma HT, Leung JC, Kwok TC, Leung PC. Bone marrow fat content in the elderly: a reversal of sex difference seen in younger subjects. *J Magn Reson Imaging* (2012) 36(1):225–30. doi:10.1002/jmri.23619
62. Ishijima H, Ishizaka H, Horikoshi H, Sakurai M. Water fraction of lumbar vertebral bone marrow estimated from chemical shift misregistration on MR imaging: normal variations with age and sex. *AJR Am J Roentgenol* (1996) 167(2):355–8. doi:10.2214/ajr.167.2.8686603
63. Kugel H, Jung C, Schulte O, Heindel W. Age- and sex-specific differences in the 1H-spectrum of vertebral bone marrow. *J Magn Reson Imaging* (2001) 13(2):263–8. doi:10.1002/1522-2586(200102)13:2<263::AID-JMRI1038>3.3.CO;2-D
64. Huovinen V, Viljakainen H, Hakkarainen A, Saukkonen T, Toiviainen-Salo S, Lundbom N, et al. Bone marrow fat unsaturation in young adults is not affected by present or childhood obesity, but increases with age: a pilot study. *Metabolism* (2015) 64(11):1574–81. doi:10.1016/j.metabol.2015.08.014
65. Baum T, Cordes C, Dieckmeyer M, Ruschke S, Franz D, Hauner H, et al. Assessment of whole spine vertebral bone marrow fat using chemical shift-encoding based water-fat MRI. *J Magn Reson Imaging* (2015) 42(4):1018–23. doi:10.1002/jmri.24854
66. Patsch JM, Li X, Baum T, Yap SP, Karampinos DC, Schwartz AV, et al. Bone marrow fat composition as a novel imaging biomarker in postmenopausal women with prevalent fragility fractures. *J Bone Miner Res* (2013) 28(8):1721–8. doi:10.1002/jbmr.1950
67. Bredella MA, Lin E, Gerweck AV, Landa MG, Thomas BJ, Torriani M, et al. Determinants of bone microarchitecture and mechanical properties in obese men. *J Clin Endocrinol Metab* (2012) 97(11):4115–22. doi:10.1210/jc.2012-2246
68. Bredella MA, Gill CM, Gerweck AV, Landa MG, Kumar V, Daley SM, et al. Ectopic and serum lipid levels are positively associated with bone marrow fat in obesity. *Radiology* (2013) 269(2):534–41. doi:10.1148/radiol.13130375
69. Bredella MA, Gerweck AV, Barber LA, Breggia A, Rosen CJ, Torriani M, et al. Effects of growth hormone administration for 6 months on bone turnover and bone marrow fat in obese premenopausal women. *Bone* (2014) 62:29–35. doi:10.1016/j.bone.2014.01.022
70. Bredella MA, Torriani M, Ghomi RH, Thomas BJ, Brick DJ, Gerweck AV, et al. Vertebral bone marrow fat is positively associated with visceral fat and inversely associated with IGF-1 in obese women. *Obesity (Silver Spring)* (2011) 19(1):49–53. doi:10.1038/oby.2010.106
71. Wongdee K, Charoenphandhu N. Update on type 2 diabetes-related osteoporosis. *World J Diabetes* (2015) 6(5):673–8. doi:10.4239/wjd.v6.i5.673
72. Cordes C, Dieckmeyer M, Ott B, Shen J, Ruschke S, Settles M, et al. MR-detected changes in liver fat, abdominal fat, and vertebral bone marrow fat after a four-week calorie restriction in obese women. *J Magn Reson Imaging* (2015) 42(5):1272–80. doi:10.1002/jmri.24908
73. Hardouin P, Marie PJ, Rosen CJ. New insights into bone marrow adipocytes: report from the first European meeting on bone marrow adiposity (BMA 2015). *Bone* (2015). doi:10.1016/j.bone.2015.11.013
74. Scheller EL, Doucette CR, Learman BS, Cawthorn WP, Khandaker S, Schell B, et al. Region-specific variation in the properties of skeletal adipocytes reveals regulated and constitutive marrow adipose tissues. *Nat Commun* (2015) 6:7808. doi:10.1038/ncomms8808

Conflict of Interest Statement: DK receives Grant Support from Phillips Healthcare. The remaining authors declare that the research was conducted in the absence of any commercial or financial relationships that could be construed as a potential conflict of interest.

frontiers in Endocrinology

REVIEW
published: 21 September 2016
doi: 10.3389/fendo.2016.00127

The Bone Marrow-Derived Stromal Cells: Commitment and Regulation of Adipogenesis

Michaela Tencerova[1,2]* *and Moustapha Kassem*[1,2,3]

[1] Department of Molecular Endocrinology, Odense University Hospital, University of Southern Denmark, Odense, Denmark, [2] Danish Diabetes Academy, Novo Nordisk Foundation, Odense, Denmark, [3] Stem Cell Unit, Department of Anatomy, Faculty of Medicine, King Saud University, Riyadh, Saudi Arabia

Bone marrow (BM) microenvironment represents an important compartment of bone that regulates bone homeostasis and the balance between bone formation and bone resorption depending on the physiological needs of the organism. Abnormalities of BM microenvironmental dynamics can lead to metabolic bone diseases. BM stromal cells (also known as skeletal or mesenchymal stem cells) [bone marrow stromal stem cell (BMSC)] are multipotent stem cells located within BM stroma and give rise to osteoblasts and adipocytes. However, cellular and molecular mechanisms of BMSC lineage commitment to adipocytic lineage and regulation of BM adipocyte formation are not fully understood. In this review, we will discuss recent findings pertaining to identification and characterization of adipocyte progenitor cells in BM and the regulation of differentiation into mature adipocytes. We have also emphasized the clinical relevance of these findings.

Keywords: bone marrow stem cells, adipogenesis, secreted factors, bone marrow microenvironment, bone marrow stem cell subpopulations

OPEN ACCESS

Edited by:
William Peter Cawthorn, University of Edinburgh, UK

Reviewed by:
Jan Tuckermann, University of Ulm, Germany
Luca Vanella, University of Catania, Italy

***Correspondence:**
Michaela Tencerova
mtencerova@health.sdu.dk

Specialty section:
This article was submitted to Bone Research, a section of the journal Frontiers in Endocrinology

Received: *04 May 2016*
Accepted: *05 September 2016*
Published: *21 September 2016*

Citation:
Tencerova M and Kassem M (2016) The Bone Marrow-Derived Stromal Cells: Commitment and Regulation of Adipogenesis. Front. Endocrinol. 7:127. doi: 10.3389/fendo.2016.00127

INTRODUCTION

Bone marrow (BM) is an important compartment of bone, which regulates bone homeostasis. BM can also be perceived as an immune organ as it contains many different cell types secreting a large number of cytokines and immune modulatory factors. Finally, BM is a metabolic organ and has recently been demonstrated to regulate a whole body energy metabolism (1, 2).

The cellular composition of BM is complex as it contains hematopoietic stem cells giving rise to myeloid lineage including osteoclasts and lymphoid lineage giving rise to immune cells. It also contains a stroma compartment containing bone marrow stromal stem cells (BMSC) (also known as skeletal or mesenchymal stem cells) and their differentiated progeny of adipocytes and osteoblasts as well as endothelial cells, pericytes and neuronal cells. The cellular composition of BM changes with age, gender, and metabolic status (3, 4).

Bone turnover/remodeling is very dynamic and energetically demanding process that consists of two main phases: bone formation mediated by osteoblasts recruited from BMSC and bone resorption mediated by osteoclasts recruited from hematopoietic progenitors. Bone resorption and bone formation are *coupled* in time and space and there is a balance between the amount of bone resorbed by osteoclasts and the amount of bone formed by osteoblasts. These processes of *coupling and balance* are tightly regulated via several factors present in BM microenvironment and also via sympathetic central nervous system (2) (**Figure 1**). Imbalance between bone resorption and bone formation leads to metabolic bone diseases, including age-related bone loss and osteoporosis.

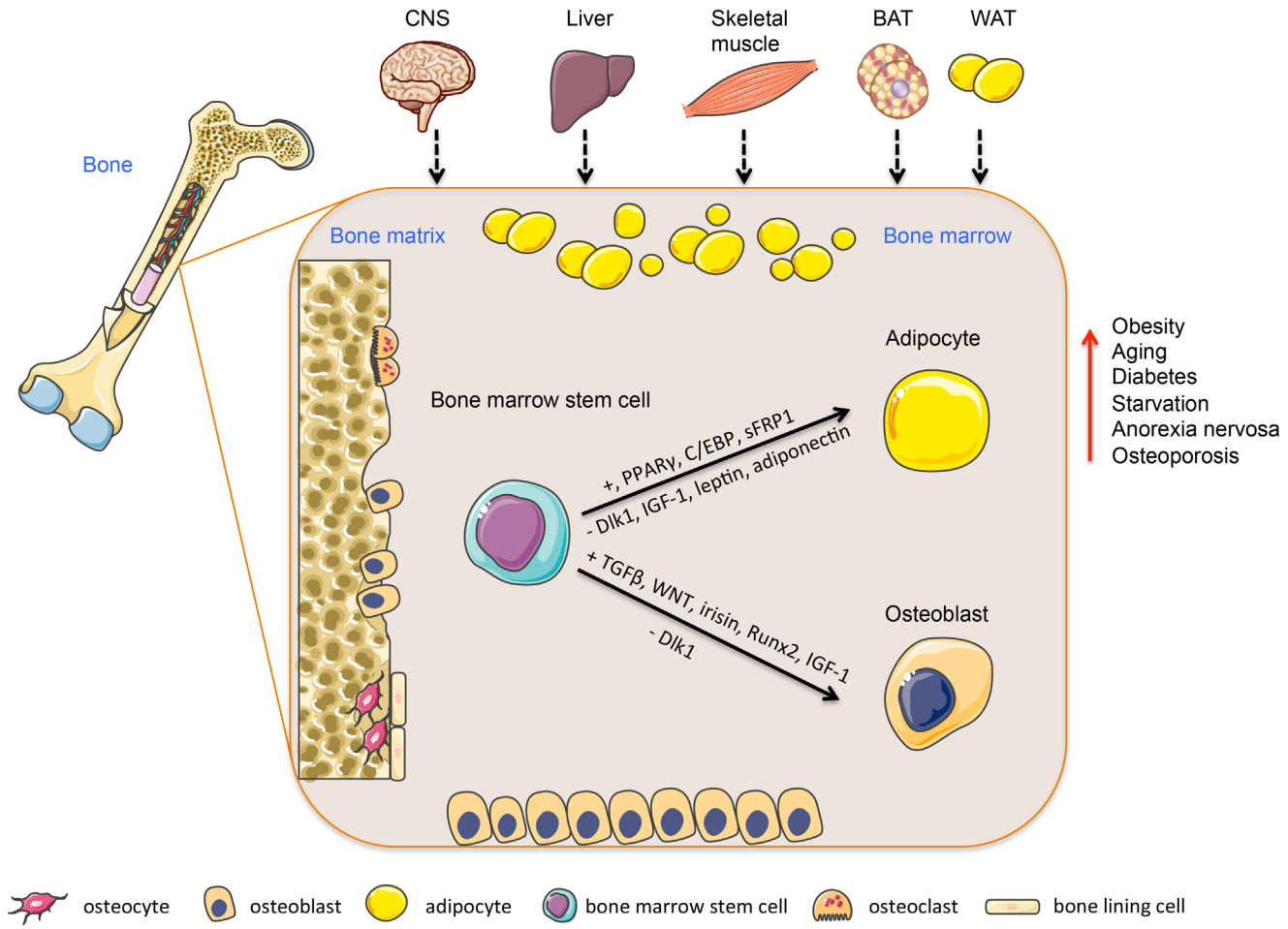

FIGURE 1 | Regulation of bone marrow stem cells differentiation into adipocytes or osteoblasts. Bone marrow is a heterogeneous organ, which consists of different cell types participating in bone homeostasis. Among them, most abundant are hematopoietic stem cells (bone resorptive osteoclasts) and mesenchymal stem cells giving rise into bone forming osteoblasts or adipocytes. This process is regulated via several transcription factors and secreted molecules (e.g., PPARs, Wnt, adiponectin, leptin), which are produced locally or released from peripheral tissues, including BAT, WAT, skeletal muscle, liver, or CNS and affecting bone marrow niche through circulation. This multiorgan crosstalk between bone and peripheral tissues plays an important role in the regulation of bone and energy metabolism. Abbreviations: CNS, central nervous system; BAT, brown adipose tissue; WAT, white adipose tissue. Adapted from SERVIER Medical Art; http://www.servier.com/Powerpoint-image-bank

During the recent years, there has been an increasing interest in understanding the biology of BM adipocyte for a number of reasons. First, it is an abundant cell type in adult BM (5). Second, an increased BM adipose tissue mass has been reported in the conditions of low bone mass, suggesting an abnormal differentiation of BMSC as a possible pathogenetic mechanism to be investigated. Finally, the biological role of BM adipocytes and their differences and similarities with extramedullary adipocytes are not known and may be relevant to bone tissue homeostasis.

In this review, we will present an overview of the BM adipocyte differentiation and its regulation by a number of factors. We will also outline a number of specific signaling pathways that regulate BMSC lineage commitment to adipocytes versus osteoblasts and that can be targeted to enhance bone formation and increase bone mass.

FROM BONE MARROW STEM CELLS TO COMMITTED ADIPOCYTIC CELLS IN THE BONE MARROW

In vitro, BMSC are plastic-adherent cells, present within BM stroma and capable of clonal expansion and differentiation to osteoblasts and adipocytes. Currently, human BM adipocytes are thought to differentiate from BMSC as evidenced by a large body of both *in vitro* and *in vivo* studies (5). In mice, recent lineage tracing studies employing genetically modified mice, provided evidence for the common stem cell hypothesis for the presence of a common stem cells for osteoblastic and adipocytic cells (6, 7). **Table 1** summaries the main characteristics of recently reported BMSC and progenitor cells identified and characterized based on lineage tracing studies employing expression of a number of markers.

TABLE 1 | List of different skeletal progenitor cells in the bone marrow identified by specific cell surface markers and mediators.

Marker	Function	Differentiation potential	Reference
Nestin	A type VI intermediate filament protein	HSC maintenance	(8)
Gremlin	Inhibitor of BMP in TGF beta signaling pathway	Osteoblast, chondrocyte, reticular cell	(9)
RANKL	Receptor activator of NFκB ligand	Adipocyte	(10)
LepR	Leptin receptor	Adipocyte	(11)
Sox9	Transcription factor	Chondrocyte	(12)
Col2	Type II collagen	Chondrocyte	(13)
CD146	Cell adhesion molecule	Osteoblast	(14)
CD34	Cell adhesion molecule	Osteoblast	(15)

Single cell clonal analysis of cultured BM stromal cells revealed, in addition to BMSC, the presence of independent committed precursors for osteoblasts and adipocytes. Our study of Post et al. demonstrated the existence of these precursors within the murine BM stroma (16). Based on clonal selection, we were able to isolate and characterize the phenotype of two different precursor cell lines isolated from BM of 2- to 3-month-old mice: one cell line is committed to adipocyte differentiation and termed ^{adipo}MSC and another one committed to osteoblast and chondrocyte differentiation and termed ^{bone}MSC. The two cell lines exhibit distinct morphology and molecular signature. Based on the differentiation marker expression between these two cell lines, we have recently reported that CD34 is differentially expressed in ^{bone}MSC and not in ^{adipo}MSC and that it can be used to prospective isolation of osteoblastic committed BMSC (15). Examples of studies using lineage tracing to identify committed precursor cells include the study of Yue et al. (11) that employed leptin receptor (LepR) to identify precursor cells with adipocyte differentiation potential. Mice with conditionally deleted LepR in limb bones enhanced osteogenesis and improved fracture healing (11). Another example is the study of Holt et al. (10) that demonstrated the presence of RANKL + preadipocytes in aged mice BM that support osteoclastogenesis. Similar findings have been confirmed in human BM (10, 17). Interestingly, some lineage tracing studies show heterogeneity of BMSC populations with respect to their differentiation potential. Gremlin 1 (Grem1) is a secreted BMP inhibitor and involved in the regulation of adipogenesis in peripheral adipose acting via PPARγ (18). Recent study of Worthley et al. identified Gremlin 1 positive precursor cells that can differentiate into osteoblasts, chondrocytes, and reticular cells, but not to adipocytes (9). All these studies demonstrate the presence of complex cellular heterogeneity within the BM microenvironment and the presence of different committed BMSC subpopulations with a different differentiation potential, whose functions in the BM can be modulated independently during aging and metabolic diseases. It is also possible that these precursor cells number and functions are modulated by physiological conditions and energy demand. Since most of the above-mentioned studies were performed in mice, it is important to define the relevance of these findings to normal human physiology.

TABLE 2 | Cellular and molecular characteristics of bone marrow and extramedullary adipocytes.

Parameters	Bone marrow adipocytes	Extramedullary adipocytes	Reference
Adipocyte size	+	++	(24)
Content of free fatty acids	+	++	(28)
Cytokine expression	↑	↓	(31)
Adipokine expression	↓	↑	(27)
Stem cell markers expression	↓	↑	(26)
Immunomodulatory properties	↑	↓	(31)

BONE MARROW ADIPOCYTES VERSUS EXTRAMEDULLARY ADIPOCYTES

Biological differences between BM medullary adipocytes and extramedullary adipocytes are not completely delineated. Several investigators have reported similarities between stromal cells isolated from the BM and subcutaneous stromal cells with respect to molecular phenotype and adipocyte differentiation capacity (19–22). However, significant differences have been observed in their responsiveness to adipocyte differentiation signals, as subcutaneous adipose tissue-derived stem cells (ASC) are better to differentiate to adipocytes compared to BMSC. BM and extramedullary adipocytes are different in cell size, expression of stem cell markers (e.g., Sox2, Nanog, Klf4), presence of extracellular matrix, free fatty acid content, proportion of immune cells in contact with adipocytes, levels of cytokine, and adipokine expression (23–28). Also BMSC have higher expression of inflammatory genes compared to ASC (29). Interestingly, the molecular signature analysis reveals that stromal cells from different tissue compartment are imprinted by their tissue of origin and ASC are enriched in adipogenesis-associated genes compared to MSC from other tissue compartments (19, 30–35). Other differences on cellular and molecular level have been reported (see listed in **Table 2**).

A recent paper of Liaw et al. has reported significant differences in lipid composition among different adipocytic cell lines derived from a variety of sources, including white and brown adipose tissue in mice and in adipocytes differentiated from 3T3-L1 cell line and ear mesenchymal cells (36). Unfortunately, the authors did not include BM adipocytes in their studies. This data highlight the differences in lipid metabolism in different adipocyte compartments, which may be mediated by exposure to different bioactive molecules in their microenvironment.

BONE MARROW STROMAL STEM CELL COMMITMENT TO ADIPOCYTIC LINEAGE AND REGULATORY FACTORS

Bone marrow stromal stem cell commitment to adipocytic lineage is a complex process, which is tightly controlled via several positive and negative regulatory factors activated possibly in a

TABLE 3 | List of selected regulatory factors for adipocyte differentiation in bone marrow and adipose-derived stem cells.

Gene name	Gene symbol	Category	Bone marrow-derived stem cells (BMSC)	Adipose-derived stem cells (ASC)	Reference
Peroxisome proliferated-activated receptor γ	PPARγ	Transcription factor	↑	↑	(37, 38)
CAAT enhancer binding protein	C/EBPα/β	Transcription factor	↑↓	↑	(37–39)
Adiponectin	Adipoq	Soluble mediator	↓	↓	(40–42)
Leptin	Lep	Soluble mediator	↓	↓	(43–45)
Secreted frizzled-related protein 1	sFRP1	Soluble mediator	↑	↑	(46, 47)
Delta like-1/preadipocyte factor 1	Dlk1/Pref-1	Soluble mediator	↓	↓	(48)
Low-density lipoprotein receptor-related protein 5	LRP5	Soluble mediator	↓	↑	(49–51)
Bone morphogenic proteins	BMPs (2,4,7)	Soluble mediator	↓↑ (depends on concentration and differentiation cocktail)	↑ (white and beige)	(52–54)
Insulin growth-like factor 1	IGF-1	Soluble mediator	↓	↑	(55, 56)
Irisin, fibronectin type III domain-containing 5	Fndc5	Soluble mediator	↓	↑ (beige)	(57–59)
Fibroblast growth factor 21	FGF-21	Soluble mediator	↑	↑	(60, 61)
Transforming growth factor beta	TGFβ	Soluble mediator	↓	↓	(62, 63)
Interleukin 1	IL1	Soluble mediator	↓	↓	(62)
Interleukin 6	IL6	Soluble mediator	↓	↓	(62)
Tumor necrosis factor α	TNFα	Soluble mediator	↓	↓	(62)
Heme-oxygenase 1	HO-1	Soluble mediator	↓	↓	(64, 65)

sequential cascade. These factors include steroid hormones, secreted cytokines/adipokines, and transcription factors. Most of these signaling molecules are known for their regulation of adipogenesis in bona fide ASC. **Table 3** summarizes the effects of selected regulatory factors on adipocyte differentiation in BMSC and ASC that are discussed in the following paragraphs.

The most characterized transcription factor and a key regulator of adipogenesis is peroxisome proliferated-activated receptor gamma (PPARγ) (37, 66). PPARγ belongs to a nuclear receptor superfamily, which is activated by lipophilic ligands. The activation of PPARγ is necessary and sufficient for adipocyte differentiation and also required for maintenance of differentiated state in BMSC and ASC (67–69). Inhibition of PPARγ *in vitro* impairs adipogenesis, while enhancing osteoblast differentiation in BMSC (67). In mice PPARγ deficiency leads to impaired development of adipose tissue when fed a high-fat diet (HFD) (70). PPARγ is also a target for insulin sensitizing drugs, such as thiazolidinediones in diabetes. However, their use for diabetic patients is associated with a decreased bone mass and increases a risk for fracture. The role of PPARγ activation in age-related increase of BM adipogenesis and decreased osteoblastogenesis has been discussed previously [for more information, see the reviews: Ref. (3, 38, 68, 71)].

Additional transcription factors involved in the regulation of adipogenesis are members of CAAT enhancer binding proteins (C/EBP) family: C/EBPα, C/EBPβ, C/EBPγ and C/EBPδ. Based on the studies performed in 3T3 cell line, C/EBP activation during adipocyte differentiation is synchronized in a temporal manner where early activation of C/EBPβ and C/EBPδ leads to induction of C/EBPα. In BMSC, the function and activation of individual transcription factors exhibited a different pattern (72). Moreover, it has been shown that an isoform of C/EBPβ, liver-enriched inhibitory protein (LIP), which lacks transcriptional binding domain, induces activation of Runx2 and promotes osteogenesis in BMSC (39). C/EBPs crosstalk with PPARγ and regulate each other via a feedback loop (38, 68). C/EBP deficient mice exhibited impaired adipogenesis and insulin sensitivity (73–75). Moreover, C/EBPβ-deficient mice displayed reduced bone mineral density with decreased trabecular number (76, 77). These findings confirm an important role of C/EBPs in the early stage of MSC differentiation and their commitment (78).

The PPARγ-regulated adipokines: leptin and adiponectin are primarily secreted by adipocytes and can regulate adipogenesis (79, 80). *In vitro* leptin inhibits adipogenesis and enhances osteoblastogenesis in human stromal marrow cells (43). On the other hand, leptin-deficient mice *ob/ob* and LepR-deficient *db/db* mice exhibit an increased BM adiposity and low bone mass (79). Leptin regulates bone mass negatively indirectly via sympathetic nervous system (44). Interestingly, selective inhibition of LepR in osteoblastic cells has no effects on bone mass, whereas hypothalamic deletion of LepR leads to a phenotype similar to that of *ob/ob* mice (81), suggesting that the main effects of leptin on bone are centrally mediated. In extramedullary adipocytes leptin impairs adipocyte function (e.g., insulin responsiveness and lipid metabolism) and inhibits lipogenesis (45). In addition, Aprath-Husmann et al. reported no effect of leptin on adipocyte differentiation in ASC of lean and obese subjects (82). Also, leptin levels increase with obesity and diabetes, diseases associated with bone fragility. Thus, leptin seems to exert multiple functions with direct and indirect effects on BM adipocytes and extramedullary adipocytes.

Adiponectin is an adipocyte-secreted factor with insulin sensitizing and anti-inflammatory effects. Adiponectin blocks adipocyte differentiation of BMSC and ASC suggesting an autocrine or paracrine negative feedback loop (40). *In vitro* adiponectin enhances osteoblast differentiation, increases osteoblast proliferation and maturation via cyclooxygenase 2 (Cox2)-dependent mechanism, and inhibits osteoclastogenesis (41, 83). However, *in vivo* effects on bone mass are more complex. Adiponectin regulates bone formation via opposite central and peripheral mechanisms through FoxO1 transcriptional factor. Adiponectin-deficient mice exhibit increased bone mass in young age but low bone mass during aging. This effect is explained by local inhibition of osteoblast proliferation and enhanced

osteoblast apoptosis. During aging, this effect is antagonized by adiponectin-mediated effects on hypothalamic neurons that lead to decreased sympathetic tone and, consequently, increased bone mass and decreased energy expenditure (80). Overexpression of adiponectin in adipose tissue causes impairment of adipogenesis and increased preadipocyte factor 1 (Pref-1) expression, which inhibits adipogenesis in mice (42).

In obesity and type 2 diabetes, circulating levels of leptin and adiponectin are differentially regulated (up- and down-regulated, respectively). However, their role in the regulation of BM adipogenesis has not been determined. Recently, Yue et al. demonstrated LepR signaling in BMSC promotes adipogenesis and inhibits osteoblastogenesis in response to diet (11). By contrast, activation of adiponectin receptor R1 (AdipR1) in osteoblasts results in enhanced bone formation via GSK-3β/β-Catenin signaling (84). AdipoR1 deficient mice exhibit impaired osteoblast differentiation. The study of Yu et al. highlighted the importance of adiponectin signaling in BMSC mobilization and recruitment during bone fracture repair via increased secretion of stromal cell-derived factor 1 (SDF-1) in mice (85). Cawthorn et al. recently reported increased secretion of adiponectin from BM adipocytes in caloric restriction state that can contribute to its circulating levels (86), suggesting an important endocrine role of BM adipocytes in the regulation of whole body energy metabolism. However, this observation needs further investigation.

Novel factors, which have been identified in our laboratory based on proteomic analysis of secreted factors by committed BM adipocytic cells (^{adipo}MSC) and committed BM osteoblastic cells (^{bone}MSC), are secreted frizzled-related protein 1 (sFRP1) and Delta-like 1, also known as preadipocyte factor 1 (Dlk1/Pref-1) (16).

Secreted frizzled-related protein 1 is an inhibitor of Wnt signaling that sequester Wnts from their receptors. *In vitro* it inhibits osteoblastogenesis and promotes adipogensis of BMSC by blocking the Wnt signaling (46) *In vivo* sFRP1 inhibited bone formation. Similar effects of sFRP1 have been reported in preadipocytes and primary adipose tissue-derived cells (87, 88).

Delta-like 1/preadipocyte factor 1 is a transmembrane protein, which belongs to a family of epidermal-growth-factor-like repeats containing proteins. Its extracellular domain is proteolytically cleaved by ADAM17/TACE and released as soluble factor circulating in body fluids include amniotic fluid and, hence, its name fetal antigen A (FA1) (89–91). Pref-1 is highly expressed in preadipocytes and its expression decreases during differentiation. Pref-1 overexpression in 3T3-L1 cells blocks adipogenesis (92). Pref-1 regulates adipocyte differentiation via FOXA2 (93), KLF6 (94), and KLF2 (95). Our group has reported that overexpression of Dlk1 in human BMSC inhibits adipocyte and osteoblastic differentiation (48). Interestingly, Dlk1/Pref-1 inhibited differentiation of MSC downstream of C/EBPβ during adipocytic differentiation and Cbfa1/Runx2 during osteoblastic differentiation, suggesting that Dlk1/Pref-1 maintains MSC in a progenitor state. Importantly, we showed a negative effect of soluble FA1 on bone formation in *ex vivo* neonatal calvaria organ cultures. Also transgenic mice with Dlk1 overexpression had reduced fat and bone mass (96). We have also recently reported that FA1 acts as a link between bone and whole body energy metabolism and it interacts with osteocalcin (97).

Additional negative regulators of adipocyte differentiation of BMSC include molecules in Wnt signaling pathway that consists of several ligands, receptors, co-receptors and transcriptional mediators, e.g., β-catenin, which blocks PPARγ and its down-stream-regulated genes (98, 99).

Low-density lipoprotein receptor-related protein 5 (LRP5) is a Wnt co-receptor and is involved in activation of canonical Wnt signaling (49, 50, 100). It has been shown to inhibit adipogenesis and promote osteoblastogenesis in BMSC. A gain of function mutation in Lrp5, a clinical condition known as a high-bone-mass phenotype, leads to inhibition of adipogenesis and enhances osteoblastogenesis, which is associated with increased bone mass. On the other hand, Lrp5 loss of function mutation causes severe osteoporosis in mice and humans (49, 50, 100, 101). Recent paper of Loh et al. (49) demonstrated enhanced adipogenesis in lower body fat, e.g., gluteal adipose tissue in high-bone-mass phenotype patients. This finding confirms the results of Palsgaard et al., who reported impaired adipogenesis in LRP5-deficient preadipocytes due to an interaction between LRP5 and insulin receptor (51).

Bone morphogenetic proteins (BMPs) are members of the transforming growth factor β (TGFβ) superfamily that were originally identified based on their ability to induce ectopic bone formation. BMPs have pleiotropic developmental actions, important for stem cell self-renewal and lineage commitment and differentiation (102). BMP4 promotes adipogenesis in peripheral adipose tissue progenitors by increasing transcription activity of PPARγ (18, 103). However, dependent on BMP concentration and receptor activation, they exert different lineage differentiation effects (104). Low concentrations of BMP-2 and BMP-7 induce adipocytic differentiation, whereas high concentrations promote differentiation toward chondrocytes and osteoblasts (105, 106). BMP signaling through type IB BMP receptor (BMPR-IB) plays a crucial role in mediating osteoblast differentiation of BMSC by a Dlx5/Runx2-mediated pathway, while activation of the type IA BMP receptor (BMPR-IA) in BMSC induces PPARs expression and promotes adipocyte differentiation (107, 108).

Another signaling pathway involved in the regulation of adipogenesis is insulin/insulin-like growth factor (IGF-1) pathway (55, 56, 109). IGF-1 has pleiotropic functions in several tissues with regulatory effects on cell proliferation and cell differentiation. It is the most abundant growth factor in the bone matrix. Deletion of IGF-1 in osteocytes caused impaired developmental bone growth in mice (110). IGF-1-osteoblast deficient animals exhibit impaired bone formation and reduction in bone mass (111). Mice treated with recombinant IGF-1 exhibited enhanced bone formation and osteogenesis via activation of mTOR signaling (112). In adipose tissue, IGF-1 plays an important role in adipocyte differentiation, especially in lineage commitment stage where insulin acts predominantly through IGF-1 receptors, which are highly expressed in preadipocytes compared to insulin receptors (113). Blocking downstream molecules in insulin signaling pathway inhibits adipogenesis in preadipocytes (56). Importantly, IGF-1 is also involved in the regulation of energy metabolism and glucose uptake in insulin responsive cells. Therefore, IGF-1 exerts multiple functions dependent on cellular energy needs. However,

its role in the regulation of energy metabolism in BMSC and BM adipocytes is not known.

Muscle-secreted proteins, known as myokines, represent a group of regulatory molecules with expanding role in crosstalk between muscle and different organs in the body and with regulatory functions on bone and energy metabolism.

Irisin is a newly identified myokine released from skeletal muscle during exercise through peroxisome proliferator-activated receptor gamma coactivator 1 (PGC1) activation that mediates expression of membrane protein Fibronectin type III domain-containing protein 5 (FNDC5). This is a precursor molecule for irisin, which is subsequently cleaved as the myokine (114). Irisin has a browning effect on white adipose tissue via upregulating uncoupling protein 1 (UCP1) through p38 MAPK and ERK (57, 114). Moreover, recent studies demonstrated that irisin positively affects skeletal system, i.e., it enhances osteoblastogenesis *in vitro* and *in vivo* (58, 59).

Fibroblast growth factor 21 (FGF21) has been identified as a circulating hepatokine with effects on glucose and lipid metabolism. FGF21 is also secreted from adipose tissue and skeletal muscle (115). It exerts a positive effect on adipogenesis via activation of PPARγ in BMSC and adipose tissue progenitors. FGF21-deficient mice exhibit high bone mass and decreased fat formation. Reciprocally, mice overexpressing FGF21 exhibit reduced bone mass (60, 61). In older men, high serum levels of FGF21 are associated with low bone mass (116).

Inflammatory cytokines are mostly produced by immune cells and play an important role in the regulation of bone remodeling and adipocyte formation.

Transforming growth factor beta is a cytokine of the TGF superfamily that promotes preadipocyte proliferation and inhibits adipocyte differentiation. Overexpression of TGFβ in mice leads to impaired adipose tissue development. On the other hand, TGFβ-deficient mice display impaired bone growth and mineralization (117). TGFβ mediates its inhibitory function on adipogenesis via SMAD3, which acts on C/EBPα (56, 118).

The effects of the pro-inflammatory cytokines: interleukin 1 (IL1), interleukin 6 (IL6), and tumor necrosis factor alpha (TNFα) on preadipocytes and BMSC are similar (62). They inhibit adipogenesis by reducing PPARγ and C/EBPα expression and by blocking insulin action via decreasing Glut4 expression in preadipocytes (119). TNFα and IL1 suppress adipocyte differentiation by activation of the TAK1/TAB1/NIK cascade, which in turn inhibits PPARγ activity (120). IL1 and TNFα inhibit adipocyte cell proliferation by activation of several distinct intracellular signaling pathways (e.g., JNK, p38 MAPK) (119, 121, 122). Moreover, IL6 maintains BMSC in undifferentiated state through ERK1/2-mediated mechanism during bone fracture healing (123). On the other hand IL6 enhances osteoblast differentiation of BMSC by decreasing Sox2 expression (124). In estrogen-deficient mouse model, IL6-deficient mice are protected from ovariectomy-induced bone loss (125), suggesting a role in mediating estrogen-deficiency-related bone loss (125).

Heme-oxigenase 1 (HO-1) is a rate-limiting enzyme with anti-inflammatory properties, activated by oxidative stress, which was reported to regulate commitment of human BMSC differentiation to osteoblastic cells. HO-1 acts as an inhibitor of adipogenesis by enhancing Wnt signaling (64). Similar effects were observed in ASC of obese mice, which were treated with HO-1 inducer that led to decreased adiposity in peripheral adipose and BM along with a positive effect on insulin sensitivity (65).

Taken together, the above-mentioned regulatory factors share similar signaling pathways for the regulation of adipocyte differentiation in BMSC and ASC. However, some of these factors, e.g., BMP, IGF-1, and LRP5 display different effects depending on the origin of MSCs, suggesting an important role of local microenvironment. These findings are relevant to the design of potential drugs for targeting BMSC in the context of regulation of bone and energy metabolism. **Figure 1** summarizes factors regulating BMSC differentiation and their associated signaling pathways.

MICRO RNA AND REGULATING GENETIC NETWORKS IN ADIPOCYTIC DIFFERENTIATION

Micro RNAs (miRNA) are evolutionary conserved short non-coding RNA molecules (containing about 22 nucleotides) that function in RNA silencing and post-transcriptional regulation of gene expression. Accumulating evidence suggests that miRNA regulate fate decisions of stem cells, including self-renewal and differentiation (126, 127).

Several groups have employed global miRNA gene expression profiling during differentiation of human BMSC to identify several miRNAs that regulate BMSC fate and that act as a molecular switch to control adipocyte and osteoblast differentiation fate. Most of miRNAs regulate gene expression of key molecules involved in BMSC differentiation, such as PPARγ, C/EBP, Runx2, Wnt/β-catenin, Lrp5/6, and so on. For example, recent study of Hamam et al. identified miR320 family, whose upregulation in human BMSC enhanced adipocyte differentiation. The biologically relevant gene targets for miR-320c are RUNX2, MIB1 (mindbomb E3 ubiquitin protein ligase 1), PAX6 (paired box 6), YWHAH, and ZWILCH (128). Other miRNAs that have been reported as regulators of adipogenesis include miR-143, -24, -31, -30c, and -642a-3p. More detailed description of their function in the regulation of BMSC differentiation is summarized in these recently published reviews (127, 129, 130). Thus, targeting different miRNAs represents a potential tool for a molecular therapy to regulate BMSC differentiation fate.

BONE MARROW ADIPOGENESIS IN AGING, OSTEOPOROSIS, AND METABOLIC DISORDERS

In vivo, it has been shown an inverse relationship between bone and fat formation in the BM cavity (1, 131, 132). For examples, observed abnormalities of bone remodeling during aging, osteoporosis, estrogen deficiency, chronic glucocorticoid (GC) treatment, immobilization, anorexia nervosa, and Cushing disease are associated with increased adipose tissue accumulation in the BM and decreased bone mass (3, 133–135). One of the cellular explanations that has been put forward to explain this inverse relationship between bone and fat tissue mass in the BM is

differentiation reprograming of BMSC toward adipocyte instead of osteoblastic fate (136–138). Moerman et al. reported that aging activates adipogenic and suppresses osteogenic differentiation programs in BMSC in mice (139). Molecular mechanism behind this reprograming machinery is not completely delineated. It has been shown that several extracellular signaling proteins have overlapping roles in BMSC adipogenesis and osteoblastogenesis by modulating the expression and/or activity of adipocyte-specific (e.g., PPARs) or osteoblast-specific (e.g., Runx2 and osterix) transcription factors. Some of these factors play opposing roles in lineage determination, while others function in complementary fashion. Schilling et al. using whole genome analyses identified several genes that could play a role in osteoblast versus adipocyte differentiation of BMSC (138).

Obesity and diabetes are highly prevalent diseases, in which bone mass is also affected (140). Several studies have demonstrated that metabolic complications of diabetes are associated with increased risk for bone fractures. However, it is not clear whether these effects are mediated by changes in BM adipose tissue. Bredella et al. found positive correlation between visceral adipose tissue and BM adiposity as measured in vertebrae of obese premenopausal women. Interestingly, this finding correlates with decreased BMD, even after correcting for the degree of obesity (141). An *in vitro* study reported that incubating BMSC with sera obtained from overweight persons promotes *in vitro* adipocyte differentiation and diminishes osteoblast differentiation (142), suggesting that secreted factors/nutrients present in circulation can affect the differentiation process of BMSC (142). In HFD-induced obesity in mice, an increased osteoclastic bone resorption associated with a lower trabecular bone mass is observed (143). Indeed, saturated fatty acids impair osteoblastogenesis, enhance adipogenesis, and affect cell survival and proliferation of human BMSC (144, 145). Other animal study reported impairment of mitochondrial function and apoptosis of BMSC in obese mice (146).

An increased BM adiposity has been reported in type 1 and type 2 diabetes (T1D and T2D). However, in T1D, there is a decrease in bone mass, whereas T2D is characterized by no change or higher bone mass and paradoxically increased risk for osteoporotic fractures (147–150). Studies are underway to examine the role of impaired glucose metabolism and its associated hyperglycemia and hyperinsulinemia on the biological functions of BMSC. This area of research has also been strengthened by the discovery of osteocalcin as a bone secreted hormone that regulates insulin secretion, proliferation of β-cells, and overall energy metabolism in mice (151, 152) and FA1 as a negative regulator of osteocalcin-induced hypoglycemia (97).

TARGETING BONE MARROW ADIPOCYTES TO INCREASE BONE MASS

Several studies have examined the possibility of reverting the adipocyte differentiation fate of BMSC to bone forming osteoblasts as an approach to increased bone mass during aging and in osteoporosis. A number of molecular studies have investigated therapeutic potential of several factors as regulators of BMSC differentiation fate, which included hormone replacement therapy/small molecules with antagonistic/agonistic effect or neutralizing antibodies.

An example is sclerostin (SOST), which is a glycoprotein produced by osteocytes and acts as an inhibitor of Wnt signaling. SOST inhibits bone formation and increases bone adiposity through possibly targeting differentiation of BMSC (153, 154). Treatment with humanized antibodies against SOST is currently in phase III trials for osteoporosis management (155). Another molecule with a similar function as SOST is Dickkopf-1 (DKK1), which negatively regulates Wnt signaling (156). Growth factors, such as BMPs or activin A, represent other anabolic agents for a potential treatment (157). Recent study of Florio et al. reported promising results on the use of bispecific antibody targeting SOST and DKK1 with an enhanced effect on bone formation in rodents and non-human primates (158). However, further clinical studies are needed to investigate the effectiveness of combined treatment, especially in patients with severe osteoporosis.

Some anti-diabetic drugs designed to improve insulin sensitivity and adipogenesis in the peripheral tissues have unfortunately the side effects on bone mass with increased fracture risk, e.g., thiazolidinediones due to partly enhanced BM adiposity (71, 159, 160). Thus, one of the research goals is to design anti-diabetic drugs with minimal negative effects on bone. Recently used anti-diabetic drugs in the clinic include the incretin-based therapies (GLP-1 receptor agonists, DPP-4 inhibitors) and drugs targeting sodium-glucose co-transporter 2 (SGLT2)-inhibitors. However, their effects on bone mass and fracture risk need to be determined (161).

CONCLUSION/FUTURE PERSPECTIVES

MSC commitment to differentiate into osteoblasts or adipocytes and, consequently, the balance between bone mass and BM adipose tissue mass is a complex and dynamic process, which is regulated and fine tuned by a large number of bioactive molecules. The sequential cascade of these processes and how they modulate BMSC differentiation is currently under intensive investigation. Future studies need to identify the biological functions of BM adipocytes not only in relation to bone remodeling but also as part of the overall regulation of energy metabolism. The findings of novel secreted molecules involved in the regulation of cellular fate of BMSC provide new possible anabolic therapies for treating clinical conditions of low bone mass and possibly disturbances in energy metabolism.

AUTHOR CONTRIBUTIONS

MT and MK researched data, wrote manuscript and reviewed the final manuscript.

ACKNOWLEDGMENTS

This work was supported by The Novo Nordisk Foundation NNF15OC0016284, Interregional EU grant Bonebank 16-1.0-15, Inovationsfonden, Denmark and OUH Research grant 15-A845. MT is supported by a Postdoctoral fellowship from the Novo Nordisk Foundation through the Danish Diabetes Academy.

REFERENCES

1. Gimble JM, Zvonic S, Floyd ZE, Kassem M, Nuttall ME. Playing with bone and fat. *J Cell Biochem* (2006) 98:251–66. doi:10.1002/jcb.20777
2. Lecka-Czernik B, Rosen CJ. Energy excess, glucose utilization, and skeletal remodeling: new insights. *J Bone Miner Res* (2015) 30:1356–61. doi:10.1002/jbmr.2574
3. Justesen J, Stenderup K, Ebbesen EN, Mosekilde L, Steiniche T, Kassem M. Adipocyte tissue volume in bone marrow is increased with aging and in patients with osteoporosis. *Biogerontology* (2001) 2:165–71. doi:10.1023/A:1011513223894
4. Rosen CJ, Ackert-Bicknell C, Rodriguez JP, Pino AM. Marrow fat and the bone microenvironment: developmental, functional, and pathological implications. *Crit Rev Eukaryot Gene Expr* (2009) 19:109–24. doi:10.1615/CritRevEukarGeneExpr.v19.i2.20
5. Gimble JM, Robinson CE, Wu X, Kelly KA. The function of adipocytes in the bone marrow stroma: an update. *Bone* (1996) 19:421–8. doi:10.1016/S8756-3282(96)00258-X
6. Kassem M, Bianco P. Skeletal stem cells in space and time. *Cell* (2015) 160:17–9. doi:10.1016/j.cell.2014.12.034
7. Chan CK, Seo EY, Chen JY, Lo D, McArdle A, Sinha R, et al. Identification and specification of the mouse skeletal stem cell. *Cell* (2015) 160:285–98. doi:10.1016/j.cell.2014.12.002
8. Mendez-Ferrer S, Michurina TV, Ferraro F, Mazloom AR, Macarthur BD, Lira SA, et al. Mesenchymal and haematopoietic stem cells form a unique bone marrow niche. *Nature* (2010) 466:829–34. doi:10.1038/nature09262
9. Worthley DL, Churchill M, Compton JT, Tailor Y, Rao M, Si Y, et al. Gremlin 1 identifies a skeletal stem cell with bone, cartilage, and reticular stromal potential. *Cell* (2015) 160:269–84. doi:10.1016/j.cell.2014.11.042
10. Holt V, Caplan AI, Haynesworth SE. Identification of a subpopulation of marrow MSC-derived medullary adipocytes that express osteoclast-regulating molecules: marrow adipocytes express osteoclast mediators. *PLoS One* (2014) 9:e108920. doi:10.1371/journal.pone.0108920
11. Yue R, Zhou BO, Shimada IS, Zhao Z, Morrison SJ. Leptin receptor promotes adipogenesis and reduces osteogenesis by regulating mesenchymal stromal cells in adult bone marrow. *Cell Stem Cell* (2016). doi:10.1016/j.stem.2016.02.015
12. Akiyama H, Kim JE, Nakashima K, Balmes G, Iwai N, Deng JM, et al. Osteochondroprogenitor cells are derived from Sox9 expressing precursors. *Proc Natl Acad Sci U S A* (2005) 102:14665–70. doi:10.1073/pnas.0504750102
13. Grant TD, Cho J, Ariail KS, Weksler NB, Smith RW, Horton WA. Col2-GFP reporter marks chondrocyte lineage and chondrogenesis during mouse skeletal development. *Dev Dyn* (2000) 218:394–400. doi:10.1002/(SICI)1097-0177(200006)218:2<394::AID-DVDY12>3.0.CO;2-I
14. Harkness L, Zaher W, Ditzel N, Isa A, Kassem M. CD146/MCAM defines functionality of human bone marrow stromal stem cell populations. *Stem Cell Res Ther* (2016) 7:4. doi:10.1186/s13287-015-0266-z
15. Abdallah BM, Al-Shammary A, Skagen P, Abu Dawud R, Adjaye J, Aldahmash A, et al. CD34 defines an osteoprogenitor cell population in mouse bone marrow stromal cells. *Stem Cell Res* (2015) 15:449–58. doi:10.1016/j.scr.2015.09.005
16. Post S, Abdallah BM, Bentzon JF, Kassem M. Demonstration of the presence of independent pre-osteoblastic and pre-adipocytic cell populations in bone marrow-derived mesenchymal stem cells. *Bone* (2008) 43:32–9. doi:10.1016/j.bone.2008.03.011
17. Takeshita S, Fumoto T, Naoe Y, Ikeda K. Age-related marrow adipogenesis is linked to increased expression of RANKL. *J Biol Chem* (2014) 289:16699–710. doi:10.1074/jbc.M114.547919
18. Gustafson B, Hammarstedt A, Hedjazifar S, Hoffmann JM, Svensson PA, Grimsby J, et al. BMP4 and BMP antagonists regulate human white and beige adipogenesis. *Diabetes* (2015) 64:1670–81. doi:10.2337/db14-1127
19. Liu TM, Martina M, Hutmacher DW, Hui JH, Lee EH, Lim B. Identification of common pathways mediating differentiation of bone marrow- and adipose tissue-derived human mesenchymal stem cells into three mesenchymal lineages. *Stem Cells* (2007) 25:750–60. doi:10.1634/stemcells.2006-0394
20. Winter A, Breit S, Parsch D, Benz K, Steck E, Hauner H, et al. Cartilage-like gene expression in differentiated human stem cell spheroids: a comparison of bone marrow-derived and adipose tissue-derived stromal cells. *Arthritis Rheum* (2003) 48:418–29. doi:10.1002/art.10767
21. Zuk PA, Zhu M, Ashjian P, De Ugarte DA, Huang JI, Mizuno H, et al. Human adipose tissue is a source of multipotent stem cells. *Mol Biol Cell* (2002) 13:4279–95. doi:10.1091/mbc.E02-02-0105
22. Vishnubalaji R, Al-Nbaheen M, Kadalmani B, Aldahmash A, Ramesh T. Comparative investigation of the differentiation capability of bone-marrow- and adipose-derived mesenchymal stem cells by qualitative and quantitative analysis. *Cell Tissue Res* (2012) 347:419–27. doi:10.1007/s00441-011-1306-3
23. Griffith JF, Yeung DK, Ahuja AT, Choy CW, Mei WY, Lam SS, et al. A study of bone marrow and subcutaneous fatty acid composition in subjects of varying bone mineral density. *Bone* (2009) 44:1092–6. doi:10.1016/j.bone.2009.02.022
24. Trubowitz S, Bathija A. Cell size and plamitate-1-14c turnover of rabbit marrow fat. *Blood* (1977) 49:599–605.
25. Tavassoli M. *Fatty Involution of Marrow and the Role of Adipose Tissue in Hemopoiesis*. Clifton, NJ: Humana (1989).
26. Poloni A, Maurizi G, Serrani F, Mancini S, Zingaretti MC, Frontini A, et al. Molecular and functional characterization of human bone marrow adipocytes. *Exp Hematol* (2013) 41:558–566e2. doi:10.1016/j.exphem.2013.02.005
27. Krings A, Rahman S, Huang S, Lu Y, Czernik PJ, Lecka-Czernik B. Bone marrow fat has brown adipose tissue characteristics, which are attenuated with aging and diabetes. *Bone* (2012) 50:546–52. doi:10.1016/j.bone.2011.06.016
28. Bojin FM, Gruia AT, Cristea MI, Ordodi VL, Paunescu V, Mic FA. Adipocytes differentiated in vitro from rat mesenchymal stem cells lack essential free fatty acids compared to adult adipocytes. *Stem Cells Dev* (2012) 21:507–12. doi:10.1089/scd.2011.0491
29. Gimble JM, Katz AJ, Bunnell BA. Adipose-derived stem cells for regenerative medicine. *Circ Res* (2007) 100:1249–60. doi:10.1161/01.RES.0000265074.83288.09
30. Aldahmash A, Zaher W, Al-Nbaheen M, Kassem M. Human stromal (mesenchymal) stem cells: basic biology and current clinical use for tissue regeneration. *Ann Saudi Med* (2012) 32:68–77.
31. Elman JS, Li M, Wang F, Gimble JM, Parekkadan B. A comparison of adipose and bone marrow-derived mesenchymal stromal cell secreted factors in the treatment of systemic inflammation. *J Inflamm (Lond)* (2014) 11:1. doi:10.1186/1476-9255-11-1
32. Shafiee A, Seyedjafari E, Soleimani M, Ahmadbeigi N, Dinarvand P, Ghaemi N. A comparison between osteogenic differentiation of human unrestricted somatic stem cells and mesenchymal stem cells from bone marrow and adipose tissue. *Biotechnol Lett* (2011) 33:1257–64. doi:10.1007/s10529-011-0541-8
33. Maumus M, Peyrafitte JA, D'Angelo R, Fournier-Wirth C, Bouloumie A, Casteilla L, et al. Native human adipose stromal cells: localization, morphology and phenotype. *Int J Obes (Lond)* (2011) 35:1141–53. doi:10.1038/ijo.2010.269
34. De Ugarte DA, Morizono K, Elbarbary A, Alfonso Z, Zuk PA, Zhu M, et al. Comparison of multi-lineage cells from human adipose tissue and bone marrow. *Cells Tissues Organs* (2003) 174:101–9. doi:10.1159/000071150
35. Kim D, Monaco E, Maki A, de Lima AS, Kong HJ, Hurley WL, et al. Morphologic and transcriptomic comparison of adipose- and bone-marrow-derived porcine stem cells cultured in alginate hydrogels. *Cell Tissue Res* (2010) 341:359–70. doi:10.1007/s00441-010-1015-3
36. Liaw L, Prudovsky I, Koza RA, Anunciado-Koza RV, Siviski ME, Lindner V, et al. Lipid profiling of in vitro cell models of adipogenic differentiation: relationships with mouse adipose tissues. *J Cell Biochem* (2016) 117(9):2182–93. doi:10.1002/jcb.25522
37. Smas CM, Sul HS. Control of adipocyte differentiation. *Biochem J* (1995) 309(Pt 3):697–710. doi:10.1042/bj3090697
38. Siersbaek R, Nielsen R, Mandrup S. Transcriptional networks and chromatin remodeling controlling adipogenesis. *Trends Endocrinol Metab* (2012) 23:56–64. doi:10.1016/j.tem.2011.10.001
39. Hata K, Nishimura R, Ueda M, Ikeda F, Matsubara T, Ichida F, et al. A CCAAT/enhancer binding protein beta isoform, liver-enriched inhibitory protein, regulates commitment of osteoblasts and adipocytes. *Mol Cell Biol* (2005) 25:1971–9. doi:10.1128/MCB.25.5.1971-1979.2005
40. Yokota T, Meka CS, Medina KL, Igarashi H, Comp PC, Takahashi M, et al. Paracrine regulation of fat cell formation in bone marrow cultures

via adiponectin and prostaglandins. *J Clin Invest* (2002) 109:1303–10. doi:10.1172/JCI0214506
41. Lee HW, Kim SY, Kim AY, Lee EJ, Choi JY, Kim JB. Adiponectin stimulates osteoblast differentiation through induction of COX2 in mesenchymal progenitor cells. *Stem Cells* (2009) 27:2254–62. doi:10.1002/stem.144
42. Bauche IB, El Mkadem SA, Pottier AM, Senou M, Many MC, Rezsohazy R, et al. Overexpression of adiponectin targeted to adipose tissue in transgenic mice: impaired adipocyte differentiation. *Endocrinology* (2007) 148:1539–49. doi:10.1210/en.2006-0838
43. Thomas T, Gori F, Khosla S, Jensen MD, Burguera B, Riggs BL. Leptin acts on human marrow stromal cells to enhance differentiation to osteoblasts and to inhibit differentiation to adipocytes. *Endocrinology* (1999) 140:1630–8. doi:10.1210/en.140.4.1630
44. Ducy P, Amling M, Takeda S, Priemel M, Schilling AF, Beil FT, et al. Leptin inhibits bone formation through a hypothalamic relay: a central control of bone mass. *Cell* (2000) 100:197–207. doi:10.1016/S0092-8674(00)81558-5
45. Harris RB. Direct and indirect effects of leptin on adipocyte metabolism. *Biochim Biophys Acta* (2014) 1842:414–23. doi:10.1016/j.bbadis.2013.05.009
46. Taipaleenmaki H, Abdallah BM, AlDahmash A, Saamanen AM, Kassem M. Wnt signalling mediates the cross-talk between bone marrow derived pre-adipocytic and pre-osteoblastic cell populations. *Exp Cell Res* (2011) 317:745–56. doi:10.1016/j.yexcr.2010.12.015
47. Abdallah BM, Kassem M. New factors controlling the balance between osteoblastogenesis and adipogenesis. *Bone* (2012) 50:540–5. doi:10.1016/j.bone.2011.06.030
48. Abdallah BM, Jensen CH, Gutierrez G, Leslie RG, Jensen TG, Kassem M. Regulation of human skeletal stem cells differentiation by Dlk1/Pref-1. *J Bone Miner Res* (2004) 19:841–52. doi:10.1359/jbmr.040118
49. Loh NY, Neville MJ, Marinou K, Hardcastle SA, Fielding BA, Duncan EL, et al. LRP5 regulates human body fat distribution by modulating adipose progenitor biology in a dose- and depot-specific fashion. *Cell Metab* (2015) 21:262–72. doi:10.1016/j.cmet.2015.01.009
50. Qiu W, Andersen TE, Bollerslev J, Mandrup S, Abdallah BM, Kassem M. Patients with high bone mass phenotype exhibit enhanced osteoblast differentiation and inhibition of adipogenesis of human mesenchymal stem cells. *J Bone Miner Res* (2007) 22:1720–31. doi:10.1359/jbmr.070721
51. Palsgaard J, Emanuelli B, Winnay JN, Sumara G, Karsenty G, Kahn CR. Cross-talk between insulin and Wnt signaling in preadipocytes: role of Wnt co-receptor low density lipoprotein receptor-related protein-5 (LRP5). *J Biol Chem* (2012) 287:12016–26. doi:10.1074/jbc.M111.337048
52. Tseng YH, Kokkotou E, Schulz TJ, Huang TL, Winnay JN, Taniguchi CM, et al. New role of bone morphogenetic protein 7 in brown adipogenesis and energy expenditure. *Nature* (2008) 454:1000–4. doi:10.1038/nature07221
53. Bowers RR, Kim JW, Otto TC, Lane MD. Stable stem cell commitment to the adipocyte lineage by inhibition of DNA methylation: role of the BMP-4 gene. *Proc Natl Acad Sci U S A* (2006) 103:13022–7. doi:10.1073/pnas.0605789103
54. Wozney JM. The bone morphogenetic protein family and osteogenesis. *Mol Reprod Dev* (1992) 32:160–7. doi:10.1002/mrd.1080320212
55. Guntur AR, Rosen CJ. IGF-1 regulation of key signaling pathways in bone. *Bonekey Rep* (2013) 2:437. doi:10.1038/bonekey.2013.171
56. Rosen ED, MacDougald OA. Adipocyte differentiation from the inside out. *Nat Rev Mol Cell Biol* (2006) 7:885–96. doi:10.1038/nrm2066
57. Zhang Y, Li R, Meng Y, Li S, Donelan W, Zhao Y, et al. Irisin stimulates browning of white adipocytes through mitogen-activated protein kinase p38 MAP kinase and ERK MAP kinase signaling. *Diabetes* (2014) 63:514–25. doi:10.2337/db13-1106
58. Colaianni G, Cuscito C, Mongelli T, Oranger A, Mori G, Brunetti G, et al. Irisin enhances osteoblast differentiation in vitro. *Int J Endocrinol* (2014) (2014):902186. doi:10.1155/2014/902186
59. Colaianni G, Cuscito C, Mongelli T, Pignataro P, Buccoliero C, Liu P, et al. The myokine irisin increases cortical bone mass. *Proc Natl Acad Sci U S A* (2015) 112:12157–62. doi:10.1073/pnas.1516622112
60. Dutchak PA, Katafuchi T, Bookout AL, Choi JH, Yu RT, Mangelsdorf DJ, et al. Fibroblast growth factor-21 regulates PPARgamma activity and the antidiabetic actions of thiazolidinediones. *Cell* (2012) 148:556–67. doi:10.1016/j.cell.2011.11.062
61. Wei W, Dutchak PA, Wang X, Ding X, Wang X, Bookout AL, et al. Fibroblast growth factor 21 promotes bone loss by potentiating the effects of peroxisome proliferator-activated receptor gamma. *Proc Natl Acad Sci U S A* (2012) 109:3143–8. doi:10.1073/pnas.1200797109
62. Okada A, Yamasaki S, Koga T, Kawashiri SY, Tamai M, Origuchi T, et al. Adipogenesis of the mesenchymal stromal cells and bone oedema in rheumatoid arthritis. *Clin Exp Rheumatol* (2012) 30:332–7.
63. Ahdjoudj S, Lasmoles F, Holy X, Zerath E, Marie PJ. Transforming growth factor beta2 inhibits adipocyte differentiation induced by skeletal unloading in rat bone marrow stroma. *J Bone Miner Res* (2002) 17:668–77. doi:10.1359/jbmr.2002.17.4.668
64. Vanella L, Sodhi K, Kim DH, Puri N, Maheshwari M, Hinds TD, et al. Increased heme-oxygenase 1 expression in mesenchymal stem cell-derived adipocytes decreases differentiation and lipid accumulation via upregulation of the canonical Wnt signaling cascade. *Stem Cell Res Ther* (2013) 4:28. doi:10.1186/scrt176
65. Li M, Kim DH, Tsenovoy PL, Peterson SJ, Rezzani R, Rodella LF, et al. Treatment of obese diabetic mice with a heme oxygenase inducer reduces visceral and subcutaneous adiposity, increases adiponectin levels, and improves insulin sensitivity and glucose tolerance. *Diabetes* (2008) 57:1526–35. doi:10.2337/db07-1764
66. MacDougald A. Transcriptional regulation of gene expression during adipocyte differentiation. *Annu Rev Biochem* (1993) 64:345–73. doi:10.1146/annurev.bi.64.070195.002021
67. Gimble JM, Robinson CE, Wu X, Kelly KA, Rodriguez BR, Kliewer SA, et al. Peroxisome proliferator-activated receptor-gamma activation by thiazolidinediones induces adipogenesis in bone marrow stromal cells. *Mol Pharmacol* (1996) 50:1087–94.
68. Rosen ED, Hsu CH, Wang X, Sakai S, Freeman MW, Gonzalez FJ, et al. C/EBPalpha induces adipogenesis through PPARgamma: a unified pathway. *Genes Dev* (2002) 16:22–6. doi:10.1101/gad.948702
69. Akune T, Ohba S, Kamekura S, Yamaguchi M, Chung UI, Kubota N, et al. PPARgamma insufficiency enhances osteogenesis through osteoblast formation from bone marrow progenitors. *J Clin Invest* (2004) 113:846–55. doi:10.1172/JCI200419900
70. Jones JR, Barrick C, Kim KA, Lindner J, Blondeau B, Fujimoto Y, et al. Deletion of PPARgamma in adipose tissues of mice protects against high fat diet-induced obesity and insulin resistance. *Proc Natl Acad Sci U S A* (2005) 102:6207–12. doi:10.1073/pnas.0306743102
71. Lecka-Czernik B. Bone loss in diabetes: use of antidiabetic thiazolidinediones and secondary osteoporosis. *Curr Osteoporos Rep* (2010) 8:178–84. doi:10.1007/s11914-010-0027-y
72. Qian SW, Li X, Zhang YY, Huang HY, Liu Y, Sun X, et al. Characterization of adipocyte differentiation from human mesenchymal stem cells in bone marrow. *BMC Dev Biol* (2010) 10:47. doi:10.1186/1471-213X-10-47
73. Linhart HG, Ishimura-Oka K, DeMayo F, Kibe T, Repka D, Poindexter B, et al. C/EBPalpha is required for differentiation of white, but not brown, adipose tissue. *Proc Natl Acad Sci U S A* (2001) 98:12532–7. doi:10.1073/pnas.211416898
74. Tanaka T, Yoshida N, Kishimoto T, Akira S. Defective adipocyte differentiation in mice lacking the C/EBPbeta and/or C/EBPdelta gene. *EMBO J* (1997) 16:7432–43. doi:10.1093/emboj/16.24.7432
75. Zuo Y, Qiang L, Farmer SR. Activation of CCAAT/enhancer-binding protein (C/EBP) alpha expression by C/EBP beta during adipogenesis requires a peroxisome proliferator-activated receptor-gamma-associated repression of HDAC1 at the C/ebp alpha gene promoter. *J Biol Chem* (2006) 281:7960–7. doi:10.1074/jbc.M510682200
76. Zanotti S, Stadmeyer L, Smerdel-Ramoya A, Durant D, Canalis E. Misexpression of CCAAT/enhancer binding protein beta causes osteopenia. *J Endocrinol* (2009) 201:263–74. doi:10.1677/JOE-08-0514
77. Staiger J, Lueben MJ, Berrigan D, Malik R, Perkins SN, Hursting SD, et al. C/EBPbeta regulates body composition, energy balance-related hormones and tumor growth. *Carcinogenesis* (2009) 30:832–40. doi:10.1093/carcin/bgn273
78. Tominaga H, Maeda S, Hayashi M, Takeda S, Akira S, Komiya S, et al. CCAAT/enhancer-binding protein beta promotes osteoblast differentiation by enhancing Runx2 activity with ATF4. *Mol Biol Cell* (2008) 19:5373–86. doi:10.1091/mbc.E08-03-0329
79. Turner RT, Kalra SP, Wong CP, Philbrick KA, Lindenmaier LB, Boghossian S, et al. Peripheral leptin regulates bone formation. *J Bone Miner Res* (2013) 28:22–34. doi:10.1002/jbmr.1734

80. Kajimura D, Lee HW, Riley KJ, Arteaga-Solis E, Ferron M, Zhou B, et al. Adiponectin regulates bone mass via opposite central and peripheral mechanisms through FoxO1. *Cell Metab* (2013) 17:901–15. doi:10.1016/j.cmet.2013.04.009
81. Shi Y, Yadav VK, Suda N, Liu XS, Guo XE, Myers MG Jr, et al. Dissociation of the neuronal regulation of bone mass and energy metabolism by leptin in vivo. *Proc Natl Acad Sci U S A* (2008) 105:20529–33. doi:10.1073/pnas.0808701106
82. Aprath-Husmann I, Rohrig K, Gottschling-Zeller H, Skurk T, Scriba D, Birgel M, et al. Effects of leptin on the differentiation and metabolism of human adipocytes. *Int J Obes Relat Metab Disord* (2001) 25:1465–70. doi:10.1038/sj.ijo.0801737
83. Oshima K, Nampei A, Matsuda M, Iwaki M, Fukuhara A, Hashimoto J, et al. Adiponectin increases bone mass by suppressing osteoclast and activating osteoblast. *Biochem Biophys Res Commun* (2005) 331:520–6. doi:10.1016/j.bbrc.2005.03.210
84. Lin YY, Chen CY, Chuang TY, Lin Y, Liu HY, Mersmann HJ, et al. Adiponectin receptor 1 regulates bone formation and osteoblast differentiation by GSK-3beta/beta-catenin signaling in mice. *Bone* (2014) 64:147–54. doi:10.1016/j.bone.2014.03.051
85. Yu L, Tu Q, Han Q, Zhang L, Sui L, Zheng L, et al. Adiponectin regulates bone marrow mesenchymal stem cell niche through a unique signal transduction pathway: an approach for treating bone disease in diabetes. *Stem Cells* (2015) 33:240–52. doi:10.1002/stem.1844
86. Cawthorn WP, Scheller EL, Learman BS, Parlee SD, Simon BR, Mori H, et al. Bone marrow adipose tissue is an endocrine organ that contributes to increased circulating adiponectin during caloric restriction. *Cell Metab* (2014) 20:368–75. doi:10.1016/j.cmet.2014.06.003
87. Lagathu C, Christodoulides C, Tan CY, Virtue S, Laudes M, Campbell M, et al. Secreted frizzled-related protein 1 regulates adipose tissue expansion and is dysregulated in severe obesity. *Int J Obes (Lond)* (2010) 34:1695–705. doi:10.1038/ijo.2010.107
88. Bennett CN, Ross SE, Longo KA, Bajnok L, Hemati N, Johnson KW, et al. Regulation of Wnt signaling during adipogenesis. *J Biol Chem* (2002) 277:30998–1004. doi:10.1074/jbc.M204527200
89. Laborda J. The role of the epidermal growth factor-like protein dlk in cell differentiation. *Histol Histopathol* (2000) 15:119–29.
90. Wang Y, Sul HS. Ectodomain shedding of preadipocyte factor 1 (Pref-1) by tumor necrosis factor alpha converting enzyme (TACE) and inhibition of adipocyte differentiation. *Mol Cell Biol* (2006) 26:5421–35. doi:10.1128/MCB.02437-05
91. Jensen CH, Krogh TN, Stoving RK, Holmskov U, Teisner B. Fetal antigen 1 (FA1), a circulating member of the epidermal growth factor (EGF) superfamily: ELISA development, physiology and metabolism in relation to renal function. *Clin Chim Acta* (1997) 268:1–20. doi:10.1016/S0009-8981(97)00152-6
92. Smas CM, Sul HS. Molecular mechanisms of adipocyte differentiation and inhibitory action of pref-1. *Crit Rev Eukaryot Gene Expr* (1997) 7:281–98. doi:10.1615/CritRevEukarGeneExpr.v7.i4.10
93. Wolfrum C, Shih DQ, Kuwajima S, Norris AW, Kahn CR, Stoffel M. Role of Foxa-2 in adipocyte metabolism and differentiation. *J Clin Invest* (2003) 112:345–56. doi:10.1172/JCI18698
94. Li D, Yea S, Li S, Chen Z, Narla G, Banck M, et al. Kruppel-like factor-6 promotes preadipocyte differentiation through histone deacetylase 3-dependent repression of DLK1. *J Biol Chem* (2005) 280:26941–52. doi:10.1074/jbc.M500463200
95. Wu J, Srinivasan SV, Neumann JC, Lingrel JB. The KLF2 transcription factor does not affect the formation of preadipocytes but inhibits their differentiation into adipocytes. *Biochemistry* (2005) 44:11098–105. doi:10.1021/bi050166i
96. Abdallah BM, Ding M, Jensen CH, Ditzel N, Flyvbjerg A, Jensen TG, et al. Dlk1/FA1 is a novel endocrine regulator of bone and fat mass and its serum level is modulated by growth hormone. *Endocrinology* (2007) 148:3111–21. doi:10.1210/en.2007-0171
97. Abdallah BM, Ditzel N, Laborda J, Karsenty G, Kassem M. DLK1 regulates whole-body glucose metabolism: a negative feedback regulation of the osteocalcin-insulin loop. *Diabetes* (2015) 64:3069–80. doi:10.2337/db14-1642
98. Logan CY, Nusse R. The Wnt signaling pathway in development and disease. *Annu Rev Cell Dev Biol* (2004) 20:781–810. doi:10.1146/annurev.cellbio.20.010403.113126
99. Liu J, Farmer SR. Regulating the balance between peroxisome proliferator-activated receptor gamma and beta-catenin signaling during adipogenesis. A glycogen synthase kinase 3beta phosphorylation-defective mutant of beta-catenin inhibits expression of a subset of adipogenic genes. *J Biol Chem* (2004) 279:45020–7. doi:10.1074/jbc.M407050200
100. Frost M, Andersen TE, Yadav V, Brixen K, Karsenty G, Kassem M. Patients with high-bone-mass phenotype owing to Lrp5-T253I mutation have low plasma levels of serotonin. *J Bone Miner Res* (2010) 25:673–5. doi:10.1002/jbmr.44
101. Cui Y, Niziolek PJ, MacDonald BT, Zylstra CR, Alenina N, Robinson DR, et al. Lrp5 functions in bone to regulate bone mass. *Nat Med* (2011) 17:684–91. doi:10.1038/nm.2388
102. Bowers RR, Lane MD. A role for bone morphogenetic protein-4 in adipocyte development. *Cell Cycle* (2007) 6:385–9. doi:10.4161/cc.6.4.3804
103. Gustafson B, Smith U. The WNT inhibitor Dickkopf 1 and bone morphogenetic protein 4 rescue adipogenesis in hypertrophic obesity in humans. *Diabetes* (2012) 61:1217–24. doi:10.2337/db11-1419
104. Yu-Hua T. Bone morphogenetic proteins and adipocyte differentiation. *Cell Sci Rev* (2007) 3:1–18.
105. Asahina I, Sampath TK, Hauschka PV. Human osteogenic protein-1 induces chondroblastic, osteoblastic, and/or adipocytic differentiation of clonal murine target cells. *Exp Cell Res* (1996) 222:38–47. doi:10.1006/excr.1996.0005
106. Wang EA, Israel DI, Kelly S, Luxenberg DP. Bone morphogenetic protein-2 causes commitment and differentiation in C3H10T1/2 and 3T3 cells. *Growth Factors* (1993) 9:57–71. doi:10.3109/08977199308991582
107. Kim YJ, Lee MH, Wozney JM, Cho JY, Ryoo HM. Bone morphogenetic protein-2-induced alkaline phosphatase expression is stimulated by Dlx5 and repressed by Msx2. *J Biol Chem* (2004) 279:50773–80. doi:10.1074/jbc.M404145200
108. Chen D, Ji X, Harris MA, Feng JQ, Karsenty G, Celeste AJ, et al. Differential roles for bone morphogenetic protein (BMP) receptor type IB and IA in differentiation and specification of mesenchymal precursor cells to osteoblast and adipocyte lineages. *J Cell Biol* (1998) 142:295–305. doi:10.1083/jcb.142.1.295
109. Czech MP, Tencerova M, Pedersen DJ, Aouadi M. Insulin signalling mechanisms for triacylglycerol storage. *Diabetologia* (2013) 56:949–64. doi:10.1007/s00125-013-2869-1
110. Sheng MH, Zhou XD, Bonewald LF, Baylink DJ, Lau KH. Disruption of the insulin-like growth factor-1 gene in osteocytes impairs developmental bone growth in mice. *Bone* (2013) 52:133–44. doi:10.1016/j.bone.2012.09.027
111. Govoni KE, Wergedal JE, Florin L, Angel P, Baylink DJ, Mohan S. Conditional deletion of insulin-like growth factor-I in collagen type 1alpha2-expressing cells results in postnatal lethality and a dramatic reduction in bone accretion. *Endocrinology* (2007) 148:5706–15. doi:10.1210/en.2007-0608
112. Xian L, Wu X, Pang L, Lou M, Rosen CJ, Qiu T, et al. Matrix IGF-1 maintains bone mass by activation of mTOR in mesenchymal stem cells. *Nat Med* (2012) 18:1095–101. doi:10.1038/nm.2793
113. Smith PJ, Wise LS, Berkowitz R, Wan C, Rubin CS. Insulin-like growth factor-I is an essential regulator of the differentiation of 3T3-L1 adipocytes. *J Biol Chem* (1988) 263:9402–8.
114. Bostrom P, Wu J, Jedrychowski MP, Korde A, Ye L, Lo JC, et al. A PGC1-alpha-dependent myokine that drives brown-fat-like development of white fat and thermogenesis. *Nature* (2012) 481:463–8. doi:10.1038/nature10777
115. Itoh N. FGF21 as a hepatokine, adipokine, and myokine in metabolism and diseases. *Front Endocrinol* (2014) 5:107. doi:10.3389/fendo.2014.00107
116. Hanks LJ, Gutierrez OM, Bamman MM, Ashraf A, McCormick KL, Casazza K. Circulating levels of fibroblast growth factor-21 increase with age independently of body composition indices among healthy individuals. *J Clin Transl Endocrinol* (2015) 2:77–82. doi:10.1016/j.jcte.2015.02.001
117. Geiser AG, Hummel CW, Draper MW, Henck JW, Cohen IR, Rudmann DG, et al. A new selective estrogen receptor modulator with potent uterine antagonist activity, agonist activity in bone, and minimal ovarian stimulation. *Endocrinology* (2005) 146:4524–35. doi:10.1210/en.2005-0024
118. Choy L, Derynck R. Transforming growth factor-beta inhibits adipocyte differentiation by Smad3 interacting with CCAAT/enhancer-binding protein (C/EBP) and repressing C/EBP transactivation function. *J Biol Chem* (2003) 278:9609–19. doi:10.1074/jbc.M212259200

119. Constant VA, Gagnon A, Landry A, Sorisky A. Macrophage-conditioned medium inhibits the differentiation of 3T3-L1 and human abdominal preadipocytes. *Diabetologia* (2006) 49:1402–11. doi:10.1007/s00125-006-0253-0
120. Suzawa M, Takada I, Yanagisawa J, Ohtake F, Ogawa S, Yamauchi T, et al. Cytokines suppress adipogenesis and PPAR-gamma function through the TAK1/TAB1/NIK cascade. *Nat Cell Biol* (2003) 5:224–30. doi:10.1038/ncb942
121. Lumeng CN, Deyoung SM, Saltiel AR. Macrophages block insulin action in adipocytes by altering expression of signaling and glucose transport proteins. *Am J Physiol Endocrinol Metab* (2007) 292:E166–74. doi:10.1152/ajpendo.00284.2006
122. Gustafson B, Smith U. Cytokines promote Wnt signaling and inflammation and impair the normal differentiation and lipid accumulation in 3T3-L1 preadipocytes. *J Biol Chem* (2006) 281:9507–16. doi:10.1074/jbc.M512077200
123. Pricola KL, Kuhn NZ, Haleem-Smith H, Song Y, Tuan RS. Interleukin-6 maintains bone marrow-derived mesenchymal stem cell stemness by an ERK1/2-dependent mechanism. *J Cell Biochem* (2009) 108:577–88. doi:10.1002/jcb.22289
124. Yoon DS, Kim YH, Lee S, Lee KM, Park KH, Jang Y, et al. Interleukin-6 induces the lineage commitment of bone marrow-derived mesenchymal multipotent cells through down-regulation of Sox2 by osteogenic transcription factors. *FASEB J* (2014) 28:3273–86. doi:10.1096/fj.13-248567
125. Poli V, Balena R, Fattori E, Markatos A, Yamamoto M, Tanaka H, et al. Interleukin-6 deficient mice are protected from bone loss caused by estrogen depletion. *EMBO J* (1994) 13:1189–96.
126. Ivey KN, Srivastava D. MicroRNAs as regulators of differentiation and cell fate decisions. *Cell Stem Cell* (2010) 7:36–41. doi:10.1016/j.stem.2010.06.012
127. Taipaleenmaki H, Bjerre Hokland L, Chen L, Kauppinen S, Kassem M. Mechanisms in endocrinology: micro-RNAs: targets for enhancing osteoblast differentiation and bone formation. *Eur J Endocrinol* (2012) 166:359–71. doi:10.1530/EJE-11-0646
128. Hamam D, Ali D, Vishnubalaji R, Hamam R, Al-Nbaheen M, Chen L, et al. microRNA-320/RUNX2 axis regulates adipocytic differentiation of human mesenchymal (skeletal) stem cells. *Cell Death Dis* (2014) 5:e1499. doi:10.1038/cddis.2014.462
129. Hamam D, Ali D, Kassem M, Aldahmash A, Alajez NM. microRNAs as regulators of adipogenic differentiation of mesenchymal stem cells. *Stem Cells Dev* (2015) 24:417–25. doi:10.1089/scd.2014.0331
130. Clark EA, Kalomoiris S, Nolta JA, Fierro FA. Concise review: MicroRNA function in multipotent mesenchymal stromal cells. *Stem Cells* (2014) 32:1074–82. doi:10.1002/stem.1623
131. Rzonca SO, Suva LJ, Gaddy D, Montague DC, Lecka-Czernik B. Bone is a target for the antidiabetic compound rosiglitazone. *Endocrinology* (2004) 145:401–6. doi:10.1210/en.2003-0746
132. Tornvig L, Mosekilde LI, Justesen J, Falk E, Kassem M. Troglitazone treatment increases bone marrow adipose tissue volume but does not affect trabecular bone volume in mice. *Calcif Tissue Int* (2001) 69:46–50. doi:10.1007/s002230020018
133. van Staa TP, Leufkens B, Cooper C. Bone loss and inhaled glucocorticoids. *N Engl J Med* (2002) 346:533–5. doi:10.1056/NEJM200202143460716
134. van Staa TP, Leufkens HG, Cooper C. The epidemiology of corticosteroid-induced osteoporosis: a meta-analysis. *Osteoporos Int* (2002) 13:777–87. doi:10.1007/s001980200108
135. Bredella MA, Fazeli PK, Miller KK, Misra M, Torriani M, Thomas BJ, et al. Increased bone marrow fat in anorexia nervosa. *J Clin Endocrinol Metab* (2009) 94:2129–36. doi:10.1210/jc.2008-2532
136. Bennett JH, Joyner CJ, Triffitt JT, Owen ME. Adipocytic cells cultured from marrow have osteogenic potential. *J Cell Sci* (1991) 99(Pt 1):131–9.
137. Song L, Tuan RS. Transdifferentiation potential of human mesenchymal stem cells derived from bone marrow. *FASEB J* (2004) 18:980–2.
138. Schilling T, Kuffner R, Klein-Hitpass L, Zimmer R, Jakob F, Schutze N. Microarray analyses of transdifferentiated mesenchymal stem cells. *J Cell Biochem* (2008) 103:413–33. doi:10.1002/jcb.21415
139. Moerman EJ, Teng K, Lipschitz DA, Lecka-Czernik B. Aging activates adipogenic and suppresses osteogenic programs in mesenchymal marrow stroma/stem cells: the role of PPAR-gamma2 transcription factor and TGF-beta/BMP signaling pathways. *Aging Cell* (2004) 3:379–89. doi:10.1111/j.1474-9728.2004.00127.x
140. Lecka-Czernik B. Marrow fat metabolism is linked to the systemic energy metabolism. *Bone* (2012) 50:534–9. doi:10.1016/j.bone.2011.06.032
141. Bredella MA, Torriani M, Ghomi RH, Thomas BJ, Brick DJ, Gerweck AV, et al. Vertebral bone marrow fat is positively associated with visceral fat and inversely associated with IGF-1 in obese women. *Obesity (Silver Spring)* (2011) 19:49–53. doi:10.1038/oby.2010.106
142. Di Bernardo G, Messina G, Capasso S, Del Gaudio S, Cipollaro M, Peluso G, et al. Sera of overweight people promote in vitro adipocyte differentiation of bone marrow stromal cells. *Stem Cell Res Ther* (2014) 5:4. doi:10.1186/scrt393
143. Cao JJ, Sun L, Gao H. Diet-induced obesity alters bone remodeling leading to decreased femoral trabecular bone mass in mice. *Ann N Y Acad Sci* (2010) 1192:292–7. doi:10.1111/j.1749-6632.2009.05252.x
144. Casado-Diaz A, Santiago-Mora R, Dorado G, Quesada-Gomez JM. The omega-6 arachidonic fatty acid, but not the omega-3 fatty acids, inhibits osteoblastogenesis and induces adipogenesis of human mesenchymal stem cells: potential implication in osteoporosis. *Osteoporos Int* (2013) 24:1647–61. doi:10.1007/s00198-012-2138-z
145. Fillmore N, Huqi A, Jaswal JS, Mori J, Paulin R, Haromy A, et al. Effect of fatty acids on human bone marrow mesenchymal stem cell energy metabolism and survival. *PLoS One* (2015) 10:e0120257. doi:10.1371/journal.pone.0120257
146. de Oliveira GP, Cortez E, Araujo GJ, de Carvalho Sabino KC, Neves FA, Bernardo AF, et al. Impaired mitochondrial function and reduced viability in bone marrow cells of obese mice. *Cell Tissue Res* (2014) 357:185–94. doi:10.1007/s00441-014-1857-1
147. Botolin S, McCabe LR. Bone loss and increased bone adiposity in spontaneous and pharmacologically induced diabetic mice. *Endocrinology* (2007) 148:198–205. doi:10.1210/en.2006-1006
148. Shanbhogue VV, Hansen S, Frost M, Jorgensen NR, Hermann AP, Henriksen JE, et al. Bone geometry, volumetric density, microarchitecture, and estimated bone strength assessed by HR-pQCT in adult patients with type 1 diabetes mellitus. *J Bone Miner Res* (2015) 30:2188–99. doi:10.1002/jbmr.2573
149. Shanbhogue VV, Hansen S, Frost M, Jorgensen NR, Hermann AP, Henriksen JE, et al. Compromised cortical bone compartment in type 2 diabetes mellitus patients with microvascular disease. *Eur J Endocrinol* (2016) 174:115–24. doi:10.1530/EJE-15-0860
150. Vestergaard P. Diabetes and bone fracture: risk factors for old and young. *Diabetologia* (2014) 57:2007–8. doi:10.1007/s00125-014-3338-1
151. Wei J, Ferron M, Clarke CJ, Hannun YA, Jiang H, Blaner WS, et al. Bone-specific insulin resistance disrupts whole-body glucose homeostasis via decreased osteocalcin activation. *J Clin Invest* (2014) 124:1–13. doi:10.1172/JCI72323
152. Wei J, Hanna T, Suda N, Karsenty G, Ducy P. Osteocalcin promotes beta-cell proliferation during development and adulthood through Gprc6a. *Diabetes* (2014) 63:1021–31. doi:10.2337/db13-0887
153. van Bezooijen RL, Roelen BA, Visser A, van der Wee-Pals L, de Wilt E, Karperien M, et al. Sclerostin is an osteocyte-expressed negative regulator of bone formation, but not a classical BMP antagonist. *J Exp Med* (2004) 199:805–14. doi:10.1084/jem.20031454
154. Ma YH, Schwartz AV, Sigurdsson S, Hue TF, Lang TF, Harris TB, et al. Circulating sclerostin associated with vertebral bone marrow fat in older men but not women. *J Clin Endocrinol Metab* (2014) 99:E2584–90. doi:10.1210/jc.2013-4493
155. McClung MR, Grauer A. Romosozumab in postmenopausal women with osteopenia. *N Engl J Med* (2014) 370:1664–5. doi:10.1056/NEJMoa1305224
156. Qiang YW, Barlogie B, Rudikoff S, Shaughnessy JD Jr. Dkk1-induced inhibition of Wnt signaling in osteoblast differentiation is an underlying mechanism of bone loss in multiple myeloma. *Bone* (2008) 42:669–80. doi:10.1016/j.bone.2007.12.006
157. Gennari L, Rotatori S, Bianciardi S, Nuti R, Merlotti D. Treatment needs and current options for postmenopausal osteoporosis. *Expert Opin Pharmacother* (2016) 17:1141–52. doi:10.1080/14656566.2016.1176147
158. Florio M, Gunasekaran K, Stolina M, Li X, Liu L, Tipton B, et al. A bispecific antibody targeting sclerostin and DKK-1 promotes bone mass accrual and fracture repair. *Nat Commun* (2016) 7:11505. doi:10.1038/ncomms11505

159. Beck GR Jr, Khazai NB, Bouloux GF, Camalier CE, Lin Y, Garneys LM, et al. The effects of thiazolidinediones on human bone marrow stromal cell differentiation in vitro and in thiazolidinedione-treated patients with type 2 diabetes. *Transl Res* (2013) 161:145–55. doi:10.1016/j.trsl.2012.08.006
160. Grey A, Beckley V, Doyle A, Fenwick S, Horne A, Gamble G, et al. Pioglitazone increases bone marrow fat in type 2 diabetes: results from a randomized controlled trial. *Eur J Endocrinol* (2012) 166:1087–91. doi:10.1530/EJE-11-1075
161. Meier C, Schwartz AV, Egger A, Lecka-Czernik B. Effects of diabetes drugs on the skeleton. *Bone* (2016) 82:93–100. doi:10.1016/j.bone.2015.04.026

Conflict of Interest Statement: The authors declare that the research was conducted in the absence of any commercial or financial relationships that could be construed as a potential conflict of interest.

frontiers in Endocrinology

REVIEW
published: 20 June 2016
doi: 10.3389/fendo.2016.00069

Fatty Infiltration of Skeletal Muscle: Mechanisms and Comparisons with Bone Marrow Adiposity

Mark W. Hamrick[1], Meghan E. McGee-Lawrence[1] and Danielle M. Frechette[2]*

[1] Department of Cellular Biology and Anatomy, Medical College of Georgia, Augusta, GA, USA, [2] Department of Biomedical Engineering, Stony Brook University, Stony Brook, NY, USA

Skeletal muscle and bone share common embryological origins from mesodermal cell populations and also display common growth trajectories early in life. Moreover, muscle and bone are both mechanoresponsive tissues, and the mass and strength of both tissues decline with age. The decline in muscle and bone strength that occurs with aging is accompanied in both cases by an accumulation of adipose tissue. In bone, adipocyte (AC) accumulation occurs in the marrow cavities of long bones and is known to increase with estrogen deficiency, mechanical unloading, and exposure to glucocorticoids. The factors leading to accumulation of intra- and intermuscular fat (myosteatosis) are less well understood, but recent evidence indicates that increases in intramuscular fat are associated with disuse, altered leptin signaling, sex steroid deficiency, and glucocorticoid treatment, factors that are also implicated in bone marrow adipogenesis. Importantly, accumulation of ACs in skeletal muscle and accumulation of intramyocellular lipid are linked to loss of muscle strength, reduced insulin sensitivity, and increased mortality among the elderly. Resistance exercise and whole body vibration can prevent fatty infiltration in skeletal muscle and also improve muscle strength. Therapeutic strategies to prevent myosteatosis may improve muscle function and reduce fall risk in the elderly, potentially impacting the incidence of bone fracture.

Keywords: bone marrow adipogenesis, myosteatosis, intramyocellular lipid, exercise

OPEN ACCESS

Edited by:
Erica L. Scheller, Washington University School of Medicine, USA

Reviewed by:
Gretchen Meyer, Washington University, USA
Amanda L. Lorbergs, Harvard Medical School, USA

****Correspondence:***
Mark W. Hamrick
mhamrick@augusta.edu

Specialty section:
This article was submitted to Bone Research, a section of the journal Frontiers in Endocrinology

Received: *02 May 2016*
Accepted: *07 June 2016*
Published: *20 June 2016*

Citation:
Hamrick MW, McGee-Lawrence ME and Frechette DM (2016) Fatty Infiltration of Skeletal Muscle: Mechanisms and Comparisons with Bone Marrow Adiposity. Front. Endocrinol. 7:69. doi: 10.3389/fendo.2016.00069

INTRODUCTION

Osteoporosis affects ~10 million people in the U.S. and results in over 1.5 million bone fractures per year. Hip fractures are a major cause of morbidity and mortality among the elderly: ~40% of those suffering a hip fracture will end up in a nursing home and 20% will never walk again. In addition, the 1-year mortality of hip fractures at age 70 is ~30%. Muscle weakness and postural instability are major contributors to the incidence of falls among the elderly, and falling is the primary etiological factor in more than 75% of hip fractures (1). Loss of muscle and bone mass with age is therefore a significant public health problem, as the morbidity that accompanies fractures in the elderly is costly both in terms of financial burden and quality of life. The mechanisms underlying loss of muscle and bone strength with age are complex and multifactorial in nature, but evidence suggests that common factors regulate the integrated growth, development, and degeneration of these two tissues. For example, skeletal muscle and bone share common embryological origins from mesodermal cell populations and also display common growth trajectories early in life. Moreover, muscle and bone

are both mechanoresponsive tissues, and the mass and strength of both tissues decline with age. Importantly, the decline in muscle and bone strength that occurs with aging is accompanied in both cases by an accumulation of adipose tissue. This accumulation of fat in non-adipose depots, such as bone, liver, and muscle, is now recognized as a common feature of aging (2). The processes driving the accumulation of bone marrow adipocytes (ACs) are becoming more well understood (3, 4); however, the factors leading to the accumulation of fat in skeletal muscle (myosteatosis) with age are not yet as well defined. Evidence, to date, does suggest that many of the factors that have been observed to stimulate bone marrow adipogenesis, such as estrogen deficiency, glucocorticoid treatment, and disuse atrophy, also induce myosteatosis. In this study, we review these findings to highlight potential therapeutic strategies for the prevention of age-related myosteatosis as an approach for reducing fall risk and hence the likelihood of bone fracture.

FACTORS CONTRIBUTING TO BONE MARROW ADIPOGENESIS

Bone cell populations are heterogeneous and include cells of both hematopoietic (e.g., megakaryocytes and osteoclasts) and mesenchymal (e.g., osteoblasts and AC) origin. Aging is accompanied by an accumulation of AC as well as increase in ACs size within the bone marrow cavity (5). Adipose tissue represents ~20% of bone marrow tissue before the third decade in life but increases to nearly 50% by the ninth decade (6). This accumulation of bone marrow fat shows a strong association with bone loss, reduced bone formation, and fracture risk (6–9). Mesenchymal progenitors (MSCs) within bone marrow can be directed toward the AC or osteoblast lineage, and conditions that favor adipogenesis such as estrogen depletion (10), disuse (11), anorexia/calorie restriction (12, 13), and exposure to microgravity (14) are also associated with reduced osteoblast differentiation.

In addition, there are a number of pharmaceutical treatments that can mediate bone marrow adipogenesis. For example, glucocorticoids and PPAR gamma agonists will stimulate adipogenesis in mesenchymal progenitors (15, 16), whereas lipid-lowering statins can inhibit adipogenic differentiation (17). Importantly, the microenvironment of the MSCs plays a key role in modulating this reciprocal switch between adipogenic or osteogenic differentiation, particularly with aging, as young MSCs transplanted into old animals or young MSCs exposed to serum of old donors will tend to differentiate down the adipogenic pathway rather than become osteogenic (18, 19). Finally, epigenetic programing also appears to play an important role in modulating bone marrow adipogenesis. For example, conditional deletion of Hdac3 in preosteoblasts increases marrow AC number and lipid storage in preosteoblasts (20). It is worth noting that marrow ACs are themselves not homogenous in their gene expression and secretory profile. For example, some marrow ACs are similar to "white" fat in being rich in saturated fatty acids, whereas other marrow ACs are more "beige-like" fat in having greater thermogenic potential (4).

FATTY INFILTRATION IN SKELETAL MUSCLE: CELLULAR AND MOLECULAR MECHANISMS

Aging in humans is accompanied by a loss of subcutaneous fat but an accumulation of AC and lipids in non-adipose depots, such as bone marrow, liver, and skeletal muscle (2). Fatty infiltration of skeletal muscle (myosteatosis) has, in particular, been recognized as an important component of aging and frailty (21–26). Lipid accumulation in muscles of the lower limb is also associated with increased fracture risk in the elderly (27). The cellular origins of fatty accumulation in muscle arise through several different pathways (**Figure 1**). One direct route is *via* the accumulation of lipid within myofibers themselves, known as intramuscular fat or intramyocellular (IMC) lipid (28–30). Accumulation of IMC lipid is now known to be associated with insulin insensitivity, inflammation, and functional deficits in skeletal muscle. Accumulation of the sphingolipid ceramide appears to have a particularly

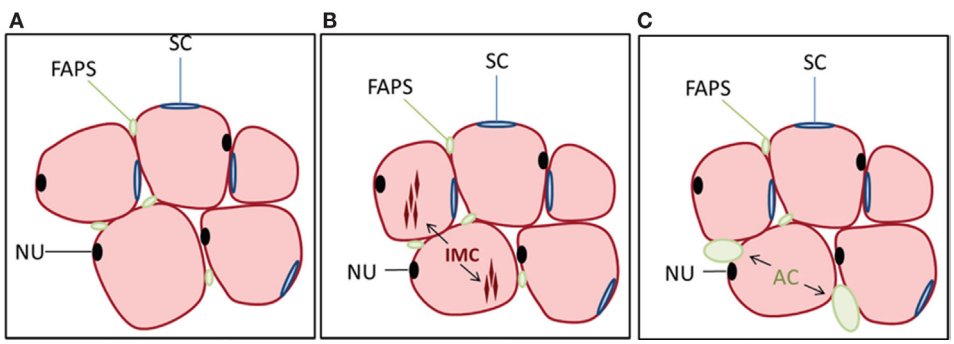

FIGURE 1 | Cell populations in muscle and their relationship to lipid accumulation. **(A)** Myofibers (pink) are multinucleated (NU, nucleus, black) and surrounded by satellite cells (SCs, blue) as well as multipotential cells of mesenchymal origin referred to as fibro-adipogenic progenitors (FAPs, green). FAPs are distinct from satellite cells and lack Pax7 expression but are Sca-1 and PDGFRα positive. Not shown are pericytes surrounding blood vessels within muscle. **(B)** Intramyocellular (IMC) lipid can accumulate within myofibers, which is one pathway for lipid deposition within skeletal muscle. **(C)** FAPs can also differentiate to adipocytes (ACs), contributing to the accumulation of intermuscular fat, often following muscle injury.

detrimental effect on skeletal muscle function (30). Recent data also suggest that the lipid metabolites diacylglycerols (DAG) are responsible for mediating insulin resistance in skeletal muscle through disrupting the insulin signaling pathway (31).

Another pathway for myosteatosis is an accumulation of AC within skeletal muscle, known as intermuscular fat. There are several stem cell populations in skeletal muscle, the most well defined being muscle satellite cells (SCs), which lie below the basil lamina of muscle fibers and contribute to myogenesis during the process of muscle regeneration. A second, more recently described, population of cells is termed fibro/adipogenic progenitors (FAPs) or mesenchymal interstitial cells [**Figure 1**; Ref. (32–35)]. These cells are distinct from SCs and lack Pax7 expression but are Sca-1 and PDGFRα positive. SCs are generally resistant to adipogenic differentiation, whereas FAPs readily differentiate into ACs under various conditions such as muscle injury or glucocorticoid treatment (34, 36). Endogenous glucocorticoid levels increase with age (37), which may contribute not only to accumulation of bone marrow ACs but also to the deposition of intermuscular fat with age. Multipotent mesenchymal stem cells and other progenitors may also contribute toward skeletal muscle adipogenesis. For example, $PW1^+$ interstitial cells (PICs) have shown adipogenic potential *in vitro* (38); however, the extent to which this population overlaps with FAPs is unclear. Additionally, type-1 pericytes expressing PDGFRα have been shown to commit to the adipogenic lineage *in vivo* in the presence of glycerol (39).

Just as glucocorticoids can stimulate adipogenesis in both bone and muscle, other signaling pathways appear to be shared that regulate adipogenesis in muscle and bone (**Figure 2**). Wnt10b is well recognized to inhibit adipogenesis and stimulate bone formation in bone tissue (40). Wnt10b also suppresses the accumulation of IMC lipid in myofibers, increases insulin sensitivity, and inhibits adipogenic differentiation of aged, muscle-derived stem cells (41, 42). Similarly, inhibition of histone deacetylases (HDAC) can inhibit the adipogenic differentiation of MSCs *in vitro* and enhance their differentiation to osteoblasts (43), and HDAC inhibitors also inhibit the adipogenic differentiation of FAPs during the process of muscle regeneration (44). Altered leptin signaling, either due to absence of leptin or leptin receptors, is associated with increased bone marrow fat (45) as well as increased intra- and intermuscular fat (**Figure 3**). The leptin receptor is a key marker of bone marrow mesenchymal stem cells that mediate marrow adipogenesis (46), and the leptin receptor is also expressed in skeletal muscle (47). Whether or not the accumulation of inter- and intramuscular fat is directly mediated by the leptin receptor is, however, not well understood. Leptin deficiency associated with calorie restriction results in increased marrow adiposity (12), as does anorexia nervosa (48), but calorie restriction decreases lipid stores and lipid droplet size in skeletal muscle (49).

Unloading through either prolonged bedrest or spaceflight increases bone marrow adipogenesis (11, 14), and prolonged bedrest also decreases muscle strength and increases IMC lipid in skeletal muscle (50), which can ultimately lead to postural instability (51). Finally, estrogen deficiency is implicated in bone loss and marrow AC accumulation in women. Estrogen deficiency increases lipid content in skeletal muscle, the expression of adipogenic genes, and decreases relative satellite cell proportions in ovariectomized rodents (52, 53). Androgen deprivation therapy also increases fatty infiltration of skeletal muscle in men with prostate cancer, although CT imaging does not enable a distinction between IMC or intermuscular lipid accumulation and so

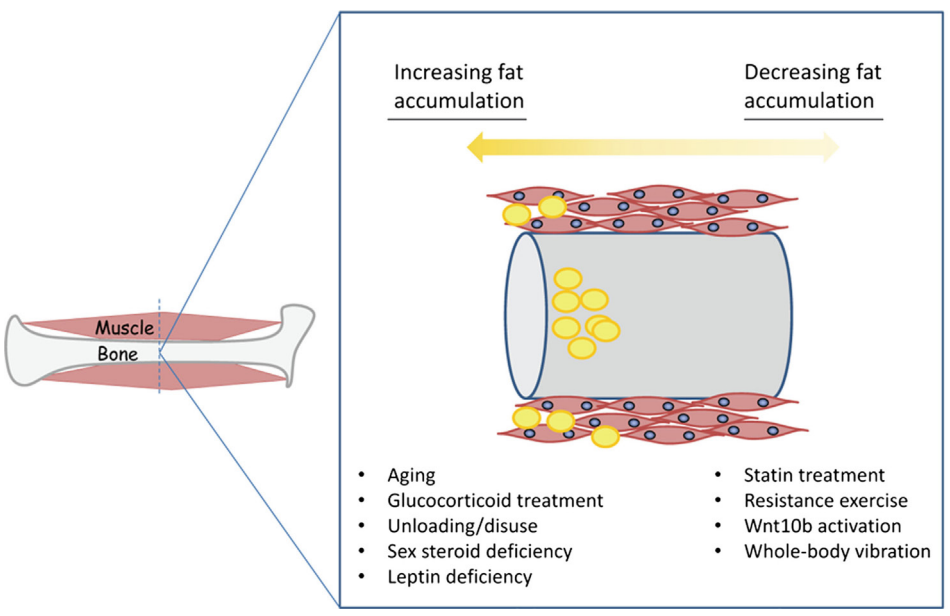

FIGURE 2 | Conditions favoring the accumulation of fat (yellow) in muscle and bone versus those conditions that can either prevent or possibly reverse fatty deposition in muscle and bone.

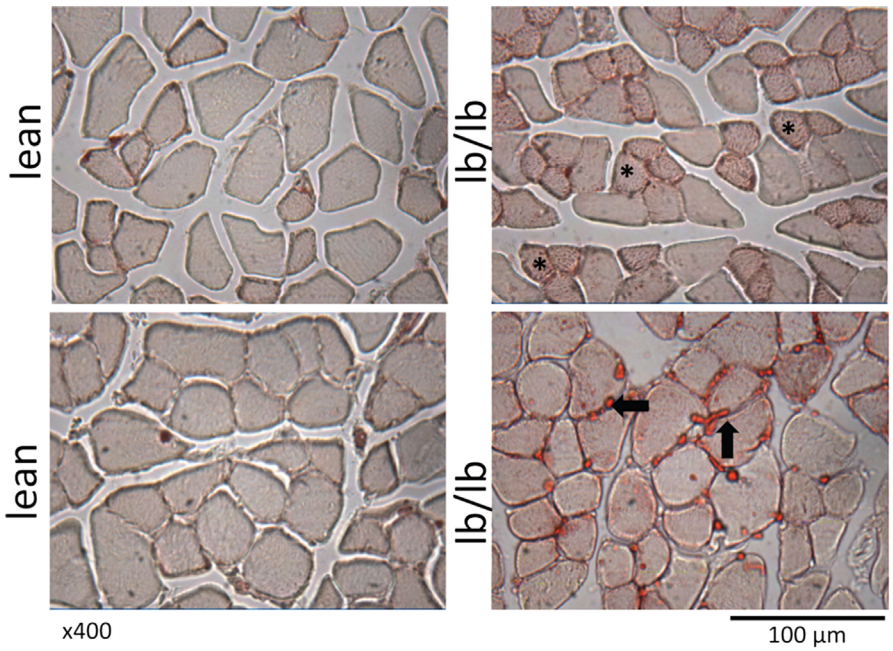

FIGURE 3 | Cross sections of muscle fibers from normal, lean mice (left), or mice that lack leptin receptors (lb/lb, right) stained for oil red O. The asterisks indicate the accumulation of intramyocellular lipid, and the arrows indicate intermuscular fat. Note also the relatively small diameter of fibers that are positive for intramyocellular lipid. POUND mice (lb/lb) lack both short and long forms of the leptin receptor and are obese and hyperphagic (47).

the actual site of lipid deposition is not clear in this case (54). Together, these findings indicate that many of the conditions that induce marrow adipogenesis and bone loss in men and women such as disuse, sex steroid deficiency, altered leptin signaling, and glucocorticoid treatment also stimulate the accumulation of ACs and IMC lipid in skeletal muscle (**Figure 2**).

FUNCTIONAL CONSEQUENCES OF FATTY INFILTRATION IN MUSCLE

Protein synthesis enhances muscle hypertrophy and the maintenance of muscle strength, whereas impaired protein synthesis contributes to muscle atrophy. Insulin is an anabolic factor for skeletal muscle, and accumulation of muscle ACs and IMC lipid decreases insulin sensitivity, impairing the capacity for normal protein synthesis in skeletal muscle (30). Thus, decreased insulin sensitivity with fatty infiltration in skeletal muscle is one pathway by which fatty infiltration can directly affect muscle mass and muscle strength. The accumulation of IMC lipid with aging or with disuse is not homogenous across different muscles or different fiber types. This may be analogous to the unequal distribution of ACs throughout bone marrow in the appendicular skeleton, where fatty infiltration begins at more distal skeletal locations (55). For example, within the posterior compartment of the leg, the gastrocnemius accumulates more lipid with age than other calf muscles (21). Type I fibers, also referred to as "slow-twitch oxidative fibers," tend to accumulate more IMC lipid with age in human subjects than fast-twitch oxidative fibers (23, 25), and fast-twitch fibers typically show greater atrophy with age than type I fibers (23, 56). It is possible that lipid accumulation alone may even support a transition of type II fibers to more of a type I phenotype (57). These changes ultimately lead to muscles with impaired contractile capacity of both type I and type II fibers, which together lead the dramatic decrease in muscle power (product of force and speed) observed with age (58).

Aging and disuse can induce the accumulation of IMC lipid, but muscle injury is associated with a marked accumulation of intermuscular fat (ACs), likely derived from the FAPs referenced above. This phenomenon has been most well described in patients with Duchene muscular dystrophy (DMD), where the prolonged cycle of muscle injury and regeneration that accompanies dystrophin deficiency ultimately results in an accumulation of ACs and fibrous tissue in areas where muscle fibers are lost (59, 60). The loss of muscle fibers and replacement with fatty and fibrous tissues leads to muscle weakness. The extent to which muscle injury with aging, which might occur with frequent eccentric muscle contractions, contributes to accumulation of intermuscular fat is not well documented. Fatty infiltration of skeletal muscle is also common following rotator cuff muscle injury and is a major factor that limits functional recovery (61). Attenuation of fatty infiltration following rotator cuff injury with statin treatment can have a protective effect on muscle atrophy in rats (62); however, a number of studies in human subjects indicate that fatty infiltration and muscle atrophy after rotator cuff repair is very difficult to reverse (63, 64). Hyperlipidemia and type 2 diabetes are independent risk factors for rotator cuff injury (65). It is certainly

possible that these risk factors may not only increase the risk of rotator cuff injury but also may contribute to an attenuated repair response following treatment by exacerbating fatty infiltration of the injured rotator cuff muscles.

DISCUSSION: TARGETING ADIPOGENESIS AND LIPID ACCUMULATION IN MUSCLE TO PREVENT FRACTURE

One of the most effective countermeasures against fatty infiltration of muscle with aging is physical activity and regular exercise. Previous work indicates that 6 months of regular aerobic exercise combined with weight loss reduced low-density muscle (lipid measurement) and improved glucose tolerance in men aged 60+ years compared with those who just exercised alone (66). Resistance training 3 days/week in adults' age 55+ years decreased thigh intramuscular adipose tissue (67), and 1 year of brisk walking prevented fatty infiltration of muscle in older subjects (68). Importantly, resumption of physical activity following periods of sedentary activity could reverse the fatty infiltration that occurred in older adults following cessation of resistance training (69). Fracture risk in women declines with higher levels of weekly physical activity (70), and hip fracture in men is more common in those individuals with low physical activity compared with men with higher levels of physical activity (71). Resistance exercise increases leg strength and power in both older (aged 70 years) men and women (72), and this increase is associated with increased muscle fiber size (73). While the effects of exercise on bone and perhaps bone marrow ACs are more modest (74), resistance training may have a positive effect on reducing fracture risk by reducing intramuscular fat and increasing muscle strength and power.

Alternative forms of mechanical signals that are safe and can help prevent accumulation of muscular or bone marrow fat may be desirable, particularly, for the elderly or injured who are unable to exercise or have increased risk of fracture. Low magnitude (<1 *g*; *g* = earth's gravitational field), whole body vibration has been observed to reduce adipose tissue as well as the expression of adipogenic genes in muscle (53, 75) while also acting as an anabolic signal and increasing muscle fiber area (76). Similarly, vibration has reduced bone marrow adiposity in a model of postmenopausal osteoporosis (77) and reduced bone marrow-derived mesenchymal stem cell commitment to the adipogenic lineage (78). Reduced indices of adipogenesis with the application of these mechanical signals as seen in both muscle and bone may occur through a similar mechanism – bias of mesenchymal stem cell or fate away from the fat differentiation pathway. These findings suggest that mechanical stimulation in a relatively low magnitude, high-frequency domain may have the potential to preserve muscle function with age by reducing the accumulation of lipids and ACs in skeletal muscle.

AUTHOR CONTRIBUTIONS

MH wrote the initial draft and prepared the manuscript illustrations. MM-L contributed additional narrative material on bone marrow adipogenesis and edited the manuscript. DF contributed narrative material on exercise and whole body vibration and on myosteatosis. DF also edited the manuscript.

ACKNOWLEDGMENTS

The authors are grateful to E. Scheller and W. Cawthorn for the opportunity to prepare this contribution. Funding to MH is provided by the National Institute on Aging (NIA AG036675) and funding to MM-L is provided by the American Diabetes Association (1-16-JDF-062). The authors thank Donna Kumiski in the Electron Microscopy and Histology Core Facility for her assistance with the staining shown in **Figure 2**.

REFERENCES

1. Järvinen TL, Sievänen H, Khan KM, Heinonen A, Kannus P. Shifting the focus in fracture prevention from osteoporosis to falls. *BMJ* (2008) 336:124–6. doi:10.1136/bmj.39428.470752.AD
2. Kirkland JL, Tchkonia T, Pirtskhalava T, Han J, Karagiannides I. Adipogenesis and aging: does aging make fat go MAD? *Exp Gerontol* (2002) 37:757–67. doi:10.1016/S0531-5565(02)00014-1
3. Rosen CJ, Bouxsein ML. Mechanisms of disease: is osteoporosis the obesity of bone? *Nat Clin Pract Rheumatol* (2006) 2:35–43. doi:10.1038/ncprheum0070
4. Hardouin P, Marie PJ, Rosen CJ. New insights into bone marrow adipocytes: report from the first European meeting on bone marrow adiposity (BMA 2015). *Bone* (2015) S8756-3282(15):414–7. doi:10.1016/j.bone.2015.11.013
5. Meunier P, Aaron J, Edouard C, Vignon G. Osteoporosis and the replacement of cell populations of the marrow by adipose tissue. *Clin Orthop Relat Res* (1971) 80:147–54. doi:10.1097/00003086-197110000-00021
6. Schellinger D, Lin CS, Hatipoglu HG, Fertikh D. Potential value of vertebral proton MR spectroscopy in determining bone weakness. *AJNR Am J Neuroradiol* (2001) 22:1620–7.
7. Justesen J, Stenderup K, Ebbesen E, Mosekilde L, Steiniche T, Kasse M. Adipocyte tissue volume in bone marrow is increased with aging and in patients with osteoporosis. *Biogerontol* (2001) 2:165–71. doi:10.1023/A:1011513223894
8. Verma S, Rajaratnam JH, Denton J, Hoyland JA, Byers RJ. Adipocytic proportion of bone marrow is inversely related to bone formation in osteoporosis. *J Clin Pathol* (2002) 55:693–8. doi:10.1136/jcp.55.9.693
9. Patsch JM, Li X, Baum T, Yap SP, Karampinos DC, Schwartz AV, et al. Bone marrow fat composition as a novel imaging biomarker in postmenopausal women with prevalent fragility fractures. *J Bone Miner Res* (2013) 28(8):1721–8. doi:10.1002/jbmr.1950
10. Nuttall M, Gimble J. Is there a therapeutic opportunity to either prevent or treat osteopenic disorders by inhibiting marrow adipogenesis? *Bone* (2000) 27:177–84. doi:10.1016/S8756-3282(00)00317-3
11. Minaire P, Meunier P, Edouard C, Berbard J, Courpron J, Bourret J. Quantitative histological data on disuse osteoporosis. *Calcif Tissue Res* (1974) 13:371–82.
12. Devlin MJ, Cloutier AM, Thomas NA, Panus DA, Lotinun S, Pinz I, et al. Caloric restriction leads to high marrow adiposity and low bone mass in growing mice. *J Bone Miner Res* (2010) 25:2078–88. doi:10.1002/jbmr.82
13. Cawthorn WP, Scheller EL, Learman BS, Parlee SD, Simon BR, Mori H, et al. Bone marrow adipose tissue is an endocrine organ that contributes to increased circulating adiponectin during caloric restriction. *Cell Metab* (2014) 20:368–75. doi:10.1016/j.cmet.2014.06.003
14. Wronski T, Morey-Holton E, Jee W. Skeletal alterations in rats during spaceflight. *Adv Space Res* (1981) 1:135–40. doi:10.1016/0273-1177(81)90254-4

15. Cui Q, Wang GJ, Balian G. Pluripotential marrow cells produce adipocytes when transplanted into steroid-treated mice. *Connect Tissue Res* (2000) 41:45–56. doi:10.3109/03008200009005641
16. Akune T, Ohba S, Kamekura S, Yamaguchi M, Chung UI, Kubota N, et al. PPAR gamma insufficiency enhances osteogenesis through osteoblast formation from bone marrow progenitors. *J Clin Invest* (2004) 113:846–55. doi:10.1172/JCI200419900
17. Li X, Cui Q, Kao C, Wang GJ, Balian G. Lovastatin inhibits adipogenic and stimulates osteogenic differentiation by suppressing PPARgamma2 and increasing Cbfa1/Runx2 expression in bone marrow mesenchymal cell cultures. *Bone* (2003) 33:652–9. doi:10.1016/S8756-3282(03)00239-4
18. Abdallah BM, Haack-Sørensen M, Fink T, Kassem M. Inhibition of osteoblast differentiation but not adipocyte differentiation of mesenchymal stem cells by sera obtained from aged females. *Bone* (2006) 39:181–8. doi:10.1016/j.bone.2005.12.082
19. Singh L, Brennan TA, Russell E, Kim JH, Chen Q, Brad Johnson F, et al. Aging alters bone-fat reciprocity by shifting in vivo mesenchymal precursor cell fate towards an adipogenic lineage. *Bone* (2016) 85:29–36. doi:10.1016/j.bone.2016.01.014
20. McGee-Lawrence ME, Carpio LR, Schulze RJ, Pierce JL, McNiven MA, Farr JN, et al. Hdac3 deficiency increases marrow adiposity and induces lipid storage and glucocorticoid metabolism in osteochondroprogenitor cells. *J Bone Miner Res* (2016) 31:116–28. doi:10.1002/jbmr.2602
21. Tuttle LJ, Sinacore DR, Mueller MJ. Intermuscular adipose tissue is muscle specific and associated with poor functional performance. *J Aging Res* (2012) 2012:172957. doi:10.1155/2012/172957
22. Delmonico MJ, Harris TB, Visser M, Park SW, Conroy MB, Velasquez-Mieyer P, et al. Longitudinal study of muscle strength, quality, and adipose tissue infiltration. *Am J Clin Nutr* (2009) 90:1579–85. doi:10.3945/ajcn.2009.28047
23. Gueugneau M, Coudy-Gandilhon C, Théron L, Meunier B, Barboiron C, Combaret L, et al. Skeletal muscle lipid content and oxidative activity in relation to muscle fiber type in aging and metabolic syndrome. *J Gerontol A Biol Sci Med Sci* (2015) 70:566–76. doi:10.1093/gerona/glu086
24. Miljkovic I, Kuipers AL, Cauley JA, Prasad T, Lee CG, Ensrud KE, et al. Greater skeletal muscle fat infiltration is associated with higher all-cause and cardiovascular mortality in older men. *J Gerontol A Biol Sci Med Sci* (2015) 70:1133–40. doi:10.1093/gerona/glv027
25. Choi SJ, Files DC, Zhang T, Wang ZM, Messi ML, Gregory H, et al. Intramyocellular lipid and impaired myofiber contraction in normal weight and obese older adults. *J Gerontol A Biol Sci Med Sci* (2016) 71:557–64. doi:10.1093/gerona/glv169
26. Reinders I, Murphy RA, Brouwer IA, Visser M, Launer L, Siggeirsdottir K, et al. Muscle quality and myosteatosis: novel associations with mortality risk: the age, gene/environment susceptibility (AGES)-Reykjavik study. *Am J Epidemiol* (2016) 183:53–60. doi:10.1093/aje/kwv153
27. Lang T, Cauley JA, Tylavsky F, Bauer D, Cummings S, Harris TB, et al. Computed tomographic measurements of thigh muscle cross-sectional area and attenuation coefficient predict hip fracture: the health, aging, and body composition study. *J Bone Miner Res* (2010) 25(3):513–9. doi:10.1359/jbmr.090807
28. Komolka K, Albrecht E, Wimmers K, Michal JJ, Maak S. Molecular heterogeneities of adipose depots – potential effects on adipose-muscle cross-talk in humans, mice and farm animals. *J Genomics* (2014) 2:31–44. doi:10.7150/jgen.5260
29. Kindler JM, Lewis RD, Hamrick MW. Skeletal muscle and pediatric bone development. *Curr Opin Endocrinol Diabetes Obes* (2015) 22:467–74. doi:10.1097/MED.0000000000000201
30. Rivas DA, McDonald DJ, Rice NP, Haran PH, Dolnikowski GG, Fielding RA. Diminished anabolic signaling response to insulin induced by intramuscular lipid accumulation is associated with inflammation in aging but not obesity. *Am J Physiol Regul Integr Comp Physiol* (2016) 310:R561–9. doi:10.1152/ajpregu.00198.2015
31. Shulman GI. Ectopic fat in insulin resistance, dyslipidemia, and cardiometabolic disease. *N Engl J Med* (2014) 371:1131–41. doi:10.1056/NEJMra1011035
32. Uezumi A, Fukada S, Yamamoto N, Takeda S, Tsuchida K. Mesenchymal progenitors distinct from satellite cells contribute to ectopic fat cell formation in skeletal muscle. *Nat Cell Biol* (2010) 12:143–52. doi:10.1038/ncb2014
33. Penton CM, Thomas-Ahner JM, Johnson EK, McAllister C, Montanaro F. Muscle side population cells from dystrophic or injured muscle adopt a fibro-adipogenic fate. *PLoS One* (2013) 8:e54553. doi:10.1371/journal.pone.0054553
34. Dong Y, Silva KA, Dong Y, Zhang L. Glucocorticoids increase adipocytes in muscle by affecting IL-4 regulated FAP activity. *FASEB J* (2014) 28:4123–32. doi:10.1096/fj.14-254011
35. Farup J, Madaro L, Puri PL, Mikkelsen UR. Interactions between muscle stem cells, mesenchymal-derived cells and immune cells in muscle homeostasis, regeneration and disease. *Cell Death Dis* (2015) 6:e1830. doi:10.1038/cddis.2015.198
36. Agley CC, Rowlerson AM, Velloso CP, Lazarus NR, Harridge SD. Human skeletal muscle fibroblasts, but not myogenic cells, readily undergo adipogenic differentiation. *J Cell Sci* (2013) 126(Pt 24):5610–25. doi:10.1242/jcs.132563
37. Weinstein RS, Wan C, Liu Q, Wang Y, Almeida M, O'Brien CA, et al. Endogenous glucocorticoids decrease skeletal angiogenesis, vascularity, hydration, and strength in aged mice. *Aging Cell* (2010) 9:147–61. doi:10.1111/j.1474-9726.2009.00545.x
38. Pannerec A, Formicola L, Besson V, Marazzi G, Sassoon DA. Defining skeletal muscle resident progenitors and their cell fate potentials. *Development* (2013) 140:2879–91. doi:10.1242/dev.089326
39. Birbrair A, Zhang T, Wang ZM, Messi ML, Enikolopov GN, Mintz A, et al. Role of pericytes in skeletal muscle regeneration and fat accumulation. *Stem Cells Dev* (2013) 22:2298–314. doi:10.1089/scd.2012.0647
40. Bennett CN, Longo KA, Wright WS, Suva LJ, Lane TF, Hankenson KD, et al. Regulation of osteoblastogenesis and bone mass by Wnt10b. *Proc Natl Acad Sci U S A* (2005) 102:3324–9. doi:10.1073/pnas.0408742102
41. Taylor-Jones JM, McGehee RE, Rando TA, Lecka-Czernik B, Lipschitz DA, Peterson CA. Activation of an adipogenic program in adult myoblasts with age. *Mech Ageing Dev* (2002) 123:649–61. doi:10.1016/S0047-6374(01)00411-0
42. Abiola M, Favier M, Christodoulou-Vafeiadou E, Pichard AL, Martelly I, Guillet-Deniau I. Activation of Wnt/beta-catenin signaling increases insulin sensitivity through a reciprocal regulation of Wnt10b and SREBP-1c in skeletal muscle cells. *PLoS One* (2009) 4(12):e8509. doi:10.1371/journal.pone.0008509
43. Xu Y, Hammerick KE, James AW, Carre AL, Leucht P, Giaccia AJ, et al. Inhibition of histone deacetylase activity in reduced oxygen environment enhances the osteogenesis of mouse adipose-derived stromal cells. *Tissue Eng Part A* (2009) 15:3697–707. doi:10.1089/ten.TEA.2009.0213
44. Saccone V, Consalvi S, Giordani L, Mozzetta C, Barozzi I, Sandoná M, et al. HDAC-regulated myomiRs control BAF60 variant exchange and direct the functional phenotype of fibro-adipogenic progenitors in dystrophic muscles. *Genes Dev* (2014) 28:841–57. doi:10.1101/gad.234468.113
45. Hamrick MW, Della-Fera MA, Choi YH, Pennington C, Hartzell D, Baile CA. Leptin treatment induces loss of bone marrow adipocytes and increases bone formation in leptin-deficient ob/ob mice. *J Bone Miner Res* (2005) 20:994–1001. doi:10.1359/JBMR.050103
46. Yue R, Zhou BO, Shimada IS, Zhao Z, Morrison SJ. Leptin receptor promotes adipogenesis and reduces osteogenesis by regulating mesenchymal stromal cells in adult bone marrow. *Cell Stem Cell* (2016) 18(6):782–96. doi:10.1016/j.stem.2016.02.015
47. Arounleut P, Bowser M, Upadhyay S, Shi X-M, Fulzele S, Johnson M, et al. Absence of functional leptin receptor isoforms in the POUND (Lepr db/lb) mouse is associated with muscle atrophy and altered myoblast proliferation and differentiation. *PLoS One* (2013) 8:e72330. doi:10.1371/annotation/3a7d6e24-137c-4603-93ca-879bec7fab80
48. Devlin MJ. Why does starvation make bones fat? *Am J Hum Biol* (2011) 23(5):577–85. doi:10.1002/ajhb.21202
49. Shaw CS, Clark J, Wagenmakers AJ. The effect of exercise and nutrition on intramuscular fat metabolism and insulin sensitivity. *Annu Rev Nutr* (2010) 30:13–34. doi:10.1146/annurev.nutr.012809.104817
50. Cree M, Paddon-Jones D, Newcomer B, Ronsen O, Aarsland A, Wolfe R, et al. Twenty-eight-day bed rest with hypercortisolemia induces peripheral insulin resistance and increases intramuscular triglycerides. *Metabolism* (2010) 59:703–10. doi:10.1016/j.metabol.2009.09.014
51. Muir J, Judex S, Qin YX, Rubin C. Postural instability caused by extended bed rest is alleviated by brief daily exposure to low magnitude mechanical signals. *Gait Posture* (2011) 33:429–35. doi:10.1016/j.gaitpost.2010.12.019

52. Leite RD, Prestes J, Bernardes CF, Shiguemoto GE, Pereira GB, Duarte JO, et al. Effects of ovariectomy and resistance training on lipid content in skeletal muscle, liver, and heart; fat depots; and lipid profile. *Appl Physiol Nutr Metab* (2009) 34:1079–86. doi:10.1139/H09-116
53. Frechette DM, Krishnamoorthy D, Adler BJ, Chan ME, Rubin CT. Diminished satellite cells and elevated adipogenic gene expression in muscle as caused by ovariectomy are averted by low-magnitude mechanical signals. *J Appl Physiol* (2015) 119:27–36. doi:10.1152/japplphysiol.01020.2014
54. Chang D, Joseph DJ, Ebert MA, Galvão DA, Taaffe DR, Denham JW, et al. Effect of androgen deprivation therapy on muscle attenuation in men with prostate cancer. *J Med Imaging Radiat Oncol* (2014) 58:223–8. doi:10.1111/1754-9485.12124
55. Scheller EL, Troiano N, Vanhoutan JN, Bouxsein MA, Fretz JA, Xi Y, et al. Use of osmium tetroxide staining with microcomputerized tomography to visualize and quantify bone marrow adipose tissue in vivo. *Methods Enzymol* (2014) 537:123–39. doi:10.1016/B978-0-12-411619-1.00007-0
56. Novotny SA, Warren GL, Hamrick MW. Aging and the muscle-bone relationship. *Physiology (Bethesda)* (2015) 30(1):8–16. doi:10.1152/physiol.00033.2014
57. Mastrocola R, Collino M, Nigro D, Chiazza F, D'Antona G, Aragno M, et al. Accumulation of advanced glycation end-products and activation of the SCAP/SREBP lipogenetic pathway occur in diet-induced obese mouse skeletal muscle. *PLoS One* (2015) 10(3):e0119587. doi:10.1371/journal.pone.0119587
58. Reid KF, Fielding RA. Skeletal muscle power: a critical determinant of physical functioning in older adults. *Exerc Sport Sci Rev* (2012) 40:4–12. doi:10.1097/JES.0b013e31823b5f13
59. Yamanouchi K, Yada E, Ishiguro N, Hosoyama T, Nishihara M. Increased adipogenicity of cells from regenerating skeletal muscle. *Exp Cell Res* (2006) 312:2701–11. doi:10.1016/j.yexcr.2006.04.014
60. Hosoyama T, Ishiguro N, Yamanouchi K, Nishihara M. Degenerative muscle fiber accelerates adipogenesis of intramuscular cells via RhoA signaling pathway. *Differentiation* (2009) 77:350–9. doi:10.1016/j.diff.2008.11.001
61. Gumucio JP, Korn MA, Saripalli AL, Flood MD, Phan AC, Roche SM, et al. Aging-associated exacerbation in fatty degeneration and infiltration after rotator cuff tear. *J Shoulder Elbow Surg* (2014) 23:99–108. doi:10.1016/j.jse.2013.04.011
62. Davis ME, Korn MA, Gumucio JP, Harning JA, Saripalli AL, Bedi A, et al. Simvastatin reduces fibrosis and protects against muscle weakness after massive rotator cuff tear. *J Shoulder Elbow Surg* (2015) 24:280–7. doi:10.1016/j.jse.2014.06.048
63. Gerber C, Schneeberger AG, Hoppeler H, Meyer DC. Correlation of atrophy and fatty infiltration on strength and integrity of rotator cuff repairs: a study in thirteen patients. *J Shoulder Elbow Surg* (2007) 16(6):691–6. doi:10.1016/j.jse.2007.02.122
64. Gladstone JN, Bishop JY, Lo IK, Flatow EL. Fatty infiltration and atrophy of the rotator cuff do not improve after rotator cuff repair and correlate with poor functional outcome. *Am J Sports Med* (2007) 35(5):719–28. doi:10.1177/0363546506297539
65. Lin TT, Lin CH, Chang CL, Chi CH, Chang ST, Sheu WH. The effect of diabetes, hyperlipidemia, and statins on the development of rotator cuff disease: a nationwide, 11-year, longitudinal, population-based follow-up study. *Am J Sports Med* (2015) 43:2126–32. doi:10.1177/0363546515588173
66. Prior SJ, Joseph LJ, Brandauer J, Katzel LI, Hagberg JM, Ryan AS. Reduction in midthigh low-density muscle with aerobic exercise training and weight loss impacts glucose tolerance in older men. *J Clin Endocrinol Metab* (2007) 92:880–6. doi:10.1210/jc.2006-2113
67. Marcus RL, Addison O, Kidde JP, Dibble LE, Lastayo PC. Skeletal muscle fat infiltration: impact of age, inactivity, and exercise. *J Nutr Health Aging* (2010) 14:362–6. doi:10.1007/s12603-010-0081-2
68. Goodpaster BH, Chomentowski P, Ward BK, Rossi A, Glynn NW, Delmonico MJ, et al. Effects of physical activity on strength and skeletal muscle fat infiltration in older adults: a randomized controlled trial. *J Appl Physiol* (2008) 105:1498–503. doi:10.1152/japplphysiol.90425.2008
69. Taaffe DR, Henwood TR, Nalls MA, Walker DG, Lang TF, Harris TB. Alterations in muscle attenuation following detraining and retraining in resistance-trained older adults. *Gerontology* (2009) 55:217–23. doi:10.1159/000182084
70. Feskanich D, Willett W, Colditz G. Walking and leisure-time activity and risk of hip fracture in postmenopausal women. *JAMA* (2002) 288:2300–6. doi:10.1001/jama.288.18.2300
71. Michaëlsson K, Olofsson H, Jensevik K, Larsson S, Mallmin H, Berglund L, et al. Leisure physical activity and the risk of fracture in men. *PLoS Med* (2007) 4(6):e199. doi:10.1371/journal.pmed.0040199
72. Fielding RA, LeBrasseur NK, Cuoco A, Bean J, Mizer K, Fiatarone Singh MA. High-velocity resistance training increases skeletal muscle peak power in older women. *J Am Geriatr Soc* (2002) 50:655–62. doi:10.1046/j.1532-5415.2002.50159.x
73. Leenders M, Verdijk LB, van der Hoeven L, van Kranenburg J, Nilwik R, van Loon LJ. Elderly men and women benefit equally from prolonged resistance-type exercise training. *J Gerontol A Biol Sci Med Sci* (2013) 68:769–79. doi:10.1093/gerona/gls241
74. Lieberman DE, Pearson OM, Polk JD, Demes B, Crompton AW. Optimization of bone growth and remodeling in response to loading in tapered mammalian limbs. *J Exp Biol* (2003) 206(Pt 18):3125–38. doi:10.1242/jeb.00514
75. Novotny SA, Mader TL, Greising AG, Lin AS, Guldberg RE, Warren GL, et al. Low intensity, high frequency vibration training to improve musculoskeletal function in a mouse model of Duchenne muscular dystrophy. *PLoS One* (2014) 9(8):e104339. doi:10.1371/journal.pone.0104339
76. Xie L, Rubin C, Judex S. Enhancement of the adolescent murine musculoskeletal system using low-level mechanical vibrations. *J Appl Physiol (1985)* (2008) 104:1056–62. doi:10.1152/japplphysiol.00764.2007
77. Krishnamoorthy D, Frechette DM, Adler BJ, Green DE, Chan ME, Rubin CT. Marrow adipogenesis and bone loss that parallels estrogen deficiency is slowed by low-intensity mechanical signals. *Osteoporos Int* (2016) 27:747–56. doi:10.1007/s00198-015-3289-5
78. Rubin CT, Capilla E, Luu YK, Busa B, Crawford H, Nolan DJ, et al. Adipogenesis is inhibited by brief, daily exposure to high-frequency, extremely low-magnitude mechanical signals. *Proc Natl Acad Sci U S A* (2007) 104:17879–84. doi:10.1073/pnas.0708467104

Conflict of Interest Statement: The authors declare that the research was conducted in the absence of any commercial or financial relationships that could be construed as a potential conflict of interest.

frontiers in Endocrinology

ORIGINAL RESEARCH
published: 03 August 2016
doi: 10.3389/fendo.2016.00108

Vanadate Impedes Adipogenesis in Mesenchymal Stem Cells Derived from Different Depots within Bone

*Frans Alexander Jacobs, Hanél Sadie-Van Gijsen, Mari van de Vyver and William Frank Ferris**

Department of Medicine, Division of Endocrinology, Faculty of Medicine and Health Sciences, Stellenbosch University, Cape Town, Western Cape, South Africa

Glucocorticoid-induced osteoporosis (GIO) is associated with an increase in bone marrow adiposity, which skews the differentiation of mesenchymal stem cell (MSC) progenitors away from osteoblastogenesis and toward adipogenesis. We have previously found that vanadate, a non-specific protein tyrosine phosphatase inhibitor, prevents GIO in rats, but it was unclear whether vanadate directly influenced adipogenesis in bone-derived MSCs. For the present study, we investigated the effect of vanadate on adipogenesis in primary rat MSCs derived from bone marrow (bmMSCs) and from the proximal end of the femur (pfMSCs). By passage 3 after isolation, both cell populations expressed the MSC cell surface markers CD90 and CD106, but not the hematopoietic marker CD45. However, although variable, expression of the fibroblast marker CD26 was higher in pfMSCs than in bmMSCs. Differentiation studies using osteogenic and adipogenic induction media (OM and AM, respectively) demonstrated that pfMSCs rapidly accumulated lipid droplets within 1 week of exposure to AM, while bmMSCs isolated from the same femur only formed lipid droplets after 3 weeks of AM treatment. Conversely, pfMSCs exposed to OM produced mineralized extracellular matrix (ECM) after 3 weeks, compared to 1 week for OM-treated bmMSCs. Vanadate (10 μM) added to AM resulted in a significant reduction in AM-induced intracellular lipid accumulation and expression of adipogenic gene markers (PPARγ2, aP2, adipsin) in both pfMSCs and bmMSCs. Pharmacological concentrations of glucocorticoids (1 μM) alone did not induce lipid accumulation in either bmMSCs or pfMSCs, but resulted in significant cell death in pfMSCs. Our findings demonstrate the existence of at least two fundamentally different MSC depots within the femur and highlights the presence of MSCs capable of rapid adipogenesis within the proximal femur, an area prone to osteoporotic fractures. In addition, our results suggest that the increased bone marrow adiposity observed in GIO may not be solely due to direct effect of glucocorticoids on bone-derived MSCs, and that an increase in femur lipid content may also arise from increased adipogenesis in MSCs residing outside of the bone marrow niche.

Keywords: mesenchymal stem cells, bone, vanadate, adipogenesis, glucocorticoids

OPEN ACCESS

Edited by:
William Peter Cawthorn, University of Edinburgh, UK

Reviewed by:
Jan Tuckermann, University of Ulm, Germany
Antonia Sophocleous, University of Edinburgh, UK

***Correspondence:**
William Frank Ferris
wferris@sun.ac.za

Specialty section:
This article was submitted to Bone Research, a section of the journal Frontiers in Endocrinology

Received: *03 May 2016*
Accepted: *22 July 2016*
Published: *03 August 2016*

Citation:
Jacobs FA, Sadie-Van Gijsen H, van de Vyver M and Ferris WF (2016) Vanadate Impedes Adipogenesis in Mesenchymal Stem Cells Derived from Different Depots within Bone. Front. Endocrinol. 7:108. doi: 10.3389/fendo.2016.00108

INTRODUCTION

Glucocorticoids (GCs) are widely used to treat a variety of inflammatory disorders, but chronic GC use can reduce bone mineral density (BMD) and lead to GC-induced osteoporosis (GIO) through an increase in bone resorption and a decrease in bone formation (1, 2). The GC-induced decrease in formation may arise from a reduction in the pool of mesenchymal stem cells (MSCs) available for osteoblastic differentiation, resulting in smaller numbers of mature bone-forming osteoblasts (1, 2).

Osteoblasts arise from multipotent MSCs, which can also differentiate into other cell-types, including adipocytes and chondrocytes (3, 4), with several lines of evidence indicating an inverse reciprocal relationship between osteoblast and adipocyte differentiation (5). Several mechanisms have been identified whereby GCs may reduce the number of osteoprogenitor cells in bone. *In vitro* studies have suggested that GCs may reduce the number of MSCs destined for osteoblastogenesis by shifting the differentiation potential of MSCs preferentially toward adipogenesis (6, 7), and this is in agreement with *in vivo* observations of GC-induced increases in marrow adiposity (8). In addition, we have previously documented the anti-proliferative effects of GCs in Naïve adipose-derived MSCs and in partially differentiated osteoblasts derived from these cells (9). Evidence from *in vivo* studies in mice and *in vitro* studies on osteoblast cell-lines indicate that GCs may also directly cause apoptosis in osteoprogenitors, osteoblasts, and osteocytes (10, 11). Taken together, these findings indicate that GCs have many deleterious effects on MSCs and on cells committed to the osteoblastic lineage, and that the prevention of these effects may restore both the number of MSCs available for osteoblastic differentiation and the number of functional osteoblasts in bone.

Earlier work in animal models found that GIO could be prevented by the non-selective protein tyrosine phosphatase inhibitor sodium orthovanadate (12), although the mechanism was not described in detail. It was subsequently shown that vanadate inhibited apoptosis of cultured osteoblasts *in vitro* and of osteocytes *in vivo* (10). Vanadate has also been shown to counteract the anti-proliferative effects of GCs on Naïve MSCs and pre-osteoblasts (9), and to inhibit adipocytic differentiation in the 3T3-L1 pre-adipocyte cell line (13). Vanadate is therefore an attractive candidate for the prevention of GIO by reversing or counteracting the effects of GCs on osteoblast precursors, possibly through a variety of mechanisms.

The aim of this study was to examine the effects of supra-physiological doses of GCs and vanadate on primary bone-derived MSCs, with a view of further understanding the etiology of GIO and how vanadate ameliorates GC-induced bone disease. Bone-derived MSCs can be isolated and cultured from various parts of long bones, including bone marrow (14), compact bone (15), the periosteal layer (16), or the epiphysis of long bones (17). However, many of these studies reported subtle differences between bone marrow-derived MSCs (bmMSCs) and MSCs derived from other areas of bone, suggesting that not all MSCs populations within bone are identical and that these different populations may respond differently during disease progression and pharmacological treatments (15–17). The typical bmMSC isolation procedure utilizes the diaphysis (shaft) of the femur, thereby excluding the proximal region of the femur, which is particularly susceptible to fracture during GIO compared to other bone sites (18, 19). We have therefore isolated MSCs from the proximal region of the femur (pfMSCs) and compared these cells with bmMSCs in order to investigate whether these two osteoprogenitor populations may differ in their responses to GCs and vanadate.

MATERIALS AND METHODS

Experimental Animals

Experiments involving animals were approved by Stellenbosch University Ethics Committee and performed in accordance with the South African Medical Research Council Guidelines on Ethics for Medical Research in compliance with the South African Animal Protection Act (Act No. 71 of 1962). Adult male Wistar rats [12 weeks old, ~250 g mass, housed at the Stellenbosch University Animal Facility and fed *ad libitum* on standard laboratory chow (Rat and Mouse Breeder Feed, Animal Specialities, Pty. Ltd., Klapmuts, South Africa)], were used for all experiments. Animals were sacrificed *via* intraperitoneal injection with 12 mg kg^{-1} sodium pentobarbitone (Eutha-naze, Bayer, South Africa) and the femora subsequently excised.

Cell Culture

Isolation of MSCs

Bone marrow-derived MSCs were isolated using a protocol that was adapted from Nadri et al. (14) and Zhu et al. (15): The tendon and muscle tissue on the femoral surface were manually removed with sterile gauze. The ends of the bones were cleaved off at the greater trochanter and saved for the isolation of pfMSCs. The bone marrow cavity was then flushed with cell isolation media [Dulbecco's Modified Eagle Medium (DMEM) (Lonza, Verviers, Belgium)] containing 1% Penicillin/Streptomycin (P/S) (Lonza) and 20% fetal bovine serum (FBS) (Biochrom, Berlin, Germany) into a 100-mm cell culture dish using a syringe. Bone marrow from both femora was pooled and subsequently incubated overnight at 37°C in 95% humidified air containing 5% CO_2. The following day, the culture was washed once with PBS to remove any non-adherent cells and debris, and subsequently cultured in growth media (DMEM with P/S supplemented with 10% FBS). For the isolation of pfMSCs, the protocol was adapted from Zhu et al. (15). The proximal region of the femur was macerated into 1 mm^3 fragments and digested at 37°C for 60 min in 10 ml Hanks' Balanced Salt Solution (Lonza) containing 0.075% (w/v) collagenase I (#CLS1, Worthington, Lakewood, NJ, USA) and 1.5% bovine serum albumin (BSA). The digested proximal femur fragments were then washed five times in DMEM and seeded in a cell culture dish with cell isolation media. After 24 h, non-adherent material was washed off with PBS and the media replaced with standard growth media.

Subculturing and Maintenance

All cell cultures were maintained at 37°C with 5% CO_2 and 95% humidified air. Once the MSC cultures reached approximately

80% confluence, the cells were dissociated using 0.5% trypsin solution (Lonza) and sub-cultured at a dilution of 1:4. MSC cultures were expanded to passage 3 before being used for further experiments.

MSC Differentiation and Cytological Staining

All constituents of the differentiation media were purchased from Sigma-Aldrich (Schnelldorf, Germany). Differentiation experiments were performed in six-well cell culture-treated dishes (Porvair, UK). For osteoblastic differentiation, the protocol was adapted from Jaiswal et al. (20). In brief, bmMSCs were cultured to confluence before being treated with osteogenic media (OM), which consisted of growth media supplemented with 50 μM ascorbic acid, 10 mM β-glycerophosphate, and 10 nM dexamethasone, with a final ethanol concentration of 0.1%. For negative vehicle controls, cells were treated with growth media containing 0.1% ethanol. OM was replaced twice a week for the duration of osteoblastic differentiation. Once osteoblastic differentiation was complete (after day 7 for bmMSCs and day 21 for pfMSCs), mineralized extracellular deposits were stained with Alizarin Red S (Amresco, USA), using a protocol adapted from Gregory et al. (21). Briefly, cells were fixed in 70% ethanol for 10 min and stained with 40 mM Alizarin Red S dissolved in water (pH adjusted to 4.1 with 5% NH_4OH). Excess stain was removed after 1 h, and the samples were washed twice with water. PBS (1 ml) was added to each stained well before image capturing using an Olympus CKX41 microscope (CKX41, CachN 10×/0.25 PhP objective) and a Canon EOS 600D camera.

For adipocytic differentiation, the protocol was adapted from Ogawa et al. (22). MSCs at passage 3 were cultured to 2 days post-confluence before being treated with adipogenic media (AM), which consisted of growth media supplemented with 1 μM dexamethasone, 50 μM ascorbic acid, 56 μM indomethacin, 10 μM insulin, and 0.5 mM 3-isobutyl-1-methylxanthine. The AM was replaced every 2–3 days for the duration of differentiation. For concomitant vanadate treatments, a stock solution of 10 mM sodium orthovanadate was dissolved in water and boiled as per manufacturer's instructions (Sigma-Aldrich, Schnelldorf, Germany), and aliquots were stored at −20°C. Intracellular lipid droplets were stained with filtered 0.7% (w/v) Oil Red O (Sigma-Aldrich) in 70% isopropanol for 30 min and subsequently washed three times with water before images were captured as described above (23). For quantification of staining, isopropanol was used to extract the bound Oil Red O, and the absorbance of the extracted dye was measured at 510 nm. To correct for differences in cell density, the cells were re-stained with 0.1% (w/v) Crystal Violet (CV) nuclear stain, which was extracted with 75% ethanol, and the absorbance of the extracted dye was measured at 570 nm. Oil Red O absorption values were normalized against corresponding crystal violet absorption values (ORO/CV) and expressed as the relative triglyceride content.

Characterization of MSC Populations using Flow Cytometry

Bone marrow-derived MSCs and pfMSCs (80% confluent; passage 3) were harvested by trypsinisation and re-suspended in PBS containing 1% BSA (Sigma-Aldrich, Berlin, Germany). Cell suspensions at a concentration of 1×10^6 cells per 100 μl were co-labeled with mouse anti-rat Alexa Fluor 647-conjugated CD106 (AbDSerotec #MCA4633A647T), FITC-conjugated CD90 (BD Pharmingen, # 554897), V450-conjugated CD45 (BD Horizon, # 561587), and PE-conjugated CD26 (BD Pharmingen, # 559641). Flow cytometry was performed on a BD FACS Canto II instrument using FACSDiva software. A total of 15 000 events were recorded prior to data analysis. Since a multicolor cytometric analysis was carried out, fluorescent compensation settings were established through a compensation experiment, and regions of positive and negative staining were determined through a fluorochrome minus one (FMO) experiment. An unstained control sample was used as a negative control for gating purposes, and to measure forward and side scatter. Data analysis was performed using Flow Jo Vx (Treestar, Oregon, USA) software.

Cell Viability

Cells at passage 3 were grown to 2 days post-confluence before being treated with 1 μM dexamethasone, in the absence or presence of 10 μM vanadate, for 7 days. For crystal violet (CV) staining, samples were fixed in 70% ethanol, stained with 0.1% CV for 5 min, and washed three times with PBS before images were captured as described above (see MSC Differentiation and Cytological Staining). Crystal violet was then extracted with 75% ethanol and the absorbance measured at 570 nm. The MTT assay protocol was adapted from the MTT-based *in vitro* toxicology assay kit from Sigma-Aldrich. Cells at passage 3 were seeded into 96-well plates and treatments commenced at 2 days post-confluence. Cells were treated for 7 days, after which 10 μl of 5 mg/ml MTT stock solution was added to each well and incubated for 2 h. The color reaction was stopped by the addition of 100 μl of 10% Triton X-100 plus 0.1N HCL in isopropanol, and samples were incubated on a plate shaker until the color product was completely dissolved. The color development was quantified spectrophotometrically at 570 nm, and background absorbance at 690 nm was subtracted from each well.

Apoptosis Detection

For the detection and quantification of apoptosis, pfMSCs were expanded to passage 3 and grown to 2 days post-confluence before being treated with 1 μM dexamethasone and/or 10 μM vanadate for 7 days. Cells were harvested by trypsinization, subjected to centrifugation at $400 \times g$ for 5 min, and cell pellets were re-suspended in PBS. Apoptosis was measured according to the PE Annexin V Apoptosis Detection Kit I (BD Pharmingen, #559763). Approximately 1×10^6 cells were co-stained with PE-conjugated annexin V (a marker of early apoptosis) and 7-amino-actinomycin (7-AAD: a marker for the loss of membrane integrity and cell death) and incubated in the dark at room temperature for 15 min. Flow cytometry was performed on the FACSCanto II flow cytometer with FACSDiva software, analyzing a total of 10,000 events per sample. Further data analysis was performed on Flow Jo Vx (Treestar) software where early apoptotic cells were characterized as annexin

V^+/7-AAD^-. Gating strategy: Unstained cells were used as a negative control, whereas cells treated with 50 μg/ml cyclohexamide (4, 24, 48 h) to induce apoptosis were used as a positive control for Annexin V staining (data not shown). The positive control for the nuclear stain, 7-AAD, was obtained through prolonged exposure of cells to trypsin in order to permeabilize the cell membrane and allow 7-AAD to penetrate the cells (data not shown).

Gene Expression Analysis (qRT-PCR)

For all gene expression analyses, cells were plated into six-well plates at passage 3. Cells were prepared for RNA extraction by lysis in Qiagen (Berlin, Germany) buffer RLT and then stored at −80°C until required. Total RNA was purified using the Qiagen RNeasy Mini kit (#74106), and 1 μg total RNA was treated with 1 U of Promega (Madison, Wisconsin, USA) RQ1 RNase-free DNase, as per manufacturer's instructions. The DNase-treated RNA samples were used as a template for cDNA synthesis, using 20-(dT) as a primer with Promega ImProm-II reverse transcriptase. Real-time semi-quantitative RT-PCR (qRT-PCR) was performed on a Rotor-Gene 6000 (Corbett Life Science) using the Quantace Sensimix No-ROX kit (Bioline, London, England). Sequences for gene-specific primers can be found in **Table 1**. Relative gene expression levels were calculated according to the ΔCt method (24) and normalized to the expression of the housekeeping gene ARBP (25).

TABLE 1 | Primer sequences used in qRT-PCR.

Gene name (*symbol*)	Ref Seq no.	Primer sequences (5′-3′)	Product size (bp)
PPARγ2 (*Pparg*) (26)	NM_013124.3	F: ACTGCCTATGAGCACTTCAC R: CAATCGGATGGTTCTTCGGA	448
C/EBPα (*Cebpa*) (26)	NM_012524.3	F: TGGACAAGAACAGCAACGAG R: AATCTCCTAGTCCTGGCTTG	360
aP2[a] (*Fabp4*) (27)	NM_053365.1	F: TGAAATCACCCCAGATGACAG R: CTCATGCCCTTTCATAAACT	185
Adipsin[b] (*Cfd*)	NM_001077642.1	F: CACGTGTGCGGTGGCACCCTG R: CCCCTGCAAGTGTCCCTGCGGT	475
ARBP (*Rplp0*) (25)	NM_022402.2	F: AAAGGGTCCTGGCTTTGTCT R: GCAAATGCAGATGGATCG	91
Fatty acid synthase[c] (*Fasn*)	NM_017332.1	F: GGCCTGGAGTCTATCATCAA R: CTGCACTCAGGGTGTGAT	148
GLUT4[c] (*Slc2a4*)	NM_012751.1	F: CTTCCTTCTATTTGCCGTCC R: TGCCCCTCAGTCATTCTCAT	190
Msx2 (*Msx2*) (28)	NM_012982.3	F: TCACCACGTCCCAGCTTCTAG R: AGCTTTTCCAGTTCCGCCTCC	178
Runx2/ Cbfa1 (*Runx2*) (29)	NM_001278483.1	F: GCGGACGAGGCAAGAGTT R: TTGGTGCTGAGTTCAGGGAG	252
Wnt10b[b] (*Wnt10b*)	NM_001108111.1	F: TTCCAGCCCCGCCTACGTCCG R: CAGTGGAAACGACAGTGGC	227

[a]*Forward primer designed by authors.*
[b]*Primers designed by authors.*
[c]*Primers derived from Qiagen RT2 Adipogenesis PCR array.*

Statistical Analysis

All statistical analyses were performed with GraphPad Prism version 5.01. All data were expressed as average ± SD, and were analyzed using one-way ANOVA and Bonferroni's multiple comparison test.

RESULTS

Characterization of Isolated MSC Populations

The cell populations isolated from bone marrow and the proximal femur were analyzed at passage 3 using flow cytometry in order to assess the homogeneity of the populations as well as the expression of cell surface markers associated with the MSC phenotype. Both bone marrow-derived and proximal femur-derived cell cultures constituted single homogeneous populations (**Figure 1A**), and both cell-types expressed the MSC cell surface markers CD90 (bmMSCs 90 ± 2.5%; pfMSCs 61 ± 9%) and CD106 (bmMSCs 72 ± 4%; pfMSCs 80 ± 5%), but not the hematopoietic marker CD45 (bmMSCs 8 ± 3%; pfMSCs 12 ± 2%) (**Figure 1B**). Despite biological variability, the overall expression of the fibroblast marker, CD26, was slightly higher in pfMSCs (53 ± 14%) ($n = 8$) than in bmMSCs (37 ± 11%) ($n = 9$) (**Figure 1B**).

Comparison of Differentiation Potential between pfMSCs and bmMSCs

Bone marrow-derived MSCs and pfMSCs were treated with OM and AM to assess the osteoblastic and adipocytic differentiation potential of the cells. BmMSCs rapidly responded to OM treatment and had completely and uniformly mineralized the extracellular matrix within 7 days, while pfMSCs formed individual mineralized nodules after 21 days of OM treatment (**Figure 2**). In contrast, pfMSCs exhibited a strong adipogenic response, with large numbers of lipid-filled cells apparent by day 7, while bmMSCs required 21 days to form intracellular lipid droplets in a few individual cells (**Figure 3**).

The Effect of Vanadate on Adipogenesis in Bone-Derived MSCs

Cytological Staining

In order to determine whether vanadate had an effect on adipogenesis in bone-derived MSCs, pfMSCs and bmMSCs were treated with AM in the absence or presence of 10 μM vanadate (treatment group AMV). Oil Red O staining was significantly decreased by approximately 50% in AMV-treated pfMSCs and bmMSCs, compared to AM-treated cells (**Figure 4**).

Gene Expression Analysis

We hypothesized that the observed partial inhibition of AM-stimulated lipid accumulation may be either due to an effect on one or more molecules in lipid sequestering or synthesizing pathways, or by globally affecting the process of adipogenesis. To ascertain whether vanadate inhibits adipogenesis, and to gain further insight into the possible mechanism(s) involved, the effect

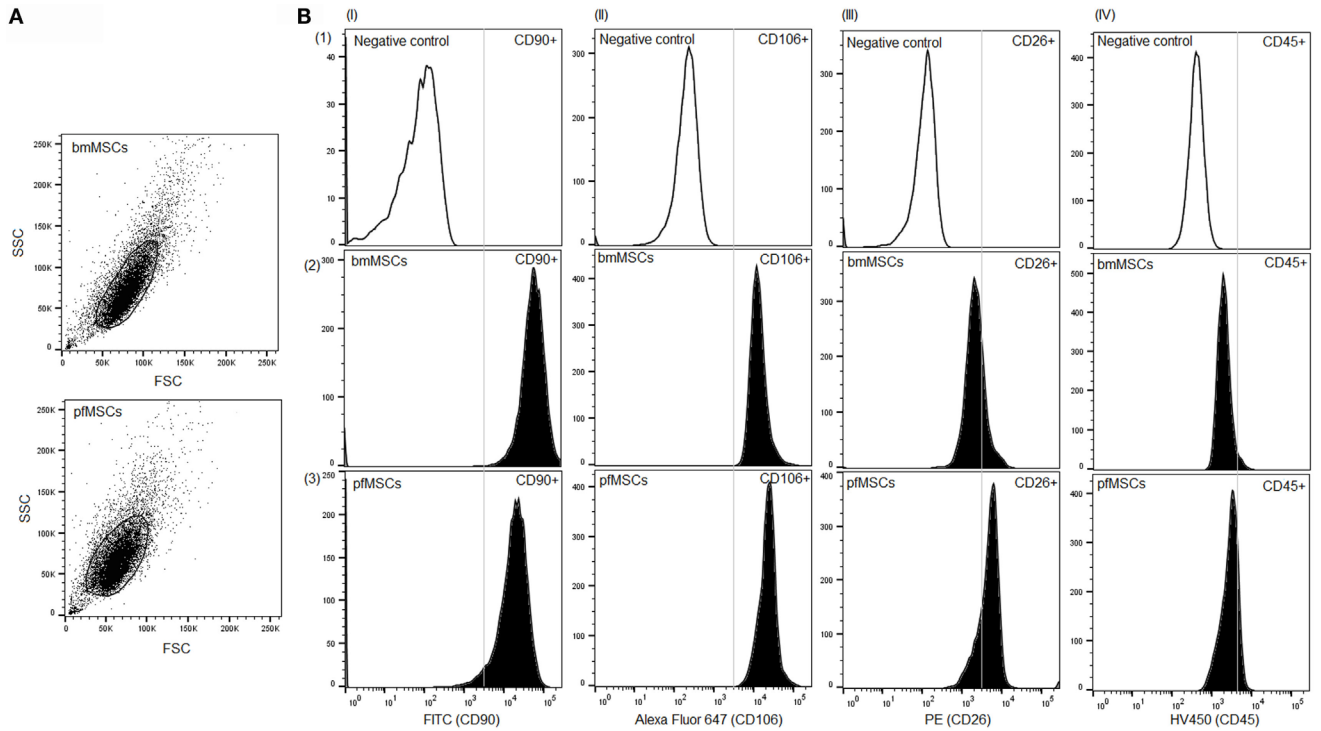

FIGURE 1 | Characterization of bone cell isolates. **(A)** A scatter plot showing homogeneous populations of bone marrow- and proximal femur-derived cells. **(B)** Cell surface expression of the mesenchymal progenitor cell marker CD90 (column I), bmMSC marker CD106 (column II), fibroblast marker CD26 (column III), and the hematopoietic marker CD45 (column IV) was examined using flow cytometry. The first row (1) represents the negative (unstained) control samples, whereas the results for surface marker expression in bmMSCs and pfMSCs are shown in rows 2 and 3, respectively. Regions of positive staining are indicated to the right-hand side of the vertical line. Experiments were repeated in duplicate on MSCs derived from nine animals ($n = 9$), and the graphs show the results for one representative animal. For each experiment 15,000 events were recorded of which 10,000 were gated and analyzed using FlowJo Vx (Treestar) software.

of vanadate on the expression of several adipogenesis-related genes was examined using qRT-PCR.

The expression of the pivotal activator of adipogenesis, PPARγ2, could not be consistently observed in untreated, Naïve pfMSCs, and was completely undetectable in Naïve bmMSCs. However, PPARγ2 expression was induced in pfMSCs after 3 days of AM treatment and was maintained until day 7 (the last time-point examined for pfMSCs) (**Figure 5A**). Vanadate did not affect the initial upregulation of PPARγ2 expression by day 3, but reduced AM-induced PPARγ2 expression by approximately 70% by day 7 (**Figure 5A**). In contrast to the rapid upregulation of PPARγ2 in pfMSCs, PPARγ2 expression was only induced in bmMSCs between 14 and 21 days of AM treatment, and this induction was reduced by 30–60% by vanadate (**Figure 5A**). C/EBPα expression was readily detectable in untreated pfMSCs and bmMSCs (Ct values between 25 and 29), and was upregulated in response to AM at all time-points tested (**Figure 5B**), although the magnitude of the response to AM varied between cell isolates. In pfMSCs, C/EBPα expression exhibited a stronger induction at day 7 of AM treatment than at day 3, and a significant down-regulation with vanadate at day 7 but not at day 3 (**Figure 5B**), similar to that observed for PPARγ2 (**Figure 5A**). In bmMSCs, vanadate also had very little effect on AM-induced C/EBPα expression at earlier time-points (days 7 and 14), but caused a 60–70% reduction in AM-induced C/EBPα expression by day 21 (**Figure 5B**). The late adipogenic markers, aP2/FABP4 (adipocyte protein-2, also known as fatty acid binding protein-4), fatty acid synthase (Fasn) and adipsin, were strongly upregulated in response to AM at day 7 in pfMSCs and day 21 in bmMSCs, although the magnitude of the responses varied dramatically. As was found for the early adipogenic markers examined, vanadate caused a significant decrease in the AM-induced expression of late adipogenic markers in both cell-types (**Figure 6**).

Inherent Differences in Gene Expression Underlying the Variation in Differentiation Potential between pfMSCs and bmMSCs

Given the similarities in the AM-mediated upregulation of adipocyte gene expression in pfMSCs and bmMSCs, and our observations that vanadate had similar inhibitory effects on lipid accumulation and adipogenic gene expression in both cell types, we concluded that it was likely that the mechanisms governing adipogenesis and lipid accumulation were largely the same in both cell types, even though adipogenesis proceeded more rapidly in pfMSCs than in bmMSCs. However, we questioned whether differential expression of specific genes before the initiation of adipogenesis could account for the increased rate of lipid

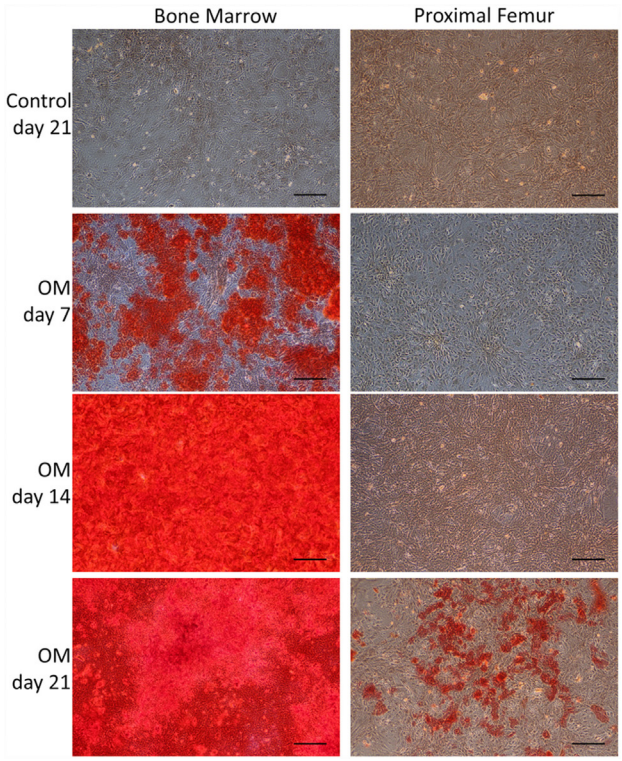

FIGURE 2 | Characterization of the osteoblastic differentiation potential of bmMSCs and pfMSCs. Cells were treated with osteogenic media (OM) as described under Section "Materials and Methods," for the number of days as indicated on the figure, and subsequently stained with Alizarin Red S. Images show representative results of three independent experiments, and were taken at 10× magnification, with the size bar = 1 mm.

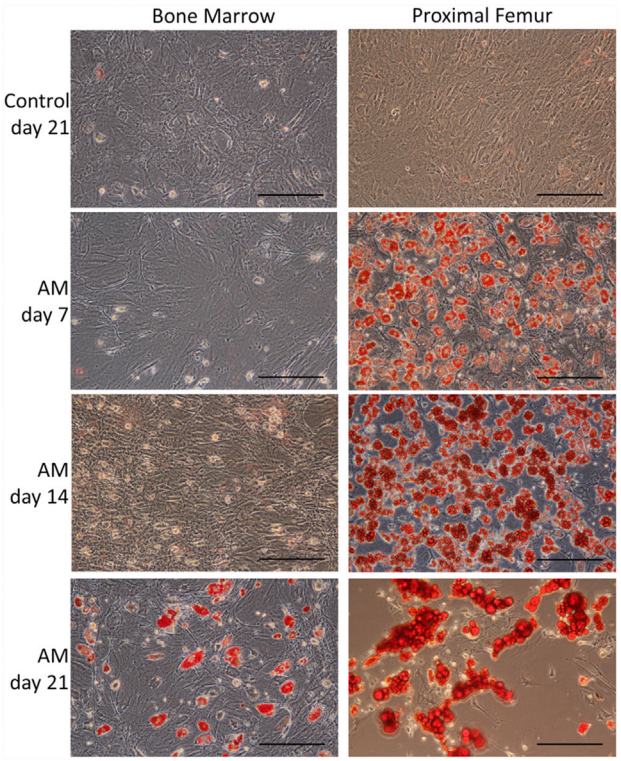

FIGURE 3 | Characterization of the adipocytic differentiation potential of bmMSCs and pfMSCs. Cells were treated with adipogenic media (AM) as described under Section "Materials and Methods," for the number of days as indicated on the figure, and subsequently stained with Oil Red O. Images show representative results of three independent experiments, and were taken at 20× magnification, with the size bar = 1 mm.

accumulation in pfMSCs, compared to bmMSCs. First, we compared the expression of adipocyte-specific genes between Naïve pfMSCs and bmMSCs using qRT-PCR. Although the expression of C/EBPα and fatty acid synthase was readily detectable in both cell types, neither was found to be differentially regulated (**Figure 7A**). Furthermore, the expression levels of aP2/FABP4 in Naïve cells varied considerably, but did not correlate with adipogenic potential (**Figure 7A**), and GLUT4 expression was found to be very low in both cell types (data not shown). It therefore appeared unlikely that the increased lipid accumulation rate of pfMSCs could be attributed to elevated adipocyte-specific gene expression in the Naïve state, and consequently the expression of anti-adipogenic genes was examined. The anti-adipogenic/pro-osteogenic factors Wnt1, Wnt3a, and sonic hedgehog (Shh) (30) were undetectable by qRT-PCR in either cell type (data not shown). Expression levels of the pro-osteogenic transcription factors Runx2 and Msx2 also did not differ between Naïve pfMSCs and bmMSCs (**Figure 7B**), although the anti-adipogenic/pro-osteogenic factor Wnt10b (31) was expressed in Naïve bmMSCs, but not pfMSCs (**Figure 7B**). Subsequently it was found that Wnt10b expression in AM-treated bmMSCs was downregulated after 14 days (**Figure 7C**), therefore preceding the induction of PPARγ2 expression. Wnt10b expression remained downregulated in AM-treated bmMSCs by day 21, but was unexpectedly also found to be downregulated by vanadate treatment (**Figure 7C**).

The Effects of GCs on Lipid Accumulation and Viability of pfMSCs and bmMSCs

Given that GC-induced osteoporosis is often associated with increased bone marrow adiposity (8), it was questioned whether GCs could directly induce adipogenesis in bone-derived MSCs. PfMSCs and bmMSCs were treated with 1 μM dexamethasone (Dex) for 21 days, but no lipid accumulation was observed (**Figure 8**). It was also hypothesized that GCs may reduce the viability of bone-derived MSCs, as it had been previously shown that glucocorticoids induced apoptosis in bone cells *in vivo* and *in vitro* (10). In-well staining of bone-derived MSCs with crystal violet or MTT demonstrated a significant decrease in cell density of pfMSC cultures that had been treated with 1 μM Dex for 7 days (**Figures 9A,B**). In addition, results from the annexin V apoptosis assay indicated an increase in the percentage of apoptotic cells in Dex-treated pfMSC cultures (**Figure 9C**). As previous work had found that vanadate could be protective against GC-induced apoptosis in an immortalized bone cell line (10), we examined

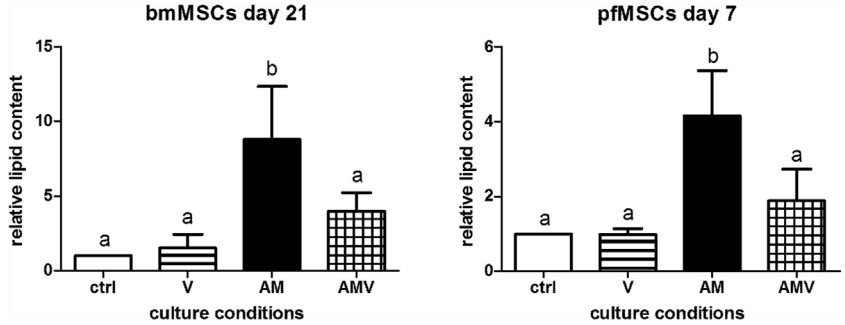

FIGURE 4 | The effect of vanadate on lipid accumulation in bmMSCs and pfMSCs. Cells were treated with adipogenic media (AM) or AM plus 10 μM vanadate (AMV) for the number of days as indicated, before being stained with Oil Red O (ORO) and counterstained with crystal violet (CV). The ORO/CV ratio for control cells was set as 1. Different lower-case letters (a vs. b) indicates statistically significant differences ($P < 0.05$, with $n = 4$ for bmMSCs and $n = 3$ for pfMSCs).

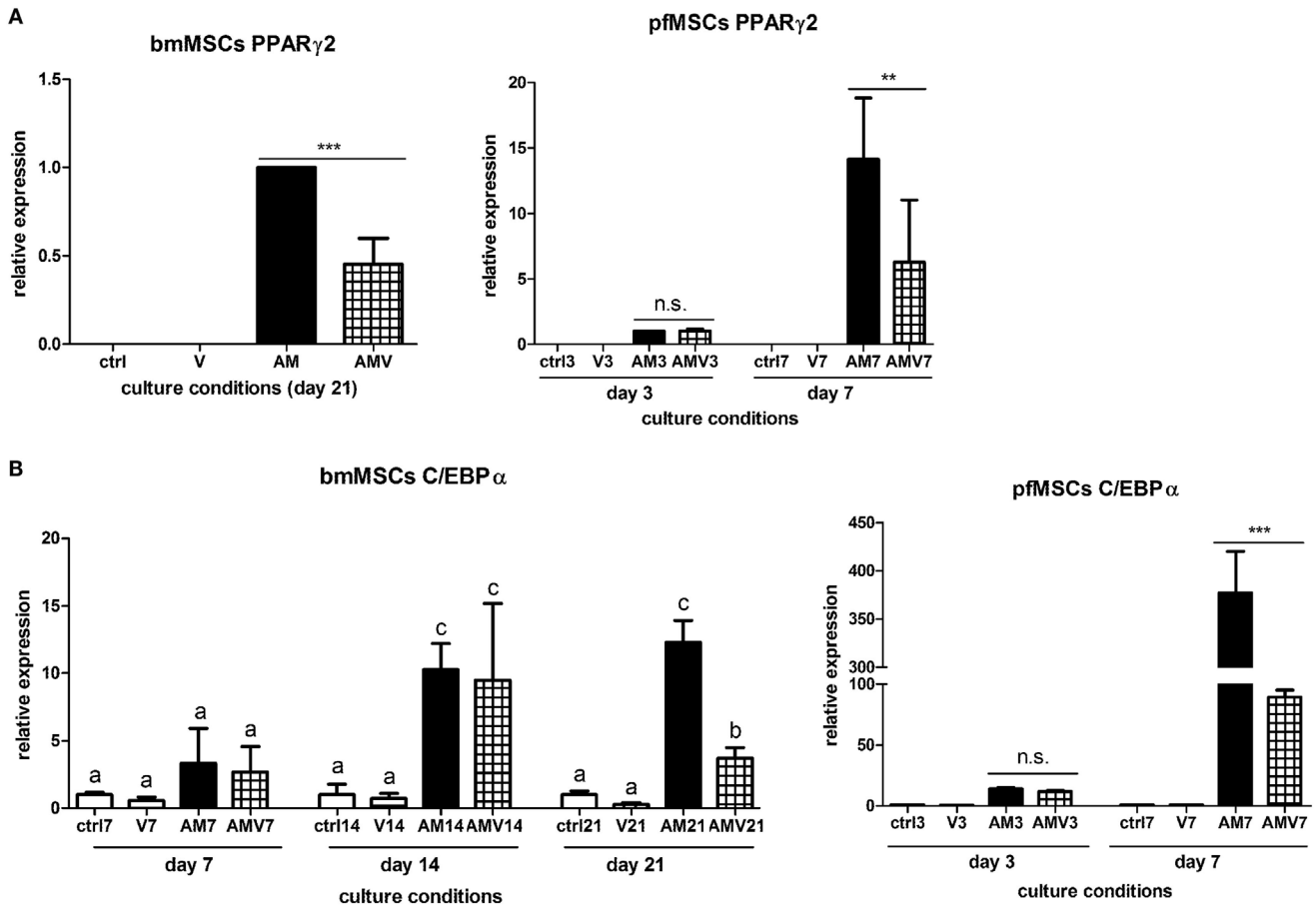

FIGURE 5 | The effect of vanadate on the expression of early markers of adipogenesis. **(A,B)** Cells were treated with adipogenic media (AM) or AM plus 10 μM vanadate (AMV) for the number of days as indicated, and the expression of PPARγ2 **(A)** and C/EBPα **(B)** were measured by qRT-PCR. All target gene measurements were normalized to the housekeeping gene acidic ribosomal phosphoprotein (ARBP). **(A)** As PPARγ2 expression was undetectable in Naïve cells, PPARγ2 expression in day 3 AM-treated pfMSCs or day 21 AM-treated bmMSCs was set as 1. The graph presents the combined data of $n = 3$ for bmMSCs and $n = 3$ for pfMSCs. **(B)** C/EBPα expression in control cells was set as 1. The graph presents representative data from one experimental repeat out of three repeats for bmMSCs and one out of four repeats for pfMSCs.

whether vanadate could counteract the apoptotic effects of Dex on pfMSCs. However, both cytological staining and apoptosis measurements showed that vanadate could not rescue pfMSCs from the negative effects of Dex treatment (**Figures 9A–C**). Vanadate treatment also had no effect on the viability of bmMSCs (**Figures 9A,B**).

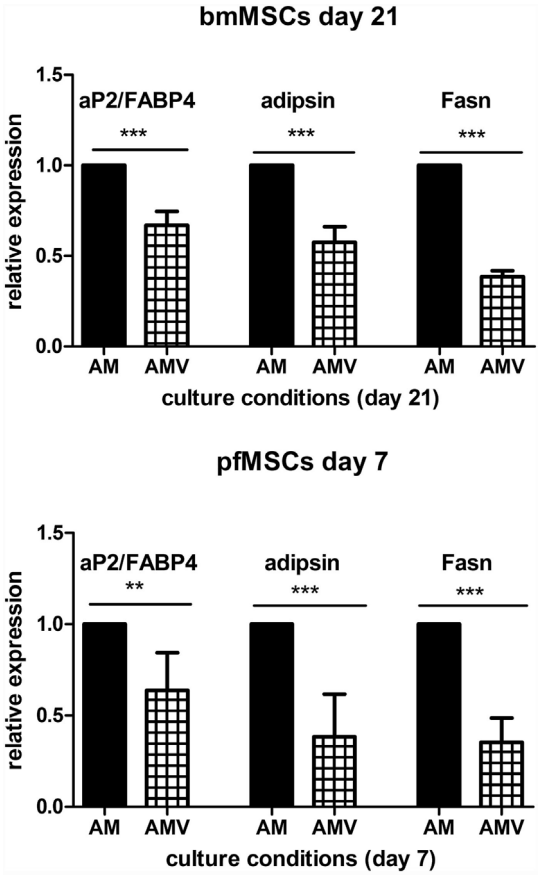

FIGURE 6 | The effect of vanadate on the expression of late markers of adipogenesis. Cells were treated with adipogenic media (AM) or AM plus 10 μM vanadate (AMV) for the number of days as indicated, and the expression of adipocyte protein-2/fatty acid binding protein-4 (aP2/FABP4), adipsin, and fatty acid synthase (Fasn) was measured with qRT-PCR. All target gene measurements were normalized to the housekeeping gene acidic ribosomal phosphoprotein (ARBP). The expression of aP2/FABP4, adipsin, and Fasn in AM-treated cells was set as 1. The graph presents the combined data of $n = 3$ for bmMSCs and $n = 4$ for pfMSCs. Statistically significant differences are indicated as $^{**}P < 0.01$ or $^{***}P < 0.001$.

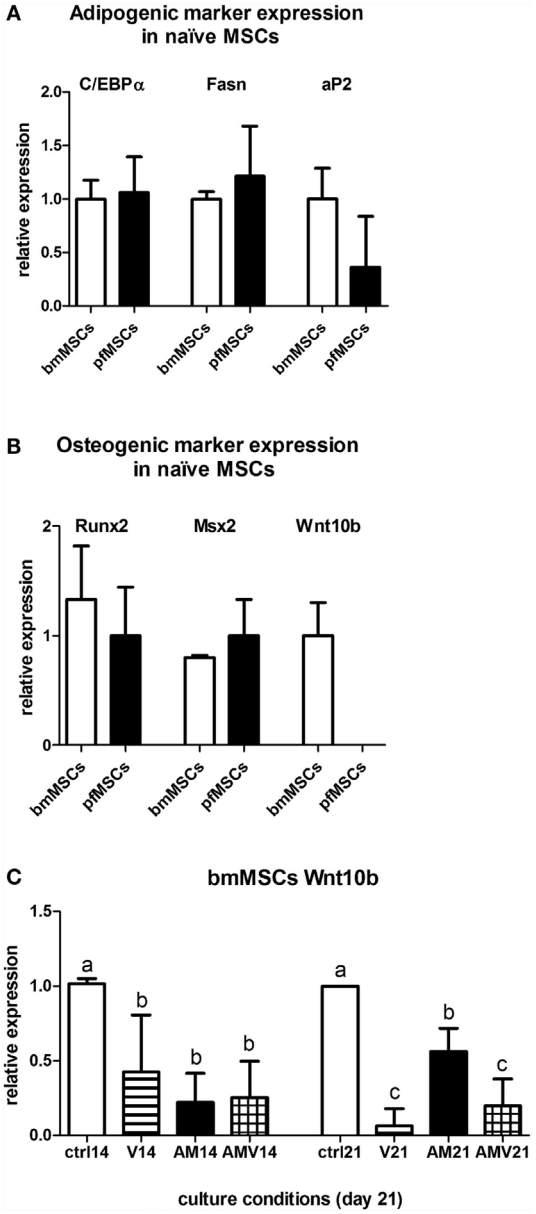

FIGURE 7 | Comparison of gene expression between bmMSCs and pfMSCs. The relative expression levels of adipogenic genes **(A)** and osteogenic genes **(B)** in Naïve bmMSCs and pfMSCs were measured by qRT-PCR. All target gene measurements were normalized to the housekeeping gene acidic ribosomal phosphoprotein (ARBP). For each target gene, the average expression in bmMSCs ($n = 3$) was set as 1, and the expression in pfMSCs ($n = 4$) calculated relative to expression in bmMSCs. **(C)** bmMSCs were treated with adipogenic media (AM) or AM plus 10 μM vanadate (AMV) as indicated, and the expression of Wnt10b was measured by qRT-PCR after 14 and 21 days. Expression in control cells was set as 1. Different lower-case letters (a vs. b vs. c) indicates statistically significant differences ($P < 0.05$, $n = 3$).

DISCUSSION

In the present study, we report for the first time the isolation and characterization of an MSC population, residing in the proximal end of rat femurs (pfMSCs) that is phenotypically similar to, but functionally distinct from bmMSCs. Compared to bmMSCs, pfMSCs exhibited a more rapid adipogenic response but a delayed and impaired osteogenic response. However, despite these apparent differences in differentiation responses, gene expression analysis indicated that the mechanisms involved in adipogenesis and lipid accumulation are likely to be the same in both cell types. It was also found that GCs strongly reduced the viability of pfMSCs by stimulating apoptosis in these cells, while bmMSCs were resistant to the cytotoxic effects of GCs. Vanadate partially inhibited adipogenesis and lipid accumulation in both cell types, but could not reverse the GC-induced cytotoxicity in pfMSCs.

Cell surface marker analysis indicated that both pfMSCs and bmMSCs were strongly positive for the mesenchymal markers CD90 (32) and CD106 (33), and negative for the hematopoietic marker CD45 (34). However, it was found that CD26 was expressed at higher levels in pfMSCs than in bmMSCs. CD26

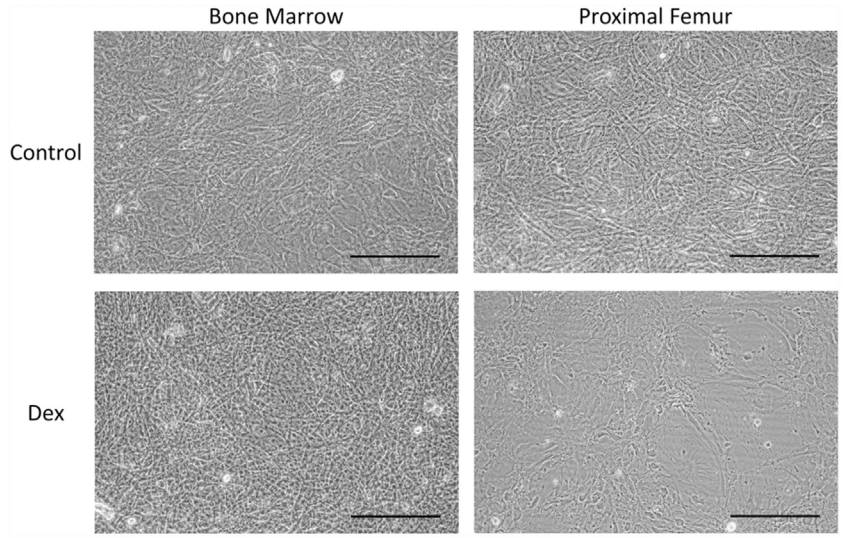

FIGURE 8 | The effect of GC treatment on bmMSCs and pfMSCs. BmMSCs and pfMSCs were treated with 1 μM dexamethasone (Dex) for 21 days, and compared to vehicle-treated cells. Images show unstained cells at 20× magnification and are representative of three independent experiments. The size bar = 1 mm.

is considered to be a fibroblast marker, and earlier work has described that CD26 and CD106 may be used to distinguish between bmMSCs and fibroblasts (33, 35). However, fibroblasts are terminally differentiated cells, whereas the maintenance of an undifferentiated phenotype, proliferative- and bipotential differentiation capacity shown in the bmMSCS and pfMSCs in the present study indicate that these are Naïve progenitor cells, suggesting that CD26 expression is not absolutely indicative of the differentiated fibroblastic phenotype.

The most dramatic difference observed between pfMSCs and bmMSCs was in the adipocytic and osteoblastic differentiation potential, with pfMSCs being highly adipogenic and bmMSCs being highly osteogenic. Unexpectedly, despite these differences in differentiation potential, neither cell types exhibited spontaneous differentiation in culture, and we found that the expression of pro-adipogenic (PPARγ2, C/EBPα) (36) and pro-osteogenic transcription factors (Runx2, Msx2) (37, 38), as well as factors related to adipocyte function (aP2/FABP4, fatty acid synthase, GLUT4) (39, 40), did not differ between Naïve pfMSCs and bmMSCs. However, we found that Wnt10b was expressed in bmMSCs, but was absent in pfMSCs.

It is well established that an inverse relationship exists between osteoblastogenesis and adipogenesis in MSCs, with signals stimulating the one process often reciprocally inhibiting the other (5, 41). Wnt10b was first identified as a crucial "off-switch" for adipogenesis *in vitro* in 3T3-L1 pre-adipocytes (42) and subsequently *in vivo* in transgenic mice (43). Conversely, it was found that Wnt10b promoted osteoblastogenesis *in vitro* in bipotential ST2 cells (31, 44) and *in vivo* in transgenic mice (44, 45). Furthermore, proximal femur bone samples from osteoporotic women with hip fractures exhibit decreased Wnt10b expression (46), providing evidence for a relationship between Wnt10b expression, the maintenance of osteoblastic differentiation and bone strength. In addition, calvarial cultures from transgenic mice with reduced Wnt10b expression displayed dominant adipogenesis and a reduction in osteoblastogenesis (47), similar to the association between Wnt10b expression and osteoblastic differentiation seen in pfMSCs and bmMSCs in the present study. It may therefore be likely that the difference in differentiation potential between pfMSCs and bmMSCs is driven, at least in part, by a dissimilarity in Wnt10b expression. However, apart from Wnt10b expression and the concomitant delay in the onset of adipogenesis in bmMSCs, compared to pfMSCs, the profile of adipogenesis-related genes expressed in response to AM did not differ between these two cell types, indicating that the mechanism of adipocyte development from these two distinct progenitor populations was highly similar.

Glucocorticoid-induced osteoporosis is often associated with a decrease in osteoblast number and an increase in bone marrow adiposity (8). Previously, it has been found that vanadate prevented GC-induced osteoporosis *in vivo* in rats by restoring osteoblast numbers and preventing osteocyte apoptosis (10, 12). However, to our knowledge, there is no information available on the effects of vanadate on adipogenesis and lipid accumulation in bone-derived MSCs. The results presented here indicate that vanadate was able to inhibit lipid accumulation and the expression of early and late adipogenesis markers in pfMSCs and bmMSCs, demonstrating that vanadate inhibited the adipogenic program, and not just the later phases of lipid accumulation, similar to that previously found in immortalized 3T3-L1 pre-adipocytes (13). However, it should be noted that AM-induced expression of the early adipogenesis markers PPARγ2 and C/EBPα was only inhibited by vanadate at later time-points, after the expression of these genes had been upregulated by AM, suggesting the possibility that vanadate-mediated inhibition of adipogenesis involves an upstream signal that is induced during the initial phases of the

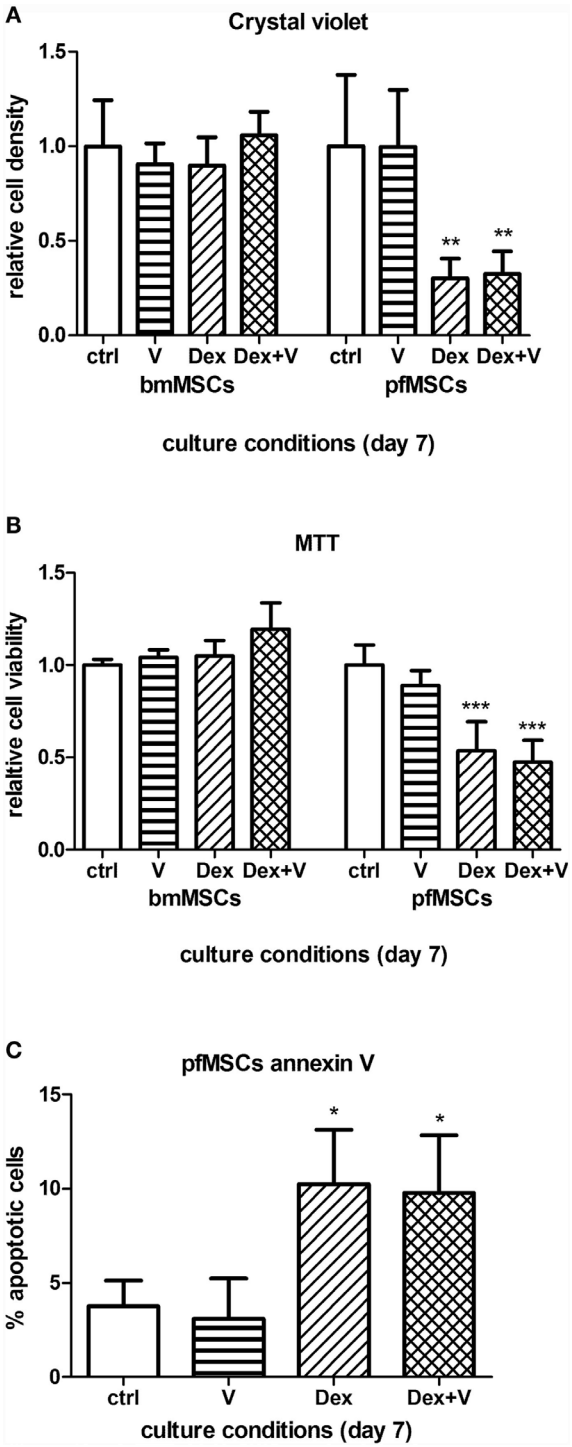

FIGURE 9 | The effects of GCs and vanadate on cell viability and apoptosis in bmMSCs and pfMSCs. Naïve cells were treated with 1 μM dexamethasone (Dex) in the absence or presence of 10 μM vanadate. **(A,B)** Cells were stained with crystal violet **(A)** or MTT **(B),** and the staining was quantified spectrophotometrically. Absorbance measurements of control cells were set as 1. **(C)** The percentage of apoptotic cells in treated pfMSC cultures was determined with flow cytometry, using annexin V as an apoptotic marker. Statistically significant differences are indicated as $^{*}P < 0.05$, $^{**}P < 0.01$, or $^{***}P < 0.001$ ($n = 3$ for bmMSCs, $n = 3$ for pfMSCs).

adipogenic response, with consequential effects only occurring later in the differentiation process. Furthermore, we observed that the vanadate-mediated inhibition of adipogenesis in bmMSCs was not associated with upregulated expression of the anti-adipogenic Wnt10b (42, 43), but that Wnt10b was unexpectedly downregulated by AM as well as by vanadate. The inhibition of adipogenesis in MSCs by vanadate is therefore not underpinned by increased Wnt10b expression, suggesting that other signals are activated by vanadate that can inhibit adipogenesis without a requirement for Wnt10b.

Our finding that bmMSCs showed no differences in cell viability when cultured in a high concentration of Dex (1 μM) suggests that cultured primary bmMSCs are resistant to the detrimental effects of high doses of GCs, even though other studies have described decreased viability, proliferation and osteogenic potential in bmMSCs isolated from GC-treated animals (7, 48). It is therefore possible that these effects of GCs are not the result of direct GC actions at a cellular level, but that they may be mediated systemically. In contrast, pfMSCs were found to be exquisitely sensitive to the cytotoxic and apoptotic effects of GCs, but these effects could not be counteracted by vanadate co-administration. This is in contrast with previous findings, which demonstrated that *in vivo* vanadate treatment could rescue osteoblasts and osteocytes from the negative effects of GCs (10, 12), again suggesting that the effects of GCs and vanadate on bone may be systemic rather than direct.

It has been noted that GC-induced osteoporosis may result in a greater increase in fractures of the vertebrae and proximal femur, compared to fractures at other sites (18, 19), and that GC-induced fat conversion takes place in the proximal femur (8). In addition, studies on patients with GC-induced osteonecrosis of the proximal femur found a decreased proliferative capacity in isolated MSCs (49) and a decrease in progenitor cell numbers in regions adjacent to the necrotic areas (50). Moreover, it was demonstrated in rabbit models that GC treatment induced both marrow fat cell hyperplasia and hypertrophy in the proximal femur (51, 52), and that GC-induced osteonecrosis was also associated with marrow fat cell hypertrophy in this region of bone (53). While our results indicated that GCs alone could not induce lipid accumulation in either pfMSCs or bmMSCs, GC treatment reduced the viability and increased apoptosis in pfMSCs, but not in bmMSCs. These findings, taken together with the highly adipogenic nature of pfMSCs, compared to bmMSCs, suggest that distinct MSC populations may exist in the proximal femur that are more susceptible to adipogenic and apoptotic signals than other bone-derived MSC populations, such as bmMSCs. In addition, it may also be possible that the fat content of the proximal femur, which is usually labeled as "marrow adiposity," may actually arise from distinct pfMSCs, rather than from bmMSCs from the diaphyseal region.

AUTHOR CONTRIBUTIONS

FJ, HS, and MV were responsible for the conceptual design of the study, experimental procedures, sample collection and analysis, interpretation of data, and preparation of the manuscript. WF contributed to the conceptual design and editing of the manuscript.

FUNDING

This work was supported by research funding from the South African National Research Foundation (NRF), the South African Medical Research Council (MRC) and the Harry Crossley Foundation. FJ was supported by a PhD bursary from the NRF and MV was supported by a postdoctoral fellowship from the Faculty of Medicine and Health Sciences, Stellenbosch University.

REFERENCES

1. Frenkel B, White W, Tuckermann J. Glucocorticoid-induced osteoporosis. *Adv Exp Med Biol* (2015) 872:179–215. doi:10.1007/978-1-4939-2895-8_8
2. Canalis E, Mazziotti G, Giustina A, Bilezikian JP. Glucocorticoid-induced osteoporosis: pathophysiology and therapy. *Osteoporos Int* (2007) 18:1319–28. doi:10.1007/s00198-007-0394-0
3. Owen M. Marrow stromal stem cells. *J Cell Sci Suppl* (1988) 10:63–76. doi:10.1242/jcs.1988.Supplement_10.5
4. Caplan AI. Mesenchymal stem cells. *J Orthop Res* (1991) 9:641–50. doi:10.1002/jor.1100090504
5. Gimble JM, Zvonic S, Floyd ZE, Kassem M, Nuttall ME. Playing with bone and fat. *J Cell Biochem* (2006) 98:251–66. doi:10.1002/jcb.20777
6. Pereira RC, Delany AM, Canalis E. Effects of cortisol and bone morphogenetic protein-2 on stromal cell differentiation: correlation with CCAAT-enhancer binding protein expression. *Bone* (2002) 30:685–91. doi:10.1016/S8756-3282(02)00687-7
7. Li J, Zhang N, Huang X, Xu J, Fernandes JC, Dai K, et al. Dexamethasone shifts bone marrow stromal cells from osteoblasts to adipocytes by C/EBPalpha promoter methylation. *Cell Death Dis* (2013) 4:e832. doi:10.1038/cddis.2013.348
8. Vande Berg BC, Malghem J, Lecouvet FE, Devogelaer JP, Maldague B, Houssiau FA. Fat conversion of femoral marrow in glucocorticoid-treated patients: a cross-sectional and longitudinal study with magnetic resonance imaging. *Arthritis Rheum* (1999) 42(7):1405–11. doi:10.1002/1529-0131(199907)42:7<1405::AID-ANR14>3.0.CO;2-W
9. Sanderson M, Sadie-Van Gijsen H, Hough S, Ferris WF. The role of MKP-1 in the anti-proliferative effects of glucocorticoids in primary rat pre-osteoblasts. *PLoS One* (2015) 10(8):e0135358. doi:10.1371/journal.pone.0135358
10. Conradie MM, de Wet H, Kotze DDR, Burrin JM, Hough FS, Hulley PA. Vanadate prevents glucocorticoid-induced apoptosis of osteoblasts in vitro and osteocytes in vivo. *J Endocrinol* (2007) 195:229–40. doi:10.1677/JOE-07-0217
11. Weinstein RS, Jilka RL, Almeida M, Roberson PK, Manolagas SC. Intermittent parathyroid hormone administration counteracts the adverse effects of glucocorticoids on osteoblast and osteocyte viability, bone formation, and strength in mice. *Endocrinology* (2010) 151:2641–8. doi:10.1210/en.2009-1488
12. Hulley PA, Conradie MM, Langeveldt CR, Hough FS. Glucocorticoid-induced osteoporosis in the rat is prevented by the tyrosine phosphatase inhibitor, sodium orthovanadate. *Bone* (2002) 31:220–9. doi:10.1016/S8756-3282(02)00807-4
13. Jin S, Zhai B, Qiu Z, Wu J, Lane MD, Liao K. c-Crk, a substrate of the insulin-like growth factor-1 receptor tyrosine kinase, functions as an early signal mediator in the adipocyte differentiation process. *J Biol Chem* (2000) 275:34344–52. doi:10.1074/jbc.M004927200
14. Nadri S, Soleimani M, Hosseni RH, Massumi M, Atashi A, Izadpanah R. An efficient method for isolation of murine bone marrow mesenchymal stem cells. *Int J Dev Biol* (2007) 51:723–9. doi:10.1387/ijdb.072352ns
15. Zhu H, Guo ZK, Jiang XX, Li H, Wang XY, Yao HY, et al. A protocol for isolation and culture of mesenchymal stem cells from mouse compact bone. *Nat Protoc* (2010) 5:550–60. doi:10.1038/nprot.2009.238
16. Yoshimura H, Muneta T, Nimura A, Yokoyama A, Koga H, Sekiya I. Comparison of rat mesenchymal stem cells derived from bone marrow, synovium, periosteum, adipose tissue, and muscle. *Cell Tissue Res* (2007) 327:449–62. doi:10.1007/s00441-006-0308-z
17. Cheng CC, Lian WS, Hsiao FS, Liu IH, Lin SP, Lee YH, et al. Isolation and characterization of novel murine epiphysis derived mesenchymal stem cells. *PLoS One* (2012) 7:e36085. doi:10.1371/journal.pone.0036085
18. Van Staa TP, Leufkens HG, Abenhaim L, Zhang B, Cooper C. Use of oral corticosteroids and risk of fractures. June, 2000. *J Bone Miner Res* (2000) 20:1487–94. doi:10.1359/jbmr.2000.15.6.993
19. Al-Osail AM, Sadat-Ali M, Al-Elq AH, Al-Omran AS, Azzam Q. Glucocorticoid-related osteoporotic fractures. *Singapore Med J* (2010) 51:948–51.
20. Jaiswal N, Haynesworth SE, Caplan AI, Bruder SP. Osteogenic differentiation of purified, culture-expanded human mesenchymal stem cells *in vitro*. *J Cell Biochem* (1997) 64:295–312. doi:10.1002/(SICI)1097-4644(199702)64:2<295::AID-JCB12>3.0.CO;2-I
21. Gregory CA, Gunn WG, Peister A, Prockop DJ. An alizarin red-based assay of mineralization by adherent cells in culture: comparison with cetylpyridinium chloride extraction. *Anal Biochem* (2004) 329:77–84. doi:10.1016/j.ab.2004.02.002
22. Ogawa R, Mizuno H, Watanabe A, Migita M, Hyakusoku H, Shimada T. Adipogenic differentiation by adipose-derived stem cells harvested from GFP transgenic mice-including relationship of sex differences. *Biochem Biophys Res Commun* (2004) 319(2):511–7. doi:10.1016/j.bbrc.2004.05.021
23. Laughton C. Measurement of the specific lipid content of attached cells in microtiter cultures. *Anal Biochem* (1986) 156:307–14. doi:10.1016/0003-2697(86)90258-7
24. Pfaffl MW. A new mathematical model for relative quantification in real-time RT-PCR. *Nucleic Acids Res* (2001) 29:e45. doi:10.1093/nar/29.9.e45
25. Van Wijngaarden P, Brereton HM, Coster DJ, Williams KA. Stability of housekeeping gene expression in the rat retina during exposure to cyclic hyperoxia. *Mol Vis* (2007) 13:1508–15.
26. Tanabe Y, Koga M, Saito M, Matsunaga Y, Nakayama K. Inhibition of adipocyte differentiation by mechanical stretching through ERK-mediated downregulation of PPARgamma2. *J Cell Sci* (2004) 117:3605–14. doi:10.1242/jcs.01207
27. Fukuen S, Iwaki M, Yasui A, Makishima M, Matsuda M, Shimomura I. Sulfonylurea agents exhibit peroxisome proliferator-activated receptor gamma agonistic activity. *J Biol Chem* (2005) 280:23653–9. doi:10.1074/jbc.M412113200
28. Kato S, Kawabata N, Suzuki N, Ohmura M, Takagi M. Bone morphogenetic protein-2 induces the differentiation of a mesenchymal progenitor cell line, ROB-C26, into mature osteoblasts and adipocytes. *Life Sci* (2009) 84:302–10. doi:10.1016/j.lfs.2008.12.011
29. Sun J, Zhang T, Zhang P, Lv L, Wang Y, Zhang J, et al. Overexpression of the PLAP-1 gene inhibits the differentiation of BMSCs into osteoblast-like cells. *J Mol Histol* (2014) 45:599–608. doi:10.1007/s10735-014-9585-0
30. Gesta S, Tseng YH, Kahn CR. Developmental origin of fat: tracking obesity to its source. *Cell* (2007) 131:242–56. doi:10.1016/j.cell.2007.10.004
31. Cawthorn WP, Bree AJ, Yao Y, Du B, Hemati N, Martinez-Santibañez G, et al. Wnt6, Wnt10a and Wnt10b inhibit adipogenesis and stimulate osteoblastogenesis through a β-catenin-dependent mechanism. *Bone* (2012) 50:477–89. doi:10.1016/j.bone.2011.08.010
32. Fickert S, Fiedler J, Brenner RE. Identification of subpopulations with characteristics of mesenchymal progenitor cells from human osteoarthritic cartilage using triple staining for cell surface markers. *Arthritis Res Ther* (2004) 6:R422–32. doi:10.1186/ar1210
33. Campioni D, Moretti S, Ferrari L, Punturieri M, Castoldi GL, Lanza F. Immunophenotypic heterogeneity of bone marrow-derived mesenchymal stromal cells from patients with hematologic disorders: correlation with bone marrow microenvironment. *Haematologica* (2006) 91(3):364–8.
34. Kishimoto T, Kikutani H, Borne A, Goyert SM, Mason D, Miyasaki M, et al. *Leucocyte Typing VI, White Cell Differentiation Antigens*. Hamden, CT: Garland Publishing (1997).
35. Cappellesso-Fleury S, Puissant-Lubrano B, Apoil PA, Titeux M, Winterton P, Casteilla L, et al. Human fibroblasts share immunosuppressive properties with bone marrow mesenchymal stem cells. *J Clin Immunol* (2010) 30(4):607–19. doi:10.1007/s10875-010-9415-4

36. Tontonoz P, Spiegelman BM. Fat and beyond: the diverse biology of PPARgamma. *Annu Rev Biochem* (2008) 77:289–312. doi:10.1146/annurev.biochem.77.061307.091829
37. Ducy P. Cbfa1: a molecular switch in osteoblast biology. *Dev Dyn* (2000) 219:461–71. doi:10.1002/1097-0177(2000)9999:9999<::AID-DVDY1074>3.0.CO;2-C
38. Satokata I, Ma L, Ohshima H, Bei M, Woo I, Mishizawa K, et al. Msx2 deficiency in mice causes pleiotropic defects in bone growth and ectodermal organ formation. *Nat Genet* (2000) 24:391–5. doi:10.1038/74231
39. Moreno-Indias I, Tinahones FJ. Impaired adipose tissue expandability and lipogenic capacities as ones of the main causes of metabolic disorders. *J Diabetes Res* (2015) 2015:970375. doi:10.1155/2015/970375
40. Assimacopoulos-Jeannet F, Cusin I, Greco-Perotto RM, Terrettaz J, Rohner-Jeanrenaud F, Zarjevski N, et al. Glucose transporters: structure, function, and regulation. *Biochimie* (1991) 73:67–70. doi:10.1016/0300-9084(91)90076-D
41. Sadie-Van Gijsen H, Hough FS, Ferris WF. Determinants of bone marrow adiposity: the modulation of peroxisome proliferator-activated receptor-γ2 activity as a central mechanism. *Bone* (2013) 56:255–65. doi:10.1016/j.bone.2013.06.016
42. Ross SE, Hemati N, Longo KA, Bennett CN, Lucas PC, Erickson RL, et al. Inhibition of adipogenesis by Wnt signaling. *Science* (2000) 289:950–3. doi:10.1126/science.289.5481.950
43. Longo KA, Wright WS, Kang S, Gerin I, Chiang SH, Lucas PC, et al. Wnt10b inhibits development of white and brown adipose tissues. *J Biol Chem* (2004) 279:35503–9. doi:10.1074/jbc.M402937200
44. Bennett CN, Longo KA, Wright WS, Suva LJ, Lane TF, Hankenson KD, et al. Regulation of osteoblastogenesis and bone mass by Wnt10b. *Proc Natl Acad Sci U S A* (2005) 102:3324–9. doi:10.1073/pnas.0408742102
45. Bennett CN, Ouyang H, Ma YL, Zeng Q, Gerin I, Sousa KM, et al. Wnt10b increases postnatal bone formation by enhancing osteoblast differentiation. *J Bone Miner Res* (2007) 22:1924–32. doi:10.1359/jbmr.070810
46. Föger-Samwald U, Vekszler G, Hörz-Schuch E, Salem S, Wipperich M, Ritschl P, et al. Molecular mechanisms of osteoporotic hip fractures in elderly women. *Exp Gerontol* (2016) 73:49–58. doi:10.1016/j.exger.2015.11.012
47. Zhou H, Mak W, Zheng Y, Dunstan CR, Seibel MJ. Osteoblasts directly control lineage commitment of mesenchymal progenitor cells through Wnt signaling. *J Biol Chem* (2008) 283:1936–45. doi:10.1074/jbc.M702687200
48. Weinstein RS, Jilka RL, Parfitt AM, Manolagas SC. Inhibition of osteoblastogenesis and promotion of apoptosis of osteoblasts and osteocytes by glucocorticoids. Potential mechanisms of their deleterious effects on bone. *J Clin Invest* (1998) 102:274–82. doi:10.1172/JCI2799
49. Wang BL, Sun W, Shi ZC, Lou JN, Zhang NF, Shi SH, et al. Decreased proliferation of mesenchymal stem cells in corticosteroid-induced osteonecrosis of femoral head. *Orthopedics* (2008) 31:444.
50. Hernigou P, Beaujean F, Lambotte JC. Decrease in the mesenchymal stem-cell pool in the proximal femur in corticosteroid-induced osteonecrosis. *J Bone Joint Surg Br* (1999) 81:349–55. doi:10.1302/0301-620X.81B2.8818
51. Li GW, Xu Z, Chen QW, Chang SX, Tian YN, Fan JZ. The temporal characterization of marrow lipids and adipocytes in a rabbit model of glucocorticoid-induced osteoporosis. *Skeletal Radiol* (2013) 42:1235–44. doi:10.1007/s00256-013-1659-7
52. Li GW, Chang SX, Fan JZ, Tian YN, Xu Z, He YM. Marrow adiposity recovery after early zoledronic acid treatment of glucocorticoid-induced bone loss in rabbits assessed by magnetic resonance spectroscopy. *Bone* (2013) 52:668–75. doi:10.1016/j.bone.2012.11.002
53. Miyanishi K, Yamamoto T, Irisa T, Yamashita A, Jingushi S, Noguchi Y, et al. Bone marrow fat cell enlargement and a rise in intraosseous pressure in steroid-treated rabbits with osteonecrosis. *Bone* (2002) 30:185–90. doi:10.1016/S8756-3282(01)00663-9

Conflict of Interest Statement: The authors declare that the research was conducted in the absence of any commercial or financial relationships that could be construed as a potential conflict of interest.

frontiers in Endocrinology

ORIGINAL RESEARCH
published: 27 July 2016
doi: 10.3389/fendo.2016.00102

Changes in Skeletal Integrity and Marrow Adiposity during High-Fat Diet and after Weight Loss

Erica L. Scheller[1,2], Basma Khoury[3], Kayla L. Moller[1], Natalie K. Y. Wee[4], Shaima Khandaker[2], Kenneth M. Kozloff[3], Simin H. Abrishami[5], Brian F. Zamarron[6] and Kanakadurga Singer[5]*

[1] Division of Bone and Mineral Diseases, Department of Medicine, Washington University, St. Louis, MO, USA, [2] Department of Molecular and Integrative Physiology, University of Michigan, Ann Arbor, MI, USA, [3] Department of Orthopaedic Surgery, University of Michigan, Ann Arbor, MI, USA, [4] Osteoporosis and Bone Biology Division, Garvan Institute of Medical Research, Darlinghurst, Sydney, NSW, Australia, [5] Division of Pediatric Endocrinology, Department of Pediatrics and Communicable Diseases, University of Michigan Medical School, Ann Arbor, MI, USA, [6] Graduate Program in Immunology, University of Michigan, Ann Arbor, MI, USA

OPEN ACCESS

Edited by:
Ann Schwartz, University of California San Francisco, USA

Reviewed by:
Jan Josef Stepan, Charles University in Prague, Czech Republic
Roberto Jose Fajardo, University of Texas Health Science Center at San Antonio, USA

***Correspondence:**
Erica L. Scheller
scheller@wustl.edu

Specialty section:
This article was submitted to Bone Research, a section of the journal Frontiers in Endocrinology

Received: *16 May 2016*
Accepted: *08 July 2016*
Published: *27 July 2016*

Citation:
Scheller EL, Khoury B, Moller KL, Wee NKY, Khandaker S, Kozloff KM, Abrishami SH, Zamarron BF and Singer K (2016) Changes in Skeletal Integrity and Marrow Adiposity during High-Fat Diet and after Weight Loss. Front. Endocrinol. 7:102. doi: 10.3389/fendo.2016.00102

The prevalence of obesity has continued to rise over the past three decades leading to significant increases in obesity-related medical care costs from metabolic and non-metabolic sequelae. It is now clear that expansion of body fat leads to an increase in inflammation with systemic effects on metabolism. In mouse models of diet-induced obesity, there is also an expansion of bone marrow adipocytes. However, the persistence of these changes after weight loss has not been well described. The objective of this study was to investigate the impact of high-fat diet (HFD) and subsequent weight loss on skeletal parameters in C57Bl6/J mice. Male mice were given a normal chow diet (ND) or 60% HFD at 6 weeks of age for 12, 16, or 20 weeks. A third group of mice was put on HFD for 12 weeks and then on ND for 8 weeks to mimic weight loss. After these dietary challenges, the tibia and femur were removed and analyzed by micro computed-tomography for bone morphology. Decalcification followed by osmium staining was used to assess bone marrow adiposity, and mechanical testing was performed to assess bone strength. After 12, 16, or 20 weeks of HFD, mice had significant weight gain relative to controls. Body mass returned to normal after weight loss. Marrow adipose tissue (MAT) volume in the tibia increased after 16 weeks of HFD and persisted in the 20-week HFD group. Weight loss prevented HFD-induced MAT expansion. Trabecular bone volume fraction, mineral content, and number were decreased after 12, 16, or 20 weeks of HFD, relative to ND controls, with only partial recovery after weight loss. Mechanical testing demonstrated decreased fracture resistance after 20 weeks of HFD. Loss of mechanical integrity did not recover after weight loss. Our study demonstrates that HFD causes long-term, persistent changes in bone quality, despite prevention of marrow adipose tissue accumulation, as demonstrated through changes in bone morphology and mechanical strength in a mouse model of diet-induced obesity and weight loss.

Keywords: obesity, bone, marrow adipose tissue, marrow fat, weight loss, leptin, high-fat diet, fracture

INTRODUCTION

Over the past two decades, the prevalence of obesity has increased in Western countries (1, 2). In the United States, currently ~68.6% of adults and approximately one-third (~31.8%) of children are overweight or obese (3). Obesity is associated with comorbidities including cardiovascular and metabolic disease, autoimmune disorders and some cancers (1, 4–6). Recent work has suggested that obesity is also detrimental to bone health (7–11), with skeletal changes that can persist even after weight loss (10, 12).

Previously, it was assumed that obesity had a purely positive effect on bone mass (13–15); increased body weight provides mechanical stimulation, resulting in skeletal loading and bone accrual. However, juxtaposed to this, there is a newly recognized metabolic component, as the adipose tissue itself can exert a negative influence on bone (14). Indeed, increases in body mass index (BMI) have been associated with decreased bone mineral density (BMD) and increased fracture risk in obese adolescents and adults (9, 16), and in obese children (17). The effect of obesity on fracture risk is site specific. The presence of soft-tissue padding from fat may contribute to decreased fracture risk in some areas (e.g., hip) while unprotected sites, such as the extremities (e.g., humerus and ankle), have increased risk (18–20).

The cross-sectional nature of previous clinical studies can only identify associations between obesity and bone, thus, rodent models are widely utilized to explore the mechanisms underlying the relationship between obesity and the skeleton. It is well established that high-fat feeding of mice leads to a reduction in cancellous bone mass (7, 12, 21, 22). This may be mediated by leptin-induced sympathetic tone, which has been implicated as strong mediator of cancellous bone loss (23–25). By comparison, the cortical phenotype in response to high-fat diet (HFD) in rodents remains unclear, with some studies indicating an increase (11), no change (12, 21, 22, 26) or a reduction in cortical bone mass (10, 27). Located within the skeleton are the bone marrow adipocytes; recent studies suggest that marrow adipose tissue (MAT) expansion occurs during high-fat feeding (28, 29). Whether MAT expansion and bone loss are somehow linked during obesity is still unclear; some studies suggest that these lineages are correlated (29–31) while Doucette et al. recently reported MAT expansion during diet-induced obesity that occurred independently of a bone phenotype (28).

In addition to the effects of obesity on bone, weight loss interventions have also been shown to have detrimental effects on bone metabolism, as reviewed by Brzozowska et al. (32). There are a range of interventions including calorie-restricted diets, exercise regimens, medications, and bariatric surgery (32, 33). Each of these interventions aim to reduce body fat and improve metabolic disease; the full extent to which these processes may alter MAT and bone mass in the context of obesity are largely unknown. Surgical interventions of bariatric surgery (Roux-en Y gastric bypass, laparoscopic adjustable gastric banding, and sleeve gastrectomy) have all been associated with a decline in bone mass despite improvements in metabolic health (32). In contrast to surgical weight loss, exercise has been shown to be quite beneficial on bone density due to increased muscle loading (34–36). The most common initial intervention clinically is calorie restriction or "dieting." Few studies have looked at weight loss in rodent models through interventions of "switching" diet. One study performed showed that switching back to a chow diet following high-fat feeding could rescue bone loss (12); however, the response of MAT and the interaction of MAT with bone loss in these models was not examined.

The objective of this study was to investigate the interaction between MAT and bone in the context of high-fat feeding and to examine the response of these tissues to dietary weight loss. We demonstrate that high-fat feeding leads to excess peripheral adiposity, MAT expansion, a reduction in bone mass and impaired bone strength. Weight loss led to a significant reduction in whole body adiposity and blocked MAT expansion; however, it failed to completely rescue defects in skeletal morphology and biomechanics. This work begins to address the potential of adipose tissue within the skeleton to have an impact on bone – working, unlike peripheral fat, from the inside out.

MATERIALS AND METHODS

Animals

Male C57Bl6/J mice (Jackson Laboratories) were given a normal chow diet (ND) (13.5% calories from fat; LabDiet 5LOD) or 60% high fat diet (HFD) (Research Diets D12492) at 6 weeks of age for a duration of 12, 16, or 20 weeks. A third group of mice was put on HFD for 12 weeks and then on ND for 8 weeks [weight loss (WL) group]. Animals were housed in a specific pathogen-free facility with a 12-h light/12-h dark cycle at ~22°C and given free access to food and water. All animal use was in compliance with the Institute of Laboratory Animal Research Guide for the Care and Use of Laboratory Animals and approved by the University Committee on Use and Care of Animals at the University of Michigan. The tibia was selected for our longitudinal analyses since it can be used to simultaneously monitor changes in rMAT (proximal tibia) and cMAT (distal tibia) within one sample (37). To compare the changes in bone within the tibia to those in the femur, as reported previously (12), we also analyzed the femurs in the 20-week groups.

Micro Computed-Tomography

Tibiae were fixed in formalin for 48-h and then placed in phosphate buffered saline (PBS). Specimens were embedded in 1% agarose and placed in a 19-mm diameter tube, and the length of the bone was scanned using a Micro Computed-Tomography (microCT) system (μCT100 Scanco Medical, Bassersdorf, Switzerland). Scan settings were: voxel size 12 μm, medium resolution, 70 kVp, 114 μA, 0.5 mm AL filter, and integration time 500 ms. Density measurements were calibrated to the manufacturer's hydroxyapatite phantom. Analysis was performed using the manufacturer's evaluation software.

Femurs were removed and frozen after wrapping in PBS-soaked gauze and then analyzed by microCT. Femora were scanned in water using cone beam computed tomography (explore Locus SP, GE Healthcare Pre-Clinical Imaging, London, ON, Canada). Scan parameters included a 0.5° increment angle, four frames averaged, an 80 kVp and 80 μA X-ray source with a 0.508 mm AI filter to

reduce beam hardening artifacts, and a beam flattener around the specimen holder. All images were reconstructed and calibrated at an 18 μm isotropic voxel size to manufacturer-supplied phantom of air, water, and hydroxyapatite (38).

Biomechanical Assessment

Following microCT scanning, femurs were loaded to failure in four-point bending using a servohydraulic testing machine (MTS 858 MiniBionix, Eden Prairie, MN, USA). All specimens were kept hydrated in lactated ringers solution-soaked gauze until mechanical testing. In the same mid-diaphyseal region analyzed by μCT, the femur was loaded in four-point bending with the posterior surface oriented under tension. The distance between the wide, upper supports was 6.26 mm, and the span between the narrow, lower supports was 2.085 mm. The vertical displacement rate of the four-point bending apparatus in the anterior–posterior direction was 0.5 mm/s. Force was recorded by a 50 lb load cell (Sensotec) and vertical displacement by an external linear variable differential transducer (LVDT, Lucas Schavitts, Hampton, VA, USA), both at 2000 Hz. A custom MATLAB script was used to analyze the raw force-displacement data and calculate all four-point bending parameters. Combining anterior–posterior bending moment of inertia data from μCT with mechanical stiffness from four point bending, the estimated elastic modulus was calculated using standard beam theory as previously described (38). The modulus of elasticity was derived based on previous methods with "L" set at 3.57 and "a" at 0.99 (39).

Quantification of Trabecular and Cortical Parameters with microCT

Tibia. Regions of interest (ROI) was located for both cortical and trabecular parameters. Analyses were performed with MicroCT software provided by Scanco Medical (Bassersdorf, Switzerland). A mid-diaphyseal cortical ROI was defined as ending at 70% of the distance between the growth plate and the tibia/fibula junction. A ROI spanning 360 μm (30-slices) proximal to this region was analyzed with standard plugins using a threshold of 280. The trabecular ROI was defined as starting 60 μm (5-slices) distal to the growth plate and ending after 600 μm total (50-slices). Trabecular analyses were performed with standard Scanco plugins with a threshold of 180.

Femur. ROI was located for both cortical and trabecular parameters. A diaphyseal cortical ROI spanning 18% of total femur length was located midway between the distal growth plate and third trochanter. Cortical bone was isolated with a fixed threshold of 2000 Hounsfield Units for all experimental groups. Parameters including cortical thickness, endosteal and periosteal perimeter, cross sectional area, marrow area, total area, anterior–posterior bending moment of inertia, and tissue mineral density (TMD) were quantified with commercially available software (MicroView v2.2 Advanced Bone Analysis Application, GE Healthcare Pre-Clinical Imaging, London, ON, Canada). A trabecular ROI 10% of total femur length was located immediately proximal to the distal femoral growth plate and defined along the inner cortical surface with a splining algorithm. Trabecular metaphyseal bone was isolated with a fixed threshold of 1200 Hounsfield Units.

Quantification of Marrow Adipose Tissue

Marrow adipose tissue volume within the tibia was assessed as described previously (37, 40). After the initial microCT scan, bones were decalcified in 14% EDTA solution, pH 7.4 for 14 days at 4°C. Decalcified bones were stained with 1% osmium tetroxide solution in Sorensen's phosphate buffer pH 7.4 at room temperature for 48 h. Osmium-stained bones were re-scanned using the Scanco microCT settings described above. For analysis of MAT within the tibia, four regions were defined as follows: (1) the proximal epiphysis between the proximal end of the tibia and the growth plate, (2) the proximal metaphysis, beginning 60 μm (5-slices) distal to the growth plate and ending after 600 μm total (50-slices), (3) the growth plate to the tibia/fibula junction (GP to T/F J), and the distal tibia between the tibia/fibula junction and the distal end of the bone. MAT volume analyses were performed with standard Scanco plugins with a threshold of 500.

Statistics

Statistical comparisons were performed in GraphPad Prism (GraphPad Software, Inc., La Jolla, CA, USA). The following planned comparisons were performed on the graphs in **Figures 1**, **2**, **3** and **5**: 12-week ND vs. HFD (two-tailed *t*-test); 16-week ND vs. HFD (two-tailed *t*-test); 20-week ND vs. HFD vs. WL (1-way ANOVA); 12-, 16-, 20-week ND (1-way ANOVA); 12-, 16-, 20-week HFD (1-way ANOVA); 12-week HFD vs. 20-week WL (two-tailed *t*-test). These results were corrected for multiple comparisons using the Benjamini-Hochberg procedure as described previously (41). For comparisons in **Figures 4**, **6** and **7**, a one-way ANOVA with Tukey's correction was applied. In **Figure 8**, linear regression was applied to test the significance of the correlations. Raw data for the skeletal morphology, marrow fat quantification, and biomechanical testing is available in Data Sets 1–3 in Supplementary Material.

RESULTS

Increases in Body Mass with High-Fat Diet Are Rescued by Weight Loss

Mice were fed normal chow diet (ND) or 60% high-fat diet (HFD), starting at 6 weeks of age, for 12, 16, or 20 weeks. A separate group of mice received 12 weeks of HFD, followed by 8 weeks of ND to mimic weight loss (**Figure 1A**). Comparison of the 12-week HFD group to the WL group was used to determine if weight loss reversed changes that were already present at 12 weeks, or, rather, prevented further deterioration induced by continued HFD.

Increases in body mass relative to ND control were apparent after 12-weeks of HFD (**Figure 1B**). Increases in body mass relative to ND control persisted at the 16- and 20-week time points (**Figure 1B**). Over time, body mass continued to increase from 12 to 16 weeks of HFD but stabilized between 16 and 20 weeks (**Figure 1B**). Body mass returned to normal after weight loss (**Figure 1B**). Weight gain was due, at least in part, to increases in liver, inguinal and gonadal white adipose tissue (WAT) mass after 20-weeks of HFD (**Figure 1C**). With weight loss, liver mass returned to normal; however, WAT mass was only partially rescued (**Figure 1C**).

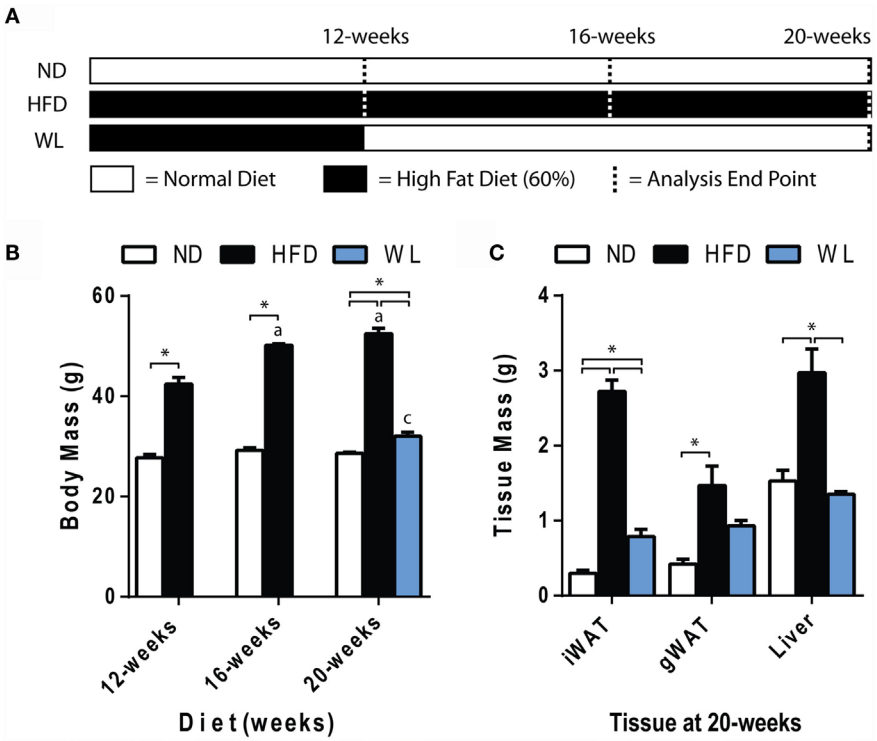

FIGURE 1 | **Body and tissue mass**. **(A)** Experiment outline. Starting at 6-weeks of age, mice were fed the indicated diets for up to 20 weeks prior to analysis. Seven groups of mice were analyzed as indicated by the dashed lines. ND: normal chow diet; HFD: high fat diet; WL: weight loss. **(B)** Body mass. $N = 7$-8 per group. **(C)** Tissue mass at 20 weeks. $N = 4$-6 per group. All graphs are mean ± SEM. "a" – significant vs. 12-week on same diet. "b" – significant vs. 16-week on same diet. "c" – significant vs. 12-week HFD. *$p < 0.050$ for the indicated comparison.

Marrow Adipose Tissue Expansion after High-Fat Diet Feeding Is Inhibited with Weight Loss

Within the tibia, MAT expansion became significant, relative to ND control, after 16 weeks of HFD (**Figures 2A,B**). With HFD, changes in the proximal tibial epiphysis mimicked what was observed between the growth plate and tibia/fibula junction, with a 5.5- and 4.3-fold increase at 16 weeks, relative to 12 weeks, respectively (**Figure 2B**). The distal tibia was similar, though there was only a 2.1-fold increase between 12 and 16 weeks of HFD, likely owing to the higher baseline MAT in this region (**Figure 2B**). No additional MAT accrual in any region of the tibia was observed between 16 and 20 weeks of HFD (**Figure 2B**).

In the weight loss group, the MAT in the regions of the proximal epiphysis and GP to T/F J was indistinguishable from that of the 20-week ND group (**Figure 2B**). However, it was also similar in magnitude to the 12-week HFD group, suggesting that switching to ND was sufficient to block HFD-induced MAT expansion – rather than reversing MAT accrual that had already occurred.

In the distal tibia, age-associated increases in MAT were noted from 12- to 16-weeks of age in the ND group. Prior to correction for multiple comparisons, MAT within the distal tibia in the WL group was higher than chow ($p = 0.019$) but less than HFD ($p = 0.050$). This suggests that weight loss blunted, but did not entirely prevent, HFD-induced MAT expansion in the distal tibia at 20-weeks (**Figure 2B**). Raw data for these comparisons is available as Data Set 1 in Supplementary Material.

In the Tibia, Trabecular Bone Quality Decreases with High-Fat Diet and Partially Improves with Weight Loss

Consistent with previous reports (42, 43), we observed an age-related decrease in trabecular bone volume fraction (BVF) and trabecular number, with a corresponding increase in spacing, in the proximal tibial metaphysis of ND control mice (**Figures 3A,C,E,G**).

Relative to ND controls, mice fed a HFD had a significant decrease in trabecular BVF, bone mineral content (BMC), and number after 12-weeks of diet (**Figures 3C,D,E**). Structure model index and trabecular spacing were reciprocally increased (**Figures 3F,G**). Trabecular thickness remained unchanged (Data Set 1 in Supplementary Material). Loss of trabecular BVF and BMC with HFD, relative to control ND, persisted at the 16- and 20-week time points (**Figures 3C–G**). Weight loss partially rescued decreases in trabecular BVF, BMC, and number (**Figures 3C–E**) and increases in spacing (**Figure 3G**).

Unlike loss of trabecular bone at 12-weeks, MAT volume was not significantly increased relative to ND control until 16- and 20-weeks of HFD (**Figure 3B**). Over time, MAT increased by 3.5-fold from 12- to 16-weeks of age in the HFD group (**Figure 3B**).

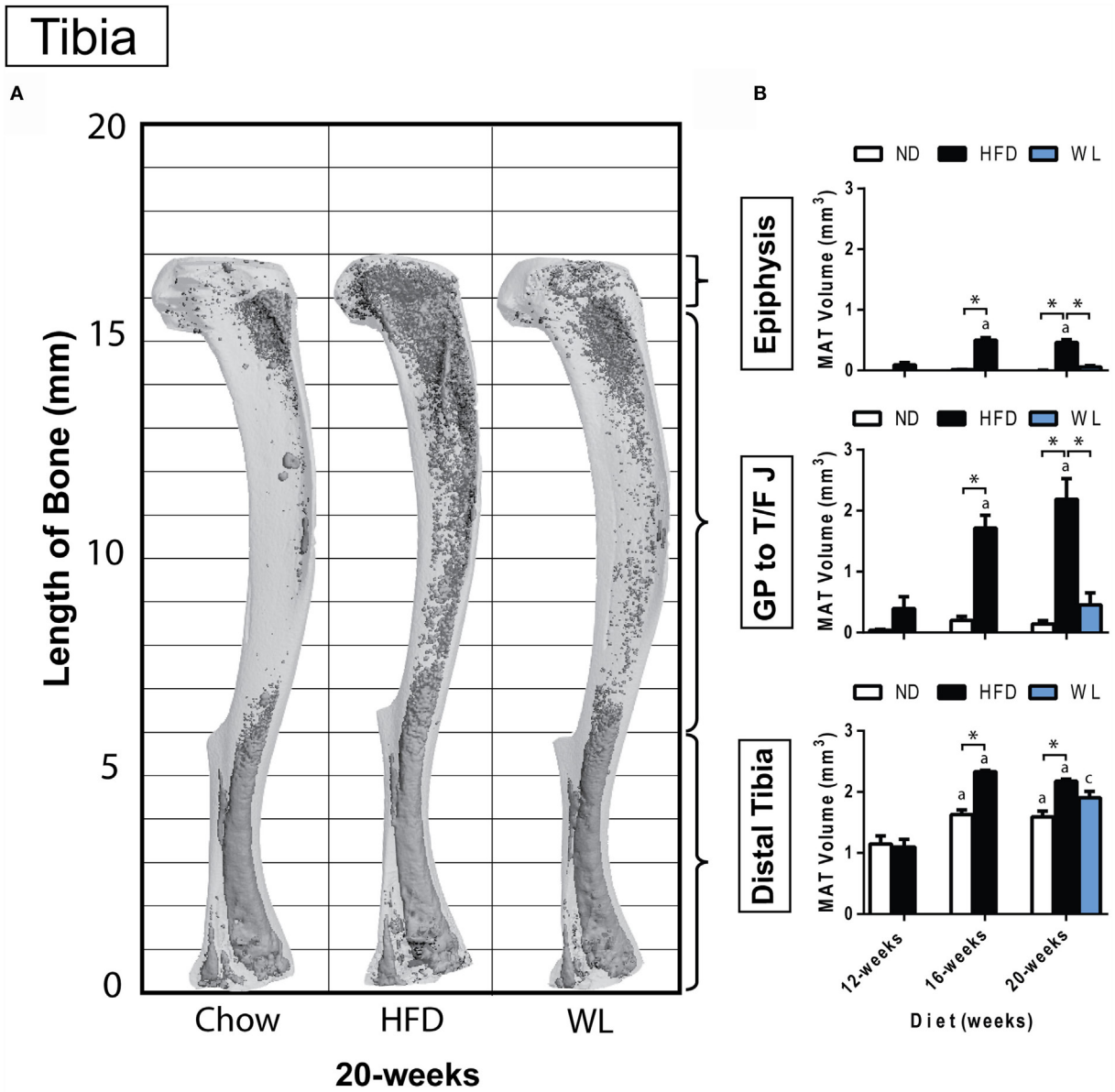

FIGURE 2 | Region-specific changes in MAT volume with HFD and WL. (A) 3D reconstruction of osmium tetroxide stained MAT (dark gray) overlaid on the tibia bone (light gray). **(B)** Region-specific quantification of MAT in the proximal tibial epiphysis, between the growth plate to tibia/fibula junction (GP to T/F J), and the distal tibia. All graphs are mean ± SEM. *N* = 3-6 per group for the proximal epiphysis; low *N* is due to accidental removal/fracture of the proximal epiphysis during processing. *N* = 6–8 for all other groups. ND, normal chow diet; HFD, high-fat diet; WL, weight loss. "a" – significant vs. 12-week on same diet. "b" – significant vs. 16-week on same diet. "c" – significant vs. 12-week HFD. *$p < 0.050$ for the indicated comparison.

No further increases were present from 16- to 20-weeks of age. Weight loss completely prevented HFD-induced MAT accumulation from 12- to 20-weeks (**Figure 3B**).

In the Femur, Trabecular Bone Quality Decreases with High-Fat Diet and after Weight Loss

Relative to ND control, HFD caused MAT expansion within the femur (**Figure 4A**). MAT expansion was absent in the WL group (**Figure 4A**). The absolute amount of MAT in the distal femoral metaphysis was ~90% less than the proximal tibia ($p < 0.0001$, *t*-test) (**Figures 3B** and **4A**). The magnitude of the loss of BVF with HFD at 20-weeks was comparable between femur and tibia (50 vs. 45%) (**Figure 4B**; Data Sets 1 and 2 in Supplementary Material). There was also a significant, HFD-induced decrease in trabecular number and increase in trabecular spacing (**Figures 4D,F**). Trabecular thickness and tissue mineral density remained unchanged (**Figures 4C,E**). With weight loss, there were no statistically significant differences in trabecular morphology,

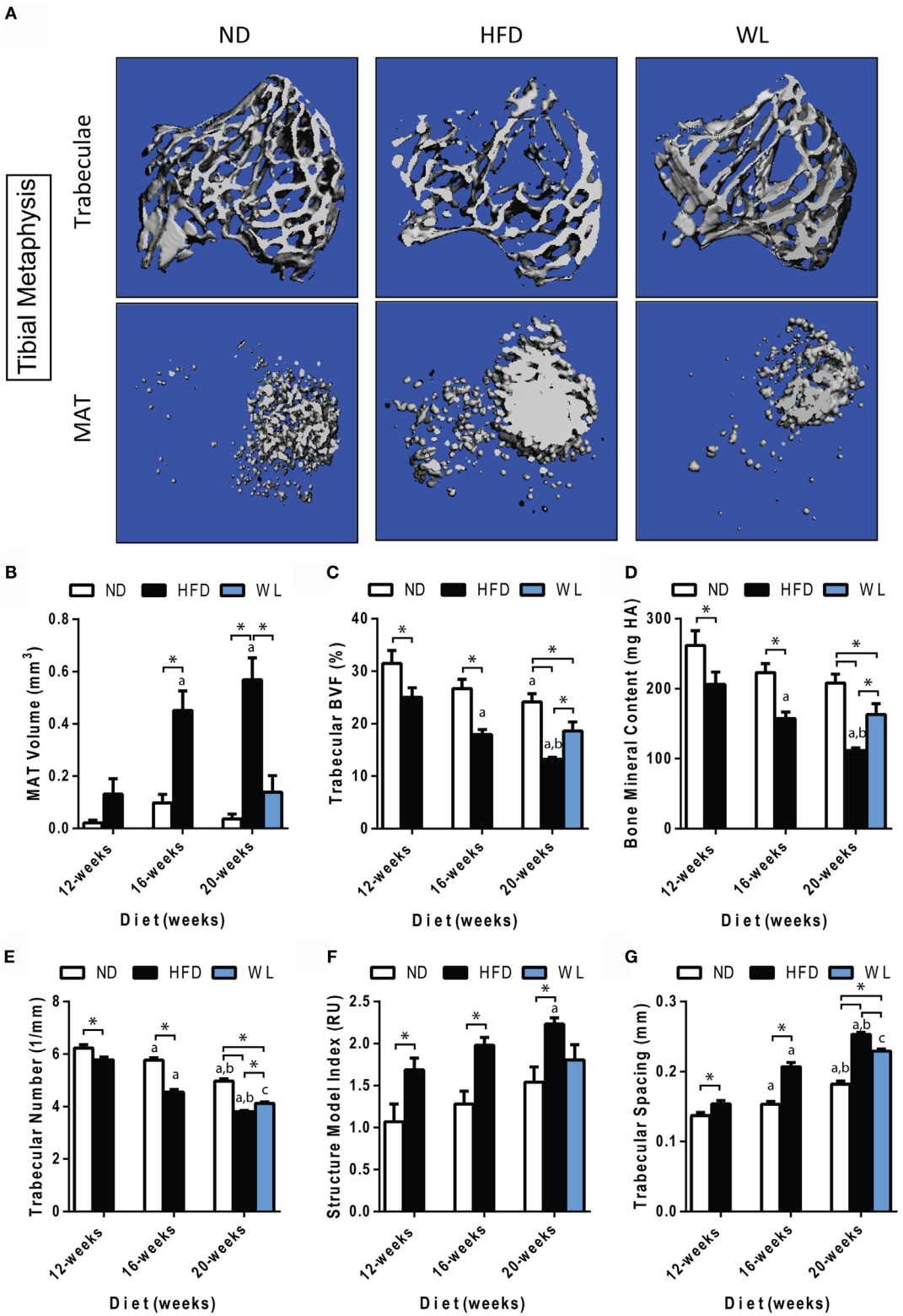

FIGURE 3 | Changes in MAT and trabecular architecture at the proximal tibial metaphysis over time. **(A)** Representative images of trabecular architecture and MAT at the 20-week time point. Images of trabeculae and MAT are from the same bone for a given diet. **(B–G)** Quantification of MAT and trabecular parameters in the proximal metaphysis of the tibia. All graphs are mean ± SEM. $N = 7–8$ per group. ND: normal chow diet; HFD: high-fat diet; WL: weight loss. "a" – significant vs. 12-week on same diet. "b" – significant vs. 16-week on same diet. "c" – significant vs. 12-week HFD. *$p < 0.050$ for the indicated comparison.

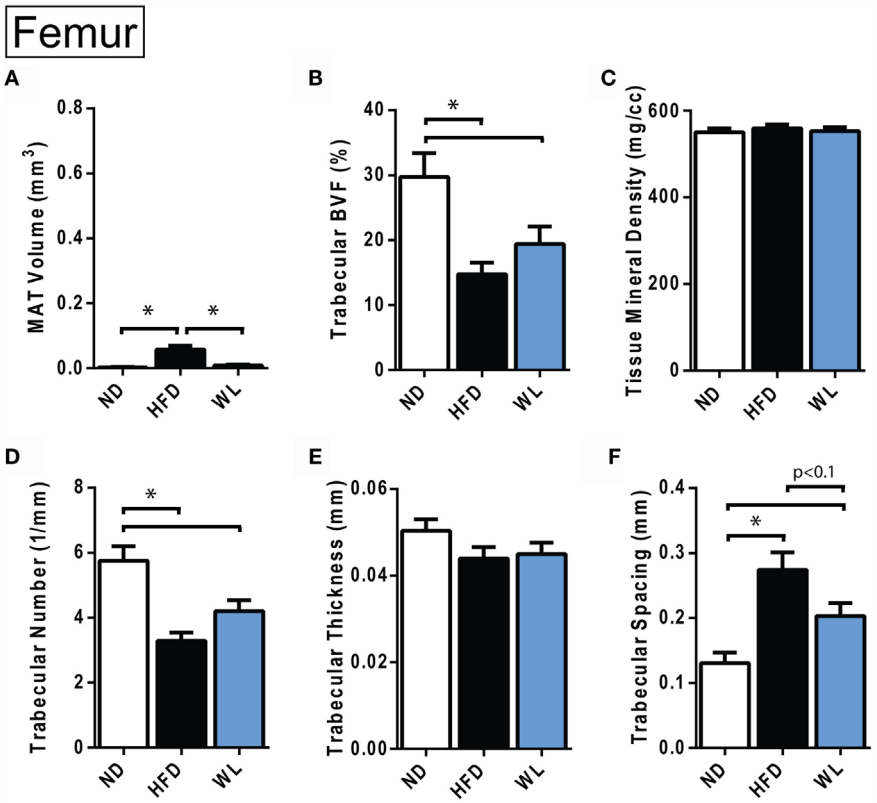

FIGURE 4 | Changes in MAT and trabecular architecture at the distal femoral metaphysis at 20-weeks. (A–F) Quantification of MAT and trabecular parameters in the distal metaphysis of the femur. All graphs are mean ± SEM. $N = 8$ per group. ND, normal chow diet; HFD, high-fat diet; WL, weight loss. *$p < 0.050$ for the indicated comparison.

relative to HFD, in the femur (**Figures 4B–F**). There was a non-significant trend toward a decrease in trabecular spacing in the WL group relative to HFD (**Figure 4F**).

Changes in Cortical Bone after High-Fat Diet and Weight Loss

Within the tibia, there were no statistically significant changes in mid-diaphyseal cortical morphology after 12, 16, or 20 weeks of HFD or after weight loss (**Figures 5A–F**). However, slight differences may have been missed after statistical correction for multiple comparisons. For example, with standard one-way ANOVA at the 20-week time point only, there was a slight decrease in cortical thickness in the 20-week HFD group relative to ND control ($p = 0.045$) (**Figure 5D**). Raw data are available in Data Set 1 in Supplementary Material.

In the femur, 20-week HFD caused a significant decrease in cortical thickness relative to ND control (**Figure 6D**). Cortical tissue mineral density was also decreased with HFD (**Figure 6F**). With weight loss, cortical thickness and total mineral density improved relative to ND (**Figures 6D,F**). No differences in total area, marrow area, cortical area, or Iyy were noted (**Figures 6A–F**). Raw data are available in Data Set 2 in Supplementary Material.

Marrow Adipose Tissue Expansion Correlates with Bone Loss in the Tibia

In the control ND group, pooled over all ages (12, 16, and 20 weeks of diet), there was a significant inverse correlation between MAT volume in the proximal metaphysis and measures of trabecular morphology including BVF, trabecular thickness, and BMC – but not with trabecular number (**Figures 7A–D**). By contrast, in the HFD group, MAT volume was negatively correlated with trabecular BVF, thickness, and BMC in addition to trabecular number (**Figures 7A–D**). Cortical thickness was significantly negatively correlated with GP to T/F J MAT volume in the HFD group only (**Figure 7E**). Cortical TMD did not correlate with MAT volume in either group (**Figure 7F**).

High-Fat Diet Causes Persistent Decreases in Biomechanical Properties of the Femur

Four-point bending was performed to assess the biomechanical integrity of HFD and WL femurs. The femurs from the 20-week HFD and WL groups broke under a reduced maximum load relative to ND, trending toward less total work to induce fracture (**Figures 8A,B**). This indicates that despite recovery of cortical

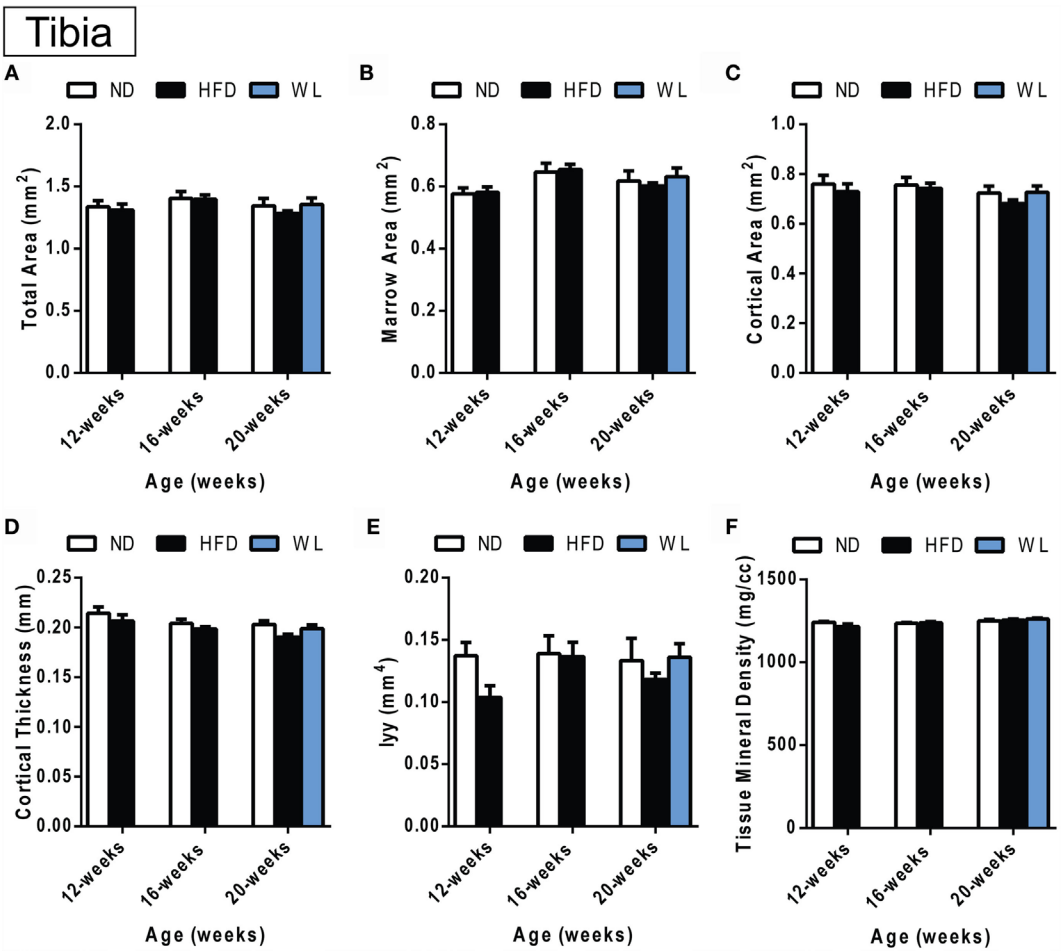

FIGURE 5 | Changes in cortical morphology at the mid-tibial diaphysis. (A–F) Quantification of cortical parameters in the mid-diaphysis of the tibia. $N = 7–8$ per group. ND: normal chow diet; HFD: high-fat diet; WL: weight loss. All graphs are mean ± SEM. "a" – significant vs. 12-week on same diet. "b" – significant vs. 16-week on same diet. "c" – significant vs. 12-week HFD. *$p < 0.050$ for the indicated comparison.

thickness and mineral density with WL (**Figure 6**), the bone quality remains impaired, leading to decreased fracture resistance and poor post-yield behavior. The yield load and post-yield work trended toward a decrease relative to ND in the HFD and WL groups, respectively ($p < 0.1$) (**Figures 8D,E**). The stiffness, post-yield displacement, and modulus of elasticity (39) were not significantly different between groups (**Figures 8C,F**) (Data Set 3 in Supplementary Material).

DISCUSSION

To our knowledge, this is the first study that has measured, within the same bone, HFD-induced MAT expansion and changes in skeletal morphology. By incorporating a weight loss group, we were also able to inhibit MAT expansion, and thus examine the impact of HFD on bone quality in the absence of MAT accumulation. In this study, HFD caused increases in body mass at 12-weeks, indicating accumulation of peripheral adiposity. This occurred prior to increases in MAT, supporting the hypothesis that dysfunction of peripheral tissues (e.g., insulin resistance) occurs prior to HFD-induced MAT expansion.

As adipocytes and osteoblasts arise from the same mesenchymal progenitor cell, the notion of "fate-switching" whereby one lineage is favored over the other has been suggested (29–31). The inhibition of osteoblast differentiation may subsequently lead to increased adipocyte production, thus presenting with a situation of reduced bone mass and increased MAT (44). It is of note that this concept fails to capture the complexity of skeletal progenitors – some of which have the capacity to differentiate into osteoblasts but not adipocytes (45). In our study we observed the well-documented inverse correlation between MAT volume and bone mass/density in the tibia (**Figure 7**). However, despite this correlation, our data do not support the hypothesis that MAT expansion is the sole mediator of bone loss with HFD. Specifically, deterioration of trabecular architecture occurred as early as 12-weeks after HFD in the tibia, while changes in MAT did not become statistically significant until 16 weeks (**Figures 2** and **3**). Furthermore,

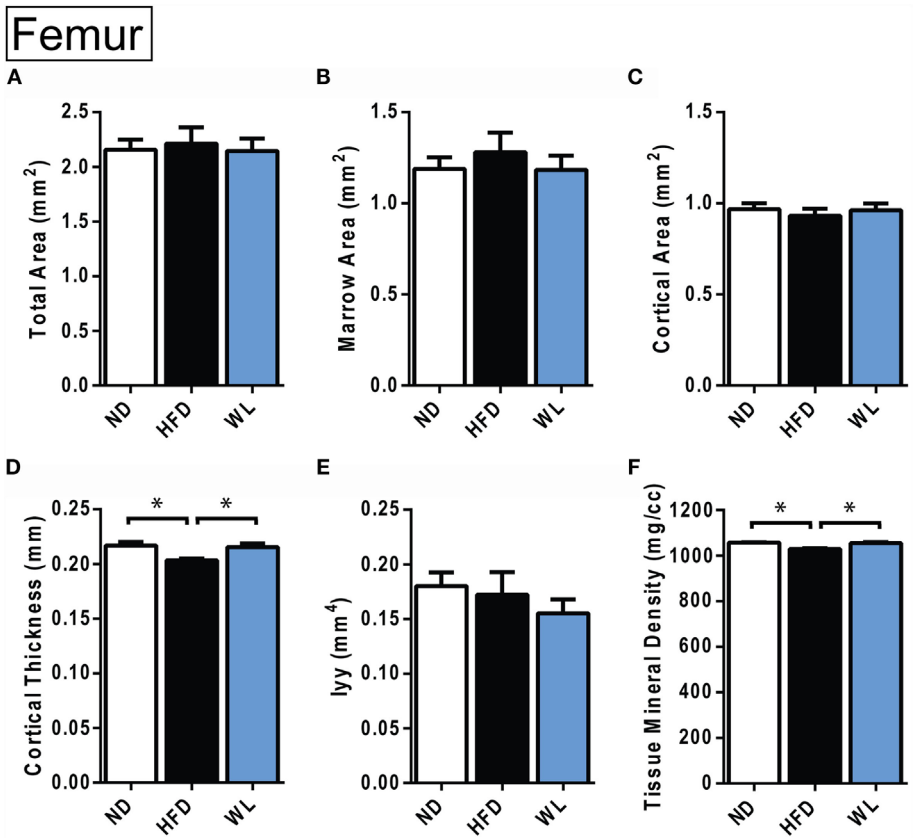

FIGURE 6 | Changes in cortical morphology at the mid-femoral diaphysis. (A–F) Quantification of cortical parameters in the mid-diaphysis of the femur. $N = 8$ per group. ND, normal chow diet; HFD, high-fat diet; WL, weight loss. All graphs are mean ± SEM. *$p < 0.050$ for the indicated comparison.

though switching from HFD to chow at 12-weeks completely prevented HFD-induced MAT accumulation in the WL group (**Figure 3B**), loss of trabecular number and corresponding increases in trabecular spacing beyond that of controls still occurred (**Figures 3E,G**). Thus, in this context, inhibition of MAT expansion by weight loss was not sufficient to block HFD-induced decreases in trabecular bone within the tibial metaphysis.

There are many MAT-independent effects with the potential to regulate bone during high-fat feeding, the presence of which may contribute to the cancellous and cortical bone loss observed in this model. Increased fat mass is associated with increased systemic markers of oxidative stress in both humans and mice (4). Increased peroxide (H_2O_2) and reduced endothelial nitric oxide synthase in a genetic model of obesity was associated with cancellous bone loss (46). Reactive oxygen species have been found to promote the association of the transcription factors FoxO with β-catenin, subsequently leading to a reduction in Wnt signaling and osteoblastic differentiation (47). Although the direct effects of leptin may also promote osteoblast proliferation and differentiation (25, 48), the central effects of leptin have been shown to mediate the opposite effects, promoting cancellous bone loss *via* the sympathetic nervous system (23, 24). Another central pathway involving increased neuropeptide Y (NPY) arising from leptin resistance during obesity is implicated in bone metabolism as mice with increased central NPY have concurrent obesity with bone loss (49) and NPY deficiency in *ob/ob* mice leads to improved cortical bone mass (50).

Lastly, there is an increase in systemic inflammation with obesity that might directly affect bone marrow osteoclasts. A major source of obesity-induced inflammation stems from an increase in bone marrow macrophages and their progenitors (51). These bone marrow-derived macrophages during obesity mediate an inflammatory environment that has been shown to stimulate osteoclastogenesis and reduce osteoblast development (52, 53), possibly due to the expansion of the common monocyte-osteoclast progenitor (54). Recently, Yue et al. have also demonstrated that leptin produced from obese adipose tissue can directly bind to leptin receptors on mesenchymal stem cells promoting differentiation of adipocytes and inhibiting osteoblast formation (29). Altogether there are a number of MAT-independent variables involved in coordinating the relationship between diet-induced obesity and bone.

Though it is not the sole mediator of bone loss with HFD, our study does not rule out the possibility that MAT, particularly when present in large excess, may exert detrimental effects on bone. Indeed, the magnitude of cancellous bone loss in the

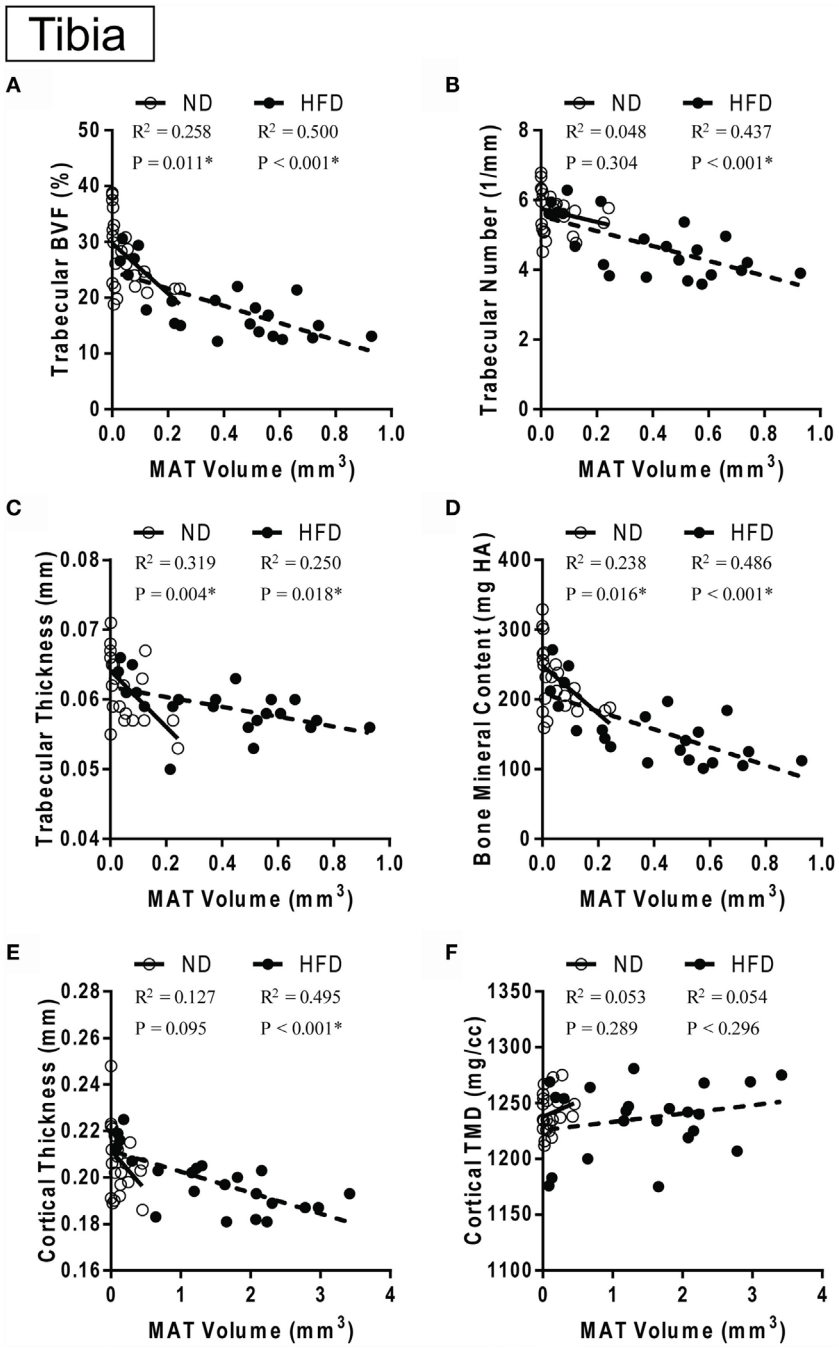

FIGURE 7 | **MAT vs. bone over time with control or high-fat diet**. **(A–D)** Correlation between marrow adipose tissue volume in the proximal metaphysis and trabecular parameters. **(E,F)** Correlation between marrow adipose tissue volume between the growth plate and tibia/fibula junction and cortical parameters in the same bone. Data grouped by diet type. ND: normal diet control for 12, 16and 20 weeks. HFD: high-fat diet for 12, 16, and 20 weeks. Linear regression. *$p < 0.050$ for the indicated diet.

tibia (**Figure 3**) and cortical bone loss in the femur (**Figure 6**) was significantly greater in the 20-week HFD group with MAT expansion than the WL group in which MAT expansion failed to occur. Comparisons between the femur and tibia provide further clues as to this relationship. Consistent with a previous report, 12-weeks of HFD followed by 8-weeks of normal chow diet (WL group) did not prevent cancellous bone loss in the distal femoral metaphysis (12). By contrast, in the same animals, weight loss partially prevented HFD-induced deterioration of trabecular BVF and BMC in the tibia (**Figure 3**). It is possible

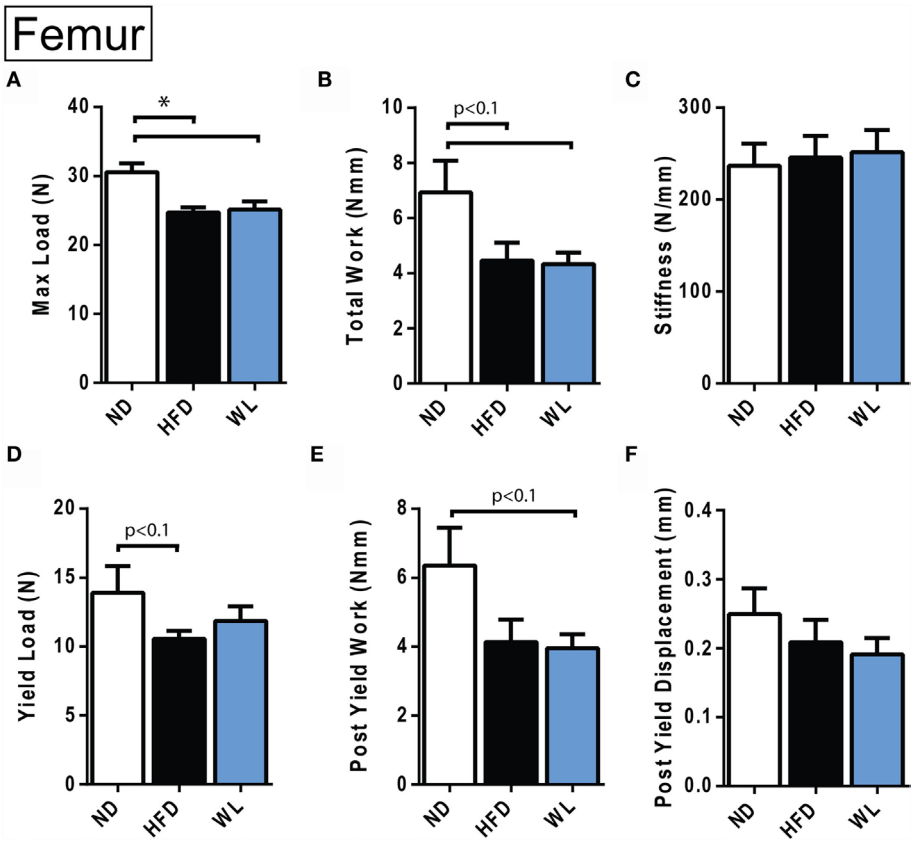

FIGURE 8 | **Femur biomechanical testing at 20 weeks**. **(A–F)** Quantification of biomechanical parameters, as assessed by four-point bending. $N = 12–14$ per group. ND, normal chow diet; HFD, high-fat diet; WL, weight loss. All graphs are mean ± SEM. $^{*}p < 0.050$ for the indicated comparison.

that this discrepancy may be explained by differences in MAT. After 20-weeks of HFD, the volume of MAT in the metaphysis of the tibia was 9.8-fold greater than in the femur. This is similar to previous work by Halade et al., despite substantial differences in their model system (10% corn oil diet for 24-weeks in 12-month-old female mice) (44). Thus, it is possible that this increase in MAT contributed to additional bone loss in the tibia, beyond that observed in the femur, subsequently leading to a difference between the HFD and WL groups. However, given previous work, the nuances of this observation remain unclear (44).

Direct interactions between MAT and bone may influence bone loss during high fat feeding. Recently, MAT was found to be a significant contributor of circulating adiponectin during calorie restriction (55), this emphasizes the potential of MAT to influence not only bone but also whole body homeostasis. Direct adipose-bone pathways have been demonstrated to influence bone mass; the main two adipokines implicated are leptin (29, 48, 56–58) and adiponectin (59–61). More locally within the bone microenvironment, *in vitro* experiments have demonstrated that the release of free fatty acids from adipocytes inhibited osteoblast differentiation and promoted apoptosis through ROS production (62). Interestingly, co-cultures of osteoblasts and osteoclasts with adipocytes suggest that in addition to reducing osteoblastogenesis, osteoclastogenesis may be increased with increased adiposity, resulting in reduced bone mass (31).

Biomechanically, weight loss after 12-weeks of HFD was insufficient to rescue impaired fracture resistance. Indeed, the maximum load endured by the HFD and WL femurs was nearly identical – despite almost complete recovery of body mass and prevention of MAT expansion in the WL group. Comparable stiffness and modulus of elasticity in the ND, WL, and HFD groups indicates that the elastic properties of the bone were not affected. However, the failure properties were similarly reduced in both the HFD and WL groups, despite differential rescue of tissue mineral density and cortical thickness, implying that femur architecture fails to explain the impaired biomechanics. This may point to dysfunction within the organic properties of the bone, such as impaired cross-linking of collagen (26), as a potential mediator of persistent HFD-induced fracture risk.

Our study demonstrates that HFD causes long-term, persistent changes in bone quality. We started HFD at an age in which skeletal development is still highly active, likely contributing to impaired bone accrual during growth. Indeed, diet-induced obesity causes greater damage in growing bones (63). This

is an important finding given the rise of obesity in pediatric populations (2, 64). Furthermore, these data demonstrate that MAT is not necessary for HFD-induced bone loss; however, MAT expansion, when present, may contribute to additional skeletal deterioration. It is likely that changes within the bone microenvironment including the adipocytes themselves are being altered but this was not examined in the current study (31, 65) and will need to be evaluated with future mechanistic investigations.

Given the rise in obesity across the age spectrum, this is a critical area of research and future studies are needed to determine the effects of weight loss (dietary or surgical) on bone density and to understand the mechanisms that drive changes in bone health. Even with the limitations a clear finding in this study is that there are some reversible and some permanent changes with HFD, followed by WL. Different regimens may be required to maintain bone health after WL, possibly with a focus on activity and diet (36).

AUTHOR CONTRIBUTIONS

ES and KS were involved in designing studies, completion of studies, data interpretation and analysis, and manuscript preparation. BK, KM, SK, KK, SA, and BZ were involved in completion of studies, data analysis, and reviewed the final manuscript.

FUNDING

This work was supported by grants from the National Institute of Health, K99-DE024178 and R00-DE024178 (ES) and K08-DK101755 (KS).

SUPPLEMENTARY MATERIAL

The Supplementary Material for this article can be found online at http://journal.frontiersin.org/article/10.3389/fendo.2016.00102

REFERENCES

1. AustralianHealthSurvey. *Australian Health Survey – Australian Bureau of Statistics*. Canberra: ABS (2011).
2. Ogden CL, Carroll MD, Fryar CD, Flegal KM. Prevalence of obesity among adults and youth: United States, 2011–2014. *NCHS Data Brief* (2015) 219:1–8.
3. Ogden CL, Carroll MD, Flegal KM. Prevalence of obesity in the United States. *JAMA* (2014) 312(2):189–90. doi:10.1001/jama.2014.6228
4. Furukawa S, Fujita T, Shimabukuro M, Iwaki M, Yamada Y, Nakajima Y, et al. Increased oxidative stress in obesity and its impact on metabolic syndrome. *J Clin Invest* (2004) 114(12):1752–61. doi:10.1172/jci21625
5. Prospective Studies C, Whitlock G, Lewington S, Sherliker P, Clarke R, Emberson J, et al. Body-mass index and cause-specific mortality in 900 000 adults: collaborative analyses of 57 prospective studies. *Lancet* (2009) 373(9669):1083–96. doi:10.1016/s0140-6736(09)60318-4
6. Gregor MF, Hotamisligil GS. Inflammatory mechanisms in obesity. *Annu Rev Immunol* (2011) 29:415–45. doi:10.1146/annurev-immunol-031210-101322
7. Fehrendt H, Linn T, Hartmann S, Szalay G, Heiss C, Schnettler R, et al. Negative influence of a long-term high-fat diet on murine bone architecture. *Int J Endocrinol* (2014) 2014:318924. doi:10.1155/2014/318924
8. Gautam J, Choudhary D, Khedgikar V, Kushwaha P, Singh RS, Singh D, et al. Micro-architectural changes in cancellous bone differ in female and male C57BL/6 mice with high-fat diet-induced low bone mineral density. *Br J Nutr* (2014) 111(10):1811–21. doi:10.1017/S0007114514000051
9. Mosca LN, Goldberg TB, da Silva VN, da Silva CC, Kurokawa CS, Bisi Rizzo AC, et al. Excess body fat negatively affects bone mass in adolescents. *Nutrition* (2014) 30(7–8):847–52. doi:10.1016/j.nut.2013.12.003
10. Shen CL, Chen L, Wang S, Chyu MC. Effects of dietary fat levels and feeding durations on musculoskeletal health in female rats. *Food Funct* (2014) 5(3):598–604. doi:10.1039/c3fo60334b
11. Lecka-Czernik B, Stechschulte LA, Czernik PJ, Dowling AR. High bone mass in adult mice with diet-induced obesity results from a combination of initial increase in bone mass followed by attenuation in bone formation: implications for high bone mass and decreased bone quality in obesity. *Mol Cell Endocrinol* (2015) 410:35–41. doi:10.1016/j.mce.2015.01.001
12. Inzana JA, Kung M, Shu L, Hamada D, Xing LP, Zuscik MJ, et al. Immature mice are more susceptible to the detrimental effects of high fat diet on cancellous bone in the distal femur. *Bone* (2013) 57(1):174–83. doi:10.1016/j.bone.2013.08.003
13. Kinjo M, Setoguchi S, Solomon DH. Bone mineral density in adults with the metabolic syndrome: analysis in a population-based U.S. sample. *J Clin Endocrinol Metab* (2007) 92(11):4161–4. doi:10.1210/jc.2007-0757
14. Ho-Pham LT, Nguyen UD, Nguyen TV. Association between lean mass, fat mass, and bone mineral density: a meta-analysis. *J Clin Endocrinol Metab* (2014) 99(1):30–8. doi:10.1210/jc.2013-319010.1210/jc.2014-v99i12-30A
15. Lloyd JT, Alley DE, Hawkes WG, Hochberg MC, Waldstein SR, Orwig DL. Body mass index is positively associated with bone mineral density in US older adults. *Arch Osteoporos* (2014) 9:175. doi:10.1007/s11657-014-0175-2
16. Compston J. Obesity and fractures. *Joint Bone Spine* (2013) 80(1):8–10. doi:10.1016/j.jbspin.2012.07.016
17. Dimitri P, Jacques RM, Paggiosi M, King D, Walsh J, Taylor ZA, et al. Leptin may play a role in bone microstructural alterations in obese children. *J Clin Endocrinol Metab* (2015) 100(2):594–602. doi:10.1210/jc.2014-3199
18. Prieto-Alhambra D, Premaor MO, Fina Aviles F, Hermosilla E, Martinez-Laguna D, Carbonell-Abella C, et al. The association between fracture and obesity is site-dependent: a population-based study in postmenopausal women. *J Bone Miner Res* (2012) 27(2):294–300. doi:10.1002/jbmr.1466
19. Tang X, Liu G, Kang J, Hou Y, Jiang F, Yuan W, et al. Obesity and risk of hip fracture in adults: a meta-analysis of prospective cohort studies. *PLoS One* (2013) 8(4):e55077. doi:10.1371/journal.pone.0055077
20. Caffarelli C, Alessi C, Nuti R, Gonnelli S. Divergent effects of obesity on fragility fractures. *Clin Interv Aging* (2014) 9:1629–36. doi:10.2147/cia.s64625
21. Cao JJ, Gregoire BR, Gao H. High-fat diet decreases cancellous bone mass but has no effect on cortical bone mass in the tibia in mice. *Bone* (2009) 44(6):1097–104. doi:10.1016/j.bone.2009.02.017
22. Cao JJ, Sun L, Gao H. Diet-induced obesity alters bone remodeling leading to decreased femoral trabecular bone mass in mice. *Ann N Y Acad Sci* (2010) 1192:292–7. doi:10.1111/j.1749-6632.2009.05252.x
23. Ducy P, Amling M, Takeda S, Priemel M, Schilling AF, Beil FT, et al. Leptin inhibits bone formation through a hypothalamic relay: a central control of bone mass. *Cell* (2000) 100(2):197–207. doi:10.1016/S0092-8674(00)81558-5
24. Takeda S, Elefteriou F, Levasseur R, Liu X, Zhao L, Parker KL, et al. Leptin regulates bone formation via the sympathetic nervous system. *Cell* (2002) 111(3):305–17. doi:10.1016/S0092-8674(02)01049-8
25. Elefteriou F, Ahn JD, Takeda S, Starbuck M, Yang X, Liu X, et al. Leptin regulation of bone resorption by the sympathetic nervous system and CART. *Nature* (2005) 434(7032):514–20. doi:10.1038/nature03398
26. Ionova-Martin SS, Wade JM, Tang S, Shahnazari M, Ager JW III, Lane NE, et al. Changes in cortical bone response to high-fat diet from adolescence to adulthood in mice. *Osteoporos Int* (2011) 22(8):2283–93. doi:10.1007/s00198-010-1432-x
27. Fujita Y, Watanabe K, Maki K. Serum leptin levels negatively correlate with trabecular bone mineral density in high-fat diet-induced obesity mice. *J Musculoskelet Neuronal Interact* (2012) 12(2):84–94.
28. Doucette CR, Horowitz MC, Berry R, MacDougald OA, Anunciado-Koza R, Koza RA, et al. A high fat diet increases bone marrow adipose tissue (MAT) but does not alter trabecular or cortical bone mass in C57BL/6J mice. *J Cell Physiol* (2015) 230(9):2032–7. doi:10.1002/jcp.24954

29. Yue R, Zhou BO, Shimada IS, Zhao Z, Morrison SJ. Leptin receptor promotes adipogenesis and reduces osteogenesis by regulating mesenchymal stromal cells in adult bone marrow. *Cell Stem Cell* (2016) 18(6):782–96. doi:10.1016/j.stem.2016.02.015
30. Hamrick MW, Della-Fera MA, Choi YH, Pennington C, Hartzell D, Baile CA. Leptin treatment induces loss of bone marrow adipocytes and increases bone formation in leptin-deficient ob/ob mice. *J Bone Miner Res* (2005) 20(6):994–1001. doi:10.1359/jbmr.050103
31. Xu F, Du Y, Hang S, Chen A, Guo F, Xu T. Adipocytes regulate the bone marrow microenvironment in a mouse model of obesity. *Mol Med Rep* (2013) 8(3):823–8. doi:10.3892/mmr.2013.1572
32. Brzozowska MM, Sainsbury A, Eisman JA, Baldock PA, Center JR. Bariatric surgery, bone loss, obesity and possible mechanisms. *Obes Rev* (2013) 14(1):52–67. doi:10.1111/j.1467-789X.2012.01050.x
33. Seimon RV, Shi YC, Slack K, Lee K, Fernando HA, Nguyen AD, et al. Intermittent moderate energy restriction improves weight loss efficiency in diet-induced obese mice. *PLoS One* (2016) 11(1):e0145157. doi:10.1371/journal.pone.0145157
34. Kohrt WM, Barry DW, Schwartz RS. Muscle forces or gravity: what predominates mechanical loading on bone? *Med Sci Sports Exerc* (2009) 41(11):2050–5. doi:10.1249/MSS.0b013e3181a8c717
35. Ma H, Turpeinen T, Silvennoinen M, Torvinen S, Rinnankoski-Tuikka R, Kainulainen H, et al. Effects of diet-induced obesity and voluntary wheel running on the microstructure of the murine distal femur. *Nutr Metab (Lond)* (2011) 8(1):1. doi:10.1186/1743-7075-8-1
36. Hunter GR, Plaisance EP, Fisher G. Weight loss and bone mineral density. *Curr Opin Endocrinol Diabetes Obes* (2014) 21(5):358–62. doi:10.1097/MED.0000000000000087
37. Scheller EL, Doucette CR, Learman BS, Cawthorn WP, Khandaker S, Schell B, et al. Region-specific variation in the properties of skeletal adipocytes reveals regulated and constitutive marrow adipose tissues. *Nat Commun* (2015) 6:7808. doi:10.1038/ncomms8808
38. Sinder BP, Salemi JD, Ominsky MS, Caird MS, Marini JC, Kozloff KM. Rapidly growing Brtl/+ mouse model of osteogenesis imperfecta improves bone mass and strength with sclerostin antibody treatment. *Bone* (2015) 71:115–23. doi:10.1016/j.bone.2014.10.012
39. Kozloff KM, Carden A, Bergwitz C, Forlino A, Uveges TE, Morris MD, et al. Brittle IV mouse model for osteogenesis imperfecta IV demonstrates postpubertal adaptations to improve whole bone strength. *J Bone Miner Res* (2004) 19(4):614–22. doi:10.1359/JBMR.040111
40. Scheller EL, Troiano N, Vanhoutan JN, Bouxsein MA, Fretz JA, Xi Y, et al. Use of osmium tetroxide staining with microcomputerized tomography to visualize and quantify bone marrow adipose tissue in vivo. *Methods Enzymol* (2014) 537:123–39. doi:10.1016/B978-0-12-411619-1.00007-0
41. Thissen D, Steinberg L, Kuang D. Quick and easy implementation of the Benjamini-Hochberg procedure for controlling the false positive rate in multiple comparisons. *J Educ Behav Stat* (2002) 27(1):77–83. doi:10.3102/10769986027001077
42. Halloran BP, Ferguson VL, Simske SJ, Burghardt A, Venton LL, Majumdar S. Changes in bone structure and mass with advancing age in the male C57BL/6J mouse. *J Bone Miner Res* (2002) 17(6):1044–50. doi:10.1359/jbmr.2002.17.6.1044
43. Glatt V, Canalis E, Stadmeyer L, Bouxsein ML. Age-related changes in trabecular architecture differ in female and male C57BL/6J mice. *J Bone Miner Res* (2007) 22(8):1197–207. doi:10.1359/jbmr.070507
44. Halade GV, Rahman MM, Williams PJ, Fernandes G. High fat diet-induced animal model of age-associated obesity and osteoporosis. *J Nutr Biochem* (2010) 21(12):1162–9. doi:10.1016/j.jnutbio.2009.10.002
45. Worthley DL, Churchill M, Compton JT, Tailor Y, Rao M, Si Y, et al. Gremlin 1 identifies a skeletal stem cell with bone, cartilage, and reticular stromal potential. *Cell* (2015) 160(1–2):269–84. doi:10.1016/j.cell.2014.11.042
46. Ohnishi T, Bandow K, Kakimoto K, Machigashira M, Matsuyama T, Matsuguchi T. Oxidative stress causes alveolar bone loss in metabolic syndrome model mice with type 2 diabetes. *J Periodontal Res* (2009) 44(1):43–51. doi:10.1111/j.1600-0765.2007.01060.x
47. Almeida M, Han L, Martin-Millan M, Plotkin LI, Stewart SA, Roberson PK, et al. Skeletal involution by age-associated oxidative stress and its acceleration by loss of sex steroids. *J Biol Chem* (2007) 282(37):27285–97. doi:10.1074/jbc.M702810200
48. Iwamoto I, Fujino T, Douchi T. The leptin receptor in human osteoblasts and the direct effect of leptin on bone metabolism. *Gynecol Endocrinol* (2004) 19(2):97–104. doi:10.1080/09513590412331284389
49. Baldock PA, Sainsbury A, Couzens M, Enriquez RF, Thomas GP, Gardiner EM, et al. Hypothalamic Y2 receptors regulate bone formation. *J Clin Invest* (2002) 109(7):915–21. doi:10.1172/jci14588
50. Wong IP, Nguyen AD, Khor EC, Enriquez RF, Eisman JA, Sainsbury A, et al. Neuropeptide Y is a critical modulator of leptin's regulation of cortical bone. *J Bone Miner Res* (2013) 28(4):886–98. doi:10.1002/jbmr.1786
51. Singer K, DelProposto J, Morris DL, Zamarron B, Mergian T, Maley N, et al. Diet-induced obesity promotes myelopoiesis in hematopoietic stem cells. *Mol Metab* (2014) 3(6):664–75. doi:10.1016/j.molmet.2014.06.005
52. Kyung TW, Lee JE, Phan TV, Yu R, Choi HS. Osteoclastogenesis by bone marrow-derived macrophages is enhanced in obese mice. *J Nutr* (2009) 139(3):502–6. doi:10.3945/jn.108.100032
53. Halade GV, El Jamali A, Williams PJ, Fajardo RJ, Fernandes G. Obesity-mediated inflammatory microenvironment stimulates osteoclastogenesis and bone loss in mice. *Exp Gerontol* (2011) 46(1):43–52. doi:10.1016/j.exger.2010.09.014
54. Pollard JW. Trophic macrophages in development and disease. *Nat Rev Immunol* (2009) 9(4):259–70. doi:10.1038/nri2528
55. Cawthorn WP, Scheller EL, Learman BS, Parlee SD, Simon BR, Mori H, et al. Bone marrow adipose tissue is an endocrine organ that contributes to increased circulating adiponectin during caloric restriction. *Cell Metab* (2014) 20(2):368–75. doi:10.1016/j.cmet.2014.06.003
56. Gordeladze JO, Drevon CA, Syversen U, Reseland JE. Leptin stimulates human osteoblastic cell proliferation, de novo collagen synthesis, and mineralization: impact on differentiation markers, apoptosis, and osteoclastic signaling. *J Cell Biochem* (2002) 85(4):825–36. doi:10.1002/jcb.10156
57. Scheller EL, Song J, Dishowitz MI, Soki FN, Hankenson KD, Krebsbach PH. Leptin functions peripherally to regulate differentiation of mesenchymal progenitor cells. *Stem Cells* (2010) 28(6):1071–80. doi:10.1002/stem.432
58. Scheller EL, Song J, Dishowitz MI, Hankenson KD, Krebsbach PH. A potential role for the myeloid lineage in leptin-regulated bone metabolism. *Horm Metab Res* (2012) 44(1):1–5. doi:10.1055/s-0031-1297971
59. Williams GA, Wang Y, Callon KE, Watson M, Lin JM, Lam JB, et al. In vitro and in vivo effects of adiponectin on bone. *Endocrinology* (2009) 150(8):3603–10. doi:10.1210/en.2008-1639
60. Kajimura D, Lee HW, Riley KJ, Arteaga-Solis E, Ferron M, Zhou B, et al. Adiponectin regulates bone mass via opposite central and peripheral mechanisms through FoxO1. *Cell Metab* (2013) 17(6):901–15. doi:10.1016/j.cmet.2013.04.009
61. Wang F, Wang PX, Wu XL, Dang SY, Chen Y, Ni YY, et al. Deficiency of adiponectin protects against ovariectomy-induced osteoporosis in mice. *PLoS One* (2013) 8(7):e68497. doi:10.1371/journal.pone.0068497
62. Dong X, Bi L, He S, Meng G, Wei B, Jia S, et al. FFAs-ROS-ERK/P38 pathway plays a key role in adipocyte lipotoxicity on osteoblasts in co-culture. *Biochimie* (2014) 101:123–31. doi:10.1016/j.biochi.2014.01.002
63. Wee N, Herzog H, Baldock PA. Diet-induced obesity alters skeletal microarchitecture and the endocrine activity of bone. In: Watson RR, Mahadevan D, editors. *Nutrition and Diet in Therapy of Bone Diseases*. Wageningen, The Netherlands: Wageningen Academic (2016). p. 375–94.
64. Australian Bureau of Statistics. *Australian Bureau of Statistics: Australian Health Survey (2011–2012)*. Canberra: ABS (2013).
65. Patsch JM, Li X, Baum T, Yap SP, Karampinos DC, Schwartz AV, et al. Bone marrow fat composition as a novel imaging biomarker in postmenopausal women with prevalent fragility fractures. *J Bone Miner Res* (2013) 28(8):1721–8. doi:10.1002/jbmr.1950

Conflict of Interest Statement: The authors declare that the research was conducted in the absence of any commercial or financial relationships that could be construed as a potential conflict of interest.

frontiers in Endocrinology

ORIGINAL RESEARCH
published: 16 August 2016
doi: 10.3389/fendo.2016.00110

Hypothalamic Leptin Gene Therapy Reduces Bone Marrow Adiposity in *ob/ob* Mice Fed Regular and High-Fat Diets

*Laurence B. Lindenmaier[1], Kenneth A. Philbrick[1], Adam J. Branscum[2], Satya P. Kalra[3], Russell T. Turner[1,4] and Urszula T. Iwaniec[1,4]**

[1] Skeletal Biology Laboratory, School of Biological and Population Health Sciences, Oregon State University, Corvallis, OR, USA, [2] Biostatistics Program, School of Biological and Population Health Sciences, Oregon State University, Corvallis, OR, USA, [3] Department of Neuroscience, McKnight Brain Institute, University of Florida, Gainesville, FL, USA, [4] Center for Healthy Aging Research, Oregon State University, Corvallis, OR, USA

Low bone mass is often associated with elevated bone marrow adiposity. Since osteoblasts and adipocytes are derived from the same mesenchymal stem cell (MSC) progenitor, adipocyte formation may increase at the expense of osteoblast formation. Leptin is an adipocyte-derived hormone known to regulate energy and bone metabolism. Leptin deficiency and high-fat diet-induced obesity are associated with increased marrow adipose tissue (MAT) and reduced bone formation. Short-duration studies suggest that leptin treatment reduces MAT and increases bone formation in leptin-deficient *ob/ob* mice fed a regular diet. Here, we determined the long-duration impact of increased hypothalamic leptin on marrow adipocytes and osteoblasts in *ob/ob* mice following recombinant adeno-associated virus (rAAV) gene therapy. Eight- to 10-week-old male *ob/ob* mice were randomized into four groups: (1) untreated, (2) rAAV-Lep, (3) rAAV-green fluorescent protein (rAAV-GFP), or (4) pair-fed to rAAV-Lep. For vector administration, mice were injected intracerebroventricularly with either rAAV-leptin gene therapy (rAAV-Lep) or rAAV-GFP (9×10^7 particles) and maintained for 30 weeks. In a second study, the impact of increased hypothalamic leptin levels on MAT was determined in mice fed high-fat diets; *ob/ob* mice were randomized into two groups and treated with either rAAV-Lep or rAAV-GFP. At 7 weeks post-vector administration, half the mice in each group were switched to a high-fat diet for 8 weeks. Wild-type (WT) controls included age-matched mice fed regular or high-fat diet. High-fat diet resulted in a threefold increase in MAT in WT mice, whereas MAT was increased by leptin deficiency up to 50-fold. Hypothalamic leptin gene therapy increased osteoblast perimeter and osteoclast perimeter with minor change in cancellous bone architecture. The gene therapy decreased MAT levels in *ob/ob* mice fed regular or high-fat diet to values similar to WT mice fed regular diet. These findings suggest that leptin plays an important role in regulating the differentiation of MSCs to adipocytes and osteoblasts, a process that may be dysregulated by high-fat diet. However, the results also illustrate that reducing MAT by increasing leptin levels does not necessarily result in increased bone mass.

Keywords: adipocyte, osteoblast, osteoclast, stem cell, osteoporosis, histomorphometry, rAAV

OPEN ACCESS

Edited by:
Erica L. Scheller, Washington University in St. Louis, USA

Reviewed by:
Robin Mark Howard Rumney, University of Sheffield, UK
Mark Hamrick, Georgia Health Sciences University, USA

****Correspondence:***
Urszula T. Iwaniec
urszula.iwaniec@oregonstate.edu

Specialty section:
This article was submitted to Bone Research, a section of the journal Frontiers in Endocrinology

Received: *19 May 2016*
Accepted: *02 August 2016*
Published: *16 August 2016*

Citation:
Lindenmaier LB, Philbrick KA, Branscum AJ, Kalra SP, Turner RT and Iwaniec UT (2016) Hypothalamic Leptin Gene Therapy Reduces Bone Marrow Adiposity in ob/ob Mice Fed Regular and High-Fat Diets. Front. Endocrinol. 7:110. doi: 10.3389/fendo.2016.00110

INTRODUCTION

Adipose tissue in bone marrow may contribute to metabolic health through its effects on local energy balance and/or its actions as an endocrine organ (1). Low bone mass is often associated with elevated bone marrow adiposity (2, 3). Bone marrow contains mesenchymal stem cells (MSCs) capable of differentiating into cells of the osteoblastic and adipocytic lineages (4). A reciprocal relationship between the number of mature osteoblasts and bone marrow adipocytes may occur as a consequence of differentiation of MSCs toward one lineage at the expense of the other lineage (5, 6). Mechanistically, peroxisome proliferator-activated receptor gamma (PPARγ), a transcription factor that plays a key role in regulation of adipogenesis and lipid uptake, has been implicated as a factor controlling MSC differentiation. Inhibition of PPARγ increases osteoblast differentiation while decreasing adipocyte differentiation. Osteoblast-targeted overexpression of PPARγ inhibits bone mass gain in male mice and increases ovariectomy-induced osteopenia in female mice (5). Furthermore, cultured adipocytes release factors capable of inducing osteoblast linage cells to differentiate into an adipocyte-like phenotype (7). Thus, excessive marrow adipose tissue (MAT) has the potential to directly and/or indirectly reduce bone mass by inhibiting osteoblast differentiation. As such, an increase in MAT may contribute to osteoporosis in conditions, such as menopause, skeletal disuse, alcohol abuse, and eating disorders (3, 8, 9).

Interestingly, anorexia and obesity both result in increased MAT (10, 11). Anorexia is commonly associated with reduced bone mineral density (BMD) and increased fracture risk. By contrast, being overweight is generally associated with increased BMD and reduced fracture risk. However, recent studies suggest that morbid obesity has negative effects on bone quality (12, 13). Thus, it is possible that the increase in MAT plays a role in the detrimental skeletal changes associated with both extremes in body weight.

Leptin, an adipokine produced in proportion to fat mass, plays a critical role in central nervous system-mediated regulation of energy homeostasis (14). Additionally, leptin plays an important positive role in skeletal growth and maturation (15, 16). Indeed, leptin signaling deficiency results in abnormal growth plate development (17) and mild osteopetrosis (18).

Leptin suppresses PPARγ expression and increases lipolysis in adipose tissue in rodents (19). In parallel, leptin increases longitudinal bone growth, osteoblastogenesis and bone formation (15, 16). Thus, the low leptin levels resulting from insufficient adipose tissue observed in anorexia may contribute to increased MAT and decreased bone formation. In contrast to anorexia, obesity typically results in increased leptin levels which, in turn, should suppress MAT. Many authors have concluded that leptin resistance plays an important role in hyperphagia and weight gain associated with obesity (20). Thus, leptin resistance may counteract the expected response to elevated leptin levels and thereby contribute to an increase in MAT during obesity. However, some new studies question whether resistance to endogenous leptin contributes to development of diet-induced obesity in mice (21, 22). If leptin resistance is a major contributor to the etiology of obesity, it may be overcome in normal rodents, at least in part, by increasing hypothalamic leptin levels. Whatever its precise role in diet-induced obesity, it is clear that leptin resistance resulting from loss of function of the leptin receptor (*db/db* mice), in addition to inducing morbid obesity, results in profound negative effects on the skeleton. Furthermore, some of these negative skeletal effects (e.g., reduced bone formation) are recapitulated, without impacting energy metabolism, following adoptive transfer of bone marrow from *db/db* mice into wild-type (WT) mice (16).

Leptin-deficient *ob/ob* and leptin receptor-deficient *db/db* mice exhibit excessive MAT in long bones (16). Short-term delivery of leptin into the hypothalamus was shown to reduce peripheral fat depots as well as MAT (23, 24). However, the long-term effects of increased leptin levels on MAT have not been well characterized. Hypothalamic leptin gene therapy has been shown to result in life-long reductions in body weight in *ob/ob* mice (25). The goal of the present study was to determine the long-duration effects of increased hypothalamic leptin, using recombinant adeno-associated virus leptin gene therapy (rAAV-Lep), on bone marrow adiposity in morbidly obese *ob/ob* mice. Given that the energy density of a diet impacts weight gain and MAT levels (26), the effects of a regular and high energy density (high fat) diet were also evaluated.

MATERIALS AND METHODS

Experimental Animals

Eight- to 10-week-old male WT C57BL/6J (B6) and leptin-deficient *ob/ob* mice on the same genetic background were obtained from Jackson Laboratory (Bar Harbor, ME, USA). This age corresponds to peak cancellous bone volume fraction in the femur metaphysis (27). The mice were maintained in accordance with the NIH Guide for the Care and Use of Laboratory Animals and the experimental protocols were approved by the Institutional Animal Care and Use Committee at the University of Florida. The mice were housed individually in a temperature (21–23°C) and light-controlled room (lights on 6:00 a.m. to 6:00 p.m.) under specific pathogen-free conditions.

Experiment 1: Effects of 30 Weeks of Hypothalamic Leptin Gene Therapy on Marrow Adiposity and Cancellous Bone Histomorphometry in *ob/ob* Mice

Following arrival, *ob/ob* mice were randomized by weight into four treatment groups: (1) untreated ($n = 6$), (2) control vector encoding green fluorescent protein (rAAV-GFP, $n = 7$), (3) rAAV-Lep ($n = 8$), or (4) pair-fed to rAAV-Lep ($n = 6$). The mice were maintained on standard mouse chow (LM-485, Teklad, Madison, WI, USA) and sacrificed 30 weeks following vector administration at 38–40 weeks of age. This age corresponds to a period immediately prior to a drastic increase in mortality in *ob/ob* mice – median lifespan in *ob/ob* mice is 55 weeks compared to 131 weeks in WT mice (25). The effects of treatment on hypothalamic leptin gene expression, body weight, food intake, hormone levels, organ weights, and cancellous and cortical bone

architecture evaluated by microcomputed tomography in this study are detailed elsewhere (25, 28).

Experiment 2: Effects of 15 Weeks of Hypothalamic Leptin Gene Therapy and 8 Weeks of High-Fat Diet on Marrow Adiposity and Cancellous Bone Histomorphometry in *ob/ob* Mice

Experiment 2 was conducted using WT and *ob/ob* mice. Following arrival, WT mice ($n = 12$) were maintained on regular chow (LM-485, Teklad, Madison, WI, USA; caloric density 3.4 kcal/g, 11% of kcal from fat) until 15–17 weeks of age and then randomized by weight into two groups: (1) control ($n = 3$) or (2) high-fat diet ($n = 9$). Mice in the control group continued to consume the regular diet *ad libitum* while mice in the high-fat group were placed on a high-fat diet (caloric density 4.7 kcal/g; 45% of kcal from fat, primarily from lard; Research Diets, New Brunswick, NJ, USA) fed *ad libitum*. The mice were sacrificed 8 weeks later at 23–25 weeks of age – an age corresponding to cessation of linear growth in B6 mice (27).

In conjunction, *ob/ob* mice were randomized by weight into two treatment groups: rAAV-Lep ($n = 16$) or control vector rAAV-GFP ($n = 14$). At 7 weeks post-vector administration, rAAV-GFP and rAAV-Lep mice were each divided into two groups: one group continued to consume regular diet and the other was switched to a high-fat diet as described above for WT mice. The mice were sacrificed 8 weeks later at 23–25 weeks of age (15 weeks following vector administration). The effect of the rAAV-Lep pretreatment and high-fat diet on hypothalamic leptin gene expression, body weight, food intake, organ weights, hormone levels, and cancellous and cortical bone architecture determined by microcomputed tomography are detailed elsewhere (28–30).

Construction and Packaging of rAAV Vectors

rAAV-leptin gene therapy and rAAV-GFP vectors were constructed and packaged as previously described (31). In brief, the vector pTR-CBA-Ob *Eco*RI fragment of pCR-rOb containing rat leptin cDNA was subcloned into rAAV vector plasmid pAAVβGEnh after deleting the *Eco*RI fragment carrying the β-glucoronidase cDNA sequence. The control vector, rAAV-GFP, was similarly constructed to encode the GFP gene.

Vector Administration

For vector administration, the mice were anesthetized with sodium pentobarbital (60 mg/kg, i.p.), placed on a Kopf stereotaxic apparatus with mouse adapter for intracerebroventricular injection, and injected intracerebroventricularly with either rAAV-Lep (9×10^7 particles in 1.5 µl) or rAAV-GFP (9×10^7 particles in 1.5 µl). The coordinates employed for microinjector placement in the third cerebroventricle were 0.3 mm posterior to bregma, 0.0 lateral to midline, and 4.2 mm below the dura (29).

Tissue Collection and Analyses

At the end of each experiment mice were anesthetized with sodium pentobarbital (60 mg/kg; i.p.) and euthanized by exsanguination. Femora were excised, cleaned of soft tissue, and stored in 70% ethanol. Femora were prepared for histomorphometric evaluation as described (32). In brief, distal femora were dehydrated in graded increases of ethanol and xylene and embedded undecalcified in methyl methacrylate. Frontal sections (4 µm thick) were cut with a vertical bed microtome (Leica 2165) and affixed to slides precoated with a 1% gelatin solution. One section/animal was stained for tartrate-resistant acid phosphatase and counterstained with toluidine blue (Sigma, St Louis, MO, USA) for assessment of bone and cell-based measurements.

Histomorphometric data were collected using the OsteoMeasure System (OsteoMetrics, Inc., Atlanta, GA, USA). The sampling site for the distal femoral metaphysis was located 0.25–1.25 mm proximal to the growth plate and 0.1 mm from cortical bone. Cancellous bone measurements included bone area fraction (bone area/tissue area, %) and the derived architectural indices of trabecular number (mm^{-1}), trabecular thickness (micrometer), and trabecular separation (micrometer). Measurements of MAT included overall marrow adiposity (adipose area/tissue area, %), adipocyte density (mm^{-2}), and adipocyte size ($micrometers^2$). Adipocytes were identified as large circular or oval-shaped cells bordered by a prominent cell membrane and lacking cytoplasmic staining due to alcohol extraction of intracellular lipids during processing. This method has been validated by fat extraction and analysis (33). Osteoblast and osteoclast perimeters were also measured and expressed as % of total bone perimeter. Osteoblasts were identified as plump cuboidal cells immediately adjacent to a thin layer of osteoid in direct contact with the bone perimeter. Osteoclasts were identified as multinucleated (two or more nuclei) cells with acid phosphatase positive (red-stained) cytoplasm in contact with the bone perimeter. Data are reported using standard two-dimensional nomenclature (34).

Statistical Analysis

Mean responses for Experiment 1 were compared among the untreated, rAAV-GFP, rAAV-Lep, and pair-fed groups using one-way analysis of variance. For Experiment 2, the effects of treatment and diet were assessed using two-way analysis of variance. Pairwise comparisons were made using *t*-tests or the Wilcoxon–Mann–Whitney test. The required conditions for valid use of linear models were assessed using Levene's test for homogeneity of variance, plots of residuals versus fitted values, normal quantile plots, and the Anderson–Darling test of normality. The Benjamini and Hochberg method (35) for maintaining the false discovery rate at 5% was used to adjust for multiple comparisons. Data analysis was performed using R version 3.3.2.

RESULTS

Experiment 1: Effects of 30 Weeks of Hypothalamic Leptin Gene Therapy on Marrow Adiposity and Cancellous Bone Histomorphometry in *ob/ob* Mice

The effects of treatment on body weight and on cancellous bone in the distal femur metaphysis are shown in **Table 1**. rAAV-Lep treatment resulted in lower body weight compared to untreated,

TABLE 1 | Effects of hypothalamic leptin gene therapy (rAAV-Lep) on body weight and cancellous bone architecture in distal femur metaphysis in *ob/ob* male mice at 30 weeks post-vector administration.

	ob/ob Mice				ANOVA FDR adjusted *P*
	Untreated ($n = 6$)	rAAV-GFP ($n = 7$)	rAAV-Lep ($n = 8$)	Pair-fed ($n = 6$)	
Body weight (g)	70 ± 2	68 ± 2	29 ± 3[a–c]	63 ± 2	<0.001*
Bone area/tissue area (%)	8.3 ± 1.1	7.2 ± 0.9	5.3 ± 1.0	5.7 ± 0.7	0.225
Trabecular thickness (μm)	35 ± 2	34 ± 1	26 ± 2[a,b]	31 ± 2	0.009
Trabecular number (mm^{-1})	2.3 ± 0.2	2.1 ± 0.2	2.0 ± 0.2	1.8 ± 0.2	0.645
Trabecular spacing (μm)	416 ± 42	470 ± 38	542 ± 71	547 ± 73	0.588

Data are mean ± SE.
**Previously reported (28).*
[a]Different from untreated, $P < 0.05$.
[b]Different from rAAV-GFP, $P < 0.05$.
[c]Different from pair-fed, $P < 0.05$.

rAAV-GFP-treated, and pair-fed mice. Significant differences in cancellous bone area fraction, trabecular number, or trabecular spacing were not detected with treatment. However, trabecular thickness was lower in rAAV-Lep-treated mice compared to untreated and rAAV-GFP-treated mice, but did not differ from pair-fed *ob/ob* mice.

The effects of treatment on MAT in the distal femur metaphysis are shown in **Figure 1**. Marrow adiposity (adipose area/tissue area) (**Figure 1A**), adipocyte density (**Figure 1B**), and adipocyte size (**Figure 1C**) were lower in rAAV-Lep-treated mice compared to untreated, rAAV-GFP-treated, and pair-fed mice. Significant differences among untreated, rAAV-GFP-treated, and pair-fed mice were not detected for any of the MAT measurements. The effects of rAAV-Lep treatment on marrow adiposity can be readily appreciated in **Figures 1D–G**.

The effects of treatment on osteoblast perimeter and osteoclast perimeter in the distal femur metaphysis are shown in **Figure 2**. Osteoblast perimeter (**Figure 2A**) and osteoclast perimeter (**Figure 2B**) were higher in rAAV-Lep-treated mice compared to untreated, rAAV-GFP-treated, and pair-fed mice. Significant differences among untreated, rAAV-GFP-treated, and pair-fed mice were not detected for either of the cellular endpoints evaluated. The effects of rAAV-Lep treatment on osteoblast and osteoclast perimeter can be appreciated in **Figures 2C–F**.

Experiment 2: Effects of 15 Weeks of Hypothalamic Leptin Gene Therapy and 8 Weeks of High-Fat Diet on Marrow Adiposity and Cancellous Bone Histomorphometry in *ob/ob* Mice

The effects of rAAV-Lep pretreatment and high-fat diet on body weight and on cancellous bone in distal femur metaphysis are shown in **Table 2**. Body weight was higher in WT mice fed high-fat diet compared to WT mice fed regular diet. Body weight was also higher in *ob/ob* mice fed high fat compared to *ob/ob* mice fed regular diet and rAAV-Lep treatment resulted in lower body weight. Cancellous bone area fraction, trabecular thickness, and trabecular number were higher and trabecular spacing was lower in WT mice fed high-fat diet compared to WT mice fed regular diet. rAAV-Lep treatment in *ob/ob* mice resulted in lower cancellous bone area fraction and trabecular thickness. Significant differences in trabecular number or trabecular spacing were not detected with treatment in the *ob/ob* mice. With the exception of trabecular thickness, which was lower, significant differences between WT mice and rAAV-Lep-treated *ob/ob* mice fed regular diets were not detected for any of the remaining cancellous endpoints evaluated.

The effects of treatment on marrow adiposity in distal femur metaphysis are shown in **Figure 3**. Marrow adiposity and adipocyte size were higher in WT mice fed high-fat diet compared to mice fed regular diet. Significant differences in adipocyte density were not detected with diet in WT mice. rAAV-Lep treatment in *ob/ob* mice resulted in lower marrow adiposity due to lower adipocyte density as well as lower adipocyte size. Significant differences in marrow adiposity, adipocyte density, or adipocyte size were not detected between WT and rAAV-Lep-treated *ob/ob* mice fed regular diet.

DISCUSSION

Leptin-deficient *ob/ob* mice were heavier and had increased MAT in distal femur metaphysis compared to WT mice. Consumption of high-fat diet resulted in increased body weight in both WT mice and *ob/ob* mice but increased MAT and cancellous bone in WT mice only. rAAV-Lep treatment decreased MAT in *ob/ob* mice. The reduction in MAT in rAAV-Lep-treated *ob/ob* mice was accompanied by increases in osteoblast-lined and osteoclast-lined bone perimeter but not by an increase in cancellous bone.

Continuous and once daily intracerebroventricular administration of leptin were similarly effective in reducing MAT in long bones of *ob/ob* mice (23, 24, 36, 37). Based on lower adipocyte number and size and increased concentration of apoptosis marker caspase-3 in bone marrow adipocytes, the reduction in MAT was likely due to a combination of reduced adipocyte differentiation, increased fat oxidation, and increased adipocyte apoptosis. A similar reduction in MAT was observed following subcutaneous leptin administration (36).

In normal female rats, hypothalamic delivery of rAAV-Lep was shown to maintain lower body weight, WAT weight, and serum leptin levels (2.7 ± 0.3 versus 1.0 ± 0.1 ng/ml) for at least 18 weeks following vector administration. By contrast, rAAV-Lep transiently reduced MAT; MAT levels were reduced at 5 weeks but returned to normal levels by 10 weeks following vector

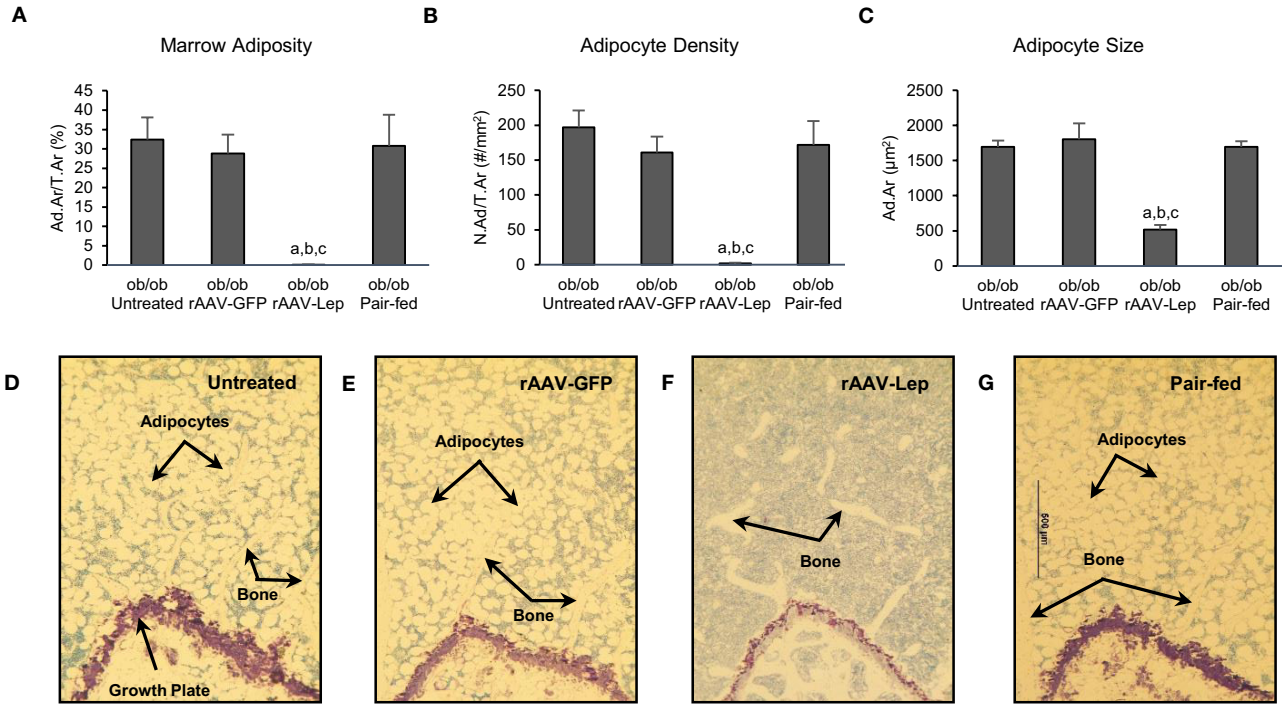

FIGURE 1 | Effects of hypothalamic leptin gene therapy (rAAV-Lep) on marrow adipose tissue in distal femur metaphysis in male *ob/ob* mice at 30 weeks post-vector administration. Bone marrow adiposity **(A)**, adipocyte density **(B)**, and adipocyte size **(C)** were decreased with rAAV-Lep treatment. The effects of treatment on marrow adipose tissue in the femoral metaphysis can be readily appreciated in representative micrographs from an untreated **(D)**, rAAV-GFP-treated **(E)**, rAAV-Lep-treated **(F)**, and pair-fed to rAAV-Lep **(G)** mouse. Please see **Figures 2C–F** for representative higher magnification images. Data are mean ± SE (n = 6–8/group). [a]Different from untreated, [b]different from rAAV-GFP, and [c]different from pair-fed, $P < 0.05$.

administration (38). Also, hypothalamic rAAV-Lep gene therapy was ineffective in lowering MAT in ovariectomized rats (39). In the present study, MAT levels in rAAV-Lep-treated *ob/ob* mice, evaluated 15 and 30 weeks following vector administration, were much lower than age-matched *ob/ob* controls and comparable to WT mice in Experiment 2. These findings suggest that (1) while very important, the physiological actions of leptin on MAT are primarily manifested at low hormone levels and (2) hyperleptinemia has little further effect on MAT. If correct, this could help explain why some studies fail to detect a relationship between blood leptin levels and MAT (1). The findings regarding the actions of leptin on MAT are remarkably similar to the actions of the hormone on bone growth, maturation, and turnover. Whereas hypothalamic rAAV-Lep gene therapy corrected the skeletal abnormalities in *ob/ob* mice, it had minimal long-term impact on bone in rodents capable of producing leptin (16, 18, 28, 39).

It was initially hypothesized that the complex skeletal phenotype of *ob/ob* mice was due to opposing actions of peripheral and central leptin on bone formation (40, 41). However, subcutaneous and intracerebroventricular delivery of leptin were found to similarly increase bone formation in *ob/ob* mice (36). Additionally, long-duration hypothalamic leptin gene therapy was shown to normalize bone microarchitecture in *ob/ob* mice; specifically, increasing hypothalamic leptin levels resulted in increased femur length and total femur bone volume but decreased cancellous bone volume fraction in lumbar vertebra (28). These latter findings imply that, in addition to increasing longitudinal bone growth, delivery of leptin into the hypothalamus results in increased bone formation as well as increased bone resorption. Thus, an imbalance between bone formation and resorption related to local environment (e.g., precursor cell populations, mechanical loads, paracrine factors, etc.) potentially explains the contrasting phenotypes that have been identified in bones of the limb and spine in *ob/ob* mice (41).

Bone- and bone compartment-specific changes in microarchitecture in response to hormonal regulators of bone metabolism and mechanical loading environment are not unique to leptin. For example, by regulating longitudinal and radial bone growth and bone turnover balance, estrogens, and androgens contribute to sexual dimorphism of the skeleton. In this regard, administration of estrogen to growing ovariectomized rats results in shorter bones with lower total bone mass but higher site-specific cancellous bone volume (42). Ovariectomized rats also experience increased MAT expansion (39). *ob/ob* mice of both genders are hypogonadal due to reduced GnRH secretion (43), a defect that is reversed following leptin treatment (25, 29). Thus, it is possible that hypogonadism contributes to MAT expansion in *ob/ob* mice. Expansion of MAT during caloric restriction in WT mice was associated with increased circulation of glucocorticoids, while caloric restriction resulted in a further increase in the already high levels of MAT in leptin-deficient *ob/ob* mice (1, 18). These findings provide evidence that multiple factors, including leptin, regulate MAT levels.

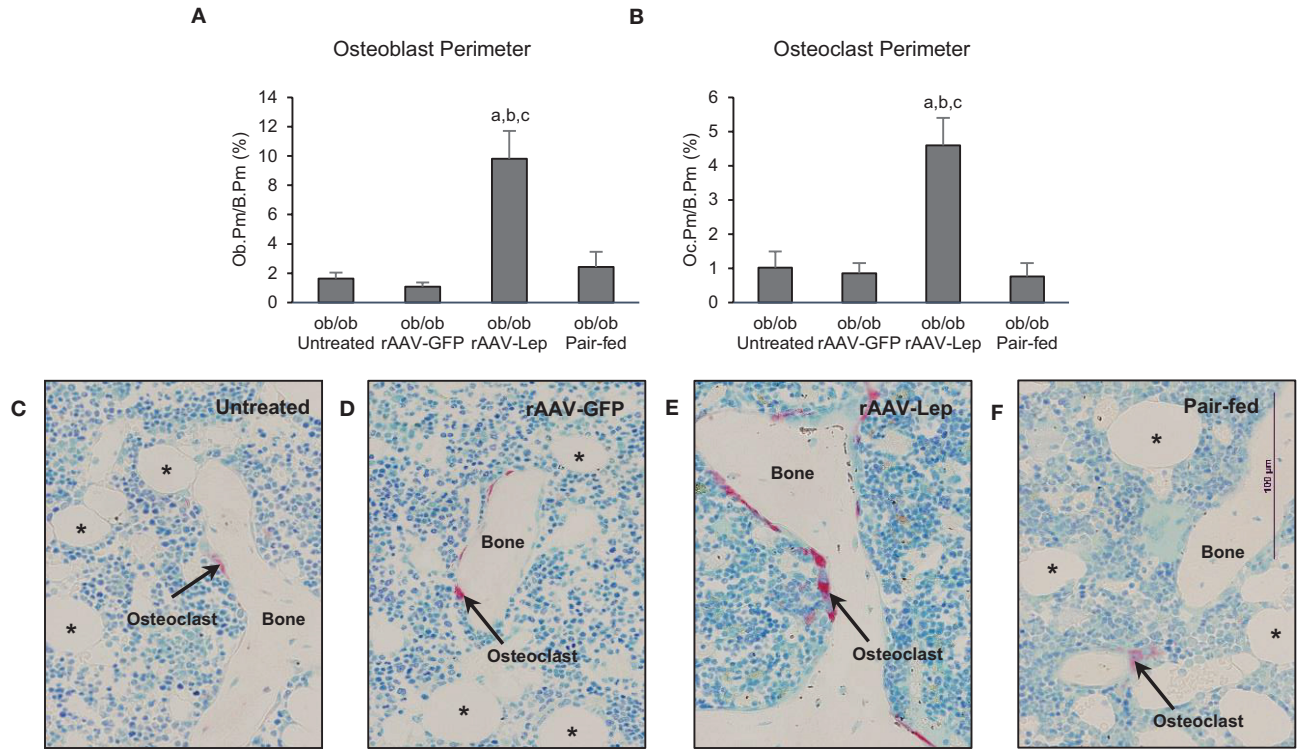

FIGURE 2 | Effects of hypothalamic leptin gene therapy (rAAV-Lep) on osteoblast perimeter, an index of bone formation, and osteoclast perimeter, an index of bone resorption, in distal femur metaphysis in male *ob/ob* mice at 30 weeks post-vector administration. Osteoblast perimeter **(A)** and osteoclast perimeter **(B)** were increased with rAAV-Lep treatment. The effects of treatment on osteoclast perimeter, an index of bone resorption, can be readily appreciated in representative micrographs from an untreated **(C)**, rAAV-GFP-treated **(D)**, rAAV-Lep-treated **(E)**, and pair-fed to rAAV-Lep **(F)** mouse. Data are mean ± SE (n = 6–8/group). [a]Different from untreated, [b]different from rAAV-GFP, and [c]different from pair-fed, $P < 0.05$. Asterisks demarcate adipocytes.

As previously mentioned, short-duration delivery of leptin into the hypothalamus increased bone formation (36). Similarly, hypothalamic leptin gene therapy increased serum osteocalcin levels and osteoblast perimeter in lumbar vertebra of *ob/ob* mice (16, 44). In the present study, hypothalamic leptin gene therapy increased osteoblast perimeter in distal femur metaphysis in *ob/ob* mice 30 weeks following vector administration. These findings indicate that leptin promotes higher levels of bone formation prior to and following restoration of normal body weight and bone mass in *ob/ob* mice (28).

The increased cancellous bone volume fraction observed at selected skeletal sites (lumbar vertebrae) in *ob/ob* mice was initially attributed to increased bone formation, suggesting that leptin was antiosteogenic (45). However, subsequent studies consistently reported decreased bone formation in *ob/ob* mice and leptin receptor-deficient *db/db* mice, and increased bone formation following intracerebroventricular delivery of leptin, leptin gene therapy, or subcutaneous administration of leptin in *ob/ob* mice (16, 37, 44). Leptin signaling-deficient (*ob/ob* and *db/db*) mice have normal or increased osteoclast number but exhibit evidence for impaired osteoclast function (16, 18). As a consequence, these mice exhibit impaired skeletal maturation due to defective resorption of calcified cartilage. Specifically, the high cancellous bone volume fraction represents mild osteopetrosis. In the present study in *ob/ob* mice, rAAV-Lep resulted in increased osteoclast-lined bone perimeter. Thus, the failure to detect an increase in cancellous bone volume fraction in the femur metaphysis in response to higher leptin levels is likely due to parallel increases in bone formation and bone resorption.

High MAT levels in *ob/ob* mice are associated with low cancellous bone turnover (16). In the present study, rAAV-Lep resulted in increases in osteoclast-lined perimeter as well as osteoblast-lined bone perimeter and greatly reduced MAT with minimal change in cancellous bone area fraction. High MAT levels are not unique to leptin deficiency. Growth hormone deficiency in rats and mice induced by hypophysectomy or deletion of the gene for growth hormone, respectively, is also associated with high MAT and low bone turnover. In the case of growth hormone deficiency, parathyroid hormone was found to increase bone formation in hypophysectomized rats without impacting MAT levels, demonstrating that bone formation induced by bone anabolic agents is not suppressed by high levels of MAT (33). Similarly, although bone formation was increased, the absence of MAT in $kit^{W/W\text{-}v}$ mice did not protect against ovariectomy-induced bone loss (46). Taken together, these findings suggest that bone resorption as well as bone formation can be impacted during changes in MAT levels and interventions that target MAT may not necessarily change bone turnover balance.

TABLE 2 | Effects of high-fat diet and rAAV-Lep pretreatment and high fat diet on terminal body weight and cancellous bone architecture in distal femur metaphysis in male WT and *ob/ob* mice, respectively.

				ob/ob Mice						
	WT mice			rAAV-GFP		rAAV-Lep		ANOVA *P*		
	Regular diet ($n = 3$)	High-fat diet ($n = 9$)	*T*-test *P*	Regular diet ($n = 5$)	High-fat diet ($n = 9$)	Regular diet ($n = 8$)	High-fat diet ($n = 8$)	Vector	Diet	Interaction
Body weight (g)	29 ± 1	38 ± 1	0.014	56 ± 2	66 ± 2	28 ± 3	33 ± 2	0.000	0.003	0.307*
Bone area/ tissue area (%)	7.1 ± 1.0	11.5 ± 0.8	0.009	7.9 ± 0.9	9.9 ± 1.0	7.1 ± 0.7	6.6 ± 0.6	0.016	0.486	0.159
Trabecular thickness (μm)	30 ± 0	38 ± 1	0.009	31 ± 1	34 ± 2	25 ± 1.1[a]	25 ± 1	0.000	0.501	0.330
Trabecular number (mm^{-1})	2.3 ± 0.3	3.0 ± 0.1	0.020	2.5 ± 0.2	2.8 ± 0.1	2.8 ± 0.2	2.6 ± 0.1	0.950	0.658	0.115
Trabecular spacing (μm)	412 ± 62	297 ± 12	0.014	379 ± 29	323 ± 16	340 ± 19	363 ± 24	0.764	0.608	0.083

Data are mean ± SE.
**Previously reported (30).*
[a]*Different from WT mice fed regular diet.*

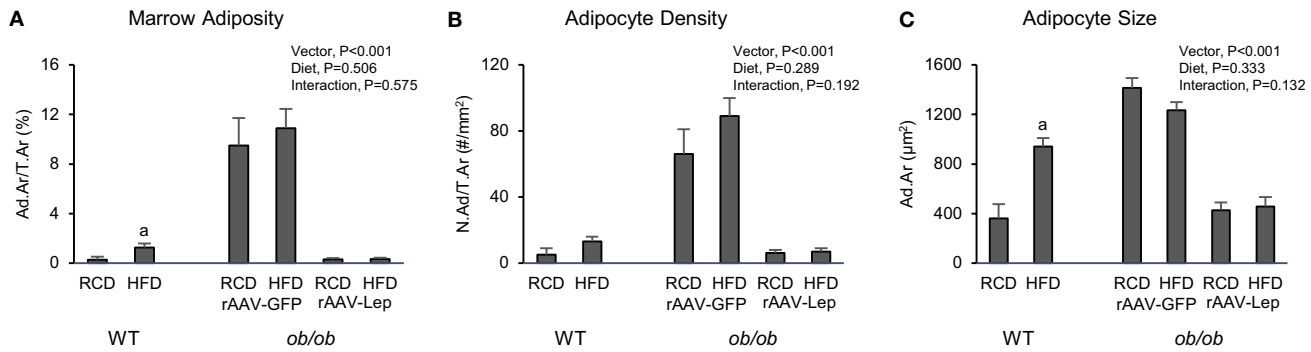

FIGURE 3 | Effects of high-fat diet and rAAV-Lep pretreatment and high-fat diet on bone marrow adiposity (A), adipocyte density (B), and adipocyte size (C) in distal femur metaphysis in male WT and *ob/ob* mice, respectively. RCD, regular control diet. HFD, high-fat diet. Data are mean ± SE ($n = 3$–9/ group). [a]Different from RCD within WT, $P < 0.05$.

A positive association between body weight and bone mass was observed in *ob/ob* as well as WT mice (30, 47). However, leptin appears to sensitize the skeleton to bone mechanical loading. This may explain why leptin-deficient mice have a low total bone mass even though they are morbidly obese and why the massive weight loss in *ob/ob* mice following leptin treatment is actually associated with a net increase in bone mass (28).

Conditional knockout of the leptin receptor in bone marrow stromal cells has been reported to result in local increases in osteogenesis and decreased adipogenesis (48). It is difficult to reconcile these findings with the skeletal phenotype of leptin receptor-deficient mice (16, 49) or with the present results demonstrating that increasing hypothalamic leptin levels profoundly reduces MAT levels. Evidence that factors secondary to leptin deficiency are responsible for the discrepancy, as suggested by Yue et al., are presently lacking and correction of many of the metabolic abnormalities associated with leptin deficiency (e.g., hyperglycemia), rather than improving, actually worsens the skeletal phenotype of *ob/ob* mice (18). Also inexplicable by Yue et al. is the finding that adoptive transfer of leptin receptor-deficient *db/db* bone marrow cells into WT mice recapitulates the low bone formation skeletal phenotype of *db/db* mice without impacting food intake or weight gain (16). It is possible that the role of leptin receptors in regulating bone metabolism depends upon stage of stromal cell differentiation (50), but this requires additional research.

A limitation of the present study is that MAT measurements were performed at a single skeletal site and MAT subtypes were not evaluated. The lipid composition and physiological function of MAT can vary with location and/or regulatory factors, such as growth hormone status (33, 51). A further limitation of most studies, including the present study, is that they have been performed housing mice at room temperature. Thermoneutral (temperature range where basal rate of energy production is at equilibrium with heat loss) in mice ranges from 26 to 34°C (52). Mild cold stress induced by room temperature housing results in dramatic cancellous bone loss at the femur metaphysis. Interestingly, mice housed at 32°C consumed ~40% less food (fed *ad libitum*) but did not differ from room temperature-housed mice in weight (53). In addition to higher bone mass, mice housed at 32°C had greatly

reduced UCP-1 gene expression in brown fat, higher serum leptin, higher MAT levels due to increased adipocyte number, higher bone formation rate to due higher osteoblast perimeter, and lower osteoclast perimeter. These findings suggest that non-shivering thermogenesis substantially influences the association between leptin, MAT, and bone cells.

In summary, hypothalamic leptin gene therapy maintained low MAT levels in *ob/ob* mice fed regular or high-fat diet. The reduction in MAT was accompanied by an increase in osteoblast-lined bone perimeter but not an increase in cancellous bone volume fraction. The increase in osteoclast-lined bone perimeter suggests that the increase in bone formation was matched by an increase in bone resorption. These findings provide further evidence that a deterministic model where reducing MAT will invariably lead to increased bone volume is not tenable. As a consequence, interventions targeted at reducing MAT may not be an effective strategy for increasing bone mass.

AUTHOR CONTRIBUTIONS

Study design: SK. Data acquisition: LL, KP, and RT. Data analysis: AB. Data interpretation: LL, KP, AB, SK, RT, and UI. Drafting of manuscript: LL, RT, and UI. Revising manuscript content: LL, KP, AB, SK, RT, and UI. Approving final version of manuscript: LL, KP, AB, SK, RT, and UI. All authors take responsibility for the integrity of this work.

ACKNOWLEDGMENTS

We thank Dr. S. Boghossian for executing the studies.

FUNDING

This study was supported by NIH AR060913, NASA NNX12AL24, and USDA 38420-17804.

REFERENCES

1. Cawthorn WP, Scheller EL, Learman BS, Parlee SD, Simon BR, Mori H, et al. Bone marrow adipose tissue is an endocrine organ that contributes to increased circulating adiponectin during caloric restriction. *Cell Metab* (2014) 20:368–75. doi:10.1016/j.cmet.2014.06.003
2. Liu Y, Tang GY, Tang RB, Peng YF, Li W. Assessment of bone marrow changes in postmenopausal women with varying bone densities: magnetic resonance spectroscopy and diffusion magnetic resonance imaging. *Chin Med J (Engl)* (2010) 123:1524–7.
3. Morita Y, Iwamoto I, Mizuma N, Kuwahata T, Matsuo T, Yoshinaga M, et al. Precedence of the shift of body-fat distribution over the change in body composition after menopause. *J Obstet Gynaecol Res* (2006) 32:513–6. doi:10.1111/j.1447-0756.2006.00437.x
4. Prockop DJ. Marrow stromal cells as stem cells for nonhematopoietic tissues. *Science* (1997) 276:71–4. doi:10.1126/science.276.5309.71
5. Akune T, Ohba S, Kamekura S, Yamaguchi M, Chung UI, Kubota N, et al. PPARgamma insufficiency enhances osteogenesis through osteoblast formation from bone marrow progenitors. *J Clin Invest* (2004) 113:846–55. doi:10.1172/JCI200419900
6. Cho SW, Yang JY, Her SJ, Choi HJ, Jung JY, Sun HJ, et al. Osteoblast-targeted overexpression of PPARgamma inhibited bone mass gain in male mice and accelerated ovariectomy-induced bone loss in female mice. *J Bone Miner Res* (2011) 26:1939–52. doi:10.1002/jbmr.366
7. Kim YY, Kim SH, Oh S, Sul OJ, Lee HY, Kim HJ, et al. Increased fat due to estrogen deficiency induces bone loss by elevating monocyte chemoattractant protein-1 (MCP-1) production. *Mol Cells* (2010) 29:277–82. doi:10.1007/s10059-010-0027-x
8. Maddalozzo GF, Turner RT, Edwards CH, Howe KS, Widrick JJ, Rosen CJ, et al. Alcohol alters whole body composition, inhibits bone formation, and increases bone marrow adiposity in rats. *Osteoporos Int* (2009) 20:1529–38. doi:10.1007/s00198-009-0836-y
9. Trudel G, Payne M, Madler B, Ramachandran N, Lecompte M, Wade C, et al. Bone marrow fat accumulation after 60 days of bed rest persisted 1 year after activities were resumed along with hemopoietic stimulation: the Women International Space Simulation for Exploration study. *J Appl Physiol (1985)* (2009) 107:540–8. doi:10.1152/japplphysiol.91530.2008
10. Bredella MA, Fazeli PK, Miller KK, Misra M, Torriani M, Thomas BJ, et al. Increased bone marrow fat in anorexia nervosa. *J Clin Endocrinol Metab* (2009) 94:2129–36. doi:10.1210/jc.2008-2532
11. Cao JJ. Effects of obesity on bone metabolism. *J Orthop Surg Res* (2011) 6:30. doi:10.1186/1749-799X-6-30
12. Cawsey S, Padwal R, Sharma AM, Wang X, Li S, Siminoski K. Women with severe obesity and relatively low bone mineral density have increased fracture risk. *Osteoporos Int* (2015) 26:103–11. doi:10.1007/s00198-014-2833-z
13. Iwaniec UT, Turner RT. Influence of body weight on bone mass, architecture, and turnover. *J Endocrinol* (2016) 230:R115–30. doi:10.1530/JOE-16-0089
14. Friedman JM, Halaas JL. Leptin and the regulation of body weight in mammals. *Nature* (1998) 395:763–70. doi:10.1038/27376
15. Steppan CM, Crawford DT, Chidsey-Frink KL, Ke H, Swick AG. Leptin is a potent stimulator of bone growth in ob/ob mice. *Regul Pept* (2000) 92:73–8. doi:10.1016/S0167-0115(00)00152-X
16. Turner RT, Kalra SP, Wong CP, Philbrick KA, Lindenmaier LB, Boghossian S, et al. Peripheral leptin regulates bone formation. *J Bone Miner Res* (2013) 28:22–34. doi:10.1002/jbmr.1734
17. Kishida Y, Hirao M, Tamai N, Nampei A, Fujimoto T, Nakase T, et al. Leptin regulates chondrocyte differentiation and matrix maturation during endochondral ossification. *Bone* (2005) 37:607–21. doi:10.1016/j.bone.2005.05.009
18. Turner RT, Philbrick KA, Wong CP, Olson DA, Branscum AJ, Iwaniec UT. Morbid obesity attenuates the skeletal abnormalities associated with leptin deficiency in mice. *J Endocrinol* (2014) 223:M1–15. doi:10.1530/JOE-14-0224
19. Qian H, Hausman GJ, Compton MM, Azain MJ, Hartzell DL, Baile CA. Leptin regulation of peroxisome proliferator-activated receptor-gamma, tumor necrosis factor, and uncoupling protein-2 expression in adipose tissues. *Biochem Biophys Res Commun* (1998) 246:660–7. doi:10.1006/bbrc.1998.8680
20. Banks WA, Farrell CL. Impaired transport of leptin across the blood-brain barrier in obesity is acquired and reversible. *Am J Physiol Endocrinol Metab* (2003) 285:E10–5. doi:10.1152/ajpendo.00468.2002
21. Balland E, Cowley MA. New insights in leptin resistance mechanisms in mice. *Front Neuroendocrinol* (2015) 39:59–65. doi:10.1016/j.yfrne.2015.09.004
22. Ottaway N, Mahbod P, Rivero B, Norman LA, Gertler A, D'Alessio DA, et al. Diet-induced obese mice retain endogenous leptin action. *Cell Metab* (2015) 21:877–82. doi:10.1016/j.cmet.2015.04.015
23. Ambati S, Li Q, Rayalam S, Hartzell DL, Della-Fera MA, Hamrick MW, et al. Central leptin versus ghrelin: effects on bone marrow adiposity and gene expression. *Endocrine* (2010) 37:115–23. doi:10.1007/s12020-009-9274-z
24. Hamrick MW, Della Fera MA, Choi YH, Hartzell D, Pennington C, Baile CA. Injections of leptin into rat ventromedial hypothalamus increase adipocyte apoptosis in peripheral fat and in bone marrow. *Cell Tissue Res* (2007) 327:133–41. doi:10.1007/s00441-006-0312-3
25. Boghossian S, Ueno N, Dube MG, Kalra P, Kalra S. Leptin gene transfer in the hypothalamus enhances longevity in adult monogenic mutant mice in the absence of circulating leptin. *Neurobiol Aging* (2007) 28:1594–604. doi:10.1016/j.neurobiolaging.2006.08.010
26. Doucette CR, Horowitz MC, Berry R, MacDougald OA, Anunciado-Koza R, Koza RA, et al. A high fat diet increases bone marrow adipose tissue (MAT) but does not alter trabecular or cortical bone mass in C57BL/6J mice. *J Cell Physiol* (2015) 230:2032–7. doi:10.1002/jcp.24954
27. Glatt V, Canalis E, Stadmeyer L, Bouxsein ML. Age-related changes in trabecular architecture differ in female and male C57BL/6J mice. *J Bone Miner Res* (2007) 22:1197–207. doi:10.1359/jbmr.070507
28. Iwaniec UT, Boghossian S, Lapke PD, Turner RT, Kalra SP. Central leptin gene therapy corrects skeletal abnormalities in leptin-deficient ob/ob mice. *Peptides* (2007) 28:1012–9. doi:10.1016/j.peptides.2007.02.001

29. Boghossian S, Dube MG, Torto R, Kalra PS, Kalra SP. Hypothalamic clamp on insulin release by leptin-transgene expression. *Peptides* (2006) 27:3245–54. doi:10.1016/j.peptides.2006.07.022
30. Iwaniec UT, Dube MG, Boghossian S, Song H, Helferich WG, Turner RT, et al. Body mass influences cortical bone mass independent of leptin signaling. *Bone* (2009) 44:404–12. doi:10.1016/j.bone.2008.10.058
31. Beretta E, Dube MG, Kalra PS, Kalra SP. Long-term suppression of weight gain, adiposity, and serum insulin by central leptin gene therapy in prepubertal rats: effects on serum ghrelin and appetite-regulating genes. *Pediatr Res* (2002) 52:189–98. doi:10.1203/00006450-200208000-00010
32. Iwaniec UT, Wronski TJ, Turner RT. Histological analysis of bone. *Methods Mol Biol* (2008) 447:325–41. doi:10.1007/978-1-59745-242-7_21
33. Menagh PJ, Turner RT, Jump DB, Wong CP, Lowry MB, Yakar S, et al. Growth hormone regulates the balance between bone formation and bone marrow adiposity. *J Bone Miner Res* (2010) 25:757–68. doi:10.1359/jbmr.091015
34. Dempster DW, Compston JE, Drezner MK, Glorieux FH, Kanis JA, Malluche H, et al. Standardized nomenclature, symbols, and units for bone histomorphometry: a 2012 update of the report of the ASBMR Histomorphometry Nomenclature Committee. *J Bone Miner Res* (2013) 28:2–17. doi:10.1002/jbmr.1805
35. Benjamini Y, Hochberg Y. Controlling the false discovery rate: a practical and powerful approach to multiple testing. *J R Statist Soc B* (1995) 57:289–300.
36. Bartell SM, Rayalam S, Ambati S, Gaddam DR, Hartzell DL, Hamrick M, et al. Central (ICV) leptin injection increases bone formation, bone mineral density, muscle mass, serum IGF-1, and the expression of osteogenic genes in leptin-deficient ob/ob mice. *J Bone Miner Res* (2011) 26:1710–20. doi:10.1002/jbmr.406
37. Hamrick MW, Della-Fera MA, Choi YH, Pennington C, Hartzell D, Baile CA. Leptin treatment induces loss of bone marrow adipocytes and increases bone formation in leptin-deficient ob/ob mice. *J Bone Miner Res* (2005) 20:994–1001. doi:10.1359/JBMR.050103
38. Iwaniec UT, Boghossian S, Trevisiol CH, Wronski TJ, Turner RT, Kalra SP. Hypothalamic leptin gene therapy prevents weight gain without long-term detrimental effects on bone in growing and skeletally mature female rats. *J Bone Miner Res* (2011) 26:1506–16. doi:10.1002/jbmr.365
39. Jackson MA, Iwaniec UT, Turner RT, Wronski TJ, Kalra SP. Effects of increased hypothalamic leptin gene expression on ovariectomy-induced bone loss in rats. *Peptides* (2011) 32:1575–80. doi:10.1016/j.peptides.2011.04.029
40. Burguera B, Hofbauer LC, Thomas T, Gori F, Evans GL, Khosla S, et al. Leptin reduces ovariectomy-induced bone loss in rats. *Endocrinology* (2001) 142:3546–53. doi:10.1210/endo.142.8.8346
41. Hamrick MW, Pennington C, Newton D, Xie D, Isales C. Leptin deficiency produces contrasting phenotypes in bones of the limb and spine. *Bone* (2004) 34:376–83. doi:10.1016/j.bone.2003.11.020
42. Turner RT, Riggs BL, Spelsberg TC. Skeletal effects of estrogen. *Endocr Rev* (1994) 15:275–300. doi:10.1210/edrv-15-3-275
43. Donato J Jr, Cravo RM, Frazao R, Elias CF. Hypothalamic sites of leptin action linking metabolism and reproduction. *Neuroendocrinology* (2011) 93:9–18. doi:10.1159/000322472
44. Kalra SP, Dube MG, Iwaniec UT. Leptin increases osteoblast-specific osteocalcin release through a hypothalamic relay. *Peptides* (2009) 30:967–73. doi:10.1016/j.peptides.2009.01.020
45. Ducy P, Amling M, Takeda S, Priemel M, Schilling AF, Beil FT, et al. Leptin inhibits bone formation through a hypothalamic relay: a central control of bone mass. *Cell* (2000) 100:197–207. doi:10.1016/S0092-8674(00)81558-5
46. Iwaniec UT, Turner RT. Failure to generate bone marrow adipocytes does not protect mice from ovariectomy-induced osteopenia. *Bone* (2013) 53:145–53. doi:10.1016/j.bone.2012.11.034
47. Philbrick KA, Turner RT, Branscum AJ, Wong CP, Iwaniec UT. Paradoxical effects of partial leptin deficiency on bone in growing female mice. *Anat Rec (Hoboken)* (2015) 298:2018–29. doi:10.1002/ar.23267
48. Yue R, Zhou BO, Shimada IS, Zhao Z, Morrison SJ. Leptin receptor promotes adipogenesis and reduces osteogenesis by regulating mesenchymal stromal cells in adult bone marrow. *Cell Stem Cell* (2016) 18:782–96. doi:10.1016/j.stem.2016.02.015
49. Williams GA, Callon KE, Watson M, Costa JL, Ding Y, Dickinson M, et al. Skeletal phenotype of the leptin receptor-deficient db/db mouse. *J Bone Miner Res* (2011) 26:1698–709. doi:10.1002/jbmr.367
50. Scheller EL, Song J, Dishowitz MI, Soki FN, Hankenson KD, Krebsbach PH. Leptin functions peripherally to regulate differentiation of mesenchymal progenitor cells. *Stem Cells* (2010) 28:1071–80. doi:10.1002/stem.432
51. Scheller EL, Doucette CR, Learman BS, Cawthorn WP, Khandaker S, Schell B, et al. Region-specific variation in the properties of skeletal adipocytes reveals regulated and constitutive marrow adipose tissues. *Nat Commun* (2015) 6:7808. doi:10.1038/ncomms8808
52. Gordon CJ. *Temperature Regulation in Laboratory Rodents*. New York, NY: Cambridge University Press (1993).
53. Iwaniec UT, Philbrick KA, Wong CP, Gordon JL, Kahler-Quesada AM, Olson DA, et al. Room temperature housing results in premature cancellous bone loss in growing female mice: implications for the mouse as a preclinical model for age-related bone loss. *Osteoporos Int* (2016). doi:10.1007/s00198-016-3634-3

Conflict of Interest Statement: The authors declare that the research was conducted in the absence of any commercial or financial relationships that could be construed as a potential conflict of interest.

frontiers in Endocrinology

ORIGINAL RESEARCH
published: 30 June 2016
doi: 10.3389/fendo.2016.00087

Marrow Adipose Tissue Expansion Coincides with Insulin Resistance in MAGP1-Deficient Mice

Tezin A. Walji[1†], Sarah E. Turecamo[1†], Alejandro Coca Sanchez[2], Bryan A. Anthony[3], Grazia Abou-Ezzi[3], Erica L. Scheller[4], Daniel C. Link[3], Robert P. Mecham[1] and Clarissa S. Craft[1,4]*

[1] Department of Cell Biology and Physiology, Washington University School of Medicine, St. Louis, MO, USA, [2] Department of Medicine and Medical Specialties, Faculty of Medicine and Health Sciences, University of Alcala de Henares, Madrid, Spain, [3] Department of Medicine, Oncology Division, Washington University School of Medicine, St. Louis, MO, USA, [4] Department of Medicine, Bone and Mineral Diseases Division, Washington University School of Medicine, St. Louis, MO, USA

Marrow adipose tissue (MAT) is an endocrine organ with the potential to influence skeletal remodeling and hematopoiesis. Pathologic MAT expansion has been studied in the context of severe metabolic challenge, including caloric restriction, high fat diet feeding, and leptin deficiency. However, the rapid change in peripheral fat and glucose metabolism associated with these models impedes our ability to examine which metabolic parameters precede or coincide with MAT expansion. Microfibril-associated glycoprotein-1 (MAGP1) is a matricellular protein that influences cellular processes by tethering signaling molecules to extracellular matrix structures. MAGP1-deficient (*Mfap2*$^{-/-}$) mice display a progressive excess adiposity phenotype, which precedes insulin resistance and occurs without changes in caloric intake or ambulation. *Mfap2*$^{-/-}$ mice were, therefore, used as a model to associate parameters of metabolic disease, bone remodeling, and hematopoiesis with MAT expansion. Marrow adiposity was normal in *Mfap2*$^{-/-}$ mice until 6 months of age; however, by 10 months, marrow fat volume had increased fivefold relative to wild-type control at the same age. Increased gonadal fat pad mass and hyperglycemia were detectable in *Mfap2*$^{-/-}$ mice by 2 months, but peaked by 6 months. The development of insulin resistance coincided with MAT expansion. Longitudinal characterization of bone mass demonstrated a disconnection in MAT volume and bone volume. Specifically, *Mfap2*$^{-/-}$ mice had reduced trabecular bone volume by 2 months, but this phenotype did not progress with age or MAT expansion. Interestingly, MAT expansion in the 10-month-old *Mfap2*$^{-/-}$ mice was associated with modest alterations in basal hematopoiesis, including a shift from granulopoiesis to B lymphopoiesis. Together, these findings indicate MAT expansion is coincident with insulin resistance, but not excess peripheral adiposity or hyperglycemia in *Mfap2*$^{-/-}$ mice; and substantial MAT accumulation does not necessitate a proportional decrease in either bone mass or bone marrow cellularity.

Keywords: marrow adipose tissue, obesity, insulin resistance, bone remodeling, hematopoiesis, microfibril-associated glycoprotein-1

Abbreviations: ECM, extracellular matrix; MAT, marrow adipose tissue; MAGP1, microfibril-associated glycoprotein-1.

OPEN ACCESS

Edited by:
Ann Schwartz, University of California San Francisco, USA

Reviewed by:
Katherine A. Staines, The Royal Veterinary College, UK
Beata Lecka-Czernik, University of Toledo, USA

***Correspondence:**
Clarissa S. Craft
clarissa.craft@wustl.edu

†Tezin A. Walji and Sarah E. Turecamo contributed equally to this work.

Specialty section:
This article was submitted to Bone Research, a section of the journal Frontiers in Endocrinology

Received: *05 May 2016*
Accepted: *22 June 2016*
Published: *30 June 2016*

Citation:
Walji TA, Turecamo SE, Sanchez AC, Anthony BA, Abou-Ezzi G, Scheller EL, Link DC, Mecham RP and Craft CS (2016) Marrow Adipose Tissue Expansion Coincides with Insulin Resistance in MAGP1-Deficient Mice. Front. Endocrinol. 7:87. doi: 10.3389/fendo.2016.00087

INTRODUCTION

Adipose tissue exists in multiple variations, the most extensively studied being: brown, white, and beige. Brown adipocytes specialize in utilizing energy to produce heat (thermogenesis), white adipocytes are energy-storing reservoirs, and beige adipocytes principally store lipids but can be stimulated to transdifferentiate into a "brown-like" state (1). Less studied is a fourth lipid storing depot, located within the skeleton, marrow adipose tissue (MAT). These skeleton-associated adipocytes arise from a unique progenitor (2) and occupy approximately 70% of the marrow space within adult human bones (3). There is an evidence that MAT adipocytes exist in two forms: regulated marrow adipocytes (rMATs) that respond in size and number to physiological challenge, and the constitutive marrow adipocytes (cMATs) that persist despite challenge (4). Marrow adipocytes are not inert space-filling cells. Rather, the ability to produce leptin and adiponectin classifies them as an endocrine organ (5, 6). These cells also release fatty acids *via* lipolysis, suggesting that they may fuel local cellular processes (7).

Pathologic MAT expansion, as a consequence of metabolic dysfunction, has been studied in several contexts, including caloric restriction, high fat diet feeding, and leptin deficiency (6, 8–10). Unfortunately, the rapid change in peripheral fat and glucose metabolism associated with these models impedes our ability to determine which metabolic parameters precede or coincide with MAT expansion. The objective of this study was to correlate parameters of metabolic disease, bone remodeling, and hematopoiesis with MAT volume. Thus, we chose a model of progressive metabolic dysfunction – mice lacking the extracellular matrix (ECM) protein microfibril-associated glycoprotein-1 (MAGP1).

The ECM is a milieu of structural proteins, proteoglycans, and adhesive glycoproteins (11). MAGPs are a non-structural component of the ECM. The biology of this family has been recently reviewed (12). Briefly, MAGP1 (*Mfap2*) is broadly expressed, including both adipose tissue and bone (13, 14), and typically associates with fibrillin-rich microfibrils. MAGP1 may also interact with collagen-VI fibers (15). Characterization of MAGP1-deficient mice ($Mfap2^{-/-}$) suggests that MAGP1 does not contribute to the mechanical integrity of its associated ECM fibers (16). Rather, MAGP1 functions as a gatekeeper of signal transduction. A significant body of evidence has demonstrated that MAGP1 interacts with ligands of the transforming growth factor beta (TGFβ) superfamily; sequestering them in the ECM (13, 14, 16, 17). In mice, MAGP1 deficiency ($Mfap2^{-/-}$) results in adipocyte hypertrophy in peripheral white adipose tissue (WAT), diabetes, and reduced bone mass (13, 14). These phenotypes are progressive, developing with age.

Using the $Mfap2^{-/-}$ model, we demonstrate that MAT expansion occurs concurrent with insulin resistance, not excessive peripheral adiposity or hyperglycemia. Bone loss in the MAGP1-deficient mice occurs without corresponding increases in MAT. Furthermore, a fivefold increase in MAT in the proximal tibia does not negatively affect bone marrow (BM) cellularity.

MATERIALS AND METHODS

Animals and Diet

All animals were C57BL/6 background males, housed in a pathogen-free animal facility and fed standard chow *ad libitum*. MAGP1-deficient mice were generated using C57BL/6-derived ES cells [$Mfap2^{tm1a(KOMP)Wtsi}$] purchased from KOMP Repository (Davis, CA, USA). ES cells were injected into blastocyst from C57BL/6 donors and transferred into pseudopregnant C57BL/6 females. Offspring were maintained on the Jackson Laboratories C57BL/6J strain. These mice are a newly derived line and are therefore different from the $Mfap2^{-/-}$ mice used in previous studies (13, 14, 16, 17). All animals were treated in accordance with animal protocols approved by the Animal Studies Committee at Washington University.

Tissue Collection

Tissues were harvested at 2, 6, and 10 months. Mouse fur was sprayed with 70% EtOH, then gonadal white adipose tissue (gWAT), and tibias were collected. Tissues were cleaned thoroughly of all contaminants (hair, connective tissue, etc.), then frozen or stored in 10% neutral buffered formalin.

Insulin Tolerance Test

For insulin tolerance tests (ITTs), mice were fasted for 6 h and then given an injection of 0.75 U/kg Humulin-R insulin (Lilly, Indianapolis, IN, USA). Insulin was delivered by intraperitoneal injection, and tail blood glucose concentration was measured using Contour strips and meters (Bayer, Whippany, NJ, USA) at the indicated intervals.

Osmium Staining and Micro-Computed Tomography

Micro-computed tomography (μCT) was completed on tibias from 2-, 6-, and 10-month-old mice. Bones were fixed in 10% neutral buffered formalin and then embedded in 2% agarose gel. Tibias were scanned at 20 μm voxel resolution using a Scanco μCT 40 (Scanco Medical AG, Zurich, Switzerland) calibrated using a hydroxyapatite phantom. Measurements of both trabecular and cortical bones were made based on reported guidelines (18). For trabecular bone, 50 slices below the growth plate were contoured to exclude the cortical bone, allowing trabecular bone volume/tissue volume (BV/TV) and bone mineral density (BMD) to be determined. For cortical bone, 20 slices – 2 mm proximal to the tibia–fibula junction were analyzed to determine cortical tissue mineral density (TMD). A threshold of 175 for trabecular bone and 260 for cortical bone (on a 0–1000 scale) was maintained. Note: two 10-month-old $Mfap2^{-/-}$ bones were excluded from study due to suspected fracture.

Tibias were then decalcified in 14% EDTA for 3 weeks. Demineralized bones were incubated in a solution containing 1% osmium and 2.5% potassium dichromate for 48 h at room temperature. After thorough washing (water), tibias were embedded in 1% agarose gel. Osmium stained bones were then scanned as above, using a Scanco μCT 40, but at 10 μm voxel resolution. Analysis was performed in the same region as the trabecular

bone (1,000 μm distal to the growth plate, 100 slices), using a threshold of 350 (on a 0–1000 scale). Osmium volume (OV) is quantification of the total OV within the region of interest. OV/TV is division of the OV by the volume of the marrow cavity within the same region.

Flow Cytometry

Blood, spleen, and BM (one each of pelvis bone, femur, and tibia) were harvested from Jackson Laboratories c57BL/6J WT and *Mfap2*$^{-/-}$ mice using standard techniques. Single cell suspensions were made, and red blood cells were lysed. Blood cells were counted using a Hemavet. BM and spleen cells were counted using a Cellometer. Ten million cells were stained and washed in FACS buffer (PBS, 1% BSA, 0.1% sodium aziade, and 2 μm EDTA). For monocyte, macrophage, and neutrophil analyses, cells from each tissue were stained with Brilliant Violet 421-conjugated F4/80 (BM8), peridinin chlorophyll protein complex (PerCP)-Cy5.5-conjugated MHC Class II (M5/114.15.2), phycoerythrin (PE)-Cy7-conjugated CD11c (N418), allophycocyanin (APC)-conjugated CD19 (1D3), APC-conjugated CD45R/B220 (RA3-6B2), APC-eFluor780-conjugated Ly-6G (Gr1, RB6-8C5), and PE-conjugated CD115 (AFS98). Two million live events were collected in the live gate and analyzed *via* FlowJo. Gating strategies can be found in Figure S1 in Supplementary Material.

Statistical Analysis

Statistical comparisons were performed using Graphpad Prism® (GraphPad Software, Inc., La Jolla, CA, USA). In **Figures 1–3**, with the exception of panel 2D, comparisons between wild-type (WT) and *Mfap2*$^{-/-}$ mice at each time point and over time within groups (WT or *Mfap2*$^{-/-}$) were performed using a regular two-way ANOVA with Holm–Sidak correction for multiple comparisons. For the ITTs in panel 2D, repeated measures two-way ANOVA with Sidak's correction was used. In **Figures 4** and **5**, results were compared with a two-tailed *t*-test. Comparisons with a *P*-value ≤0.05 were considered statistically significant.

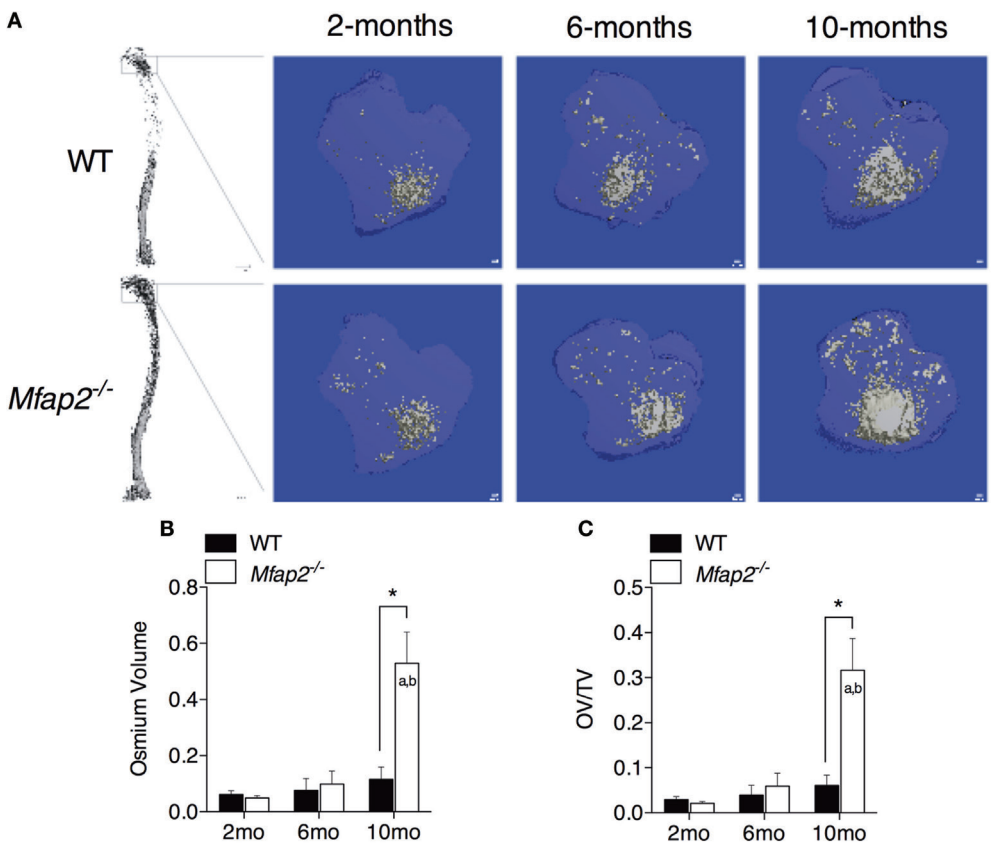

FIGURE 1 | MAT expansion in *Mfap2*$^{-/-}$ mice. (A) Micro-computed tomography (μCT) visualization of osmium stained lipid within the decalcified proximal tibia. **(B,C)** Region analyzed for osmium volume (OV) was 1 mm distal to the growth plate. OV/TV is osmium volume divided by the marrow cavity volume in the same region. Mean ± SEM; Sample sizes for WT and *Mfap2*$^{-/-}$ mice, respectively: 2 months: $n = 8, 8$; 6 months: $n = 6, 8$; and 10 months: $n = 8, 6$. Statistical significance at each time point and within groups (WT or *Mfap2*$^{-/-}$) over time was determined by two-way ANOVA with Holm–Sidak's correction for multiple comparisons (*$p \leq 0.05$, *a* = significant relative to 2 months of same genotype, and *b* = significant relative to 6 months of same genotype). Scale bar is 100 μm. Note: two 10-month-old *Mfap2*$^{-/-}$ bones were excluded from study due to suspected fracture.

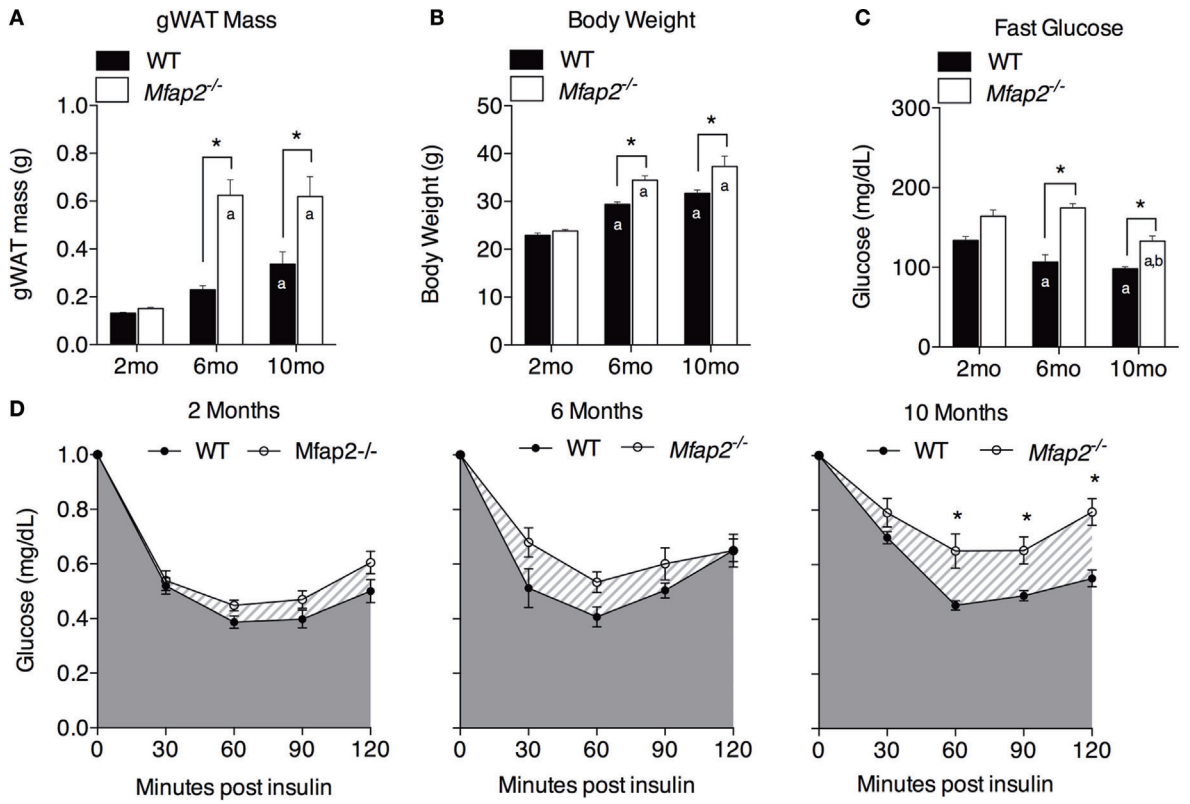

FIGURE 2 | Characterization of metabolic disorder in *Mfap2*$^{-/-}$mice. (A) Gonadal white adipose tissue (WAT) was harvested at 2 months (n = 10, 8), 6 months (n = 6, 8), and 10 months (n = 8, 8). **(B)** Total body weight at 2 months (n = 10, 8), 6 months (n = 7, 9), and 10 months (n = 8, 8). **(C)** Fasted (6 h) blood glucose concentration at 2 months (n = 10, 8), 6 months (n = 6, 8), and 10 months (n = 8, 8). **(D)** Insulin sensitivity results at 2 months (n = 10, 8), 6 months (n = 5, 8), and 10 months (n = 8, 8). Blood glucose data were normalized to time point 0 (before insulin injection). Mean ± SEM; statistical significance in **(A–C)** at each time point and within groups (WT or *Mfap2*$^{-/-}$) over time was determined by two-way ANOVA with Holm–Sidak's correction for multiple comparisons. Statistical significance in **(D)** was determined by repeated-measured two-way ANOVA with Sidak's correction (*$p \leq 0.05$, a = significant relative to 2 months of same genotype, and b = significant relative to 6 months of same genotype). Sample sizes shown above are for WT and *Mfap2*$^{-/-}$ mice, respectively.

RESULTS

Pathologic MAT Expansion in *Mfap2*$^{-/-}$ Mice

To compare parameters of metabolic disease with MAT expansion, a longitudinal study was performed in MAGP1-deficient (*Mfap2*$^{-/-}$) mice that are susceptible to metabolic syndrome. Marrow adiposity was determined by μCT imaging of osmium stained lipid within the proximal tibia (**Figure 1A**). Quantification of total marrow lipid OV and OV normalized to total marrow cavity volume (OV/TV) is shown in **Figures 1B,C**. Marrow adiposity was found to be indistinguishable in either young (2 months) or adult (6 months) *Mfap2*$^{-/-}$ mice, relative to WT mice. However, aged 10-month-old *Mfap2*$^{-/-}$ mice displayed a fivefold increase in marrow lipid (OV and OV/TV) relative to WT animals. WT C57BL/6 mice have only a modest, statistically insignificant, increase (54%) in MAT between 6 and 10 months.

Characterization of Metabolic Dysfunction in *Mfap2*$^{-/-}$ Mice

Previously, we demonstrated that MAGP1 deficiency results in excess adiposity and reduced bone mass (13, 14, 16). Consistent with previous results, 2-month-old *Mfap2*$^{-/-}$ mice had only a modest 15% increase in white fat (as measured by gonadal fat pad mass, **Figure 2A**). However, by 6 months, *Mfap2*$^{-/-}$ mice had a 2.7-fold increase in fat mass, relative to WT mice. Extending our study to 10 months of age, we found that the differential in fat mass stabilizes, indicated by a 1.8-fold increase *Mfap2*$^{-/-}$ gonadal fat pad mass relative to WT mice. Total body weight reinforced this finding (**Figure 2B**). *Mfap2*$^{-/-}$ body weight was insignificantly increased at 2 months, but a significant (17%) increase in *Mfap2*$^{-/-}$ weight was found at 6 months. Similar to the fat mass measurement, the weight differential between WT and *Mfap2*$^{-/-}$ mice stabilized, remaining increased by 17% relative to baseline, at 10 months. Six-hour fasting blood glucose was significantly elevated in *Mfap2*$^{-/-}$ mice by 2 months (12%, **Figure 2C**). By 6 months, fasted blood glucose was 63% higher in *Mfap2*$^{-/-}$ mice relative to WT mice. However, by 10 months, there was only a 35% increase in *Mfap2*$^{-/-}$ blood glucose relative to WT. To characterize metabolic function, ITTs were performed on WT and *Mfap2*$^{-/-}$ mice at all ages (**Figure 2D**). In contrast to fat mass, body weight, and fasting blood glucose, insulin resistance did not reach statistical significance until the *Mfap2*$^{-/-}$ mice were 10-month old. Thus, *Mfap2*$^{-/-}$ mice

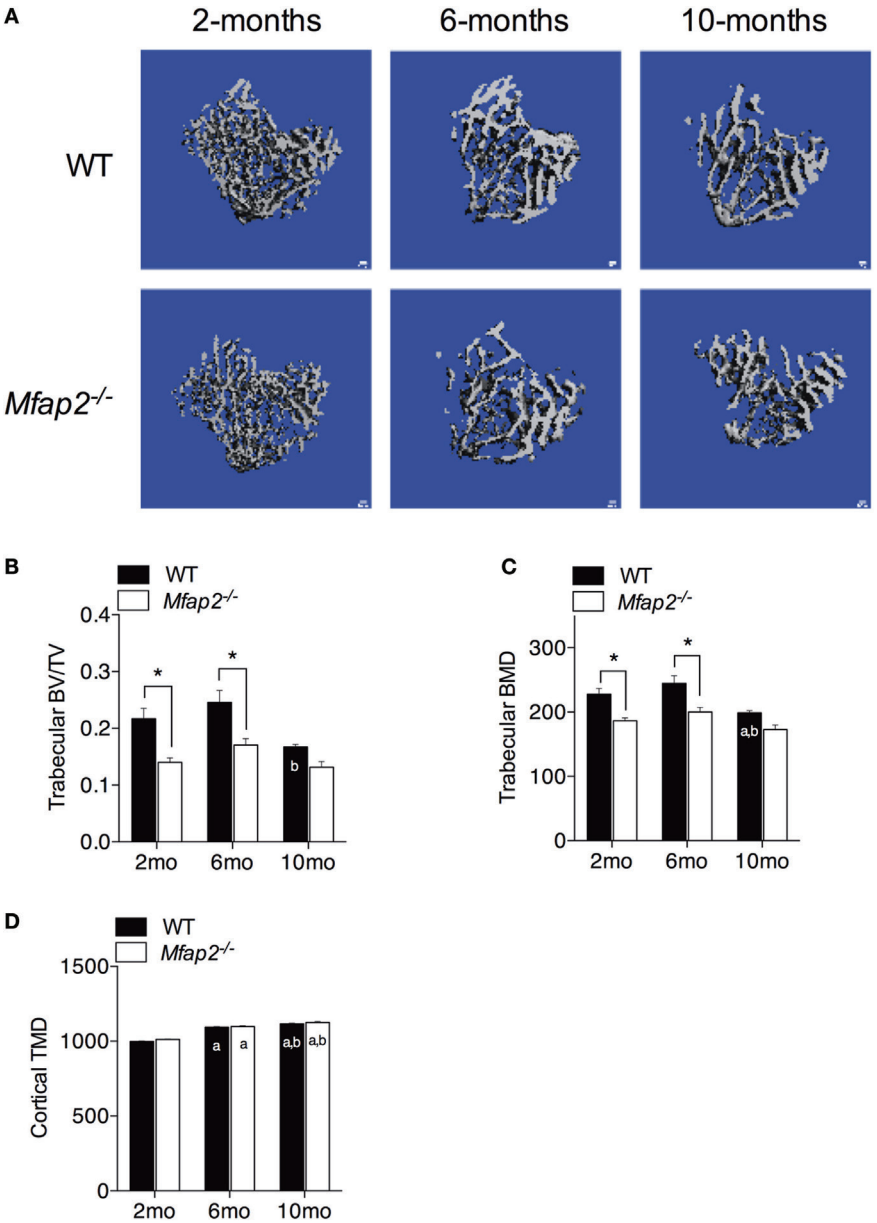

FIGURE 3 | Skeletal changes in *Mfap2*$^{-/-}$ mice. Tibias were harvested at 2, 6, and 10 months. Micro-comupted tomography was used to determine the ratio of bone volume to total volume (BV/TV) and bone mineral density (BMD/TMD). **(A–C)** For trabecular bone, 1 mm distal to the growth plate was analyzed. **(D)** For cortical bone, tissue mineral density (TMD) was determined by contouring 400 μm located 2 mm proximal to the tibia–fibula junction. Sample size for WT and *Mfap2*$^{-/-}$ mice, respectively, are 2 months $n = 8, 8$; 6 months $n = 6, 8$; and 10 months $n = 8, 6$. Mean ± SEM; statistical significance at each time point and within groups (WT or *Mfap2*$^{-/-}$) over time was determined by two-way ANOVA with Holm–Sidak's correction for multiple comparisons (*$p \leq 0.05$, *a* = significant relative to 2 months of same genotype, and *b* = significant relative to 6 months of same genotype). Scale bar is 100 μm. Note: two 10-month-old *Mfap2*$^{-/-}$ bones were excluded from study due to suspected fracture.

are severely hyperglycemic by 6 months in age, but not insulin resistant until 10 months.

Relationship between MAT Expansion and Bone Mass

Tibial bone morphology was assessed by μCT prior to osmium staining for MAT quantification (**Figure 3A**). Trabecular bone analysis was performed using the same region of interest analyzed for MAT (**Figures 3B,C**). Reduced trabecular bone volume (BV/TV) and BMD were detectable in *Mfap2*$^{-/-}$ mice by 2 months. Aging of WT mice from 6 to 10 months was associated with statistically significant reductions in trabecular bone volume (−32%, **Figure 3B**) and mineral density (−19%, **Figure 3C**), but not a statistically significant increase in MAT (**Figure 1C**). During this time, *Mfap2*$^{-/-}$ mice had a 22% reduction in BV/

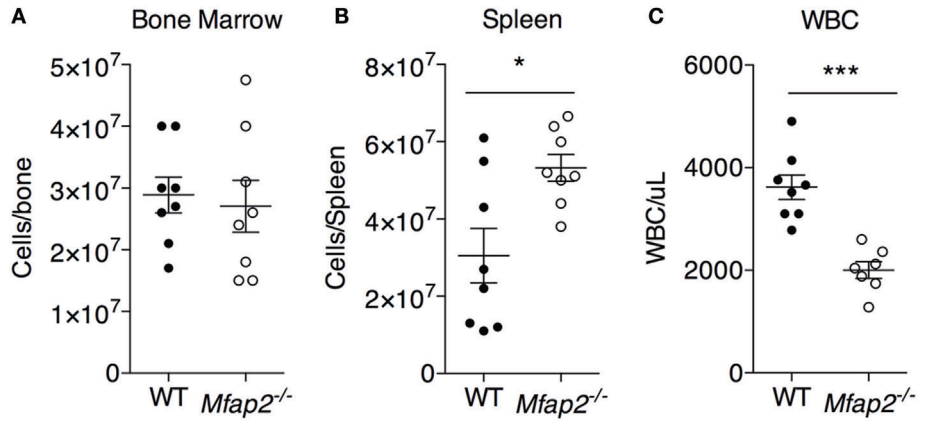

FIGURE 4 | MAT expansion and hematopoiesis. To address the consequence of pathologic MAT expansion on hematopoiesis, the cellularity of the **(A)** bone marrow, **(B)** spleen, and **(C)** blood [white blood cells (WBCs)] were measured at 10 months. Sample size for WT and *Mfap2*$^{-/-}$ mice, respectively, are $n = 8, 8$ **(A,B)** or $n = 8, 7$ **(C)**. Mean ± SEM; Student's *t*-test was done for single comparison (*$p \leq 0.05$ and ***$p \leq 0.001$).

TV (**Figure 3B**), but a 5.2-fold increase in MAT volume (OV/TV, **Figure 1C**). Cortical bone density was maintained during aging and unchanged by MAT accumulation (**Figure 3D**). In fact, cortical BMD was highest at 10 months in both WT and *Mfap2*$^{-/-}$ mice. Additional μCT indices of bone structure can be found in Tables S1 and S2 in Supplementary Material.

MAT Expansion and Hematopoiesis

To address the impact of pathologic MAT expansion on hematopoietic function, we measured the cellularity of the BM and spleen as well as the number of circulating white blood cells (WBCs) at 10 months of age. BM cellularity was not significantly reduced in *Mfap2*$^{-/-}$ mice, despite the fivefold increase in MAT (**Figure 4A**). However, spleen cellularity was slightly elevated and WBC count was decreased in *Mfap2*$^{-/-}$ mice (**Figures 4B,C**). To further investigate these findings, flow cytometry was used to assess hematopoietic lineage distribution. Within the BM of *Mfap2*$^{-/-}$ mice, there was a modest increase in macrophages, myeloid-derived dendritic cells (MDCs), and B-cells (+61, +78, and +18%, respectively) and a corresponding decrease in neutrophils relative to WT mice (−13%) (**Figure 5A**). In the spleen, there was a significant increase in MDCs (+250%) and decrease in neutrophils (−72%), with a trend to increased B-cells (**Figure 5B**). Finally, in the blood, we observed an increase in monocytes (+216%) and a modest decrease in B-cells (−15%) in *Mfap2*$^{-/-}$ mice (**Figure 5C**).

DISCUSSION

Once viewed as inert, space-filling structures, BM adipocytes are now recognized as metabolically active cells with the potential to influence bone remodeling and hematopoiesis. The relationship between MAT volume and peripheral fat mass has been addressed previously (9, 10). In rodents, weight gain resulting from HFD feeding is associated with significant MAT expansion. However, extreme peripheral fat loss due to caloric restriction also correlates with increased marrow adiposity (6). The rapid change in adiposity impedes our understanding of whether changes in peripheral adipose tissue lipid storage shift lipids to the marrow, or if metabolic changes such as insulin resistance contribute to MAT expansion. To address this question, we performed a longitudinal study of mice predisposed to excess, age-associated fat accumulation without dietary intervention.

Microfibril-associated glycoprotein-1 is a matricellular protein that associates with ECM structures but does not contribute to their biophysical properties. Instead, MAGP1 affords fibrillar structures the capacity to regulate signal transduction by tethering growth factors to the ECM [reviewed in Ref. (12)]. MAGP1 is expressed in adipose tissue. MAGP1 deficiency in mice (*Mfap2*$^{-/-}$) causes adipocyte hypertrophy in peripheral WAT, which contributes to obesity and then insulin resistance (13). MAGP1 is also highly expressed by osteoblasts in the bone. Loss of MAGP1 *in vivo* leads to increased osteoclast number and reduced bone mass (14). In this study, MAT expansion did not occur coincident with bone loss or excess peripheral adiposity in *Mfap2*$^{-/-}$ mice; osteopenia was detectable by 2 months and excess adiposity by 6 months in *Mfap2*$^{-/-}$ mice whereas pathologic MAT expansion was not detectable until 10 months of age. This suggests that MAGP1 deficiency in bone is sufficient to cause abnormal bone remodeling but is unlikely to be mediating the changes in MAT. Instead, MAT expansion coincided with insulin resistance in *Mfap2*$^{-/-}$ mice. Our findings are of importance because they address three confounding factors of MAT biology: the mechanisms that drive MAT expansion, the relationship between MAT expansion and bone loss, and whether MAT is detrimental to hematopoiesis.

The coincidence of MAT expansion with insulin resistance suggests that insulin may limit MAT adipocyte size or number. Insulin signaling in marrow adipocytes has not been reported, thus, we cannot comment on insulin's direct action on lipid storage or adipogenesis in these specialized cells. However, the pathophysiology of insulin resistance could induce a secondary complication (e.g., hyperlipidemia) that drives subsequent

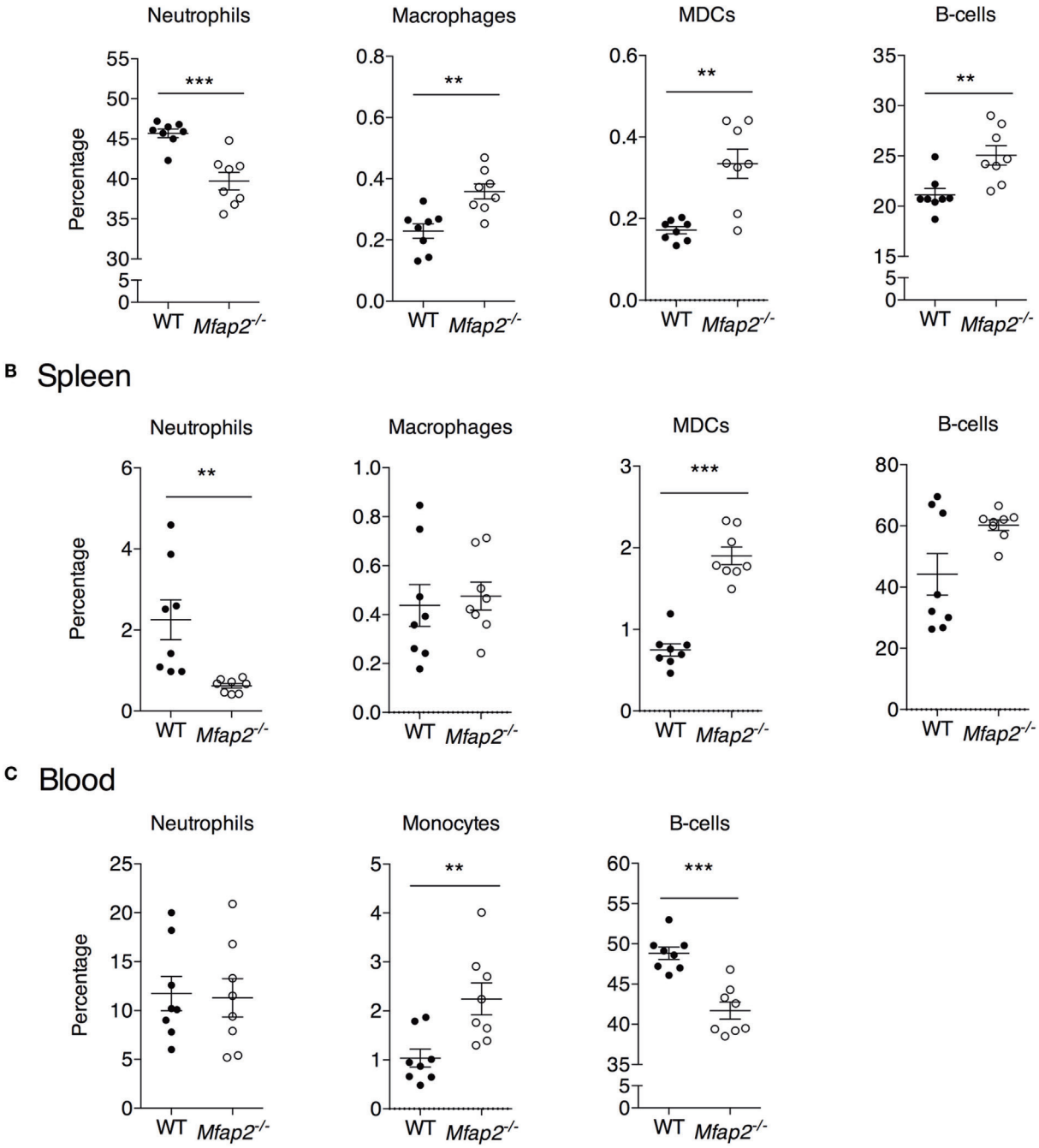

FIGURE 5 | Neutrophil, macrophage, myeloid-derived dendritic cell, monocyte, and B cell frequency within the (A) bone marrow, (B) spleen, and (C) blood at 10 months. Neutrophils: B220$^-$, Gr1$^+$. Macrophage: B220$^-$, Gr1$^-$, MHCII$^+$, F4/80$^+$, and CD11c$^-$. Dendritic cell: B220$^-$, Gr1$^-$, MHCII$^+$, F4/80$^-$, and CD11c$^+$. Monocyte: B220$^-$, Gr1$^-$, and F4/80$^+$. Sample sizes for WT and *Mfap2*$^{-/-}$ mice, respectively, are $n = 8$ and 8. Mean ± SEM; Student's *t*-test was done for single comparison (*$p \leq 0.05$, **$p \leq 0.01$, and ***$p \leq 0.001$).

MAT expansion. Insulin is a potent inhibitor of lipolysis, the breakdown of triglyceride stores, in traditional white adipocytes. Insulin resistance is therefore associated with elevated circulating free fatty acids (FFA) and excess energy storage in atypical sites (e.g., muscle and liver) (19). It is possible that marrow adipocytes respond to elevated FFA associated with insulin resistance by storing them as triglycerides. Rodent models of type 1 diabetes (T1DM) also display significant MAT accumulation (20–22),

providing a second example of perturbed insulin signaling associating with hyperlipidemia and MAT expansion.

The relationship between marrow adiposity and bone mass is highly debated. Published reports have shown that MAT expansion can coincide with increased, reduced, or unchanged bone volume (9, 10, 23–27).

Substantial *in vitro* evidence demonstrates that adipocytes and osteoblasts arise from the same mesenchymal progenitor. If true, maturation of mesenchymal stem cells through the adipocyte lineage should be at the expense of the osteoblast lineage. However, *in vivo* evidence is conflicting. Specifically, lineage tracing of marrow adipocytes has demonstrated that the osteoblasts are derived from a Gremlin-1 positive mesenchymal progenitor cell, but these Gremlin-1 positive cells do not differentiate into adipocytes (28). This would allow osteoblast cell numbers to exist independent of marrow adipocyte number. The marrow cavity is also a relatively defined space, and it would, therefore, seem that expansion of MAT must occur at the expense of something else, such as bone. Our study supports a disconnection between MAT volume and bone volume. When WT and *Mfap2*$^{-/-}$ mice age from 6 to 10 months, there is an increase in MAT and decrease in BV/TV. However, loss of trabecular BV/TV from 6 to 10 months is actually greater in WT mice, despite *Mfap2*$^{-/-}$ mice having a greater accrual of MAT. Specifically, in WT mice, BV/TV loss is 32% and MAT volume increases 54%; however, MAT volume in *Mfap2*$^{-/-}$ mice is increased 530% but BV/TV is decreased only 22%.

Marrow adipocytes are considered as members of the hematopoietic niche. Marrow adiposity and hematopoiesis have been studied in the context of marrow ablation by irradiation and chemotherapy. From these studies, it was concluded that the filling of the marrow with fat impedes marrow reconstitution and hematopoiesis (29–31). The current study investigated the consequence of pathologic MAT expansion on existing hematopoietic cells (not reconstitution). We found a significant reduction in circulating WBCs and a small increase in spleen cellularity, indicators of BM failure and extramedullary hematopoiesis. Further study is needed to determine whether MAT expansion in this model leads to a loss of functional hematopoietic stem cells. Unexpectedly, however, total BM cellularity was unchanged. This may be due to shifts in marrow composition to favor loss of fluid space and vascular tone with MAT expansion to allow subsequent preservation of hematopoiesis. We also examined whether fat expansion within the marrow would cause a recruitment (or retention) of macrophages. Macrophages are recruited to peripheral adipose tissue to allow remodeling of adipose tissue during expansion, and because of this, obesity is linked to fat inflammation (32). Indeed, we found a slight increase in macrophage frequency within *Mfap2*$^{-/-}$ BM. However, the implications of this finding are unclear. Future studies are needed to examine the remodeling of the MAT adipocyte niche in response to obesity.

The goal of this project was to determine the association between pathologic MAT expansion and peripheral indicators of metabolic dysfunction without the use of modified diet. We also addressed the relationship between MAT expansion and bone mass, and the consequence of pathologic MAT expansion on hematopoiesis. We found that MAT volume was not linked directly to peripheral fat accumulation and, instead, coincided with insulin resistance. Furthermore, we found that bone loss occurred, regardless of MAT expansion, in *Mfap2*$^{-/-}$ relative to WT at all ages. Lastly, we show that MAT expansion is associated with modest alterations in basal hematopoiesis, including a shift from granulopoiesis to B lymphopoiesis.

AUTHOR CONTRIBUTIONS

TW and ST contributed equally to this work. TW, ST, AS, and BA designed and performed the experiments as well as analyzed the data. TW, ST, and CC wrote the manuscript. GA-E and DL analyzed and interpreted FACS data. CC, ES, RM, and DL provided research materials and contributed to editing of the manuscript.

ACKNOWLEDGMENTS

We thank Dan Leib for his help in developing the osmium μCT imaging technique, and Kayla Moller for her generation of the 3-dimensional μCT images. This work was supported by National Institutes of Health grants HL-053325 and HL-105314 to RM, and K99-DE024178 to ES. An American Diabetes Association grant 7-13-JF-16 to CC. Washington University Nutrition and Obesity Research Center award P30-DK-056341 to CC, and Washington University's Musculoskeletal Research Center award JIT2014_Craft_1 to CC. Technical support was provided by the Mouse Phenotyping Core, the Adipocyte Biology and Molecular Nutrition Core of the Nutrition and Obesity Research Center (grant P30-DK-056341), the Morphology Core of the Digestive Disease Research Core Center (grant P30-DK-52574), and the Washington University Musculoskeletal Research Center structure and strength core (grant P30-AR-057235).

SUPPLEMENTARY MATERIAL

The Supplementary Material for this article can be found online at http://journal.frontiersin.org/article/10.3389/fendo.2016.00087

REFERENCES

1. Sanchez-Gurmaches J, Hung CM, Guertin DA. Emerging complexities in adipocyte origins and identity. *Trends Cell Biol* (2016) 26:313–26. doi:10.1016/j.tcb.2016.01.004
2. Berry R, Rodeheffer MS, Rosen CJ, Horowitz MC. Adipose tissue residing progenitors (adipocyte lineage progenitors and adipose derived stem cells (ADSC)). *Curr Mol Biol Rep* (2015) 1:101–9. doi:10.1007/s40610-015-0018-y
3. Steiner RM, Mitchell DG, Rao VM, Murphy S, Rifkin MD, Burk DL, et al. Magnetic resonance imaging of bone marrow: diagnostic value in diffuse hematologic disorders. *Magn Reson Q* (1990) 6:17–34.
4. Scheller EL, Doucette CR, Learman BS, Cawthorn WP, Khandaker S, Schell B, et al. Region-specific variation in the properties of skeletal adipocytes reveals regulated and constitutive marrow adipose tissues. *Nat Commun* (2015) 6:7808. doi:10.1038/ncomms8808
5. Cawthorn WP, Scheller EL, Parlee SD, Pham HA, Learman BS, Redshaw CM, et al. Expansion of bone marrow adipose tissue during caloric restriction is

associated with increased circulating glucocorticoids and not with hypoleptinemia. *Endocrinology* (2016) 157:508–21. doi:10.1210/en.2015-1477
6. Cawthorn WP, Scheller EL, Learman BS, Parlee SD, Simon BR, Mori H, et al. Bone marrow adipose tissue is an endocrine organ that contributes to increased circulating adiponectin during caloric restriction. *Cell Metab* (2014) 20:368–75. doi:10.1016/j.cmet.2014.06.003
7. Lecka-Czernik B. Marrow fat metabolism is linked to the systemic energy metabolism. *Bone* (2012) 50:534–9. doi:10.1016/j.bone.2011.06.032
8. Hamrick MW, Della-Fera MA, Choi YH, Pennington C, Hartzell D, Baile CA. Leptin treatment induces loss of bone marrow adipocytes and increases bone formation in leptin-deficient ob/ob mice. *J Bone Miner Res* (2005) 20:994–1001. doi:10.1359/JBMR.050103
9. Doucette CR, Horowitz MC, Berry R, MacDougald OA, Anunciado-Koza R, Koza RA, et al. A high fat diet increases bone marrow adipose tissue (MAT) but does not alter trabecular or cortical bone mass in C57BL/6J mice. *J Cell Physiol* (2015) 230:2032–7. doi:10.1002/jcp.24954
10. Lecka-Czernik B, Stechschulte LA, Czernik PJ, Dowling AR. High bone mass in adult mice with diet-induced obesity results from a combination of initial increase in bone mass followed by attenuation in bone formation; implications for high bone mass and decreased bone quality in obesity. *Mol Cell Endocrinol* (2015) 410:35–41. doi:10.1016/j.mce.2015.01.001
11. Frantz C, Stewart KM, Weaver VM. The extracellular matrix at a glance. *J Cell Sci* (2010) 123:4195–200. doi:10.1242/jcs.023820
12. Mecham RP, Gibson MA. The microfibril-associated glycoproteins (MAGPs) and the microfibrillar niche. *Matrix Biol* (2015) 47:13–33. doi:10.1016/j.matbio.2015.05.003
13. Craft CS, Pietka TA, Schappe T, Coleman T, Combs MD, Klein S, et al. The extracellular matrix protein MAGP1 supports thermogenesis and protects against obesity and diabetes through regulation of TGF-β. *Diabetes* (2014) 63:1920–32. doi:10.2337/db13-1604
14. Craft CS, Zou W, Watkins M, Grimston S, Brodt MD, Broekelmann TJ, et al. Microfibril-associated glycoprotein-1, an extracellular matrix regulator of bone remodeling. *J Biol Chem* (2010) 285:23858–67. doi:10.1074/jbc.M110.113019
15. Finnis ML, Gibson MA. Microfibril-associated glycoprotein-1 (MAGP-1) binds to the pepsin-resistant domain of the alpha3(VI) chain of type VI collagen. *J Biol Chem* (1997) 272:22817–23. doi:10.1074/jbc.272.36.22817
16. Weinbaum JS, Broekelmann TJ, Pierce RA, Werneck CC, Segade F, Craft CS, et al. Deficiency in microfibril-associated glycoprotein-1 leads to complex phenotypes in multiple organ systems. *J Biol Chem* (2008) 283:25533–43. doi:10.1074/jbc.M709962200
17. Craft CS, Broekelmann TJ, Zou W, Chappel JC, Teitelbaum SL, Mecham RP. Oophorectomy-induced bone loss is attenuated in MAGP1-deficient mice. *J Cell Biochem* (2012) 113:93–9. doi:10.1002/jcb.23331
18. Bouxsein ML, Boyd SK, Christiansen BA, Guldberg RE, Jepsen KJ, Müller R. Guidelines for assessment of bone microstructure in rodents using micro-computed tomography. *J Bone Miner Res* (2010) 25:1468–86. doi:10.1002/jbmr.141
19. Karpe F, Dickmann JR, Frayn KN. Fatty acids, obesity, and insulin resistance: time for a reevaluation. *Diabetes* (2011) 60:2441–9. doi:10.2337/db11-0425
20. Botolin S, McCabe LR. Inhibition of PPARgamma prevents type I diabetic bone marrow adiposity but not bone loss. *J Cell Physiol* (2006) 209:967–76. doi:10.1002/jcp.20804
21. Botolin S, Faugere MC, Malluche H, Orth M, Meyer R, McCabe LR. Increased bone adiposity and peroxisomal proliferator-activated receptor-gamma2 expression in type I diabetic mice. *Endocrinology* (2005) 146:3622–31. doi:10.1210/en.2004-1677
22. Botolin S, McCabe LR. Bone loss and increased bone adiposity in spontaneous and pharmacologically induced diabetic mice. *Endocrinology* (2007) 148:198–205. doi:10.1210/en.2006-1006
23. Bredella MA, Fazeli PK, Miller KK, Misra M, Torriani M, Thomas BJ, et al. Increased bone marrow fat in anorexia nervosa. *J Clin Endocrinol Metab* (2009) 94:2129–36. doi:10.1210/jc.2008-2532
24. Ecklund K, Vajapeyam S, Feldman HA, Buzney CD, Mulkern RV, Kleinman PK, et al. Bone marrow changes in adolescent girls with anorexia nervosa. *J Bone Miner Res* (2010) 25:298–304. doi:10.1359/jbmr.090805
25. Schwartz AV, Sigurdsson S, Hue TF, Lang TF, Harris TB, Rosen CJ, et al. Vertebral bone marrow fat associated with lower trabecular BMD and prevalent vertebral fracture in older adults. *J Clin Endocrinol Metab* (2013) 98:2294–300. doi:10.1210/jc.2012-3949
26. Yeung DK, Griffith JF, Antonio GE, Lee FK, Woo J, Leung PC. Osteoporosis is associated with increased marrow fat content and decreased marrow fat unsaturation: a proton MR spectroscopy study. *J Magn Reson Imaging* (2005) 22:279–85. doi:10.1002/jmri.20367
27. Cohen A, Dempster DW, Stein EM, Nickolas TL, Zhou H, McMahon DJ, et al. Increased marrow adiposity in premenopausal women with idiopathic osteoporosis. *J Clin Endocrinol Metab* (2012) 97:2782–91. doi:10.1210/jc.2012-1477
28. Worthley DL, Churchill M, Compton JT, Tailor Y, Rao M, Si Y, et al. Gremlin 1 identifies a skeletal stem cell with bone, cartilage, and reticular stromal potential. *Cell* (2015) 160:269–84. doi:10.1016/j.cell.2014.11.042
29. Green DE, Adler BJ, Chan ME, Rubin CT. Devastation of adult stem cell pools by irradiation precedes collapse of trabecular bone quality and quantity. *J Bone Miner Res* (2012) 27:749–59. doi:10.1002/jbmr.1505
30. Green DE, Adler BJ, Chan ME, Lennon JJ, Acerbo AS, Miller LM, et al. Altered composition of bone as triggered by irradiation facilitates the rapid erosion of the matrix by both cellular and physicochemical processes. *PLoS One* (2013) 8:e64952. doi:10.1371/journal.pone.0064952
31. Zhu RJ, Wu MQ, Li ZJ, Zhang Y, Liu KY. Hematopoietic recovery following chemotherapy is improved by BADGE-induced inhibition of adipogenesis. *Int J Hematol* (2013) 97:58–72. doi:10.1007/s12185-012-1233-4
32. Dam V, Sikder T, Santosa S. From neutrophils to macrophages: differences in regional adipose tissue depots. *Obes Rev* (2016) 17:1–17. doi:10.1111/obr.12335

Conflict of Interest Statement: The authors declare that the research was conducted in the absence of any commercial or financial relationships that could be construed as a potential conflict of interest.

frontiers in Endocrinology

REVIEW
published: 14 July 2016
doi: 10.3389/fendo.2016.00094

Exercise Regulation of Marrow Adipose Tissue

*Gabriel M. Pagnotti[1] and Maya Styner[2]**

[1] Department of Biomedical Engineering, Stony Brook University, Stony Brook, NY, USA, [2] Department of Medicine, University of North Carolina, Chapel Hill, NC, USA

Despite association with low bone density and skeletal fractures, marrow adipose tissue (MAT) remains poorly understood. The marrow adipocyte originates from the mesenchymal stem cell (MSC) pool that also gives rise to osteoblasts, chondrocytes, and myocytes, among other cell types. To date, the presence of MAT has been attributed to preferential biasing of MSC into the adipocyte rather than osteoblast lineage, thus negatively impacting bone formation. Here, we focus on understanding the physiology of MAT in the setting of exercise, dietary interventions, and pharmacologic agents that alter fat metabolism. The beneficial effect of exercise on musculoskeletal strength is known: exercise induces bone formation, encourages growth of skeletally supportive tissues, inhibits bone resorption, and alters skeletal architecture through direct and indirect effects on a multiplicity of cells involved in skeletal adaptation. MAT is less well studied due to the lack of reproducible quantification techniques. In recent work, osmium-based 3D quantification shows a robust response of MAT to both dietary and exercise intervention in that MAT is elevated in response to high-fat diet and can be suppressed following daily exercise. Exercise-induced bone formation correlates with suppression of MAT, such that exercise effects might be due to either calorie expenditure from this depot or from mechanical biasing of MSC lineage away from fat and toward bone, or a combination thereof. Following treatment with the anti-diabetes drug rosiglitazone – a PPARγ-agonist known to increase MAT and fracture risk – mice demonstrate a fivefold higher femur MAT volume compared to the controls. In addition to preventing MAT accumulation in control mice, exercise intervention significantly lowers MAT accumulation in rosiglitazone-treated mice. Importantly, exercise induction of trabecular bone volume is unhindered by rosiglitazone. Thus, despite rosiglitazone augmentation of MAT, exercise significantly suppresses MAT volume and induces bone formation. That exercise can both suppress MAT volume and increase bone quantity, notwithstanding the skeletal harm induced by rosiglitazone, underscores exercise as a powerful regulator of bone remodeling, encouraging marrow stem cells toward the osteogenic lineage to fulfill an adaptive need for bone formation. Thus, exercise represents an effective strategy to mitigate the deleterious effects of overeating and iatrogenic etiologies on bone and fat.

Keywords: exercise, marrow adipose tissue, quantitative image analysis, bone microarchitecture, lipid, PPARγ, rosiglitazone, exercise

OPEN ACCESS

Edited by:
William Peter Cawthorn, University of Edinburgh, UK

Reviewed by:
Petra Simic, Massachusetts Institute of Technology, USA
Jonathan Gooi, The University of Melbourne, Australia

****Correspondence:***
Maya Styner
mstyner@med.unc.edu

Specialty section:
This article was submitted to Bone Research, a section of the journal Frontiers in Endocrinology

Received: *21 May 2016*
Accepted: *04 July 2016*
Published: *14 July 2016*

Citation:
Pagnotti GM and Styner M (2016) Exercise Regulation of Marrow Adipose Tissue. Front. Endocrinol. 7:94. doi: 10.3389/fendo.2016.00094

MARROW ADIPOSE TISSUE

Increased marrow adipose tissue (MAT) is associated with states of impaired bone formation (1, 2) and dysfunctional hematopoiesis (3–5), although its physiological role remains unclear. In humans, pathologists have noted that MAT increases in healthy subjects with age, beginning in the distal long bones and accruing proximally such that by age 25, approximately 70% of the marrow space is filled with MAT (4). In addition to physiologic MAT, which accrues with aging, this fat depot – housed within bone – is abundant in states of low bone density: osteoporosis (6), anorexia nervosa (7), skeletal unloading (8, 9), and anti-diabetes therapies (10), conditions that are also associated with skeletal fractures. Adipocytes within the marrow originate from the mesenchymal stem cell (MSC) pool that also gives rise to osteoblasts, chondrocytes, and myocytes, among other cell types (11, 12). Recent work suggests that increased marrow fat can also be demonstrated in the setting of preserved or increased bone density (high-fat feeding or obesity) (13–15) and, thus, challenges the premise that the relationship between MAT and bone volume is reciprocal. The MAT/bone relationship is further complicated by the identification of a new population of Grem1$^+$ MSC (16), a phenotype capable of differentiating into osteoblasts and chondrocytes, but not adipocytes: the Grem1$^+$ population differs from the LepR$^+$ MSC, which do generate marrow adipocytes. Whether senile marrow invasion with adipocytes represents a later predominance of a LepR$^+$ MSC population is unknown but complicates considerations as to the physiologic and/or pathologic role of MAT.

In the case of diet-induced obesity, marrow fat also increases compared to normal weight controls, but whether this contributes to bone fragility is unclear (17). Nevertheless, if the burden of fat across the marrow space is inevitable, then perhaps what's more worthy of an investigation is the quality of the MAT being generated, possibly representing a direct reflection of the health of the surrounding bone. Importantly, the unsaturation index of MAT increases with aging, and thus, this feature of MAT may shed light on its physiology; nonetheless, unsaturation index of MAT is unaffected by physical activity (18). While subcutaneous white fat depots store excess energy and provide a clear evolutionary advantage during times of scarcity (19), MAT's purpose remains indeterminate, harboring characteristics of both white and brown fat (20). WAT serves as a source of adipokines and inflammatory markers that have both positive (e.g., adiponectin) (21) and negative (22) effects on metabolic and cardiovascular endpoints. Visceral abdominal fat is a distinct depot of WAT that is proportionally associated with negative metabolic and cardiovascular morbidity (23), regenerates cortisol (24), and has been linked to reduced bone formation (25, 26). WAT substantially differs from brown adipose tissue (BAT), as defined by a panel of proteins that support BAT's thermogenic role (27). MAT, by virtue of its specific marrow location and its adipocyte origin from at least LepR$^+$ marrow MSC, is clearly demarcated from non-bone fat depots by higher expression of bone transcription factors (28) and likely represents a unique fat phenotype (29). Recently, MAT was noted to produce a greater proportion of adiponectin – an adipokine associated with improved metabolism – than WAT (30), suggesting an endocrine function for MAT as distinct depot, akin, but different from that of WAT. Moreover, deficiency of histone deacetylase 3 (Hdac3), known to play a major role in skeletal development and lipid metabolism, increases MAT volume, implicating this important transcriptional regulator in MAT development (31). Potentially, MAT might serve multiple functions, reflecting those of both white and brown fat, storing lipid in preexisting adipocytes, secreting adipokines, and generating heat. Exercise universally affects the metabolism of both WAT (32) and more recently BAT (33, 34); thus, exercise intervention can be harnessed as a powerful tool to query the poorly understood physiology of MAT.

MEASUREMENT AND QUANTIFICATION OF MARROW ADIPOSE TISSUE

In order to quantify and characterize the effects of exercise on MAT, various analytic methods were considered. Until recently, qualitative measurements of MAT have relied on bone histology (35, 36), which is subject to site selection bias and cannot adequately quantify the volume of fat in the marrow. Nevertheless, histological techniques and fixation make possible *in situ* visualization of MAT, quantification of adipocyte size, and MAT's association with the surrounding endosteum, milieu of cells, and secreted factors (37–39).

Recent advances in cell surface and intracellular marker identification and single-cell microfluidic analyses have led to greater resolution and high-throughput *ex vivo* quantification. Flow cytometric quantification can be used to purify adipocytes from the stromal vascular fraction of most fat depots (40). Early research with such machinery cited adipocytes as too large (50–200 mm) and fragile for cytometer-based purification, as their cytoskeleton lacks rigidity, rendering them susceptible to lysis; however, recent advances have been made to mitigate this (41). One may distinguish discrete adipocyte subpopulations from other cells by utilizing internal lipid content and surface biomarker identification. Filtration of the marrow (pore size = 150 μm) permits adequate flowthrough for adipocytes and smaller cellular contents. Subsequent centrifugation of the suspension aids in isolating adipocytes. Maintaining laminar flow and optimal temperatures when sorting has led to greater viability and precision. However, accumulation of lipid and protein content can adhere to the sheath tubing, thereby clogging the instrumentation (42). High-binding affinity of protein to antibodies bound by fluorescent probes used in FACS has made the identification of MAT and the cells that cohabitate the marrow increasingly specific, though these measurements provide little information on adipocyte location within the marrow microenvironment.

To improve our understanding of MAT, novel imaging techniques have recently been developed as a means to visualize and quantify MAT, *in situ*. Although proton magnetic resonance spectroscopy (1H-MRS) has been used with success to quantify vertebral MAT in humans (43), it is more difficult to employ in laboratory animals (44). Magnetic resonance imaging (MRI) provides MAT assessment in the vertebral skeleton (45) in conjunction with μCT-based marrow density measurements (46). A volumetric method to identify, quantify, and localize

MAT in rodent bone has been recently developed, requiring osmium staining of bones and μCT imaging (47), followed by image analysis of osmium-bound lipid volume (in cubic millimeter) relative to bone volume (see **Figure 1**) (13, 48). Briefly, femurs stripped of connective tissue are decalcified, immersed in osmium tetroxide, and placed in potassium dichromate (49). Bones are scanned using μCT imaging (resolution 10 μm × 10 μm × 10 μm). Image processing consists of rigid image coalignment (**Figures 1B,D**, Slicer) (50), regional masking, allowing consistent regional measurements and superimposed visualizations. Additional bone masks are established in a semi-automatic contouring of the femur. As osmium is significantly more dense than bone [Hounsfield units (HU) ~ 700–2000], HU thresholds are set to capture low osmium from 2000 to 3000 HU, mid osmium from 3000 to 4000 HU (**Figures 1E,F**, green), and high osmium from 4000 to 5000 HU (**Figures 1E,F**, blue), and quantified accordingly (cubic millimeter). The lowest threshold is set above dense cortical bone (2000 HU) (51), and, thus, the contribution of potentially mislabeled cortical bone to the osmium volume is negligible (51, 52). Following quantification, the femur is subdivided into anatomical regions wherein regional osmium volume is normalized to bone volume. Aligned bone images are then averaged across all images as a reference for visualization. Average images are also computed for each group to obtain color-coded visualizations of the osmium densities to allow additional visual comparison of MAT between groups (**Figure 2**). This technique provides reproducible quantification and visualization of MAT, enabling the ability to quantify changes in MAT with diet, exercise, and agents that constrain precursor lineage allocation.

EXERCISE REGULATION OF MARROW ADIPOSE TISSUE IN THE SETTING OF HIGH-FAT FEEDING

Marrow adipose tissue volume has recently been demonstrated to increase during short-term, high-fat feeding in rodents relative to the total bone volume (13), rising more rapidly than calorie induction of visceral fat depot size (53). A positive association between obesity and MAT was noted in rodents (15) and humans (43). In fact, obese individuals generally present with higher bone density (54–62) and are unlikely to experience classical osteoporotic fragility fractures (63). Because MAT has been associated with states of low bone density and increased fracture risk (6, 8, 64), the impact of fat in the marrow likely varies depending on its etiology. As obesity associates with increased bone density and lower fracture, MAT in obesity could represent a distinct fat depot that supports skeletal anabolism.

The *Nurse's Health Study* showed that exercise affords a morbidity and mortality benefit that is independent of weight loss or calorie expenditure (65). One well-known effect of exercise is to improve bone strength, limiting the impact of postmenopausal osteoporosis (66). Exploring the salutary effects of exercise on bone and MAT in the setting of HFD, small animal models have been employed to address the degree of responsivity under said conditions. In one such experiment, 6 weeks of daily voluntary running exercise suppresses MAT accumulation in mice fed both a regular and HFD (13), in contrast to their non-exercised counterparts. While HFD does not perturb trabecular bone parameters as compared to control, significant gains in trabecular bone

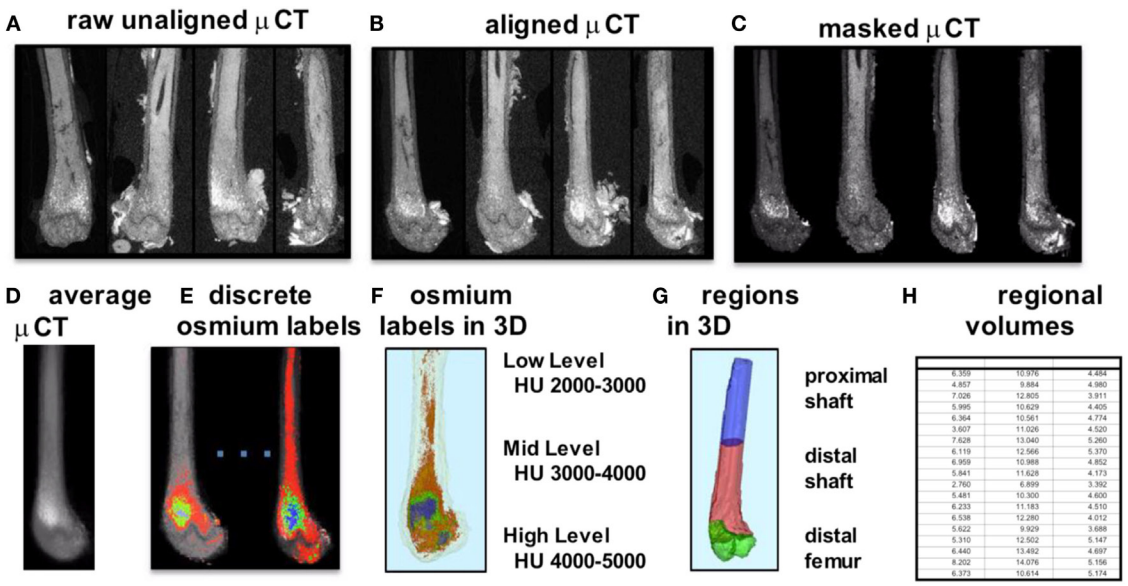

FIGURE 1 | Overview of method for visualization and quantification of marrow adipose tissue (MAT). Osmium-stained femorae are visualized *via* μCT. Femorae **(A)** are rigidly aligned **(B)**. Bone masks **(C)** are averaged **(D)**. Osmium within the bone mask is quantified as volumetric (cubic millimeter) measurements of low (red), mid (green), and high (blue) osmium-containing regions in the femur and **(E)** overlaid on μCT images for viewing. 3D rendering of osmium regions **(F)** with same coloring as **(E)**, colors slightly offset due to transparent bone mask. In **(G)**, the femur is subdivided into three anatomical regions of interest. **(H)** is a pictorial representation of a data spreadsheet containing regional osmium measurements as osmium volume normalized to bone volume (in %).

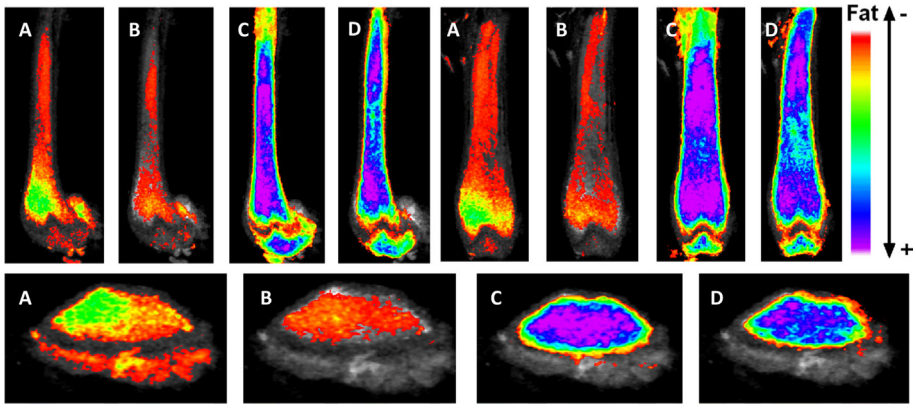

FIGURE 2 | Exercise suppresses marrow adipose tissue accumulation, despite PPARγ agonist treatment. Visualization of osmium (lipid-binder) stain by μCT in sagittal (top left), coronal (top right), and axial (bottom) planes in the femur of C57BL/6 mice. Visualization is performed by superimposing and averaging the images of each femur ($n = 5$ per group) and colored labeling of osmium according to Hounsfield unit (HU) density. The four experimentals are as follows: control **(A)**, rosiglitazone **(B)**, control-exercise **(C)**, and rosiglitazone-exercise **(D)**.

volume and trabecular thickness are noted in tibiae of exercised animals. Cortical bone parameters are unaltered by HFD and exercise in this short-term study. Thus, the trabecular compartment might be more receptive to both metabolic disarray and to mechanical signals from exercise than cortical bone, especially when challenged with elevated MAT *via* HFD.

EXERCISE REGULATION OF MARROW ADIPOSE TISSUE IN THE SETTING OF ROSIGLITAZONE

It is accepted that elevated MAT due to PPARγ-agonist treatment in mice (48, 49, 67) and humans (68, 69) is due to PPARγ-induction of adipogenesis from marrow MSC. *In vitro*, rosiglitazone (PPARγ-agonist)-treated MSCs resist mechanically stimulated adipogenesis when treated with a dynamic load (70). *In vivo*, it was previously hypothesized that exercise might not overcome pathologically induced MAT in the setting of rosiglitazone; however, interestingly, exercise suppresses MAT even in the face of powerful adipogenic biasing (*via* MSC) in rosiglitazone-treated mice (48). While rosiglitazone significantly elevates cortical porosity in proximal tibiae, bone quantity is unaffected in these young mice. Exercise associates with increased trabecular bone volume fraction and trabecular thickness in control and rosiglitazone-treated mice (48). This further highlights the positive impact of exercise and mechanical signals on healthy bone as well as bone challenged by pharmacologic agents shown to facilitate marrow adiposity as well as cortical porosities.

EXERCISE AND MECHANICAL REGULATION OF BONE QUALITY AND QUANTITY

Exercise and Musculoskeletal Mass

Of the many health benefits attributed to exercise – improved neurological endpoints (71, 72), cardiovascular health (73), reduced inflammation (74–77), and decreased risk for chronic disease development, perhaps, most immediately and visually apparent is its ability to augment musculoskeletal mass (78–81). Exercise is known to encourage anabolic responses in musculoskeletal tissue (i.e., bone, muscle, ligament, and tendon) (82) as a consequence of successive bouts of musculoskeletal-loading. Indeed, skeletal tissue is known to adapt to meet loading demands (83), altering its bone remodeling strategy to sustain maximum loads. Prominent and varied forces are exerted across the appendicular and axial skeleton (84) through exercise: the musculoskeletal construct, thereby, acts as a conduit for transducing muscle contractive perturbations at the bone surface at both low frequencies (e.g., bicep flexion) and high frequencies (type II fast-twitch muscle). At the cellular level, these responses are mediated by a wide spectrum of mechanical stimuli of both high- and low-magnitude stresses, information that is internalized by cells through cytoskeletal and transmembrane-bound integrins linking the extracellular environment with the genetic machinery encased within the nucleus (85–90). Thus, these mechanical factors transcribe osteo-, chondro-, or myogenic (91) growth factors (RunX2) while deterring pathways conducive to adipogenesis (PPARγ) (70, 92–95). We now know that these signals propagate across the Wnt/β–Catenin transduction pathways (96), upregulating expression of genes that drive osteogenic (RunX2) and chondrogenic (SOX9) growth, while also being positioned across other complex signaling pathways involving other signals of interest, such as MAPK, pRB, FGFs, and TGF-β. The ability of mechanical stimuli to regulate musculoskeletal mass is likely multifactorial, occurring through repression of fat generation as well as bone resorptive pathways (97), while at the same time stimulating musculoskeletal anabolism. Additionally, exercise has been shown to improve resistance to fracture, specifically through the separation of exercise into shorter regimens (98).

Skeletal Unloading

The importance of mechanical information on bone adaptation can also be exemplified by observing the response of musculoskeletal tissue and the underlying cellular dynamics in the

absence of mechanical cues (99–101). Whereas exercise delivers large quanta of mechanical information, as a function of disuse (chronic bed rest, microgravity, or reduced physical activity) (102, 103), regulation of musculoskeletal tissue homeostasis is compromised, instead elevating conditions wherein muscle, tendon, and ligament (and fat) undergo catalysis and rapid resorption of bone. Together, these tissue-level responses heighten the occurrence of osteoporotic bone and degree of fracture risk: these outcomes are in direct response to lapses in mechanical input (104–107). Whether chronic skeletal unloading encourages a specific MAT phenotype remains unclear, yet, studies have definitively shown that extended bed rest drives an increased marrow adipogenesis (108). In the absence of mechanical cues, PPARγ and receptor activator of nuclear factor-Kappa-B ligand (RANKL), which promotes osteoclast-mediated bone resorption, are both elevated, indicating an effect that could be stemmed upon reintroduction of mechanical stimuli.

Mechanical Effect on Bone and Fat Precursors

Both *in vitro* and *in vivo* studies have demonstrated that MSCs and early, non-committed progenitors exhibit unquestionable responsivity to mechanical loading (93, 109). Osteocytes (88, 110), osteoblasts (111, 112), and pre-osteoblast MC3T3 cells (113) in the marrow are other known mechanosensitive cells and contribute to the complex transduction of mechanical information driving osteogenic gene expression. While mechanical signals can inhibit osteoclastogenesis and subsequent bone resorption through direct effects on osteocyte and MSC expression of RANKL, it is known that mechanical effects on bone remodeling also involve regulation of MSC differentiation toward osteogenesis (93, 114, 115) facilitated by Wnt/β–Catenin signaling and uncommitted precursors. This is, in part, due to the plasticity of stem cells to differentiate specifically toward one mesenchymal lineage over another as dictated by environmental cues, such as exogenous mechanical stimuli (93), local substrate rigidity (113, 116, 117), and regional cytokine signaling gradients (11, 118). These factors drive MSC and other resident marrow cells toward fulfilling their role in musculoskeletal homeostasis by promoting formation of bone and other critical tissues that support skeletal health in lieu of engaging pathways conducive to adipogenesis. Exercise not only encourages MSC proliferation but downstream lineages are also influenced as well: lipid droplets and adipocyte cell diameters are reduced while driving osteogenic potential through upregulated alkaline phosphatase activity (119). *In vivo* studies show decreased adipocytes and increased pre-osteoblasts in the marrow of running rats (38) and climbing mice (120).

Rodent studies highlight increased bone formation rates in response to exercise and mechanical signals *via* dynamic histomorphometry (104), including running exercise (121–124). These responses persist through incorporation of non-exercise mechanical loading interventions [low-magnitude mechanical signals (LMMS)], which have been demonstrated to increase bone formation rates in loaded tibiae of mice (125, 126). In consideration of the phenotypic differences in lineage subtypes across niches, the bone marrow-derived MSC has recently been suggested to have unique, focal-specific properties (127). Therefore, it is important to weigh the contribution of precursor cells and other progenitors in the presence of mature adipocytes or the marrow, when considering the effect mechanical stimuli may have on their interaction with the surrounding milieu.

Low-Magnitude Mechanical Signals Effect on Bone and Marrow Adiposity

While physical activity presents an ideal strategy to introduce exogenous low-frequency, high-magnitude mechanical cues to musculoskeletal tissue, this approach is impractical for those patients with compromised bone microarchitecture (i.e., osteoporosis, osteopenia) (105, 109, 128–130) or muscle instability (131–133), populations that could benefit the most from their effects. Alternatively, mechanical signals delivered to the skeleton in the form of high-frequency, LMMS (fast-twitch muscles controlling balance and posture) can be introduced outside of the context of physical activity (134). For instance, low strain (<100 με) displacements contribute more toward maintaining musculoskeletal health than higher magnitude strains and can be delivered whole-body using platforms to oscillate in the high-frequency domain (20–100 Hz), while maintaining a low-magnitude (i.e., sub-gravitational) acceleration. In doing so, these platforms partially reintroduce the spectral content of muscle contraction (105, 135), thereby exerting a beneficial quotient of exercise without risking fracture to bone resulting from extreme loads prevalent in exercise. Moreover, when separated into multiple administrations, the effects of both exercise and LMMS are amplified (95), encouraging enhancement in the responsiveness of MSC. Importantly, in humans, the non-pharmacologic therapy LMMS prevent bone loss due to Crohn's disease (136), in children recovering from various cancers (137), and in other disabling conditions where bone losses are apparent (138, 139).

EXERCISE AND THE BROWNING OF MARROW ADIPOSE TISSUE

Upon initiation of exercise, there is an increase in uptake and oxidation of lipids in skeletal muscle (140). When exercise intensity increases, fuel selection shifts toward an increase in carbohydrate and decrease in fat utilization. In contrast, endurance training is associated with a shift toward an enhanced lipid utilization (140). BAT, initially observed in hibernating mammals and human infants, dissipates energy in the form of heat through non-shivering thermogenesis (141). Inducible brown fat depots – beige fat – have been discovered within the white adipose tissue of adult humans (142). On exposure to cold or β-adrenergic stimulation, these beige/brite fat cells express high levels of mitochondrial uncoupling protein UCP1 and fat globules become multilocular (143), characteristics of the brown fat phenotype. Irisin, a muscle-derived hormone induced by exercise, also activates UCP1 expression and browning of white adipose tissue (33): coactivator PPAR-γ coactivator-1 α (PGC1-α) stimulates irisin, and transgenic mice overexpressing PGC1-α exhibit increased energy expenditure despite no changes in food intake or activity (33). Overall, there is evidence that fat depots

can alter phenotype to serve functional demands. Since exercise browns white adipose depots (33), it is conceivable that exercise might result in analogous browning of MAT. Indeed, running exercise increased UCP1 in bone mRNA (48). UCP1 is localized in the mitochondrial inner membrane of mammalian BAT and is, therefore, a specific marker for BAT (144). This increase in UCP1 with exercise may indicate a brown phenotype within MAT adipocytes; however, this requires further confirmation. Interestingly, exercise-induced increases in UCP1 expression may correlate with increases in irisin (33), although irisin's role in exercise physiology remains unclear (145). Finally, recent work suggests that irisin may have direct effects on bone in addition to its known effect on adipocytes, and thus irisin's role in skeletal health remains an area of active investigation (146–148).

CONCLUSION

Marrow adipose tissue, housed within bone and interspersed with hematopoietic elements, remains a poorly understood fat depot, likely due to its anatomic location, rendering it inaccessible and thus challenging to quantify. Clinicians are particularly interested in the physiology of this fat depot due to its association with low bone density states and pharmacologic agents that increase fracture risk. As more robust volumetric imaging and quantification tools emerge [e.g., osmium-μCT Ref. (13, 48)], precise determinations can be made regarding MAT physiology and relationship to bone health. Interestingly, these methodologies have pointed to an increase in MAT in the setting of high-fat feeding (13), without an impact on bone quantity. Additionally, we are now able to visualize the effect of pharmacologic PPARγ activation with rosiglitazone on bone and to appreciate the significant encroachment of marrow fat (**Figure 2**) as well as to quantify these dramatic findings. Interestingly, both regimented exercise and LMMS serve to counter the effects of obesity and potent pharmacologic agents on bone remodeling. Further, in evaluating the response of MAT to mechanical stimuli, we highlight a positive effect toward normalizing bone parameters and, in doing so, constraining expansion of MAT across the marrow. It is possible that exercise serves to "brown" MAT as indicated in Ref. (48); however, further work is needed to establish the metabolic purpose of MAT in the setting of exercise. It remains unclear whether exercise-induced bone formation biases MSCs away from adipogenesis in order to recruit osteoblasts or whether alternative mechanisms are involved. *In vitro*, MSCs are highly responsive to mechanical signals during differentiation; indeed, mechanical loading slows adipogenesis (38, 92, 93, 149–151). Conversely, MSCs under microgravity conditions decrease osteogenic differentiation in favor of fat formation, an event accompanied by elevated nuclear expression of PPARγ (152). Thus, in the setting of mechanical input or exercise, bone formation is increased and marrow fat is suppressed, highlighting a likely mechanistic relationship between MAT and bone in the setting of mechanical stimulation. Other pathways are likely involved in the exercise regulation of MAT: lipogenesis, lipid uptake, skeletal anabolism, regulation of hematopoiesis in the bone marrow, and regulation of adipokines and cytokines. The elucidation of these pathways and their role in MAT/bone regulation in the setting of exercise remains an area of active investigation.

AUTHOR CONTRIBUTIONS

MS and GP wrote this review together as a team. Each author contributed approximately 50% to the writing of this review.

FUNDING

Funding for this work was provided by NIAMS: AR062097 and NIDDK: P30DK056350.

REFERENCES

1. Verma S, Rajaratnam JH, Denton J, Hoyland JA, Byers RJ. Adipocytic proportion of bone marrow is inversely related to bone formation in osteoporosis. *J Clin Pathol* (2002) 55(9):693–8. doi:10.1136/jcp.55.9.693
2. Yeung DK, Griffith JF, Antonio GE, Lee FK, Woo J, Leung PC. Osteoporosis is associated with increased marrow fat content and decreased marrow fat unsaturation: a proton MR spectroscopy study. *J Magn Reson Imaging* (2005) 22(2):279–85. doi:10.1002/jmri.20367
3. Meunier P, Aaron J, Edouard C, Vignon G. Osteoporosis and the replacement of cell populations of the marrow by adipose tissue. A quantitative study of 84 iliac bone biopsies. *Clin Orthop Relat Res* (1971) 80:147–54. doi:10.1097/00003086-197110000-00021
4. Kricun ME. Red-yellow marrow conversion: its effect on the location of some solitary bone lesions. *Skeletal Radiol* (1985) 14(1):10–9. doi:10.1007/BF00361188
5. Duque G. As a matter of fat: new perspectives on the understanding of age-related bone loss. *IBMS Bonekey* (2007) 4(4):129–40. doi:10.1138/20070257
6. Cohen A, Dempster DW, Stein EM, Nickolas TL, Zhou H, McMahon DJ, et al. Increased marrow adiposity in premenopausal women with idiopathic osteoporosis. *J Clin Endocrinol Metab* (2012) 97(8):2782–91. doi:10.1210/jc.2012-1477
7. Fazeli PK, Horowitz MC, MacDougald OA, Scheller EL, Rodeheffer MS, Rosen CJ, et al. Marrow fat and bone – new perspectives. *J Clin Endocrinol Metab* (2013) 98(3):935–45. doi:10.1210/jc.2012-3634
8. Wronski TJ, Morey ER. Skeletal abnormalities in rats induced by simulated weightlessness. *Metab Bone Dis Relat Res* (1982) 4(1):69–75. doi:10.1016/0221-8747(82)90011-X
9. Ahdjoudj S, Lasmoles F, Holy X, Zerath E, Marie PJ. Transforming growth factor beta2 inhibits adipocyte differentiation induced by skeletal unloading in rat bone marrow stroma. *J Bone Miner Res* (2002) 17(4):668–77. doi:10.1359/jbmr.2002.17.4.668
10. Rubin MR, Manavalan JS, Agarwal S, McMahon DJ, Nino A, Fitzpatrick LA, et al. Effects of rosiglitazone vs metformin on circulating osteoclast and osteogenic precursor cells in postmenopausal women with type 2 diabetes mellitus. *J Clin Endocrinol Metab* (2014) 99(10):E1933–42. doi:10.1210/jc.2013-3666
11. Pittenger MF, Mackay AM, Beck SC, Jaiswal RK, Douglas R, Mosca JD, et al. Multilineage potential of adult human mesenchymal stem cells. *Science* (1999) 284(5411):143–7. doi:10.1126/science.284.5411.143
12. Muruganandan S, Roman AA, Sinal CJ. Adipocyte differentiation of bone marrow-derived mesenchymal stem cells: cross talk with the osteoblastogenic program. *Cell Mol Life Sci* (2009) 66(2):236–53. doi:10.1007/s00018-008-8429-z
13. Styner M, Thompson WR, Galior K, Uzer G, Wu X, Kadari S, et al. Bone marrow fat accumulation accelerated by high fat diet is suppressed by exercise. *Bone* (2014) 64C:39–46. doi:10.1016/j.bone.2014.03.044
14. Doucette CR, Horowitz MC, Berry R, MacDougald OA, Anunciado-Koza R, Koza RA, et al. A high fat diet increases bone marrow adipose tissue (MAT) but does not alter trabecular or cortical bone mass in C57BL/6J mice. *J Cell Physiol* (2015) 230(9):2032–7. doi:10.1002/jcp.24954

15. Lecka-Czernik B, Stechschulte LA, Czernik PJ, Dowling AR. High bone mass in adult mice with diet-induced obesity results from a combination of initial increase in bone mass followed by attenuation in bone formation; implications for high bone mass and decreased bone quality in obesity. *Mol Cell Endocrinol* (2015) 410:35–41. doi:10.1016/j.mce.2015.01.001
16. Worthley DL, Churchill M, Compton JT, Tailor Y, Rao M, Si Y, et al. Gremlin 1 identifies a skeletal stem cell with bone, cartilage, and reticular stromal potential. *Cell* (2015) 160(1–2):269–84. doi:10.1016/j.cell.2014.11.042
17. Adler BJ, Kaushansky K, Rubin CT. Obesity-driven disruption of haematopoiesis and the bone marrow niche. *Nat Rev Endocrinol* (2014) 10(12):737–48. doi:10.1038/nrendo.2014.169
18. Huovinen V, Viljakainen H, Hakkarainen A, Saukkonen T, Toiviainen-Salo S, Lundbom N, et al. Bone marrow fat unsaturation in young adults is not affected by present or childhood obesity, but increases with age: a pilot study. *Metabolism* (2015) 64(11):1574–81. doi:10.1016/j.metabol.2015.08.014
19. Bellisari A. Evolutionary origins of obesity. *Obes Rev* (2008) 9(2):165–80. doi:10.1111/j.1467-789X.2007.00392.x
20. Krings A, Rahman S, Huang S, Lu Y, Czernik PJ, Lecka-Czernik B. Bone marrow fat has brown adipose tissue characteristics, which are attenuated with aging and diabetes. *Bone* (2012) 50(2):546–52. doi:10.1016/j.bone.2011.06.016
21. Ye R, Scherer PE. Adiponectin, driver or passenger on the road to insulin sensitivity? *Mol Metab* (2013) 2(3):133–41. doi:10.1016/j.molmet.2013.04.001
22. Tilg H, Moschen AR. Adipocytokines: mediators linking adipose tissue, inflammation and immunity. *Nat Rev Immunol* (2006) 6(10):772–83. doi:10.1038/nri1937
23. Wronska A, Kmiec Z. Structural and biochemical characteristics of various white adipose tissue depots. *Acta Physiol (Oxf)* (2012) 205(2):194–208. doi:10.1111/j.1748-1716.2012.02409.x
24. Masuzaki H, Paterson J, Shinyama H, Morton NM, Mullins JJ, Seckl JR, et al. A transgenic model of visceral obesity and the metabolic syndrome. *Science* (2001) 294(5549):2166–70. doi:10.1126/science.1066285
25. Bredella MA, Lin E, Gerweck AV, Landa MG, Thomas BJ, Torriani M, et al. Determinants of bone microarchitecture and mechanical properties in obese men. *J Clin Endocrinol Metab* (2012) 97(11):4115–22. doi:10.1210/jc.2012-2246
26. Cohen A, Dempster DW, Recker RR, Lappe JM, Zhou H, Zwahlen A, et al. Abdominal fat is associated with lower bone formation and inferior bone quality in healthy premenopausal women: a transiliac bone biopsy study. *J Clin Endocrinol Metab* (2013) 98(6):2562–72. doi:10.1210/jc.2013-1047
27. Wu J, Cohen P, Spiegelman BM. Adaptive thermogenesis in adipocytes: is beige the new brown? *Genes Dev* (2013) 27(3):234–50. doi:10.1101/gad.211649.112
28. Al-Nbaheen M, Vishnubalaji R, Ali D, Bouslimi A, Al-Jassir F, Megges M, et al. Human stromal (mesenchymal) stem cells from bone marrow, adipose tissue and skin exhibit differences in molecular phenotype and differentiation potential. *Stem Cell Rev* (2013) 9(1):32–43. doi:10.1007/s12015-012-9365-8
29. Gimble JM, Zvonic S, Floyd ZE, Kassem M, Nuttall ME. Playing with bone and fat. *J Cell Biochem* (2006) 98(2):251–66. doi:10.1002/jcb.20777
30. Cawthorn WP, Scheller EL, Learman BS, Parlee SD, Simon BR, Mori H, et al. Bone marrow adipose tissue is an endocrine organ that contributes to increased circulating adiponectin during caloric restriction. *Cell Metab* (2014) 20(2):368–75. doi:10.1016/j.cmet.2014.06.003
31. McGee-Lawrence ME, Carpio LR, Schulze RJ, Pierce JL, McNiven MA, Farr JN, et al. Hdac3 deficiency increases marrow adiposity and induces lipid storage and glucocorticoid metabolism in osteochondroprogenitor cells. *J Bone Miner Res* (2016) 31(1):116–28. doi:10.1002/jbmr.2602
32. Gollisch KS, Brandauer J, Jessen N, Toyoda T, Nayer A, Hirshman MF, et al. Effects of exercise training on subcutaneous and visceral adipose tissue in normal- and high-fat diet-fed rats. *Am J Physiol Endocrinol Metab* (2009) 297(2):E495–504. doi:10.1152/ajpendo.90424.2008
33. Bostrom P, Wu J, Jedrychowski MP, Korde A, Ye L, Lo JC, et al. A PGC1-alpha-dependent myokine that drives brown-fat-like development of white fat and thermogenesis. *Nature* (2012) 481(7382):463–8. doi:10.1038/nature10777
34. Stanford KI, Middelbeek RJ, Goodyear LJ. Exercise effects on white adipose tissue: beiging and metabolic adaptations. *Diabetes* (2015) 64(7):2361–8. doi:10.2337/db15-0227
35. Bielohuby M, Matsuura M, Herbach N, Kienzle E, Slawik M, Hoeflich A, et al. Short-term exposure to low-carbohydrate, high-fat diets induces low bone mineral density and reduces bone formation in rats. *J Bone Miner Res* (2010) 25(2):275–84. doi:10.1359/jbmr.090813
36. Spatz JM, Ellman R, Cloutier AM, Louis L, van Vliet M, Suva LJ, et al. Sclerostin antibody inhibits skeletal deterioration due to reduced mechanical loading. *J Bone Miner Res* (2013) 28(4):865–74. doi:10.1002/jbmr.1807
37. Rosen CJ, Ackert-Bicknell CL, Adamo ML, Shultz KL, Rubin J, Donahue LR, et al. Congenic mice with low serum IGF-I have increased body fat, reduced bone mineral density, and an altered osteoblast differentiation program. *Bone* (2004) 35(5):1046–58. doi:10.1016/j.bone.2004.07.008
38. David V, Martin A, Lafage-Proust MH, Malaval L, Peyroche S, Jones DB, et al. Mechanical loading down-regulates peroxisome proliferator-activated receptor gamma in bone marrow stromal cells and favors osteoblastogenesis at the expense of adipogenesis. *Endocrinology* (2007) 148(5):2553–62. doi:10.1210/en.2006-1704
39. Naveiras O, Nardi V, Wenzel PL, Hauschka PV, Fahey F, Daley GQ. Bone-marrow adipocytes as negative regulators of the haematopoietic microenvironment. *Nature* (2009) 460(7252):259–63. doi:10.1038/nature08099
40. Majka SM, Miller HL, Sullivan T, Erickson PF, Kong R, Weiser-Evans M, et al. Adipose lineage specification of bone marrow-derived myeloid cells. *Adipocyte* (2012) 1(4):215–29. doi:10.4161/adip.21496
41. Majka SM, Miller HL, Helm KM, Acosta AS, Childs CR, Kong R, et al. Analysis and isolation of adipocytes by flow cytometry. *Methods Enzymol* (2014) 537:281–96. doi:10.1016/B978-0-12-411619-1.00015-X
42. Bernstein RL, Hyun WC, Davis JH, Fulwyler MJ, Pershadsingh HA. Flow cytometric analysis of mature adipocytes. *Cytometry* (1989) 10(4):469–74. doi:10.1002/cyto.990100416
43. Bredella MA, Torriani M, Ghomi RH, Thomas BJ, Brick DJ, Gerweck AV, et al. Vertebral bone marrow fat is positively associated with visceral fat and inversely associated with IGF-1 in obese women. *Obesity (Silver Spring)* (2011) 19(1):49–53. doi:10.1038/oby.2010.106
44. de Paula FJ, Dick-de-Paula I, Bornstein S, Rostama B, Le P, Lotinun S, et al. VDR haploinsufficiency impacts body composition and skeletal acquisition in a gender-specific manner. *Calcif Tissue Int* (2011) 89(3):179–91. doi:10.1007/s00223-011-9505-1
45. Fazeli PK, Bredella MA, Freedman L, Thomas BJ, Breggia A, Meenaghan E, et al. Marrow fat and preadipocyte factor-1 levels decrease with recovery in women with anorexia nervosa. *J Bone Miner Res* (2012) 27(9):1864–71. doi:10.1002/jbmr.1640
46. Rantalainen T, Nikander R, Heinonen A, Cervinka T, Sievanen H, Daly RM. Differential effects of exercise on tibial shaft marrow density in young female athletes. *J Clin Endocrinol Metab* (2013) 98(5):2037–44. doi:10.1210/jc.2012-3748
47. Scheller EL, Troiano N, Vanhoutan JN, Bouxsein MA, Fretz JA, Xi Y, et al. Use of osmium tetroxide staining with microcomputerized tomography to visualize and quantify bone marrow adipose tissue in vivo. *Methods Enzymol* (2014) 537:123–39. doi:10.1016/B978-0-12-411619-1.00007-0
48. Styner M, Pagnotti GM, Galior K, Wu X, Thompson WR, Uzer G, et al. Exercise regulation of marrow fat in the setting of PPARgamma agonist treatment in female C57BL/6 mice. *Endocrinology* (2015) 156(8):2753–61. doi:10.1210/en.2015-1213
49. Liu L, Aronson J, Huang S, Lu Y, Czernik P, Rahman S, et al. Rosiglitazone inhibits bone regeneration and causes significant accumulation of fat at sites of new bone formation. *Calcif Tissue Int* (2012) 91(2):139–48. doi:10.1007/s00223-012-9623-4
50. Fedorov A, Beichel R, Kalpathy-Cramer J, Finet J, Fillion-Robin JC, Pujol S, et al. 3D slicer as an image computing platform for the quantitative imaging network. *Magn Reson Imaging* (2012) 30(9):1323–41. doi:10.1016/j.mri.2012.05.001
51. Schreiber JJ, Anderson PA, Rosas HG, Buchholz AL, Au AG. Hounsfield units for assessing bone mineral density and strength: a tool for osteoporosis management. *J Bone Joint Surg Am* (2011) 93(11):1057–63. doi:10.2106/JBJS.J.00160
52. Aamodt A, Kvistad KA, Andersen E, Lund-Larsen J, Eine J, Benum P, et al. Determination of Hounsfield value for CT-based design of custom femoral stems. *J Bone Joint Surg Br* (1999) 81(1):143–7. doi:10.1302/0301-620X.81B1.8880

53. Reid IR, Ames R, Evans MC, Sharpe S, Gamble G, France JT, et al. Determinants of total body and regional bone mineral density in normal postmenopausal women – a key role for fat mass. *J Clin Endocrinol Metab* (1992) 75(1):45–51. doi:10.1210/jcem.75.1.1619030
54. Dawson-Hughes B, Shipp C, Sadowski L, Dallal G. Bone density of the radius, spine, and hip in relation to percent of ideal body weight in postmenopausal women. *Calcif Tissue Int* (1987) 40(6):310–4. doi:10.1007/BF02556691
55. Ribot C, Tremollieres F, Pouilles JM, Bonneu M, Germain F, Louvet JP. Obesity and postmenopausal bone loss: the influence of obesity on vertebral density and bone turnover in postmenopausal women. *Bone* (1987) 8(6):327–31. doi:10.1016/8756-3282(87)90062-7
56. Liel Y, Edwards J, Shary J, Spicer KM, Gordon L, Bell NH. The effects of race and body habitus on bone mineral density of the radius, hip, and spine in premenopausal women. *J Clin Endocrinol Metab* (1988) 66(6):1247–50. doi:10.1210/jcem-66-6-1247
57. Kin K, Kushida K, Yamazaki K, Okamoto S, Inoue T. Bone mineral density of the spine in normal Japanese subjects using dual-energy X-ray absorptiometry: effect of obesity and menopausal status. *Calcif Tissue Int* (1991) 49(2):101–6. doi:10.1007/BF02565129
58. Harris S, Dallal GE, Dawson-Hughes B. Influence of body weight on rates of change in bone density of the spine, hip, and radius in postmenopausal women. *Calcif Tissue Int* (1992) 50(1):19–23. doi:10.1007/BF00297292
59. Tremollieres FA, Pouilles JM, Ribot C. Vertebral postmenopausal bone loss is reduced in overweight women: a longitudinal study in 155 early postmenopausal women. *J Clin Endocrinol Metab* (1993) 77(3):683–6. doi:10.1210/jcem.77.3.8370689
60. May H, Murphy S, Khaw KT. Age-associated bone loss in men and women and its relationship to weight. *Age Ageing* (1994) 23(3):235–40. doi:10.1093/ageing/23.3.235
61. Khosla S, Atkinson EJ, Riggs BL, Melton LJ III. Relationship between body composition and bone mass in women. *J Bone Miner Res* (1996) 11(6):857–63. doi:10.1002/jbmr.5650110618
62. Evans AL, Paggiosi MA, Eastell R, Walsh JS. Bone density, microstructure and strength in obese and normal weight men and women in younger and older adulthood. *J Bone Miner Res* (2015) 30(5):920–8. doi:10.1002/jbmr.2407
63. De Laet C, Kanis JA, Oden A, Johanson H, Johnell O, Delmas P, et al. Body mass index as a predictor of fracture risk: a meta-analysis. *Osteoporos Int* (2005) 16(11):1330–8. doi:10.1007/s00198-005-1863-y
64. Devlin MJ. Why does starvation make bones fat? *Am J Hum Biol* (2011) 23(5):577–85. doi:10.1002/ajhb.21202
65. Hu FB, Willett WC, Li T, Stampfer MJ, Colditz GA, Manson JE. Adiposity as compared with physical activity in predicting mortality among women. *N Engl J Med* (2004) 351(26):2694–703. doi:10.1056/NEJMoa042135
66. Dalsky GP, Stocke KS, Ehsani AA, Slatopolsky E, Lee WC, Birge SJ Jr. Weight-bearing exercise training and lumbar bone mineral content in postmenopausal women. *Ann Intern Med* (1988) 108(6):824–8. doi:10.7326/0003-4819-108-6-824
67. Lecka-Czernik B, Moerman EJ, Grant DF, Lehmann JM, Manolagas SC, Jilka RL. Divergent effects of selective peroxisome proliferator-activated receptor-gamma 2 ligands on adipocyte versus osteoblast differentiation. *Endocrinology* (2002) 143(6):2376–84. doi:10.1210/en.143.6.2376
68. Ackert-Bicknell CL, Shockley KR, Horton LG, Lecka-Czernik B, Churchill GA, Rosen CJ. Strain-specific effects of rosiglitazone on bone mass, body composition, and serum insulin-like growth factor-I. *Endocrinology* (2009) 150(3):1330–40. doi:10.1210/en.2008-0936
69. Grey A, Beckley V, Doyle A, Fenwick S, Horne A, Gamble G, et al. Pioglitazone increases bone marrow fat in type 2 diabetes: results from a randomized controlled trial. *Eur J Endocrinol* (2012) 166(6):1087–91. doi:10.1530/EJE-11-1075
70. Case N, Thomas J, Xie Z, Sen B, Styner M, Rowe D, et al. Mechanical input restrains PPARgamma2 expression and action to preserve mesenchymal stem cell multipotentiality. *Bone* (2013) 52(1):454–64. doi:10.1016/j.bone.2012.08.122
71. Taubert M, Villringer A, Lehmann N. Endurance exercise as an "endogenous" neuro-enhancement strategy to facilitate motor learning. *Front Hum Neurosci* (2015) 9:692. doi:10.3389/fnhum.2015.00692
72. Klein C, Jonas W, Iggena D, Empl L, Rivalan M, Wiedmer P, et al. Exercise prevents high-fat diet-induced impairment of flexible memory expression in the water maze and modulates adult hippocampal neurogenesis in mice. *Neurobiol Learn Mem* (2016) 131:26–35. doi:10.1016/j.nlm.2016.03.002
73. Myers J. Cardiology patient pages. Exercise and cardiovascular health. *Circulation* (2003) 107(1):e2–5. doi:10.1161/01.CIR.0000048890.59383.8D
74. Bjorholt PG, Hoyeraal HM, Munthe E, Pahle J, Kogstad O, Sydnes OA, et al. Physical activity in the treatment of inflammatory rheumatic disorders. *Scand J Soc Med Suppl* (1982) 29:235–9.
75. Woods JA, Davis JM. Exercise, monocyte/macrophage function, and cancer. *Med Sci Sports Exerc* (1994) 26(2):147–56. doi:10.1249/00005768-199402000-00004
76. You T, Arsenis NC, Disanzo BL, Lamonte MJ. Effects of exercise training on chronic inflammation in obesity: current evidence and potential mechanisms. *Sports Med* (2013) 43(4):243–56. doi:10.1007/s40279-013-0023-3
77. Khoo J, Dhamodaran S, Chen DD, Yap SY, Chen RY, Tian HH. Exercise-induced weight loss is more effective than dieting for improving adipokine profile, insulin resistance, and inflammation in obese men. *Int J Sport Nutr Exerc Metab* (2015) 25(6):566–75. doi:10.1123/ijsnem.2015-0025
78. Woo SL, Gomez MA, Amiel D, Ritter MA, Gelberman RH, Akeson WH. The effects of exercise on the biomechanical and biochemical properties of swine digital flexor tendons. *J Biomech Eng* (1981) 103(1):51–6. doi:10.1115/1.3138246
79. Turner CH, Robling AG. Mechanisms by which exercise improves bone strength. *J Bone Miner Metab* (2005) 23(Suppl):16–22. doi:10.1007/BF03026318
80. Wallace IJ, Kwaczala AT, Judex S, Demes B, Carlson KJ. Physical activity engendering loads from diverse directions augments the growing skeleton. *J Musculoskelet Neuronal Interact* (2013) 13(3):283–8.
81. Hinton PS, Nigh P, Thyfault J. Effectiveness of resistance training or jumping-exercise to increase bone mineral density in men with low bone mass: a 12-month randomized, clinical trial. *Bone* (2015) 79:203–12. doi:10.1016/j.bone.2015.06.008
82. Judex S, Gross TS, Zernicke RF. Strain gradients correlate with sites of exercise-induced bone-forming surfaces in the adult skeleton. *J Bone Miner Res* (1997) 12(10):1737–45. doi:10.1359/jbmr.1997.12.10.1737
83. Frost HM. Bone "mass" and the "mechanostat": a proposal. *Anat Rec* (1987) 219(1):1–9. doi:10.1002/ar.1092190104
84. Rubin C, Lanyon LE. Regulation of bone mass by mechanical strain magnitude. *Calcif Tissue Int* (1985) 37:411–7. doi:10.1007/BF02553711
85. Tjandrawinata RR, Vincent VL, Hughes-Fulford M. Vibrational force alters mRNA expression in osteoblasts. *FASEB J* (1997) 11(6):493–7.
86. Ko KS, McCulloch CA. Intercellular mechanotransduction: cellular circuits that coordinate tissue responses to mechanical loading. *Biochem Biophys Res Commun* (2001) 285(5):1077–83. doi:10.1006/bbrc.2001.5177
87. Rubin J, Rubin C, Jacobs CR. Molecular pathways mediating mechanical signaling in bone. *Gene* (2006) 367:1–16. doi:10.1016/j.gene.2005.10.028
88. Thompson WR, Uzer G, Brobst K, Xie Z, Sen B, Yen S, et al. Osteocyte specific responses to soluble and mechanical stimuli in a stem cell derived culture model. *Sci Rep* (2015) 5:11049. doi:10.1038/srep11049
89. Uzer G, Thompson WR, Sen B, Xie Z, Yen SS, Miller S, et al. Cell mechanosensitivity to extremely low magnitude signals is enabled by a LINCed nucleus. *Stem Cells* (2015) 33(6):2063–76. doi:10.1002/stem.2004
90. Uzer G, Fuchs RK, Rubin J, Thompson WR. Concise review: plasma and nuclear membranes convey mechanical information to regulate mesenchymal stem cell lineage. *Stem Cells* (2016) 34(6):1455–63. doi:10.1002/stem.2342
91. Murfee WL, Hammett LA, Evans C, Xie L, Squire M, Rubin C, et al. High-frequency, low-magnitude vibrations suppress the number of blood vessels per muscle fiber in mouse soleus muscle. *J Appl Physiol (1985)* (2005) 98(6):2376–80. doi:10.1152/japplphysiol.01135.2004
92. Sen B, Xie Z, Case N, Ma M, Rubin C, Rubin J. Mechanical strain inhibits adipogenesis in mesenchymal stem cells by stimulating a durable beta-catenin signal. *Endocrinology* (2008) 149(12):6065–75. doi:10.1210/en.2008-0687
93. Luu YK, Capilla E, Rosen CJ, Gilsanz V, Pessin JE, Judex S, et al. Mechanical stimulation of mesenchymal stem cell proliferation and differentiation promotes osteogenesis while preventing dietary-induced obesity. *J Bone Miner Res* (2009) 24(1):50–61. doi:10.1359/jbmr.080817
94. Styner M, Sen B, Xie Z, Case N, Rubin J. Indomethacin promotes adipogenesis of mesenchymal stem cells through a cyclooxygenase independent mechanism. *J Cell Biochem* (2010) 111(4):1042–50. doi:10.1002/jcb.22793

95. Sen B, Xie Z, Case N, Styner M, Rubin CT, Rubin J. Mechanical signal influence on mesenchymal stem cell fate is enhanced by incorporation of refractory periods into the loading regimen. *J Biomech* (2011) 44(4):593–9. doi:10.1016/j.jbiomech.2010.11.022
96. Case N, Rubin J. Beta-catenin – a supporting role in the skeleton. *J Cell Biochem* (2010) 110(3):545–53. doi:10.1002/jcb.22574
97. Wallace BA, Cumming RG. Systematic review of randomized trials of the effect of exercise on bone mass in pre- and postmenopausal women. *Calcif Tissue Int* (2000) 67(1):10–8. doi:10.1007/s00223001089
98. Warden SJ, Hurst JA, Sanders MS, Turner CH, Burr DB, Li J. Bone adaptation to a mechanical loading program significantly increases skeletal fatigue resistance. *J Bone Miner Res* (2005) 20(5):809–16. doi:10.1359/JBMR.041222
99. Ozcivici E, Luu YK, Adler B, Qin YX, Rubin J, Judex S, et al. Mechanical signals as anabolic agents in bone. *Nat Rev Rheumatol* (2010) 6(1):50–9. doi:10.1038/nrrheum.2009.239
100. Gupta S, Vijayaraghavan S, Uzer G, Judex S. Multiple exposures to unloading decrease bone's responsivity but compound skeletal losses in C57BL/6 mice. *Am J Physiol Regul Integr Comp Physiol* (2012) 303(2):R159–67. doi:10.1152/ajpregu.00499.2011
101. Cabahug-Zuckerman P, Frikha-Benayed D, Majeska RJ, Tuthill A, Yakar S, Judex S, et al. Osteocyte apoptosis caused by hindlimb unloading is required to trigger osteocyte RANKL production and subsequent resorption of cortical and trabecular bone in mice femurs. *J Bone Miner Res* (2016) 31(7):1356–65. doi:10.1002/jbmr.2807
102. Globus RK, Bikle DD, Morey-Holton E. The temporal response of bone to unloading. *Endocrinology* (1986) 118(2):733–42. doi:10.1210/endo-118-2-733
103. Bikle DD, Sakata T, Halloran BP. The impact of skeletal unloading on bone formation. *Gravit Space Biol Bull* (2003) 16(2):45–54.
104. Rubin C, Xu G, Judex S. The anabolic activity of bone tissue, suppressed by disuse, is normalized by brief exposure to extremely low-magnitude mechanical stimuli. *FASEB J* (2001) 15(12):2225–9. doi:10.1096/fj.01-0166com
105. Rubin C, Turner AS, Muller R, Mittra E, McLeod K, Lin W, et al. Quantity and quality of trabecular bone in the femur are enhanced by a strongly anabolic, noninvasive mechanical intervention. *J Bone Miner Res* (2002) 17(2):349–57. doi:10.1359/jbmr.2002.17.2.349
106. Judex S, Garman R, Squire M, Busa B, Donahue LR, Rubin C. Genetically linked site-specificity of disuse osteoporosis. *J Bone Miner Res* (2004) 19(4):607–13. doi:10.1359/JBMR.040110
107. Squire M, Brazin A, Keng Y, Judex S. Baseline bone morphometry and cellular activity modulate the degree of bone loss in the appendicular skeleton during disuse. *Bone* (2008) 42(2):341–9. doi:10.1016/j.bone.2007.09.052
108. Trudel G, Payne M, Madler B, Ramachandran N, Lecompte M, Wade C, et al. Bone marrow fat accumulation after 60 days of bed rest persisted 1 year after activities were resumed along with hemopoietic stimulation: the Women International Space Simulation for Exploration study. *J Appl Physiol* (2009) 107(2):540–8. doi:10.1152/japplphysiol.91530.2008
109. Pagnotti GM, Adler BJ, Green DE, Chan ME, Frechette DM, Shroyer KR, et al. Low magnitude mechanical signals mitigate osteopenia without compromising longevity in an aged murine model of spontaneous granulosa cell ovarian cancer. *Bone* (2012) 51(3):570–7. doi:10.1016/j.bone.2012.05.004
110. You L, Temiyasathit S, Lee P, Kim CH, Tummala P, Yao W, et al. Osteocytes as mechanosensors in the inhibition of bone resorption due to mechanical loading. *Bone* (2008) 42(1):172–9. doi:10.1016/j.bone.2007.09.047
111. Tanaka SM, Li J, Duncan RL, Yokota H, Burr DB, Turner CH. Effects of broad frequency vibration on cultured osteoblasts. *J Biomech* (2003) 36(1):73–80. doi:10.1016/S0021-9290(02)00245-2
112. Garman R, Rubin C, Judex S. Small oscillatory accelerations, independent of matrix deformations, increase osteoblast activity and enhance bone morphology. *PLoS One* (2007) 2(7):e653. doi:10.1371/journal.pone.0000653
113. Khatiwala CB, Peyton SR, Metzke M, Putnam AJ. The regulation of osteogenesis by ECM rigidity in MC3T3-E1 cells requires MAPK activation. *J Cell Physiol* (2007) 211(3):661–72. doi:10.1002/jcp.20974
114. Xie L, Jacobson JM, Choi ES, Busa B, Donahue LR, Miller LM, et al. Low-level mechanical vibrations can influence bone resorption and bone formation in the growing skeleton. *Bone* (2006) 39(5):1059–66. doi:10.1016/j.bone.2006.05.012
115. Qiu W, Andersen TE, Bollerslev J, Mandrup S, Abdallah BM, Kassem M. Patients with high bone mass phenotype exhibit enhanced osteoblast differentiation and inhibition of adipogenesis of human mesenchymal stem cells. *J Bone Miner Res* (2007) 22(11):1720–31. doi:10.1359/jbmr.070721
116. Altman GH, Horan RL, Martin I, Farhadi J, Stark PR, Volloch V, et al. Cell differentiation by mechanical stress. *FASEB J* (2002) 16(2):270–2. doi:10.1096/fj.01-0656fje
117. Subramony SD, Dargis BR, Castillo M, Azeloglu EU, Tracey MS, Su A, et al. The guidance of stem cell differentiation by substrate alignment and mechanical stimulation. *Biomaterials* (2013) 34(8):1942–53. doi:10.1016/j.biomaterials.2012.11.012
118. Porada CD, Zanjani ED, Almeida-Porad G. Adult mesenchymal stem cells: a pluripotent population with multiple applications. *Curr Stem Cell Res Ther* (2006) 1(3):365–9. doi:10.2174/157488806778226821
119. Maredziak M, Smieszek A, Chrzastek K, Basinska K, Marycz K. Physical activity increases the total number of bone-marrow-derived mesenchymal stem cells, enhances their osteogenic potential, and inhibits their adipogenic properties. *Stem Cells Int* (2015) 2015:379093. doi:10.1155/2015/379093
120. Menuki K, Mori T, Sakai A, Sakuma M, Okimoto N, Shimizu Y, et al. Climbing exercise enhances osteoblast differentiation and inhibits adipogenic differentiation with high expression of PTH/PTHrP receptor in bone marrow cells. *Bone* (2008) 43(3):613–20. doi:10.1016/j.bone.2008.04.022
121. Yeh JK, Liu CC, Aloia JF. Effects of exercise and immobilization on bone formation and resorption in young rats. *Am J Physiol* (1993) 264(2 Pt 1):E182–9.
122. Huang TH, Lin SC, Chang FL, Hsieh SS, Liu SH, Yang RS. Effects of different exercise modes on mineralization, structure, and biomechanical properties of growing bone. *J Appl Physiol (1985)* (2003) 95(1):300–7. doi:10.1152/japplphysiol.01076.2002
123. Iwamoto J, Shimamura C, Takeda T, Abe H, Ichimura S, Sato Y, et al. Effects of treadmill exercise on bone mass, bone metabolism, and calciotropic hormones in young growing rats. *J Bone Miner Metab* (2004) 22(1):26–31. doi:10.1007/s00774-003-0443-5
124. Wallace JM, Ron MS, Kohn DH. Short-term exercise in mice increases tibial post-yield mechanical properties while two weeks of latency following exercise increases tissue-level strength. *Calcif Tissue Int* (2009) 84(4):297–304. doi:10.1007/s00223-009-9228-8
125. Judex S, Boyd S, Qin YX, Turner S, Ye K, Muller R, et al. Adaptations of trabecular bone to low magnitude vibrations result in more uniform stress and strain under load. *Ann Biomed Eng* (2003) 31(1):12–20. doi:10.1114/1.1535414
126. Srinivasan S, Agans SC, King KA, Moy NY, Poliachik SL, Gross TS. Enabling bone formation in the aged skeleton via rest-inserted mechanical loading. *Bone* (2003) 33(6):946–55. doi:10.1016/j.bone.2003.07.009
127. Wallace IJ, Pagnotti GM, Rubin-Sigler J, Naeher M, Copes LE, Judex S, et al. Focal enhancement of the skeleton to exercise correlates with responsivity of bone marrow mesenchymal stem cells rather than peak external forces. *J Exp Biol* (2015) 218(Pt 19):3002–9. doi:10.1242/jeb.118729
128. Judex S, Donahue LR, Rubin C. Genetic predisposition to low bone mass is paralleled by an enhanced sensitivity to signals anabolic to the skeleton. *FASEB J* (2002) 16(10):1280–2. doi:10.1096/fj.01-0913fje
129. Rubin C, Recker R, Cullen D, Ryaby J, McCabe J, McLeod K. Prevention of postmenopausal bone loss by a low-magnitude, high-frequency mechanical stimuli: a clinical trial assessing compliance, efficacy, and safety. *J Bone Miner Res* (2004) 19(3):343–51. doi:10.1359/JBMR.0301251
130. Wallace IJ, Rubin CT, Lieberman DE. Osteoporosis. *Evol Med Public Health* (2015) 2015(1):343. doi:10.1093/emph/eov032
131. Huang RP, Rubin CT, McLeod KJ. Changes in postural muscle dynamics as a function of age. *J Gerontol A Biol Sci Med Sci* (1999) 54(8):B352–7. doi:10.1093/gerona/54.8.B352
132. Qin YX, Lam H, Ferreri S, Rubin C. Dynamic skeletal muscle stimulation and its potential in bone adaptation. *J Musculoskelet Neuronal Interact* (2010) 10(1):12–24.
133. Muir J, Judex S, Qin YX, Rubin C. Postural instability caused by extended bed rest is alleviated by brief daily exposure to low magnitude mechanical signals. *Gait Posture* (2011) 33(3):429–35. doi:10.1016/j.gaitpost.2010.12.019
134. Rubin C, Judex S, Hadjiargyrou M. Skeletal adaptation to mechanical stimuli in the absence of formation or resorption of bone. *J Musculoskelet Neuronal Interact* (2002) 2(3):264–7.
135. Rubin C, Turner AS, Bain S, Mallinckrodt C, McLeod K. Anabolism. Low mechanical signals strengthen long bones. *Nature* (2001) 412(6847):603–4. doi:10.1038/35088119

136. Leonard MB, Shults J, Long J, Baldassano RN, Brown JK, Hommel K, et al. Effect of low-magnitude mechanical stimuli on bone density and structure in pediatric Crohn's disease: a randomized placebo-controlled trial. *J Bone Miner Res* (2016) 31(6):1177–88. doi:10.1002/jbmr.2799
137. Mogil RJ, Kaste SC, Ferry RJ Jr, Hudson MM, Mulrooney DA, Howell CR, et al. Effect of low-magnitude, high-frequency mechanical stimulation on BMD among young childhood cancer survivors: a randomized clinical trial. *JAMA Oncol* (2016). doi:10.1001/jamaoncol.2015.6557
138. Ward K, Alsop C, Caulton J, Rubin C, Adams J, Mughal Z. Low magnitude mechanical loading is osteogenic in children with disabling conditions. *J Bone Miner Res* (2004) 19(3):360–9. doi:10.1359/JBMR.040129
139. Gilsanz V, Wren TA, Sanchez M, Dorey F, Judex S, Rubin C. Low-level, high-frequency mechanical signals enhance musculoskeletal development of young women with low BMD. *J Bone Miner Res* (2006) 21(9):1464–74. doi:10.1359/jbmr.060612
140. Kiens B. Skeletal muscle lipid metabolism in exercise and insulin resistance. *Physiol Rev* (2006) 86(1):205–43. doi:10.1152/physrev.00023.2004
141. Cannon B, Nedergaard J. Brown adipose tissue: function and physiological significance. *Physiol Rev* (2004) 84(1):277–359. doi:10.1152/physrev.00015.2003
142. Nedergaard J, Bengtsson T, Cannon B. Unexpected evidence for active brown adipose tissue in adult humans. *Am J Physiol Endocrinol Metab* (2007) 293(2):E444–52. doi:10.1152/ajpendo.00691.2006
143. Wu J, Bostrom P, Sparks LM, Ye L, Choi JH, Giang AH, et al. Beige adipocytes are a distinct type of thermogenic fat cell in mouse and human. *Cell* (2012) 150(2):366–76. doi:10.1016/j.cell.2012.05.016
144. Nicholls DG, Bernson VS, Heaton GM. The identification of the component in the inner membrane of brown adipose tissue mitochondria responsible for regulating energy dissipation. *Experientia Suppl* (1978) 32:89–93. doi:10.1007/978-3-0348-5559-4_9
145. Albrecht E, Norheim F, Thiede B, Holen T, Ohashi T, Schering L, et al. Irisin – a myth rather than an exercise-inducible myokine. *Sci Rep* (2015) 5:8889. doi:10.1038/srep08889
146. Colaianni G, Cuscito C, Mongelli T, Pignataro P, Buccoliero C, Liu P, et al. The myokine irisin increases cortical bone mass. *Proc Natl Acad Sci U S A* (2015) 112(39):12157–62. doi:10.1073/pnas.1516622112
147. Colaianni G, Grano M. Role of Irisin on the bone-muscle functional unit. *Bonekey Rep* (2015) 4:765. doi:10.1038/bonekey.2015.134
148. Yong Qiao X, Nie Y, Xian Ma Y, Chen Y, Cheng R, Yao Yinrg W, et al. Irisin promotes osteoblast proliferation and differentiation via activating the MAP kinase signaling pathways. *Sci Rep* (2016) 6:18732. doi:10.1038/srep18732
149. Sen B, Styner M, Xie Z, Case N, Rubin CT, Rubin J. Mechanical loading regulates NFATc1 and beta-catenin signaling through a GSK3beta control node. *J Biol Chem* (2009) 284(50):34607–17. doi:10.1074/jbc.M109.039453
150. Sen B, Guilluy C, Xie Z, Case N, Styner M, Thomas J, et al. Mechanically induced focal adhesion assembly amplifies anti-adipogenic pathways in mesenchymal stem cells. *Stem Cells* (2011) 29(11):1829–36. doi:10.1002/stem.732
151. Styner M, Meyer MB, Galior K, Case N, Xie Z, Sen B, et al. Mechanical strain downregulates C/EBPbeta in MSC and decreases endoplasmic reticulum stress. *PLoS One* (2012) 7(12):e51613. doi:10.1371/journal.pone.0051613
152. Zayzafoon M, Gathings WE, McDonald JM. Modeled microgravity inhibits osteogenic differentiation of human mesenchymal stem cells and increases adipogenesis. *Endocrinology* (2004) 145(5):2421–32. doi:10.1210/en.2003-1156

Conflict of Interest Statement: The authors declare that the research was conducted in the absence of any commercial or financial relationships that could be construed as a potential conflict of interest.

frontiers in Endocrinology

PERSPECTIVE
published: 16 September 2016
doi: 10.3389/fendo.2016.00125

Increased Bone Marrow Adiposity in a Context of Energy Deficit: The Tip of the Iceberg?

*Olfa Ghali[1,2], Nathalie Al Rassy[1,2], Pierre Hardouin[1,2] and Christophe Chauveau[1,2]**

[1] Laboratoire de Physiopathologie des Maladies Osseuses Inflammatoires, Université de Lille, Boulogne-sur-Mer, France, [2] Laboratoire de Physiopathologie des Maladies Osseuses Inflammatoires, Université du Littoral Côte d'Opale, Boulogne-sur-Mer, France

Elevated bone marrow adiposity (BMA) is defined as an increase in the proportion of the bone marrow (BM) cavity volume occupied by adipocytes. This can be caused by an increase in the size and/or number of adipocytes. BMA increases with age in a bone-site-specific manner. This increase may be linked to certain pathophysiological situations. Osteoporosis or compromised bone quality is frequently associated with high BMA. The involvement of BM adipocytes in bone loss may be due to commitment of mesenchymal stem cells to the adipogenic pathway rather than the osteogenic pathway. However, adipocytes may also act on their microenvironment by secreting factors with harmful effects for the bone health. Here, we review evidence that in a context of energy deficit (such as anorexia nervosa (AN) and restriction rodent models) bone alterations can occur in the absence of an increase in BMA. In severe cases, bone alterations are even associated with gelatinous BM transformation. The relationship between BMA and energy deficit and the potential regulators of this adiposity in this context are also discussed. On the basis of clinical studies and preliminary results on animal model, we propose that competition between differentiation into osteoblasts and differentiation into adipocytes might trigger bone loss at least in moderate-to-severe AN and in some calorie restriction models. Finally, some of the main questions resulting from this hypothesis are discussed.

Keywords: bone marrow adiposity regulation, osteoporosis, gelatinous bone marrow transformation, mesenchymal stem cell differentiation, anorexia nervosa

OPEN ACCESS

Edited by:
William Peter Cawthorn, University of Edinburgh, UK

Reviewed by:
Elaine Dennison, University of Southampton, UK
Jan Josef Stepan, Charles University in Prague, Czech Republic
Maureen Devlin, University of Michigan, USA

****Correspondence:***
Christophe Chauveau
chauveau@univ-littoral.fr

Specialty section:
This article was submitted to Bone Research, a section of the journal Frontiers in Endocrinology

Received: *04 May 2016*
Accepted: *30 August 2016*
Published: *16 September 2016*

Citation:
Ghali O, Al Rassy N, Hardouin P and Chauveau C (2016) Increased Bone Marrow Adiposity in a Context of Energy Deficit: The Tip of the Iceberg? Front. Endocrinol. 7:125. doi: 10.3389/fendo.2016.00125

INTRODUCTION

The bone marrow (BM) is predominantly composed of two fractions, namely the hematopoietic and stromal fractions. Mesenchymal progenitor cells reside in the stromal fraction of the BM and can differentiate primarily into osteoblasts and adipocytes (1).

Bone marrow adiposity (BMA) is defined as the proportion of the BM cavity volume occupied by adipocytes. A rise in the BMA can be caused by an increase in the size and/or number of adipocytes (2). BMA levels differ for males vs. females; they are usually higher in women than in men, and higher in female animal models than in males (3). It is also well known that BMA increases with age in a bone-site-specific manner. At birth, the BM is largely hematopoietic (red marrow) but is gradually converted to fatty (yellow) marrow over the lifespan (4–7). The age-related progression of BMA in the axial skeleton differs from that observed in the appendicular skeleton.

The fat fraction in iliac crest biopsies is relatively low during childhood but increases gradually with age (8). In contrast, BMA in long bones of the limbs starts to rise during the first few years of life, with progressive colonization of the medullar cavity from the diaphysis. This process is complete at the age of 25 years or so (9).

These observations suggest that (i) the presence of adipocytes in the BM is a physiological, age-related phenomenon, and (ii) these adipocytes may have positive effects. In fact, adipocytes can supply energy for the high level of bone remodeling required during puberty (10, 11). Furthermore, BM adipocytes may be involved in thermogenesis and heat dissipation because they display some of the characteristic features of brown adipocytes (12). However, an increase in BMA may be linked to certain pathophysiological situations. In fact, osteoporosis or compromised bone quality related to mechanical unloading (13), aging (14), menopause (15), diabetes (16, 17), obesity (18, 19), or anorexia nervosa (AN) (20) is frequently associated with high BMA [for a review, see the article by Hardouin et al. (21) in this special issue].

Two hypotheses have been proposed to explain the bone alterations induced by BMA increase: (i) the elevated BMA observed in osteoporotic patients is caused by a shift in mesenchymal stem cell commitment from the osteogenic pathway to the adipogenic pathway at the expense of bone formation (22–24) and (ii) BM adipocytes can regulate the BM microenvironment and act negatively on the balance between bone formation and bone resorption (11, 25–27) and hematopoiesis (28–31).

A better understanding of the quantitative and/or qualitative changes in BM adipocytes during osteoporosis might enable the development of novel therapeutic strategies. Of the various pathologic contexts associated with osteoporosis, AN is of particular interest. Although osteoporosis in AN has been extensively described, the present article discusses changes in BMA and the regulation of this process in a context of energy deficit and, then, proposes some perspectives for research in this specific field.

BMA AND ENERGY DEFICIT

Anorexia nervosa is a major public health concern; it is the psychiatric disease with the highest mortality rate. Given that AN often coincides with puberty, this condition markedly interferes with bone mass gain and has a long-term impact on bone quality (32). In particular, studying AN may reveal novel, hitherto unsuspected links between BMA and bone mass. First, secondary osteoporosis in AN is often associated with an increase in BMA that contrasts with a decrease in the adiposity of other fatty tissues (**Table 1**). Second, some studies (but not others) have found that levels of inflammation markers are not elevated in patients with AN (despite amenorrhea) (33, 34). Given that most patients with AN have a low bone mass, inflammation-independent mechanisms may be involved in this bone loss.

However, the fact that a link between energy deficit and increased BMA is not always observed raises questions as to the relevance of BMA in AN. Indeed, several studies of osteoporotic patients with AN did not observe elevated BMA (**Table 1**). In fact, the studies having found an increase in BMA tended to feature patients with a higher body mass index (BMI) than those in studies that did not observe this increase. Moreover, a number of studies that categorized patients into BMI classes highlighted a relationship between the severity of body weight loss and changes in the BMA (40, 43, 44). Interestingly, Abella et al.'s histological study of patient biopsies described a hypoplastic BM in which an increase in both the fat fraction and adipocyte diameter was associated with moderate body weight loss (40). The researchers also observed areas of unaffected or hypoplastic BM and focal gelatinous degeneration in patients with intermediate levels of body weight losses (40). Last, the most severe cases featured a high microadipocyte count in a hyaluronic acid matrix. It is noteworthy that, in one of the patients in Abella et al.'s study, the BM's appearance normalized after the resumption of food intake and the return to an appropriate bodyweight (40). Vande Berg et al. used magnetic resonance imaging to highlight the presence of serous-like BM at different skeletal sites in anorectic patients (44). They distinguished between two groups as a function of the presence (group A) or absence (group B) of a water-like pattern in the marrow spaces. The individual BMI values in the group A were all under 13.5 kg/m^2, whereas six of the eight patients in group B had a BMI above 15 kg/m^2. Abella et al. did not find an intergroup difference in disease duration, which suggests that body weight loss is a key factor in BM alterations (39–41, 46).

This short overview of the relationship between BMA alterations and the severity of the body weight loss highlights the complexity of the processes leading to these alterations and probably, thereafter, to bone loss. Studies of animal models should provide some clues to these processes. In rodent models of food restriction or calorie restriction, only four published studies have focused on BMA (**Table 2**). First, Hamrick et al. studied the effects of a 40% food restriction in 14-week-old male mice (60). The 10-week protocol led to a body weight loss of 30% (relative to control mice) and the total disappearance of BM adipocytes in the distal femur and lumbar vertebra (60) (two adipocyte-poor medullar sites). Despite this lack of adipocytes, the cortical thickness fell in the femur and lumbar vertebra, and the trabecular thickness fell in the femur (60). However, Devlin et al.'s 2010 study of the effects of a 9-week, 30% food restriction in 3-week-old male mice highlighted decreases of 11 and 27% in the bone volume/total volume (BV/TV) ratio and in cortical thickness, respectively (61). Although this protocol induced a relative body weight loss of 40% (compared with control mice), the food-restricted animals were nevertheless 80% heavier at the end of the protocol than at the start. The main impact on bone microarchitecture was observed in the femur, where the BM adipocyte density was 700% higher than in control animals. Third, Baek and Bloomfield fed 6-month-old Sprague-Dawley female rats a calorie-restricted diet for 12 weeks (62). At the end of this period, the calorie-restricted rats displayed body weight losses of 20% (relative to day 0) and 25% (relative to control rats). The volumetric bone mineral density of the proximal tibia was 14% below that of control mice, while the BMA in the proximal femur had doubled. More recently, Cawthorn et al. showed that 6 weeks of a 30% calorie-restricted diet in 9-week-old female mice induced a final increase in tibia BMA of 700% vs. mice able to feed *ad libitum* (27). In our separation-based model of AN (SBA), 8-week-old female mice were housed singly and submitted to time-restricted feeding (in

TABLE 1 | Variations in BMA and the presence of gelatinous BM transformation in patients with AN, as reported in case–control studies and case reports.

	N	Age	BMI	BMA measurement site	Method for measuring BMA	Change in BMA	Presence of GBMT
	Anorexic/ normal	Anorexic/normal	Anorexic/normal				
Bredella et al. (35)	14/12	29.5 ± 7.1/30.8 ± 6.6	17.7 ± 1/22.1 ± 1.7	Femoral diaphysis	(1)H-MRS	↑	ND
Fazeli et al. (36)	7/15	33.1 ± 2.8	18.2 ± 0.6/21.9 ± 0.4	Lumbar vertebra Proximal femoral epiphysis Proximal femoral metaphysis Proximal femoral diaphysis	(1)H-MRS	↑ → → →	ND
Ecklund et al. (37)	30/–	16.1 ± 1.6/16.3 ± 1.6	16.9 ± 1.5/22.3 ± 2.0	Distal femoral metaphysic Proximal tibia metaphysis	MRI and relaxometry	↑ ↑	ND
Bredella et al. (20)	10/10	29.8 ± 7.6/30.8 ± 6.6	17.6 ± 1/21.9 ± 1.7	Lumbar vertebra Proximal femoral epiphysis Proximal femoral metaphysis Proximal femoral diaphysis	(1)H-MRS	↑ → ↑ ↑	ND
Mayo-Smith et al. (38)	15/58	15–33/18–44	ND/ND	Lumbar spine (L1-L4)	Dual energy CT scanning	↑	ND
Geiser et al. (39)	20/19	15–56/21–56	14.5/22	Femoral epiphysis Femoral diaphysis Lumbar spine	(1)H-MRS and relaxometry	↓ → →	ND
Abella et al. (40)	44/–	22.5 ± 5.3/–	ND/–	Iliac crest	Histology	↑ in 35% of cases	In 50% of cases
Boutin et al. (41)	10/–	17–57/–	ND/–	Many different bone sites	MRI	ND	In all cases
Lambert et al. (42)	10/19	17.2 ± 0.7/18.7 ± 0.5	14 ± 0.5/22.3 ± 0.4	Lumbar spine, pelvis, proximal femur	MRI	ND	40% of cases
Vande Berg et al. (43)	19/–	15–35/–	–/–	Proximal to distal lower limb	MRI	ND	79% of cases
Vande Berg et al. (44)	14/–	27 ± 10/–	13.9 ± 2.6/–	Lumbar spine, pelvis, proximal femur	MRI	ND	43% of cases
Mant and Faragher (45)	6/–	16–44	ND	Iliac crest	Histology	ND	83% of cases
Case reports of AN with GBMT[a]	18		12.1 ± 1.5/9.3–16	Iliac crest for half of the cases. Proximal femur, pelvis, foot or not specified for the other cases	Histology, cytology[b]	↓	All cases

BMI, body mass index; BMA, bone marrow adiposity; GBMT, gelatinous bone marrow transformation; H-MRS, proton magnetic resonance spectroscopy; ND, not determined; MRI, magnetic resonance imaging; CT, computed tomography; ND, not determined; AN, anorexia nervosa.

Arrows: the variations in patients with AN differed significantly from those observed in control subjects.

[a]*Data from 15 case reports on GBMT in patients with AN (46–59).*

[b]*Except for two cases where MRI was applied.*

TABLE 2 | Variations in BM adipose tissue (BMAT) content in calorie-restricted rodent models.

Characteristics of the model	Period of protocol	BW	Bone	BMAT content	Reference
Male mice 40%, food restriction	From 14 to 24 weeks of age	–30% vs. *ad libitum*	Low cortical and low trabecular thickness (femur)	–100% (distal femur)	Hamrick et al. (60)
Male mice 30%, calorie restriction	From 3 to 12 weeks of age	–40% vs. *ad libitum* +80% vs. day 0	Low cortical thickness and low trabecular BV/TV (femur)	+700% (distal femur)	Devlin et al. (61)
Female rats	From 6 to 9 months of age	–25% vs. *ad libitum* –20% vs. day 0	Low trabecular volumetric bone mineral density but non-significant changes in cortical bone (tibia)	+100% (proximal femur)	Baek and Bloomfield (62)
Female mice, 30% calorie restriction	From 9 to 15 weeks of age	–23% vs. *ad libitum* –3% vs. day 0	Low trabecular thickness and low cortical volume (tibia)	+700% (tibia, above fibula junction)	Cawthorn et al. (27)
Female mice, time-restricted feeding	From 8 to 18 weeks of age	–40% vs. *ad libitum* –25% vs. day 0	Low trabecular BV/TV and thickness, low cortical thickness (tibia)	Non-significant (proximal tibia)	Zgheib et al. (63) and unpublished data

order to avoid a compensatory increase in food intake and, thus, attain a daily food intake close to that of *ad libitum* mice) (63). The calorie-restricted animals rapidly lost around 25% of their initial body weight, which corresponded to a body weight loss of 40% (relative to control mice) after 10 weeks of the protocol. The bone mass gain observed in control mice was curtailed after 2 weeks of the protocol (63). After 10 weeks, the tibia trabecular BV/TV ratio, trabecular thickness, and cortical thickness were, respectively, 32, 31, and 15% lower in SBA mice than in control mice. However, the BMA level in the proximal tibia was similar to that observed in control mice (unpublished data). These results showed (as did Hamrick et al.'s study) that energy deficit can

induce bone alterations in the absence of an obvious increase in BMA (60). Interestingly, Cawthorn et al. showed very recently that, in rabbit, CR leads to bone loss, even without increases in BMA (64).

To learn more from these animal datasets about BMA regulation, one can attempt to compare them. The five above-mentioned studies assessed rodents of different genders and at different ages. The well-known differences between male and female physiology and the differences in BMA variation with age make it difficult to compare males with females (65). For the studies of male animals, the difference in observed BMA changes between Hamrick et al.'s study and Devlin et al.'s study might be linked to the age difference. One might conclude that calorie restriction induces a large increase in BMA in young male rodents only. However, it is also noteworthy that there is a late-onset BMA increase in male control mice; this might reduce the possible BMA increase in older animals (as observed at the end of Hamrick et al.'s study). When considering the three studies of female rodents, Baek's work was performed on rats aged up to 9 months. It is difficult to compare old female rats with the 8- and 9-week-old C57Bl/6 female mice used by Cawthorn et al. and Zgheib et al., respectively. The main differences consisted in the body weight changes (relative to the start of the study) and the BMA changes in the tibia. Cawthorn et al. observed a stable body weight and a 700% increase in BMA, whereas Zgheib et al. observed a 25% decrease in body weight but no significant change in BMA. Given that these two models were similar enough to enable a valid comparison, one can hypothesize that the magnitude of body weight loss influences the change in BMA most strongly in young adult female mice.

POTENTIAL REGULATORS OF BMA IN A CONTEXT OF ENERGY DEFICIT

As described above, it appears that BMA may be modulated by age, gender, and the severity of the energy deficit. However, it is important to bear in mind that BMA can also be affected by many different biological factors, including hormones, growth factors, and pharmacologic agents. Although the molecular mechanisms involved in BMA regulation have not been fully defined, they appear to converge on the modulation of peroxisome proliferator activated receptor gamma 2 (PPARγ2) expression and/or activity.

When considering potential regulators of BMA in subjects with a severely reduced calorie intake, it has been shown that dysregulation of the growth hormone insulin-like growth factor 1 axis and low leptin levels can stimulate BM adipogenesis (19, 61, 66). Moreover, starvation prompts the mobilization of fat stores, which might activate PPARγ2 and stimulate adipocyte differentiation in the BM (27). Furthermore, calorie restriction in a mouse model resulted in low expression and activity of runt-related transcription factor 2 (Runx2) and tafazzin (TAZ), both of which are pro-osteogenic transcriptional factors in BM stromal cells (67, 68).

Several other investigators have established links between BMA and pre-adipocyte factor 1 (Pref1). Indeed, circulating Pref1 concentrations are higher in women with AN than in healthy controls (66). In women who have recovered from AN, Pref1 levels are significantly lower than in normal-weight controls (66). Hence, it is possible that elevated Pref1 levels in AN may be involved in the increase in BMA.

It is also known that the production of reactive oxygen species (ROS) is greater in AN patients than in control subjects (69). ROS greatly influence the generation and survival of bone cells (70). *In vitro* studies of bone metabolism have shown that oxidative stress inhibits osteoblastic differentiation and induces apoptosis (71, 72).

Interestingly, women with AN have higher cortisol levels than healthy controls (73, 74). Cortisol levels are also predictive of a low bone mineral density in AN (73). In animal models, Cawthorn et al. showed that both BMA and glucocorticoids increase during CR in mice, but neither of these increases during CR in rabbits, suggesting a narrow link between these two phenomena (64). Experiments *in vitro* suggest that corticosteroids lead to adipogenesis by activating PPARγ2 and blocking the Wnt signaling pathway (75, 76). These findings also suggest that cortisol, Pref1, and leptin are all potential BMA regulators in a context of energy deficit.

Furthermore, women with AN have low estrogen levels (77, 78). Postmenopausal estrogen deficit has been linked to high BMA (79). *In vitro* studies have demonstrated that estradiol induces a pro-osteogenic lineage shift in BM stromal cells, whereas estrogen deficit in aging mice was found to induce a decrease in the expression and activity of the pro-osteogenic, anti-adipogenic factor sirtuin type 1 (80, 81). One can, thus, conclude that estrogen is likely to be involved in the regulation of BMA.

Moreover, it is important to note that BM adipose tissue (BMAT) expansion contributes significantly to the elevated serum adiponectin levels and skeletal muscle adaptation observed during CR (27). Indeed, the study by Cawthorn et al. suggested that BMAT is a major source of circulating adiponectin in states of leanness, and that (through endocrine functions) BMAT can have extraskeletal, systemic effects (27). Thus, adiponectin may also regulate BMA in this context.

Last, it is probable that ongoing and/or future research will prompt us to take account of new factors that regulate adiposity in a context of energy deficit.

PERSPECTIVES

This short overview of the relationship between BMA alterations and the severity of body weight loss highlights the complexity of the underlying processes and the mechanism of subsequent bone loss.

With a view to designing BMA-focused therapeutic strategies against osteoporosis in a context of energy deficit, one major question is "*do BM adipocytes trigger bone loss in a context of energy deficit*?" Several studies of patients with AN have shown that average-to-severe body weight loss tends to lead to normal or decreased BMA. This suggests that (i) the BMA increase observed in patients with mild body weight loss may be a late marker of changes that occur in BM and that result in low bone mass, and (ii) the absence of an increase in BMA does not necessarily mean that the skeleton is healthy. Some studies of CR animal models have shown that bone quality can decrease when the BMA is stable or even when it falls. This finding suggests

that (at least in these models) hypotheses based on the effect of factors released by mature adipocytes on the BM microenvironment are not the most realistic. If the latter phenomenon is nevertheless involved, it might have a secondary role in the downregulation of bone physiology. Thus, BM adipocytes might not trigger bone loss in moderate-to-severe AN and in some CR models. Next, hypotheses involving competition between differentiation into osteoblasts and differentiation into adipocytes should be considered. Interestingly, our analysis of the differentiation capabilities of BM stromal cells from SBA and control mice found that the SBA cells displayed a huge increase in adipogenesis at the expense of osteoblastogenesis (unpublished data). This was observed in SBA mice that displayed normal or low BMA, which led us to suppose that the BM of these mice contains many pre-adipocytes that are not able to synthesize and store lipids *in vivo*. These preliminary results strengthen the second hypothesis, although further experiments will be required to confirm these observations and to determine which factors in the culture medium trigger this pre-adipocyte maturation and adipocyte activity. The glucose concentration appears to be a relevant candidate factor. However, favoring hypotheses based on the importance of pre-adipocytes raises another question: "*Do pre-adipocytes influence their microenvironment?*" The characterization of stromal cells at the earliest stage in culture might help to answer this question.

If one acknowledges that a shift in the differentiation of BM stromal cells toward the adipocyte lineage is the main BM event during bone mass loss in a context of energy deficit, the next question would be "*how is this commitment regulated?*" One way of addressing this question would be to develop CR models with different levels of body weight loss. One could then compare BMA, bone quality/turnover, concentrations of circulating hormones known to have effects on adipogenesis and osteoblastogenesis, and the BM stromal cells' differentiation capabilities.

Tools are already available for studying how the differentiation of BM stromal cells is reprogrammed in animal models of CR and how differentiation is linked to the associated low bone mass. However, the development of novel tools for the *in vivo* assessment of specific cell types in the BM (such as pre-adipocytes) remains a true challenge.

AUTHOR CONTRIBUTIONS

OG, NAR, PH, and CC discussed the concept, compiled the literature, and wrote the paper.

FUNDING

NAR's PhD is founded by ULCO and Lebanon CNRS.

REFERENCES

1. Song L, Tuan RS. Transdifferentiation potential of human mesenchymal stem cells derived from bone marrow. *FASEB J* (2004) 18(9):980–2. doi:10.1096/fj.03-1100fje
2. Rozman C, Feliu E, Berga L, Reverter JC, Climent C, Ferrán MJ. Age-related variations of fat tissue fraction in normal human bone marrow depend both on size and number of adipocytes: a stereological study. *Exp Hematol* (1989) 17(1):34–7.
3. Hardouin P, Rharass T, Lucas S. Bone marrow adipose tissue: to be or not to be a typical adipose tissue? *Front Endocrinol* (2016) 7:85. doi:10.3389/fendo.2016.00085
4. Moore SG, Dawson KL. Red and yellow marrow in the femur: age-related changes in appearance at MR imaging. *Radiology* (1990) 175(1):219–23. doi:10.1148/radiology.175.1.2315484
5. Griffith JF, Yeung DKW, Ma HT, Leung JCS, Kwok TCY, Leung PC. Bone marrow fat content in the elderly: a reversal of sex difference seen in younger subjects. *J Magn Reson Imaging* (2012) 36(1):225–30. doi:10.1002/jmri.23619
6. Shen W, Chen J, Gantz M, Punyanitya M, Heymsfield SB, Gallagher D, et al. MRI-measured pelvic bone marrow adipose tissue is inversely related to DXA-measured bone mineral in younger and older adults. *Eur J Clin Nutr* (2012) 66(9):983–8. doi:10.1038/ejcn.2012.35
7. Wren TAL, Chung SA, Dorey FJ, Bluml S, Adams GB, Gilsanz V. Bone marrow fat is inversely related to cortical bone in young and old subjects. *J Clin Endocrinol Metab* (2011) 96(3):782–6. doi:10.1210/jc.2010-1922
8. Verma S, Rajaratnam JH, Denton J, Hoyland JA, Byers RJ. Adipocytic proportion of bone marrow is inversely related to bone formation in osteoporosis. *J Clin Pathol* (2002) 55(9):693–8. doi:10.1136/jcp.55.9.693
9. Blebea JS, Houseni M, Torigian DA, Fan C, Mavi A, Zhuge Y, et al. Structural and functional imaging of normal bone marrow and evaluation of its age-related changes. *Semin Nucl Med* (2007) 37(3):185–94. doi:10.1053/j.semnuclmed.2007.01.002
10. Lecka-Czernik B. Marrow fat metabolism is linked to the systemic energy metabolism. *Bone* (2012) 50(2):534–9. doi:10.1016/j.bone.2011.06.032
11. Kawai M, Rosen CJ. Bone: adiposity and bone accrual-still an established paradigm? *Nat Rev Endocrinol* (2010) 6(2):63–4. doi:10.1038/nrendo.2009.249
12. Krings A, Rahman S, Huang S, Lu Y, Czernik PJ, Lecka-Czernik B. Bone marrow fat has brown adipose tissue characteristics, which are attenuated with aging and diabetes. *Bone* (2012) 50(2):546–52. doi:10.1016/j.bone.2011.06.016
13. Ahdjoudj S, Lasmoles F, Holy X, Zerath E, Marie PJ. Transforming growth factor beta2 inhibits adipocyte differentiation induced by skeletal unloading in rat bone marrow stroma. *J Bone Miner Res* (2002) 17(4):668–77. doi:10.1359/jbmr.2002.17.4.668
14. Justesen J, Stenderup K, Ebbesen EN, Mosekilde L, Steiniche T, Kassem M. Adipocyte tissue volume in bone marrow is increased with aging and in patients with osteoporosis. *Biogerontology* (2001) 2(3):165–71. doi:10.1023/A:1011513223894
15. Yeung DKW, Griffith JF, Antonio GE, Lee FKH, Woo J, Leung PC. Osteoporosis is associated with increased marrow fat content and decreased marrow fat unsaturation: a proton MR spectroscopy study. *J Magn Reson Imaging* (2005) 22(2):279–85. doi:10.1002/jmri.20367
16. Botolin S, McCabe LR. Bone loss and increased bone adiposity in spontaneous and pharmacologically induced diabetic mice. *Endocrinology* (2007) 148(1):198–205. doi:10.1210/en.2006-1006
17. Piccinin MA, Khan ZA. Pathophysiological role of enhanced bone marrow adipogenesis in diabetic complications. *Adipocyte* (2014) 3(4):263–72. doi:10.4161/adip.32215
18. Schafer AL, Li X, Schwartz AV, Tufts LS, Wheeler AL, Grunfeld C, et al. Changes in vertebral bone marrow fat and bone mass after gastric bypass surgery: a pilot study. *Bone* (2015) 74:140–5. doi:10.1016/j.bone.2015.01.010
19. Bredella MA, Torriani M, Ghomi RH, Thomas BJ, Brick DJ, Gerweck AV, et al. Vertebral bone marrow fat is positively associated with visceral fat and inversely associated with IGF-1 in obese women. *Obesity (Silver Spring)* (2011) 19(1):49–53. doi:10.1038/oby.2010.106
20. Bredella MA, Fazeli PK, Miller KK, Misra M, Torriani M, Thomas BJ, et al. Increased bone marrow fat in anorexia nervosa. *J Clin Endocrinol Metab* (2009) 94(6):2129–36. doi:10.1210/jc.2008-2532
21. Hardouin P, Pansini V, Cortet B. Bone marrow fat. *Jt Bone Spine* (2014) 81(4):313–9. doi:10.1016/j.jbspin.2014.02.013
22. Nishimura R, Hata K, Ikeda F, Ichida F, Shimoyama A, Matsubara T, et al. Signal transduction and transcriptional regulation during mesenchymal

cell differentiation. *J Bone Miner Metab* (2008) 26(3):203–12. doi:10.1007/s00774-007-0824-2
23. Owen M. Marrow stromal stem cells. *J Cell Sci Suppl* (1988) 10:63–76. doi:10.1242/jcs.1988.Supplement_10.5
24. Pittenger MF, Mackay AM, Beck SC, Jaiswal RK, Douglas R, Mosca JD, et al. Multilineage potential of adult human mesenchymal stem cells. *Science* (1999) 284(5411):143–7. doi:10.1126/science.284.5411.143
25. Uckan D, Kilic E, Sharafi P, Kazik M, Kaya F, Erdemli E, et al. Adipocyte differentiation defect in mesenchymal stromal cells of patients with malignant infantile osteopetrosis. *Cytotherapy* (2009) 11(4):392–402. doi:10.1080/14653240802582083
26. Lecka-Czernik B. PPARs in bone: the role in bone cell differentiation and regulation of energy metabolism. *Curr Osteoporos Rep* (2010) 8(2):84–90. doi:10.1007/s11914-010-0016-1
27. Cawthorn WP, Scheller EL, Learman BS, Parlee SD, Simon BR, Mori H, et al. Bone marrow adipose tissue is an endocrine organ that contributes to increased circulating adiponectin during caloric restriction. *Cell Metab* (2014) 20(2):368–75. doi:10.1016/j.cmet.2014.06.003
28. Naveiras O, Nardi V, Wenzel PL, Hauschka PV, Fahey F, Daley GQ. Bone-marrow adipocytes as negative regulators of the haematopoietic microenvironment. *Nature* (2009) 460(7252):259–63. doi:10.1038/nature08099
29. Belaid-Choucair Z, Lepelletier Y, Poncin G, Thiry A, Humblet C, Maachi M, et al. Human bone marrow adipocytes block granulopoiesis through neuropilin-1-induced granulocyte colony-stimulating factor inhibition. *Stem Cells* (2008) 26(6):1556–64. doi:10.1634/stemcells.2008-0068
30. Yan Q-W, Yang Q, Mody N, Graham TE, Hsu C-H, Xu Z, et al. The adipokine lipocalin 2 is regulated by obesity and promotes insulin resistance. *Diabetes* (2007) 56(10):2533–40. doi:10.2337/db07-0007
31. Kern PA, Saghizadeh M, Ong JM, Bosch RJ, Deem R, Simsolo RB. The expression of tumor necrosis factor in human adipose tissue. Regulation by obesity, weight loss, and relationship to lipoprotein lipase. *J Clin Invest* (1995) 95(5):2111–9. doi:10.1172/JCI117899
32. Herzog W, Minne H, Deter C, Leidig G, Schellberg D, Wüster C, et al. Outcome of bone mineral density in anorexia nervosa patients 11.7 years after first admission. *J Bone Miner Res* (1993) 8(5):597–605. doi:10.1002/jbmr.5650080511
33. Solmi M, Veronese N, Favaro A, Santonastaso P, Manzato E, Sergi G, et al. Inflammatory cytokines and anorexia nervosa: a meta-analysis of cross-sectional and longitudinal studies. *Psychoneuroendocrinology* (2015) 51:237–52. doi:10.1016/j.psyneuen.2014.09.031
34. Corcos M, Guilbaud O, Chaouat G, Cayol V, Speranza M, Chambry J, et al. Cytokines and anorexia nervosa. *Psychosom Med* (2001) 63(3):502–4. doi:10.1097/00006842-200105000-00021
35. Bredella MA, Fazeli PK, Daley SM, Miller KK, Rosen CJ, Klibanski A, et al. Marrow fat composition in anorexia nervosa. *Bone* (2014) 66:199–204. doi:10.1016/j.bone.2014.06.014
36. Fazeli PK, Bredella MA, Freedman L, Thomas BJ, Breggia A, Meenaghan E, et al. Marrow fat and preadipocyte factor-1 levels decrease with recovery in women with anorexia nervosa. *J Bone Miner Res* (2012) 27(9):1864–71. doi:10.1002/jbmr.1640
37. Ecklund K, Vajapeyam S, Feldman HA, Buzney CD, Mulkern RV, Kleinman PK, et al. Bone marrow changes in adolescent girls with anorexia nervosa. *J Bone Miner Res* (2010) 25(2):298–304. doi:10.1359/jbmr.090805
38. Mayo-Smith W, Rosenthal DI, Goodsitt MM, Klibanski A. Intravertebral fat measurement with quantitative CT in patients with Cushing disease and anorexia nervosa. *Radiology* (1989) 170(3 Pt 1):835–8. doi:10.1148/radiology.170.3.2916039
39. Geiser F, Mürtz P, Lutterbey G, Träber F, Block W, Imbierowicz K, et al. Magnetic resonance spectroscopic and relaxometric determination of bone marrow changes in anorexia nervosa. *Psychosom Med* (2001) 63(4):631–7. doi:10.1097/00006842-200107000-00016
40. Abella E, Feliu E, Granada I, Millá F, Oriol A, Ribera JM, et al. Bone marrow changes in anorexia nervosa are correlated with the amount of weight loss and not with other clinical findings. *Am J Clin Pathol* (2002) 118(4):582–8. doi:10.1309/2Y7X-YDXK-006B-XLT2
41. Boutin RD, White LM, Laor T, Spitz DJ, Lopez-Ben RR, Stevens KJ, et al. MRI findings of serous atrophy of bone marrow and associated complications. *Eur Radiol* (2015) 25(9):2771–8. doi:10.1007/s00330-015-3692-5
42. Lambert M, Hubert C, Depresseux G, Vande Berg B, Thissen JP, Nagant de Deuxchaisnes C, et al. Hematological changes in anorexia nervosa are correlated with total body fat mass depletion. *Int J Eat Disord* (1997) 21(4):329–34. doi:10.1002/(SICI)1098-108X(1997)21:4<329::AID-EAT4>3.0.CO;2-Q
43. Vande Berg BC, Malghem J, Lecouvet FE, Lambert M, Maldague BE. Distribution of serous like bone marrow changes in the lower limbs of patients with anorexia nervosa: predominant involvement of the distal extremities. *AJR Am J Roentgenol* (1996) 166(3):621–5. doi:10.2214/ajr.166.3.8623638
44. Vande Berg BC, Malghem J, Devuyst O, Maldague BE, Lambert MJ. Anorexia nervosa: correlation between MR appearance of bone marrow and severity of disease. *Radiology* (1994) 193(3):859–64. doi:10.1148/radiology.193.3.7972838
45. Mant MJ, Faragher BS. The haematology of anorexia nervosa. *Br J Haematol* (1972) 23(6):737–49. doi:10.1111/j.1365-2141.1972.tb03488.x
46. Cornbleet PJ, Moir RC, Wolf PL. A histochemical study of bone marrow hypoplasia in anorexia nervosa. *Virchows Arch A Pathol Anat Histol* (1977) 374(3):239–47. doi:10.1007/BF00427118
47. Devuyst O, Lambert M, Rodhain J, Lefebvre C, Coche E. Haematological changes and infectious complications in anorexia nervosa: a case-control study. *Q J Med* (1993) 86(12):791–9.
48. Bailly D, Lambin I, Garzon G, Parquet PJ. Bone marrow hypoplasia in anorexia nervosa: a case report. *Int J Eat Disord* (1994) 16(1):97–100. doi:10.1002/1098-108X(199407)16:1<97::AID-EAT2260160112>3.0.CO;2-N
49. Mehler PS, Howe SE. Serous fat atrophy with leukopenia in severe anorexia nervosa. *Am J Hematol* (1995) 49(2):171–2. doi:10.1002/ajh.2830490219
50. Feugier P, Guerci A, Boman F, Stockemer V, Lederlin P. Transformation gélatineuse de la moelle osseuse. À propos de trois observations. *Rev Méd Interne* (1995) 16(1):15–9. doi:10.1016/0248-8663(96)80660-6
51. Nonaka D, Tanaka M, Takaki K, Umeno M, Okamura T, Taketa H. Gelatinous bone marrow transformation complicated by self-induced malnutrition. *Acta Haematol* (1998) 100(2):88–90. doi:10.1159/000040872
52. Orlandi E, Boselli P, Covezzi R, Bonaccorsi G, Guaraldi GP. Reversal of bone marrow hypoplasia in anorexia nervosa: case report. *Int J Eat Disord* (2000) 27(4):480–2. doi:10.1002/(SICI)1098-108X(200005)27:4<480::AID-EAT14>3.0.CO;2-3
53. Nishio S, Yamada H, Yamada K, Okabe H, Okuya T, Yonekawa O, et al. Severe neutropenia with gelatinous bone marrow transformation in anorexia nervosa: a case report. *Int J Eat Disord* (2003) 33(3):360–3. doi:10.1002/eat.10143
54. Boullu-Ciocca S, Darmon P, Sébahoun G, Silaghi A, Dutour-Meyer A. Gelatinous bone marrow transformation in anorexia nervosa. *Ann Endocrinol* (2005) 66(1):7–11. doi:10.1016/S0003-4266(05)81680-4
55. Tins B, Cassar-Pullicino V. Marrow changes in anorexia nervosa masking the presence of stress fractures on MR imaging. *Skeletal Radiol* (2006) 35(11):857–60. doi:10.1007/s00256-005-0053-5
56. Mohamed M, Khalafallah A. Gelatinous transformation of bone marrow in a patient with severe anorexia nervosa. *Int J Hematol* (2012) 97(2):157–8. doi:10.1007/s12185-012-1255-y
57. Rivière E, Pillot J, Saghi T, Clouzeau B, Castaing Y, Gruson D, et al. Gelatinous transformation of the bone marrow and acute hepatitis in a woman suffering from anorexia nervosa. *Rev Méd Interne* (2012) 33(7):e38–40. doi:10.1016/j.revmed.2011.11.011
58. Morii K, Yamamoto T, Kishida H, Okushin H. Gelatinous transformation of bone marrow in patients with anorexia nervosa. *Intern Med* (2013) 52(17):2005–6. doi:10.2169/internalmedicine.52.0912
59. Villate A, Iquel S, Legac E. Gelatinous transformation of the bone marrow: a retrospective monocentric case series of 12 patients. *Rev Méd Interne* (2015) 37(7):448–52. doi:10.1016/j.revmed.2015.10.349
60. Hamrick MW, Ding K-H, Ponnala S, Ferrari SL, Isales CM. Caloric restriction decreases cortical bone mass but spares trabecular bone in the mouse skeleton: implications for the regulation of bone mass by body weight. *J Bone Miner Res* (2008) 23(6):870–8. doi:10.1359/jbmr.080213
61. Devlin MJ, Cloutier AM, Thomas NA, Panus DA, Lotinun S, Pinz I, et al. Caloric restriction leads to high marrow adiposity and low bone mass in growing mice. *J Bone Miner Res* (2010) 25(9):2078–88. doi:10.1002/jbmr.82
62. Baek K, Bloomfield SA. Blocking β-adrenergic signaling attenuates reductions in circulating leptin, cancellous bone mass, and marrow adiposity seen with

dietary energy restriction. *J Appl Physiol (1985)* (2012) 113(11):1792–801. doi:10.1152/japplphysiol.00187.2012
63. Zgheib S, Méquinion M, Lucas S, Leterme D, Ghali O, Tolle V, et al. Long-term physiological alterations and recovery in a mouse model of separation associated with time-restricted feeding: a tool to study anorexia nervosa related consequences. *PLoS One* (2014) 9(8):e103775. doi:10.1371/journal.pone.0103775
64. Cawthorn WP, Scheller EL, Parlee SD, Pham HA, Learman BS, Redshaw CM, et al. Expansion of bone marrow adipose tissue during caloric restriction is associated with increased circulating glucocorticoids and not with hypoleptinemia. *Endocrinology* (2016) 157(2):508–21. doi:10.1210/en.2015-1477
65. Scheller EL, Doucette CR, Learman BS, Cawthorn WP, Khandaker S, Schell B, et al. Region-specific variation in the properties of skeletal adipocytes reveals regulated and constitutive marrow adipose tissues. *Nat Commun* (2015) 6:7808. doi:10.1038/ncomms8808
66. Fazeli PK, Bredella MA, Misra M, Meenaghan E, Rosen CJ, Clemmons DR, et al. Preadipocyte factor-1 is associated with marrow adiposity and bone mineral density in women with anorexia nervosa. *J Clin Endocrinol Metab* (2010) 95(1):407–13. doi:10.1210/jc.2009-1152
67. Hong J-H, Yaffe MB. TAZ: a beta-catenin-like molecule that regulates mesenchymal stem cell differentiation. *Cell Cycle* (2006) 5(2):176–9. doi:10.4161/cc.5.2.2362
68. Guo X, Yang W, Ni J, He M, Yang L. A role for suppressed bone formation favoring catch-up fat in the pathophysiology of catch-up growth after food restriction. *Eur J Nutr* (2011) 50(8):645–55. doi:10.1007/s00394-011-0174-7
69. Victor VM, Rovira-Llopis S, Saiz-Alarcon V, Sangüesa MC, Rojo-Bofill L, Bañuls C, et al. Altered mitochondrial function and oxidative stress in leukocytes of anorexia nervosa patients. *PLoS One* (2014) 9(9):e106463. doi:10.1371/journal.pone.0106463
70. Hamada Y, Fujii H, Fukagawa M. Role of oxidative stress in diabetic bone disorder. *Bone* (2009) 45(Suppl 1):S35–8. doi:10.1016/j.bone.2009.02.004
71. Bai X, Lu D, Bai J, Zheng H, Ke Z, Li X, et al. Oxidative stress inhibits osteoblastic differentiation of bone cells by ERK and NF-kappaB. *Biochem Biophys Res Commun* (2004) 314(1):197–207. doi:10.1016/j.bbrc.2003.12.073
72. Fatokun AA, Stone TW, Smith RA. Hydrogen peroxide-induced oxidative stress in MC3T3-E1 cells: the effects of glutamate and protection by purines. *Bone* (2006) 39(3):542–51. doi:10.1016/j.bone.2006.02.062
73. Lawson EA, Donoho D, Miller KK, Misra M, Meenaghan E, Lydecker J, et al. Hypercortisolemia is associated with severity of bone loss and depression in hypothalamic amenorrhea and anorexia nervosa. *J Clin Endocrinol Metab* (2009) 94(12):4710–6. doi:10.1210/jc.2009-1046
74. Lawson EA, Misra M, Meenaghan E, Rosenblum L, Donoho DA, Herzog D, et al. Adrenal glucocorticoid and androgen precursor dissociation in anorexia nervosa. *J Clin Endocrinol Metab* (2009) 94(4):1367–71. doi:10.1210/jc.2008-2558
75. Greenberger JS. Corticosteroid-dependent differentiation of human marrow preadipocytes in vitro. *In Vitro* (1979) 15(10):823–8. doi:10.1007/BF02618309
76. Ohnaka K, Tanabe M, Kawate H, Nawata H, Takayanagi R. Glucocorticoid suppresses the canonical Wnt signal in cultured human osteoblasts. *Biochem Biophys Res Commun* (2005) 329(1):177–81. doi:10.1016/j.bbrc.2005.01.117
77. Pafumi C, Ciotta L, Farina M, Bosco P, Chiarenza M, Pernicone G, et al. Evaluation of bone mass in young amenorrheic women with anorexia nervosa. *Minerva Ginecol* (2002) 54(6):487–91.
78. Estour B, Germain N, Diconne E, Frere D, Cottet-Emard J-M, Carrot G, et al. Hormonal profile heterogeneity and short-term physical risk in restrictive anorexia nervosa. *J Clin Endocrinol Metab* (2010) 95(5):2203–10. doi:10.1210/jc.2009-2608
79. Syed FA, Oursler MJ, Hefferanm TE, Peterson JM, Riggs BL, Khosla S. Effects of estrogen therapy on bone marrow adipocytes in postmenopausal osteoporotic women. *Osteoporos Int* (2008) 19(9):1323–30. doi:10.1007/s00198-008-0574-6
80. Okazaki R, Inoue D, Shibata M, Saika M, Kido S, Ooka H, et al. Estrogen promotes early osteoblast differentiation and inhibits adipocyte differentiation in mouse bone marrow stromal cell lines that express estrogen receptor (ER) alpha or beta. *Endocrinology* (2002) 143(6):2349–56. doi:10.1210/en.143.6.2349
81. Elbaz A, Rivas D, Duque G. Effect of estrogens on bone marrow adipogenesis and Sirt1 in aging C57BL/6J mice. *Biogerontology* (2009) 10(6):747–55. doi:10.1007/s10522-009-9221-7

Conflict of Interest Statement: The authors declare that the research was conducted in the absence of any commercial or financial relationships that could be construed as a potential conflict of interest.

frontiers in Endocrinology

ORIGINAL RESEARCH
published: 21 September 2016
doi: 10.3389/fendo.2016.00128

Increased Circulating Adiponectin in Response to Thiazolidinediones: Investigating the Role of Bone Marrow Adipose Tissue

*Richard J. Sulston[1], Brian S. Learman[2], Bofeng Zhang[2], Erica L. Scheller[2], Sebastian D. Parlee[2], Becky R. Simon[3], Hiroyuki Mori[2], Adam J. Bree[2], Robert J. Wallace[4], Venkatesh Krishnan[5], Ormond A. MacDougald[2,3,6] and William P. Cawthorn[1,2,5]**

[1] University/British Heart Foundation Centre for Cardiovascular Science, The Queen's Medical Research Institute, University of Edinburgh, Edinburgh, UK, [2] Department of Molecular & Integrative Physiology, University of Michigan Medical School, Ann Arbor, MI, USA, [3] Program in Cellular and Molecular Biology, University of Michigan Medical School, Ann Arbor, MI, USA, [4] Department of Orthopaedics, University of Edinburgh, Edinburgh, UK, [5] Musculoskeletal Research, Lilly Research Laboratories, Indianapolis, IN, USA, [6] Department of Internal Medicine, University of Michigan Medical School, Ann Arbor, MI, USA

OPEN ACCESS

Edited by:
Basem M. Abdallah, University of Southern Denmark, Denmark

Reviewed by:
Melissa Orlandin Premaor, Universidade Federal de Santa Maria, Brazil
Jan Tuckermann, University of Ulm, Germany

***Correspondence:**
William P. Cawthorn
w.cawthorn@ed.ac.uk

Specialty section:
This article was submitted to Bone Research, a section of the journal Frontiers in Endocrinology

Received: 14 June 2016
Accepted: 05 September 2016
Published: 21 September 2016

Citation:
Sulston RJ, Learman BS, Zhang B, Scheller EL, Parlee SD, Simon BR, Mori H, Bree AJ, Wallace RJ, Krishnan V, MacDougald OA and Cawthorn WP (2016) Increased Circulating Adiponectin in Response to Thiazolidinediones: Investigating the Role of Bone Marrow Adipose Tissue. Front. Endocrinol. 7:128. doi: 10.3389/fendo.2016.00128

Background: Bone marrow adipose tissue (MAT) contributes to increased circulating adiponectin, an insulin-sensitizing hormone, during caloric restriction (CR), but whether this occurs in other contexts remains unknown. The antidiabetic thiazolidinediones (TZDs) also promote MAT expansion and hyperadiponectinemia, even without increasing adiponectin expression in white adipose tissue (WAT).

Objectives: To test the hypothesis that MAT expansion contributes to TZD-associated hyperadiponectinemia, we investigated the effects of rosiglitazone, a prototypical TZD, in wild-type (WT) or *Ocn*-Wnt10b mice. The latter resist MAT expansion during CR, leading us to postulate that they would also resist this effect of rosiglitazone.

Design: Male and female WT or *Ocn*-Wnt10b mice (C57BL/6J) were treated with or without rosiglitazone for 2, 4, or 8 weeks, up to 30 weeks of age. MAT content was assessed by osmium tetroxide staining and adipocyte marker expression. Circulating adiponectin was determined by ELISA.

Results: In WT mice, rosiglitazone caused hyperadiponectinemia and MAT expansion. Compared to WT mice, *Ocn*-Wnt10b mice had significantly less MAT in distal tibiae and sometimes in proximal tibiae; however, interpretation was complicated by the leakage of osmium tetroxide from ruptures in some tibiae, highlighting an important technical consideration for osmium-based MAT analysis. Despite decreased MAT in *Ocn*-Wnt10b mice, circulating adiponectin was generally similar between WT and *Ocn*-Wnt10b mice; however, in females receiving rosiglitazone for 4 weeks, hyperadiponectinemia was significantly blunted in *Ocn*-Wnt10b compared to WT mice. Notably, this was also the only group in which tibial adiponectin expression was lower than in WT mice, suggesting a close association between MAT adiponectin production and circulating adiponectin. However, rosiglitazone significantly increased adiponectin protein expression in WAT,

suggesting that WAT contributes to hyperadiponectinemia in this context. Finally, rosiglitazone upregulated uncoupling protein 1 in brown adipose tissue (BAT), but this protein was undetectable in tibiae, suggesting that MAT is unlikely to share thermogenic properties of BAT.

Conclusion: TZD-induced hyperadiponectinemia is closely associated with increased adiponectin production in MAT but is not prevented by the partial loss of MAT that occurs in *Ocn*-Wnt10b mice. Thus, more robust loss-of-MAT models are required for future studies to better establish MAT's elusive functions, both on an endocrine level and beyond.

Keywords: bone marrow adipose tissue, white adipose tissue, brown adipose tissue, thiazolidinedione, rosiglitazone, adiponectin, beige adipocyte, UCP1

INTRODUCTION

Adipose tissue is typically classified into two broad subtypes, white adipose tissue (WAT) and brown adipose tissue (BAT). WAT is commonly known for its role in energy storage and release and is now established as a major endocrine organ. BAT also mediates some endocrine functions but is more widely known for its ability to mediate adaptive thermogenesis (1). Through these functions, both WAT and BAT impact metabolic homeostasis; hence, the global burden of obesity and metabolic disease has motivated extensive study of these tissues (2).

In addition to WAT and BAT, adipocytes also exist in the bone marrow, and such marrow adipose tissue (MAT) has been estimated to account for over 10% of total adipose tissue mass in lean, healthy humans (3). We recently revealed that MAT characteristics are region-specific, such that MAT can be classified into two broad subtypes: regulated MAT (rMAT), which exists in more proximal skeletal sites and consists of adipocytes interspersed with hematopoietic BM; and constitutive MAT (cMAT), which exists in more distal regions (e.g., distal tibia, caudal vertebrae) and appears histologically similar to WAT, with few visible hematopoietic cells (4). These MAT subtypes also differ in their lipid composition and response to external stimuli (4). Both rMAT and cMAT appear to be developmentally and functionally distinct to WAT and BAT, and therefore MAT may represent a third general class of adipose tissue (5, 6). Despite these advances, knowledge of MAT formation and function remains relatively limited (2). However, research from others and us suggests that, like WAT, MAT is an endocrine organ that can exert local and systemic effects (3, 7).

The appreciation of WAT as an endocrine organ derives largely from the discovery in the mid-1990s of two adipocyte-derived hormones, leptin and adiponectin, each of which impacts metabolic homeostasis (8–10). These two hormones have since been mentioned in over 40,000 publications, reflecting the extensive depth of WAT research. Circulating leptin concentrations correlate directly with body fat percentage and are therefore increased in obesity. In contrast, adiponectin concentrations are decreased in obesity and insulin-resistance; hence, hypoadiponectinemia is now an established biomarker for increased risk of cardiometabolic disease. Conversely, circulating adiponectin is elevated in conditions of leanness and insulin sensitivity, such as during caloric restriction (CR) (2). This counterintuitive observation has been dubbed the "adiponectin paradox": why should circulating adiponectin increase when the amount of WAT, the presumed source of adiponectin, is decreased? Moreover, CR can cause hyperadiponectinemia without increasing expression or secretion of adiponectin from WAT (2), suggesting that other tissues contribute to this effect. Our recent research has highlighted a potential explanation for this paradox, revealing, unexpectedly, that MAT is a source of circulating adiponectin during CR (3).

Our studies into MAT and CR were motivated by the striking observation that, in contrast to WAT and BAT, MAT accumulates during CR (3, 11, 12). The biochemical phenotype of this CR-responsive MAT remains to be elucidated; however, we have since shown that these increases occur predominantly in regions of rMAT rather than cMAT (2). This phenomenon led us to investigate if MAT contributes to increased circulating adiponectin during CR. After confirming that MAT expresses and secretes adiponectin (3), we then tested if MAT accumulation is required for CR-associated hyperadiponectinemia. To do so, we used *Ocn*-Wnt10b mice, a transgenic model in which the secreted ligand, Wnt10b, is expressed in osteoblasts from the *Ocn* promoter (13). Because Wnt10b simulates osteoblastogenesis and inhibits adipogenesis, these mice have increased bone formation and decreased bone marrow volume (3, 13). We found that *Ocn*-Wnt10b mice also resist CR-associated MAT expansion, both in rMAT and cMAT (2, 3). Notably, hyperadiponectinemia during CR is also blunted in these mice, despite no differences in adiponectin expression in WAT (3). Finally, impaired MAT expansion also coincides with blunted hyperadiponectinemia in a separate mouse model of CR (14) and during CR in rabbits (12). Together, these observations suggest that MAT expansion is required for CR-induced hyperadiponectinemia, supporting the conclusion that MAT is a source of circulating adiponectin in this context.

To further investigate this endocrine function, we sought to determine if MAT also influences circulating adiponectin beyond CR. For example, increases in both MAT and circulating adiponectin occur in many other conditions, including aging, estrogen deficiency, type 1 diabetes, cancer treatment, and in response to fibroblast growth factor-21 or glucocorticoid therapy

(2). Notably, these increases also coincide during treatment with thiazolidinediones (TZDs), a class of insulin-sensitizing, antidiabetic drugs that act as agonists for the nuclear hormone receptor, peroxisome proliferator-activated receptor gamma (PPARγ) (15, 16). Binding and subsequent activation of PPARγ causes it to activate the expression of its transcriptional targets, including adiponectin and other lipid-metabolism-associated genes such as fatty acid-binding protein 4 (*Fabp4*) (17). Thus, TZDs, such as rosiglitazone, significantly increase circulating adiponectin in rodent models and human patients (18, 19). Importantly, preclinical studies suggest that such hyperadiponectinemia is required for the full insulin-sensitizing effects of TZDs (20). Despite the beneficial effects of TZDs in improving glucose tolerance, their clinical use has been restricted owing to increased risk of myocardial infarction and bone fractures (21, 22); the latter may relate to the ability of TZDs to drive MAT expansion. If so, MAT expansion may be detrimental to the clinical utility of these drugs. However, it is notable that TZDs can increase circulating adiponectin without increasing adiponectin expression in WAT (23, 24), and that some studies suggest that TZD action is independent of WAT (25). Thus, given the contribution of MAT to increased circulating adiponectin during CR, we hypothesized that MAT also contributes to TZD-induced hyperadiponectinemia. If so, MAT expansion may play a role in the beneficial insulin-sensitizing effects of TZDs.

Herein, we investigated this hypothesis by feeding wild-type (WT) and *Ocn*-Wnt10b mice a Western diet to induce obesity and glucose intolerance, followed by treatment with rosiglitazone, a prototypical TZD. We postulated that, as in CR, these mice would resist TZD-induced MAT expansion. As secondary analyses, we also investigated the contribution of WAT to TZD-mediated hyperadiponectinemia and the possibility, suggested previously (26), that MAT has BAT-like properties. Our results shed light on MAT's characteristics and highlight technical considerations that will be important for future research into MAT formation and function.

MATERIALS AND METHODS

Animals and Animal Care

Ocn-Wnt10b mice (Wnt10b) or non-transgenic controls (WT) were on a C57BL/6J background and were bred in-house, as described previously (13). The University of Michigan Committee on the Use and Care of Animals approved all animal experiments, with daily care of mice and rabbits overseen by the Unit for Laboratory Animal Medicine (ULAM).

Diets and Rosiglitazone (TZD) Treatment

Male WT ($n = 18$), male Wnt10b ($n = 22$), female WT ($n = 20$), and female Wnt10b ($n = 15$) mice were fed a standard laboratory chow diet (Research Diets, D12450B) from weaning until 10 weeks of age. From 10 to 22 weeks of age, all mice were fed a high-fat, high-sucrose Western diet (Research Diets D12079B), with the goal of promoting diet-induced obesity and glucose intolerance. The rationale for this was that, if *Ocn*-Wnt10b mice resisted hyperadiponectinemia, they might also be less responsive to the metabolic effects of TZD treatment. Thus, mice were fed a Western diet prior to TZD treatment, with the aim of allowing detection of metabolic improvements upon TZD administration. At 18 weeks of age, mice were fasted overnight; body mass and fasting glucose were then recorded and body fat, lean mass, and free fluid were measured in conscious mice using an NMR analyzer (Minispec LF90II; Bruker Optics, Billerica, MA, USA). These measurements were then used as a basis to assign mice to four evenly matched groups (with similar body mass, fat mass, and fasting glucose), with each group corresponding to a different duration of rosiglitazone (TZD) treatment. Mice were then treated with or without TZD from 22 to 30 weeks of age. TZD was administered in the diet (Research Diets D12112601) by supplementing diet D12450B with rosiglitazone at 0.175 mg/g diet; based on daily consumption of D12450B, this concentration was estimated to give a final dose per mouse of 15 mg/kg body mass per day. This approach is similar to that used in previous studies investigating rosiglitazone-induced MAT accumulation (26–28). The four experimental groups were as follows: control mice (0 weeks' TZD), which continued to receive Western diet D12079B from 22 to 30 weeks of age; 2 weeks' TZD mice, which received D12079B from 22 to 28 weeks and D12112601 from 28 to 30 weeks; 4 weeks' TZD mice, which received D12079B from 22 to 26 weeks and D12112601 from 26 to 30 weeks; and 8 weeks' TZD mice, which received D12112601 from 22 to 30 weeks. Numbers of mice per group and diet durations are described further in **Table 1**. At 29.5 weeks of age, blood glucose concentrations were recorded after an overnight fast to assess the effects of TZD treatment. At 30 weeks of age, serum was sampled, mice were humanely euthanized, and tissues were isolated for further analysis.

Blood Collection and Serum Adiponectin Analysis

Blood was sampled from the lateral tail vein of mice using Microvette CB 300 capillary collection tubes (Sarstedt, Newton,

TABLE 1 | Summary of groups for control or TZD treatment.

Weeks of TZD	Ages (weeks) fed Western diet (D12450B)	Ages (weeks) fed TZD diet (D12112601)	Group sizes for each sex and genotype
0	22–30	N/A	WT male, 5; *Ocn*-Wnt10b male, 5 WT female, 6; *Ocn*-Wnt10b female, 4
2	22–28	28–30	WT male, 3; *Ocn*-Wnt10b male, 7 WT female, 5; *Ocn*-Wnt10b female, 3
4	22–26	26–30	WT male, 5; *Ocn*-Wnt10b male, 5 WT female, 5; *Ocn*-Wnt10b female, 3
8	N/A	22–30	WT male, 5; *Ocn*-Wnt10b male, 5 WT female, 4; *Ocn*-Wnt10b female, 5

NC, USA). Blood glucose was measured using an Accu-Chek Aviva glucometer. To obtain serum, blood samples were allowed to clot on ice for 2 h before centrifuging at 3,800 RCF for 5 min at 4°C. Serum adiponectin was determined using an ELISA kit (catalog no. MRP300) from R&D Systems (Bio-Techne Ltd., Abingdon, UK) according to the manufacturer's instructions.

Osmium Tetroxide Staining and μCT Analysis

Tibiae were isolated and, after removal of external soft tissue, fixed in formalin at 4°C. Fixed tibiae were decalcified in 14% EDTA for 14 days and then washed in Sorensen's Phosphate buffer (81 mM KH_2PO_4, 19 mM $Na_2HPO_4 \cdot 7H_2O$, pH 7.4). Decalcified tibiae were stored in Sorensen's Phosphate buffer at 4°C until ready to be stained with osmium tetroxide. To do so, osmium tetroxide solution (2% w/v; Agar Scientific, UK) was diluted 1:1 in Sorensen's Phosphate buffer. Tibiae were then stained in this 1% osmium tetroxide solution for 48 h at room temperature, then washed, and stored in Sorensen's Phosphate buffer at 4°C prior to micro computed tomography (μCT) analysis.

Micro Computed Tomography Analysis

Layers of four to five stained tibiae were arranged in parallel in 1% agarose in a 30-mL universal tube and mounted in a Skyscan 1172 desktop micro CT (Bruker, Kontich, Belgium). The samples were then scanned through 360° using a step of 0.40° between exposures. A voxel resolution of 12.05 μm was obtained in the scans using the following control settings: 54 kV source voltage, 185 μA source current with an exposure time of 885 ms. A 0.5-mm aluminum filter and two-frame averaging were used to optimize the scan. After scanning, the data were reconstructed using Skyscan software NRecon v1.6.9.4 (Bruker, Kontich, Belgium). The reconstruction thresholding window was optimized to encapsulate the target image. Volumetric analysis was performed using CT Analyser v1.13.5.1 (Bruker, Kontich, Belgium).

Real-time Quantitative PCR

RNA was extracted from tissue using RNA STAT60 reagent (Tel-Test, Inc.) according to the manufacturer's instructions. Synthesis of cDNA was done using TaqMan reverse transcription reagents (Thermo Fisher Scientific) using 1 μg of RNA template per reaction, as per manufacturer's instructions. Transcript expression was then analyzed by quantitative PCR (qPCR) in 10 μL duplicate reactions using qPCRBIO SyGreen Mix (part number PB20.11; PCR Biosystems, UK) and 1–4 μL of cDNA template. Reactions were loaded into 384-well qPCR plates (part number 72.1985.202; Sarstedt, UK) and run on a Light Cycler 480 (Roche). Transcript expression was calculated based on a cDNA titration loaded on each plate and was presented relative to expression of the housekeeping gene *Ppia.* Primers for *Adipoq* and *Ppia* were described and validated previously (3).

Immunoblot Analysis

Frozen tissue was processed as described previously (12). The resulting protein lysates were separated by size using gradient (4–12%) polyacrylamide gels (BioRad). Protein was then transferred to Immobilon-FL membrane (Millipore) for 150 min at 350 mA, 4°C, using a Criterion wet-transfer system (BioRad). Post-transfer, the membranes were blocked in 5% milk for 1 h at room temperature, then immunoblotted with primary antibody in 5% bovine serum albumin overnight at 4°C. Membranes were then incubated in 1:15,000-diluted fluorescently labeled secondary antibody (LiCor) for 1 h at room temperature. Signal was detected using the LiCor Odyssey system and band intensities quantified using LiCor Image Studio Lite software. The following primary antibodies were used: rabbit anti-adiponectin antibody (Sigma, A6354-200UL) diluted 1:1,000 in 5% BSA; rabbit anti-uncoupling protein 1 (UCP1) antibody (Sigma, U6382) diluted 1:10,000 in 2.5% milk; and rabbit anti-β-actin antibody (Abcam, ab8227) diluted 1:1,000 in 5% BSA.

Data Presentation and Statistical Analysis

Data are presented as box and whisker plots overlaid with individual data points for each animal. Boxes indicate the 25th and 75th percentiles; whiskers display the range; and horizontal lines in each box represent the median. Group sizes are described in **Table 1**. Statistical analysis was done using GraphPad Prism 6 software, with significant differences assessed by two-way ANOVA using a Tukey or Sidak *post hoc* test for multiple comparisons, as appropriate. A P-value <0.05 was considered statistically significant. A significant influence of TZD treatment, across all treatment groups, is indicated by †. For multiple comparisons, asterisks (*) indicate significant differences between genotypes within each TZD group, while hash signs (#) indicate significance between TZD-treated and non-TZD-treated controls within each genotype.

RESULTS

Effects of TZD on WAT Mass and Fasting Glucose Do Not Differ between WT and *Ocn*-Wnt10b Mice

Circulating adiponectin is decreased in states of obesity and glucose intolerance (29), while TZDs modulate both fat mass and glucose homeostasis. Therefore, after treating WT and *Ocn*-Wnt10b mice with or without rosiglitazone for 2, 4, or 8 weeks, we first assessed body mass, fat mass, and fasting glucose, primarily as readouts of TZD action but also as parameters that might influence circulating adiponectin. While body masses of female or male mice did not differ with TZD treatment (**Figures 1A,C**), across both genotypes, TZD was associated with significant loss of gonadal WAT (gWAT), a visceral adipose depot, in both females ($P = 0.027$) and males ($P = 0.006$) (**Figures 1B,D**). Conversely, the mass of inguinal WAT (iWAT), a subcutaneous depot, significantly increased with TZD treatment in males ($P = 0.002$) (**Figure 1D**). Analysis of fasting glucose revealed no effects of TZD in female mice (**Figure 1E**), whereas TZD significantly decreased fasting glucose across WT and *Ocn*-Wnt10b males (**Figure 1F**). These findings are consistent with previous studies demonstrating that rosiglitazone decreases gWAT mass (26, 27), increases subcutaneous WAT (30), and ameliorates hyperglycemia (16);

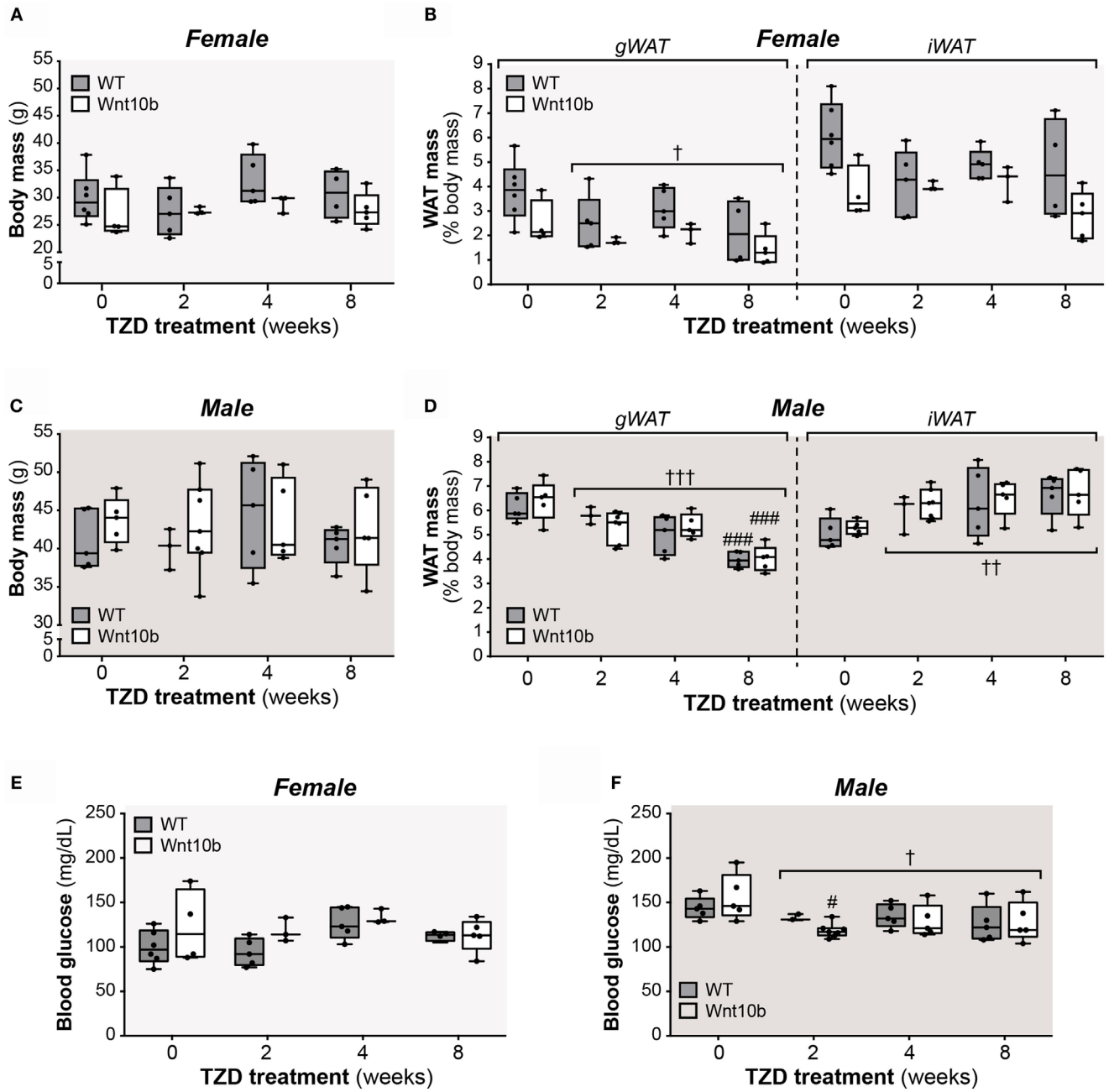

FIGURE 1 | **Effects of rosiglitazone on body mass, fat mass, and fasting glucose**. Male and female mice were fed a control Western diet only or a Western diet supplemented with rosiglitazone for 2, 4, or 8 weeks, as described in Section "Materials and Methods." **(A,C)** Body masses of females **(A)** and males **(C)** were recorded prior to necropsy at 30 weeks of age. **(B,D)** Masses of iWAT and gWAT were recorded at necropsy for female **(B)** and male mice **(D)** and are shown as percentage of total body mass. **(E,F)** Fasting blood glucose, as recorded at 29.5 weeks of age. For **(A–F)**, a significant influence of TZD treatment, across all treatment groups, is indicated by † ($P < 0.05$), †† ($P < 0.01$) or ††† ($P < 0.001$). Within each genotype, significant differences between untreated controls (0-week TZD) and individual durations of TZD treatment are indicated by ### ($P < 0.001$). Within each TZD treatment group (0-, 2-, 4-, or 8-week TZD), there were no statistically significant differences between WT and *Ocn*-Wnt10b mice.

however, it is unclear why rosiglitazone influenced iWAT mass and fasting glucose in males but not in females. In contrast to these effects of rosiglitazone, body mass, WAT mass, or fasting glucose did not differ between WT and *Ocn*-Wnt10b mice within each TZD treatment group (**Figures 1A–F**). Thus, differences in peripheral adiposity or glucose homeostasis, which can influence circulating adiponectin, did not occur between WT and *Ocn*-Wnt10b mice.

TZD Increases rMAT and cMAT Volume in WT Mice, and These Effects Are Partially Blunted in *Ocn*-Wnt10b Mice

Having characterized these peripheral metabolic parameters, we next investigated the impact of TZD on MAT expansion and whether this differs between WT and *Ocn*-Wnt10b mice. To do so, we first used an approach based on staining tibiae with osmium tetroxide, which covalently binds to unsaturated lipids within bone marrow and thereby acts as a strong contrast agent for MAT detection by μCT (31). As shown in **Figure 2A**, osmium staining in the proximal diaphysis, corresponding to rMAT, was markedly increased in females of both genotypes following 4- or 8-week TZD treatment. Statistical analyses confirmed that, across all groups of females, TZD significantly influenced the volume of rMAT, as well as that of cMAT and total MAT ($P < 0.0001$ for each) (**Figures 2B,C**). Multiple comparisons were then made to assess the effect of each duration of TZD treatment in each genotype of mice, relative to untreated controls. This revealed that, in female WT mice, TZD treatment for 4 or 8 weeks significantly increased rMAT volume in proximal tibiae and cMAT volume in distal tibiae (**Figures 2A,B**). Thus, total tibial MAT volume was also significantly increased by 4- or 8-week TZD in WT females (**Figure 2C**). Similar effects of TZD were also observed in *Ocn*-Wnt10b females (**Figures 2A–C**), and rMAT volume did not significantly differ between genotypes (**Figure 2B**). However, cMAT volume was markedly lower in *Ocn*-Wnt10b females within each TZD treatment group (**Figure 2B**). Total tibial MAT volume was also significantly decreased in *Ocn*-Wnt10b compared to WT females following 8 weeks' TZD (**Figure 2C**).

Compared to the female mice, osmium staining was less pronounced in the rMAT of TZD-treated males (**Figure 2D**). Nevertheless, statistical analysis across all groups of males revealed a significant influence of TZD on the volumes of rMAT ($P = 0.0015$), cMAT ($P = 0.0006$), and total MAT ($P = 0.0003$) (**Figures 2E,F**). Multiple comparisons further revealed that, in WT males, treatment with TZD for 8 weeks, but not shorter durations, significantly increased volumes of rMAT, cMAT, and total MAT (**Figures 2E,F**). This also occurred for cMAT and total MAT, but not rMAT, in *Ocn*-Wnt10b males (**Figures 2E,F**). As found for female mice, male *Ocn*-Wnt10b mice had significantly decreased cMAT volume compared to their WT counterparts (**Figure 2E**), and this also occurred for total MAT volume in the 0-, 4-, and 8-week TZD groups (**Figure 2F**).

Cortical Bone Ruptures Significantly Decrease Detectable rMAT Volume

The above observations suggest that *Ocn*-Wnt10b males and females partially resist TZD-induced MAT expansion, predominantly as a result of a lower cMAT volume than WT mice. Indeed, rMAT volume did not differ between genotypes in any of the TZD treatment groups. However, when analyzing the μCT scans, we noticed that the decalcified cortical bone had ruptured in tibiae from all male mice and in a subset of females. The ruptures always occurred in proximal tibial diaphysis, as indicated by representative scans of non-ruptured (intact) and ruptured tibiae (**Figure 3A**). Cross sections show that ruptures allowed escape of the bone marrow, resulting in decreased osmium staining compared to intact tibiae (**Figure 3A**). This loss of signal suggests that the ruptures might have confounded measurement of MAT volume. To address this, we quantified the volumes of cMAT, rMAT, and total MAT in female tibiae, comparing bones from non-TZD-treated mice (all of which were intact) with intact or ruptured bones from TZD-treated mice. The volume of cMAT did not differ between intact and ruptured bones (**Figure 3B**), indicating that these ruptures did not affect detection of cMAT in the distal tibia. However, in TZD-treated WT mice, the detectable volume of rMAT and total MAT was significantly lower in ruptured compared to intact bones (**Figure 3B**). Indeed, in both WT and *Ocn*-Wnt10b mice, TZD-induced expansion of rMAT and total MAT was strongly significant for intact bones, but not when ruptures were present (**Figure 3B**). This impaired rMAT detection likely explains why TZD-induced rMAT expansion was less marked in male than in female mice (**Figure 2B** vs. **Figure 2E**), because all male bones were ruptured. Importantly, for intact tibiae, TZD-induced expansion of rMAT and total MAT was significantly blunted in *Ocn*-Wnt10b compared to WT mice (**Figure 3B**). This suggests that, in addition to decreased cMAT (**Figures 2B,E**), *Ocn*-Wnt10b mice are at least mildly resistant to rMAT expansion during TZD treatment.

Adipocyte Transcript Expression in Tibiae Confirms TZD-Induced MAT Expansion

Given the confounding influence of these bone ruptures, we next pursued other approaches to further assess tibial MAT content. MAT expansion during CR or rosiglitazone treatment has previously been monitored by qPCR analysis of adipocyte marker expression in intact bones, including transcripts for adiponectin (*Adipoq*) and fatty acid-binding protein 4 (*Fabp4*) (3, 26). Thus, we next used qPCR to assess *Adipoq* and *Fabp4* expression in whole tibiae. As shown in **Figures 4A–D**, across all groups of female or males, expression of *Adipoq* and *Fabp4* was significantly affected by TZD treatment ($P < 0.0001$ for each). Multiple comparisons confirmed that 4- or 8-week TZD significantly increased *Adipoq* in WT males and females (**Figures 4A,C**) and *Fabp4* in males and females of each genotype (**Figures 4B,D**). TZD treatment for 2 weeks was also associated with increased *Adipoq* in *Ocn*-Wnt10b males (**Figure 4C**); increased *Fabp4* in WT females (**Figure 4B**); and increased *Fabp4* in males of each genotype (**Figure 4D**). Transcript expression within each TZD treatment group generally did not differ between WT and *Ocn*-Wnt10b mice, with the exception of decreased *Adipoq* in 4-week TZD females (**Figure 4A**) and decreased *Fabp4* in 8-week TZD males (**Figure 4D**). However, two-way ANOVA revealed that genotype significantly influenced *Fabp4* in females ($P = 0.0184$) and males ($P = 0.0339$), while there was a significant genotype–TZD interaction that influenced *Adipoq* expression in females ($P = 0.0193$) and males ($P = 0.0297$).

Collectively, these results suggest that TZD increases tibial adipocyte content and that there is some level of resistance to this effect in *Ocn*-Wnt10b mice. Thus, together with the osmium

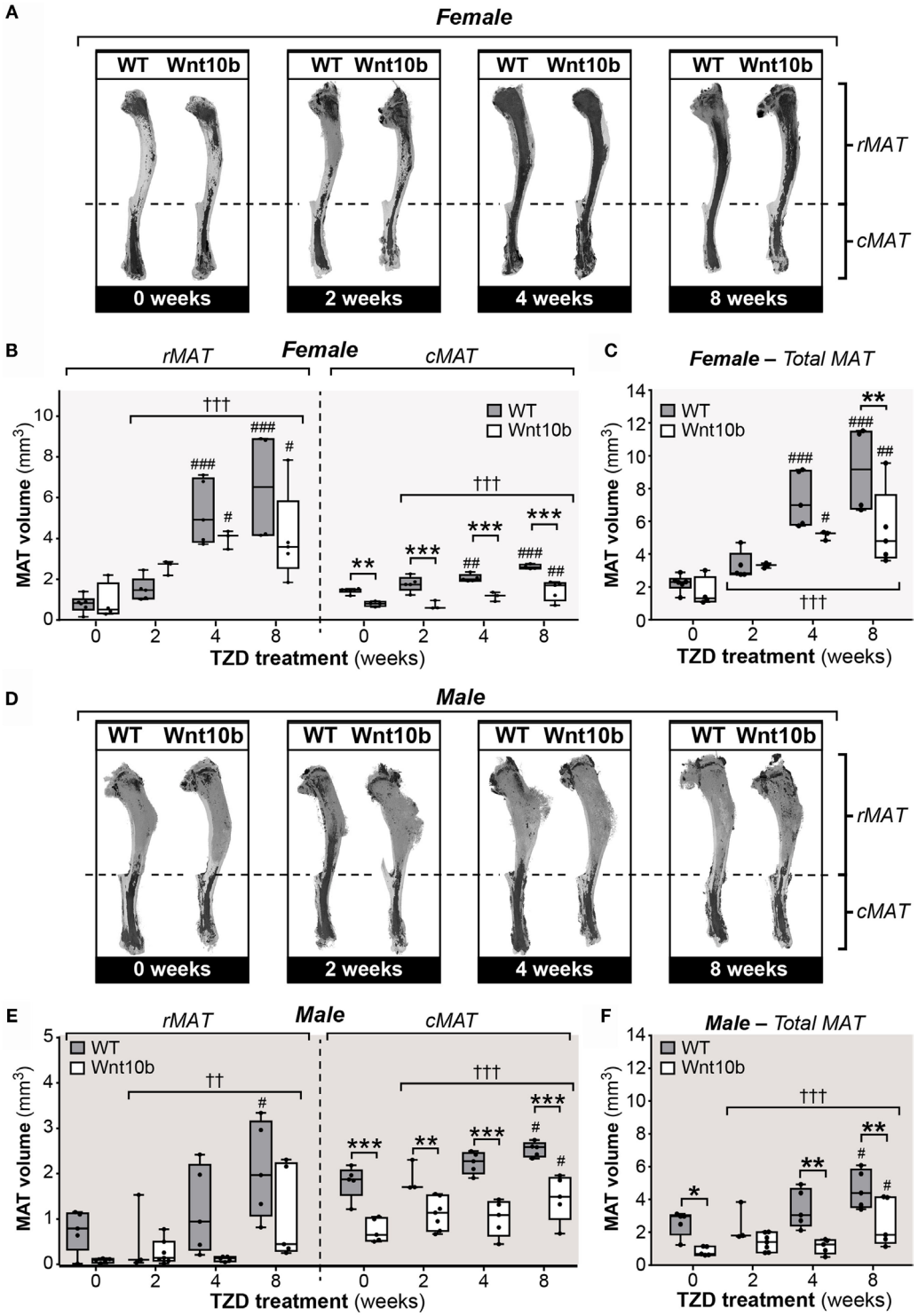

FIGURE 2 | **Rosiglitazone increases rMAT and cMAT volume in WT mice and cMAT expansion is blunted in *Ocn*-Wnt10b mice**. Male and female tibiae were dissected at necropsy. For each mouse, one tibia was decalcified in EDTA, stained with 1% osmium tetroxide, and analyzed by μCT scanning, as described in Section "Materials and Methods." **(A,D)** Representative μCT scans of stained tibiae from female **(A)** and male mice **(D)**. The dashed line indicates the tibia–fibula junction as the boundary between rMAT and cMAT. **(B,C,E,F)** For female **(B,C)** and male mice **(E,F)**, μCT scans were used to determine the volumes of rMAT (proximal to tibia–fibula junction), cMAT (distal to tibia–fibula junction), and total MAT (whole tibia), as indicated. In **(B,E)**, volumes of rMAT and cMAT are presented on the same *y*-axis scale. A significant influence of TZD treatment, across all treatment groups, is indicated by † ($P < 0.05$), †† ($P < 0.01$) or ††† ($P < 0.001$). Within each genotype, significant differences between TZD-treated mice and untreated controls are indicated by # ($P < 0.05$), ## ($P < 0.01$) or ### ($P < 0.001$). Within each TZD treatment group, statistically significant differences between WT and *Ocn*-Wnt10b mice are indicated by * ($P < 0.05$), ** ($P < 0.01$), or *** ($P < 0.001$).

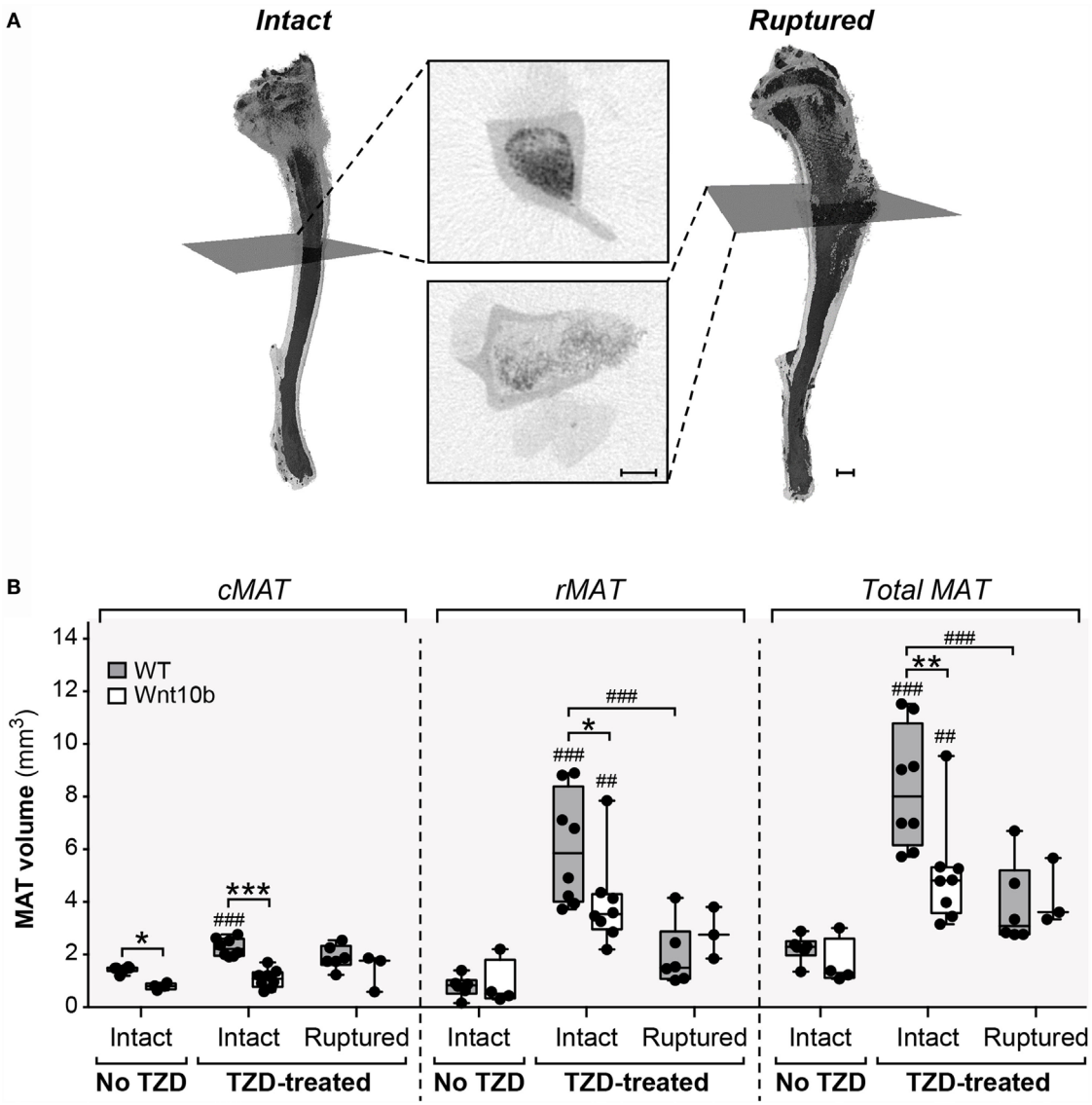

FIGURE 3 | **Cortical bone ruptures significantly decrease detectable rMAT volume**. All male and some female tibiae had ruptured cortical bone near the proximal end, causing a large reduction in signal. **(A)** Representative 3D models of intact (non-ruptured) and ruptured tibiae from 8-week-TZD-treated females, with cross-sectional images showing loss of MAT signal (dark regions within bone marrow cavity). Gray squares across the 3D models indicate the slices from which cross-sectional images are taken. Scale bars = 500 μm. **(B)** Tibiae from female WT or *Ocn*-Wnt10b mice were categorized into bones from mice untreated with TZD, all of which were intact; intact bones from TZD-treated mice; and ruptured bones from TZD-treated mice. The volume of cMAT, rMAT, and total MAT in these bones was determined from μCT scans. Statistically significant differences between untreated (intact), TZD-treated (intact), and TZD-treated (ruptured) samples are indicated by ## ($P < 0.01$) or ### ($P < 0.001$). Within each group, statistically significant differences between WT and *Ocn*-Wnt10b mice are indicated by * ($P < 0.05$), ** ($P < 0.01$), or *** ($P < 0.001$).

tetroxide analyses of MAT volume (**Figures 2** and **3**), it seems likely that *Ocn*-Wnt10b mice partially resist TZD-induced MAT expansion, but this is not prevented entirely.

TZD Induces Hyperadiponectinemia to a Similar Extent in WT and *Ocn*-Wnt10b Mice

Given this mild resistance of *Ocn*-Wnt10b mice to MAT expansion, we next investigated if TZD-induced hyperadiponectinemia was altered in these mice. To do so, we used an ELISA to measure serum adiponectin concentrations. Across both genotypes and all TZD groups, treatment with TZD was associated with significantly increased circulating adiponectin ($P < 0.0001$ for males or females) (**Figure 5**). Genotypic differences were not detected in males; however, in females, there was a significant influence of genotype ($P = 0.0466$) and a significant interaction between genotype and TZD treatment ($P = 0.0248$), indicating that effects of TZD differ between WT and *Ocn*-Wnt10b females. Consistent with this, multiple comparisons showed significantly

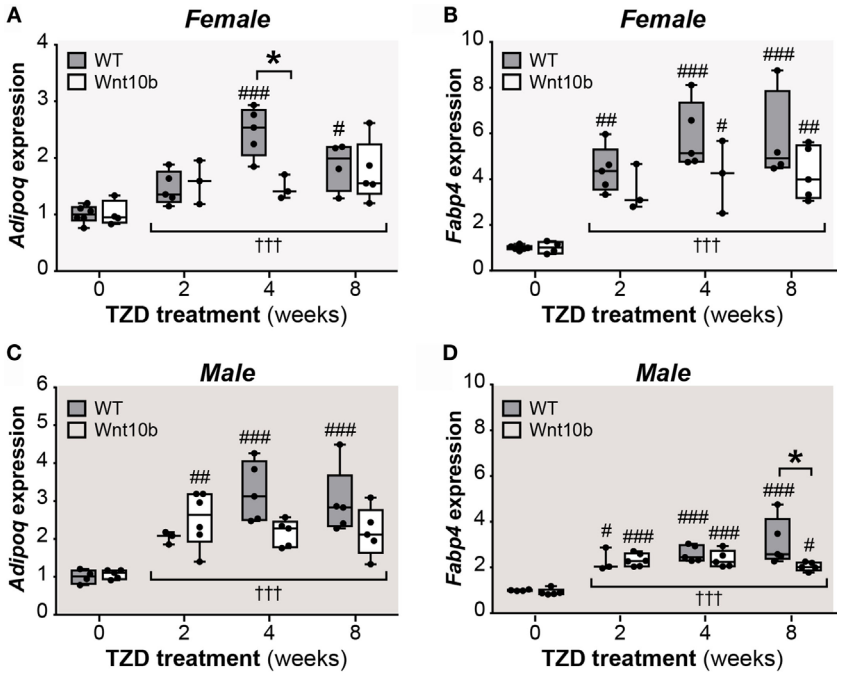

FIGURE 4 | TZD increases adipocyte marker expression in tibiae, suggesting MAT expansion. Male and female tibiae were dissected at necropsy, and total RNA was isolated from one tibia of each mouse. Expression of *Adipoq* **(A,C)** and *Fabp4* transcripts **(B,D)** in female and male mice was determined by qPCR and is presented normalized *Ppia* mRNA expression. Statistical significance is presented, as described in **Figure 2**, for the influence of TZD across all groups, and for differences between TZD-treated and untreated mice (within each genotype) or WT and *Ocn*-Wnt10b mice (within each TZD group).

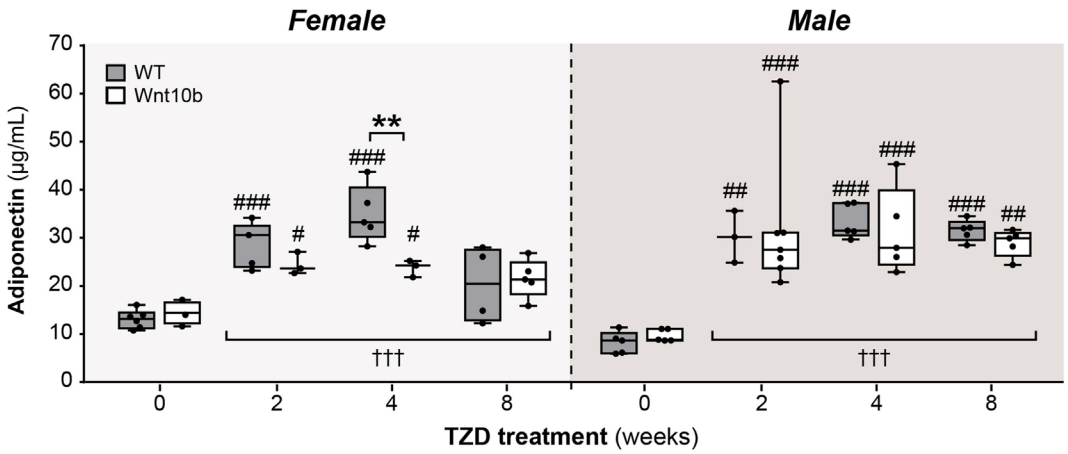

FIGURE 5 | TZD induces hyperadiponectinemia to a similar extent in WT and *Ocn*-Wnt10b mice. Serum was isolated from mice at 30 weeks of age and ELISA used to determine concentrations of total adiponectin in female and male mice, as indicated. For each sex, statistical significance for the influence of TZD across all groups, and for differences between TZD-treated and untreated mice (within each genotype) or WT and *Ocn*-Wnt10b mice (within each TZD group), are presented as described for **Figure 2**.

decreased circulating adiponectin in *Ocn*-Wnt10b compared to WT females following 4 weeks' TZD (**Figure 5**). Thus, while TZD-induced hyperadiponectinemia was similar between WT and *Ocn*-Wnt10b males, this effect of TZD was mildly blunted in female *Ocn*-Wnt10b mice.

TZD Increases Adiponectin Protein Expression in WAT

The above observations demonstrate that, despite having significantly decreased cMAT and being partially resistant to TZD-induced rMAT expansion, *Ocn*-Wnt10b mice undergo

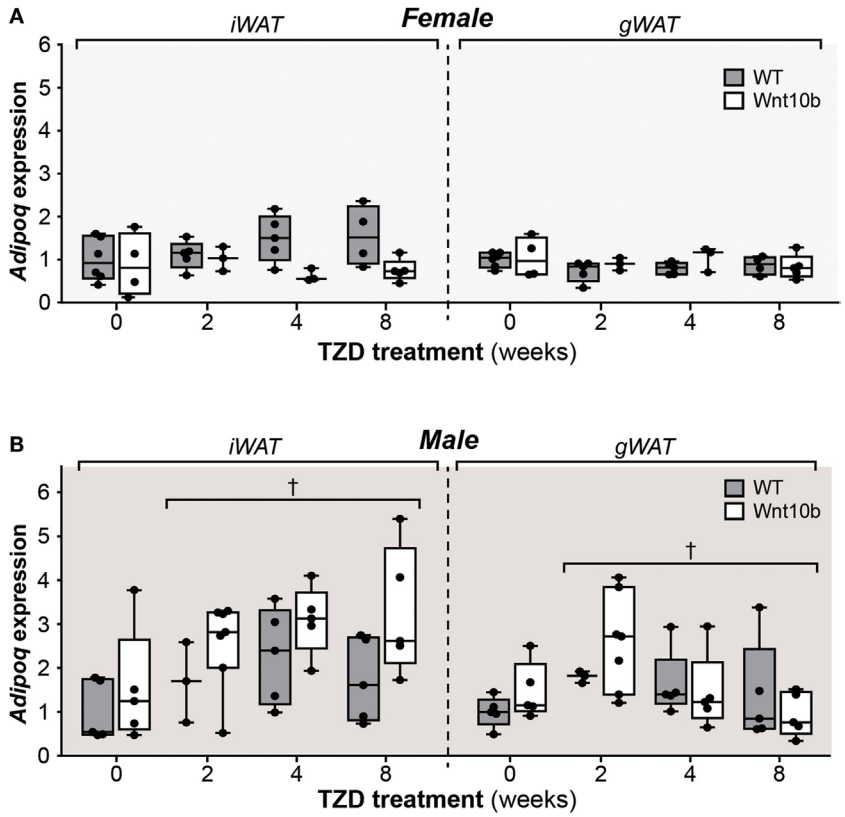

FIGURE 6 | **Rosiglitazone treatment or Wnt10b transgene expression does not alter adiponectin transcript expression in WAT**. At necropsy, iWAT and gWAT were dissected, and total RNA was isolated from portions of each tissue. Expression of *Adipoq* in female **(A)** and male mice **(B)** was determined by qPCR and is presented normalized *Ppia* mRNA expression. Across all groups, statistically significant effects of TZD are presented as described for **Figure 2**, while significant effects of genotype are described in the text. There were no statistically significant differences between TZD-treated and untreated mice (within each genotype) or between WT and *Ocn*-Wnt10b mice (within each TZD group), as determined by two-way ANOVA.

hyperadiponectinemia to a similar extent to their WT counterparts. Thus, factors beyond MAT might have a greater influence over TZD-induced hyperadiponectinemia. To address this possibility, we next investigated the effects of TZD and genotype on adiponectin expression in WAT. In WT and *Ocn*-Wnt10b females, TZD did not influence *Adipoq* expression in iWAT or gWAT, either when comparing individual treatment durations or when effects were assessed across all groups (**Figure 6A**). However, in female iWAT, *Adipoq* transcripts varied significantly by genotype ($P = 0.0095$), with expression diverging as TZD duration increased (**Figure 6A**). Given that Wnt10b transgene expression is restricted to osteoblasts, this genotypic difference in WAT was unexpected. Across all groups of males, TZD treatment had a minor influence on *Adipoq* transcript levels in both iWAT and gWAT ($P = 0.0269$ and $P = 0.0461$, respectively), although multiple comparisons found no significant effects of TZD between individual treatment groups (**Figure 6B**). As for females, male iWAT also exhibited genotypic variation ($P = 0.0096$), although in this case *Adipoq* expression tended to be greater in *Ocn*-Wnt10b than in WT mice (**Figure 6B**).

These findings show that WAT *Adipoq* expression is influenced only modestly by TZD, in contrast to the marked TZD-mediated increases in circulating adiponectin (**Figure 5**). Indeed, our above observations in female mice are consistent with previous reports demonstrating that TZDs can increase circulating adiponectin without increasing *Adipoq* expression in WAT (23, 24). However, other studies have reported a disparity between adiponectin expression at the transcript and protein level (32, 33). Therefore, we next used fluorescence-based immunoblotting to detect and quantify adiponectin protein expression. As shown in **Figure 7A**, across all groups of female mice, there was a significant influence of TZD on adiponectin protein expression in iWAT and gWAT ($P < 0.0001$ for both), with adiponectin typically increased in WAT of TZD-treated mice compared to untreated controls. Multiple comparisons further confirmed that, for females of each genotype, TZD treatment for 2 or 8 weeks significantly increased adiponectin protein in gWAT or iWAT, respectively (**Figure 7A**). As for females, across all groups of male mice, TZD had a significant influence on adiponectin protein in iWAT ($P = 0.004$) and gWAT ($P = 0.0004$) (**Figure 7B**). Based on multiple comparisons, adiponectin was significantly elevated in iWAT and gWAT of WT males after 2 weeks of TZD, and in gWAT of *Ocn*-Wnt10b males after 2 or 4 weeks of TZD (**Figure 7B**). These results demonstrate that rosiglitazone significantly increases expression

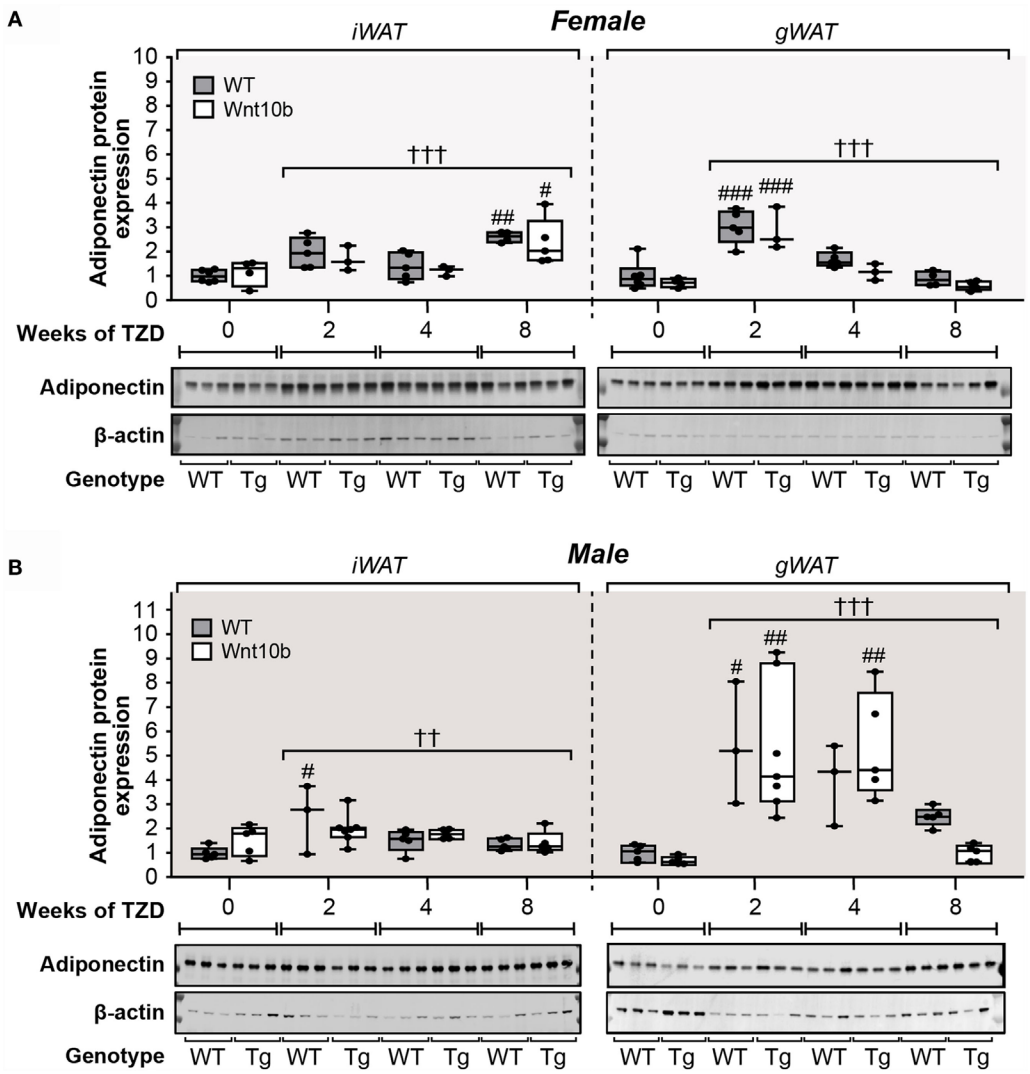

FIGURE 7 | **Rosiglitazone increases adiponectin protein expression in WAT in a depot- and sex-specific manner**. At necropsy, iWAT and gWAT were dissected, and total protein was isolated from portions of each tissue. Lysates were separated by SDS-PAGE and expression of adiponectin protein determined by immunoblotting; β-actin expression was analyzed as a loading control. Immunoblots shown in **(A,B)** are representative of three mice per group. Samples from *Ocn*-Wnt10b mice are labeled "Tg." Band intensities from these blots and further blots of the remaining samples were quantified using Image Studio Lite software. Adiponectin expression was then normalized to expression of β-actin for **(A)** Males and **(B)** Females, with representative blots shown beneath. For each sex, statistically significant differences between TZD-treated and untreated mice (within each genotype) or between WT and *Ocn*-Wnt10b mice (within each TZD group) are presented as described for **Figure 2**.

of adiponectin protein in WAT of female and male mice. Thus, it seems likely that, with this regimen of rosiglitazone treatment, WAT makes at least a partial contribution to TZD-induced hyperadiponectinemia.

TZD Induces UCP1 Protein Expression in BAT but Not in WAT or Tibiae

While these studies focused on the relationship between MAT and adiponectin, they also provided the opportunity to assess other properties of MAT; indeed, it remains unclear to what extent MAT's characteristics overlap with those of WAT and BAT. The key function of BAT is to mediate adaptive thermogenesis *via* uncoupled respiration, which is dependent on expression of uncoupling protein 1 (UCP1). TZDs dose-dependently increase UCP1 protein and *Ucp1* transcripts in BAT and can upregulate *Ucp1* in WAT and whole tibiae (26, 34). Based on the latter, it has been suggested that MAT may have BAT-like characteristics (26). However, others have argued that elevated *Ucp1* expression alone, without assessment of UCP1 protein, is insufficient evidence for a tissue's thermogenic capacity (35). Indeed, the relative protein expression of UCP1 between MAT and BAT remains to be firmly established. Thus, to further study the BAT-like properties of MAT, we next analyzed UCP1 expression in BAT, WAT, and tibiae, both at the transcript and protein level.

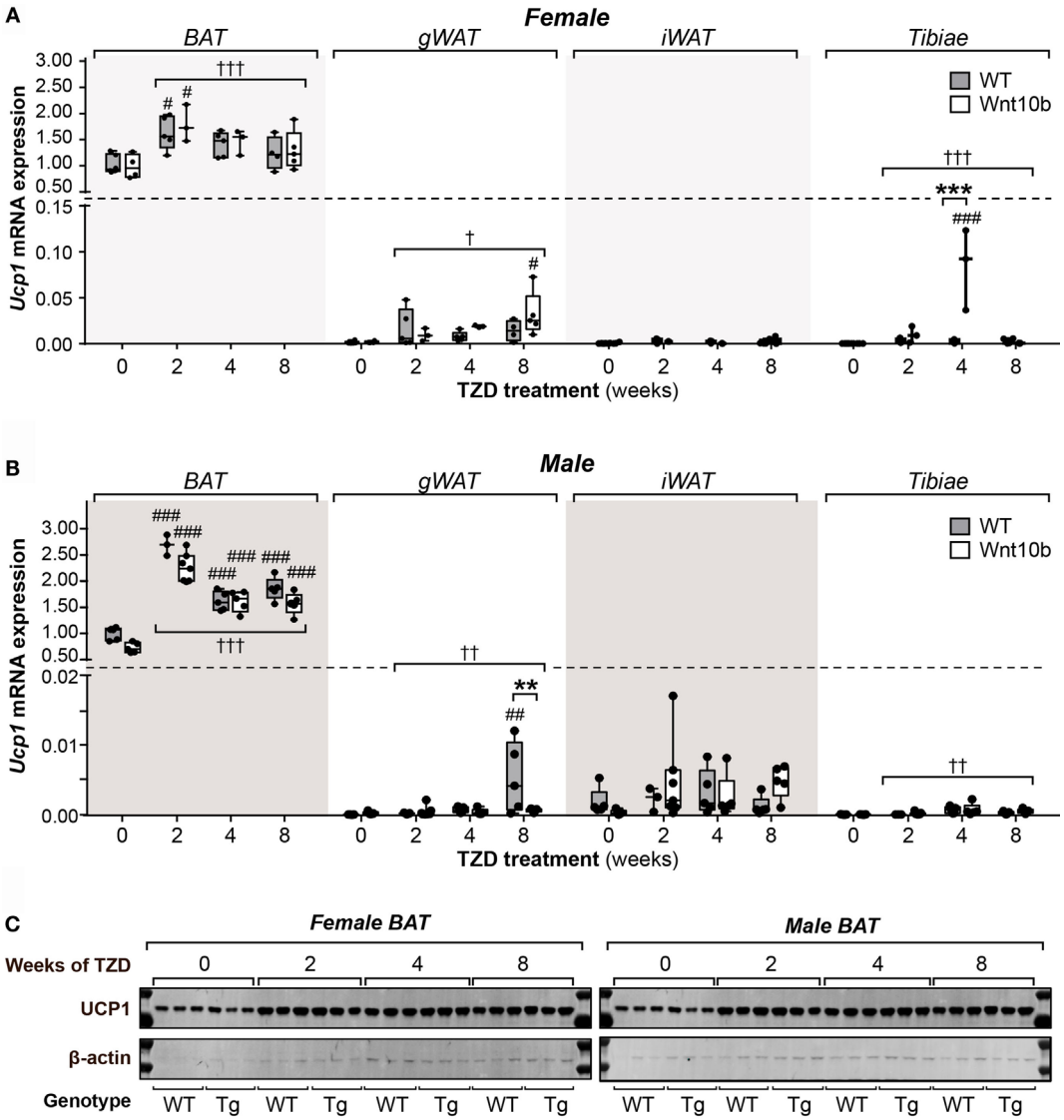

FIGURE 8 | Rosiglitazone increases UCP1 mRNA and protein in BAT not in WAT or tibiae. Total RNA and protein were isolated from interscapular BAT, gWAT, iWAT, and whole tibiae. **(A,B)** *Ucp1* transcript expression in each tissue of female **(A)** and male mice **(B)** was quantified by qPCR and normalized to expression of *Ppia* mRNA. In each tissue, statistically significant differences between TZD-treated and untreated mice (within each genotype) or between WT and *Ocn*-Wnt10b mice (within each TZD group) were determined by two-way ANOVA and are presented as described for **Figure 2**. **(C)** Protein lysates from BAT were separated by SDS-PAGE and expression of UCP1 protein determined by immunoblotting; β-actin expression was analyzed as a loading control. Immunoblots are representative of three mice per group. Samples from *Ocn*-Wnt10b mice are labeled "Tg." UCP1 protein could not be detected in gWAT, iWAT, or tibiae (data not shown).

As shown in **Figures 8A,B**, across all groups of female or male mice, TZD strongly influenced *Ucp1* expression in BAT (females, $P = 0.0002$; males, $P < 0.0001$). Multiple comparisons further confirmed that, relative to untreated controls, each duration of TZD significantly increased BAT *Ucp1* in males of each genotype (**Figure 8B**), while this also occurred for females with 2 weeks' TZD treatment (**Figure 8A**). Across-group effects of TZD were also detected in female gWAT ($P = 0.014$), female tibiae ($P < 0.0001$), male gWAT ($P = 0.0051$), and male tibiae ($P = 0.0017$), wherein TZD-treated groups typically had greater *Ucp1* expression than untreated controls (**Figures 8A,B**). Analysis of genotypic differences *via* multiple comparisons confirmed that, relative to untreated mice, *Ucp1* was significantly elevated in *Ocn*-Wnt10b female tibiae or gWAT after 4 or 8 weeks' TZD, respectively, and in WT male gWAT, after 8 weeks' TZD (**Figures 8A,B**). Each of these groups also had significantly greater *Ucp1* expression than their untreated WT or *Ocn*-Wnt10b counterparts, respectively; however, such genotypic differences were uncommon, and genotype generally did not influence *Ucp1* expression in any of the tissues analyzed.

These data demonstrate that rosiglitazone increases *Ucp1* expression in BAT, gWAT, and tibiae, consistent with results in previous studies (26, 34). However, relative to expression in BAT, *Ucp1* expression in untreated mice was over 500-fold lower in gWAT, 1,500-fold lower in iWAT, and 10,000-fold lower in tibiae (**Figures 8A,B**). Thus, even with TZD treatment, *Ucp1* expression in these tissues is negligible, raising questions over its functional relevance. To further address this, we next analyzed UCP1 expression at the protein level. As shown in **Figure 8C**, in females and males of either genotype, TZD robustly increased UCP1 expression in BAT; however, in gWAT, iWAT, or whole tibiae, we could not detect UCP1 protein expression (data not shown). Together, these observations suggest that MAT is unlikely to possess the thermogenic properties of BAT.

DISCUSSION

Herein, we pursued studies in *Ocn*-Wnt10b mice to investigate the hypothesis that MAT expansion contributes to TZD-induced hyperadiponectinemia. We found that, regardless of TZD treatment, *Ocn*-Wnt10b mice have significantly less cMAT than WT mice and likely resist TZD-induced rMAT accumulation. Despite this loss of cMAT and mild resistance to rMAT expansion, circulating adiponectin is generally similar between WT and *Ocn*-Wnt10b mice. Moreover, we found that TZD significantly increases adiponectin protein expression in WAT. Together, these findings suggest that WAT, rather than MAT, is the key mediator of TZD-induced hyperadiponectinemia, at least under these conditions of TZD treatment. However, as discussed in Section "Contribution of MAT and WAT to TZD-Induced Hyperadiponectinemia," further consideration of these findings suggests that MAT makes at least some contribution to TZD-induced hyperadiponectinemia. As a secondary aim, we also addressed the hypothesis that MAT has BAT-like properties. We found that, in contrast to BAT, UCP1 protein is undetectable in tibiae, suggesting that MAT is unlikely to have the thermogenic capacity of BAT.

As further discussed below, these findings shed new light on the function of MAT and have implications worth considering for future MAT research.

Contribution of MAT and WAT to TZD-Induced Hyperadiponectinemia

We previously identified MAT as a source of increased circulating adiponectin during CR, a conclusion based, in part, on the finding that *Ocn*-Wnt10b mice resist both CR-associated MAT expansion and hyperadiponectinemia (2, 3).

Herein, we find that, regardless of TZD treatment, cMAT volume is significantly lower in *Ocn*-Wnt10b than in WT mice. Unfortunately, tibial ruptures confounded measurement of rMAT volume; however, analysis of intact tibiae, without ruptured samples, suggests strongly that *Ocn*-Wnt10b mice also partially resist rMAT accumulation in response to TZD treatment. Despite this loss of cMAT and mild resistance to rMAT expansion, circulating adiponectin is generally similar between WT and *Ocn*-Wnt10b mice. Superficially, this suggests that MAT expansion *per se* does not contribute to hyperadiponectinemia under these TZD treatment conditions. However, this conclusion is less certain when several other key factors are taken into account.

One such factor is the likely contribution of WAT. Unlike during CR, adiponectin protein expression in WAT is increased under these conditions of TZD treatment, which may override any effects of suppressed MAT expansion. These increases are more pronounced for adiponectin protein than for *Adipoq* transcripts, with TZD affecting the *Adipoq* transcripts only in male WAT (**Figure 6**). These findings echo previous reports of sex-specific differences in WAT adiponectin expression, and of a disconnect between adiponectin expression at the transcript and protein level (32, 33). Notably, these effects on WAT are inconsistent with the finding that TZDs can increase circulating adiponectin without increasing adiponectin expression in WAT (23, 24). This disparity is likely a result of the higher dose of rosiglitazone used in our study. Indeed, WAT adiponectin expression is unaltered by lower TZD doses (24, 36) but significantly increased at higher rosiglitazone concentrations (18). Thus, as discussed further below ("Implications of TZD Dose on the Capacity of *Ocn*-Wnt10b Mice to Resist MAT Expansion and Hyperadiponectinemia"), a lower dose of rosiglitazone would likely be required if we were to further investigate the contribution of MAT to TZD-associated hyperadiponectinemia.

Considering these findings, it seems likely that WAT makes at least some contribution to hyperadiponectinemia under these conditions of rosiglitazone treatment. However, the effect of TZD on WAT adiponectin expression (**Figures 6** and **7**) is far less consistent and pronounced than that which occurs for circulating adiponectin concentrations (**Figure 5**). In contrast, these changes in circulating adiponectin are closely reflected by the increases in tibial adiponectin expression (**Figure 4**). For example, when comparing *Ocn*-Wnt10b and WT mice, circulating adiponectin is lower only in the 4-week TZD females (**Figure 5**); hence, it is striking that this is also the only group in which tibial adiponectin expression is lower in *Ocn*-Wnt10b mice (**Figure 4A**). Together, these observations show that circulating adiponectin is closely associated with tibial adiponectin expression and less tightly associated with gross changes in rMAT and cMAT volume. This underscores the importance of analyzing MAT through multiple approaches, including transcriptional markers, rather than focusing solely on MAT volume *via* osmium tetroxide staining. Perhaps, more importantly, this close association suggests that adiponectin production from MAT contributes, at least in part, to TZD-induced hyperadiponectinemia.

Implications of TZD Dose on the Capacity of *Ocn*-Wnt10b Mice to Resist MAT Expansion and Hyperadiponectinemia

Previous studies have used a wide range of doses of rosiglitazone to investigate its impact on adiponectin or bone marrow adiposity. For example, Nawrocki et al. treated mice with 10 mg/kg/day to examine the effects on circulating adiponectin and glucose homeostasis (20), while 20 mg/kg/day was used in two more recent studies investigating effects of rosiglitazone on bone marrow adiposity (26, 27). A much lower dose of 3 mg/kg/day was also found to cause MAT expansion in mice, but whether

this promotes hyperadiponectinemia was not reported (28, 37). Thus, in the present study, we used 15 mg/kg/day to ensure robust effects on MAT and circulating adiponectin. As in the above studies (26–28), we did so by administering rosiglitazone in the diet, based on measurements of body mass and estimated daily food intake. However, because of variation in body masses and daily food consumption, some mice may have exceeded the target dose of 15 mg/kg/day. As discussed above, this relatively high dose may explain the increased adiponectin expression in WAT, thereby complicating interpretation of any contribution from MAT. Such high doses may also have overwhelmed the ability of *Ocn*-Wnt10b mice to more robustly resist MAT expansion. Thus, a lower rosiglitazone dose may limit these confounding effects and thereby be more suitable for addressing our hypothesis in *Ocn*-Wnt10b mice.

Limitations of *Ocn*-Wnt10b Mice as a Model Resistant to MAT Expansion

One reason that we have not pursued such follow-up studies is that *Ocn*-Wnt10b mice may be too limited a model in which to robustly address MAT's endocrine functions. For example, while CR- or TZD-induced MAT expansion is blunted in these mice, such expansion is still marked in comparison to untreated *Ocn*-Wnt10b controls (**Figures 2** and **3**) (3). Moreover, distal tibiae of *Ocn*-Wnt10b mice remain laden with MAT (**Figures 2A,D**) and, while cMAT volume is lower in *Ocn*-Wnt10b mice, this likely reflects restrictions imposed by decreased bone marrow volume (3), rather than resulting from a direct inhibition of adipogenesis. Thus, as we have recently argued elsewhere (7), future research of MAT would benefit enormously from development of new mouse models that more robustly resist MAT formation, developmentally and/or in response to CR, TZDs, or other stimuli that promote MAT expansion.

Confounding Effects of Bone Ruptures on Osmium Tetroxide-Based rMAT Analysis

The present study reveals that cortical bone ruptures can confound osmium-based MAT detection. This issue, which has not been reported previously, provides further support for taking a multifaceted approach to MAT analysis. While TZDs can cause bone loss and fractures (38), it is unlikely that the ruptures occurred *in vivo* over the course of rosiglitazone treatment: such an injury would have dramatically impacted mobility and behavior of the mice, which was not apparent during daily inspections; and the ruptures also occurred in tibiae of males untreated with rosiglitazone, demonstrating that they are not a consequence of TZD treatment. Instead, it is likely that ruptures occurred *ex vivo* as a result of methodological issues. In particular, after fixing tibiae in formalin post-necropsy there was a very long time span, ~30 months, before most of these bones were decalcified and analyzed by osmium tetroxide staining. This holdup largely resulted from delays associated with one of our lead authors moving to a new institution, during which time the fixed tibiae were stored in PBS at 4°C and shipped by air from the USA to the UK. Although these storage conditions would not be expected to promote cortical ruptures, it is notable that no ruptures occurred in a subset of female tibiae that were stored in PBS for a shorter duration (~12 months), without air transport, before decalcification and osmium analysis. Moreover, at both the University of Michigan and the University of Edinburgh, we have analyzed hundreds of osmium-stained mouse bones from other studies, none of which has undergone such long-term storage or air transport, and among which no ruptures have ever been detected. Thus, one possibility is that exposure to low air pressure during air transport can cause a pressure differential that promotes bone ruptures. It remains possible that other factors also contributed to this phenomenon; however, our findings strongly suggest that fixed bones should not undergo long-term storage or exposure to low atmospheric pressure if MAT volume is to be determined accurately using osmium tetroxide staining.

BAT-Like Thermogenic Function Is Unlikely in MAT

There is extensive interest in "beige" or "brite" (brown-in-white) adipocytes, which develop in WAT in response to diverse external stimuli, including cold exposure or TZD treatment, and which share some properties of brown adipocytes (39–41). This so-called "browning" of WAT can increase energy consumption and may thereby contribute to TZD-associated improvement in metabolic health. Therefore, whether MAT can also undergo browning or has BAT-like characteristics has been a subject of some interest. Krings et al. found that, in mice treated for 4 weeks with rosiglitazone (20 mg/kg/day), transcript expression of brown adipocyte markers is increased in tibiae, supporting the possibility that MAT has BAT-like characteristics (26). This is consistent with our finding that rosiglitazone influences tibial *Ucp1* mRNA expression (**Figure 8**). However, Krings et al. further highlighted that, compared to BAT, *Ucp1* expression is 16,000-fold lower in tibiae, which agrees closely with our data showing a 10,000- to 25,000-fold decrease in tibiae compared to BAT. In addition, even with rosiglitazone treatment, we find that *Ucp1* transcripts remain 400- to 7,000-fold lower in tibiae than in BAT (**Figures 8A,B**). Crucially, at this level of *Ucp1* expression, we could not detect UCP1 protein, whereas rosiglitazone-induced increases in UCP1 protein in BAT are readily detectable (**Figure 8C**).

UCP1 is the hallmark of brown adipocytes and the key mediator of adaptive thermogenesis, and therefore the above findings strongly suggest that bone marrow adipocytes are unlikely to possess BAT-like thermogenic properties. One limitation of our study, and that of Krings et al., is that we analyzed whole bones rather than isolated marrow adipocytes. However, both brown and beige adipocytes are further defined by their high mitochondrial content and the multilocular morphology of their lipid droplets (41), neither of which is observed in bone marrow adipocytes (3, 4, 12, 42). This raises further doubts about the notion that MAT has BAT-like characteristics, an issue that we recently discussed in greater depth elsewhere (5). Nevertheless, it remains possible that, under a different TZD treatment regimen or in response to other stimuli, MAT is capable of undergoing browning. Indeed, while we were unable to detect UCP1 protein in WAT or whole tibiae, previous studies have detected UCP1 in

WAT following TZD treatment (41). Moreover, effects of TZDs on *Ucp1* expression in BAT are dose-dependent (34). This supports the possibility that TZD-mediated browning of WAT and MAT requires an optimal regimen of TZD treatment, in which case the conditions in our study may simply have been unsuitable for inducing a browning response. Thus, there is ample scope for future studies to further investigate whether MAT has BAT-like properties, both at the molecular and functional levels.

Other Strengths and Limitations of This Study

This study is the first to address the novel hypothesis that MAT contributes to hyperadiponectinemia in conditions beyond CR. The experimental design is strengthened by including both male and female mice, as well as by analysis of several durations of TZD treatment. The discovery of the confounding effects of cortical ruptures is partly a strength, in that it highlights an important technical consideration for future MAT research; however, presently this was a limitation because it prevented thorough measurement of rMAT volume. As discussed above, another limitation is that the dose of rosiglitazone may have been too high, and may have varied slightly between mice because of differences in body mass and daily food intake. Administration of lower doses by daily injection or oral gavage could be one approach to overcome this issue. Finally, a key limitation of this study is that our findings are based on only a single cohort of mice. Ideally, these experiments would be repeated in a second cohort, with particular care taken to avoid cortical ruptures; this would allow more robust determination of rMAT volume in *Ocn*-Wnt10b mice. However, as noted above ("Limitations of *Ocn*-Wnt10b Mice as a Model Resistant to MAT Expansion"), *Ocn*-Wnt10b mice may not be sufficiently robust as a model of impaired MAT formation. For example, adipocyte marker expression in tibiae is generally similar between WT and *Ocn*-Wnt10b mice (**Figure 4**). This limitation of the *Ocn*-Wnt10b model undermines the rationale for repeating the present studies in a second cohort. Instead, we feel strongly that it would be more productive and scientifically beneficial to focus efforts on developing new mouse models that more robustly resist MAT expansion. Such models could then be used to better address the present hypothesis, as well as other aspects of MAT function.

Beyond these particular issues, one broader limitation is that our experiments were based only in mice; it remains unclear if the relationship between TZD-induced MAT expansion and hyperadiponectinemia also exists in humans. It is well established that TZDs increase circulating adiponectin in humans (16), but their effects on MAT are less clear. Indeed, one study finds that rosiglitazone *decreases* bone marrow adiposity in the lumbar vertebrae (43), whereas a more recent report finds that pioglitazone, another TZD, increases femoral and lumbar vertebral bone marrow adiposity (44). Unfortunately, neither of these studies assessed circulating adiponectin, and there remain very few clinical studies assessing the effect of TZDs on MAT. Thus, there is a strong rationale for future research to establish how TZDs affect MAT accumulation in humans and whether this is associated with changes in circulating adiponectin.

CONCLUSION

There are four main conclusions from our study. First, under these TZD treatment conditions, it is likely that both WAT and MAT make some contribution to TZD-induced hyperadiponectinemia. Second, UCP1 expression in MAT is negligible, and therefore MAT is unlikely to have the thermogenic capacity of BAT. Third, cortical bone ruptures confound measurement of MAT volume by osmium tetroxide staining, and therefore care must be taken when processing bones for such analysis. Moreover, osmium-based assessment of MAT volume can differ from measurement of MAT content based on expression of bone marrow adipocyte transcripts; hence, multiple approaches should be used to assess MAT content, including analysis of molecular markers, rather than relying solely on osmium tetroxide staining. Finally, while *Ocn*-Wnt10b mice have been useful as a model resistant to MAT formation, development of more robust loss-of-MAT models would be of great benefit to future MAT research.

AUTHOR CONTRIBUTIONS

RS and WC designed all figures and wrote the manuscript, with ES, HM, and OM providing additional critical revisions. WC, BL, ES, VK, and OM contributed to the conception and design of the experiments. BL oversaw mouse breeding and colony management. RS, BL, BZ, ES, SP, BS, HM, AB, RW, OM, and WC contributed to data acquisition, analysis, and/or interpretation. All authors gave final approval for publication of the manuscript and agree to be accountable for all aspects of the work presented herein.

FUNDING

This work was supported by grants from the National Institutes of Health (R24 DK092759 to OM; K99-DE024178 to ES; R25 DK088752 to BZ; S10-RR026475-01 to the University of Michigan School of Dentistry microCT Core; and P30 DK089503 to the Michigan Nutrition Obesity Research Center, which oversaw NMR analysis of mouse body composition and provided a Pilot/Feasibility grant to HM). RS is supported by a British Heart Foundation 4-year PhD Studentship. WC is supported by a Career Development Award (MR/M021394/1) from the Medical Research Council (UK) and by a Chancellor's Fellowship from the University of Edinburgh, and previously by a Lilly Innovation Fellowship Award and a Postdoctoral Research Fellowship from the Royal Commission for the Exhibition of 1851 (UK). SP and BS were supported by a Training Grant from the University of Michigan Training Program in Organogenesis (T32-HD007505). Analysis of microCT imaging data was supported by a Bioinformatics Award provided through a British Heart Foundation Centre of Research Excellence grant.

REFERENCES

1. Rosen ED, Spiegelman BM. What we talk about when we talk about fat. *Cell* (2014) 156(1–2):20–44. doi:10.1016/j.cell.2013.12.012
2. Scheller EL, Burr AA, MacDougald OA, Cawthorn WP. Inside out: bone marrow adipose tissue as a source of circulating adiponectin. *Adipocyte* (2016) 5(3):251–69. doi:10.1080/21623945.2016.1149269
3. Cawthorn WP, Scheller EL, Learman BS, Parlee SD, Simon BR, Mori H, et al. Bone marrow adipose tissue is an endocrine organ that contributes to increased circulating adiponectin during caloric restriction. *Cell Metab* (2014) 20(2):368–75. doi:10.1016/j.cmet.2014.06.003
4. Scheller EL, Doucette CR, Learman BS, Cawthorn WP, Khandaker S, Schell B, et al. Region-specific variation in the properties of skeletal adipocytes reveals regulated and constitutive marrow adipose tissues. *Nat Commun* (2015) 6:7808. doi:10.1038/ncomms8808
5. Scheller EL, Cawthorn WP, Burr AA, Horowitz MC, MacDougald OA. Marrow adipose tissue: trimming the fat. *Trends Endocrinol Metab* (2016) 27(6):392–403. doi:10.1016/j.tem.2016.03.016
6. Suchacki KJ, Cawthorn WP, Rosen CJ. Bone marrow adipose tissue: formation, function and regulation. *Curr Opin Pharmacol* (2016) 28:50–6. doi:10.1016/j.coph.2016.03.001
7. Sulston RJ, Cawthorn WP. Bone marrow adipose tissue as an endocrine organ: close to the bone? *Horm Mol Biol Clin Investig* (2016). doi:10.1515/hmbci-2016-0012
8. Zhang Y, Proenca R, Maffei M, Barone M, Leopold L, Friedman JM. Positional cloning of the mouse obese gene and its human homologue. *Nature* (1994) 372(6505):425–32. doi:10.1038/372425a0
9. Scherer PE, Williams S, Fogliano M, Baldini G, Lodish HF. A novel serum protein similar to C1q, produced exclusively in adipocytes. *J Biol Chem* (1995) 270(45):26746–9. doi:10.1074/jbc.270.45.26746
10. Hu E, Liang P, Spiegelman BM. AdipoQ is a novel adipose-specific gene dysregulated in obesity. *J Biol Chem* (1996) 271(18):10697–703. doi:10.1074/jbc.271.18.10697
11. Devlin MJ. Why does starvation make bones fat? *Am J Hum Biol* (2011) 23(5):577–85. doi:10.1002/ajhb.21202
12. Cawthorn WP, Scheller EL, Parlee SD, Pham HA, Learman BS, Redshaw CM, et al. Expansion of bone marrow adipose tissue during caloric restriction is associated with increased circulating glucocorticoids and not with hypoleptinemia. *Endocrinology* (2016) 157(2):508–21. doi:10.1210/en.2015-1477
13. Bennett CN, Ouyang H, Ma YL, Zeng Q, Gerin I, Sousa KM, et al. Wnt10b increases postnatal bone formation by enhancing osteoblast differentiation. *J Bone Miner Res* (2007) 22(12):1924–32. doi:10.1359/jbmr.070810
14. Zgheib S, Mequinion M, Lucas S, Leterme D, Ghali O, Tolle V, et al. Long-term physiological alterations and recovery in a mouse model of separation associated with time-restricted feeding: a tool to study anorexia nervosa related consequences. *PLoS One* (2014) 9(8):e103775. doi:10.1371/journal.pone.0103775
15. Lehmann JM, Moore LB, Smith-Oliver TA, Wilkison WO, Willson TM, Kliewer SA. An antidiabetic thiazolidinedione is a high affinity ligand for peroxisome proliferator-activated receptor γ (PPARγ). *J Biol Chem* (1995) 270(22):12953–6. doi:10.1074/jbc.270.22.12953
16. Yki-Jarvinen H. Thiazolidinediones. *N Engl J Med* (2004) 351(11):1106–18. doi:10.1056/NEJMra041001
17. Cabre A, Lazaro I, Girona J, Manzanares JM, Marimon F, Plana N, et al. Fatty acid binding protein 4 is increased in metabolic syndrome and with thiazolidinedione treatment in diabetic patients. *Atherosclerosis* (2007) 195(1):e150–8. doi:10.1016/j.atherosclerosis.2007.04.045
18. Maeda N, Takahashi M, Funahashi T, Kihara S, Nishizawa H, Kishida K, et al. PPARgamma ligands increase expression and plasma concentrations of adiponectin, an adipose-derived protein. *Diabetes* (2001) 50(9):2094–9. doi:10.2337/diabetes.50.9.2094
19. Yu JG, Javorschi S, Hevener AL, Kruszynska YT, Norman RA, Sinha M, et al. The effect of thiazolidinediones on plasma adiponectin levels in normal, obese, and type 2 diabetic subjects. *Diabetes* (2002) 51(10):2968–74. doi:10.2337/diabetes.51.10.2968
20. Nawrocki AR, Rajala MW, Tomas E, Pajvani UB, Saha AK, Trumbauer ME, et al. Mice lacking adiponectin show decreased hepatic insulin sensitivity and reduced responsiveness to peroxisome proliferator-activated receptor gamma agonists. *J Biol Chem* (2006) 281(5):2654–60. doi:10.1074/jbc.M505311200
21. Nissen SE, Wolski K. Effect of rosiglitazone on the risk of myocardial infarction and death from cardiovascular causes. *N Engl J Med* (2007) 356(24):2457–71. doi:10.1056/NEJMoa072761
22. Loke YK, Singh S, Furberg CD. Long-term use of thiazolidinediones and fractures in type 2 diabetes: a meta-analysis. *Can Med Assoc J* (2009) 180(1):32–9. doi:10.1503/cmaj.080486
23. Rasouli N, Yao-Borengasser A, Miles LM, Elbein SC, Kern PA. Increased plasma adiponectin in response to pioglitazone does not result from increased gene expression. *Am J Physiol Endocrinol Metab* (2006) 290(1):E42–6. doi:10.1152/ajpendo.00240.2005
24. Pita J, Panadero A, Soriano-Guillén L, Rodríguez E, Rovira A. The insulin sensitizing effects of PPAR-γ agonist are associated to changes in adiponectin index and adiponectin receptors in Zucker fatty rats. *Regul Pept* (2012) 174(1–3):18–25. doi:10.1016/j.regpep.2011.11.004
25. Burant CF, Sreenan S, Hirano K, Tai TA, Lohmiller J, Lukens J, et al. Troglitazone action is independent of adipose tissue. *J Clin Invest* (1997) 100(11):2900–8. doi:10.1172/JCI119839
26. Krings A, Rahman S, Huang S, Lu Y, Czernik PJ, Lecka-Czernik B. Bone marrow fat has brown adipose tissue characteristics, which are attenuated with aging and diabetes. *Bone* (2012) 50(2):546–52. doi:10.1016/j.bone.2011.06.016
27. Lazarenko OP, Rzonca SO, Hogue WR, Swain FL, Suva LJ, Lecka-Czernik B. Rosiglitazone induces decreases in bone mass and strength that are reminiscent of aged bone. *Endocrinology* (2007) 148(6):2669–80. doi:10.1210/en.2006-1587
28. Ackert-Bicknell CL, Shockley KR, Horton LG, Lecka-Czernik B, Churchill GA, Rosen CJ. Strain-specific effects of rosiglitazone on bone mass, body composition, and serum insulin-like growth factor-I. *Endocrinology* (2009) 150(3):1330–40. doi:10.1210/en.2008-0936
29. Turer AT, Scherer PE. Adiponectin: mechanistic insights and clinical implications. *Diabetologia* (2012) 55(9):2319–26. doi:10.1007/s00125-012-2598-x
30. Carey DG, Cowin GJ, Galloway GJ, Jones NP, Richards JC, Biswas N, et al. Effect of rosiglitazone on insulin sensitivity and body composition in type 2 diabetic patients [corrected]. *Obes Res* (2002) 10(10):1008–15. doi:10.1038/oby.2002.137
31. Scheller EL, Troiano N, Vanhoutan JN, Bouxsein MA, Fretz JA, Xi Y, et al. Use of osmium tetroxide staining with microcomputerized tomography to visualize and quantify bone marrow adipose tissue in vivo. *Methods Enzymol* (2014) 537:123–39. doi:10.1016/B978-0-12-411619-1.00007-0
32. Combs TP, Berg AH, Rajala MW, Klebanov S, Iyengar P, Jimenez-Chillaron JC, et al. Sexual differentiation, pregnancy, calorie restriction, and aging affect the adipocyte-specific secretory protein adiponectin. *Diabetes* (2003) 52(2):268–76. doi:10.2337/diabetes.52.2.268
33. Wiesenborn DS, Menon V, Zhi X, Do A, Gesing A, Wang Z, et al. The effect of calorie restriction on insulin signaling in skeletal muscle and adipose tissue of Ames dwarf mice. *Aging (Albany NY)* (2014) 6(10):900–12. doi:10.18632/aging.100700
34. Kelly LJ, Vicario PP, Thompson GM, Candelore MR, Doebber TW, Ventre J, et al. Peroxisome proliferator-activated receptors gamma and alpha mediate in vivo regulation of uncoupling protein (UCP-1, UCP-2, UCP-3) gene expression. *Endocrinology* (1998) 139(12):4920–7. doi:10.1210/endo.139.12.6384
35. Nedergaard J, Cannon B. UCP1 mRNA does not produce heat. *Biochim Biophys Acta* (2013) 1831(5):943–9. doi:10.1016/j.bbalip.2013.01.009
36. Moore GB, Pickavance LC, Briscoe CP, Clapham JC, Buckingham RE, Wilding JP. Energy restriction enhances therapeutic efficacy of the PPARgamma agonist, rosiglitazone, through regulation of visceral fat gene expression. *Diabetes Obes Metab* (2008) 10(3):251–63. doi:10.1111/j.1463-1326.2007.00697.x
37. Styner M, Pagnotti GM, Galior K, Wu X, Thompson WR, Uzer G, et al. Exercise regulation of marrow fat in the setting of PPAR gamma agonist treatment in female C57BL/6 mice. *Endocrinology* (2015) 156(8):2753–61. doi:10.1210/en.2015-1213
38. Riche DM, King ST. Bone loss and fracture risk associated with thiazolidinedione therapy. *Pharmacotherapy* (2010) 30(7):716–27. doi:10.1592/phco.30.7.716
39. Petrovic N, Walden TB, Shabalina IG, Timmons JA, Cannon B, Nedergaard J. Chronic peroxisome proliferator-activated receptor gamma (PPARgamma) activation of epididymally derived white adipocyte cultures

reveals a population of thermogenically competent, UCP1-containing adipocytes molecularly distinct from classic brown adipocytes. *J Biol Chem* (2010) 285(10):7153–64. doi:10.1074/jbc.M109.053942
40. Ohno H, Shinoda K, Spiegelman BM, Kajimura S. PPAR agonists induce a white-to-brown fat conversion through stabilization of PRDM16 protein. *Cell Metab* (2012) 15(3):395–404. doi:10.1016/j.cmet.2012.01.019
41. Harms M, Seale P. Brown and beige fat: development, function and therapeutic potential. *Nat Med* (2013) 19(10):1252–63. doi:10.1038/nm.3361
42. Tavassoli M. Ultrastructural development of bone marrow adipose cell. *Acta Anat (Basel)* (1976) 94(1):65–77. doi:10.1159/000144545
43. Harslof T, Wamberg L, Moller L, Stodkilde-Jorgensen H, Ringgaard S, Pedersen SB, et al. Rosiglitazone decreases bone mass and bone marrow fat. *J Clin Endocrinol Metab* (2011) 96(5):1541–8. doi:10.1210/jc.2010-2077
44. Grey A, Beckley V, Doyle A, Fenwick S, Horne A, Gamble G, et al. Pioglitazone increases bone marrow fat in type 2 diabetes: results from a randomized controlled trial. *Eur J Endocrinol* (2012) 166(6):1087–91. doi:10.1530/EJE-11-1075

Conflict of Interest Statement: RS, BL, BZ, ES, SP, BS, HM, AB, and RW have nothing to disclose. WC held a postdoctoral fellowship funded by Eli Lilly and Company. VK is employed by Eli Lilly and Company. OM has received research funding from Eli Lilly and Company.

frontiers in Endocrinology

MINI REVIEW
published: 14 July 2016
doi: 10.3389/fendo.2016.00090

Bone Marrow Adipose Tissue: A New Player in Cancer Metastasis to Bone

Emma V. Morris[1] *and Claire M. Edwards*[1,2]*

[1] Nuffield Department of Surgical Sciences, University of Oxford, Oxford, UK, [2] Nuffield Department of Orthopaedics, Rheumatology and Musculoskeletal Sciences, University of Oxford, Oxford, UK

The bone marrow is a favored site for a number of cancers, including the hematological malignancy multiple myeloma, and metastasis of breast and prostate cancer. This specialized microenvironment is highly supportive, not only for tumor growth and survival but also for the development of an associated destructive cancer-induced bone disease. The interactions between tumor cells, osteoclasts and osteoblasts are well documented. By contrast, despite occupying a significant proportion of the bone marrow, the importance of bone marrow adipose tissue is only just emerging. The ability of bone marrow adipocytes to regulate skeletal biology and hematopoiesis, combined with their metabolic activity, endocrine functions, and proximity to tumor cells means that they are ideally placed to impact both tumor growth and bone disease. This review discusses the recent advances in our understanding of how marrow adipose tissue contributes to bone metastasis and cancer-induced bone disease.

Keywords: cancer-induced bone disease, marrow adipose tissue, multiple myeloma, prostate cancer, bone metastasis

OPEN ACCESS

Edited by:
William Peter Cawthorn, University of Edinburgh, UK

Reviewed by:
Melissa Orlandin Premaor, Federal University of Santa Maria, Brazil
Michaela Ruth Reagan, Maine Medical Center Research Institute, USA

***Correspondence:**
Claire M. Edwards
claire.edwards@ndorms.ox.ac.uk

Specialty section:
This article was submitted to Bone Research, a section of the journal Frontiers in Endocrinology

Received: *26 May 2016*
Accepted: *29 June 2016*
Published: *14 July 2016*

Citation:
Morris EV and Edwards CM (2016) Bone Marrow Adipose Tissue: A New Player in Cancer Metastasis to Bone. Front. Endocrinol. 7:90. doi: 10.3389/fendo.2016.00090

INTRODUCTION

For the majority of cancers, surgical removal of an isolated primary tumor can be curative. However, once tumor cells establish residence in other organs patient mortality is markedly increased. Once detached from the primary site, a single or cluster of tumor cells can circulate the body and establish secondary lesions in distant sites. Metastasis is a highly inefficient process with <0.1% of disseminating cells surviving to form secondary lesions (1). This implies that healthy tissues display a level of hostility toward invading tumor cells, and so in order to survive and repopulate new sites these cells need to have adapted to seek out more permissive environments to occupy. Interestingly, it has long been recognized that each type of tumor has a distinct pattern of dissemination. In 1889, Stephen Paget published a paper proposing that disseminating cancer cells or "seeds" would only colonize secondary sites or "soils" that were compatible with their growth (2). This theory was challenged in the 1920s by James Ewing who proposed that the colonization of secondary sites could be explained purely by circulatory patterns between the primary and secondary sites (3). In fact, these theories are not mutually exclusive, as there is evidence to support both (1). Systemic breast cancer commonly metastasizes to the bones, lungs, liver, and brain most of which do not have a direct circulatory link to breast tissue. Advanced prostate cancer also selectively metastasizes to bone. By contrast, patients suffering from colon cancer often develop initial metastases in the liver (4). Therefore, mechanical factors that govern the amount of cancer cells delivered to an organ, and compatibility factors such as whether the organ preferentially supports the growth of a specific tumor cell type, contribute to cancer spread (5). Once a cancer cell has successfully seeded itself, it is then dependent on the

molecular interactions between it and the environment of the new organ. The more permissive the environment, the more likely the tumor cell is able to take advantage and thrive.

THE BONE MICROENVIRONMENT

Bone or bone marrow is a major target organ for metastasis, providing a fertile "soil" for circulating tumor cells to settle and repopulate. It is the preferential site of a number of solid tumor metastases including breast and prostate, of which 70–80% of advanced cases have bone involvement (6, 7). It is also the site of the fatal hematological malignancy, multiple myeloma. The bone consists of a number of different cell types, including endothelial cells and nerve cells, cells of hematopoietic origin, such as hematopoietic stem cells, osteoclasts macrophages, and lymphocytes, as well as cells from mesenchymal origin, such as chondrocytes, osteoblasts, and adipocytes. Together these cells provide a supportive niche via cellular cross-talk that maintains healthy bone. It is thought that cancer cells are able to hijack this support network to transform what was initially a beneficial niche into a deadly one. Considerable research efforts have been made, attempting to understand the complexity of the bone microenvironment and defining the exact contribution of each cell type in tumor growth and metastasis. Mundy and colleagues greatly broadened our understanding of this by introducing the concept of the "vicious-cycle" involving bi-directional interactions of tumor cells and bone cells, resulting in osteolysis and in turn, tumor growth. Breast cancer cells produce parathyroid hormone-related peptide (PTHrP) that activates osteoblasts to produce receptor activator of nuclear factor kappa-B ligand (RANKL) and downregulate osteoprotegerin (OPG). This in turn activates osteoclast precursors, leading to osteolysis. The breakdown of the bone matrix releases bone-derived growth factors, such as transforming growth factor-β and insulin-like growth factor 1, and raises extracellular calcium concentrations. The growth factors bind to receptors on the cell surface of the tumor cells and activate SMAD and MAPK signaling, extracellular calcium binds and activates calcium pumps leading to tumor cell proliferation and the production of PTHrP, thereby causing a vicious cycle of events that result in osteolytic lesions and the progression of cancer metastasis (8–10). This theory explained how bone cells and cancer cells could have a reciprocal relationship. However, it does not take into consideration the contribution of the other resident cells of the bone marrow, such as the cells of the immune system, which have also been shown to play an important part in cancer progression (11, 12). In recent years, the contribution of bone marrow adipocytes (BMAs) has also come into question. Cancer primarily occurs in older people whose bone marrow is highly populated by adipocytes. In early childhood, the bone marrow exists in a predominantly red/hematopoietic osteogenic state (13) and there are few if any detectable adipocytes, however, by the age of 25, ~70% of bone marrow volume is filled with adipose tissue (14). This constitutes around 2 kg of marrow adipose tissue in a healthy adult that represents over 10% of total adipose mass (15). Longitudinal analysis of patients from birth to 90 years have demonstrated that even after this initial exponential accumulation, there continues to be a gradual increase in adipocyte number throughout adult life (16). These cells were previously thought to be inert space filling bystanders (17). However, recently that way of thinking has changed and it is becoming clear that adipocytes have a definite and significant contribution to the bone microenvironment and, thus, the establishment of metastatic disease.

BONE MARROW ADIPOCYTES

Over the last century, our knowledge and understanding of the role of BMAs has been slowly growing. At the beginning of the nineteenth century, it was determined that the skeleton is filled with areas consisting of yellow or red marrow that are distributed in a defined pattern (18). A number of decades later, it was shown using elegant ultrastructural studies that BMAs develop from a unique progenitor when compared to white adipocytes (19), and that there are two distinct populations of BMAs that respond differently to hematopoietic demands (20). This phenomenon was also shown by Scheller and colleagues that marrow adipose tissue may exist in two isoforms, "constitutive" that forms early on in development in sites such as the distal tibia, and "regulated" that tends to develop with aging and is located interspersed with hematopoietic cells at sites such as the proximal femur and lumbar vertebrae (21). The fact that marrow adipose tissue develops in a conserved, spatial, and temporal manner implies that it is the product of a defined developmental event; suggesting that it has a distinct physiological function. Its phenotype resembles both brown and white adipose tissue; and unlike white adipose tissue, it is not strictly associated with BMI or body fat. It is known to be increased in patients suffering from anorexia nervosa, despite their lean appearance (22). It is also elevated in young mice in response to calorie restriction (23). The main functions of bone marrow adipose tissue are to serve as an energy reservoir and secrete fatty acids, cytokines, and adipokines. BMAs store energy in the form of lipid and release triglycerides and fatty acids in response to energy demands. They are smaller than their visceral counterparts; however, due to enhanced triacylglycerol synthesis the net effect of fatty acid uptake is similar (24). BMAs are both an endocrine target and have endocrine-like functions: responding to growth hormones insulin and thyroid hormone, as well as releasing cytokines such as IL-6, IL-1β, and TNF-α (25). They also secrete adipokines, among them leptin and adiponectin, which regulate calorie uptake and insulin sensitivity, respectively. They can potentially influence neighboring cells via autocrine, paracrine, and endocrine signaling (26) making them an influential component of the bone microenvironment. BMAs arise from multipotent mesenchymal progenitors; these cells have the capacity to differentiate into several cell types, including myocytes, chondrocytes, osteoblasts, and adipocytes (27, 28). It is thought that downstream of these multipotent progenitors, bipotent osteoblast–adipocytes progenitors form an intermediate in the process of cell commitment to these two cell lineages (29). These bipotent cells are stimulated to commit to either cell lineage by the presence of adipogenic vs. osteogenic factors within the bone microenvironment that activate their respective transcriptional programs (30, 31). This creates an inverse reciprocal relationship between osteoblastogenesis and adipogenesis, with factors that promote one of these processes usually inhibiting the other. Many

have likened it to a see-saw, when one process goes up the other often comes down and vice versa (32). It has also been suggested that mature osteoblasts and adipocytes are able to dedifferentiate and transdifferentiate from one phenotype to the other (33). Work by Martin and colleagues also demonstrated that BMAs are able to influence their environment by secreting extracellular vesicles containing adipogenic mRNA transcripts. These could be taken up and expressed by neighboring osteoblasts, thereby weakening their lineage commitment (34, 35). The net result of this close relationship is that if the balance tips in flavor of adipogenesis, osteoblast number may be reduced, resulting in a decrease in bone, so compromising bone strength. BMAs are not only negative regulators of bone formation but also serve to inhibit hematopoiesis. The number of BMAs has been shown to be inversely correlated with the hematopoietic activity of the marrow (36). The evidence to support the notion that BMAs play a metabolic role in the bone is quite clear; however, the influence they have in the context of cancer development and progression is still poorly understood.

WHITE ADIPOSE TISSUE; A GROWING CONTRIBUTOR TO CANCER RISK AND PROGRESSION

White adipose tissue (WAT) was the first adipose tissue type to be heavily studied in relation to cancer development and progression. In 2002, the International Agency for Research on Cancer (IARC) conducted an evaluation on whether there was a link between weight and cancer. They concluded that the risk of developing some cancers was increased with weight gain (37). Since then, there have been numerous studies investigating the association between increased adiposity and cancer, suggesting that obesity is associated with an increased risk of developing a number of different tumor types, such as colon, breast, and endometrial cancer (38–40). As adipose tissue expands, adipocytes enlarge to store excess energy intake. This causes an increased production of a number of different adipokines and inflammatory cytokines coupled with a decrease in adiponectin, as well as a diminished ability of adipocytes to store surplus-free fatty acids. These changes are associated with dysfunctional WAT that often leads to insulin resistance. In turn, the suppression of lipolysis by insulin is inhibited in insulin resistance, resulting in an increased release of free fatty acids, thereby setting up a vicious cycle of events (40). Lipids are crucial for malignant tumors as they are necessary for the synthesis of membrane constituents; they are also an effective bioenergetic source when metabolic demands are high. In 2011, Nieman et al. demonstrated that adipocytes–ovarian cancer cell co-culture led to the direct transfer of lipids from adipocytes to ovarian cancer cells and promoted *in vitro* and *in vivo* tumor growth. Furthermore, co-culture induced lipolysis in adipocytes and β-oxidation in cancer cells, suggesting that the adipocytes act as an energy source for the cancer cells (41). Adipocytes were also shown to promote the direct migration of prostate cancer cells (42), as well as promote colon cancer proliferation (43). Similar findings have been reported in breast cancer studies, which demonstrate that adipocytes located close to invasive cancer cells are essential for breast tumor development and progression (44). Moreover, adipocytes promote drug resistance in HER2 positive breast cancer cells, suggesting that they bestow a level of protection upon tumor cells (45). Dysfunctional WAT appears to have a tumor-promoting role; it may be that cancer cells that have been in close proximity to adipocytes are primed to settle in an adipocyte-rich secondary site, making the bone a hospitable and permissive environment (**Figure 1**).

BONE MARROW ADIPOCYTES; FUELING CANCER PROGRESSION

Once WAT had been identified as a driver of cancer progression, the contribution of adipocytes from different anatomical sites came into question. There are now a number of publications highlighting the importance of BMAs as a lipid source that can be utilized by cancer cells to promote proliferation, migration, and invasion (46, 47). A key factor implicated in Nieman's 2011 study was fatty acid binding protein 4 (FABP4); a lipid chaperone that mediates lipid trafficking and transfer of free fatty acids, predominantly expressed in adipocytes, macrophages, and endothelial cells (41). Herroon et al. took these findings further using a mouse model of diet-induced marrow adiposity and demonstrated that FABP4 along with interleukin 1β and its target gene, oxidative stress protein, heme oxygenase 1 (HMOX-1) was also upregulated in prostate cancer cells that were in direct contact with BMAs (46). Taken together, these studies support the fact that cancer cells are able to utilize marrow adipocyte-supplied lipids to thrive in skeletal sites. They also open up a number of questions as to whether BMAs are utilized in the same manner as WAT or whether they offer different environmental advantages to some cancer types over others.

ADIPOKINES/CYTOKINES

Similarly to WAT, BMAs are not only an effective source of energy they also secrete a plethora of bioactive substances, such as IL-1β, IL-6, leptin, adiponectin, VCAM-1, TNF-α, and VEGF (25). As well as being important in the context of maintaining healthy bone, these secreted cytokines, adipokines, and growth factors can also influence cancer cell behavior and survival. Increased IL-1β secretion coupled with increased leptin expression was shown to recruit breast cancer cells to colonize in bone marrow adipose tissue (47). IL-6, TNF-α, CXCL12, and leptin were shown to promote cell proliferation and migration, as well as inhibit apoptosis and activate autophagy to promote chemotherapy resistance in multiple myeloma (25, 48–51). In prostate cancer, the chemokines, CXCL1 and CXCL2, have been implicated in the progression of associated bone disease by activating osteoclastogenesis and thus promoting tumor cell survival (52). Similarly, in melanoma increased IL-6 triggered an increase in osteoclastogenesis resulting in tumor cell proliferation (53). BMAs clearly influence cancer cell establishment and progression in bone. However, they also play a known tumor-suppressive role. BMAs are the largest source of circulating adiponectin in the body, far more than white adipose tissue (54). Adiponectin has been shown

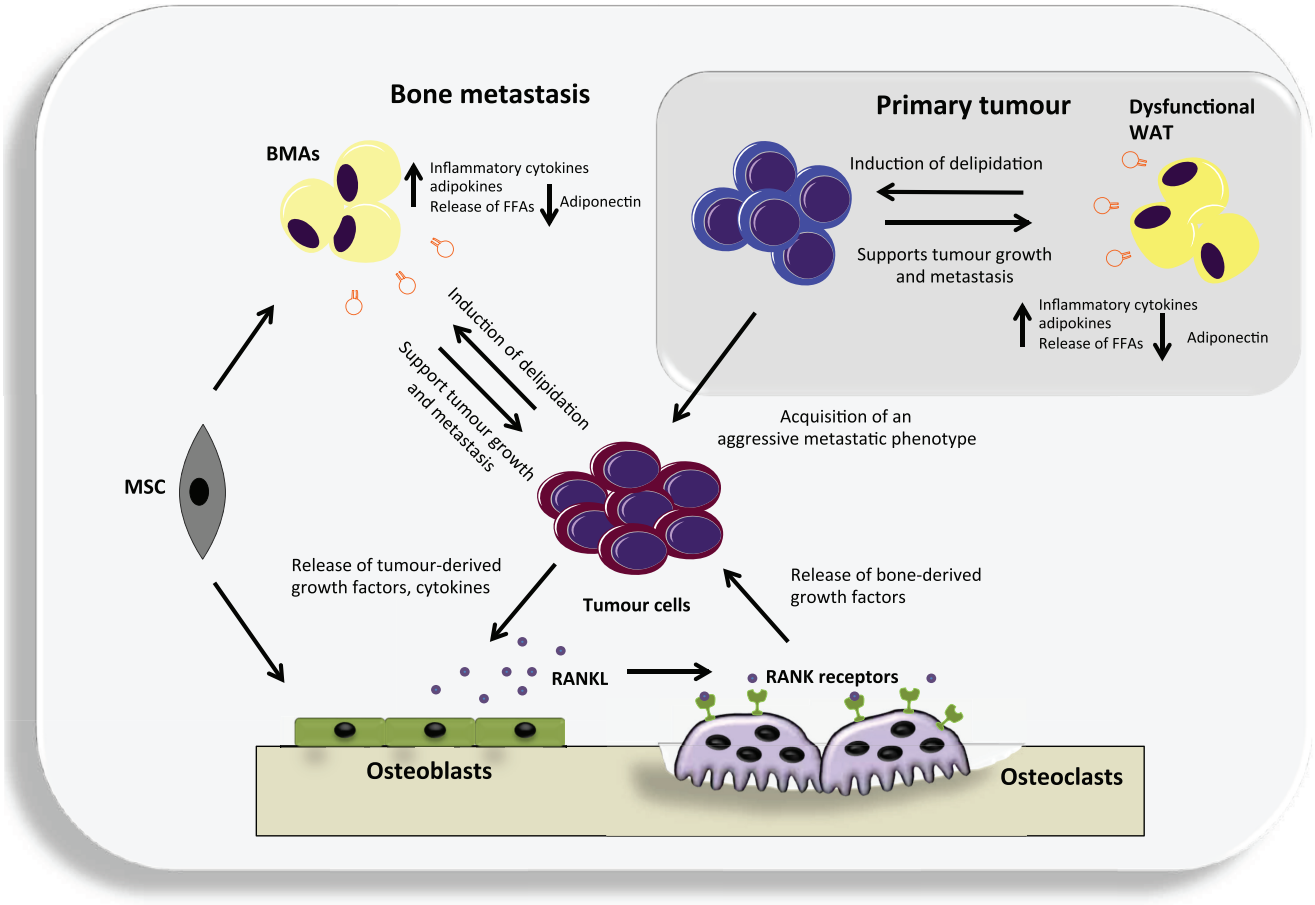

FIGURE 1 | An overview of the potential contribution of both white adipose tissue (WAT) and bone marrow adipocytes (BMAs) to the vicious cycle of bone metastases. Dysfunctional WAT releases an increased level of a number of adipokines and pro-inflammatory cytokines that can support tumor growth. In turn, cancer cells may cause delipidation of adipocytes to fuel their growth and the acquisition of an aggressive metastatic phenotype. They can then metastasize to the adipocyte-rich environment of the bone where they may continue to utilize BMAs generated from mesenchymal stem cells (MSC) that reside in the bone, as a source of fuel. Cancer cells residing in the bone produce various cytokines and growth factors that primarily target osteoblasts, causing them to increase their production of receptor activator of nuclear factor kappa-B ligand (RANKL). RANKL in turn targets the RANK receptor expressed by osteoclast precursors and leads to differentiated and activated osteoclasts. The osteoclasts degrade the bone releasing numerous factors. Many of these factors act positively upon the cancer cells resulting in a vicious cycle.

to exert anti-tumor effects (55, 56), and its levels are inversely correlated with a number of different cancers, such as myeloma, breast, prostate, colon, and endometrial cancer (57, 58), and are associated with poor prognosis (59). Interestingly, unlike other adipokines, such as leptin, circulating adiponectin levels are also decreased in obesity, which appears to be somewhat paradoxical as the numbers of adipocytes are increased. Reduced circulating adiponectin in obesity is likely derived from dysfunctional adipocytes that have decreased adiponectin expression and secretion, which may be the result of mitochondrial dysfunction or increased inflammation, hypoxia or endoplasmic reticulum stress due to the challenge of a high fat diet (60). These findings trigger the question as to what causes the downregulation of adiponectin expression in cancer? Is it a consequence of cancer progression or a cause? Do cancer cells secrete factors that directly regulate adiponectin levels? Are adiponectin levels compromised before cancer development by conditions, such as obesity, that allow for a more permissive environment? More research needs to be done to address these questions and to validate whether adiponectin signaling may be a future therapeutic target.

TARGETING BONE MARROW ADIPOCYTES

Given the mounting evidence to support the negative role of BMAs in cancer progression, as is further discussed in the context of myeloma by Falyank et al. (61), targeting these cells either alone or in combination with conventional therapeutics may be a promising approach. Due to the ability of cancer cells to induce lipidation of BMAs to support their energy expenditure, drugs are now being developed that target essential molecules of fatty acid synthesis and uptake. Chemical or RNAi mediated inhibition of fatty acid synthase, acetyl-CoA-carboxylase or ATP-citrate lyase

was shown to attenuate cancer cell proliferation and cell survival in both *in vitro* and *in vivo* models (62–64). Another approach is to regulate the balance between osteogenesis and adipogenesis by targeting PPARγ or glucocorticoid receptor signaling, thereby preventing an increase in marrow adiposity (65). The modulation of adipokines although still in its infancy has also shown encouraging effects. Leptin receptor antagonists were shown to inhibit tumor cell growth in a model of triple-negative breast cancer (66). Enhancement of circulating adiponectin levels by the apolipoprotein mimetic L-4F caused cancer cell death in a mouse model of multiple myeloma (55). Furthermore, a peptide-based adiponectin receptor agonist ADP 355 was shown to suppress the growth of orthotopic human breast cancer xenografts by ~31% (67). As we begin to gain more knowledge of the exact contribution of BMAs to disease progression, targeting strategies will inevitably become clearer. First, though we need to understand whether BMAs are simply power stations that fuel an inevitable process? If they were removed from the equation, would the cancer cells still home to the bone and thrive? Or are BMAs an integral part of the metastatic process, fertilizing the soil so circulating cancer cells can settle and progress. Interestingly, marrow adipose tissue unlike white adipose tissue increases in times of starvation. Calorie restriction has been show to not only increase marrow adiposity but also extend lifespan in a number of diverse species, such as rodents and primates (68, 69), and is associated with a decrease in cancer risk (70). These findings suggest that BMAs have a protective function that is contradictory to the evidence to suggest that they promote cancer progression. However, one question that remains unresolved is whether the BMAs generated by weight gain and sedentary behavior are the same as those generated by calorie restriction? It may be that BMAs generated by calorie restriction are more metabolically aware and, therefore, less responsive to cancer cell manipulation. However more research needs to be done to explore these possibilities. Targeting BMAs as part of a combination therapy may prove to be a valuable tool; however, first there needs to be a greater understanding of the balance between the tumor-promoting and tumor-suppressive effects of these cells.

CONCLUSION

As the field of marrow adiposity advances and we come to fully appreciate and understand the influence BMAs have on disease progression, drugs that target these cells may start to come into their own and open up new therapeutic avenues. These advances will hopefully move us one step closer to successfully treating lethal metastatic cancer.

AUTHOR CONTRIBUTIONS

All authors listed have made substantial, direct, and intellectual contribution to the work and approved it for publication.

FUNDING

This work was supported by Bloodwise, the International Myeloma Foundation and a Marie Curie Career Integration Grant from the European Union Seventh Framework Programme.

REFERENCES

1. Fidler IJ. The pathogenesis of cancer metastasis: the 'seed and soil' hypothesis revisited. *Nat Rev Cancer* (2003) 3(6):453–8. doi:10.1038/nrc1098
2. Paget S. The distribution of secondary growths in cancer of the breast. 1889. *Cancer Metastasis Rev* (1989) 8(2):98–101.
3. Ewing J. *Neoplastic Diseases. A Treatise on Tumours*. 3rd ed. Philadelphia: W.B. Saunders Co. Ltd (1928).
4. Sheth KR, Clary BM. Management of hepatic metastases from colorectal cancer. *Clin Colon Rectal Surg* (2005) 18(3):215–23. doi:10.1055/s-2005-916282
5. Chambers AF, Groom AC, MacDonald IC. Dissemination and growth of cancer cells in metastatic sites. *Nat Rev Cancer* (2002) 2(8):563–72. doi:10.1038/nrc865
6. Kuchuk I, Hutton B, Moretto P, Ng T, Addison CL, Clemons M. Incidence, consequences and treatment of bone metastases in breast cancer patients-experience from a single cancer centre. *J Bone Oncol* (2013) 2(4):137–44. doi:10.1016/j.jbo.2013.09.001
7. Coleman RE. Metastatic bone disease: clinical features, pathophysiology and treatment strategies. *Cancer Treat Rev* (2001) 27(3):165–76. doi:10.1053/ctrv.2000.0210
8. Mundy GR. Mechanisms of bone metastasis. *Cancer* (1997) 80(8 Suppl): 1546–56. doi:10.1002/(SICI)1097-0142(19971015)80:8+<1546::AID-CNCR4>3.0.CO;2-I
9. Mundy GR. Metastasis to bone: causes, consequences and therapeutic opportunities. *Nat Rev Cancer* (2002) 2(8):584–93. doi:10.1038/nrc867
10. Le Pape F, Vargas G, Clezardin P. The role of osteoclasts in breast cancer bone metastasis. *J Bone Oncol* (2016). doi:10.1016/j.jbo.2016.02.008
11. Park SI, Soki FN, McCauley LK. Roles of bone marrow cells in skeletal metastases: no longer bystanders. *Cancer Microenviron* (2011) 4(3):237–46. doi:10.1007/s12307-011-0081-8
12. D'Amico L, Roato I. The impact of immune system in regulating bone metastasis formation by osteotropic tumors. *J Immunol Res* (2015) 2015:143526. doi:10.1155/2015/143526
13. Custer CP. Studies on the structure and function of bone marrow. Part I. *J Lab Clin Med* (1932) 17:951–60.
14. Custer RP, Ahlfeldt FE. Studies on the structure and function of bone marrow II. *J Lab Clin Med* (1932) 17:960–2.
15. Scheller EL, Burr AA, MacDougald OA, Cawthorn WP. Inside out: bone marrow adipose tissue as a source of circulating adiponectin. *Adipocyte* (2016). doi:10.1080/21623945.2016.1149269
16. Fazeli PK, Horowitz MC, MacDougald OA, Scheller EL, Rodeheffer MS, Rosen CJ, et al. Marrow fat and bone – new perspectives. *J Clin Endocrinol Metab* (2013) 98(3):935–45. doi:10.1210/jc.2012-3634
17. Kawai M, Sousa KM, MacDougald OA, Rosen CJ. The many facets of PPARgamma: novel insights for the skeleton. *Am J Physiol Endocrinol Metab* (2010) 299(1):E3–9. doi:10.1152/ajpendo.00157.2010
18. Piney A. The anatomy of the bone marrow. *BMJ* (1922) 2:792–5.
19. Tavassoli M. Ultrastructural development of bone marrow adipose cell. *Acta Anat* (1976) 94(1):65–77. doi:10.1159/000144545
20. Tavassoli M. Marrow adipose cells. Histochemical identification of labile and stable components. *Arch Pathol Lab Med* (1976) 100(1):16–8.
21. Scheller EL, Rosen CJ. What's the matter with MAT? Marrow adipose tissue, metabolism, and skeletal health. *Ann N Y Acad Sci* (2014) 1311:14–30. doi:10.1111/nyas.12327
22. Bredella MA, Fazeli PK, Miller KK, Misra M, Torriani M, Thomas BJ, et al. Increased bone marrow fat in anorexia nervosa. *J Clin Endocrinol Metab* (2009) 94(6):2129–36. doi:10.1210/jc.2008-2532
23. Devlin MJ, Cloutier AM, Thomas NA, Panus DA, Lotinun S, Pinz I, et al. Caloric restriction leads to high marrow adiposity and low bone mass in growing mice. *J Bone Miner Res* (2010) 25(9):2078–88. doi:10.1002/jbmr.82

24. Trubowitz S, Bathija A. Cell size and plamitate-1-14c turnover of rabbit marrow fat. *Blood* (1977) 49(4):599–605.
25. Caers J, Deleu S, Belaid Z, De Raeve H, Van Valckenborgh E, De Bruyne E, et al. Neighboring adipocytes participate in the bone marrow microenvironment of multiple myeloma cells. *Leukemia* (2007) 21(7):1580–4. doi:10.1038/sj.leu.2404658
26. Rosen CJ, Ackert-Bicknell C, Rodriguez JP, Pino AM. Marrow fat and the bone microenvironment: developmental, functional, and pathological implications. *Crit Rev Eukaryot Gene Expr* (2009) 19(2):109–24. doi:10.1615/CritRevEukarGeneExpr.v19.i2.20
27. Owen M. Marrow stromal stem cells. *J Cell Sci Suppl* (1988) 10:63–76. doi:10.1242/jcs.1988.Supplement_10.5
28. Zhang Y, Khan D, Delling J, Tobiasch E. Mechanisms underlying the osteo- and adipo-differentiation of human mesenchymal stem cells. *ScientificWorldJournal* (2012) 2012:793823. doi:10.1100/2012/793823
29. Hasegawa T, Oizumi K, Yoshiko Y, Tanne K, Maeda N, Aubin JE. The PPARgamma-selective ligand BRL-49653 differentially regulates the fate choices of rat calvaria versus rat bone marrow stromal cell populations. *BMC Dev Biol* (2008) 8:71. doi:10.1186/1471-213X-8-71
30. Hardaway AL, Herroon MK, Rajagurubandara E, Podgorski I. Bone marrow fat: linking adipocyte-induced inflammation with skeletal metastases. *Cancer Metastasis Rev* (2014) 33(0):527–43. doi:10.1007/s10555-013-9484-y
31. Lecka-Czernik B, Rosen CJ, Kawai M. Skeletal aging and the adipocyte program: new insights from an "old" molecule. *Cell Cycle* (2010) 9(18):3648–54. doi:10.4161/cc.9.18.13046
32. Gimble JM, Nuttall ME. Bone and fat: old questions, new insights. *Endocrine* (2004) 23(2–3):183–8. doi:10.1385/ENDO:23:2-3:183
33. Song L, Tuan RS. Transdifferentiation potential of human mesenchymal stem cells derived from bone marrow. *FASEB J* (2004) 18(9):980–2. doi:10.1096/fj.03-1100fje
34. Brümmendorf T, Rathjen F. Cell adhesion molecules 1: immunoglobulin superfamily. *Protein Profile* (1995) 2:963–1056.
35. Martin PJ, Haren N, Ghali O, Clabaut A, Chauveau C, Hardouin P, et al. Adipogenic RNAs are transferred in osteoblasts via bone marrow adipocytes-derived extracellular vesicles (EVs). *BMC Cell Biol* (2015) 16:10. doi:10.1186/s12860-015-0057-5
36. Naveiras O, Nardi V, Wenzel PL, Hauschka PV, Fahey F, Daley GQ. Bone-marrow adipocytes as negative regulators of the haematopoietic microenvironment. *Nature* (2009) 460(7252):259–63. doi:10.1038/nature08099
37. Vainio H, Kaaks R, Bianchini F. Weight control and physical activity in cancer prevention: international evaluation of the evidence. *Eur J Cancer Prev* (2002) 11(Suppl 2):S94–100.
38. Slattery ML, Curtin K, Wolff RK, Herrick JS, Caan BJ, Samowitz W. Diet, physical activity, and body size associations with rectal tumor mutations and epigenetic changes. *Cancer Causes Control* (2010) 21(8):1237–45. doi:10.1007/s10552-010-9551-4
39. Maccio A, Madeddu C, Gramignano G, Mulas C, Floris C, Massa D, et al. Correlation of body mass index and leptin with tumor size and stage of disease in hormone-dependent postmenopausal breast cancer: preliminary results and therapeutic implications. *J Mol Med (Berl)* (2010) 88(7):677–86. doi:10.1007/s00109-010-0611-8
40. Prieto-Hontoria PL, Perez-Matute P, Fernandez-Galilea M, Bustos M, Martinez JA, Moreno-Aliaga MJ. Role of obesity-associated dysfunctional adipose tissue in cancer: a molecular nutrition approach. *Biochim Biophys Acta* (2011) 1807(6):664–78. doi:10.1016/j.bbabio.2010.11.004
41. Nieman KM, Kenny HA, Penicka CV, Ladanyi A, Buell-Gutbrod R, Zillhardt MR, et al. Adipocytes promote ovarian cancer metastasis and provide energy for rapid tumor growth. *Nat Med* (2011) 17(11):1498–503. doi:10.1038/nm.2492
42. Laurent V, Guerard A, Mazerolles C, Le Gonidec S, Toulet A, Nieto L, et al. Periprostatic adipocytes act as a driving force for prostate cancer progression in obesity. *Nat Commun* (2016) 7:10230. doi:10.1038/ncomms10230
43. Amemori S, Ootani A, Aoki S, Fujise T, Shimoda R, Kakimoto T, et al. Adipocytes and preadipocytes promote the proliferation of colon cancer cells in vitro. *Am J Physiol Gastrointest Liver Physiol* (2007) 292(3):G923–9. doi:10.1152/ajpgi.00145.2006
44. Tan J, Buache E, Chenard MP, Dali-Youcef N, Rio MC. Adipocyte is a non-trivial, dynamic partner of breast cancer cells. *Int J Dev Biol* (2011) 55(7–9):851–9. doi:10.1387/ijdb.113365jt
45. Duong MN, Cleret A, Matera EL, Chettab K, Mathé D, Valsesia-Wittmann S, et al. Adipose cells promote resistance of breast cancer cells to trastuzumab-mediated antibody-dependent cellular cytotoxicity. *Breast Cancer Res* (2015) 17(1):57. doi:10.1186/s13058-015-0569-0
46. Herroon MK, Rajagurubandara E, Hardaway AL, Powell K, Turchick A, Feldmann D, et al. Bone marrow adipocytes promote tumor growth in bone via FABP4-dependent mechanisms. *Oncotarget* (2013) 4(11):2108–23. doi:10.18632/oncotarget.1482
47. Templeton ZS, Lie WR, Wang W, Rosenberg-Hasson Y, Alluri RV, Tamaresis JS, et al. Breast cancer cell colonization of the human bone marrow adipose tissue niche. *Neoplasia* (2015) 17(12):849–61. doi:10.1016/j.neo.2015.11.005
48. Gado K, Domjan G, Hegyesi H, Falus A. Role of INTERLEUKIN-6 in the pathogenesis of multiple myeloma. *Cell Biol Int* (2000) 24(4):195–209. doi:10.1006/cbir.2000.0497
49. Jourdan M, Tarte K, Legouffe E, Brochier J, Rossi JF, Klein B. Tumor necrosis factor is a survival and proliferation factor for human myeloma cells. *Eur Cytokine Netw* (1999) 10(1):65–70.
50. Hideshima T, Chauhan D, Hayashi T, Podar K, Akiyama M, Gupta D, et al. The biological sequelae of stromal cell-derived factor-1alpha in multiple myeloma. *Mol Cancer Ther* (2002) 1(7):539–44.
51. Liu Z, Xu J, He J, Liu H, Lin P, Wan X, et al. Mature adipocytes in bone marrow protect myeloma cells against chemotherapy through autophagy activation. *Oncotarget* (2015) 6(33):34329–41. doi:10.18632/oncotarget.6020
52. Hardaway AL, Herroon MK, Rajagurubandara E, Podgorski I. Marrow adipocyte-derived CXCL1 and CXCL2 contribute to osteolysis in metastatic prostate cancer. *Clin Exp Metastasis* (2015) 32(4):353–68. doi:10.1007/s10585-015-9714-5
53. Chen GL, Luo Y, Eriksson D, Meng X, Qian C, Bauerle T, et al. High fat diet increases melanoma cell growth in the bone marrow by inducing osteopontin and interleukin 6. *Oncotarget* (2016) 7(18):26653–69. doi:10.18632/oncotarget.8474
54. Cawthorn WP, Scheller EL, Learman BS, Parlee SD, Simon BR, Mori H, et al. Bone marrow adipose tissue is an endocrine organ that contributes to increased circulating adiponectin during caloric restriction. *Cell Metab* (2014) 20(2):368–75. doi:10.1016/j.cmet.2014.06.003
55. Fowler JA, Lwin ST, Drake MT, Edwards JR, Kyle RA, Mundy GR, et al. Host-derived adiponectin is tumor-suppressive and a novel therapeutic target for multiple myeloma and the associated bone disease. *Blood* (2011) 118(22):5872–82. doi:10.1182/blood-2011-01-330407
56. Jarde T, Caldefie-Chezet F, Goncalves-Mendes N, Mishellany F, Buechler C, Penault-Llorca F, et al. Involvement of adiponectin and leptin in breast cancer: clinical and in vitro studies. *Endocr Relat Cancer* (2009) 16(4):1197–210. doi:10.1677/ERC-09-0043
57. Izadi V, Farabad E, Azadbakht L. Serum adiponectin level and different kinds of cancer: a review of recent evidence. *ISRN Oncol* (2012) 2012:982769. doi:10.5402/2012/982769
58. Dalamaga M, Karmaniolas K, Panagiotou A, Hsi A, Chamberland J, Dimas C, et al. Low circulating adiponectin and resistin, but not leptin, levels are associated with multiple myeloma risk: a case-control study. *Cancer Causes Control* (2009) 20(2):193–9. doi:10.1007/s10552-008-9233-7
59. Katira A, Tan PH. Evolving role of adiponectin in cancer-controversies and update. *Cancer Biol Med* (2016) 13(1):101–19. doi:10.28092/j.issn.2095-3941.2015.0092
60. Ye R, Scherer PE. Adiponectin, driver or passenger on the road to insulin sensitivity? *Mol Metab* (2013) 2(3):133–41. doi:10.1016/j.molmet.2013.04.001
61. Falyank C, Fairfield H, Reagan MR. Signaling interplay between bone marrow adipose tissue and multiple myeloma cells. *Front Endocrinol* (2016) 7:67. doi:10.3389/fendo.2016.00067
62. Wang W, Zhao X, Wang H, Liang Y. Increased fatty acid synthase as a potential therapeutic target in multiple myeloma. *J Zhejiang Univ Sci B* (2008) 9(6):441–7. doi:10.1631/jzus.B0740640
63. Chajes V, Cambot M, Moreau K, Lenoir GM, Joulin V. Acetyl-CoA carboxylase alpha is essential to breast cancer cell survival. *Cancer Res* (2006) 66(10):5287–94. doi:10.1158/0008-5472.CAN-05-1489
64. Zaidi N, Swinnen JV, Smans K. ATP-citrate lyase: a key player in cancer metabolism. *Cancer Res* (2012) 72(15):3709–14. doi:10.1158/0008-5472.CAN-11-4112
65. Lecka-Czernik B, Ackert-Bicknell C, Adamo ML, Marmolejos V, Churchill GA, Shockley KR, et al. Activation of peroxisome proliferator-activated

receptor gamma (PPARgamma) by rosiglitazone suppresses components of the insulin-like growth factor regulatory system in vitro and in vivo. *Endocrinology* (2007) 148(2):903–11. doi:10.1210/en.2006-1121
66. Otvos L Jr, Surmacz E. Targeting the leptin receptor: a potential new mode of treatment for breast cancer. *Expert Rev Anticancer Ther* (2011) 11(8):1147–50. doi:10.1586/era.11.109
67. Otvos L Jr, Haspinger E, La Russa F, Maspero F, Graziano P, Kovalszky I, et al. Design and development of a peptide-based adiponectin receptor agonist for cancer treatment. *BMC Biotechnol* (2011) 11:90. doi:10.1186/1472-6750-11-90
68. Weindruch R. The retardation of aging by caloric restriction: studies in rodents and primates. *Toxicol Pathol* (1996) 24(6):742–5. doi:10.1177/019262339602400618
69. Colman RJ, Beasley TM, Kemnitz JW, Johnson SC, Weindruch R, Anderson RM. Caloric restriction reduces age-related and all-cause mortality in rhesus monkeys. *Nat Commun* (2014) 5:3557. doi:10.1038/ncomms4557
70. Hursting SD, Smith SM, Lashinger LM, Harvey AE, Perkins SN. Calories and carcinogenesis: lessons learned from 30 years of calorie restriction research. *Carcinogenesis* (2010) 31(1):83–9. doi:10.1093/carcin/bgp280

Conflict of Interest Statement: The authors declare that the research was conducted in the absence of any commercial or financial relationships that could be construed as a potential conflict of interest.

frontiers in Endocrinology

REVIEW
published: 17 June 2016
doi: 10.3389/fendo.2016.00067

Signaling Interplay between Bone Marrow Adipose Tissue and Multiple Myeloma cells

*Carolyne Falank[1], Heather Fairfield[1] and Michaela R. Reagan[1,2,3]**

[1] Reagan Laboratory, Maine Medical Center Research Institute, Scarborough, ME, USA, [2] School of Biomedical Sciences and Engineering, University of Maine, Orono, ME, USA, [3] School of Medicine, Tufts University, Boston, MA, USA

In the year 2000, Hanahan and Weinberg (1) defined the six Hallmarks of Cancer as: self-sufficiency in growth signals, evasion of apoptosis, insensitivity to antigrowth mechanisms, tissue invasion and metastasis, limitless replicative potential, and sustained angiogenesis. Eleven years later, two new Hallmarks were added to the list (avoiding immune destruction and reprograming energy metabolism) and two new tumor characteristics (tumor-promoting inflammation and genome instability and mutation) (2). In multiple myeloma (MM), a destructive cancer of the plasma cell that grows predominantly in the bone marrow (BM), it is clear that all these hallmarks and characteristics are in play, contributing to tumor initiation, drug resistance, disease progression, and relapse. Bone marrow adipose tissue (BMAT) is a newly recognized contributor to MM oncogenesis and disease progression, potentially affecting MM cell metabolism, immune action, inflammation, and influences on angiogenesis. In this review, we discuss the confirmed and hypothetical contributions of BMAT to MM development and disease progression. BMAT has been understudied due to technical challenges and a previous lack of appreciation for the endocrine function of this tissue. In this review, we define the dynamic, responsive, metabolically active BM adipocyte. We then describe how BMAT influences MM in terms of: lipids/metabolism, hypoxia/angiogenesis, paracrine or endocrine signaling, and bone disease. We then discuss the connection between BMAT and systemic inflammation and potential treatments to inhibit the feedback loops between BM adipocytes and MM cells that support MM progression. We aim for researchers to use this review to guide and help prioritize their experiments to develop better treatments or a cure for cancers, such as MM, that associate with and may depend on BMAT.

Keywords: bone marrow adipose, BMAT, MAT, adipocyte, microenvironment, multiple myeloma, fatty acids, bone metastasis

OPEN ACCESS

Edited by:
Erica Lynn Scheller, Washington University School of Medicine, USA

Reviewed by:
Graziana Colaianni, University of Bari, Italy
Izabela Podgorski, Wayne State University School of Medicine, USA

****Correspondence:***
Michaela R. Reagan
mreagan@mmc.org

Specialty section:
This article was submitted to Bone Research, a section of the journal Frontiers in Endocrinology

Received: *03 May 2016*
Accepted: *03 June 2016*
Published: *17 June 2016*

Citation:
Falank C, Fairfield H and Reagan MR (2016) Signaling Interplay between Bone Marrow Adipose Tissue and Multiple Myeloma cells. Front. Endocrinol. 7:67. doi: 10.3389/fendo.2016.00067

INTRODUCTION

Within the last few years, researchers have begun to explore the mechanistic relationship between bone marrow (BM) adipose and adjacent tumors such as multiple myeloma (MM), which is a cancer characterized by clonal proliferation of transformed plasma cells (3). The clinical potential of such a research avenue is yet unknown, but preclinical data suggest that targeting BM adipose tissue (BMAT) could be an effective cancer treatment. BMAT also interacts with bone cells and other immune cells, highlighting indirect ways in which BMAT may affect MM disease progression

(**Figures 1** and **2**). Clearly, there needs to be more research in this area. MM cells accumulate within the BM and are highly dependent on this unique biochemical and cellular niche, as we have recently reported (4). Only recently, the idea that adipocytes may accelerate or support MM has come to researchers' attention. The BM adipocyte may play a role in MM bone homing, tumor progression, drug resistance, recurrence, or osteolysis, due to local paracrine, endocrine, or metabolic signals. Just as understanding the relationship between osteoclasts and tumor cells led to the development of highly effective antiresorptive agents (bisphosphonates), and understanding the relationship between osteoblasts and MM cells has led to bone anabolic agent research, we propose that a clearer perception of the BMAT–MM cell relationship would identify novel ways to more effectively treat or prevent MM or MM-associated bone disease.

As adipose tissue is one of the main components within the BM niche, especially in old age, obesity, and upon radiation, there is clearly a need to characterize BMAT–MM relations. In this review, we discuss the current evidence regarding the signaling pathways driving effects of BMAT on myelomagenesis and progression. This review should guide future research strategies toward developing novel therapies to target MM or MM-induced bone disease through focusing on BMAT and its derivatives. For an overview of the contributions of the other components of the BM, we refer the reader to a few other recent reviews (4–6).

DEFINING MULTIPLE MYELOMA AND MYELOMA-ASSOCIATED BONE DISEASE

Multiple myeloma is a cancer resulting from the accumulation of genetic mutations within an immune cell, called a plasma cell. Along the uncontrolled myeloma cell growth, MM also causes disruption of the BM and cancer-induced bone disease (4). Myeloma accounts for ~1–2% of cancers and ~13–15% of all blood cancers (7) and is characterized by clonal proliferation of tumor cells in the BM, monoclonal protein spikes in the blood or urine, and organ shutdown (3). In August 2015, a revised staging system was released for myeloma from the International Myeloma working group that categorized MM as stage I, II, or III, based on disease risk levels, such as chromosomal abnormalities and serum lactate dehydrogenase (LDH) levels (8). At a median follow-up of 46 months, the society found a 5-year overall survival rate of 82% in stage I, 62% in stage II, and 40% in stage III. The 5-year progression-free survival rates were 55, 36, and 24%, respectively, for these groups. Although treatments for MM have significantly improved since the disease was first

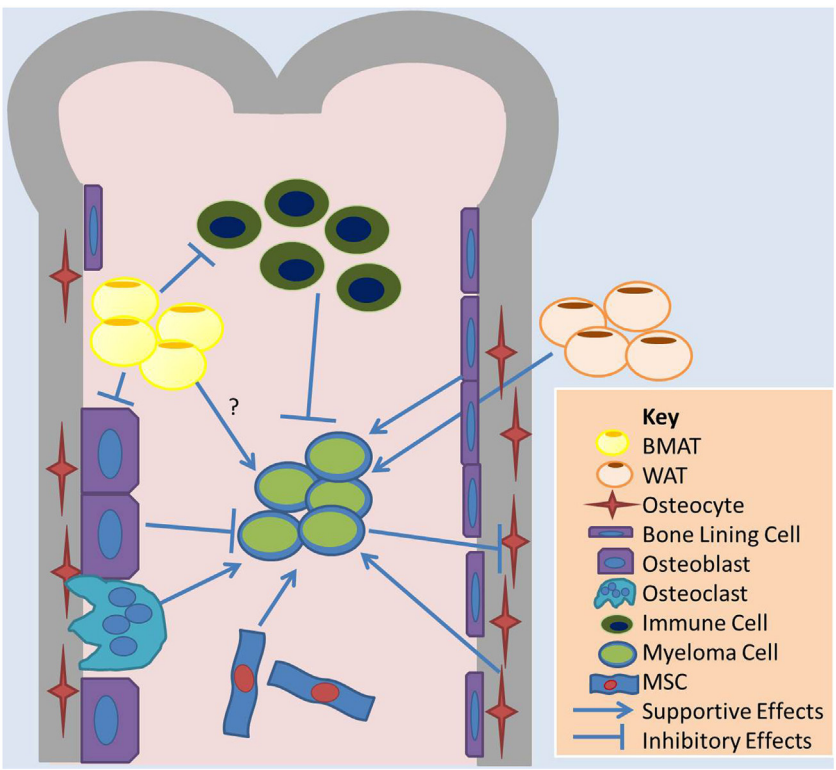

FIGURE 1 | **Overview of cell–cell interactions relevant to BMAT and adipose effects on MM**. Bone marrow adipose tissue (BMAT) may contribute to multiple myeloma (MM) growth in the marrow through indirect mechanisms, such as influences on other cells in the marrow, or direct mechanisms. BMAT has some evidence of inhibiting osteoblasts and the anticancer effects of immune cells and supporting osteoclasts and MM cell. White adipocytes, the basis of white adipose tissue (WAT), may also contribute to tumor growth in the bone marrow through systemic signaling pathways. MM cells also induce apoptosis in osteocytes, which may support MM cells. Bone lining cells and mesenchymal stromal cells (MSCs), as well as osteoclasts, support MM while osteoblasts may induce dormancy in MM cells.

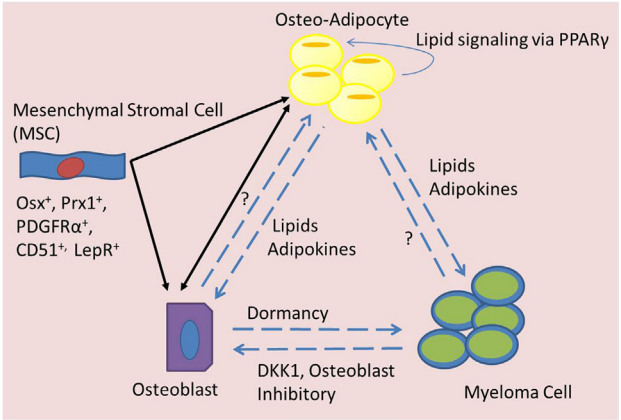

FIGURE 2 | Signaling mediators of BMAT in MM. Bone marrow mesenchymal stromal cells (MSCs) can differentiate into adipocytes or osteoblasts, which may have an elasticity and ability to transdifferentiate across lineage lines and also signal to each other (black arrows). Both osteo-adipocytes (adipocytes in the bone marrow) and osteoblasts are able to signal to each other and to myeloma cells (blue dotted arrows). Myeloma cells are known to inhibit osteoblasts, but their effects on osteo-adipocytes are unknown. Osteoblasts seem to induce dormancy in myeloma cells, but their effects on adipocytes are unknown. Osteo-adipocytes produce lipids and adipokines that likely influence MM and bone cells. Lipids from osteo-adipocytes can act as PPARγ ligands and may thus stimulate a positive feedback loop, inducing more BMAT accumulation in the marrow.

named in 1873 by J. von Rustizky (9), MM remains considered an incurable cancer. The disease is more common in males than females, African–Americans than Caucasians, older rather than younger people (the median age at diagnosis is 70), and in individuals with a family history of lymphatohematopoietic cancers (3). Obesity also has been found to be risk factor for MM in numerous studies and a pooled analysis of 20 prospective studies (10).

Myeloma arises from an asymptomatic precursor disease termed monoclonal gammopathy of undefined significance (MGUS) that progresses to smoldering myeloma and, eventually, overt, symptomatic myeloma (3). While early chromosomal abnormalities, such as immunoglobulin heavy chain translocations or trisomies, are present in both MGUS and MM, secondary translocations or mutations involving oncogenes (e.g., *MMSET, MYC, MAFB, IRF4*, *FGFR3*, *RAS* family members, among many others) (11) or tumor suppressors (e.g., *CDKN2A, CDKN2C*, or *TP53*) are unique to MM and absent in MGUS (12). Interestingly, deep sequencing of 203 tumor–normal paired samples revealed intratumor genetic heterogeneity with recurrent mutation occurring early or late during tumor evolution to be common in MM (12). Other pathways, such as the phosphatidylinositol 3-kinase (PI3K) pathway (important for cell division, growth, survival, and motility), can also be hyperactivated in MM (due to external signaling from the bone milieu) and serve as a good target, despite a lack of mutations in the pathway (13). Cells from the immune system also appear to be abnormal in MM and contribute to MM progression through expression of proteins such as TNFSF14 (6, 14) or by inducing T-cell immunosenescence (15). In sum, the genetic heterogeneity in MM may limit effectiveness of tumor-targeted therapy, indicating that better results may be obtained by targeting the bone microenvironment to impede MM and MM-induced bone disease.

Multiple myeloma-induced bone disease is the general term for the destruction of bone (associated with severe pain, pathologic fractures, and spinal cord compression) that occurs during myeloma colonization of the BM. Upon engrafting within the BM niche, MM cells accelerate osteoclastogenesis through expression of molecules, such as RANKL, MMP-13 (16), and Decoy receptor 3 (DcR3), a member of the tumor necrosis factor (TNF) receptor superfamily (17). MM cells also inhibit osteoblastogenesis, disrupting the normal equilibrium between these two processes (18), through expression of Dickkopf-1 (DKK-1) and inducing upregulation of SOST in local osteocytes. Chemokines and cytokines associated with osteolysis in MM include CCL3, CCL20, and Activin-A (19). Increased osteoclastic activity leads to hypercalcemia (elevated calcium in the blood) and bone lesions. Therefore, the mnemonic for the signs and symptoms of MM is CRAB: C, elevated Calcium in the blood stream; R, renal failure due to elevated circulating protein (immunoglobulin); A, anemia, or lack of red blood cells due to tumor crowding into the BM; and B, bone lesions (4). Much research has been directed toward inhibiting the "vicious cycle" of osteoclast activation using bisphosphonates, OPG, or RANKL antibodies (denosumab) (6, 20–22). Using bone anabolic agents to regrow bone by stimulating osteoblasts (23) is another therapy for healing bone lesions and potentially inducing quiescence in MM cells (24). Lately, research has also focused on targeting MM cell homing to the BM, either through targeting the unique BM vasculature (25, 26), the molecules (e.g., sugars) and proteins on this vasculature (27, 28), or the chemokines (e.g., SDF1) within the BM (29–31). Other marrow cellular components, such as mesenchymal stromal cells (MSCs) (5, 32–34), osteocytes (35), and adipocytes, as described in this review, are also potential new avenues to regrow bone, inhibit bone loss, or inhibit MM survival or proliferation.

DEFINING THE BM ADIPOCYTE

The anatomy and physiology of adipose tissue, as reviewed by Colaianni et al. (36), can direct energy storage (in white adipose), energy use (in brown adipose, for heat generation), or a combination of these and other functions yet to be discovered, as seen in BMAT. BMAT is a distinct adipose depot distinguishable from other adipose depots based on differences in phenotype, stress and diet response, physiological roles, gene expression, and origin. It has been found to affect the disease course of cancer, osteoporosis, and other pathologies of the bone (37). Composed of BM adipocytes and infiltrating inflammatory cells, BMAT has a gene expression pattern that overlaps with both white adipose tissue (WAT) and brown adipose tissue (BAT) (38). Like WAT, BMAT stores energy in the form of unilocular intracellular lipid droplets, opposed to multilocular droplets, as seen in BAT (39). Yet, WAT and BMAT are different in some other regards: BMAT expression of certain proteins [e.g., Dio2, peroxisome proliferator-activated receptor (PPAR) gamma coactivator

1-alpha (PGC-1α), and FOXC2] (40) is much higher than WAT expression, and while WAT volume decreases during starvation, BMAT volume increases perhaps highlighting its evolutionary role as the last energy store during starvation (41, 42). Gene expression level is also different for WAT and BMAT, as seen in the following genes: uncoupling protein 1 (UCP1), type II iodothyronine deiodinase (Dio2), PGC-1α, PR domain containing 16 (PRDM16), Forkhead box protein C2 (FOXC2), and leptin (43). Yet, these adipose depots are similar in other regards. For example, in response to obesity in mice and humans, both WAT and BMAT volumes increase due to increased adipocyte size and quantity, suggesting that both may act as reservoirs for excess energy storage (44, 45). Overall, due to the hard-to-access location of BMAT, its interspersion with many other BM cells, and its absence from hematoxylin and eosin stain histology slides due to processing challenges, BMAT has been inadvertently ignored in the BM niche for years and is thus poorly understood relative to other adipose depots.

Adipose depot properties also diverge within the BM and are both cell- and microenvironment-dependent. Adipose in the distal long bone BM is termed "constitutive marrow adipose tissue" (cMAT) and proximal adipose is termed "regulated marrow adipose tissue" (rMAT), as it is commonly "regulated," or modified, rather than constitutively present (37). This suggests that BM adipocytes may be either location dependent or composed of two subpopulations of adipocytes; this remains under investigation. In rabbits, humans, and mice, MAT develops differently based on its location in the skeleton (46). *cMAT,* often termed "yellow adipose" due to its yellow appearance in the marrow, is found in the distal tibia and tail (caudal vertebra) of rodents and forms at birth, whereas *rMAT* accumulates with aging in proximal femora and more proximal vertebrae. *cMAT* volume can be measured by MRI in humans or by osmium microcomputed tomography in rodents and is constitutively present (47, 48). *cMAT* is proportional to bone mass in many cases; for example, the distal tibia, which is loaded with *cMAT* relative to the proximal tibia, and the caudal vertebrae, again loaded with cMAT relative to the lumbar vertebrae, also have more trabecular bone mass (46, 49). Interestingly, these sites with high cMAT/yellow MAT (distal tibia metaphysis, first lumbar vertebra), compared to regions with more red marrow (proximal tibia metaphysis or fifth caudal vertebra), also appear protected from bone loss induced by ovariectomy in rats (50).

Constitutive marrow adipose tissue may negatively impact hematopoiesis and maintain hematopoetic stem cells (HSCs) in a quiescent state (51). *rMAT* is often, but not always, correlated with low bone mass and is regulated by factors including diet, drugs, age, and other endocrine and paracrine influences (42, 52–56). Interestingly, both cell-autonomous factors and the BM microenvironment appear to govern BMAT formation. In one study, although differentiation potential was found to be generally decreased in BM-MSCs, donor age was found to affect osteogenic differentiation of BM MSCs more than it affects adipogenic differentiation (57, 58). In another study, human adipose-derived stem cells showed a shift in favor of adipogenesis with increased age (59). Yet, as demonstrated in a transplant study of BM cells into old and young mice, researchers found older hosts induced greater adipogenic lineage allocation than younger hosts did for the same transplanted MSCs, demonstrating the context and source influences on adipogenesis (60).

Lineage tracing experiments demonstrate that BMAT arises from an osterix-positive BM mesenchymal progenitor cell, common to osteoblasts, chondrocytes, and other BM stromal cells (61) (**Figure 2**). Interestingly, BM adipocytes cells are more closely related to osteoblasts and chondrocytes than are peripheral WAT adipocytes (62). One study found that a quiescent, leptin receptor-positive ($LepR^+$) progenitor cell [stem cell factor (SCF) and CXCL12 expressing, and Nestin low] is the progenitor cell for most BM adipocytes, osteoblasts, and chondrocytes. This cell is also the progenitor to new cells formed after irradiation or fracture in the bone (61). These progenitors also express Prx1, PDGFRα, and CD51 markers expressed by BM-MSCs, emphasizing the need for more thorough bone progenitor classification (61). The plasticity or elasticity between different progenitors and their progeny may complicate the unequivocal identification of phylogenic lines, and differences between mouse and human cells and proteins may also further complicate these studies. A better understanding of the lineage pathways of BM cells would provide insight into a wide array of pathophysiologies.

BONE MARROW ADIPOCYTE INFLUENCES ON MM

High body mass index (BMI) is correlated with an increased risk of developing MM and is associated with higher levels of BM adiposity, perhaps creating an optimal microenvironment, or "soil," in which MM can engraft and grow (63–65). BM adipocytes isolated from MM patient femoral biopsies have been shown to support myeloma growth *in vitro* and may protect MM cells from chemotherapy-induced apoptosis (66, 67). These results suggest that elevated adipocyte numbers support MM advancement. By excreting free fatty acids (FFAs) and producing a plethora of signaling molecules [e.g., adipokines (leptin, adiponectin, adipsin, etc.) and growth factors (e.g., IL-6, TNFα, MCP-1, insulin-like growth factor 1 (IGF-1), and insulin)], BM adipocytes are both an energy source and an endocrine signaling factory (**Figures 3** and **4**). Many of these BMAT-derived signaling molecules may promote myelomagenesis and enhance tumor growth (42, 68) (**Figure 3**). In this section, we explore the potential contributions of BMAT to MM progression.

Lipids and Cellular Metabolism

When metastatic ovarian cells colonize the omentum (the fatty membrane surrounding the stomach and abdominal organs), they induce adipocytes to release lipids, which are subsequently utilized as energy for tumor cell proliferation. This process transforms the soft, flexible omentum fat pad into a hardened, tumor-infiltrated membrane with few remaining adipocytes in a process termed "omental caking" (69). This same phenomenon may occur in adipose-rich BM cavities, and fuel-switching in MM cells and the use of fatty acids could prove advantageous to MM cells owing to the high energy content of lipids and lipid-induced cell signaling changes that lead to drug resistance. Yet,

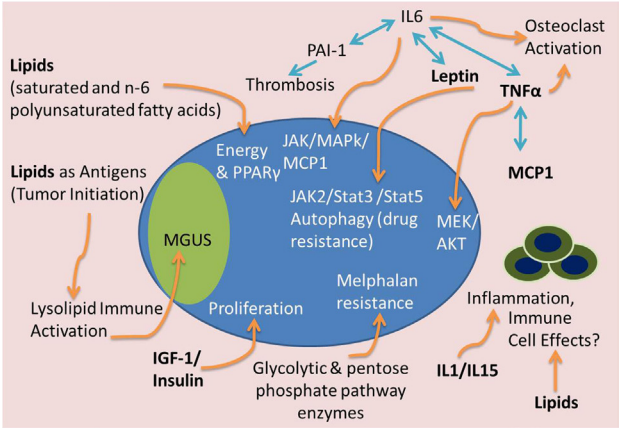

FIGURE 3 | **Tumor-supportive effects of BMAT**. Many factors from BMAT may induce MM tumor growth and disease progression. Lipids may serve as a fuel source for tumor cells, antigens to stimulate precursor disease initiation [i.e., monoclonal gammopathy of undefined significance (MGUS)], or inhibitors of the immune system. IGF-1 and insulin can accelerate tumor proliferation. IL-1 and IL-15 can have effects on immune cells and inflammatory molecules to support MM growth and immune evasion. Complex interactions between TNFα, IL-6, leptin, PAI-1, and MCP-1 can lead to osteoclast activation, thrombosis, and JAK/Stat/MAPk signaling to cause osteolysis, thrombosis and tumor cell migration, drug resistance, and proliferation. Glycolytic and pentose phosphate pathway enzyme upregulation, potentially found in high energy states, can also lead to melphalan resistance in MM cells.

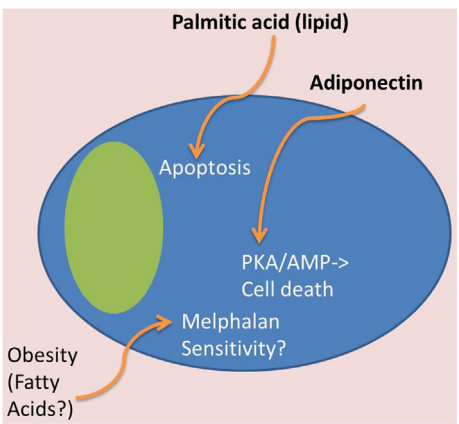

FIGURE 4 | **Tumor-suppressive effects of BMAT**. In contrast to **Figure 3**, certain adipocyte-derived factors may have tumor-suppressive effects. For example, obese patients may have tumor cells that are more melphalan sensitive, which may be due to lipid effects on MM cells. Also, certain lipids, such as palmitic acid, can induce apoptosis in MM cells, and adiponectin, derived from adipose tissue, can induce cell death through the PKA/AMP signaling pathways.

this story is not clear cut. For example, despite the fact that obesity correlates with increased risk of MM, one study found that obese and severely obese patients had superior overall survival and progression-free survival after high-dose melphalan and autologous hematopoietic stem cell transplantation compared with normal and overweight patients (70). Yet, other research found that melphalan-resistant MM cells upregulate glycolytic and pentose phosphate pathway (PPP) enzymes and downregulate tricarboxylic acid (TCA) cycle proteins (71). Together, these reports suggest that high BMI patients fuel MM cells via fatty acids, while hyperglycolytic diabetic patients could support MM cells via glycolysis, and that either metabolic pathways could support drug resistance. Additionally, some lipids, such as palmitic acid, have shown direct anti-myeloma effects (72).

Recent new data suggest that certain drugs, such as arsenic trioxide (As_2O_3), may induce anti-MM effects by affecting the sphingolipid pathways in MM cells. U266 MM cells treated with As_2O_3 displayed decreased lipid metabolites in this pathway including dihexosylceramide (Hex2Cer), sphingosine-1-phosphate (S1P), and sphinganine-1-phosphate (dhS1P) (73). As sphingolipids are a major group of membrane bioactive lipids, these changes could not only affect FFA metabolism but also membrane fluidity and cell–cell signaling. Further, complexity arises from the fact that sphingolipids and their metabolites also act as signal transduction messengers, regulating diverse cellular events such as cell cycle arrest or apoptosis, proliferation, cancer development, and multidrug resistance, as recently reviewed in Ref. (74). Increased fatty acid levels (saturated and n-6 polyunsaturated fatty acids) have also been observed in MM patient versus healthy donor blood serum (75). Lipid profiles differ between MM cells and plasma cells, such as the levels of glycerophospholipids [specifically phosphatidylcholine (16:0/20:4)] (76), which suggest potential therapeutic avenues based on lipid biochemistry.

Autophagy, the process by which intracellular proteins and organelles are degraded in lysosomes, is a protective process through which MM cells protect themselves from unfolded or misfolded proteins (77). Certain lipids can induce autophagy in hematological malignancies, but other lipids can induce tumor cell survival, proliferation, or cell death, so it is important to understand how different sphingolipids and their metabolizing enzymes cooperatively exert their functions (74). Modulating cholesterol metabolism in myeloma cells, in particular the sterols zymosternol and desmosterol, has also been shown to mediate autophagy signaling (78). Overall, it is clear that lipids may affect autophagy of MM cells.

New data also suggest that lipids may be drivers of monoclonal gammopathies, such as MM and MGUS, by acting as antigens for plasma-cell-derived antibodies (**Figure 3**). Evidence of this comes from data showing that clonal immunoglobulin in 33% of sporadic human monoclonal gammopathies is specific for the lysolipids lysoglucosylceramide (LGL1) and lysophosphatidylcholine (LPC) (79). Nair et al. reported that substrate reduction ameliorated Gaucher's disease-associated gammopathy in mice and suggest that long-term immune activation by lysolipids may underlie both sporadic monoclonal gammopathies and Gaucher's disease-associated gammopathies (79). This work was built on genetic analyses over the past two decades of immunoglobulin mutations in MM cells that found myelomagenesis to be an antigen-driven process (80). Implications of these findings are that decreasing key lipids responsible for myeloma initiation potentially represents a novel preventative

measure for at-risk populations. Moreover, the recent evidence finds that adipocyte-derived lipids, rather than adipokines, mediate obesity-related changes in macrophage phenotypes, highlighting the influential effects of adipocyte-derived lipids of the microenvironment (81).

Lipids also function as PPARγ agonists, and the PPARγ pathway has evident tumor-promoting properties in multiple cancers, as recently reviewed in Ref. (82) (**Figures 3** and **4**). Although the receptor-independent effects of PPARγ ligands compound our understanding of PPARγ in MM, the PPARγ agonist function of certain lipids likely creates a positive feedback loop both accelerating BM adipogenesis and directly supporting MM. Recent data have also found that the PPARγ agonist pioglitazone (PIO) enhances the cytotoxic effect of the histone deacetylase inhibitor (HDACi) and valproic acid (VPA) on MM cells, *in vitro* and *in vivo*, suggesting that agonizing PPARγ while inhibiting HDACs could decrease MM growth (83). Similarly, the PPARγ agonist rosiglitazone (RGZ) suppressed the expression of angiogenic factors in MM cells (HIF-1α and IGF-1) and inhibited proliferation and reduced viability of RPMI-8226 cells in a concentration- and time-dependent manner (84). RGZ also inhibited the expression of pAKT and downregulated the expression levels of phosphorylated extracellular signal-regulated kinase (pERK) in MM cells (84). However, PPARγ has a strong osteoclastogenic effect that would likely worsen osteolysis for MM patients, highlighting a downside of using RGZ in MM.

In contrast to the above, the PGC-1α is upregulated in myeloma cells grown in a high glucose media (modeling myeloma growth in hyperglycemic patients). It also contributes to chemotherapy (dexamethasone or bortezomib) resistance. These two properties suggest that inhibiting, rather than activating, the PPARγ pathway in MM cells (and controlling hyperglycemia) may improve the efficacy of chemotherapy in MM patients with diabetes. PGC-1α also increases vascular endothelial growth factor gene (VEGF) and GLUT-4 expression in MM cells suggesting that inhibition of PGC-1α in MM cells could decrease angiogenesis and glucose uptake, potentially slowing MM cell proliferation (85). Despite the growing knowledge in this area, it is still unclear how best to modulate the PPARγ pathway to inhibit MM disease progression in patients.

Adipocyte Cell Signaling Pathways

In addition to lipid molecules, there are a vast number of proteins derived from adipocytes that may influence MM tumor growth, as described here.

Adipokine and Growth Factors Affecting MM Cells

Adipocyte-derived cytokines (adipokines) within the local microenvironment may also uniquely stimulate the growth of MM cells or contribute to other aspects of the disease (86). Some of the major humoral factors and adipokines that WAT and BMAT secrete are TNFα, monocyte chemoattractant protein-1 (MCP-1), plasminogen activator inhibitor-1 (PAI-1), resistin, leptin, and adiponectin (87, 88) (**Figure 3**). TNFα is a known MM-supportive, osteoclast-activating, and osteoblast-inhibitory factor (89). TNFα treatments induce MEK and AKT phosphorylation in MM cells and stimulate the production of IL-6. This causes a forward feedback loop that drives MM cell growth and survival (90). An autocrine TNFα-MCP-1 loop has also been identified in MM cells, which was found to stimulate MM cell migration (91) (**Figure 3**).

Plasminogen activator inhibitor-1 causes increased risk of thrombosis, as it inhibits fibrinolysis, the physiological process that degrades blood clots (**Figure 3**). PAI-1 has been shown to be elevated in MM patients and appears to contribute to the greater risk of pulmonary embolism and blood clots in these patients (92). Some results suggest that patients with MM have decreased fibrinolytic activity mainly due to increased PAI-1 activity (92). In sum, these data suggest a link between adipocyte-specific cytokines, autocrine signaling, and obesity-linked cancer.

Adipocyte-Derived Hormones

Body weight is controlled by energy intake and expenditure, which are tightly regulated by communication between the brain and adipose depots through molecules such as adipocyte-derived hormones. Some hormones signal satiety (leptin) and represent high energy stores; others indicate hunger resulting from low blood glucose, inducing caloric intake as the hypothalamus receives these signals and regulates behavioral responses (93). Key adipokines such as adiponectin, leptin, and resistin are often present in skewed levels in various disease states (94–98). Abnormal adipokine levels and leptin-induced changes in gene expression profiles have been observed in MM, suggesting that these may be drivers or useful biomarkers of the disease (99–103).

Adiponectin

Adiponectin is an anti-inflammatory cytokine primarily produced by adipocytes but found to be secreted by additional cell types, including osteoblasts and BM MSCs (104). It is decreased in obesity (105–107) and has been shown to inhibit MM disease progression (100, 108) (**Figure 4**). In fact, low levels of adiponectin are associated with obesity, cardiovascular disease, and diabetes and are a risk factor for breast cancer (109). Circulating adiponectin was also decreased in patients with MGUS who then progressed to overt, symptomatic MM when compared to those with MGUS that did not develop MM (110). This study also showed that C57Bl6/KaLwRijHsd mice, which are permissive to 5T murine myeloma cells, have significantly lower adiponectin gene expression and adiponectin protein in their BM and lower total serum adiponectin compared to the non-permissive, but closely related C57BL6/J mice (110). Moreover, pharmacological stimulation of adiponectin in tumor-bearing mice led to a decrease in tumor burden and increased survival (110). Importantly, in humans, low circulating adiponectin and resistin, but not leptin, are associated with MM (99, 100, 108). Adiponectin has been shown to inhibit proliferation of MM through an increase in cell death *via* activation of the protein kinase A/AMP-activated pathways (111) (**Figure 4**). In sum, these are important findings that demonstrate the potential relevance of increasing adiponectin for MM and associated bone disease therapy.

Bone marrow adipose tissue, WAT, and BAT-derived adipocytes express relatively similar amounts of the anti-myeloma protein adiponectin on the mRNA level (40), but on the protein

level, and *in vivo*, adiponectin secretion is greater from MAT than from WAT (42). Moreover, BMAT specifically increases its production of adiponectin in times of starvation and in patients with cancer therapy (42). Expression of *adipoq,* the gene encoding adiponectin, in tibiae and femurs has been found to mirror changes in serum adiponectin, which suggests that circulating adiponectin levels are directly related to adiponectin production from BMAT (42). Therefore, adiponectin appears to be one of the major BMAT-derived molecules responsible for signaling from BMAT to MM cells.

Leptin

Leptin, a peptide hormone produced and secreted by adipocytes, has primarily been characterized for its role in the regulation of hunger response and metabolic activity (112). The main signaling capability of leptin is through the long form of its receptor, which is expressed in peripheral and brain tissues, although its primary function has been identified as signaling through the hypothalamus (112). Signaling through its receptor, leptin stimulates JAK/STAT cascades, mainly JAK2/STAT3 and JAK2/STAT5, to signal satiety (**Figure 3**). Congenital leptin deficiency in both mice and humans results in early obesity due to severe hyperphagia, but can be corrected with leptin replacement therapies (113, 114). In patients with obesity, circulating leptin levels are significantly higher than in normal age- and sex-matched patients, suggesting that a level of leptin resistance exists in these obese patients (115). Plasma leptin levels were found to be increased in both newly diagnosed male and female MM patients compared to healthy controls (100), and leptin levels are decreased in response to disease treatment (102). Similar to the effects of lipids mentioned above, autophagy, can also be induced by adipocyte-derived hormones (116) (**Figure 3**). Adipocytes have been found to upregulate the expression of autophagic proteins in MM cells *via* leptin and adipsin, leading to chemoresistance, suppression of caspase cleavage, and suppression of apoptosis in melphalan-treated MM cells *in vitro* and *in vivo* (67).

Resistin, Insulin, Insulin-Like Growth Factor 1, and Androgens

Data on resistin do not translate as well from mice to human as leptin appears to, and the relationship between resistin and adiposity is not consistent between humans and mice (117).

Still, in both species, resistin is elevated in obesity, regulates insulin sensitivity, and is positively associated with insulin resistance and glucose tolerance (118). In clinical studies, low circulating resistin levels are associated with MM risk (108). Yet, another study found no significant differences in circulating serum resistin levels between newly diagnosed MM patients and healthy controls (100). Insulin and IGF-1 are, however, both adipose-derived growth factors that stimulate proliferation for MM cells (68, 119) (**Figure 3**). Lastly, adipose tissue is one of the major sources of aromatase, an enzyme also expressed in the gonads, which synthesizes estrogens from androgen precursors. Adipose-derived aromatase and the subsequent synthesis of estrogen could contribute to MM growth, as certain MM cells have been found to express estrogen receptors and proliferate in response to estrogen (78). However, the bone anabolic effects of estrogen suggest that this enzyme could combat myeloma-induced bone disease. In sum, the net effects that adipocyte-derived hormones potentiate on MM and MM-induced bone disease are currently an open area of research.

BMAT and Hypoxia: Tumor Growth and Drug Resistance

The relationship between BMAT and hypoxia is likely an important, dynamic, and bidirectional relationship that contributes to MM development and drug resistance. As oxygen tension ranges from 21 (in normoxia) to 12% in peripheral blood and ~1.3 to 3% (hypoxia) in the BM, based on the proximity to the vasculature and endosteum (120), it is probable that BMAT-MM *in vitro* experiments, and perhaps all BM cultures, will give more translational data if they are performed in hypoxic rather normoxic conditions (121). This is because hypoxia can drive proliferation of stem cells *via* HIF1 signaling (122), induce drug resistance in MM cells, and affect MM cell homing and egress from the BM (123–126). Some data demonstrate that hypoxia decreases adipogenic differentiation (127), and severe hypoxia (1% O_2) inhibits adipogenic, chondrogenic, and osteogenic differentiation of human BM-MSCs (128). Pachón-Peña et al. found that hypoxia increased adipose-derived stem cell (hASC) proliferation and migration from lean, but not obese, patients (129), so patient type is likely important in how cells respond to hypoxia. hASC donor BMI has also been found to dictate adipogenic potential, immunophenotypic profile, and response to oxygen tension *in vitro* (129). Other studies have confirmed that obesity, and FFAs specifically, decrease stem cell multipotency (130). Overall, there appears to be an interaction coefficient between donor BMI/lipids and response to hypoxia for stem cells, suggesting that multiparameter experiments should be designed to capture these complex, non-linear interactions.

Hypoxia itself is an important factor in tumor drug resistance and is associated with poor prognosis. However, due to the challenges associated with measuring oxygen tension within the BM, it is not yet clear how, or if, the oxygen gradients in the BM specifically dictate the locations of osteolysis (131). Hypoxia activates the VEGF (132), a major stimulator of angiogenesis and neovascularization, as well as a direct inducer of MM cell growth, survival, and migration (133). Neovascularization is common in the bones of myeloma patient and in mice in areas infiltrated with myeloma cells and provides more exit routes for tumor cell intravasation and increased nutrient delivery to sustain tumor growth (134). Targeting vasculogenesis and VEGF signaling has been found to be successful to decrease tumor burden in *in vivo* models (25). VEGF concentration in the BM significantly correlates with BM microvascular density, percentage of tumor cells in bone biopsy, and hypercalcemia (135). VEGF is also significantly increased in patients after treatment who progress versus those with a partial or complete remission (135). Since adipose tissue has been shown to express high levels of VEGF, it is likely that BMAT is an important source for VEGF family members in the BM, supporting aberrant microvessel growth and neovascularization and directly fueling MM cell proliferation (136, 137). Paracrine signaling of VEGFA from BMAT to MM

cells may also be fueled through autocrine signaling, as MM cells also demonstrate high VEGFA expression and production levels (124).

As MM cells are often resistant to hypoxia-induced cell death, antiangiogenic factors do not seem to be highly effective for this type of tumor cell, despite the correlations between BM vessels and disease progression. Hypoxia protects tumor cells from apoptosis through an increase in local VEGF concentrations and subsequent increases in tumor cell MAPK/ERK signaling (138). In MM cells, hypoxia increases HIF1α and activates the PI3K/Akt/mammalian target protein of rapamycin (mTOR) pathway (139). MM cells in the BM also show high glucose uptake, similar to most tumors, as demonstrated by 18F-FDG PET imaging and increased glucose transport protein 3 (GLUT3) expression (140). As the metabolic shift from oxidative metabolism to glycolysis occurs based on both energy and oxygen sources, it is clear that the fuel type (lipid versus glucose), expression of glucose transporter, and glycolytic enzymes, as well as oxygen tension, direct tumor cell metabolism and fuel switching. Therefore, lipids and adipose tissue affect MM cell metabolism depending on oxygen availability. Specifically, decreasing local lipid concentrations may simply switch tumor cell metabolism from fatty-acid oxidation to glycolysis and not necessarily decrease tumor proliferation, or, fuel switching coupled with oxygen tension control may prove a viable therapeutic avenue through which to tackle MM. As a final consideration here, intermittent hypoxia also affects adipose tissue macrophage polarization and tumor infiltration, suggesting that immune changes should also be considered when investigating metabolic and hypoxic-based interventions in MM (141).

Bone Marrow Adipocytes and Skeletal Remodeling

The growing evidence associating elevated BMAT with low bone density suggests that BM adipocytes may contribute to bone loss in MM or that bone loss may contribute to increased BM adiposity. Either dynamic could support MM growth and increased risk of fracture (**Figure 2**). In humans (142–145) and rodents (146–149), there is often an inverse correlation between BMAT and bone quantity. Decreased bone volume or mass coinciding with higher BMAT is consistently observed across sexes, ages, models, and underlying disease etiologies (54). Moreover, many pharmacologic strategies cause opposing effects on bone and adipose tissue [glucocorticoids, hormone replacement therapies, radiation, and thiazolidinediones (TZD)] (150). Higher BMAT has been found to correlate with lower trabecular bone mineral density (BMD) in older women, but not men, and higher marrow fat is associated with prevalent vertebral fracture in men, even after adjustment for BMD (145). Lumbar spine BMD has been found to negatively correlate with BMAT (151). High BMAT also leads to disrupted hematopoiesis and reduced BMD in other studies and may increase the risk of bone metastasis, potentially resulting from an increase in receptor activator of NFκB-ligand (RANKL) and downregulation of osteoprotegerin, as observed in aging-related marrow adipogenesis (44, 152, 153).

In moving beyond correlation into causation, recent evidence demonstrates that adipocytes actively inhibit osteogenesis, based on lower mineralization, alkaline phosphatase activity, and expression of osteogenic (Runx2, osteocalcin) mRNA markers, using conditioned media experiments with hMSCs (154). Adipocytes can also induce osteoblast apoptosis (154). One pathway found to govern the effects of adipokines on osteoblasts is the PI3-kinase-FoxO1 pathway (155). Both decreased osteoblast function and induced apoptosis were enhanced by dexamethasone treatment of adipocytes, and both processes appear to be driven by the lipotoxic effect of two FFAs, stearate and palmitate, which may act as PPARγ-ligands (inhibiting osteogenesis), and can induce ROS in human cells (154). These findings demonstrate that increased BMAT may decrease osteogenesis, thus contributing to bone disease in MM patients, although this has not yet been explored in myeloma patient MSCs. Overall, the effects of BMAT specifically on MM-induced bone disease and osteolysis may be substantial and promising as a new therapeutic target.

Bone Marrow Adipocytes and Hematopoiesis

As BM adipocytes are interspersed throughout the vascular and endosteal niches responsible for guiding the lineage commitment of HSCs, they may also affect hematopoiesis both *via* local and systemic effects. Research on human iliac crest-derived marrow adipocytes found that these cells have the ability to support $CD34^+$ hematopoietic progenitor cells *in vitro* (39). BMAT is also intimately associated with the blood-forming marrow. Primary human BMAT adipocytes, purified from the iliac crest, have the ability to support differentiation of $CD34^+$ hematopoietic progenitor cells in long-term culture *in vitro* (39). Yet, other data suggest that BMAT may be inhibitory toward hematopoiesis; this has been observed in mouse experiments where BMAT induced hematopoietic cell quiescence and decreased the number of progenitor marrow cells (51). Adipocyte-derived factors are also known to inhibit B lymphopoiesis (156).

The number of adult BM adipocytes was found to correlate inversely with the hematopoietic activity of the marrow and decrease marrow transplant cell engraftment after irradiation (51). Yet, in another study, mice treated with a TZD called "Troglitazone," which causes massive BMAT expansion, hematopoietic progenitor frequency was not altered, and, in fact, preadipocytes were found to support hematopoetic cells *in vitro* (77). Thus, it is unclear if MAT always has a negative influence on the hematopoietic niche, or if this is time, location, or disease dependent.

INFLUENCES OF MYELOMA ON BMAT

Bone marrow MSCs can give rise to BM adipocytes and osteoblasts, as dictated through expression of proteins in major transcriptional regulatory pathways such as PPARγ and Wnt, respectively. It is not well understood how MM cells alter BMAT or MSC cell fate, but a study from 2007 revealed that MM-MSCs retain their capacity to differentiate down adipogenic and osteogenic lineages, although quantification of this differentiation

(e.g., with oil red O or alizarin red staining) was not performed (157). Studies since then have observed a decreased ability for MM-MSCs to proliferate and undergo osteogenic differentiation (5, 32), suggesting that their adipogenic capacity may be altered. It is also possible that MM cells utilize the lipids stored in BMAT to fuel their proliferation and migration, as other tumor cells (ovarian cells) have been found to do in other adipose depots (the omentum) (158). This utilization would decrease the amount of lipid stored in these cells, though this is an observation that has yet to be examined. Research into the bidirectional communication between MM cells and BMAT is needed to determine how MM cells affect BMAT as well as the ramifications of these interactions on tumor growth and osteolysis.

LINKING BMAT AND SYSTEMIC INFLAMMATION

Bone marrow adipose tissue is linked to systemic inflammation through mechanisms that include the production of proinflammatory cytokines and lipids able to undergo oxidation. Obesity and aging both correlate with increased systemic inflammation, increased risk of MM, and increased BMAT. This leads to a few potential hypotheses: (1) that BMAT drives MM through local and/or systemic effects (e.g., on inflammation), or (2) that elevated BMAT and MM correlate because both are driven by a common or linked underlying mechanism, e.g., obesity, aging, or decreased immune function. Currently, either hypothesis could prove true. While WAT imparts systemic/endocrine influences, BMAT may produce systemic as well as local, paracrine, and cell–cell contact-based effects on tumors. The close proximity of BMAT and MM cells suggests potential contact-mediated bidirectional signaling between these cells, which is absent from WAT–MM cell interactions. However, WAT appears to be comprised of cells that derive from the marrow (up to 35%) (159); the signaling parallels and lineage tracing links between WAT and BMAT confound determining the specific contributions of each toward MM progression or myelomagenesis. Although more research examining the specific contributions of each depot are needed, much evidence suggests that immune system alterations resulting from elevated BMAT or WAT could contribute to MM progression (44, 152, 160).

In breast cancer, obesity-related host factors, such as components of the secretome (e.g., insulin, IGF-1, leptin, adiponectin, steroid hormones, cytokines, vascular regulators, and inflammation-related molecules), explain the causative link between increased risk of breast cancer in postmenopausal women and poor prognosis in pre- and postmenopausal women (161). Many of these same factors are also systemic signals that could explain the link between obesity and increased MM risk. However, proinflammatory cytokines that are derived from adipose tissue, such as IL-1 (162), can be difficult to identify as anti-myeloma or myeloma-supportive, because of the complex roles of the immune system in cancer. In general, immune cells attack and can eliminate myeloma cells. But systemic inflammation can also contribute to tumor growth if regulatory T-cells or myeloid suppressor cells (which are cells that suppress other immune cells) are increased. Other adipocyte-derived factors are proinflammatory and support natural killer cells, such as IL-15 (163). As genetically modified, *ex vivo*-expanded natural killer cells are being used as a treatment for MM and many cancers, IL-15 and adipocyte-induced support of NK cells may in fact have anti-myeloma consequences (164). Yet, IL-15, along with other angiogenic factors (VEGF, IL-6, and HGF), is also significantly increased in MM patient blood serum reflecting a correlation between angiogenesis and MM (164). From this perspective, IL-15 and these other adipocyte-derived factors appear to support tumor growth through both direct effects and also increased tumor vascularization. MSC adipogenic differentiation has also been found to be modulated by natural killer cells (165), suggesting that a forward feedback loop between inflammation and adipogenesis may be at work. These data suggest that adipocytes not only are affected by, but also affect, the immune system. For a review on systemic and BMAT-induced inflammation and its contributions to tumor growth and survival, dysregulated bone remodeling, and activation of inflammatory pathways in tumor cells (e.g., CCL2/CCR2- and COX-2-dependent pathways), refer to the review by Hardaway et al. (166).

Lipids are essential components of cell membranes and represent an energy-rich fuel source. However, lipids are frequently targeted by reactive oxygen species (ROS), such as free radicals. This leads to the oxidation of lipids in a chain reaction known as lipid peroxidation, which has been associated with a wide range of diseases, including cancer, diabetes, and neurological disorders (167). Many of the products of free radical chain oxidation are unstable, but stable isoprostanes have become the gold standard measurable biomarker for oxidative stress (167). One well-studied lipid electrophile, 4-NHE, is generated from lipid peroxidation and mediates a variety of biological processes (e.g., DNA damage, mutagenesis, inflammatory response, cell growth, and apoptosis) through a range of pathways (ER stress, stress-responsive MAP kinase signaling, NF-kB signaling, and DNA damage response signaling) (167). Malondialdehyde (MDA) is another product of lipid peroxidation; it is highly mutagenic (168). MDA and 4-NHE are two molecules responsible for lipid-initiated genetic disruption that could support MM development through numerous pathways, such as the oxidative stress-driven activation of the PI3K/AKT pathway and inactivation of the tumor suppressor gene *PTEN* (169). Oxidative stress can also lead to increased PPAR, Cox-2, MAPK, and PKC signaling; any of these pathways could support myelomagenesis or disease progression (170). As antioxidants can abrogate oxidative-stress-induced apoptosis of osteoblasts, they may represent a potential therapeutic avenue in MM (154).

TREATMENTS TARGETING BMAT

There is immense potential in targeting BMAT or BMAT-derived factors, to combat myeloma initiation, progression, relapse, chemoresistance, and osteolysis. Based on preclinical data regarding the roles of adiponectin in MM, recombinant or biologically isolated adiponectin treatment for MM patients with low adiponectin levels may hold great potential as a therapeutic treatment. Similarly, decreasing BMAT-derived factors that are MM-supportive using inhibitors or antibodies may be a potential

future BMAT-targeted therapy. Another way to target BMAT may be to target those signaling pathways that push MSCs down the adipogenic rather than osteogenic lineage, thus flipping the commitment lineage switch. One such pathway is the Wnt signaling pathway, which supports osteogenic differentiation and inhibits adipogenic differentiation. As we know that sclerostin, a Wnt inhibitor, is elevated in the BM of MM patients, it is possible that antisclerostin antibodies would not only increase bone volumes but also decrease BMAT in MM patient marrow, creating a less hospitable microenvironment for MM cells to colonize (171, 172). Other potential target lineage switches that induce osteogenesis and limit adipogenesis are parathyroid hormone receptor (PTH), TAZ/YAP (173), and numerous zinc finger proteins (174).

It is important to consider the link between BMAT and bone when analyzing adipose-directed therapies, because treatments that affect bone could affect BMAT (and *vice versa*). As there appears to be a reciprocal relationship between BMAT and bone formation in both healthy and diseased conditions (175, 176), increasing bone mass may be one novel way to decrease BMAT and also strengthen bones that are weakened by MM. It is becoming clear that the skeleton has a complex, non-linear, and genotype-dependent relationship with energy utilization and MAT (151, 177). Exercise has been shown to significantly suppress BMAT volume and induce bone formation in certain mouse models, suggesting that a healthy diet and increased exercise or strength training program could create a two-pronged attack to strengthen bones and decrease BMAT in MGUS or MM patients (178). The antidiabetic drug metformin can also decrease BMAT in mice that are fed with a high fat diet (Michaela R. Reagan and CJ Rosen, unpublished data). It can also modestly improve bone volume (179) as well as directly affect metabolism of tumor cells (180). These data suggest that metformin may be another potential multidimensional therapeutic. The topic of metformin effects on cancer has been reviewed recently (181).

Altering lipid levels, ratios, or content systemically or in the BM may also hold great promise as an anti-myeloma treatment. For instance, Abdi et al. demonstrated that omega-3 fatty acids [n-3 polyunsaturated eicosapentaenoic acid (EPA) and docosahexaenoic acid (DHA)] induced apoptosis and increased sensitivity to bortezomib in MM cells preclinically, without affecting normal human peripheral mononuclear cells viability (182). These lipids modulated multiple signaling pathways including NFκB, Notch, Hedgehog, oxidative stress, and Wnt. They also induced apoptosis through mitochondrial perturbation and caspase-3 activation (182). Combined with the data above on oxidative stress, these data suggest that supplements such as vitamins (antioxidants) and fish oil, and/or diets rich in fish, fruits, and vegetables, should be explored as preventative measures in the development of MM. However, carefully designed trials are necessary to best optimize treatment regimes, as some antioxidants, such as vitamin C and flavonoids in vegetables, fruits, and green tea, can neutralize and should not be used with bortezomib, a commonly prescribed anti-myeloma proteasome inhibitor (183).

CONCLUSION

As reviewed herein, BMAT appears to affect MM through an array of different mechanisms. We have described what is currently understood about the BM adipocyte and BMAT. We next highlighted the ways in which BMAT may support MM, for example, through bioactive lipids (as a fuel source, signaling molecule, and a substrate for lipid peroxidation), and myeloma-supportive adipokines (e.g., IL-6, TNFα, MCP-1, PAI-1, IL-6, resistin, and leptin). We also provided an overview of adiponectin, a protein that is decreased during obesity and has anti-myeloma properties making it an attractive potential therapeutic in MM. The complex relationship between hypoxia, BMAT, angiogenesis, and myeloma in the BM was discussed. Influence of BMAT on bone health and osteogenesis was delineated, and our current understandings of potential ways in which MM cells may affect BMAT were outlined. The review investigates the relationship between BMAT and systemic inflammation in relation to MM. Lastly, we suggested possible therapeutic avenues through which BMAT could be targeted, similarly to how osteoblasts and osteoclasts, and factors derived from these cells, have been successfully targeted in MM. Targeting lipid metabolism of cancer cells and adipocytes in combination with standard antimyeloma therapies will likely reveal novel therapeutic avenues through which to attack hematological malignancies. In sum, we are optimistic about the development of new combination therapies and preventative methods that take into account the roles of the BM adipocyte in MM and other bone-metastatic cancers. The path toward improved therapies will be built on basic scientific research of BMAT roles in cancer.

AUTHOR CONTRIBUTIONS

CF, HF, and MR contributed to the conception, drafting, writing, and editing of this work.

ACKNOWLEDGMENTS

The authors thank Dr. Michael Erard, Scientific Editor and Writing consultant at Maine Medical Center Research Institute (MMCRI) for editorial assistance. We apologize to colleagues whose work could not be cited due to space constraints.

FUNDING

The authors' work is supported by Start-up funds, a pilot project grant and support from NIH/NIGMS (P30 GM106391 and P30GM103392), and the NIH/NIDDK (R24 DK092759-01) at Maine Medical Center Research Institute.

REFERENCES

1. Hanahan D, Weinberg RA. The hallmarks of cancer. *Cell* (2000) 100:57–70. doi:10.1016/S0092-8674(00)81683-9
2. Hanahan D, Weinberg RA. Hallmarks of cancer: the next generation. *Cell* (2011) 144:646–74. doi:10.1016/j.cell.2011.02.013
3. Palumbo A, Anderson K. Multiple myeloma. *N Engl J Med* (2011) 364: 1046–60. doi:10.1056/NEJMra1011442

4. Fairfield H, Falank C, Avery L, Reagan MR. Multiple myeloma in the marrow: pathogenesis and treatments. *Ann N Y Acad Sci* (2016) 1364:32–51. doi:10.1111/nyas.13038
5. Reagan MR, Ghobrial IM. Multiple myeloma-mesenchymal stem cells: characterization, origin, and tumor-promoting effects. *Clin Cancer Res* (2012) 18:342–9. doi:10.1158/1078-0432.CCR-11-2212
6. Kawano Y, Moschetta M, Manier S, Glavey S, Görgün GT, Roccaro AM, et al. Targeting the bone marrow microenvironment in multiple myeloma. *Immunol Rev* (2015) 263:160–72. doi:10.1111/imr.12233
7. Alexander DD, Mink PJ, Adami H-O, Cole P, Mandel JS, Oken MM, et al. Multiple myeloma: a review of the epidemiologic literature. *Int J Cancer* (2007) 120(Suppl):40–61. doi:10.1002/ijc.22718
8. Palumbo A, Avet-Loiseau H, Oliva S, Lokhorst HM, Goldschmidt H, Rosinol L, et al. Revised international staging system for multiple myeloma: a report from international myeloma working group. *J Clin Oncol* (2015) 33:2863–9. doi:10.1200/JCO.2015.61.2267
9. Wright JH. A case of multiple myeloma. *J Boston Soc Med Sci* (1900) 4:195–204.5.
10. Teras LR, Kitahara CM, Birmann BM, Hartge PA, Wang SS, Robien K, et al. Body size and multiple myeloma mortality: a pooled analysis of 20 prospective studies. *Br J Haematol* (2014) 166:667–76. doi:10.1111/bjh.12935
11. Qian H, Buza-Vidas N, Hyland CD, Jensen CT, Antonchuk J, Månsson R, et al. Critical role of thrombopoietin in maintaining adult quiescent hematopoietic stem cells. *Cell Stem Cell* (2007) 1:671–84. doi:10.1016/j.stem.2007.10.008
12. Lohr JG, Stojanov P, Carter SL, Cruz-Gordillo P, Lawrence MS, Auclair D, et al. Widespread genetic heterogeneity in multiple myeloma: implications for targeted therapy. *Cancer Cell* (2014) 25:91–101. doi:10.1016/j.ccr.2013.12.015
13. Sahin I, Azab F, Mishima Y, Moschetta M, Tsang B, Glavey SV, et al. Targeting survival and cell trafficking in multiple myeloma and Waldenstrom macroglobulinemia using pan-class I PI3K inhibitor, buparlisib. *Am J Hematol* (2014) 89:1030–6. doi:10.1002/ajh.23814
14. Brunetti G, Rizzi R, Oranger A, Gigante I, Mori G, Taurino G, et al. LIGHT/TNFSF14 increases osteoclastogenesis and decreases osteoblastogenesis in multiple myeloma-bone disease. *Oncotarget* (2014) 5:12950–67. doi:10.18632/oncotarget.2633
15. Suen H, Brown R, Yang S, Weatherburn C, Ho PJ, Woodland N, et al. Multiple myeloma causes clonal T-cell immunosenescence: identification of potential novel targets for promoting tumour immunity and implications for checkpoint blockade. *Leukemia* (2016). doi:10.1038/leu.2016.84
16. Fu J, Li S, Feng R, Ma H, Sabeh F, Roodman GD, et al. Multiple myeloma-derived MMP-13 mediates osteoclast fusogenesis and osteolytic disease. *J Clin Invest* (2016) 126:1759–72. doi:10.1172/JCI80276
17. Colucci S, Brunetti G, Mori G, Oranger A, Centonze M, Mori C, et al. Soluble decoy receptor 3 modulates the survival and formation of osteoclasts from multiple myeloma bone disease patients. *Leukemia* (2009) 23:2139–46. doi:10.1038/leu.2009.136
18. Reagan MR, Liaw L, Rosen CJ, Ghobrial IM. Dynamic interplay between bone and multiple myeloma: emerging roles of the osteoblast. *Bone* (2015) 75:161–9. doi:10.1016/j.bone.2015.02.021
19. Palma BD, Guasco D, Pedrazzoni M, Bolzoni M, Accardi F, Costa F, et al. Osteolytic lesions, cytogenetic features and bone marrow levels of cytokines and chemokines in multiple myeloma patients: role of chemokine (C-C motif) ligand 20. *Leukemia* (2016) 30:409–16. doi:10.1038/leu.2015.259
20. Raje N, Vadhan-Raj S, Willenbacher W, Terpos E, Hungria V, Spencer A, et al. Evaluating results from the multiple myeloma patient subset treated with denosumab or zoledronic acid in a randomized phase 3 trial. *Blood Cancer J* (2016) 6:e378. doi:10.1038/bcj.2015.96
21. Croucher PI, McDonald MM, Martin TJ. Bone metastasis: the importance of the neighbourhood. *Nat Rev Cancer* (2016) 16:373–86. doi:10.1038/nrc.2016.44
22. Vanderkerken K, De Leenheer E, Shipman C, Asosingh K, Willems A, Van Camp B, et al. Recombinant osteoprotegerin decreases tumor burden and increases survival in a murine model of multiple myeloma. *Cancer Res* (2003) 63:287–9.
23. Swami A, Reagan MR, Basto P, Mishima Y, Kamaly N, Glavey S, et al. Engineered nanomedicine for myeloma and bone microenvironment targeting. *Proc Natl Acad Sci U S A* (2014) 111:10287–92. doi:10.1073/pnas.1401337111
24. Lawson MA, McDonald MM, Kovacic NN, Hua Khoo W, Terry RTL, Down J, et al. Osteoclasts control re-activation of dormant myeloma cells by remodeling the endosteal niche. *Nat Commun* (2015) 6:8983. doi:10.1038/ncomms9983
25. Moschetta M, Mishima Y, Kawano Y, Manier S, Paiva B, Palomera L, et al. Targeting vasculogenesis to prevent progression in multiple myeloma. *Leukemia* (2016) 30:1103–15. doi:10.1038/leu.2016.3
26. Moschetta M, Mishima Y, Sahin I, Manier S, Glavey S, Vacca A, et al. Role of endothelial progenitor cells in cancer progression. *Biochim Biophys Acta* (2014) 1846:26–39. doi:10.1016/j.bbcan.2014.03.005
27. Glavey SV, Huynh D, Reagan MR, Manier S, Moschetta M, Kawano Y, et al. The cancer glycome: carbohydrates as mediators of metastasis. *Blood Rev* (2015) 29:269–79. doi:10.1016/j.blre.2015.01.003
28. Glavey SV, Manier S, Natoni A, Sacco A, Moschetta M, Reagan MR, et al. The sialyltransferase ST3GAL6 influences homing and survival in multiple myeloma. *Blood* (2014) 124(11):1765–76. doi:10.1182/blood-2014-03-560862
29. Azab AK, Quang P, Azab F, Pitsillides C, Thompson B, Chonghaile T, et al. P-selectin glycoprotein ligand regulates the interaction of multiple myeloma cells with the bone marrow microenvironment. *Blood* (2011) 119:1468–78. doi:10.1182/blood-2011-07-368050
30. Roccaro AM, Sacco A, Purschke WG, Moschetta M, Buchner K, Maasch C, et al. SDF-1 inhibition targets the bone marrow niche for cancer therapy. *Cell Rep* (2014) 9:118–28. doi:10.1016/j.celrep.2014.08.042
31. Azab AK, Runnels JM, Pitsillides C, Moreau A-S, Azab F, Leleu X, et al. CXCR4 inhibitor AMD3100 disrupts the interaction of multiple myeloma cells with the bone marrow microenvironment and enhances their sensitivity to therapy. *Blood* (2009) 113:4341–51. doi:10.1182/blood-2008-10-186668
32. Reagan MR, Mishima Y, Glavey SV, Zhang Y, Manier S, Lu ZN, et al. Investigating osteogenic differentiation in multiple myeloma using a novel 3D bone marrow niche model. *Blood* (2014) 124:3250–9. doi:10.1182/blood-2014-02-558007
33. Roccaro AM, Sacco A, Maiso P, Azab AK, Tai Y-T, Reagan M, et al. BM mesenchymal stromal cell-derived exosomes facilitate multiple myeloma progression. *J Clin Invest* (2013) 123:1542–55. doi:10.1172/JCI66517
34. Manni S, Toscani D, Mandato E, Brancalion A, Quotti Tubi L, Macaccaro P, et al. Bone marrow stromal cell-fueled multiple myeloma growth and osteoclastogenesis are sustained by protein kinase CK2. *Leukemia* (2014) 28:2094–7. doi:10.1038/leu.2014.178
35. Delgado-Calle J, Anderson J, Cregor MD, Hiasa M, Chirgwin JM, Carlesso N, et al. Bidirectional Notch signaling and osteocyte-derived factors in the bone marrow microenvironment promote tumor cell proliferation and bone destruction in multiple myeloma. *Cancer Res* (2016) 76:1089–100. doi:10.1158/0008-5472.CAN-15-1703
36. Colaianni G, Colucci S, Grano M. 1st ed. In: Lenzi A, Migliaccio S, Maria Donini L, editors. *Multidisciplinary Approach to Obesity: From Assessment to Treatment*. Switzerland: Springer International Publishing (2015). Available from: http://www.springer.com/us/book/9783319090443
37. Scheller EL, Rosen CJ. What's the matter with MAT? Marrow adipose tissue, metabolism, and skeletal health. *Ann N Y Acad Sci* (2014) 1311:14–30. doi:10.1111/nyas.12327
38. Lecka-Czernik B. Marrow fat metabolism is linked to the systemic energy metabolism. *Bone* (2012) 50:534–9. doi:10.1016/j.bone.2011.06.032
39. Poloni A, Maurizi G, Serrani F, Mancini S, Zingaretti MC, Frontini A, et al. Molecular and functional characterization of human bone marrow adipocytes. *Exp Hematol* (2013) 41:558–566.e2. doi:10.1016/j.exphem.2013.02.005
40. Lecka-Czernik B, Stechschulte LA. Bone and fat: a relationship of different shades. *Arch Biochem Biophys* (2014) 561:124–9. doi:10.1016/j.abb.2014.06.010
41. Devlin MJ, Cloutier AM, Thomas NA, Panus DA, Lotinun S, Pinz I, et al. Caloric restriction leads to high marrow adiposity and low bone mass in growing mice. *J Bone Miner Res* (2010) 25:2078–88. doi:10.1002/jbmr.82
42. Cawthorn WP, Scheller EL, Learman BS, Parlee SD, Simon BR, Mori H, et al. Bone marrow adipose tissue is an endocrine organ that contributes to increased circulating adiponectin during caloric restriction. *Cell Metab* (2014) 20:368–75. doi:10.1016/j.cmet.2014.06.003
43. Xuan D, Han Q, Tu Q, Zhang L, Yu L, Murry D, et al. Epigenetic modulation in periodontitis: interaction of adiponectin and JMJD3-IRF4 axis in macrophages. *J Cell Physiol* (2016) 231:1090–6. doi:10.1002/jcp.25201

44. Adler BJ, Kaushansky K, Rubin CT. Obesity-driven disruption of haematopoiesis and the bone marrow niche. *Nat Rev Endocrinol* (2014) 10:737–48. doi:10.1038/nrendo.2014.169
45. Doucette CR, Horowitz MC, Berry R, MacDougald OA, Anunciado-Koza R, Koza RA, et al. A high fat diet increases bone marrow adipose tissue (MAT) but does not alter trabecular or cortical bone mass in C57BL/6J mice. *J Cell Physiol* (2015) 230(9):2032–7. doi:10.1002/jcp.24954
46. Scheller EL, Cawthorn WP, Burr AA, Horowitz MC, MacDougald OA. Marrow adipose tissue: trimming the fat. *Trends Endocrinol Metab* (2016) 27:392–403. doi:10.1016/j.tem.2016.03.016
47. Scheller EL, Troiano N, Vanhoutan JN, Bouxsein MA, Fretz JA, Xi Y, et al. Use of osmium tetroxide staining with microcomputerized tomography to visualize and quantify bone marrow adipose tissue in vivo. *Methods Enzymol* (2014) 537:123–39. doi:10.1016/B978-0-12-411619-1.00007-0
48. Bredella MA, Lin E, Gerweck AV, Landa MG, Thomas BJ, Torriani M, et al. Determinants of bone microarchitecture and mechanical properties in obese men. *J Clin Endocrinol Metab* (2012) 97:4115–22. doi:10.1210/jc.2012-2246
49. Miyakoshi N, Sato K, Abe T, Tsuchida T, Tamura Y, Kudo T. Histomorphometric evaluation of the effects of ovariectomy on bone turnover in rat caudal vertebrae. *Calcif Tissue Int* (1999) 64:318–24. doi:10.1007/s002239900626
50. Li M, Shen Y, Qi H, Wronski TJ. Comparative study of skeletal response to estrogen depletion at red and yellow marrow sites in rats. *Anat Rec* (1996) 245:472–80. doi:10.1002/(SICI)1097-0185(199607)245:3<472:AID-AR3>3.0.CO;2-U
51. Naveiras O, Nardi V, Wenzel PL, Hauschka PV, Fahey F, Daley GQ. Bone-marrow adipocytes as negative regulators of the haematopoietic microenvironment. *Nature* (2009) 460:259–63. doi:10.1038/nature08099
52. Bornstein S, Brown SA, Le PT, Wang X, DeMambro V, Horowitz MC, et al. FGF-21 and skeletal remodeling during and after lactation in C57BL6 mice. *Endocrinology* (2014) 155:3516–26. doi:10.1210/en.2014-1083
53. Ackert-Bicknell CL, Shockley KR, Horton LG, Lecka-Czernik B, Churchill GA, Rosen CJ. Strain-specific effects of rosiglitazone on bone mass, body composition, and serum insulin-like growth factor-I. *Endocrinology* (2009) 150:1330–40. doi:10.1210/en.2008-0936
54. Reagan MR, Rosen CJ. Navigating the bone marrow niche: translational insights and cancer-driven dysfunction. *Nat Rev Rheumatol* (2015) 12:154–68. doi:10.1038/nrrheum.2015.160
55. Rosen CJ, Ackert-Bicknell C, Rodriguez JP, Pino AM. Marrow fat and the bone microenvironment: developmental, functional, and pathological implications. *Crit Rev Eukaryot Gene Expr* (2009) 19:109–24. doi:10.1016/j.bbi.2008.05.010
56. Fazeli PK, Horowitz MC, MacDougald OA, Scheller EL, Rodeheffer MS, Rosen CJ, et al. Marrow fat and bone-new perspectives. *J Clin Endocrinol Metab* (2013) 98:935–45. doi:10.1210/jc.2012-3634
57. Roura S, Farré J, Soler-Botija C, Llach A, Hove-Madsen L, Cairó JJ, et al. Effect of aging on the pluripotential capacity of human CD105+ mesenchymal stem cells. *Eur J Heart Fail* (2006) 8:555–63. doi:10.1016/j.ejheart.2005.11.006
58. Kretlow JD, Jin Y-Q, Liu W, Zhang WJ, Hong T-H, Zhou G, et al. Donor age and cell passage affects differentiation potential of murine bone marrow-derived stem cells. *BMC Cell Biol* (2008) 9:60. doi:10.1186/1471-2121-9-60
59. Maredziak M, Marycz K, Tomaszewski KA, Kornicka K, Henry BM. The influence of aging on the regenerative potential of human adipose derived mesenchymal stem cells. *Stem Cells Int* (2016) 2016:1–15. doi:10.1155/2016/2152435
60. Singh L, Brennan TA, Russell E, Kim J-H, Chen Q, Brad Johnson F, et al. Aging alters bone-fat reciprocity by shifting in vivo mesenchymal precursor cell fate towards an adipogenic lineage. *Bone* (2016) 85:29–36. doi:10.1016/j.bone.2016.01.014
61. Zhou BO, Yue R, Murphy MM, Peyer JG, Morrison SJ. Leptin-receptor-expressing mesenchymal stromal cells represent the main source of bone formed by adult bone marrow. *Cell Stem Cell* (2014) 15:154–68. doi:10.1016/j.stem.2014.06.008
62. Liu Y, Strecker S, Wang L, Kronenberg MS, Wang W, Rowe DW, et al. Osterix-cre labeled progenitor cells contribute to the formation and maintenance of the bone marrow stroma. *PLoS One* (2013) 8:e71318. doi:10.1371/journal.pone.0071318
63. Pan SY, Johnson KC, Ugnat A-M, Wen SW, Mao Y. Association of obesity and cancer risk in Canada. *Am J Epidemiol* (2004) 159:259–68. doi:10.1093/aje/kwh041
64. Wallin A, Larsson SC. Body mass index and risk of multiple myeloma: a meta-analysis of prospective studies. *Eur J Cancer* (2011) 47:1606–15. doi:10.1016/j.ejca.2011.01.020
65. Islam R, Altundag K, Kurt M, Altundag O, Turen S. Association between obesity and multiple myeloma in postmenopausal women may be attributed to increased aromatization of androgen in adipose tissue. *Med Hypotheses* (2005) 65:1001–2. doi:10.1016/j.mehy.2005.05.014
66. Caers J, Deleu S, Belaid Z, De Raeve H, Van Valckenborgh E, De Bruyne E, et al. Neighboring adipocytes participate in the bone marrow microenvironment of multiple myeloma cells. *Leukemia* (2007) 21:1580–4. doi:10.1038/sj.leu.2404658
67. Liu Z, Xu J, He J, Liu H, Lin P, Wan X, et al. Mature adipocytes in bone marrow protect myeloma cells against chemotherapy through autophagy activation. *Oncotarget* (2015) 6:34329–41. doi:10.18632/oncotarget.6020
68. Sprynski AC, Hose D, Caillot L, Réme T, Shaughnessy JD, Barlogie B, et al. The role of IGF-1 as a major growth factor for myeloma cell lines and the prognostic relevance of the expression of its receptor. *Blood* (2009) 113:4614–26. doi:10.1182/blood-2008-07-170464
69. Clark R, Krishnan V, Schoof M, Rodriguez I, Theriault B, Chekmareva M, et al. Milky spots promote ovarian cancer metastatic colonization of peritoneal adipose in experimental models. *Am J Pathol* (2013) 183:576–91. doi:10.1016/j.ajpath.2013.04.023
70. Vogl DT, Wang T, Pérez WS, Stadtmauer EA, Heitjan DF, Lazarus HM, et al. Effect of obesity on outcomes after autologous hematopoietic stem cell transplantation for multiple myeloma. *Biol Blood Marrow Transplant* (2011) 17:1765–74. doi:10.1016/j.bbmt.2011.05.005
71. Zub KA, Sousa MM, Sarno A, Sharma A, Demirovic A, Rao S, et al. Modulation of cell metabolic pathways and oxidative stress signaling contribute to acquired melphalan resistance in multiple myeloma cells. *PLoS One* (2015) 10:e0119857. doi:10.1371/journal.pone.0119857
72. Nagata Y, Ishizaki I, Waki M, Ide Y, Hossen MA, Ohnishi K, et al. Palmitic acid, verified by lipid profiling using secondary ion mass spectrometry, demonstrates anti-multiple myeloma activity. *Leuk Res* (2015) 39:638–45. doi:10.1016/j.leukres.2015.02.011
73. Zou J, Ma X, Zhang G, Shen L, Zhou L, Yu Y, et al. Evaluation of the change in sphingolipids in the human multiple myeloma cell line U266 and gastric cancer cell line MGC-803 treated with arsenic trioxide. *J Chromatogr B Analyt Technol Biomed Life Sci* (2015) 1004:98–107. doi:10.1016/j.jchromb.2015.09.015
74. Kitatani K, Taniguchi M, Okazaki T. Role of sphingolipids and metabolizing enzymes in hematological malignancies. *Mol Cells* (2015) 38:482–95. doi:10.14348/molcells.2015.0118
75. Jurczyszyn A, Czepiel J, Gdula-Argasińska J, Paśko P, Czapkiewicz A, Librowski T, et al. Plasma fatty acid profile in multiple myeloma patients. *Leuk Res* (2015) 39:400–5. doi:10.1016/j.leukres.2014.12.010
76. Hossen MA, Nagata Y, Waki M, Ide Y, Takei S, Fukano H, et al. Decreased level of phosphatidylcholine (16:0/20:4) in multiple myeloma cells compared to plasma cells: a single-cell MALDI-IMS approach. *Anal Bioanal Chem* (2015) 407:5273–80. doi:10.1007/s00216-015-8741-z
77. Spindler TJ, Tseng AW, Zhou X, Adams GB. Adipocytic cells augment the support of primitive hematopoietic cells in vitro but have no effect in the bone marrow niche under homeostatic conditions. *Stem Cells Dev* (2014) 23:434–41. doi:10.1089/scd.2013.0227
78. Sola B, Poirot M, de Medina P, Bustany S, Marsaud V, Silvente-Poirot S, et al. Antiestrogen-binding site ligands induce autophagy in myeloma cells that proceeds through alteration of cholesterol metabolism. *Oncotarget* (2013) 4:911–22. doi:10.18632/oncotarget.1066
79. Nair S, Branagan AR, Liu J, Boddupalli CS, Mistry PK, Dhodapkar MV. Clonal immunoglobulin against lysolipids in the origin of myeloma. *N Engl J Med* (2016) 374:555–61. doi:10.1056/NEJMoa1508808
80. Vescio RA, Cao J, Hong CH, Lee JC, Wu CH, Der Danielian M, et al. Myeloma Ig heavy chain V region sequences reveal prior antigenic selection and marked somatic mutation but no intraclonal diversity. *J Immunol* (1995) 155:2487–97.
81. Klein-Wieringa IR, Andersen SN, Kwekkeboom JC, Giera M, de Lange-Brokaar BJE, van Osch GJVM, et al. Adipocytes modulate the phenotype of human macrophages through secreted lipids. *J Immunol* (2013) 191:1356–63. doi:10.4049/jimmunol.1203074

82. Krishnan A, Nair SA, Pillai MR. Biology of PPAR gamma in cancer: a critical review on existing lacunae. *Curr Mol Med* (2007) 7:532–40. doi:10.2174/156652407781695765
83. Aouali N, Broukou A, Bosseler M, Keunen O, Schlesser V, Janji B, et al. Epigenetic activity of peroxisome proliferator-activated receptor gamma agonists increases the anticancer effect of histone deacetylase inhibitors on multiple myeloma cells. *PLoS One* (2015) 10:e0130339. doi:10.1371/journal.pone.0130339
84. Rui M, Huang Z, Liu Y, Wang Z, Liu R, Fu J, et al. Rosiglitazone suppresses angiogenesis in multiple myeloma via downregulation of hypoxia-inducible factor-1α and insulin-like growth factor-1 mRNA expression. *Mol Med Rep* (2014) 10:2137–43. doi:10.3892/mmr.2014.2407
85. Cao D, Zhou H, Zhao J, Jin L, Yu W, Yan H, et al. PGC-1α integrates glucose metabolism and angiogenesis in multiple myeloma cells by regulating VEGF and GLUT-4. *Oncol Rep* (2014) 31:1205–10. doi:10.3892/or.2014.2974
86. Kim SY, Min HJ, Park HK, Oh B, Kim TY, She CJ, et al. Increased copy number of the interleukin-6 receptor gene is associated with adverse survival in multiple myeloma patients treated with autologous stem cell transplantation. *Biol Blood Marrow Transplant* (2011) 17:810–20. doi:10.1016/j.bbmt.2011.01.002
87. Greco EA, Lenzi A, Migliaccio S. The obesity of bone. *Ther Adv Endocrinol Metab* (2015) 6:273–86. doi:10.1177/2042018815611004
88. Sakurai T, Ogasawara J, Kizaki T, Sato S, Ishibashi Y, Takahashi M, et al. The effects of exercise training on obesity-induced dysregulated expression of adipokines in white adipose tissue. *Int J Endocrinol* (2013) 2013:801743. doi:10.1155/2013/801743
89. Galson DL, Silbermann R, Roodman GD. Mechanisms of multiple myeloma bone disease. *Bonekey Rep* (2012) 1:135. doi:10.1038/bonekey.2012.135
90. Lee C, Oh J-I, Park J, Choi J-H, Bae E-K, Lee HJ, et al. TNF α mediated IL-6 secretion is regulated by JAK/STAT pathway but not by MEK phosphorylation and AKT phosphorylation in U266 multiple myeloma cells. *Biomed Res Int* (2013) 2013:580135. doi:10.1155/2013/580135
91. Jöhrer K, Janke K, Krugmann J, Fiegl M, Greil R. Transendothelial migration of myeloma cells is increased by tumor necrosis factor (TNF)-alpha via TNF receptor 2 and autocrine up-regulation of MCP-1. *Clin Cancer Res* (2004) 10:1901–10. doi:10.1158/1078-0432.CCR-1053-03
92. Yağci M, Sucak GT, Haznedar R. Fibrinolytic activity in multiple myeloma. *Am J Hematol* (2003) 74:231–7. doi:10.1002/ajh.10433
93. Schwartz MW, Woods SC, Porte D, Seeley RJ, Baskin DG. Central nervous system control of food intake. *Nature* (2000) 404:661–71. doi:10.1038/35007534
94. Ouchi N, Parker JL, Lugus JJ, Walsh K. Adipokines in inflammation and metabolic disease. *Nat Rev Immunol* (2011) 11:85–97. doi:10.1038/nri2921
95. Jarrar MH, Baranova A, Collantes R, Ranard B, Stepanova M, Bennett C, et al. Adipokines and cytokines in non-alcoholic fatty liver disease. *Aliment Pharmacol Ther* (2007) 27:412–21. doi:10.1111/j.1365-2036.2007.03586.x
96. Mattu HS, Randeva HS. Role of adipokines in cardiovascular disease. *J Endocrinol* (2012) 216:T17–36. doi:10.1530/JOE-12-0232
97. Sood A. Obesity, adipokines, and lung disease. *J Appl Physiol* (2009) 108:744–53. doi:10.1152/japplphysiol.00838.2009
98. Waluga M, Hartleb M, Boryczka G, Kukla M, Zwirska-Korczala K. Serum adipokines in inflammatory bowel disease. *World J Gastroenterol* (2014) 20:6912–7. doi:10.3748/wjg.v20.i22.6912
99. Hofmann JN, Liao LM, Pollak MN, Wang YY, Pfeiffer RM, Baris D, et al. A prospective study of circulating adipokine levels and risk of multiple myeloma. *Blood* (2012) 120:4418–20. doi:10.1182/blood-2012-06-438606
100. Reseland JE, Reppe S, Olstad OK, Hjorth-Hansen H, Brenne AT, Syversen U, et al. Abnormal adipokine levels and leptin-induced changes in gene expression profiles in multiple myeloma. *Eur J Haematol* (2009) 83:460–70. doi:10.1111/j.1600-0609.2009.01311.x
101. Dalamaga M, Diakopoulos KN, Mantzoros CS. The role of adiponectin in cancer: a review of current evidence. *Endocr Rev* (2012) 33:547–94. doi:10.1210/er.2011-1015
102. Alexandrakis MG, Passam FH, Sfiridaki A, Pappa CA, Moschandrea JA, Kandidakis E, et al. Serum levels of leptin in multiple myeloma patients and its relation to angiogenic and inflammatory cytokines. *Int J Biol Markers* (2004) 19:52–7.
103. Mouzaki A, Panagoulias I, Dervilli Z, Zolota V, Spadidea P, Rodi M, et al. Expression patterns of leptin receptor (OB-R) isoforms and direct in vitro effects of recombinant leptin on OB-R, leptin expression and cytokine secretion by human hematopoietic malignant cells. *Cytokine* (2009) 48:203–11. doi:10.1016/j.cyto.2009.07.006
104. Berner HS, Lyngstadaas SP, Spahr A, Monjo M, Thommesen L, Drevon CA, et al. Adiponectin and its receptors are expressed in bone-forming cells. *Bone* (2004) 35:842–9. doi:10.1016/j.bone.2004.06.008
105. Arita Y, Kihara S, Ouchi N, Takahashi M, Maeda K, Miyagawa J, et al. Paradoxical decrease of an adipose-specific protein, adiponectin, in obesity. *Biochem Biophys Res Commun* (1999) 257:79–83. doi:10.1006/bbrc.1999.0255
106. Hotta K, Funahashi T, Arita Y, Takahashi M, Matsuda M, Okamoto Y, et al. Plasma concentrations of a novel, adipose-specific protein, adiponectin, in type 2 diabetic patients. *Arterioscler Thromb Vasc Biol* (2000) 20:1595–9. doi:10.1161/01.ATV.20.6.1595
107. Kern PA, Di Gregorio GB, Lu T, Rassouli N, Ranganathan G. Adiponectin expression from human adipose tissue: relation to obesity, insulin resistance, and tumor necrosis factor-expression. *Diabetes* (2003) 52:1779–85. doi:10.2337/diabetes.52.7.1779
108. Dalamaga M, Karmaniolas K, Panagiotou A, Hsi A, Chamberland J, Dimas C, et al. Low circulating adiponectin and resistin, but not leptin, levels are associated with multiple myeloma risk: a case-control study. *Cancer Causes Control* (2009) 20:193–9. doi:10.1007/s10552-008-9233-7
109. Miyoshi Y, Funahashi T, Kihara S, Taguchi T, Tamaki Y, Matsuzawa Y, et al. Association of serum adiponectin levels with breast cancer risk. *Clin Cancer Res* (2003) 9:5699–704.
110. Fowler JA, Lwin ST, Drake MT, Edwards JR, Kyle RA, Mundy GR, et al. Host-derived adiponectin is tumor-suppressive and a novel therapeutic target for multiple myeloma and the associated bone disease. *Blood* (2011) 118:5872–82. doi:10.1182/blood-2011-01-330407
111. Medina EA, Oberheu K, Polusani SR, Ortega V, Velagaleti GVN, Oyajobi BO. PKA/AMPK signaling in relation to adiponectin's antiproliferative effect on multiple myeloma cells. *Leukemia* (2014) 28:2080–9. doi:10.1038/leu.2014.112
112. Zhou Y, Rui L. Leptin signaling and leptin resistance. *Front Med* (2013) 7:207–22. doi:10.1007/s11684-013-0263-5
113. Montague CT, Farooqi IS, Whitehead JP, Soos MA, Rau H, Wareham NJ, et al. Congenital leptin deficiency is associated with severe early-onset obesity in humans. *Nature* (1997) 387:903–8. doi:10.1038/43185
114. Farooqi IS, Jebb SA, Langmack G, Lawrence E, Cheetham CH, Prentice AM, et al. Effects of recombinant leptin therapy in a child with congenital leptin deficiency. *N Engl J Med* (1999) 341:879–84. doi:10.1056/NEJM199909163411204
115. Kopelman PG. Obesity as a medical problem. *Nature* (2000) 404:635–43. doi:10.1038/35007508
116. Hoang B, Benavides A, Shi Y, Frost P, Lichtenstein A. Effect of autophagy on multiple myeloma cell viability. *Mol Cancer Ther* (2009) 8:1974–84. doi:10.1158/1535-7163.MCT-08-1177
117. Arner P. Resistin: yet another adipokine tells us that men are not mice. *Diabetologia* (2005) 48:2203–5. doi:10.1007/s00125-005-1956-3
118. Ukkola O. Resistin – a mediator of obesity-associated insulin resistance or an innocent bystander? *Eur J Endocrinol* (2002) 147:571–4. doi:10.1530/eje.0.1470571
119. Sprynski AC, Hose D, Kassambara A, Vincent L, Jourdan M, Rossi JF, et al. Insulin is a potent myeloma cell growth factor through insulin/IGF-1 hybrid receptor activation. *Leukemia* (2010) 24:1940–50. doi:10.1038/leu.2010.192
120. Spencer JA, Ferraro F, Roussakis E, Klein A, Wu J, Runnels JM, et al. Direct measurement of local oxygen concentration in the bone marrow of live animals. *Nature* (2014) 508:269–73. doi:10.1038/nature13034
121. Amorin B, Alegretti AP, de Souza Valim V, da Silva AMP, da Silva MAL, Sehn F, et al. Characteristics of mesenchymal stem cells under hypoxia. *CellBio* (2013) 2:11–9. doi:10.4236/cellbio.2013.21002
122. Kakudo N, Morimoto N, Ogawa T, Taketani S, Kusumoto K. Hypoxia enhances proliferation of human adipose-derived stem cells via HIF-1α activation. *PLoS One* (2015) 10:e0139890. doi:10.1371/journal.pone.0139890
123. Borsi E, Perrone G, Terragna C, Martello M, Dico AF, Solaini G, et al. Hypoxia inducible factor-1 alpha as a therapeutic target in multiple myeloma. *Oncotarget* (2014) 5:1779–92. doi:10.18632/oncotarget.1736

124. Yata K, Otsuki T, Kurebayashi J, Uno M, Fujii T, Yawata Y, et al. Expression of angiogenic factors including VEGFs and the effects of hypoxia and thalidomide on human myeloma cells. *Int J Oncol* (2003) 22:165–73. doi:10.3892/ijo.22.1.165
125. Muz B, de la Puente P, Azab F, Luderer M, Azab AK. Hypoxia promotes stem cell-like phenotype in multiple myeloma cells. *Blood Cancer J* (2014) 4:e262. doi:10.1038/bcj.2014.82
126. Azab AK, Hu J, Quang P, Azab F, Pitsillides C, Awwad R, et al. Hypoxia promotes dissemination of multiple myeloma through acquisition of epithelial to mesenchymal transition-like features. *Blood* (2012) 119:5782–94. doi:10.1182/blood-2011-09-380410
127. Zhang Y, Marsboom G, Toth PT, Rehman J. Mitochondrial respiration regulates adipogenic differentiation of human mesenchymal stem cells. *PLoS One* (2013) 8:e77077. doi:10.1371/journal.pone.0077077
128. Cicione C, Muiños-López E, Hermida-Gómez T, Fuentes-Boquete I, Díaz-Prado S, Blanco FJ. Effects of severe hypoxia on bone marrow mesenchymal stem cells differentiation potential. *Stem Cells Int* (2013) 2013:232896. doi:10.1155/2013/232896
129. Pachón-Peña G, Serena C, Ejarque M, Petriz J, Duran X, Oliva-Olivera W, et al. Obesity determines the immunophenotypic profile and functional characteristics of human mesenchymal stem cells from adipose tissue. *Stem Cells Transl Med* (2016) 5:464–75. doi:10.5966/sctm.2015-0161
130. Wu C-L, Diekman BO, Jain D, Guilak F. Diet-induced obesity alters the differentiation potential of stem cells isolated from bone marrow, adipose tissue and infrapatellar fat pad: the effects of free fatty acids. *Int J Obes (Lond)* (2013) 37:1079–87. doi:10.1038/ijo.2012.171
131. Hu J, Van Valckenborgh E, Menu E, De Bruyne E, Vanderkerken K. Understanding the hypoxic niche of multiple myeloma: therapeutic implications and contributions of mouse models. *Dis Model Mech* (2012) 5:763–71. doi:10.1242/dmm.008961
132. Forsythe JA, Jiang BH, Iyer NV, Agani F, Leung SW, Koos RD, et al. Activation of vascular endothelial growth factor gene transcription by hypoxia-inducible factor 1. *Mol Cell Biol* (1996) 16:4604–13. doi:10.1128/MCB.16.9.4604
133. Podar K, Anderson KC. The pathophysiologic role of VEGF in hematologic malignancies: therapeutic implications. *Blood* (2005) 105:1383–95. doi:10.1182/blood-2004-07-2909
134. Yaccoby S, Barlogie B, Epstein J. Primary myeloma cells growing in SCID-hu mice: a model for studying the biology and treatment of myeloma and its manifestations. *Blood* (1998) 92:2908–13.
135. Bolkun L, Lemancewicz D, Sobolewski K, Mantur M, Semeniuk J, Kulczynska A, et al. The evaluation of angiogenesis and matrix metalloproteinase-2 secretion in bone marrow of multiple myeloma patients before and after the treatment. *Adv Med Sci* (2013) 58:118–25. doi:10.2478/v10039-012-0048-0
136. Zhang QX, Magovern CJ, Mack CA, Budenbender KT, Ko W, Rosengart TK. Vascular endothelial growth factor is the major angiogenic factor in omentum: mechanism of the omentum-mediated angiogenesis. *J Surg Res* (1997) 67:147–54. doi:10.1006/jsre.1996.4983
137. Soukas A, Socci ND, Saatkamp BD, Novelli S, Friedman JM. Distinct transcriptional profiles of adipogenesis in vivo and in vitro. *J Biol Chem* (2001) 276:34167–74. doi:10.1074/jbc.M104421200
138. Baek JH, Jang JE, Kang CM, Chung HY, Kim ND, Kim KW. Hypoxia-induced VEGF enhances tumor survivability via suppression of serum deprivation-induced apoptosis. *Oncogene* (2000) 19:4621–31. doi:10.1038/sj.onc.1203814
139. Wang F, Zhang W, Guo L, Bao W, Jin N, Liu R, et al. Gambogic acid suppresses hypoxia-induced hypoxia-inducible factor-1α/vascular endothelial growth factor expression via inhibiting phosphatidylinositol 3-kinase/Akt/mammalian target protein of rapamycin pathway in multiple myeloma cells. *Cancer Sci* (2014) 105:1063–70. doi:10.1111/cas.12458
140. de Waal EGM, Slart RHJA, Leene MJ, Kluin PM, Vellenga E. 18F-FDG PET increases visibility of bone lesions in relapsed multiple myeloma: is this hypoxia-driven? *Clin Nucl Med* (2015) 40:291–6. doi:10.1097/RLU.0000000000000629
141. Almendros I, Gileles-Hillel A, Khalyfa A, Wang Y, Zhang SX, Carreras A, et al. Adipose tissue macrophage polarization by intermittent hypoxia in a mouse model of OSA: effect of tumor microenvironment. *Cancer Lett* (2015) 361:233–9. doi:10.1016/j.canlet.2015.03.010
142. Kugel H, Jung C, Schulte O, Heindel W. Age- and sex-specific differences in the 1H-spectrum of vertebral bone marrow. *J Magn Reson Imaging* (2001) 13:263–8. doi:10.1002/1522-2586(200102)13:2<263::AID-JMRI1038>3.3.CO;2-D
143. Griffith JF, Yeung DKW, Antonio GE, Wong SYS, Kwok TCY, Woo J, et al. Vertebral marrow fat content and diffusion and perfusion indexes in women with varying bone density: MR evaluation. *Radiology* (2006) 241:831–8. doi:10.1148/radiol.2413051858
144. Griffith JF, Yeung DKW, Antonio GE, Lee FKH, Hong AWL, Wong SYS, et al. Vertebral bone mineral density, marrow perfusion, and fat content in healthy men and men with osteoporosis: dynamic contrast-enhanced MR imaging and MR spectroscopy. *Radiology* (2005) 236:945–51. doi:10.1148/radiol.2363041425
145. Schwartz AV, Sigurdsson S, Hue TF, Lang TF, Harris TB, Rosen CJ, et al. Vertebral bone marrow fat associated with lower trabecular BMD and prevalent vertebral fracture in older adults. *J Clin Endocrinol Metab* (2013) 98:2294–300. doi:10.1210/jc.2012-3949
146. McGee-Lawrence ME, Carpio LR, Schulze RJ, Pierce JL, McNiven MA, Farr JN, et al. Hdac3 deficiency increases marrow adiposity and induces lipid storage and glucocorticoid metabolism in osteochondroprogenitor cells. *J Bone Miner Res* (2015) 31:116–28. doi:10.1002/jbmr.2602
147. Sinha P, Aarnisalo P, Chubb R, Ono N, Fulzele K, Selig M, et al. Loss of Gsα early in the osteoblast lineage favors adipogenic differentiation of mesenchymal progenitors and committed osteoblast precursors. *J Bone Miner Res* (2014) 29:2414–26. doi:10.1002/jbmr.2270
148. Urs S, Henderson T, Le P, Rosen CJ, Liaw L. Tissue-specific expression of Sprouty1 in mice protects against high-fat diet-induced fat accumulation, bone loss and metabolic dysfunction. *Br J Nutr* (2012) 108:1025–33. doi:10.1017/S0007114511006209
149. Motyl KJ, Raetz M, Tekalur SA, Schwartz RC, McCabe LR. CCAAT/enhancer binding protein β-deficiency enhances type 1 diabetic bone phenotype by increasing marrow adiposity and bone resorption. *Am J Physiol Regul Integr Comp Physiol* (2011) 300:R1250–60. doi:10.1152/ajpregu.00764.2010
150. Colaianni G, Brunetti G, Faienza MF, Colucci S, Grano M. Osteoporosis and obesity: role of Wnt pathway in human and murine models. *World J Orthop* (2014) 5:242–6. doi:10.5312/wjo.v5.i3.242
151. de Paula FJA, de Araújo IM, Carvalho AL, Elias J, Salmon CEG, Nogueira-Barbosa MH. The relationship of fat distribution and insulin resistance with lumbar spine bone mass in women. *PLoS One* (2015) 10:e0129764. doi:10.1371/journal.pone.0129764
152. Templeton ZS, Lie W-R, Wang W, Rosenberg-Hasson Y, Alluri RV, Tamaresis JS, et al. Breast cancer cell colonization of the human bone marrow adipose tissue niche. *Neoplasia* (2015) 17:849–61. doi:10.1016/j.neo.2015.11.005
153. Takeshita S, Fumoto T, Naoe Y, Ikeda K. Age-related marrow adipogenesis is linked to increased expression of RANKL. *J Biol Chem* (2014) 289:16699–710. doi:10.1074/jbc.M114.547919
154. Wang D, Haile A, Jones LC. Dexamethasone-induced lipolysis increases the adverse effect of adipocytes on osteoblasts using cells derived from human mesenchymal stem cells. *Bone* (2013) 53:520–30. doi:10.1016/j.bone.2013.01.009
155. Kajimura D, Lee HW, Riley KJ, Arteaga-Solis E, Ferron M, Zhou B, et al. Adiponectin regulates bone mass via opposite central and peripheral mechanisms through foxo1. *Cell Metab* (2013) 17:901–15. doi:10.1016/j.cmet.2013.04.009
156. Kennedy DE, Knight KL. Inhibition of B lymphopoiesis by adipocytes and IL-1-producing myeloid-derived suppressor cells. *J Immunol* (2015) 195:2666–74. doi:10.4049/jimmunol.1500957
157. Arnulf B, Lecourt S, Soulier J, Ternaux B, Lacassagne M-N, Crinquette A, et al. Phenotypic and functional characterization of bone marrow mesenchymal stem cells derived from patients with multiple myeloma. *Leukemia* (2007) 21:158–63. doi:10.1038/sj.leu.2404466
158. Nieman KM, Kenny HA, Penicka CV, Ladanyi A, Buell-Gutbrod R, Zillhardt MR, et al. Adipocytes promote ovarian cancer metastasis and provide energy for rapid tumor growth. *Nat Med* (2011) 17:1498–503. doi:10.1038/nm.2492
159. Gavin KM, Gutman JA, Kohrt WM, Wei Q, Shea KL, Miller HL, et al. De novo generation of adipocytes from circulating progenitor cells in mouse

and human adipose tissue. *FASEB J* (2015) 30:1096–108. doi:10.1096/fj.15-278994
160. Devlin MJ, Rosen CJ. The bone-fat interface: basic and clinical implications of marrow adiposity. *Lancet Diabetes Endocrinol* (2015) 3:141–7. doi:10.1016/S2213-8587(14)70007-5
161. Ford NA, Devlin KL, Lashinger LM, Hursting SD. Deconvoluting the obesity and breast cancer link: secretome, soil and seed interactions. *J Mammary Gland Biol Neoplasia* (2013) 18:267–75. doi:10.1007/s10911-013-9301-9
162. Dinarello CA. Interleukin-1 in the pathogenesis and treatment of inflammatory diseases. *Blood* (2011) 117:3720–32. doi:10.1182/blood-2010-07-273417
163. Liou Y-H, Wang S-W, Chang C-L, Huang P-L, Hou M-S, Lai Y-G, et al. Adipocyte IL-15 regulates local and systemic NK cell development. *J Immunol* (2014) 193:1747–58. doi:10.4049/jimmunol.1400868
164. Szmania S, Lapteva N, Garg T, Greenway A, Lingo J, Nair B, et al. Ex vivo-expanded natural killer cells demonstrate robust proliferation in vivo in high-risk relapsed multiple myeloma patients. *J Immunother* (2015) 38:24–36. doi:10.1097/CJI.0000000000000059
165. Rezzadeh KS, Hokugo A, Jewett A, Kozlowska A, Segovia LA, Zuk P, et al. Natural killer cells differentiate human adipose-derived stem cells and modulate their adipogenic potential. *Plast Reconstr Surg* (2015) 136:503–10. doi:10.1097/PRS.0000000000001536
166. Hardaway AL, Herroon MK, Rajagurubandara E, Podgorski I. Bone marrow fat: linking adipocyte-induced inflammation with skeletal metastases. *Cancer Metastasis Rev* (2014) 33:527–43. doi:10.1007/s10555-013-9484-y
167. Yin H, Xu L, Porter NA. Free radical lipid peroxidation: mechanisms and analysis. *Chem Rev* (2011) 111:5944–72. doi:10.1021/cr200084z
168. Esterbauer H, Eckl P, Ortner A. Possible mutagens derived from lipids and lipid precursors. *Mutat Res* (1990) 238:223–33. doi:10.1016/0165-1110(90)90014-3
169. Chalhoub N, Baker SJ. PTEN and the PI3-kinase pathway in cancer. *Annu Rev Pathol* (2009) 4:127–50. doi:10.1146/annurev.pathol.4.110807.092311
170. Martinez-Useros J, Garcia-Foncillas J. Obesity and colorectal cancer: molecular features of adipose tissue. *J Transl Med* (2016) 14:21. doi:10.1186/s12967-016-0772-5
171. Eda H, Santo L, Wein MN, Hu DZ, Cirstea DD, Nemani N, et al. Regulation of sclerostin expression in multiple myeloma by Dkk-1; a potential therapeutic strategy for myeloma bone disease. *J Bone Miner Res* (2016) 31(6):1225–34. doi:10.1002/jbmr.2789
172. Brunetti G, Oranger A, Mori G, Specchia G, Rinaldi E, Curci P, et al. Sclerostin is overexpressed by plasma cells from multiple myeloma patients. *Ann N Y Acad Sci* (2011) 1237:19–23. doi:10.1111/j.1749-6632.2011.06196.x
173. Urs S, Venkatesh D, Tang Y, Henderson T, Yang X, Friesel RE, et al. Sprouty1 is a critical regulatory switch of mesenchymal stem cell lineage allocation. *FASEB J* (2010) 24:3264–73. doi:10.1096/fj.10-155127
174. Wei S, Zhang L, Zhou X, Du M, Jiang Z, Hausman GJ, et al. Emerging roles of zinc finger proteins in regulating adipogenesis. *Cell Mol Life Sci* (2013) 70:4569–84. doi:10.1007/s00018-013-1395-0
175. Shen W, Velasquez G, Chen J, Jin Y, Heymsfield SB, Gallagher D, et al. Comparison of the relationship between bone marrow adipose tissue and volumetric bone mineral density in children and adults. *J Clin Densitom* (2014) 17:163–9. doi:10.1016/j.jocd.2013.02.009
176. Martin RB, Zissimos SL. Relationships between marrow fat and bone turnover in ovariectomized and intact rats. *Bone* (1991) 12:123–31. doi:10.1016/8756-3282(91)90011-7
177. Bonnet N, Somm E, Rosen CJ. Diet and gene interactions influence the skeletal response to polyunsaturated fatty acids. *Bone* (2014) 68:100–7. doi:10.1016/j.bone.2014.07.024
178. Styner M, Pagnotti GM, Galior K, Wu X, Thompson WR, Uzer G, et al. Exercise regulation of marrow fat in the setting of PPARγ agonist treatment in female C57BL/6 mice. *Endocrinology* (2015) 156:2753–61. doi:10.1210/en.2015-1213
179. Meier C, Schwartz AV, Egger A, Lecka-Czernik B. Effects of diabetes drugs on the skeleton. *Bone* (2016) 82:93–100. doi:10.1016/j.bone.2015.04.026
180. Hanson DJ, Nakamura S, Amachi R, Hiasa M, Oda A, Tsuji D, et al. Effective impairment of myeloma cells and their progenitors by blockade of monocarboxylate transportation. *Oncotarget* (2015) 6:33568–86. doi:10.18632/oncotarget.5598
181. Kasznicki J, Sliwinska A, Drzewoski J. Metformin in cancer prevention and therapy. *Ann Transl Med* (2014) 2:57. doi:10.3978/j.issn.2305-5839.2014.06.01
182. Abdi J, Garssen J, Faber J, Redegeld FA. Omega-3 fatty acids, EPA and DHA induce apoptosis and enhance drug sensitivity in multiple myeloma cells but not in normal peripheral mononuclear cells. *J Nutr Biochem* (2014) 25:1254–62. doi:10.1016/j.jnutbio.2014.06.013
183. Jia L, Liu F-T. Why bortezomib cannot go with "green"? *Cancer Biol Med* (2013) 10:206–13. doi:10.7497/j.issn.2095-3941.2013.04.004

Conflict of Interest Statement: The authors declare that the research was conducted in the absence of any commercial or financial relationships that could be construed as a potential conflict of interest.

frontiers in Endocrinology

METHODS
published: 06 July 2016
doi: 10.3389/fendo.2016.00084

New 3D-Culture Approaches to Study Interactions of Bone Marrow Adipocytes with Metastatic Prostate Cancer Cells

*Mackenzie Katheryn Herroon[1], Jonathan Driscoll Diedrich[1,2] and Izabela Podgorski[1,2]**

[1] Department of Pharmacology, Wayne State University School of Medicine, Detroit, MI, USA, [2] Karmanos Cancer Institute, Wayne State University School of Medicine, Detroit, MI, USA

Adipocytes are a major component of the bone marrow that can critically affect metastatic progression in bone. Understanding how the marrow fat cells influence growth, behavior, and survival of tumor cells requires utilization of *in vitro* cell systems that can closely mimic the physiological microenvironment. Herein, we present two new three-dimensional (3D) culture approaches to study adipocyte–tumor cell interactions *in vitro*. The first is a transwell-based system composed of the marrow-derived adipocytes in 3D collagen I gels and reconstituted basement membrane-overlayed prostate tumor cell spheroids. Tumor cells cultured under these 3D conditions are continuously exposed to adipocyte-derived factors, and their response can be evaluated by morphological and immunohistochemical analyses. We show via immunofluorescence analysis of metabolism-associated proteins that under 3D conditions tumor cells have significantly different metabolic response to adipocytes than tumor cells grown in 2D culture. We also demonstrate that this model allows for incorporation of other cell types, such as bone marrow macrophages, and utilization of dye-quenched collagen substrates for examination of proteolysis-driven responses to adipocyte- and macrophage-derived factors. Our second 3D culture system is designed to study tumor cell invasion toward the adipocytes and the consequent interaction between the two cell types. In this model, marrow adipocytes are separated from the fluorescently labeled tumor cells by a layer of collagen I. At designated time points, adipocytes are stained with BODIPY and confocal *z*-stacks are taken through the depth of the entire culture to determine the distance traveled between the two cell types over time. We demonstrate that this system can be utilized to study effects of candidate factors on tumor invasion toward the adipocytes. We also show that immunohistochemical analyses can be performed to evaluate the impact of direct interaction of prostate tumor cells with adipocytes. Our models underline the importance of using the appropriate culture conditions to mimic physiological interactions between marrow adipocytes and metastatic tumor cells. These systems have a potential to be utilized for analyses of various factors that may be regulated by the adipocytes in bone. Their application likely extends beyond metastatic prostate cancer to other tumors that colonize the bone marrow microenvironment.

Keywords: bone marrow adipocytes, bone metastasis, prostate cancer, 3D culture, 3D invasion, *in vitro* models

OPEN ACCESS

Edited by:
William Peter Cawthorn, University of Edinburgh, UK

Reviewed by:
Stuart Rushworth, University of East Anglia, UK
Bonnie Loveless King, Stanford University, USA

***Correspondence:**
Izabela Podgorski
ipodgors@med.wayne.edu

Specialty section:
This article was submitted to Bone Research, a section of the journal Frontiers in Endocrinology

Received: *14 May 2016*
Accepted: *20 June 2016*
Published: *06 July 2016*

Citation:
Herroon MK, Diedrich JD and Podgorski I (2016) New 3D-Culture Approaches to Study Interactions of Bone Marrow Adipocytes with Metastatic Prostate Cancer Cells. Front. Endocrinol. 7:84. doi: 10.3389/fendo.2016.00084

INTRODUCTION

Adipocytes constitute a significant portion of adult bone marrow and their number increases with age, obesity, and metabolic dysfunction (1–3). Growing evidence positively links the abundance of fat cells in the marrow with metastatic progression. Adipocyte-rich bone marrow appears to contribute to skeletal colonization and growth in a number of secondary cancers, including prostate (4, 5), breast (6), multiple myeloma (7, 8), and melanoma tumors (9). It is believed that adipocytes enhance the fertility of the bone metastatic niche by serving as a source of growth factors, chemokines, and lipid mediators (10, 11). Specifically, they have been shown to (1) upregulate lipid transporters and drive lipid uptake by tumor cells (5), (2) promote osteoclast differentiation and maturation (4, 9), and (3) induce authophagy-driven tumor cell survival, all processes that ultimately allow the metastatic cancers to thrive in the bone marrow niche (8). Despite these emerging data clearly pointing to marrow fat cells as one of the critical determinants of tumor cell fate in bone, their functional contribution to the growth and aggressiveness of metastatic tumors in bone is not well understood. Studies investigating the interactions between the tumor cells and adipocytes in the bone marrow have been limited and thorough mechanistic evaluations on how fat cells affect the phenotype, metabolism, and function of the surrounding cells in the metastatic niche are lacking.

The majority of the studies examining adipocyte–tumor cell interactions to date have utilized pre-adipocyte cell lines or adipocytes derived from visceral or breast adipose tissues (12–16) depots, which are known to be distinctively different from bone marrow fat (17). There have only been a handful of studies, including our own, that have examined the interactions of bone marrow mesenchymal cell-derived or primary bone adipocytes with metastatic tumor cells (4, 5, 7–9). Although all of these investigations resulted in important findings linking marrow adipocytes with metastatic progression, the caveat is that they have all been performed using two-dimensional (2D) culture approaches. It is becoming increasingly recognized that 2D layer cultures, although convenient and reasonably inexpensive, do not adequately mimic the limited diffusion-driven access to nutrients, growth factors, and signaling molecules in the tumor microenvironment (18). Under physiological conditions, exposure of solid tumors to microenvironmental factors, such as oxygen, nutrients, stress, and therapeutic treatments, is heterogeneous and regulated by their three-dimensional (3D) spatial conformation (19). The importance of employing 3D models to model tumor architecture has proven critical to understanding the mechanisms behind tumor phenotype, behavior, and response to therapy (19–22). Emphasis has also grown on considering the contribution of host cells in the tumor microenvironment to cancer progression, and various *in vitro* models that focus on stromal–epithelial interactions and immune cell involvement have emerged (21, 23–27).

Three-dimensional, multi-cellular cell culture models have become well-accepted tools for dissecting complex molecular mechanisms of tumor progression that may not be possible to dissect *in vivo*. There have also been many advancements in the development of 3D culture systems that mimic specific tumor niches, including very complex and dynamic microenvironments such as bone (28). Models intended to interrogate the mechanisms of skeletal metastases range from culture of tumor cells and specific bone-derived cells on biologically derived or synthetic matrices, through the use of patient-derived xenografts and direct culture of tumor cells with bone explants (21, 28). However, aside from one recently reported *in vitro* system designed to evaluate bone marrow adipose colonization by breast cancer cells (6), there have been no *in vitro* 3D models that consider involvement of marrow adipocytes.

Here, we describe new *in vitro* approaches designed to study the interaction of prostate cancer cells with bone marrow-derived adipocytes. Our methods employ murine bone marrow mesenchymal cells differentiated into adipocytes in 3D collagen I gel and grown in a Transwell system with 3D-cultures of prostate carcinoma cells. We show that in this system, which allows continuous exchange of factors between the two cell types, adipocytes promote 3D growth of tumor spheroids. We also demonstrate that the cell culture approaches we are employing in this model allow for easy manipulation and are suitable for imunocytochemical analyses. We show examples of immunofluorescence analyses of metabolism-associated factors, such as carbonic anhydrase 9 (CA9) and hexokinase 2 (HK2) that reveal distinctively different expression profiles between 2D and 3D cultures exposed to adipocytes. We also demonstrate the suitability of our model to study proteolysis by live prostate carcinoma cells and potentially other components of bone marrow microenvironment, such as bone marrow macrophages. Finally, we also describe a design of a 3D invasion assay that allows direct monitoring of the attraction of prostate tumor cells to marrow adipocytes and can be utilized to evaluate potential inhibitors that target this interaction. Our models provide new approaches to dissect the functional role of marrow-derived adipocytes in tumor cell growth and aggressiveness.

MATERIALS AND METHODS

Materials

Dulbecco's modified Eagle's medium (DMEM), minimum essential medium (MEMα), and other chemicals, unless otherwise stated, were obtained from Sigma (St. Louis, MO, USA). HyClone fetal bovine serum (FBS) was from ThermoFisher (Pittsburg, PA, USA). Trypsin–EDTA, Alexa Fluor 488-conjugated goat anti-rat and anti-rabbit IgG, MitoTracker Deep Red FM, CellTracker Orange (CTO), DQ collagen type IV, BODIPY (493/503), Hoechst Dye, and Gentamicin (G418) were from Invitrogen (Carlsbad, CA, USA). StemXVivo Adipogenic Supplement was from R&D Systems (Minneapolis, MN, USA). Rosiglitazone was from Cayman Chemical Company (Ann Arbor, MI, USA). PureCol collagen type I was from Advanced Biomatrix (San Diego, CA, USA). Cultrex™ (rBM; reduced growth factor) was from Trevigen (Gaithersburg, MD, USA). Rat monoclonal F4/80 was from Abcam (Cambridge, MA, USA). Rabbit monoclonal carbonic anhydrase 9 (CA9) and hexokinase II (HK2) were from Cell Signaling Technology (Danvers, MA, USA). Transwell systems (Costar™ Transwell™ Permeable

Supports with 0.4-μm pore size) were from Corning (Corning, NY, USA). FABP4 inhibitor (BMS309403) was from Calbiochem (San Diego, CA, USA). Atglistatin was from Axon Medchem (Groningen, Netherlands).

Cell Lines

PC3, an androgen independent cell line derived from a bone metastasis of a high-grade prostate adenocarcinoma, was purchased from American Type Culture Collection (ATCC; Manassas, VA, USA). The PC3-DsRed cell line was established by stable transfection with pDsRed2-N1 vector (Clontech Laboratories, Palo Alto, CA, USA), containing the neomycin-resistant gene. Transfection was performed using Lipofectamine 2000 and pooled populations of stable cells were selected, expanded, and maintained in medium supplemented with 400 mg/ml of G418 (29). L929 cells (source of M-CSF for macrophages, purchased from ATCC) were cultured until confluent and conditioned medium was collected, centrifuged, and stored at −80°C until ready for use. PC3 and L929 cells were cultured in DMEM supplemented with 10% FBS, 10 mM HEPES, and 100 U/ml penicillin–streptomycin. All cells were maintained in a 37°C humidified incubator ventilated with 5% CO_2.

Isolation and Preparation of Primary Murine Bone Marrow Adipocytes and Macrophages

Collection of murine cells was performed in accordance with the protocol approved by the institutional Animal Investigational Committee of Wayne State University and NIH guidelines (Protocol # 15-12-025; IP, PI). Primary mouse bone marrow stromal cells (mBMSC) were isolated from femurs and tibiae of 6- to 8-week-old FVB/N mice and induced to become bone marrow adipocytes according to our previously published protocols (5). Specifically, bone marrow from each tibia and femur was flushed with of DMEM containing 20% FBS (4 ml/bone) using a 26-gauge needle. Marrow suspension was mixed and broken apart using a 20-gauge needle and seeded into a 6-well cell culture plate (~3 ml/well). After 24 h, non-adherent cells were removed by replacing the medium. Cells were cultured to confluency by changing the medium every 2–3 days and then expanded to larger dishes as needed. For adipogenic differentiation, mBMSCs (~600,000/well) were mixed with bovine collagen I and seeded in six-well plates (500 μl/well) for Transwell coculture or 60-mm dishes (500 μl, ~1,300,000/dish) for 3D invasion assays. Approximately 48–72 h later, upon reaching confluency, cells were treated with adipogenic cocktail (30% StemXVivo Adipogenic Supplement, 1 μM insulin, 2 μM Rosiglitazone; DMEM and 10% FBS) for 8–10 days (5).

For the preparation of bone marrow macrophages (BMMs), bone marrow was flushed from femurs and tibiae of 10- to 12-week-old FVB/N male mice with BMM growth medium (MEMα containing 20% FBS and 30% L929-conditioned media as the source of M-CSF; 4 ml/bone) using a 26-gauge needle (30). The cell suspension was mixed with an additional 20 ml of BMM medium using a 20-gauge needle and plated onto three 100-mm Petri dishes (12 ml/dish). Cells were cultured for 4–5 days in a 37°C humidified incubator ventilated with 5% CO_2 to obtain differentiated BMMs.

2D Tumor Cell-Adipocyte Coculture Using a Transwell System

Bone marrow adipocytes were differentiated in six-well plates as described above. On the day of the Transwell setup, tumor cells were plated on acid-washed glass coverslips (12 mm in diameter) coated with reconstituted basement membrane (rBM; Cultrex™; Trevigen). Briefly, 100 μl of 1 mg/ml rBM was added per coverslip and allowed to polymerize for 45 min at RT, then the excess was removed via suction, and the coverslips were allowed to dry for 15 min at RT before cells were plated. PC3 cells (30,000–50,000) were plated in 500 μl of normal growth medium and allowed to settle for a minimum of 4 h at 37°C. Adipocytes were prepared for Transwell coculture by washing 3× with PBS and adding 2 ml of DMEM supplemented with 5% FBS. Transwell membranes were placed above the adipocyte culture according to manufacturer's instructions and coverslips with attached tumor cells (2× coverslips per transwell) were placed on each membrane with medium gently added on top (2 ml). The control coverslips were cultured separately in DMEM supplemented with 5% FBS. All cells were allowed to grow for 48 h at 37°C.

3D Tumor Cell-Adipocyte Coculture Using a Transwell System

Adipocytes were prepared as described above for the 2D system. The experimental approach to prepare 3D cultures of prostate carcinoma cells has been adapted from the original protocols for breast cancer progression models developed by the Brugge laboratory (31). Non-diluted rBM (15.35 mg/ml) was used for the preparation of all cultures. In brief, acid-washed coverslips were placed in 35 mm dishes, and 45 μl of rBM was carefully added on top of each coverslip, making a continuous surface without going over the edge of the coverslip. The dishes were placed in 37°C for 15 min to polymerize, then 60 μl of PC3 cell suspension was placed on top of each rBM-coated coverslip (30,000–35,000 cells/coverslip). The dishes were placed in a 37°C incubator for 45 min–1 h to allow the cells to settle and attach to the matrix. After cells were attached, 2–3 ml of media (5% FBS, 2% rBM overlay) was added to the 35-mm dish control coverslips. For 3D Transwell cultures, one 3D coverslip (covering only ~24% of the membrane and thus allowing free flow of factors and nutrients) was placed on each Transwell membrane positioned above the differentiated adipocyte culture, and 2 ml of medium was gently added (**Figure 1**). Cells were allowed to grow for 48–120 h depending on experimental design.

Immunofluorescence Analyses

For the analysis of the expression and localization of carbonic anhydrase 9 (CA9) (**Figure 2**), control and Transwell coverslips from 2D and 3D cultures were washed with PBS, fixed with cold methanol, and incubated with rabbit monoclonal anti-CA9 antibody (1:50) at 4°C overnight. To label the mitochondria, coverslips were washed with PBS, and incubated with 200 nM MitoTracker Deep Red for 30–45 min at 37°C prior to fixation.

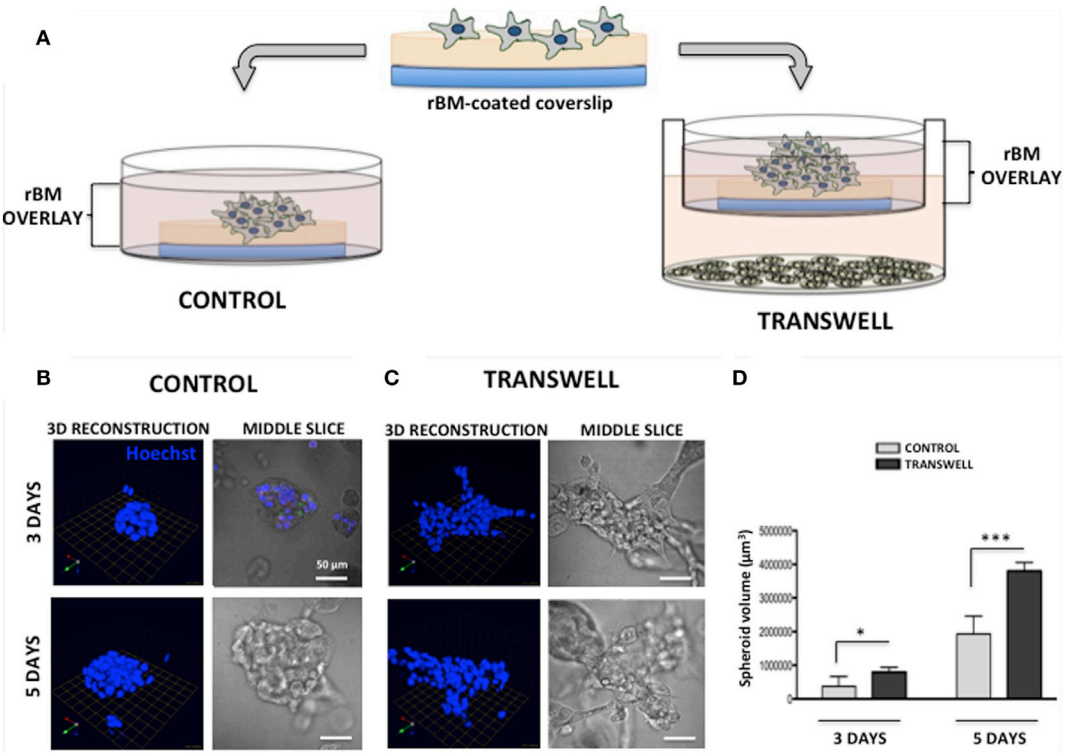

FIGURE 1 | Three-dimensional (3D) culture of prostate tumor spheroids in the absence or presence of bone marrow-derived adipocytes. **(A)** Schematic representation of 3D culture of tumor cells alone plated on reconstituted basement membrane (rBM)-coated coverslips with rBM overlay of 2% rBM and cultured alone (left) or in transwell with bone marrow adipocytes (right). **(B)** 3D reconstruction and DIC (differential interference contrast) images of the middle slice depicting morphology of the spheroids of PC3 cells grown for 3 (top) and 5 (bottom) days in control conditions or **(C)** in transwell coculture with adipocytes. 40× images; bar, 50 µm; nuclei are labeled with Hoechst dye (blue); green arrow (*X*), red arrow (*Y*), and blue arrow (*Z*) indicate orientation of the spheroid in 3D space. **(D)** Quantification of spheroid volume using Volocity software; data are shown in cubic micrometers and represent the mean (±SD) of three independent experiments with at least three independent spheroids measured/experiment; $^{*}p < 0.05$ and $^{***}p < 0.001$ are considered statistically significant.

For immunodetection of hexokinase 2 (HK2) (**Figure 3**), cells were washed with PBS, fixed with cold methanol, and stained with rabbit monoclonal anti-HK2 antibody (1:100) at 4°C overnight. Alexa Fluor 488-conjugated goat anti-rabbit IgG (1:1000) was used as a secondary antibody for both CA9 and HK2 immunostaining. For 2D cultures, DAPI was used as a nuclear stain, and coverslips were mounted using Vectashield mounting medium (Vector Laboratories) before imaging with Zeiss LSM 510 META NLO confocal microscope using 40× oil immersion lens. Coverslips from 3D cultures were left in PBS in 35-mm dishes, Hoechst Dye (1:1000) was added for labeling of nuclei, and imaging was performed at an extended depth of focus with a Zeiss LSM 510 META NLO confocal microscope using a 40× dipping lens.

Imaging the Infiltration of Bone Marrow Macrophage into 3D Tumor Spheroids

Primary BMMs were differentiated from murine bone marrow cells, as described above. To examine their ability to infiltrate the pre-formed tumor spheroids in the absence or presence of adipocytes, the 3D tumor-adipocyte Transwell cocultures were set up and cultured for 3 days, as described above. To distinguish tumor cells from macrophages, PC3 cells were pre-labeled with CTO (1:1000 in serum-free media for 1 h at 37°C) prior to plating on rBM-covered coverslips. After 3-day culture, medium with rBM overlay was removed from the Transwell or control dishes, 60 µl of cell suspension containing 150,000 BMMs was plated on top of each coverslip and allowed to settle for 45min-1 h at 37°C, then new medium (containing 2% rBM overlay) was reapplied. Cells were allowed to grow for additional 2 days (**Figure 4**) before cultures were fixed in 3.7% formaldehyde and immunostained for murine macrophage marker F4/80 using rat anti-mouse F4/80 antibody (1:50). Alexa Fluor 488 conjugated goat anti-rat IgG (1:1000) was used as a secondary antibody. Hoechst Dye (1:1000) was added for labeling of nuclei, and imaging was performed at an extended depth of focus with Zeiss LSM 510 META NLO confocal microscope using a 40× dipping lens.

Imaging Proteolysis by Live Prostate Tumor Cells in the Absence or Presence of Infiltrating BMMs

Cleavage of DQ-collagen IV substrate by live PC3 cells grown in a control or Transwell coculture with adipocytes

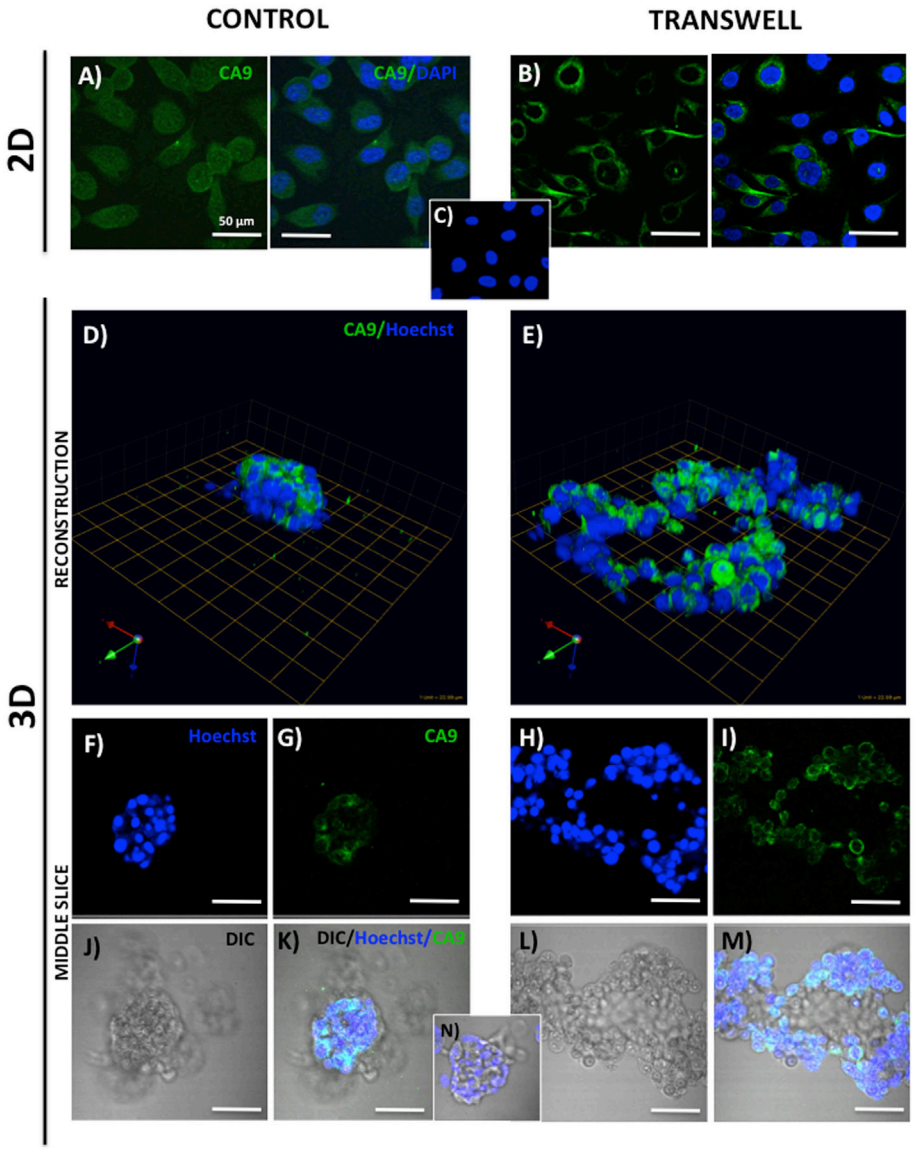

FIGURE 2 | Expression of carbonic anhydrase 9 (CA9) in 2D and 3D cultures of PC3 cells grown alone or in transwell coculture with adipocytes. Immunofluorescence analysis of CA9 expression (green) in monolayer PC3 cultures grown alone **(A)** or in transwell with adipocytes **(B)**. **(C)** 2D no primary CA9 antibody control; DAPI was used as nuclear marker (Blue). 3D reconstruction of CA9 expression in tumor spheroids grown alone **(D)** or in transwell with adipocytes **(E)**; green arrow (*X*), red arrow (*Y*), and blue arrow (*Z*) indicate orientation of the spheroid in 3D space. Middle slice through *z*-stack showing CA9 expression in spheroids cultured alone **(F,G,J,K)** or in transwell with adipocytes **(H,I,L,M)**. Hoechst dye was used for labeling nuclei [**(F,H)**; blue], CA9 [**(G,I)**; green], DIC [**(J,L)**; differential interference contrast], and merged images **(K,M)**. **(N)** 3D culture; no CA9 primary antibody control; 40× images; bar, 50 µm.

in the presence or absence of BMMs was assayed in real time and quantified based on published protocols (32–34). Briefly, single cell suspensions of tumor cells (30,000–35,000) were plated on top of coverslips coated with rBM containing DQ-collagen IV (1:30) and overlayed with 2% rBM. Cells were grown alone or in Transwell coculture with adipocytes for 3 days prior to addition of pre-labeled BMMs (**Figure 5**). After an additional 2-day culture, Hoechst dye was added as nuclear marker and DQ-IV proteolysis under all culture conditions was imaged live at an extended depth of focus with Zeiss LSM 510 META NLO confocal microscope using a 40× dipping lens.

Coculture of Bone Marrow Macrophages with Prostate Tumor Cells in a 3D Transwell System

To examine the effects of BMMs on 3D growth and proteolysis by prostate tumor cells cocultured with marrow adipocytes, we pre-labeled differentiated BMMs by incubating them with a

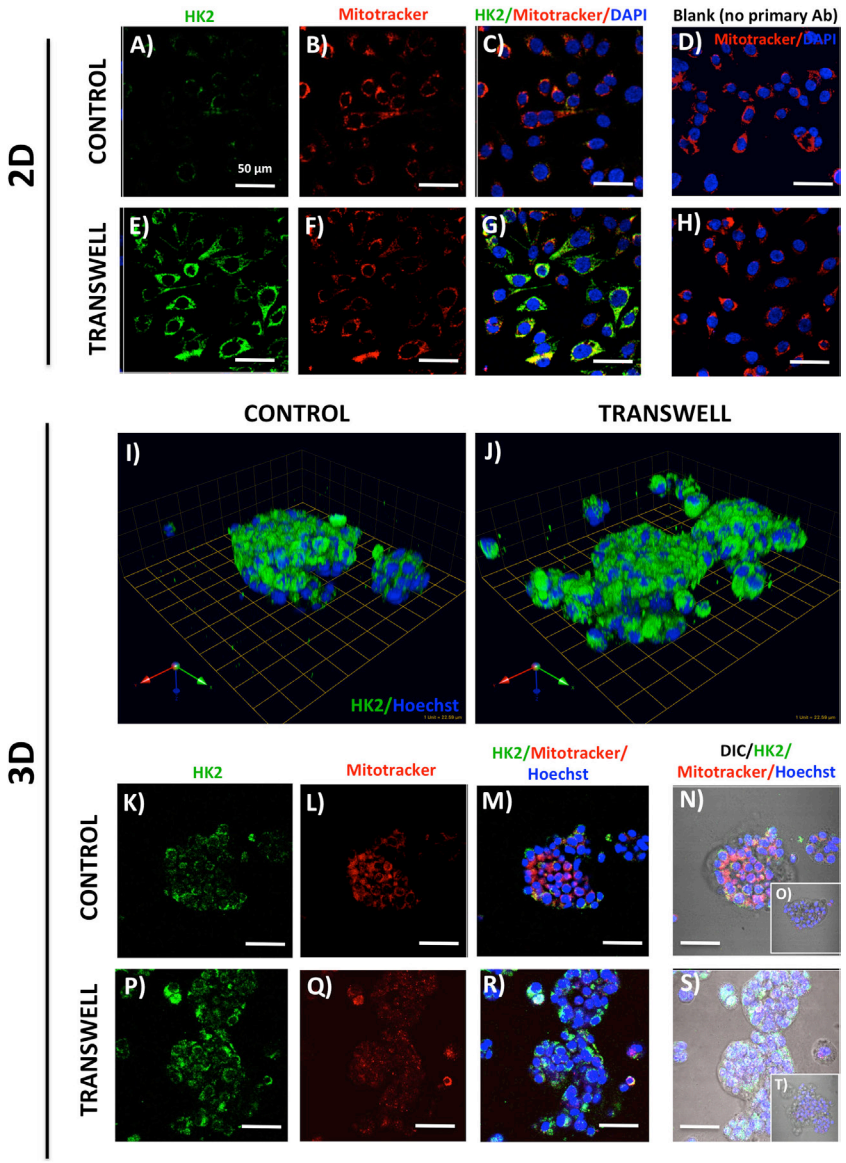

FIGURE 3 | Hexokinase 2 (HK2) expression and in 2D and 3D cultures of PC3 cells grown alone or in transwell coculture with adipocytes. Expression of HK2 [**(A)**, green] and MitoTracker [**(B)**, red] merged **(C)** in PC3 cells grown alone **(A–C)** or in transwell **(E–G)** in 2D coculture. **(D,H)** No HK2 primary antibody controls; DAPI was used as nuclear marker (blue). **(I,J)** 3D reconstruction of CA9 expression in tumor spheroids grown alone **(I)** or in transwell with adipocytes **(J)**; green arrow (*X*), red arrow (*Y*), and blue arrow (*Z*) indicate orientation of the spheroid in 3D space. HK2 and MitoTracker fluorescence to show HK2 localization to the mitochondria in PC3 cells cultured alone **(K–N)** or in Transwell with adipocytes **(P–S)**. **(O,T)** No HK2 primary antibody controls; 40× images; bar, 50 µm.

1:1000 dilution of with CellTracker Orange (CTO) in serum-free medium for 1 h at 37°C. Labeled BMMs were then washed 3× with PBS and maintained in normal BMM medium overnight until use. On the day of 3D Transwell setup, adipocytes and prostate tumor cells were prepared as described above. Coverslips were coated with rBM and 75,000 BMMs mixed with 30,000 PC3 cells were plated together on top of a coated coverslip, as described above. As before, one 3D coverslip was placed on each Transwell membrane positioned above differentiated adipocyte culture, and 2 ml of medium was gently added (**Figure 6**). Cells were allowed to grow for 3 days, and DQ-IV proteolysis was imaged live at an extended depth of focus with a Zeiss LSM 510 META NLO confocal microscope using a 40× dipping lens.

3D Invasion Assays

Bone marrow-derived mBMSC cells were mixed with collagen I matrix and plated in 60-mm dishes (500 µl/dish; ~1,300,000/500 µl). Cells were differentiated into adipocytes over the course of 8–10 days as described above. Post-differentiation, each plate was washed 3× with PBS, with all PBS carefully removed before 1 ml of collagen I was added on top and allowed to polymerize at 37°C for 45 min–1 h. A total

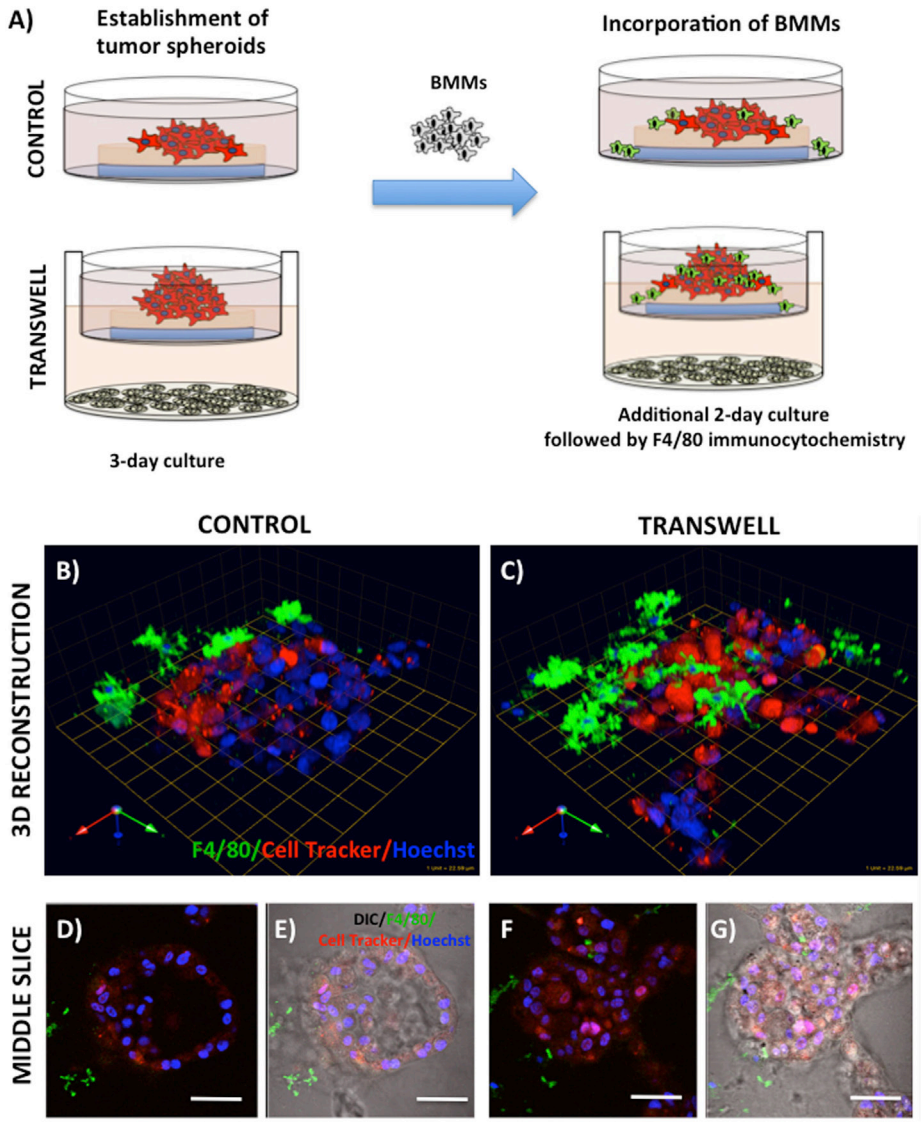

FIGURE 4 | **Infiltration of bone marrow macrophages (BMMs) into 3D cultures of PC3 cells exposed to adipocytes**. **(A)** Schematic representation of experimental design. 3D cultures were grown alone or in transwell coculture with adipocytes for three days prior to addition of bone marrow macrophages and culture for an additional 2 days. **(B,C)** 3D reconstruction of tumor spheroids infiltrated with BMMs in the absence **(B)** or presence of adipocytes **(C)**; F4/80: macrophage marker (green); CellTracker Orange: PC3 cell label (red); Hoechst: nuclear label (blue); green arrow (*X*), red arrow (*Y*), and blue arrow (*Z*) indicate orientation of the spheroid in 3D space. Middle slice through *z*-stack showing F4/80, cell tracker, and Hoechst staining of PC3 spheroids with or without BMMs grown in control conditions **(D,E)** or in transwell with adipocytes **(F,G)**; 40× images; bar, 50 μm

of 4 ml of medium, containing 400,000 dsRed-expressing PC3 cells, was gently added on top. Cultures were maintained in a 37°C humidified incubator ventilated with 5% CO_2 for up to 96 h. At designated time-points, plates were washed with PBS, fixed for 45 min with 3.7% formaldehyde at RT, stained with BODIPY (493/503) (1:1000, 1 h at RT), nuclei were marked with Hoechst dye, and imaged at an extended depth of focus with a Zeiss LSM 510 META NLO confocal microscope using a 20× dipping lens (**Figure 7**). For inhibitor studies (**Figure 8**), FABP4 inhibitor (BMS309403; 1 μM) and Atglistatin (10 μM) were added to both the collagen I layer between the adipocytes and the tumor cells as well as the medium, and were replenished in the medium daily.

Image Reconstruction and Fluorescence Quantification

All images were captured using a Zeiss LSM510 META NLO confocal microscope (Carl Zeiss AG, Göttingen, Germany). For 2D cultures, a 40× oil immersion lens was used, and a single slice was captured. 3D cultures were imaged in 35 mm dishes with a 40× water immersion lens, and *z*-stacks of 2–4 μm optical

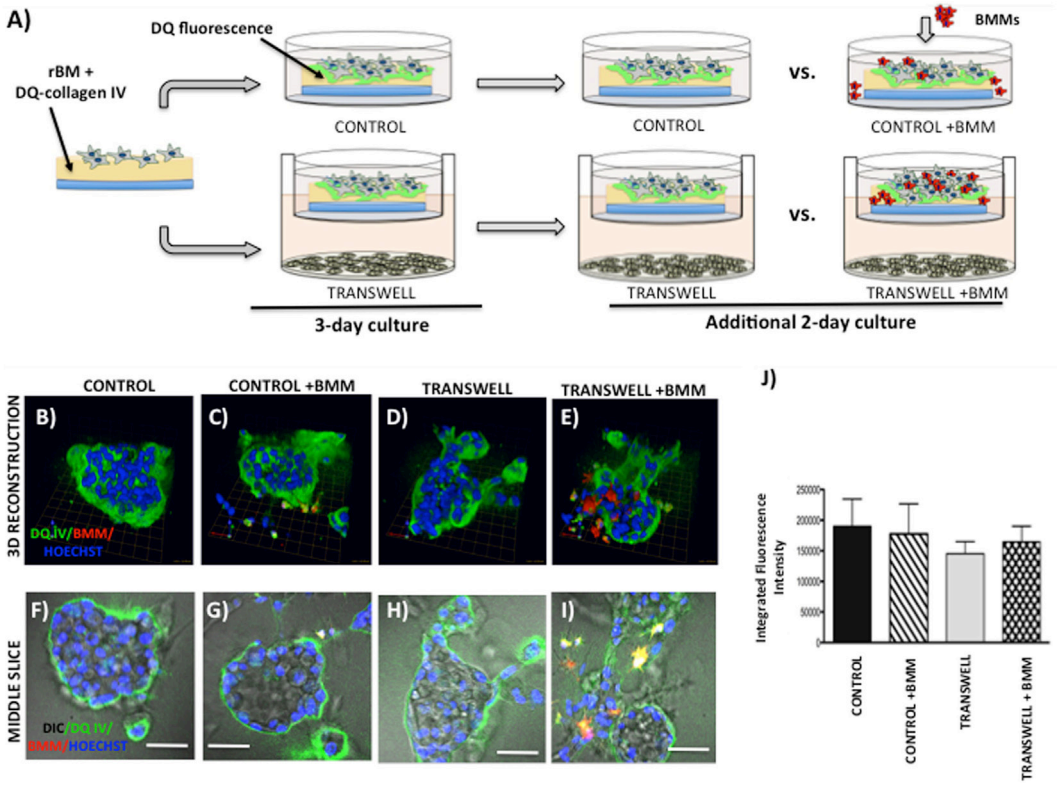

FIGURE 5 | **Live proteolysis by 3D prostate tumor cell cultures in the absence or presence of infiltrating macrophages**. **(A)** Schematic representation of experimental design. 3D cultures were seeded on rBM containing DQ-Collagen IV substrate and grown alone or in transwell coculture with adipocytes for 3 days prior to addition of bone marrow macrophages and culture for an additional 2 days. **(B–E)** 3D reconstruction of DQIV proteolysis by tumor spheroids cultured alone **(B)** or infiltrated with BMMs **(C)** in the absence or presence of adipocytes **(D,E)**; DQ-Collagen IV cleavage products (green), CellTracker Orange: PC3 cell label (red); Hoechst: nuclear label (blue); green arrow (*X*), red arrow (*Y*), and blue arrow (*Z*) indicate orientation of the spheroid in 3D space. **(F–I)** Middle slice through *z*-stack showing DQIV fluorescence, CellTracker Orange, and Hoechst staining of PC3 spheroids with or without BMMs grown in control conditions **(F,G)** or in transwell with adipocytes **(H,I)**; 40× images; bar, 50 μm. **(J)** Quantification of DQ-Collagen IV proteolysis shown as fluorescence intensity per cell in the entire volume; nuclei were stained with Hoechst 33342 (*blue*) at the time of imaging and counted. Data are shown as average (±SD) of three independent experiments with at least three independent spheroids measured/experiment.

slices were captured. 3D reconstruction of optical slices was performed using Volocity software (PerkinElmer, Waltham, MA, USA). For quantification of DQ-IV proteolysis, Volocity software was used to determine integrated intensity per image by dividing the total sum of green fluorescence signal (thresholded using intensity) by the number of nuclei in the image. At least three replicates were measured per condition. The totals in each group were averaged and shown as mean ± SEM.

Measurement and Quantification of Invasion

Invasion cultures in 60 mm dishes were imaged using a 20× water immersion lens, and *z*-stacks of 4 μm increments were captured. 3D reconstruction of optical slices was performed using Volocity software. For quantification of distance traveled by the tumor cells, images were opened in Zeiss LSM Image Browser. After removing the DIC channel, the Ortho tool was used to select and measure the distance from the middle of PC3 (red) layer to the middle of the adipocyte (green) layer. Distances between PC3 and adipocyte layers were recorded from at least three biological triplicates. For inhibitor studies, distances were shown as percent of distance at baseline (4-h control).

Statistical Analyses

All data analyses were performed using GraphPad Prism Software version 6.05. Data were presented as mean ± SD and statistically analyzed using unpaired Student's *t*-test. For three or more groups, one-way analysis of variance was used.

RESULTS

Three-Dimensional Culture of Prostate Tumor Spheroids in the Absence or Presence of Bone Marrow-Derived Adipocytes

Adipocytes are metabolically active cells that have been shown to promote growth and aggressiveness of several cancers, particularly those that grow in adipocyte-rich microenvironments

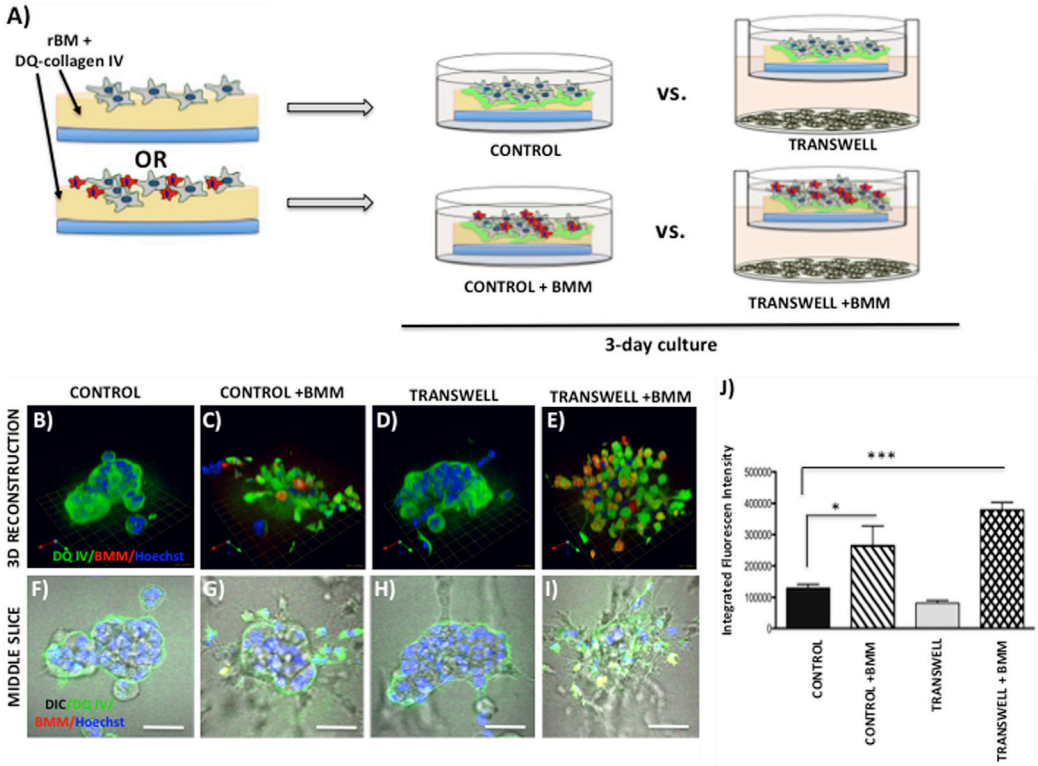

FIGURE 6 | Contribution of bone marrow macrophages to proteolysis of DQ-Collagen IV by tumor cells exposed to bone marrow adipocytes. **(A)** Schematic representation of experimental design. Tumor cells were mixed with BMMs, and 3D cultures were seeded on rBM containing DQ-Collagen IV substrate and grown alone or in transwell coculture with adipocytes for 3 days. **(B–E)** 3D reconstruction of DQIV proteolysis by tumor spheroids seeded alone **(B)** or with BMMs **(C)** in the absence or presence of adipocytes **(D,E)**; DQ-Collagen IV cleavage products (green), CellTracker Orange: PC3 cell label (red); Hoechst: nuclear label (blue); green arrow (*X*), red arrow (*Y*), and blue arrow (*Z*) indicate orientation of the spheroid in 3D space. **(F–I)** Middle slice through *z*-stack showing DQIV fluorescence, CellTracker Orange, and Hoechst staining of PC3 spheroids with or without BMMs grown in control conditions **(F,G)** or in transwell with adipocytes **(H,I)**; 40× images; bar, 50 μm. **(J)** Quantification of DQ-Collagen IV proteolysis, quantified in each 3D reconstructed spheroid using Volocity Software, is shown as fluorescence intensity per cell in the entire volume; nuclei were stained with Hoechst 33342 (*blue*) at the time of imaging and counted. Data are shown as average (±SD) of three independent experiments with at least three independent spheroids measured/experiment. $^{*}p < 0.05$ and $^{***}p < 0.001$ are considered statistically significant.

such as the breast or ovary (10, 35, 36). The fat cells residing specifically in the bone marrow have been increasingly credited with the ability to support and promote metastatic growth in bone (4–9). We have shown previously that exposure of prostate tumor cells to marrow adipocyte-supplied factors increases their proliferation and invasiveness (5). Here, to better mimic physiological conditions and to allow exploration of molecular mechanisms of adipocyte involvement in metastatic tumor growth in bone, we developed a cell culture model that allows 3D growth of prostate cancer cells exposed to adipocytes.

Seeding of the single-cell suspensions of PC3 prostate carcinoma cells on rBM-coated coverslips with 2% rBM overlay results in a formation of tumor spheroids (**Figure 1**). Cells cultured in their normal growth medium (CONTROL) form compacted, rounded spheroids after 3-day culture (**Figure 1B**, top panels). In contrast, tumor cells grown in a Transwell coculture with marrow adipocytes (TRANSWELL) form much larger and more disorganized clusters (**Figure 1C**, top panels). Longer, 5-day culture of PC3 cells results in further growth under either of the conditions, with Transwell cultures exhibiting significantly more robust proliferation and acquiring much more disordered morphology compared with control cultures (**Figures 1B,C**, bottom panels). Quantification of 3D volumes of the spheroids confirms the growth-promoting effects of adipocytes on tumor cells and indicates potential utility of this experimental system for interrogation of adipocyte–tumor cell interactions (**Figure 1D**).

Modeling Metabolic Responses to Marrow Adipocytes

One way that adipocytes can affect tumor cell behavior is by regulating cancer cell metabolism (37). Adipocyte-supplied lipids have been shown to feed into the glycolytic pathway and (38–40) and induce the Warburg effect in tumor cells (41–45). One of the master regulators of metabolic reprograming is hypoxia inducible factor (HIF), a key driver of hypoxic stress (46). Bone marrow adipocytes have a capability of inducing HIF-1α signaling in prostate tumor cells grown in 2D monolayer culture (Podgorski

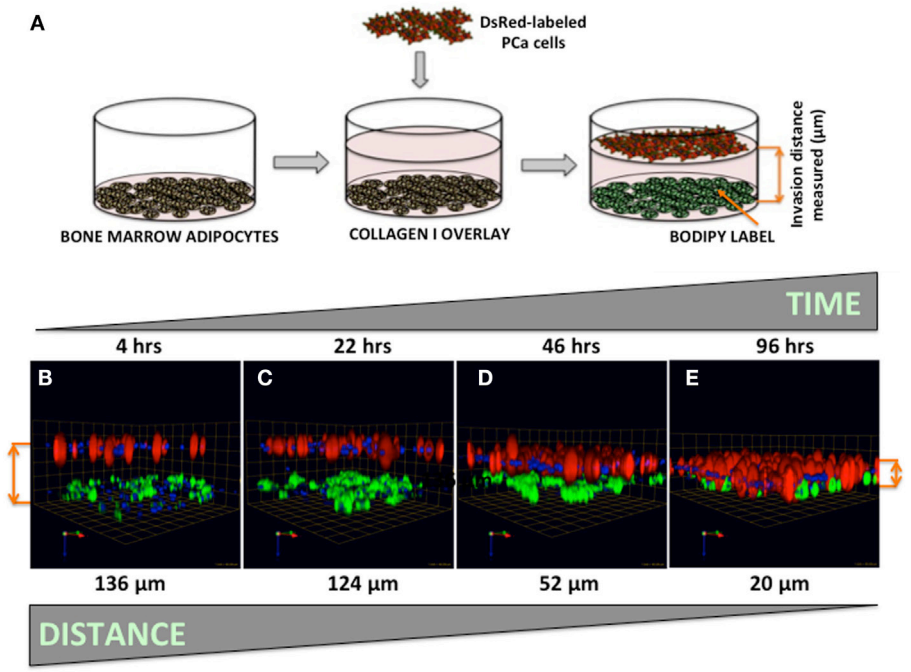

FIGURE 7 | Three-dimensional invasion of tumor cells toward bone marrow adipocytes. **(A)** Diagram depicting the experimental setup. Tumor cells invaded through collagen I matrix toward bone marrow adipocytes. Adipocytes (BODIPY, green); Tumor cells (DsRed; red) for 4 h **(B)**, 22 h **(C)**, 46 h **(D)**, and 96 h **(E)** and decreasing distance between the tumor cells and adipocytes over time is shown in micrometers. Green arrow (*X*), red arrow (*Y*), and blue arrow (*Z*) indicate orientation of the spheroid in 3D space.

et al., unpublished results[1]). It is, however, well-recognized that tissue dimensionality and associated oxygen status have a potential to profoundly affect hypoxic response in tumor cells (19, 47). Therefore, we examined the utility of our 3D Transwell model to measure hypoxia response to adipocytes. Our 3D cultures established on glass coverslips are easily fixable and suitable for immunocytochemical analyses. We used carbonic anhydrase 9 (CA9), a HIF-1α target gene (48), as a measure of hypoxic response in our system. The immunofluorescence analysis of CA9 protein revealed a significant increase and typical membrane localization in 2D tumor cell cultures exposed to adipocytes (**Figures 2A,B**), indicating activation of HIF-1α signaling. Interestingly, cells grown in 3D culture showed robust CA9 expression even under control conditions (**Figure 2D**). However, although tumor cells grown in transwell coculture with adipocytes expectedly formed significantly larger, disorganized structures (**Figures 2E,H,I,L,M**), there was no visible increase in CA9 expression compared with spheroids grown under control conditions (**Figures 2D,F,G,J,K**). This was further confirmed by the quantification of CA9 fluorescence/nuclei in each of the 3D structures (data not shown). 3D growth alone appears to activate HIF-1α signaling, which is consistent with the reports of heterogeneous oxygen distribution in 3D cultures (47). This speaks to the importance of considering tissue architecture while examining metabolic responses within the tumor microenvironment. Further studies are underway to validate these findings.

One important consequence of HIF-1α activation is the induction of glycolytic phenotype in tumor cells. We performed immunofluorescence analysis of expression and localization of hexokinase-2 (HK2), a critical enzyme in the first step of glycolysis, that elicits its functions by binding to the voltage-dependent anion channels (VDAC) in the outer mitochondrial membrane (49, 50). Low HK2 expression was detected in monolayer cultures of PC3 cells (**Figure 3A**), with robust increases in HK2 fluorescence upon exposure to adipocytes (**Figure 3E**). This is consistent with adipocyte-induced Warburg phenotype in these cells (see footnote text 1). Mitotracker labeling (**Figures 3B–D,F–H**) showed no observable differences in the number of mitochondria between the control and Transwell conditions. The majority of the HK2 appeared to co-localize with mitochondria (**Figures 3C,G**), which is consistent with the literature evidence demonstrating that approximately 80% of total HK2 is bound to the mitochondrial VDAC (51).

In stark contrast to the monolayer cultures, a significant HK2 expression was observed in PC3 3D spheroids even under control conditions (**Figures 3I,K–N**). This indicates a potential enhancement of glycolytic phenotype, consistent with activation of HIF-1α signaling by 3D culture (**Figure 2**). High HK2 fluorescence closely mirroring mitochondrial pattern was also observed in 3D cultures grown under Transwell conditions (**Figures 3J,P–S**).

[1]Diedrich J, Rajagurubandara E, Herroon MK, Mahapatra G, Huttemann M, Podgorski I (unpublished results).

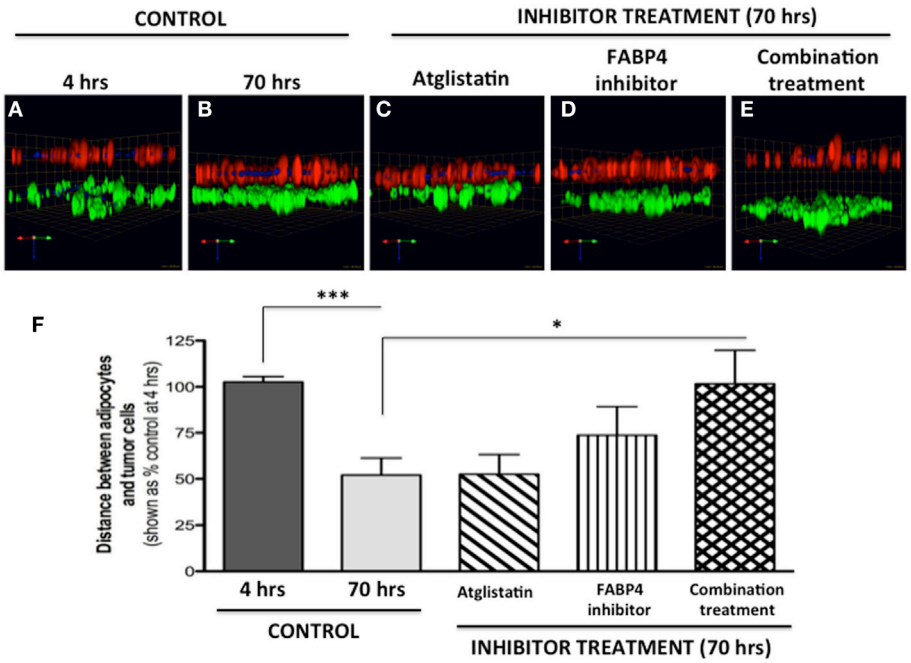

FIGURE 8 | Inhibition of tumor cell invasion toward adipocytes with FABP4 inhibitor and Atglistatin. **(A,B)** Invasion under control conditions at 4 h **(A)** and 70 h **(B)**. Adipocytes (BODIPY, green); Tumor cells (DsRed; red). **(C)** Invasion in the presence of 10 μM Atglistatin, **(D)** 1 μM FABP4 inhibitor, **(E)** Invasion in the presence of FABP4 inhibitor and Atglistatin in combination. Green arrow (*X*), red arrow (*Y*), and blue arrow (*Z*) indicate orientation of the spheroid in 3D space **(F)** Quantification of the average distance between PC3 cells and adipocytes under all experimental conditions. Distances between PC3 and adipocyte layer (in micrometers) were measured using the Zeiss LSM Image Browser software. Data were analyzed using GraphPad Prizm and shown as the mean of three independent experiments ± SD (relative to baseline invasion at 4 h). $^{*}p < 0.05$ and $^{***}p < 0.001$ are considered statistically significant.

However, HK2 fluorescence intensity was not significantly higher than in control cultures, indicating no significant enhancement of HK2 levels by coculture with adipocytes (data not shown).

Examining Effects of Marrow Adipocyte Presence on Tumor Response to Bone Marrow Macrophages

Bone represents a complex, dynamic microenvironment and establishment of metastatic lesions in the skeleton requires tumor cell interactions with a number of cell types in the marrow. To examine the suitability of our cell culture system to study multi-cell interactions, we incorporated BMMs into 3D tumor spheroids growing under control and Transwell conditions (**Figure 4A**). Pre-labeling of PC3 tumor cells with CTO allowed visualization of the tumor growing in 3D culture (**Figures 4B,C**). We tracked the incorporation of BMMs into the tumor spheroid by F4/80 immunofluorescence staining. Tumors growing under Transwell conditions with adipocytes attracted more macrophages than those cultured under control conditions (**Figures 4B,C**; green fluorescence). Incorporation of BMMs into the spheroid was also visible in the optical slices taken in the middle of the spheroid (**Figures 4D–G**). These observations suggest that adipocytes might be inducing phenotypic changes in the tumor cells and/or macrophages to promote the BMM affinity for the tumor. Further studies are needed to confirm this hypothesis.

Imaging Live Tumor Cell-Driven Proteolysis in the Presence of Marrow Adipocytes

To grow and thrive in their surrounding environments, tumors have to interact with the extracellular matrix (ECM) via biochemical and mechanical processes. Proteolysis of the ECM is one of the key aspects of tumor invasion (52, 53), and we have previously shown that exposure to adipocyte-derived factors increases invasive potential of prostate carcinoma cells (5). One way to effectively visualize ECM proteolysis by the tumor cells and other cell types residing in the tumor microenvironment is through a confocal microscopy assay utilizing quenched-fluorescent (DQ) proteins, an approach developed by the Sloane laboratory over a decade ago (53). We have previously utilized this technique to demonstrate that prostate carcinoma cells are capable of degrading quenched fluorescent derivatives of collagen IV (basement membrane) and collagen I (organic matrix of the bone) (33). Therefore, we used this approach to determine whether exposure to adipocyte-derived factors affects the collagen IV degradation in our model. PC3 cells plated on rBM containing DQ-IV were allowed to establish into spheroids by growing for 3 days under control or Transwell conditions before adding CTO-labeled BMMs and allowing cultures to continue for additional 2 days (**Figure 5A**). Degradation of the DQ-collagen IV, observed as green fluorescence, was captured and quantified at the end of 5-day culture. In agreement with

our previous findings (33), fluorescent cleavage products of DQ-collagen IV were found both intracellularly and pericellularly (**Figures 5B–E**). Similar levels of fluorescence were detected in PC3 cells cultured alone (without BMMs) regardless if they were under control or Transwell conditions (**Figures 5B,D,F,H,J**), suggesting no measurable contribution of adipocytes to tumor-driven proteolysis.

Since macrophages are important sources of proteases and key contributors to tumor-associated proteolysis (34, 53), we also measured and quantified the DQ-IV fluorescence following the 2-day coculture of pre-established tumor spheroids exposed to macrophages (**Figures 5C,E,G,I,J**). Surprisingly, despite the significant infiltration of BMMs into tumor spheroids exposed to adipocytes in a Transwell coculture and visible BMM-associated proteolysis (**Figures 5E,I**), there was no significant increase in overall tumor-associated DQ-IV degradation compared with cultures grown without macrophages (**Figure 5J**).

Interestingly, when macrophages were incorporated into the culture at the time of seeding the tumor cells (**Figure 6A**), significant changes were observed in the morphology of the resulting spheroids and in the tumor-associated proteolysis. Specifically, under control conditions, addition of BMMs led to formation of less compacted and more disorganized tumor spheroids compared with tumor cells cultured alone (**Figures 6B,F** vs. **Figures 6C,G**). This change in morphology was also associated with a significant increase in DQ-IV proteolysis (**Figure 6J**). Even more pronounced effects of BMMs were observed in cultures exposed to adipocytes in the Transwell system (**Figure 6D,H** vs. **Figures 6E,I**). Formation of highly disorganized tumor cell/BMM clusters with high levels of DQ-IV fluorescence (**Figure 6J**) suggested potentially important contribution of adipocytes to tumor- and BMM-driven proteolytic activity in this model.

Quantifying Tumor Cell Invasion Toward Adipocytes in Three-Dimensional System

Our previous work has shown that prostate carcinoma cells exposed to media conditioned by marrow adipocytes take up the fat cell-supplied lipids in a process that results in accelerated tumor growth and invasiveness (5). Prostate tumor cells have been reported to be attracted to adipocyte-rich areas of the bone marrow, where metastases commonly occur (54, 55), and the translocation of adipocyte-stored lipids has been linked to increased tumor cell motility (56). The mechanisms behind the tumor cell attraction to marrow fat cells, however, remain poorly understood. Here, we have designed a simple 3D system in which tumor cell invasion toward adipocytes can be easily visualized, measured, and quantified (**Figure 7A**). We used collagen I, the predominant component of bone, as the matrix separating BODIPY-labeled bone marrow adipocytes (bottom) and DsRed-expressing PC3 cells (top). Tumor cells invaded through collagen I matrix over the course of 96 h (**Figures 7B–E**), with complete merging of the two cell types at the 96-h time point.

We next tested two compounds with potential to affect adipocyte–tumor cell interactions: a selective inhibitor of fatty acid-binding protein 4 (FABP4) (BMS309403) (5), and Atglistatin, a selective inhibitor of Adipocyte Triglyceride LIpase (ATGL) (57). We chose to inhibit FABP4 based on our previous studies demonstrating upregulation of this lipid transporter in prostate tumor cells exposed to marrow adipocytes, and the apparent efficacy of BMS309403 in inhibiting prostate tumor cell invasion in the 2D Boyden chamber assay (5). We also used Atglistatin as the means of inhibiting adipocyte-driven lipolysis, which we have shown to be induced by prostate tumor cells (see footnote text 1). As expected, under control conditions, the distance between PC3 cells and marrow adipocytes was significantly reduced after 70 h, compared with the baseline at 4 h (**Figures 8A,B**). Atglistatin alone did not seem to have any effect on tumor cell invasion toward the adipocytes (**Figure 8C**). Despite potent inhibition of PC3 invasion in 2D (5), only modest inhibition of tumor invasion was observed with FABP4 inhibitor in a 3D assay (**Figure 8D**), a result potentially due to differences in matrix and experimental conditions between the two assays. Notably, however, the use of both inhibitors in combination significantly inhibited tumor invasion and restored the distance between the two cell types to the levels measured at 4 h (**Figures 8E,F**). This suggests a potential link between lipid hydrolysis and transport between adipocytes and tumor cells that needs further investigation.

DISCUSSION

The functional role of bone marrow adipocytes in the growth and aggressiveness of skeletal tumors is an understudied and not well-understood area of cancer research. There is a great need for *in vitro* 3D models that can address the complexity of the bone tumor microenvironment, yet allow dissection of the mechanisms behind the contribution of specific cell types to the metastatic growth. There has been a growing effort to generate 3D models that would represent a bridge between the 2D monolayer cultures and *in vivo* tumor microenvironment, with the idea of capturing the physiological complexity, multiplicity of cell types, ECM composition, and temporal and spatial distribution of soluble factors in the bone microenvironment (21, 28, 58–61). Many of these models have been key to demonstrating the importance of 3D tumor architecture in mechanistic understanding of basic cancer biology and, especially, in evaluating tumor response to therapy (22, 58, 61). Regretfully, however, none of these models to date have addressed the contribution of fat cells, one of most abundant cell types in the adult bone marrow to growth, phenotype, and behavior of metastatic tumor cells in bone.

The *in vitro* approaches we describe herein provide a simple way of examining interactions between bone marrow adipocytes and metastatic tumor cells in a physiologically relevant manner. Our Transwell system combines 3D culture of bone marrow-derived adipocytes with 3D culture of prostate tumor cells to allow paracrine interactions and sharing of nutrients and secreted factors by the two cell types. We show via immunofluorescence analysis of metabolism-associated proteins that under 3D conditions tumor cells have significantly different metabolic responses to adipocytes than tumor cells grown in a monolayer culture. This underlines the importance of employing 3D culture conditions to mimic physiological interactions between marrow

adipocytes and metastatic tumor cells. It is noteworthy that the simple design of our 3D system allows easy manipulation, processing, and analysis of the resulting cultures. Because tumor cell cultures are established on glass coverslips they are immediately available for immunocytochemistry and confocal imaging. These samples can also be recovered from the coverslips and processed for protein and RNA analyses (data not shown), allowing for additional data to support the confocal imaging results. We have also shown the suitability of this system to image proteolysis by living cells. We used DQ Collagen IV as a representative component of the basement membrane, but this approach can be easily modified for use with other DQ-labeled matrices, such as DQ Collagen I [a major protein in the bone (33, 62)], or with activity-based probes (63).

Contribution of other bone marrow-derived cell types is an important consideration in the design of physiologically relevant cell culture models. Our data show that BMMs can be easily incorporated into our coculture system. More importantly, we reveal that macrophages are attracted to tumor spheroids exposed to adipocyte-derived factors, and their coculture with tumor cells results in a more aggressive morphology and an enhanced ECM proteolysis by both cell types. This speaks to the importance of multi-cellular design in modeling the effects of specific cell types on tumor phenotype and behavior. Our system allows the manipulation of the design to vary cell types, numbers, and ECM components. Studies are currently ongoing to examine the effects of direct interaction of marrow macrophages with adipocytes on tumor cell growth and aggressiveness.

Previous studies have indicated that prostate tumor cells are attracted to adipocyte-rich areas in the bone marrow (54, 55). Our 3D invasion assay results confirm this attraction and provide a simple approach to evaluate potential targets involved in this process. We utilized our invasion system to inhibit the lipid transporter FABP4, and the main adipocyte lipase ATGL and revealed that ATGL-driven lipolysis and FABP4-driven lipid transport might be important for tumor cell–adipocyte interaction in the bone marrow microenvironment. This not only opens new avenues for investigation but also speaks to the potential utility of this assay as an initial screen to identify factors behind tumor cell invasiveness toward the marrow adipocytes. Many G protein-coupled receptors (GPRCs), including chemokine receptors and receptors of bioactive lipids, have been implicated in tumor cell growth and invasiveness (64). Given the fact that adipocytes are an abundant source of chemokines and lipids, their role in modulating the invasive capacity of tumor cells via GPCRs could be studied in this system. It is also important to mention that this approach is easily modifiable in terms of matrix type and thickness, time of invasion and cell types used, representing a useful tool to examine the functional effects of marrow adipocytes on tumor cell invasiveness.

We acknowledge that our models have limitations. First, we are utilizing adipocytes differentiated from bone marrow mesenchymal cells, which may not be entirely representative of adipocyte population in bone. Emerging data now show that there might be differences in bone marrow fat depending on localization in the bone (17), and we would not be able to capture these differences with our model. Second, we are utilizing murine bone marrow cells in combination with human tumor cells, which may not be entirely clinically relevant. Species-specific osteotropism is an important factor to be considered in design of physiologically relevant models (65). This would be particularly important when utilizing this model to study the effects of adipocyte-derived cytokines and chemokines on tumor cells. Adipokines, such as hepatocyte growth factor (HGF) or interleukin-6 (IL-6) are known to activate their receptors in a species-specific manner (66, 67). Nevertheless, it is important to mention that murine cells in our system can be easily replaced with human derived mesenchymal bone marrow cells to eliminate this issue.

Our model does not entirely recapitulate the bone tumor microenvironment found in the patient with metastatic disease, but it provides a controllable, testable system for examination of the molecular mechanisms behind adipocyte involvement in tumor progression in bone. We believe that the models described herein provide a good compromise between currently utilized 2D adipocyte-tumor cell cocultures and *in vivo* mouse models, where dissection of the specific contribution of adipocytes is not possible. Further development of these *in vitro* culture systems and combining them with other bone metastasis-focused cell culture models will open new strategies to increase our understanding of the role of marrow adipose tissue in metastatic progression.

AUTHOR CONTRIBUTIONS

MH carried out most of the data acquisition and analyses and participated in writing of the manuscript. JD carried out some data acquisition and participated in data analyses and writing of the manuscript. IP wrote the manuscript and participated in some of the data acquisition and analyses.

ACKNOWLEDGMENTS

The authors thank Dr. Kamiar Moin and the Microscopy, Imaging and Cytometry Resources Core (MICR) for assistance with confocal microscopy analyses. Grant support was provided by NIH/NCI 1 R01 CA181189-01 (IP, PI), NIH 5T32CA009531-29 (JD, trainee), and P30 CA 22453 (MICR).

REFERENCES

1. Berry R, Rodeheffer MS, Rosen CJ, Horowitz MC. Adipose tissue residing progenitors (adipocyte lineage progenitors and adipose derived stem cells (ADSC)). *Curr Mol Biol Rep* (2015) 1(3):101–9. doi:10.1007/s40610-015-0018-y
2. Georgiou KR, Hui SK, Xian CJ. Regulatory pathways associated with bone loss and bone marrow adiposity caused by aging, chemotherapy, glucocorticoid therapy and radiotherapy. *Am J Stem Cells* (2012) 1(3):205–24.
3. Cawthorn WP, Scheller EL, Learman BS, Parlee SD, Simon BR, Mori H, et al. Bone marrow adipose tissue is an endocrine organ that contributes to increased circulating adiponectin during caloric restriction. *Cell Metab* (2014) 20(2):368–75. doi:10.1016/j.cmet.2014.06.003
4. Hardaway AL, Herroon MK, Rajagurubandara E, Podgorski I. Marrow adipocyte-derived CXCL1 and CXCL2 contribute to osteolysis in metastatic prostate cancer. *Clin Exp Metastasis* (2015) 32(4):353–68. doi:10.1007/s10585-015-9714-5

5. Herroon MK, Rajagurubandara E, Hardaway AL, Powell K, Turchick A, Feldmann D, et al. Bone marrow adipocytes promote tumor growth in bone via FABP4-dependent mechanisms. *Oncotarget* (2013) 4(11):2108–23. doi:10.18632/oncotarget.1482
6. Templeton ZS, Lie WR, Wang W, Rosenberg-Hasson Y, Alluri RV, Tamaresis JS, et al. Breast cancer cell colonization of the human bone marrow adipose tissue niche. *Neoplasia* (2015) 17(12):849–61. doi:10.1016/j.neo.2015.11.005
7. Caers J, Deleu S, Belaid Z, De Raeve H, Van Valckenborgh E, De Bruyne E, et al. Neighboring adipocytes participate in the bone marrow microenvironment of multiple myeloma cells. *Leukemia* (2007) 21(7):1580–4. doi:10.1038/sj.leu.2404658
8. Liu Z, Xu J, He J, Liu H, Lin P, Wan X, et al. Mature adipocytes in bone marrow protect myeloma cells against chemotherapy through autophagy activation. *Oncotarget* (2015) 6(33):34329–41. doi:10.18632/oncotarget.6020
9. Chen GL, Luo Y, Eriksson D, Meng X, Qian C, Bäuerle T, et al. High fat diet increases melanoma cell growth in the bone marrow by inducing osteopontin and interleukin 6. *Oncotarget* (2016) 7(18):26653–69. doi:10.18632/oncotarget.8474
10. Hardaway AL, Herroon MK, Rajagurubandara E, Podgorski I. Bone marrow fat: linking adipocyte-induced inflammation with skeletal metastases. *Cancer Metastasis Rev* (2014) 33(2–3):527–43. doi:10.1007/s10555-013-9484-y
11. Morris E, Edwards C. The role of bone marrow adipocytes in bone metastasis. *J Bone Oncol* (2016). doi:10.1016/j.jbo.2016.03.006
12. Picon-Ruiz M, Pan C, Drews-Elger K, Jang K, Besser AH, Zhao D, et al. Interactions between adipocytes and breast cancer cells stimulate cytokine production and drive Src/Sox2/miR-302b-mediated malignant progression. *Cancer Res* (2016) 76(2):491–504. doi:10.1158/0008-5472.CAN-15-0927
13. Salameh TS, Le TT, Nichols MB, Bauer E, Cheng J, Camarillo IG. An ex vivo co-culture model system to evaluate stromal-epithelial interactions in breast cancer. *Int J Cancer* (2013) 132(2):288–96. doi:10.1002/ijc.27672
14. Santander AM, Lopez-Ocejo O, Casas O, Agostini T, Sanchez L, Lamas-Basulto E, et al. Paracrine interactions between adipocytes and tumor cells recruit and modify macrophages to the mammary tumor microenvironment: the role of obesity and inflammation in breast adipose tissue. *Cancers (Basel)* (2015) 7(1):143–78. doi:10.3390/cancers7010143
15. Wang C, Gao C, Meng K, Qiao H, Wang Y. Human adipocytes stimulate invasion of breast cancer MCF-7 cells by secreting IGFBP-2. *PLoS One* (2015) 10(3):e0119348. doi:10.1371/journal.pone.0119348
16. Dirat B, Bochet L, Dabek M, Daviaud D, Dauvillier S, Majed B, et al. Cancer-associated adipocytes exhibit an activated phenotype and contribute to breast cancer invasion. *Cancer Res* (2011) 71(7):2455–65. doi:10.1158/0008-5472.CAN-10-3323
17. Scheller EL, Cawthorn WP, Burr AA, Horowitz MC, MacDougald OA. Marrow adipose tissue: trimming the fat. *Trends Endocrinol Metab* (2016) 27(6):392–403. doi:10.1016/j.tem.2016.03.016
18. Pampaloni F, Reynaud EG, Stelzer EH. The third dimension bridges the gap between cell culture and live tissue. *Nat Rev Mol Cell Biol* (2007) 8(10):839–45. doi:10.1038/nrm2236
19. Weiswald LB, Bellet D, Dangles-Marie V. Spherical cancer models in tumor biology. *Neoplasia* (2015) 17(1):1–15. doi:10.1016/j.neo.2014.12.004
20. Chambers KF, Mosaad EM, Russell PJ, Clements JA, Doran MR. 3D cultures of prostate cancer cells cultured in a novel high-throughput culture platform are more resistant to chemotherapeutics compared to cells cultured in monolayer. *PLoS One* (2014) 9(11):e111029. doi:10.1371/journal.pone.0111029
21. Fong EL, Wan X, Yang J, Morgado M, Mikos AG, Harrington DA, et al. A 3D in vitro model of patient-derived prostate cancer xenograft for controlled interrogation of in vivo tumor-stromal interactions. *Biomaterials* (2016) 77:164–72. doi:10.1016/j.biomaterials.2015.10.059
22. Lovitt CJ, Shelper TB, Avery VM. Advanced cell culture techniques for cancer drug discovery. *Biology (Basel)* (2014) 3(2):345–67. doi:10.3390/biology3020345
23. Strand DW, Hayward SW. Modeling stromal-epithelial interactions in disease progression. *Discov Med* (2010) 9(49):504–11.
24. Shamir ER, Ewald AJ. Three-dimensional organotypic culture: experimental models of mammalian biology and disease. *Nat Rev Mol Cell Biol* (2014) 15(10):647–64. doi:10.1038/nrm3873
25. Nyga A, Neves J, Stamati K, Loizidou M, Emberton M, Cheema U. The next level of 3D tumour models: immunocompetence. *Drug Discov Today* (2016). doi:10.1016/j.drudis.2016.04.010
26. Sameni M, Anbalagan A, Olive MB, Moin K, Mattingly RR, Sloane BF. MAME models for 4D live-cell imaging of tumor: microenvironment interactions that impact malignant progression. *J Vis Exp* (2012) (60):3661. doi:10.3791/3661
27. Dovas A, Patsialou A, Harney AS, Condeelis J, Cox D. Imaging interactions between macrophages and tumour cells that are involved in metastasis in vivo and in vitro. *J Microsc* (2013) 251(3):261–9. doi:10.1111/j.1365-2818.2012.03667.x
28. Salamanna F, Contartese D, Maglio M, Fini M. A systematic review on in vitro 3d bone metastases models. A new horizon to recapitulate the native clinical scenario? *Oncotarget* (2016). doi:10.18632/oncotarget.8394
29. Podgorski I, Linebaugh BE, Koblinski JE, Rudy DL, Herroon MK, Olive MB, et al. Bone marrow-derived cathepsin K cleaves SPARC in bone metastasis. *Am J Pathol* (2009) 175(3):1255–69. doi:10.2353/ajpath.2009.080906
30. Herroon MK, Rajagurubandara E, Rudy DL, Chalasani A, Hardaway AL, Podgorski I. Macrophage cathepsin K promotes prostate tumor progression in bone. *Oncogene* (2013) 32(12):1580–93. doi:10.1038/onc.2012.166
31. Shaw KR, Wrobel CN, Brugge JS. Use of three-dimensional basement membrane cultures to model oncogene-induced changes in mammary epithelial morphogenesis. *J Mammary Gland Biol Neoplasia* (2004) 9(4):297–310. doi:10.1007/s10911-004-1402-z
32. Jedeszko C, Sameni M, Olive MB, Moin K, Sloane BF. Visualizing protease activity in living cells: from two dimensions to four dimensions. *Curr Protoc Cell Biol* (2008) Chapter 4:Unit4.20. doi:10.1002/0471143030.cb0420s39
33. Podgorski I, Linebaugh BE, Sameni M, Jedeszko C, Bhagat S, Cher ML, et al. Bone microenvironment modulates expression and activity of cathepsin B in prostate cancer. *Neoplasia* (2005) 7(3):207–23. doi:10.1593/neo.04349
34. Sameni M, Dosescu J, Moin K, Sloane BF. Functional imaging of proteolysis: stromal and inflammatory cells increase tumor proteolysis. *Mol Imaging* (2003) 2(3):159–75. doi:10.1162/153535003322556903
35. Nieman KM, Romero IL, Van Houten B, Lengyel E. Adipose tissue and adipocytes support tumorigenesis and metastasis. *Biochim Biophys Acta* (2013) 1831(10):1533–41. doi:10.1016/j.bbalip.2013.02.010
36. Diedrich J, Gusky HC, Podgorski I. Adipose tissue dysfunction and its effects on tumor metabolism. *Horm Mol Biol Clin Investig* (2015) 21(1):17–41. doi:10.1515/hmbci-2014-0045
37. Martinez-Outschoorn UE, Sotgia F, Lisanti MP. Power surge: supporting cells "fuel" cancer cell mitochondria. *Cell Metab* (2012) 15(1):4–5. doi:10.1016/j.cmet.2011.12.011
38. Vaughan M. The production and release of glycerol by adipose tissue incubated in vitro. *J Biol Chem* (1962) 237:3354–8.
39. Maeda N, Funahashi T, Shimomura I. Metabolic impact of adipose and hepatic glycerol channels aquaporin 7 and aquaporin 9. *Nat Clin Pract Endocrinol Metab* (2008) 4(11):627–34. doi:10.1038/ncpendmet0980
40. Langin D. Control of fatty acid and glycerol release in adipose tissue lipolysis. *C R Biol* (2006) 329(8):598–607. doi:10.1016/j.crvi.2005.10.008
41. Schwartz B, Yehuda-Shnaidman E. Putative role of adipose tissue in growth and metabolism of colon cancer cells. *Front Oncol* (2014) 4:164. doi:10.3389/fonc.2014.00164
42. Watson DG, Tonelli F, Alossaimi M, Williamson L, Chan E, Gorshkova I, et al. The roles of sphingosine kinases 1 and 2 in regulating the Warburg effect in prostate cancer cells. *Cell Signal* (2013) 25(4):1011–7. doi:10.1016/j.cellsig.2013.01.002
43. Tonelli F, Alossaimi M, Natarajan V, Gorshkova I, Berdyshev E, Bittman R, et al. The roles of sphingosine kinase 1 and 2 in regulating the metabolome and survival of prostate cancer cells. *Biomolecules* (2013) 3(2):316–33. doi:10.3390/biom3020316
44. Manzi L, Costantini L, Molinari R, Merendino N. Effect of dietary omega-3 polyunsaturated fatty acid DHA on glycolytic enzymes and Warburg phenotypes in cancer. *Biomed Res Int* (2015) 2015:137097. doi:10.1155/2015/137097
45. Baenke F, Peck B, Miess H, Schulze A. Hooked on fat: the role of lipid synthesis in cancer metabolism and tumour development. *Dis Model Mech* (2013) 6(6):1353–63. doi:10.1242/dmm.011338
46. Kroemer G, Pouyssegur J. Tumor cell metabolism: cancer's Achilles' heel. *Cancer Cell* (2008) 13(6):472–82. doi:10.1016/j.ccr.2008.05.005
47. DelNero P, Lane M, Verbridge SS, Kwee B, Kermani P, Hempstead B, et al. 3D culture broadly regulates tumor cell hypoxia response and angiogenesis via pro-inflammatory pathways. *Biomaterials* (2015) 55:110–8. doi:10.1016/j.biomaterials.2015.03.035

48. Chiche J, Brahimi-Horn MC, Pouyssegur J. Tumour hypoxia induces a metabolic shift causing acidosis: a common feature in cancer. *J Cell Mol Med* (2010) 14(4):771–94. doi:10.1111/j.1582-4934.2009.00994.x
49. Mathupala SP, Ko YH, Pedersen PL. Hexokinase II: cancer's double-edged sword acting as both facilitator and gatekeeper of malignancy when bound to mitochondria. *Oncogene* (2006) 25(34):4777–86. doi:10.1038/sj.onc.1209603
50. Pedersen PL, Mathupala S, Rempel A, Geschwind JF, Ko YH. Mitochondrial bound type II hexokinase: a key player in the growth and survival of many cancers and an ideal prospect for therapeutic intervention. *Biochim Biophys Acta* (2002) 1555(1–3):14–20. doi:10.1016/S0005-2728(02)00248-7
51. Arora KK, Pedersen PL. Functional significance of mitochondrial bound hexokinase in tumor cell metabolism. Evidence for preferential phosphorylation of glucose by intramitochondrially generated ATP. *J Biol Chem* (1988) 263(33):17422–8.
52. Sahai E. Mechanisms of cancer cell invasion. *Curr Opin Genet Dev* (2005) 15(1):87–96. doi:10.1016/j.gde.2004.12.002
53. Sloane BF, Sameni M, Podgorski I, Cavallo-Medved D, Moin K. Functional imaging of tumor proteolysis. *Annu Rev Pharmacol Toxicol* (2006) 46:301–15. doi:10.1146/annurev.pharmtox.45.120403.095853
54. Brown MD, Hart CA, Gazi E, Bagley S, Clarke NW. Promotion of prostatic metastatic migration towards human bone marrow stoma by Omega 6 and its inhibition by omega 3 PUFAs. *Br J Cancer* (2006) 94(6):842–53. doi:10.1038/sj.bjc.6603030
55. Gazi E, Gardner P, Lockyer NP, Hart CA, Brown MD, Clarke NW. Direct evidence of lipid translocation between adipocytes and prostate cancer cells with imaging FTIR microspectroscopy. *J Lipid Res* (2007) 48(8):1846–56. doi:10.1194/jlr.M700131-JLR200
56. Brown MD, Hart C, Gazi E, Gardner P, Lockyer N, Clarke N. Influence of omega-6 PUFA arachidonic acid and bone marrow adipocytes on metastatic spread from prostate cancer. *Br J Cancer* (2010) 102(2):403–13. doi:10.1038/sj.bjc.6605481
57. Mayer N, Schweiger M, Romauch M, Grabner GF, Eichmann TO, Fuchs E, et al. Development of small-molecule inhibitors targeting adipose triglyceride lipase. *Nat Chem Biol* (2013) 9(12):785–7. doi:10.1038/nchembio.1359
58. Fitzgerald KA, Guo J, Tierney EG, Curtin CM, Malhotra M, Darcy R, et al. The use of collagen-based scaffolds to simulate prostate cancer bone metastases with potential for evaluating delivery of nanoparticulate gene therapeutics. *Biomaterials* (2015) 66:53–66. doi:10.1016/j.biomaterials.2015.07.019
59. Holen I, Nutter F, Wilkinson JM, Evans CA, Avgoustou P, Ottewell PD. Human breast cancer bone metastasis in vitro and in vivo: a novel 3D model system for studies of tumour cell-bone cell interactions. *Clin Exp Metastasis* (2015) 32(7):689–702. doi:10.1007/s10585-015-9737-y
60. Marlow R, Dontu G. Modeling the breast cancer bone metastatic niche in complex three-dimensional cocultures. *Methods Mol Biol* (2015) 1293:213–20. doi:10.1007/978-1-4939-2519-3_12
61. Xu X, Farach-Carson MC, Jia X. Three-dimensional in vitro tumor models for cancer research and drug evaluation. *Biotechnol Adv* (2014) 32(7):1256–68. doi:10.1016/j.biotechadv.2014.07.009
62. Herroon MK, Sharma R, Rajagurubandara E, Turro C, Kodanko JJ, Podgorski I. Photoactivated inhibition of cathepsin K in a 3D tumor model. *Biol Chem* (2016) 397(6):571–82. doi:10.1515/hsz-2015-0274
63. Ben-Aderet L, Merquiol E, Fahham D, Kumar A, Reich E, Ben-Nun Y, et al. Detecting cathepsin activity in human osteoarthritis via activity-based probes. *Arthritis Res Ther* (2015) 17:69. doi:10.1186/s13075-015-0586-5
64. Dorsam RT, Gutkind JS. G-protein-coupled receptors and cancer. *Nat Rev Cancer* (2007) 7(2):79–94. doi:10.1038/nrc2069
65. Kuperwasser C, Dessain S, Bierbaum BE, Garnet D, Sperandio K, Gauvin GP, et al. A mouse model of human breast cancer metastasis to human bone. *Cancer Res* (2005) 65(14):6130–8. doi:10.1158/0008-5472.CAN-04-1408
66. Jeffers M, Rong S, Vande Woude GF. Hepatocyte growth factor/scatter factor-met signaling in tumorigenicity and invasion/metastasis. *J Mol Med (Berl)* (1996) 74(9):505–13. doi:10.1007/BF00204976
67. Hammacher A, Ward LD, Weinstock J, Treutlein H, Yasukawa K, Simpson RJ. Structure-function analysis of human IL-6: identification of two distinct regions that are important for receptor binding. *Protein Sci* (1994) 3(12):2280–93. doi:10.1002/pro.5560031213

Conflict of Interest Statement: The authors declare that the research was conducted in the absence of any commercial or financial relationships that could be construed as a potential conflict of interest.

Advantages of publishing in Frontiers

OPEN ACCESS
Articles are free to read, for greatest visibility

COLLABORATIVE PEER-REVIEW
Designed to be rigorous – yet also collaborative, fair and constructive

FAST PUBLICATION
Average 85 days from submission to publication (across all journals)

COPYRIGHT TO AUTHORS
No limit to article distribution and re-use

TRANSPARENT
Editors and reviewers acknowledged by name on published articles

SUPPORT
By our Swiss-based editorial team

IMPACT METRICS
Advanced metrics track your article's impact

GLOBAL SPREAD
5'100'000+ monthly article views and downloads

LOOP RESEARCH NETWORK
Our network increases readership for your article

Frontiers
EPFL Innovation Park, Building I • 1015 Lausanne • Switzerland
Tel +41 21 510 17 00 • Fax +41 21 510 17 01 • info@frontiersin.org
www.frontiersin.org

Find us on